



PHD

Synthesis of Novel Chromium based Catalyst Systems, and Investigation of their Activity in the Trimerisation of alpha-Olefins

I'Anson, Ian A

Award date:
2009

Awarding institution:
University of Bath

[Link to publication](#)

Alternative formats

If you require this document in an alternative format, please contact:
openaccess@bath.ac.uk

Copyright of this thesis rests with the author. Access is subject to the above licence, if given. If no licence is specified above, original content in this thesis is licensed under the terms of the Creative Commons Attribution-NonCommercial 4.0 International (CC BY-NC-ND 4.0) Licence (<https://creativecommons.org/licenses/by-nc-nd/4.0/>). Any third-party copyright material present remains the property of its respective owner(s) and is licensed under its existing terms.

Take down policy

If you consider content within Bath's Research Portal to be in breach of UK law, please contact: openaccess@bath.ac.uk with the details. Your claim will be investigated and, where appropriate, the item will be removed from public view as soon as possible.

Synthesis of Novel Chromium based Catalyst Systems, and Investigation of their Activity in the Trimerisation of α - Olefins

by

Ian Alan I'Anson

A thesis submitted for the degree of Doctor of Philosophy

University of Bath

Department of Chemistry

July 2007

COPYRIGHT

Attention is drawn to the fact that copyright of this thesis rests with its author. This copy of the thesis has been supplied on condition that anyone who consults it is understood to recognise that its copyright rests with its author and that no quotation from the thesis and no information derived from it may be published without the prior written consent of the author.

This thesis may not be consulted, photocopied or lent to other libraries without the permission of the author or BASF for 3 years from the date of acceptance of the thesis.

Declaration:

The work described in this thesis was carried out at the University of Bath, Department of Chemistry, between October 2003 and July 2007. All the work is my own, unless otherwise stated, and it has not been submitted previously for a degree at this or any other university.

Financial Support:

BASF is gratefully acknowledged for providing funding for the work described in this thesis.

Acknowledgements:

There are countless people to whom I owe thanks for their assistance during the course of my studies at Bath, and alas not all could be included here.

I owe a particular debt of gratitude to Dr. Randolph Köhn, for allowing me to be part of his research group, for imparting so much knowledge across the field of chemical research, and for his considerable patience on those not infrequent occasions when my inexperience (not to mention downright foolishness!), has impaired progress. Finally I have to thank him for patiently and conscientiously proof reading the reams of notes that ultimately coalesced into the document presented herein.

I would also like to thank Dr. Gabriele Kociok-Köhn for her assistance in obtaining single-crystal X-ray crystallographic data, sometimes from crystals of such quality that a less determined individual would have abandoned them.

I would like to thank Dr. Fredy Speiser, Graeme Nawn and Lorena Tomas Laudo for making the lab a fun and hospitable working environment, and for generally putting up with me. This latter acknowledgement applies also to Dr. Steve Richards, and Dr. Luke Turner.

Thanks are owed to the administrative and support staff, without whom no-one's research would be possible, and special thanks are also owed to my parents, for their patience and support over the past few months, while I've been preparing this document.

Abstract: *Selective α -olefin trimerisation catalysts are of substantial and increasing commercial significance. Novel chromium based catalyst systems, based on derivatives and analogues of the previously developed chromium III complexes of 1,3,5-triazacyclohexanes, have been investigated, with particular emphasis on the synthesis and reactivity of the potential ligand type $RB(R'NCH_2)_2$, and on the incorporation of weakly coordinating anionic functionalities into the active complexes.*

Abbreviations:

The following abbreviations are used throughout this document:

HDPE:	High density polyethylene
MDPE:	Medium density polyethylene
LDPE:	Low density polyethylene
LLDPE:	Linear low density polyethylene
MAO:	Methylaluminoxane
FTIR:	Fourier transform infrared spectroscopy
Cp:	Cyclopentadienyl anion
Cp*:	1,2,3,4,5-pentamethylcyclopentadienyl anion
SHOP:	Shell higher olefin process
BM:	Bohr magneton
TAC:	1,3,5-triazacyclohexane
NMR:	Nuclear magnetic resonance
THF:	Tetrahydrofuran
DCM:	Dichloromethane
DFT:	Density functional theory
DMSO:	Dimethylsulphoxide
ppm:	Parts per million
RMM:	Relative molecular mass
MF:	Molecular Formula

Contents:

1. Introduction:	1
1.1 Polymerisation Catalysts:	1
1.1.1 Ziegler-Natta Type Catalyst:	1
1.1.2 Kaminsky Metallocenes:	2
1.1.3 Phillips Catalyst:	4
1.2 Phillips Catalyst Model Systems:	8
1.2.1 Homogeneous Model- 2,4-pentane- <i>N,N'</i> -bis(aryl)ketiminatochromium dichloride:	8
1.2.2 Vapour Phase Collision Modeling:	9
1.2.3 Homogeneous Model- 1-(1,2,3,4,5-pentamethyl)cyclopentadienyl-2,2,5,5-tetramethyl-1-chromo-2,5-bis-phosphinocyclopentane Cation:	10
1.3 Ethylene Trimerisation Catalysts:	11
1.3.1 Phillips Ethylene Trimerisation Catalyst:	13
1.3.2 Other Model Systems:	13
1.3.2.1 2,6-diphenylphenol, Chromium (III) 2-ethylhexanoate:	16
1.3.2.2 η^5 -(Aryldimethyl)methylcyclopentadienyltitanium Chloride: η^5 - $C_5H_4CMe_2RTiCl_3$:	17
1.3.2.3 1,2,3,4,5-Pentaphenylcyclopentadienyl Chromium Hexanoate:	21
1.3.3 Complexes based on Multidentate Ligands:	23
1.3.3.1 1,4,7-Trimethyl-1,4,7-Triazacyclononane Chromium Chloride:	23
1.3.3.2 Tris(pyrazolyl)methane Chromium Chloride:	24
1.3.3.3 Methyl-bis(diaryl)phosphinoamine Complexes: $Ar_2PN(Me)PAr_2$:	25
1.3.3.4 S and N Donor Mixed Systems:	26
1.4 Chromium Complexes of 1,3,5-Triazacyclohexanes:	29
1.4.1 The Effect of Paramagnetism on In Situ Characterization of Chromium III Complexes:	33
1.5 1,3,5-Triazacyclohexanes- Synthesis and Reactivity	34

1.6 Proposed Development of Anionic Ligands:.....	41
Introduction- Summary:	44
2. Results and Discussion:	45
2.1 Triazacyclohexanes bearing Tetrarylborate Anionic Functionalities:.....	45
2.2 1-(<i>p</i> -(Trisarylboron)oxymethyl)phenyl-3,5-dialkyl-1,3,5-triazacyclohexanes:.....	52
2.3 B-N Bonded Anionic Ligands:.....	54
2.3.1 Azaboranes:.....	54
2.3.2 Diazaboranes:.....	56
2.3.2.1 Reactivity of 1-phenyl-2,5-di- <i>tert</i> -butyl-1-bora-2,5-diazacyclopentane with <i>n</i> -Butyl Lithium:.....	63
2.3.2.2 Reactivity of 1-phenyl-2,5-di- <i>tert</i> -butyl-1-bora-2,5-diazacyclopentane with Hexylmagnesium Bromide:.....	64
2.3.2.3 Reactivity of 1-phenyl-2,5-di- <i>tert</i> -butyl-1-bora-2,5-diazacyclopentane with Methanol.....	64
2.3.2.4 Reactivity of 1-phenyl-2,5-di- <i>tert</i> -butyl-1-bora-2,5-diazacyclopentane with (De-ionised) Water:.....	66
2.3.2.5 Reactivity of 1-phenyl-2,5-di- <i>tert</i> -butyl-1-bora-2,5-diazacyclopentane with Tetramethylammonium Fluoride:.....	66
2.3.2.6 Reactivity of 1-phenyl-2,5-di- <i>tert</i> -butyl-1-bora-2,5-diazacyclopentane with Sodium <i>n</i> -Butoxide:.....	69
2.3.3 Triazaboranes:.....	70
2.3.3.1 Reactivity of Tris(diethyl)aminoborane with Methylmagnesium Chloride:.....	73
2.3.3.2: Reactivity of tris(diethyl)aminoborane with <i>n</i> -Butyl lithium:.....	74
2.3.3.3: Reactivity of Tris(diethyl)aminoborane with Tetramethylammonium Fluoride:.....	74
2.3.3.4: Reactivity of (diethyl)aminoborane with Lithium Diethylamide:.....	75
2.3.4 Theoretical Considerations of B-N bonded species:.....	75
2.3.5 Complexation to Chromium III:.....	85
2.3.6: Trioxyboranes:.....	88
2.4 Cyclic Ureas:.....	92
2.4.1 Reaction of 1-keto-2,5-di- <i>tert</i> -butyl-2,5-diazacyclopentane with <i>n</i> -butyl lithium:.....	94

2.4.2 Reaction of 1-keto-2,5-di-tert-butyl-2,5-diazacyclopentane with hexylmagnesium bromide:.....	94
2.4.3: Attempted Complexation of 1-keto-2,5-di-tert-butyl-2,5-diazacyclopentane and hexylmagnesium bromide to Chromium III Chloride:.....	95
2.5 Synthesis of N,N'-dialkylethylenediamines:.....	98
2.5.1 N,N'-Bis(2-ethylhexyl)ethylenediamine Synthesis:.....	98
2.5.2 N,N'-Bis(phenethyl)ethylenediamine Synthesis:.....	98
2.6 Catalytic Properties of Chromium Complexes:.....	99
Results and Discussion- Summary:	99
3. Experimental:	100
<i>General:</i>	100
3.1 Synthesis of Sodium n-Butoxide:.....	100
3.2 Synthesis of Hexylmagnesium Bromide:.....	101
3.3 Synthesis of Bis-phenethylethylenediamine:.....	101
3.4 Synthesis of Bis(2-Ethyl)hexylethylenediamine:.....	102
3.5 Example Procedure: Synthesis of Symmetric Triazacyclohexanes- Synthesis of 1,3,5-trimethyl-1,3,5-triazacyclohexane:.....	103
3.6 Preparation of 1,3,5-trimethyl-1,3,5-triazacyclohexane Hydrobromide Crystals:.....	104
3.7 Example procedure: Synthesis of Unsymmetric Triazacyclohexanes- Synthesis of 1,3-dimethyl-5-(4-bromo)phenyl-1,3,5-triazacyclohexane:.....	104
3.8 Synthesis of 1,3-dimethyl-5-(4-trimethylsilyl)phenyl-1,3,5-triazacyclohexane:.....	105
3.9 Reaction of 1,3,5-trimethyl-1,3,5-triazacyclohexane with Boron Trifluoride Diethyletherate:.....	106
3.10 Reaction of 1,3,5-tribenzyl-1,3,5-triazacyclohexane with Tris(pentafluoro)phenylborane Diethyletherate:.....	107
3.11 Synthesis of N-(trimethyl)silyl-4-bromoaniline:.....	107
3.12 Synthesis of N,N-bis-(trimethyl)silyl-4-bromoaniline:.....	108
3.13 Synthesis of 4-(N,N'-bis-(trimethyl)silyl)aminophenyl Lithium:.....	109
3.14 Synthesis of N,N-bis-(trimethyl)silyl-p-(trimethyl)silylaniline:.....	109
3.15 Synthesis of 4-(trimethyl)silylaniline Hydrochloride:.....	110

3.16 (Synthesis of Lithium <i>N,N</i> -bis-(trimethyl)silyl-4-(tris(pentafluoro)phenylborato)aniline)]Et ₂ O] ₂ :	111
3.17 (Synthesis of Lithium 4-aminophenyltris(pentafluoro)phenylborate hydrochloride)]Et ₂ O] ₂ :	113
3.18 Attempted Synthesis of 1-(3-(sodium oxy)methyl)phenyl-3,5-(2-ethyl)hexyl-1,3,5-triazacyclohexane:	114
3.19 Complexation of Product and Chromium III Chloride:	115
3.20 Synthesis of 1,1-diphenyl-2,5-diethyl-1-sila-2,5-diazacyclopentane:	116
3.21 Attempted Complexation of 1,1-diphenyl-2,5-diethyl-1-sila-2,5-diazacyclopentane:	117
3.22 Example Procedure: Synthesis of 1-Phenyl-2,5-di-tert-butyl-1-bora-2,5-diazacyclopentane:	117
3.23 Attempted Complexation of 1-Phenyl-2,5-di-tert-butyl-1-bora-2,5-diazacyclopentane:	119
3.24 Example Procedure- Synthesis of 1-chloro-2,5-di-tert-butyl-1-bora-2,5-diazacyclopentane:	119
3.25 Preparation of 1-bromo-2,5-di-tert-butyl-1-bora-2,5-diazacyclopentane Crystals:	120
3.26 Synthesis of Bis(diethyl)aminophenylborane:	120
3.27 Synthesis of Tris(diethyl)aminoborane:	121
3.28 Attempted Reaction of Tris(diethyl)aminoborane with Methylmagnesium chloride:	122
3.29 Attempted Reaction of Tris(diethyl)aminoborane with Lithium Diethylamide:	123
3.30 Attempted Reaction of Tris(diethyl)aminoborane with Tetramethylammonium Fluoride:	123
3.31 Attempted Reaction of Tris(diethyl)aminoborane with <i>n</i> -butyl Lithium:	124
3.32 Reaction of 1-Phenyl-2,5-di-tert-butyl-1-bora-2,5-diazacyclopentane with Tetramethylammonium Fluoride:	125
3.33 Complexation of 1-Phenyl-2,5-di-tert-butyl-1-bora-2,5-diazacyclopentane and Tetramethylammonium Fluoride, with Chromium III Chloride:	127
3.34 Reactivity of 1-phenyl-2,5-di-tert-butyl-1-bora-2,5-diazacyclopentane with De-ionised Water:	128
3.35 Attempted Reaction of 1-Phenyl -2,5-di-tert-butyl-1-bora-2,5-diazacyclopentane with Methanol:	129

3.36 Attempted Reaction of 1-Phenyl -2,5-di-tert-butyl-1-bora-2,5-diazacyclopentane with sodium n-butoxide:.....	130
3.37 Attempted Reaction of 1-Phenyl -2,5-di-tert-butyl-1-bora-2,5-diazacyclopentane with Hexylmagnesium Bromide:.....	131
3.38 Complexation of 1-Phenyl-2,5-di-tert-butyl-1-bora-2,5-diazacyclopentane with hexylmagnesium bromide:.....	132
3.39 Attempted Reaction of 1-Phenyl-2,5-di-tert-butyl-1-bora-2,5-diazacyclopentane with n-Butyl Lithium:.....	133
3.40 Attempted Reaction of Trimethyl(pentafluoro)phenylsilane with Boron Tribromide:.....	134
3.41 Attempted Reaction of Trimethyl(pentafluoro)phenylsilane with Boron Trichloride:.....	135
3.42 Attempted Reaction of 3,5-bis(trifluoromethyl)phenyltrimethylsilane with Boron Tribromide:.....	135
3.43 Attempted Reaction of 3,5-bis(trifluoromethyl)phenyltrimethylsilane with Boron Trichloride:.....	136
3.44 Synthesis of Sodium Phenyl (Bis-hydroxy)Butoxyborate:.....	136
3.45 Complexation of Sodium Phenyl (Bis-hydroxy)Butoxyborate:.....	137
3.46 Synthesis of 1-keto-2,5-di-tert-butyl-2,5-diazacyclopentane:.....	137
3.47 Complexation of 1-keto-2,5-di-tert-butyl-2,5-diazacyclopentane:.....	138
3.48 Attempted Reaction of 1-keto-2,5-di-tert-butyl-2,5-diazacyclopentane with Hexylmagnesium Bromide:.....	138
3.49 Complexation of 1-keto-2,5-di-tert-butyl-2,5-diazacyclopentane and Hexylmagnesium Bromide with Chromium III Chloride:.....	139
3.50 Attempted Reaction of 1-keto-2,5-di-tert-butyl-2,5-diazacyclopentane with n-butyl Lithium:.....	140
3.51 Synthesis of N-lithium-N'-phenylpiperazine:.....	141
3.52 Synthesis of N-phenyl-N'-trimethylsilylpiperazine:.....	141
3.53 Attempted Synthesis of Lithium N-triphenylborato-N'-phenylpiperazine:.....	142
3.54 Determination of Concentration of Grignard Reagent in THF soln. Example method: Hexylmagnesium Bromide in THF:.....	142
3.55 Determination of Magnetic Moment (and hence Oxidation State) of a Chromium Complex in Solution, by an Approximation of the Evans Method:.....	143
4. Catalysis- NMR interpretation:.....	146

Calculation of Mass % Conversion of 1-hexene to Products- Example Spectrum:	
Catalysis of Ethylene Trimerisation by 1,3,5-Tris-dodecyl-1,3,5-triazacyclohexane:	146
Calculation of Mean Olefinic to Aliphatic Proton Ratio in 1-hexene Reaction	
Products:	148
Comparative Estimate of Product Chain Length:	151
Comparative Analysis of Trimerisation Properties 1,3,5-Tris-Dodecyl-1,3,5-triazacyclohexene- Chromium III Chloride Complex:	152
Trimerisation Properties of 1-keto-2,5-di-<i>tert</i>-butyl-2,5-diazacyclopentane-Chromium III Chloride complex + Hexylmagnesium Bromide:	154
Trimerisation Properties of 1-keto-2,5-di-<i>tert</i>-butyl-2,5-diazacyclopentane-Chromium III Chloride Complex:	155
Trimerisation Properties of 1,3,5-tris(2-ethyl)hexyl-1,3,5-triazacyclohexane, sodium 3-aminobenzylalcoholate + Chromium III Chloride:	156
Trimerisation Properties of 1,3,5-tris(2-ethyl)hexyl-1,3,5-triazacyclohexane, sodium 3-aminobenzylalcoholate + Chromium III Chloride + 1 eq.	
Tris(pentafluoro)phenylborane:	158
Trimerisation Properties of 1-phenyl-2,5-di-<i>tert</i>-butyl-1-bora-2,5-diazacyclopentane- Chromium III Chloride Complex + Tetramethylammonium Fluoride:	159
Trimerisation Properties of 1-Phenyl-2,5-di-<i>tert</i>-butyl-1-bora-2,5-diazacyclopentane- Chromium III Chloride Complex:	160
Trimerisation Properties of 1-phenyl-2,5-di-<i>tert</i>-butyl-1-bora-2,5-diazacyclopentane- Chromium III Chloride Complex + Hexylmagnesium Bromide:	162
Trimerisation Properties of Sodium Phenyl(bis-hydroxy)butoxyborate-Chromium III Chloride Complex:	163
Conclusion:	165
References:	169

1. Introduction:

The polymerization of olefins is a commercially highly significant process, given the variety of polymers that can thus be synthesized and their utility in the manufacture of industrial and domestic products. Due to its low cost and comparative ease of manufacture, polyethylene is the largest volume polymer consumed in the world today,¹ and exists in a variety of forms. These include HDPE (High Density Polyethylene), MDPE (Medium Density Polyethylene), LDPE (Low Density Polyethylene) and LLDPE (Linear Low Density Polyethylene), the structures and attendant physical properties of which vary according to the mean chain length, and chain length distribution; and the extent of branching of the polymer chains.² Several commercially significant industrial catalytic processes exist for the polymerization of ethylene, developed during the latter half of the 20th century- particularly the Phillips Catalyst, the Ziegler-Natta Catalyst and Kaminsky Metallocenes; and there have been a large number of more recent developments stemming from ongoing research in the field. There is also considerable interest in the development of selective olefin trimerisation processes, for applications such as the synthesis of 1-hexene from ethylene. These developments will be detailed later in this chapter. Linear α -olefins are useful intermediates in the synthesis of branched polymers, detergents etc.

1.1 Polymerisation Catalysts:

1.1.1 Ziegler-Natta Type Catalyst:

The Ziegler-Natta type comprises a variety of transition metal-based catalysts. While V, Zr, and Hf based systems are known,³ typically the system is based on Titanium Chlorides. In the 1950s Karl Ziegler developed systems based on $\text{TiCl}_3/\text{Et}_2\text{AlCl}$ and $\text{TiCl}_4/\text{AlEt}_3$, for the polymerisation of ethylene. The solid catalyst system is suspended in a solvent, through which the olefin is passed, resulting in the rapid production of linear polymers. Giulio Natta subsequently refined the process, extending it to the polymerisation of propylene for the synthesis of stereoregular (isotactic and syndiotactic) polymers.

The mechanism of catalysis has not been unequivocally established,⁴ but is widely believed to involve migratory insertion of an ethyl substituent to a coordinated α -olefin on a complex formed by the association of the catalyst and co-catalyst, this being the Cossee-Arlman Mechanism, see figure 1.1:⁵

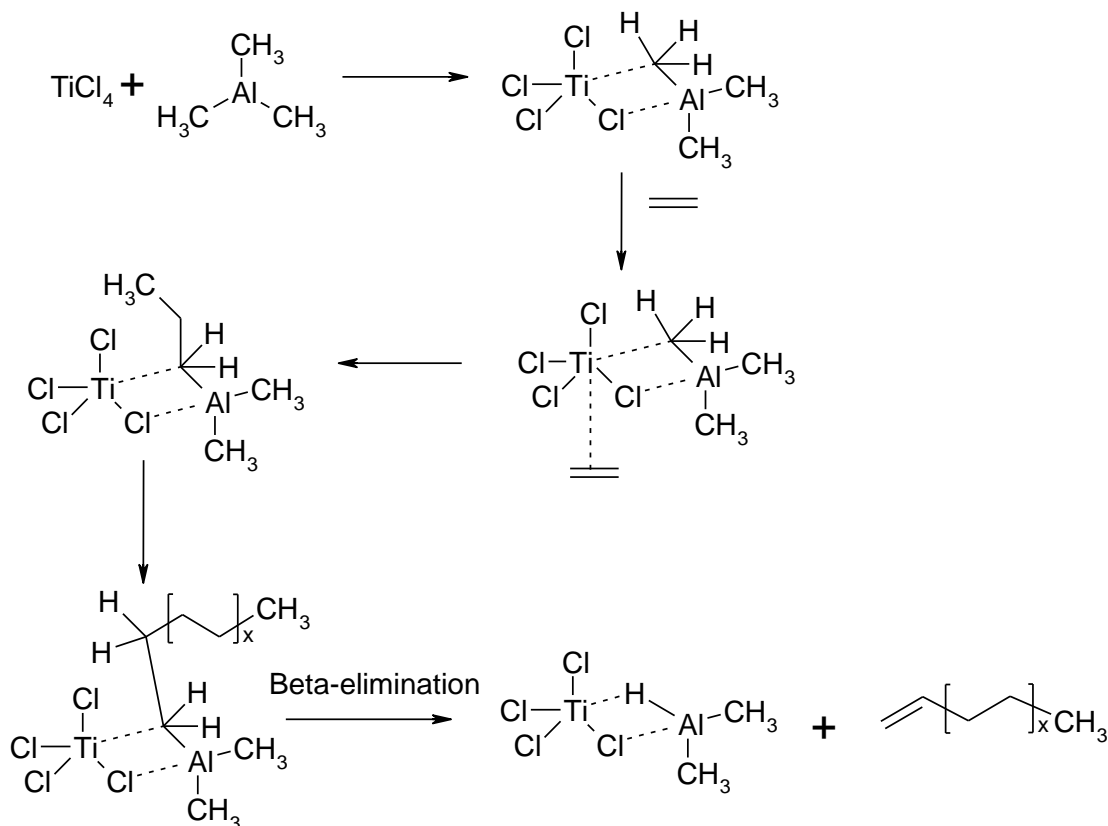


Figure 1.1: Catalytic Cycle for the Ziegler-Natta Catalysed Polymerisation of Ethylene.

The titanium chloride in the above system exists as a crystal lattice, in which the requisite coordinative unsaturation occurs at crystal defects. The generic Ziegler-Natta catalyst comprises a transition metal compound from groups IV to VII and an organometallic compound of a metal from groups I to III.⁶

The principal disadvantage of Ziegler-Natta type catalysts is that the scope for controlling the growth of the polymer chains, is limited, achievable only by selective poisoning of active sites. Greater opportunities are presented by Kaminsky Metallocenes.

1.1.2 Kaminsky Metallocenes:

The Kaminsky class of metallocenes was first developed by Kaminsky's research group at the University of Hamburg in the 1970s. The accidental addition of water to the system $\text{Cp}_2\text{ZrCl}_2/\text{AlMe}_3$ resulted in the hydrolysis of the trimethyl aluminium to form MAO. The result was an extremely active ethylene polymerisation catalyst. Metallocenes exhibiting catalytic activity for polymerisation in the presence of MAO are thus referred to as 'Kaminsky Metallocenes'.⁷

The polymerisation is believed to proceed via a variation of the Cossee-Arlman Mechanism, as seen in the case of the Ziegler-Natta catalyst, see figure 1.2:

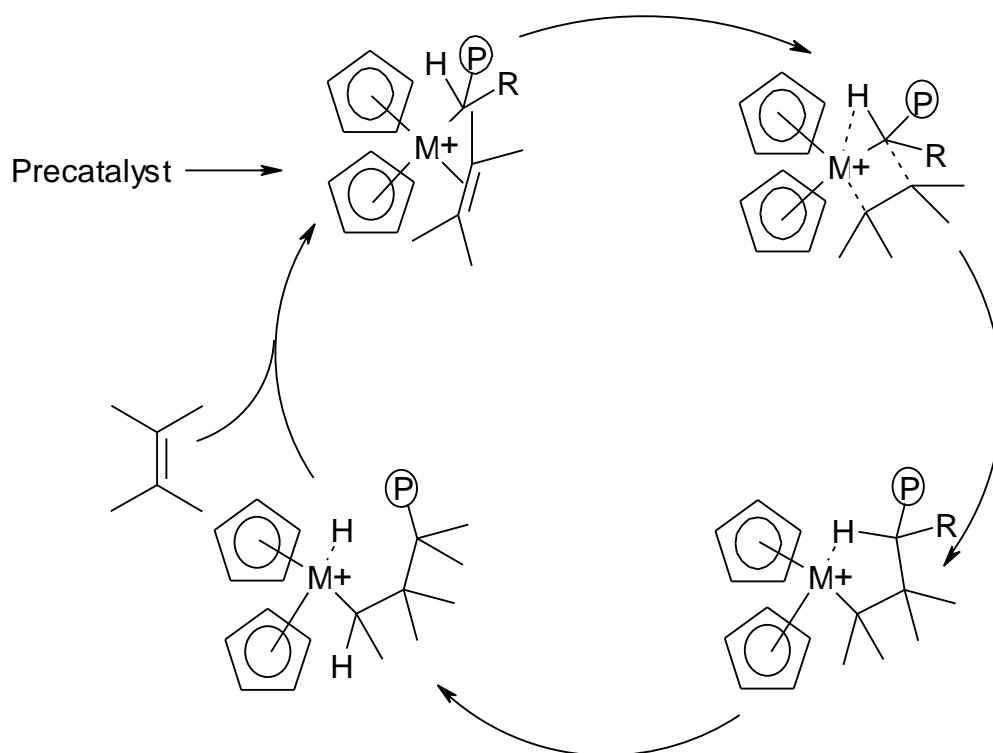


Figure 1.2: Cossee-Arlman Catalytic Cycle for Polymerisation by Kaminsky Metallocene.

Metallocenes have since been developed as co-catalysts for a variety of monomers. Stereo-rigid complexes have been developed, either through the use of bridged metallocenes, or in a more recent development, rotationally hindered unbridged ligands,³ exhibiting stereoselective polymerisation activity of α -olefins, eg,

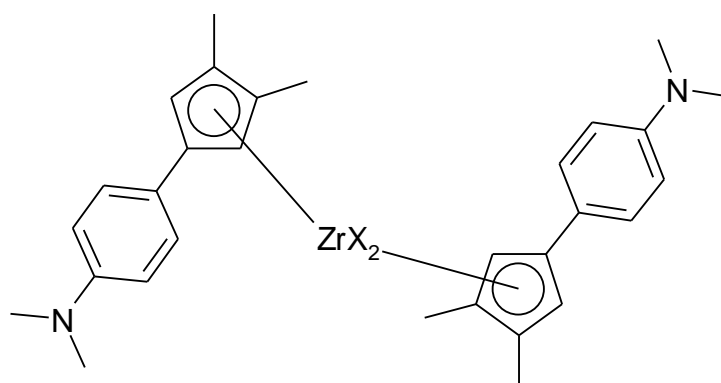


Figure 1.3: Example of a Stereoselective Polymerization Catalyst.

1.1.3 Phillips Catalyst:

The Phillips Catalyst was developed by Hogan and Banks at Phillips Petroleum Co. in the 1950s, and still represents one of the major industrial processes for the synthesis of HDPE. This is a heterogeneous catalyst based on Chromium Trioxide chemisorbed onto silica. It is prepared by addition of an approximately 2 wt% aqueous solution of chromic acid to silica, followed by drying and calcination in oxygen to give the active species.⁸ See figure 1.4:

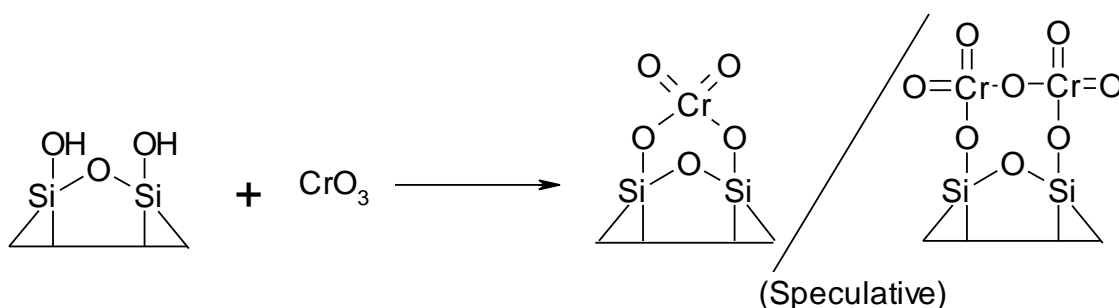


Figure 1.4. Preparation of Phillips Catalyst, active species.

It is unusual in not requiring an MAO or other alkyl aluminium co-catalyst. The catalyst is highly active for the polymerisation of ethylene. There is continuing debate as to the mechanism of the polymerisation reaction, since CrO₃ may be chemisorbed to the surface in multiple binding modes, and since the reaction occurs at the surface, while it is observable by various analytical tools, it is difficult to determine the active species. Various studies have been undertaken in an effort to investigate the catalytic

activity, both by spectroscopic observation and computer modeling. Zecchina *et al.*⁸ report FTIR studies of the oligomerisation of alkynes by a model Phillips Catalyst. They infer from their results the cyclisation of three simultaneously coordinated alkynes, see figures 1.5a, 1.5b:

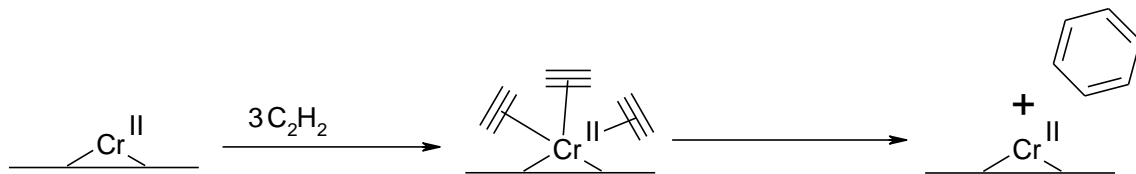


Figure 1.5a: Cyclisation of Acetylene by Phillips Catalyst

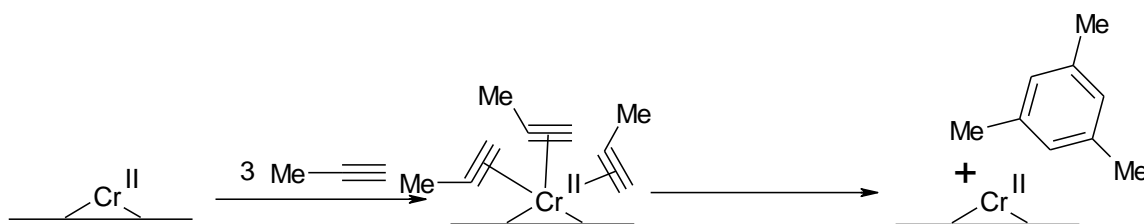


Figure 1.5b: Cyclisation of Propyne by Phillips Catalyst.

IR spectroscopic studies do not detect any intermediate prior to formation of the arene, on the measurable time scale (5 s), nor are any by-products detected, and so simultaneous coordination of all three alkynes is assumed. This suggests high coordinative unsaturation of the active Chromium species, but assumes that the latter is mononuclear and discounts the possibility that an intermediate too fleeting for the time scale of the experiment may occur.

Espelid *et al.*⁹ use computer simulations to investigate the polymerization and trimerisation properties of a model Phillips Catalyst.

The active species is modeled as a surface chemisorbed dinuclear cluster, $\text{Cr}_2\text{O}_4(\text{SiH}_2)_2$, see figure 1.6:

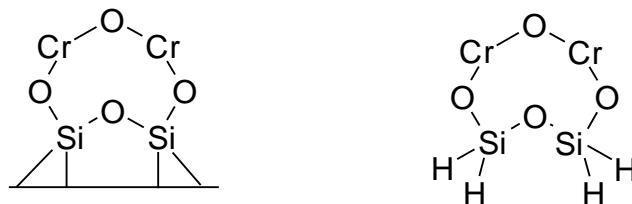


Figure 1.6: Surface Bound Active Catalyst, as proposed by Espelid *et al.* (left), modeled as $\text{Cr}_2\text{O}_4(\text{SiH}_2)_2$ (right).

A series of adsorption and rearrangement steps are proposed, based on DFT calculations, which collectively describe the following catalytic cycles, see figure 1.7:

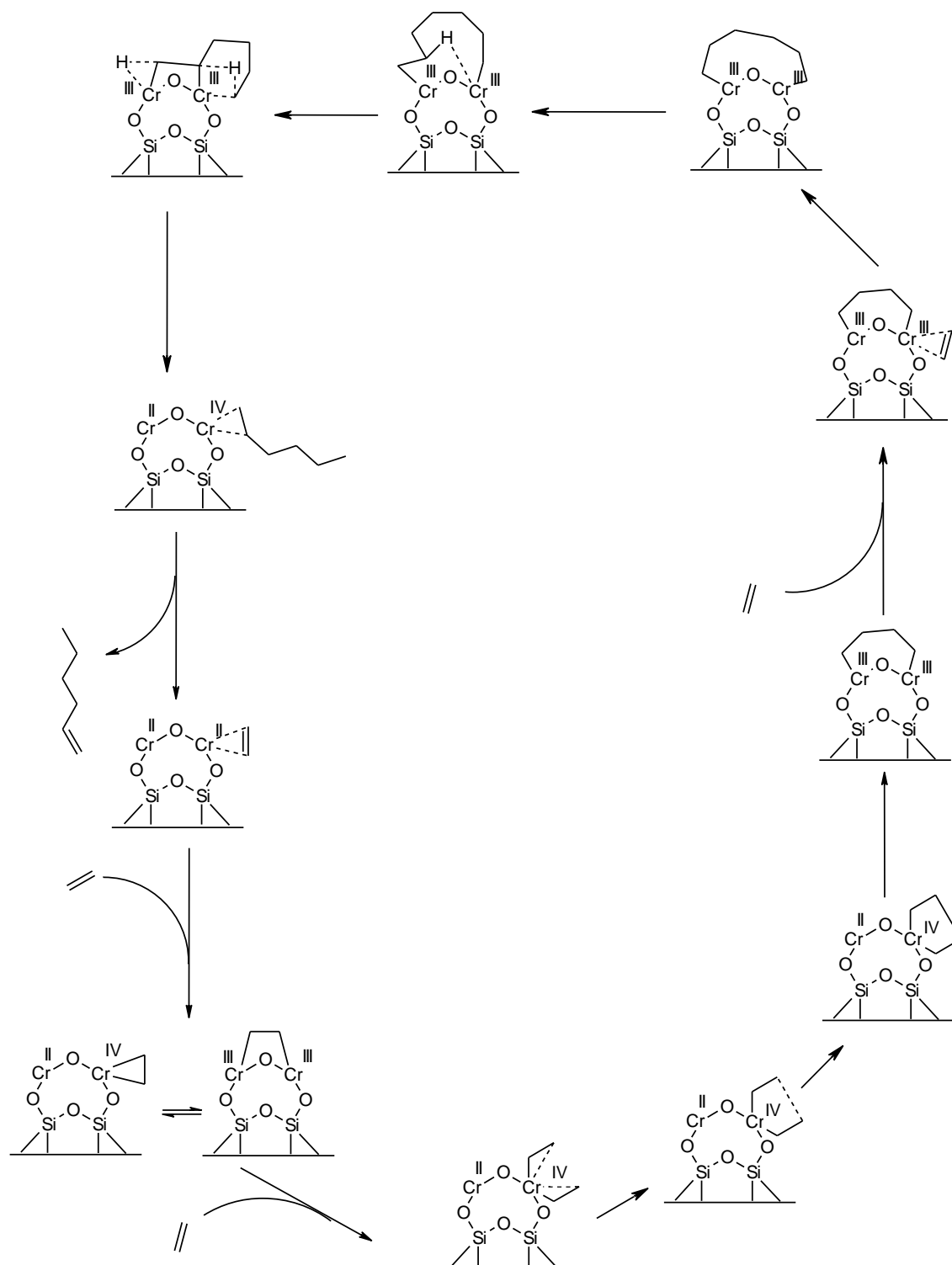


Figure 1.7: Proposed Catalytic Cycle for the Trimerisation of Ethylene by the Phillips Catalyst, based on DFT Calculations.

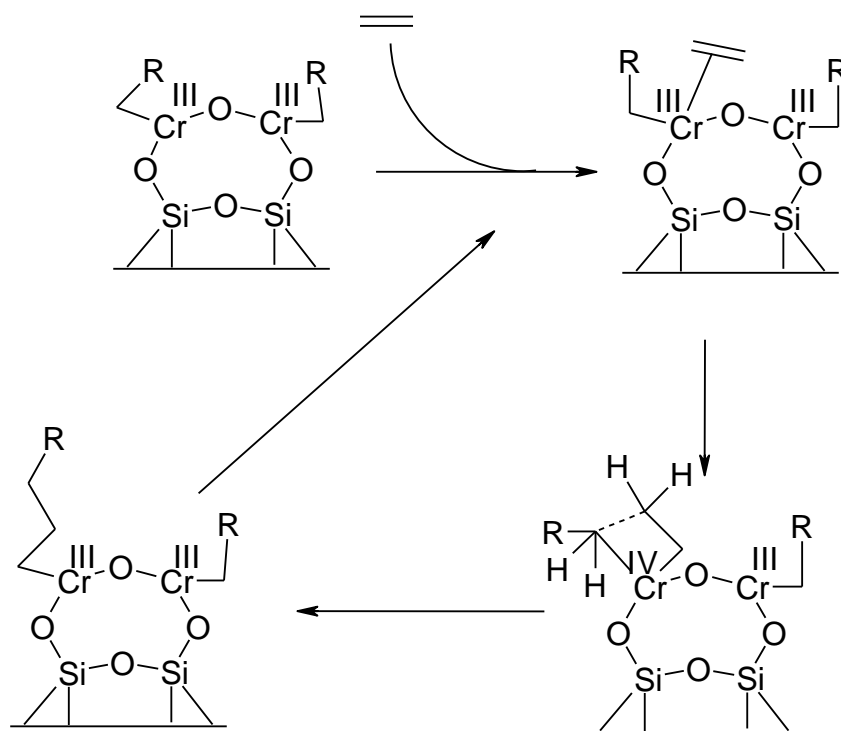


Figure 1.8: Proposed Mechanism for the Polymerisation of Ethylene by the Phillips Catalyst.

Their results suggest that two competing mechanisms are responsible for the polymerization of ethylene and the trimerisation observed in the early stages of the reaction. The selectivity for trimerisation is proposed to originate via a metallacyclic intermediate, which is consistent with the lack of an observed Schultz-Flory distribution of products, as would be expected for variants of the Cossee-Arlman mechanism.

In contrast to the above chain-transfer polymerisation mechanism, recent investigation of the metallacyclic mechanism gives weight to the suggestion that the polymerisation mechanism may also be metallacyclic in nature.¹⁰ In any case, there is little fundamental distinction between the chain-transfer and metallacyclic mechanism for polymerisation; both effectively feature chain growth by ethylene insertion into the Cr-C bond.

Besides computer modeling, various other attempts have been made to investigate the mechanism of activity of the Phillips catalyst, by use of homogeneous and heterogeneous model systems. Some examples follow:

1.2 Phillips Catalyst Model Systems:

Several model systems attempting to mimic the mechanism and activity of the Phillips Catalyst are reported, some of which are reviewed here:

1.2.1 Homogeneous Model- 2,4-pentane-*N,N'*-bis(aryl)ketiminatochromium dichloride:

MacAdams *et al.*¹¹ report a homogeneous model system based on 2,4-pentane-*N,N'*-bis(aryl)ketiminatochromium dichloride, as an approximation to the heterogeneous system derived from chemisorption of chromium trioxide to silica, see figure 1.9:

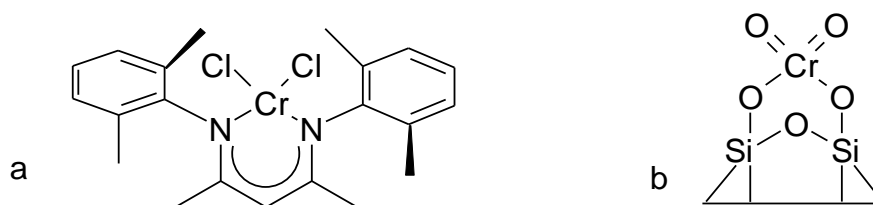


Figure 1.9: 2,4-pentane-*N,N'*-bis(aryl)ketiminatochromium dichloride 'a', where aryl = 2,6-Me₂Ph, as a Model for the postulated Heterogeneous Precatalyst, 'b'.

Their previous investigations concerning 2,4-pentane-*N,N'*-biphenylketiminato complexes of chromium, titanium and vanadium, showed activity for the polymerization of ethylene, and limited activity for copolymerization of ethylene and higher α -olefins,¹² in the presence of an activator. They were unable to isolate an active species for this system however.

Employing 2,4-pentane-*N,N'*-bis(2,6-dimethyl)phenylketiminatochromium dichloride as a starting point, they report structural characterization of a cationic chromium alkyl catalyst that is active in the absence of an activator. The active complex 2,4-pentane-*N,N'*-bis(2,6-dimethyl)phenylketiminato(trimethylsilyl)methylchromium diethyletherate, was characterised by single crystal X-ray diffraction. See figure 1.10:

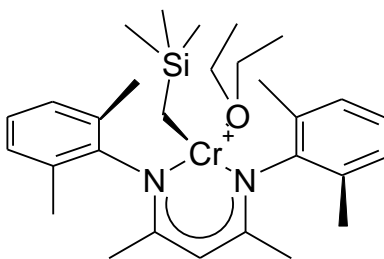


Figure 1.10: 2,4-Pentane-*N,N'*-bis(2,6-dimethyl)phenylketiminato(trimethylsilyl)methylchromium Diethyletherate

This species exhibits activity for the polymerization of ethylene and copolymerization of ethylene and α -olefins. The authors postulate that the active species represents the above complex after dissociation of the diethyl ether, due to the effect on activity of addition of Et_2O and THF to the solution during catalytic runs, and the fact that dilution of the catalyst increased its specific activity, as would be expected assuming the dissociation equilibrium for the ether adduct was concentration dependent.

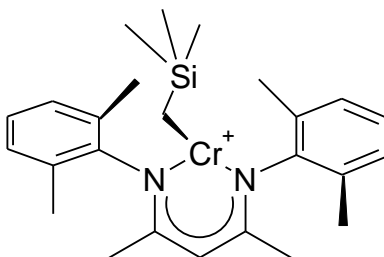


Figure 1.11: Proposed Active Species.

1.2.2 Vapour Phase Collision Modeling:

Hanmura *et al.*¹³ report a study of the vapour phase collision induced dissociation energies of $\text{CrOH}(\text{C}_2\text{H}_4)_2^+$ and $\text{CrOH}(\text{C}_4\text{H}_8)^+$. They determined that the dissociation energy of the product of addition of two equivalents of ethylene to CrOH^+ was equal to the dissociation energy of the product of addition of 1 equivalent of 1-butene to CrOH^+ , and that the two species were therefore equivalent, ie the addition of ethylene to CrOH^+ results in its dimerisation to 1-butene. From this they propose that the active site for ethylene polymerization on the Phillips catalyst is a chromium atom bound to an O atom, or an OH group on the silica surface. The former appears more likely, because as we shall see later, several homogeneous model systems exhibiting

polymerization activity are reported, containing functionalities analogous to Cr-O-Si, only.

1.2.3 Homogeneous Model- 1-(1,2,3,4,5-pentamethyl)cyclopentadienyl-2,2,5,5-tetramethyl-1-chroma-2,5-bis-phosphinocyclopentane Cation:

Theopold¹⁴ reports the polymerization of ethylene by the active species $(\text{Me}_2\text{PCH}_2)\text{Cr}(\text{Me})\text{Cp}^{*+}$, where Cp^* is the 1,2,3,4,5-pentamethylcyclopentadienyl anion. See figure 1.12:

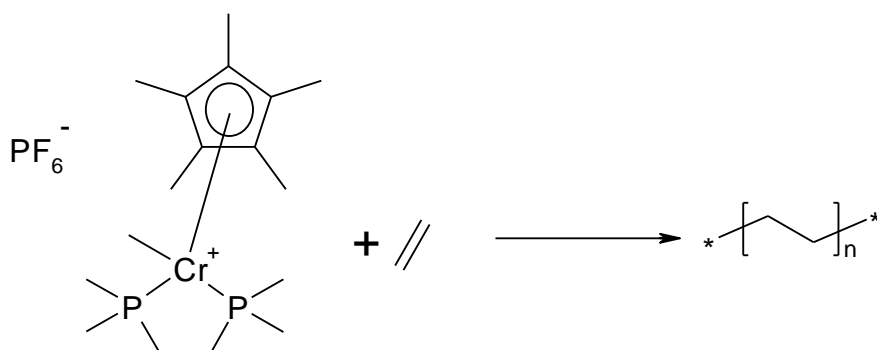


Figure 1.12: Polymerisation of Ethylene by $(\text{Me}_2\text{PCH}_2)_2\text{Cr}(\text{Me})\text{Cp}^*\text{PF}_6$

The neutral chromium II species, obtained by reduction of the chromium III complex by Na/Hg, exhibits no activity for polymerization, which fact supports chromium III as the active species in Phillips-type catalytic cycles. There are notable similarities between this homogeneous model system and that of MacAdams et al.¹¹ ie the chromium centre is strongly bound to two equivalent functional groups, in this case phosphines, rather than imines, and access to the free sites on the metal centre is restricted by adjacent steric bulk, in this case due to the Cp^* ligand, in the case of MacAdams's ligand, the aryl substituents. This lends further support to the supposition that the active species in the Philips catalyst system is the mononuclear chromium centre, bound to silica. See figure 1.13:

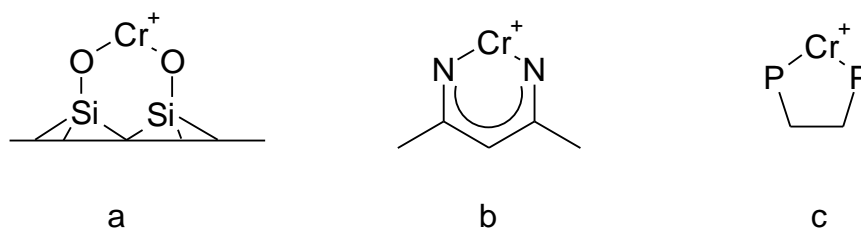


Figure 1.13: Comparison of Active Sites: a- Phillips catalyst, b- MacAdams¹¹, c- Theopold.¹⁴

While there is no comparable steric bulk around the Phillips catalyst active site, this is not significant, assuming the function of the steric bulk around the homogeneous models is to prevent dimerisation. In the case of the Phillips catalyst that is of course, irrelevant, as all the active sites are separately anchored onto the silica substrate.

For a more comprehensive review of the Phillips Catalyst and related systems, see M.P. McDaniel, *Advanced Catalysis*, 1985, 33, 47-98.

1.3 Ethylene Trimerisation Catalysts:

Catalysed selective trimerisation of ethylene, as opposed to merely a statistical distribution of oligomers, is regarded as proceeding via the general metallacyclic mechanism shown in figure 1.14:

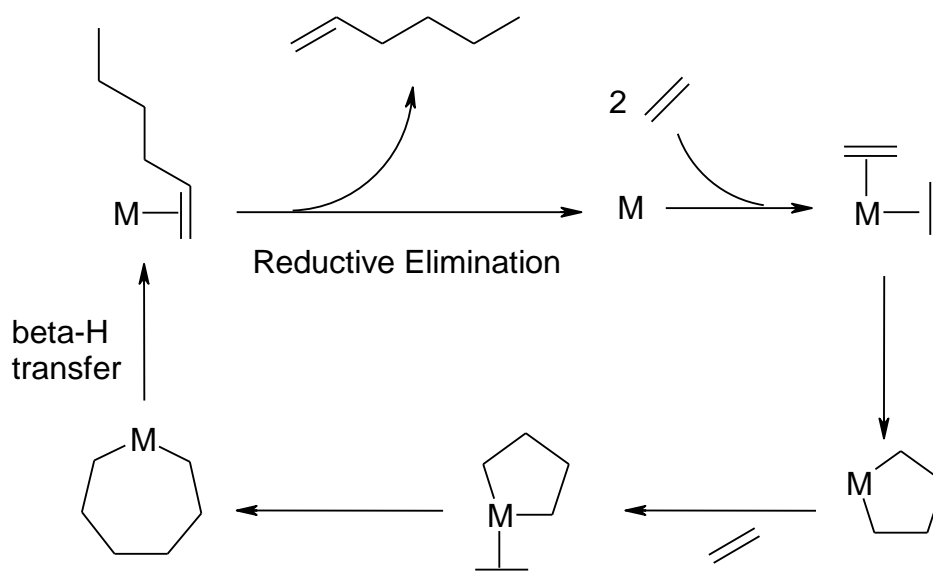


Figure 1.14: Metallacyclic Ethylene Trimerisation Mechanism.

The active species simultaneously coordinates two α -olefin species, which undergo rearrangement to a metallacyclopentane. The resultant free site on the metal centre coordinates a third olefin, which inserts to form metallacycloheptane. This forms a linear trimer by β -hydrogen transfer, which is then decomplexed, restoring the active species and producing 1-hexene. This model system is consistent with the observed product distribution for selective catalysis, where selectivity for trimerisation approaching 100% is often achieved, and the by-products are insignificantly small amounts of dimers and tetramers. Where polymerization is observed in the same system it is considered to occur via a separate metallacyclic or linear chain growth mechanism. (See Cossee-Arlman mechanism, ‘1.12 Kaminsky Metallocenes’ and ‘1.11 Ziegler Natta Type Catalyst’)

Direct experimental observations in support of this mechanism are rare, though it is supported by the work of Emrich *et al.*¹⁵, who report the isolation of stabilized metallacyclopentane and metallacycloheptane derivatives of Chromium and observation of their chemical behaviour, which are consistent with theory. The complex 1-(2-(dimethyl)amino)ethyl-2,3,4,5-tetramethylcyclopentadienylchromium dichloride was reacted with 1,4-dilithiobutane and with 1,6-dichloromagnesiohexane, yielding respectively, the metallacyclopentane and metallacycloheptane. See figure 1.15:

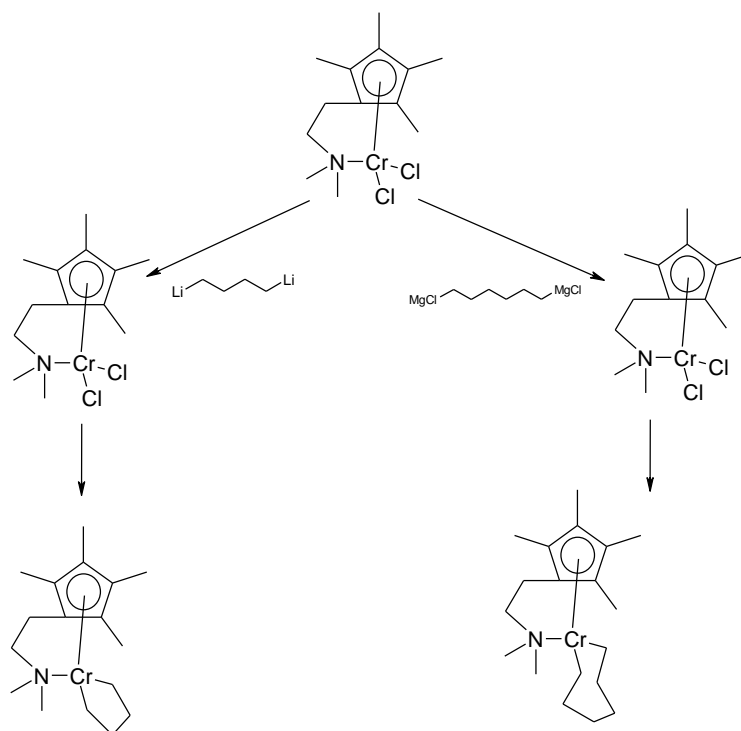


Figure 1.15: Chromium Metallacycle Syntheses.

It was noted that the metallacyclopentane was more stable than the metallacycloheptane, as expected, and that the latter decomposes to produce 1-hexene. Furthermore, the production of 1-hexene and 1-butene is inferred from the protonolysis of the products, of reaction of the metallacyclopentane with ethylene.

1.3.1 Phillips Ethylene Trimerisation Catalyst:

In addition to catalyzing the polymerization of ethylene, the Phillips polymerization catalyst was observed to produce a small amount of 1-hexene as a by-product, as well as exhibiting butyl side-chains in the polymer produced, which are consistent with the copolymerization of 1-hexene with ethylene, See '*Phillips Catalyst*'). Investigation of the effects of temperature and pressure and various additives ultimately led to the development of the Phillips Ethylene Trimerisation Catalyst. By combining Cr(III) 2-ethylhexanoate with 2,5-dimethylpyrrole, diethylaluminium chloride and triethylaluminium in toluene, Phillips were able to achieve catalyst activity above 156,000 g/g Cr/h.¹⁶ (This is currently the only truly selective ethylene trimerisation process undergoing commercial exploitation).

1.3.2 Other Model Systems:

In the past, 1-hexene has been synthesised commercially, mainly by Fischer-Tropsch synthesis using syngas ($\text{CO} + \text{H}_2$), derived from methane or coal;¹⁷ or by oligomerisation of ethylene, eg, Royal Dutch Shell's 'SHOP process',¹⁸ which generates products in the range $\text{C}_4\text{-C}_{10}$ by catalysed oligomerisation. The product initially comprises a broad range of linear α -olefins; the unwanted fractions are removed, isomerised to internal olefins, then undergo metathesis with ethylene, allowing them to be recycled. Such a strategy is, of course less efficient than the selective trimerisation of ethylene, and in recent years, growing academic and industrial interest in ethylene trimerisation catalysis has resulted in a wide variety of organometallic complexes being shown to be catalytically active for the trimerisation of ethylene to 1-hexene, see figure 1.16:

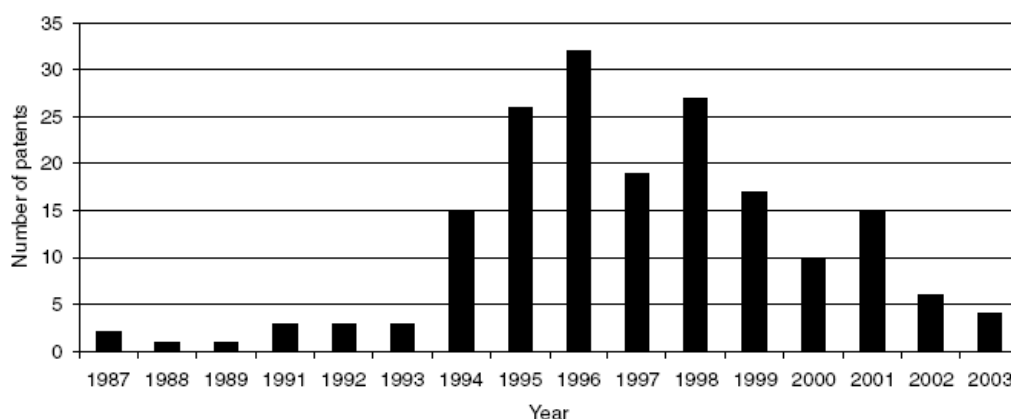


Figure 1.16: Selective Olefin Trimerisation Patents per Year.¹⁶

The Phillips trimerisation catalyst currently represents the only selective ethylene trimerisation catalyst undergoing commercial exploitation, a facility in Qatar, having been operational for some 2 years at the time of writing, and producing some 47,000 tonnes of 1-hexene per annum.¹⁹

In recent years, a variety of novel ethylene trimerisation catalyst systems have been investigated, the overwhelming majority of which are based on chromium. This is unsurprising if one considers that the Phillips Catalyst has likely been used as a starting point when considering the development of new catalysts with comparable properties.

Heterogeneous catalyst systems, such as the Phillips Catalyst itself, typically comprise a well defined ligand species being combined with a chromium source and an activator, such as an alkylaluminium or MAO (NB. there is no ligand species in the Phillips Polymerisation Catalyst itself). Though the constituents of the catalyst are known, the resultant complex is usually poorly defined.

Homogeneous systems on the other hand allow for a better defined system, since the precatalyst can often be characterised extensively, eg. by mass spectroscopy or X-ray crystallography. Although the active species cannot be unequivocally characterised, this does allow for some investigation into aspects of the mechanism of catalysis, although much of the existing data is theoretical, due in no small part to the difficulties of analyzing paramagnetic species such as chromium III, and the complex redox chemistry involved in the catalytic cycle.

For the various hemilabile, homogeneous ethylene trimerisation catalysts it is possible to propose a general mechanism, (accepting that there may be some variations, eg. trimer elimination could be a step-wise or a concerted process).

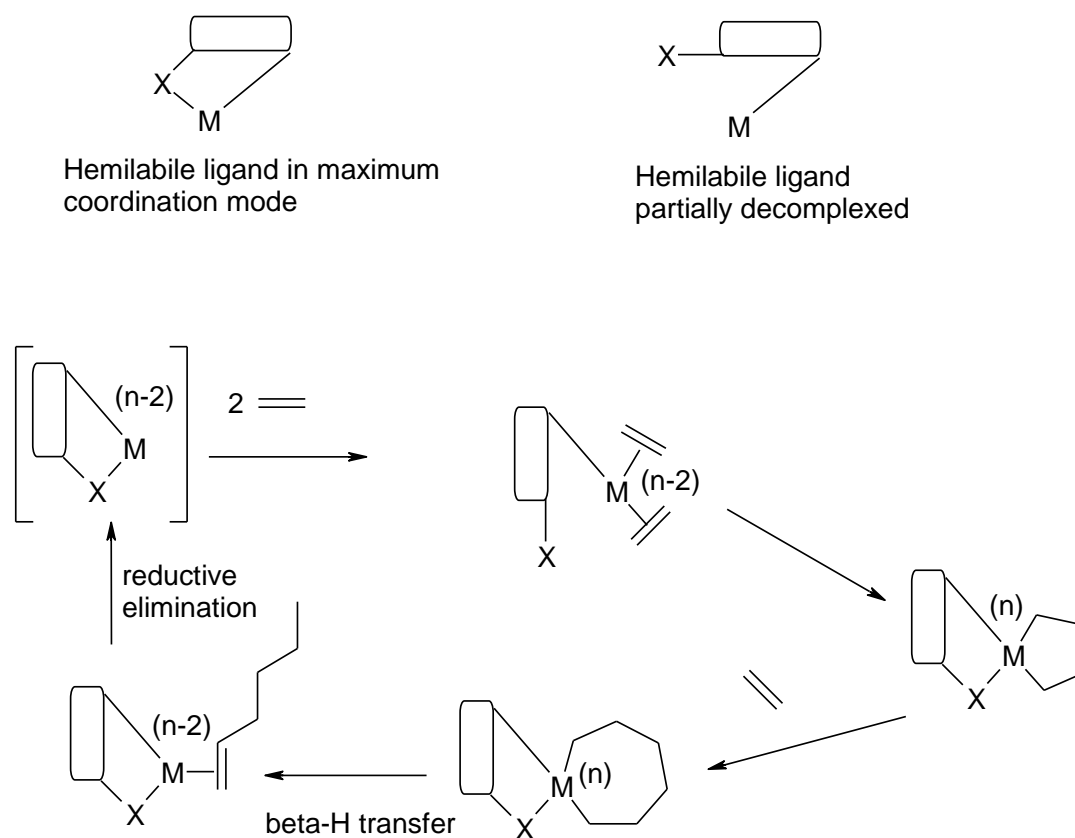


Figure 1.17: General mechanism of α -olefin trimerisation by hemilabile ligand complex. (Illustration employs ethylene for clarity).

A number of general requirements can be determined for complexes capable of effecting the above catalytic process:

1. Since the active species in these systems is considered to be obtained by oxidation (and alkylation) of the precatalyst, the barrier to oxidation, ie the relevant redox potential, must be relatively small, eg Ti (II) \rightarrow Ti (IV) (Tobisch *et al.*²⁰), Cr (I) \rightarrow Cr (III) (Köhn *et al.*²¹).
2. The active species must be capable of forming a metallacycle by simultaneous coordination of two olefinic groups (for incorporation into the cycle). This coordination mode is facilitated by a stable 2-coordinate bonding mode on the part of the ligand. (See figure 1.17). Thus the ligand must be hemilabile, and the 3-coordinate bonding mode must be energetically comparable to the 2-coordinate mode, in order to

prevent either dimerisation of the active species or promotion of a linear chain growth polymerization mechanism.²²

3. Further olefin insertion into the intermediate metallacycloheptane is not necessarily energetically disfavoured, but can be discouraged by the constraints imposed by steric bulk in the ligand design. On the other hand, elimination of 1-butene from the metallacyclopentane intermediate is energetically disfavoured due to the effect of conformational restrictions on concerted β -hydrogen transfer.²⁰

1.3.2.1 2,6-diphenylphenol, Chromium (III) 2-ethylhexanoate:

A recent communication by Morgan *et al.*²³ reports a catalyst system for the trimerisation of ethylene comprising 2,6-diphenylphenol, Chromium (III) 2-ethylhexanoate and triethylaluminium. Like the Phillips trimerisation catalyst, the ligand is monodentate, the coordinating species here being a substituted phenol, rather than a substituted pyrrole. A number of variations of the ligand are also reported, see figure 1.18:

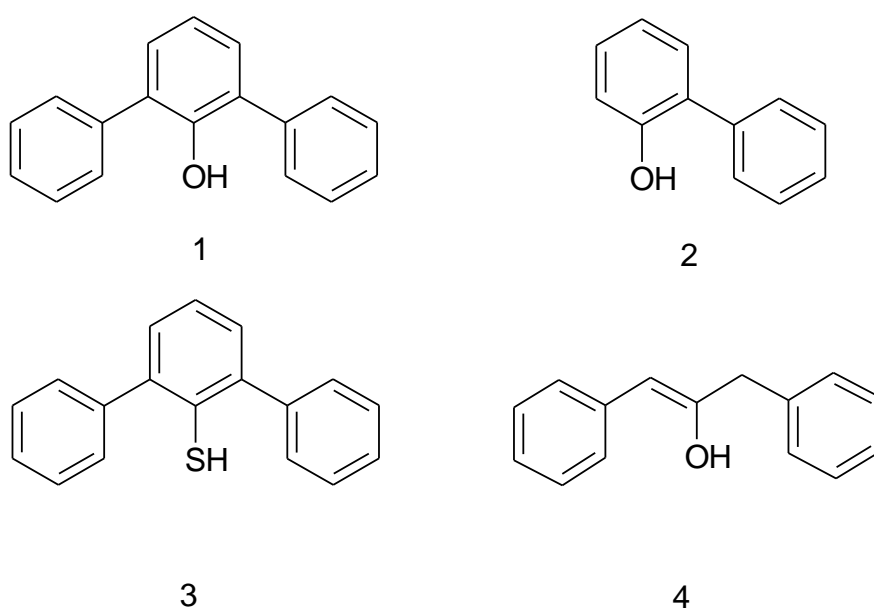


Figure 1.18: 1: 2,6-Diphenylphenol, 2: 2-Phenylphenol, 3: 2,6-Diphenylthiophenol, 4: 1,3-Diphenylacetone (Enol Tautomer).

2,6-diphenylphenol, 1 is reported as forming the most active catalyst. The addition of methoxy substituents to 1 at the *ortho* positions, where they might be capable of

coordination to the chromium centre resulted in an inactive species, while when substituted at the *para* positions they merely reduced the catalyst's activity relative to the unsubstituted version. 2-phenylphenol, 2, did not form an active catalyst, and neither did the more weakly coordinating analogue of 1, 2,6-diphenylthiophenol, 3. 1,3-diphenylacetone, 4 is sterically and electronically similar to 1, and is reported to form an active catalyst. This suggests that the steric bulk of the ligand and the presence of a conjugatively stabilized alcohol functionality are essential to the activity of the complex.

While the catalyst is reasonably active in xylene, its activity is dramatically enhanced by the use of anisole as the solvent. The nature of the chromium species is reported to differ dramatically in the two different solvent systems, as evidenced by the difference in magnetic susceptibility of the complex in each case: μ_{eff} in xylene- 5.17 BM, versus μ_{eff} in anisole- 3.61 BM.

The selectivity for trimerisation over polymerization is not as high as in some other systems, producing 13.6 wt% of polymer under the conditions of greatest catalytic activity. Presumably the steric bulk of the ligand represents a greater hindrance to the Cossee-Arlman polymerization mechanism than to the metallacyclic trimerisation mechanism.

1.3.2.2 η^5 -(Aryldimethyl)methylcyclopentadienyltitanium Chloride: η^5 - $\text{C}_5\text{H}_4\text{CMe}_2\text{RTiCl}_3$.

Cyclopentadienyl titanium complexes have been variously employed as catalysts in the polymerization of ethylene and other α -olefins.

Variations of the cyclopentadienyl complex incorporating a pendent arene substituent capable of weak coordination to the metal centre have been investigated recently.¹⁶ The effect of the substituent on the catalytic properties of the complex varies according to the nature of the bridge between aryl side-group and Cp functionality. The effect of the aryl side-group in the case of ethylene is to render the complex highly selective for trimerisation catalysis, though it merely reduces polymerization activity in the case of propene or styrene.²⁴

Deckers *et al.*²⁵ report a comparative study of the trimerisation versus polymerization properties of the catalyst system η^5 - $\text{C}_5\text{H}_4\text{CMe}_2\text{RTiCl}_3/\text{MAO}$, where R

= Me, Ph. Where R = Me, the complex behaves predominately as an ethylene polymerization catalyst, presumably by a variation of the Cossee-Arlman mechanism, see figure 1.19:

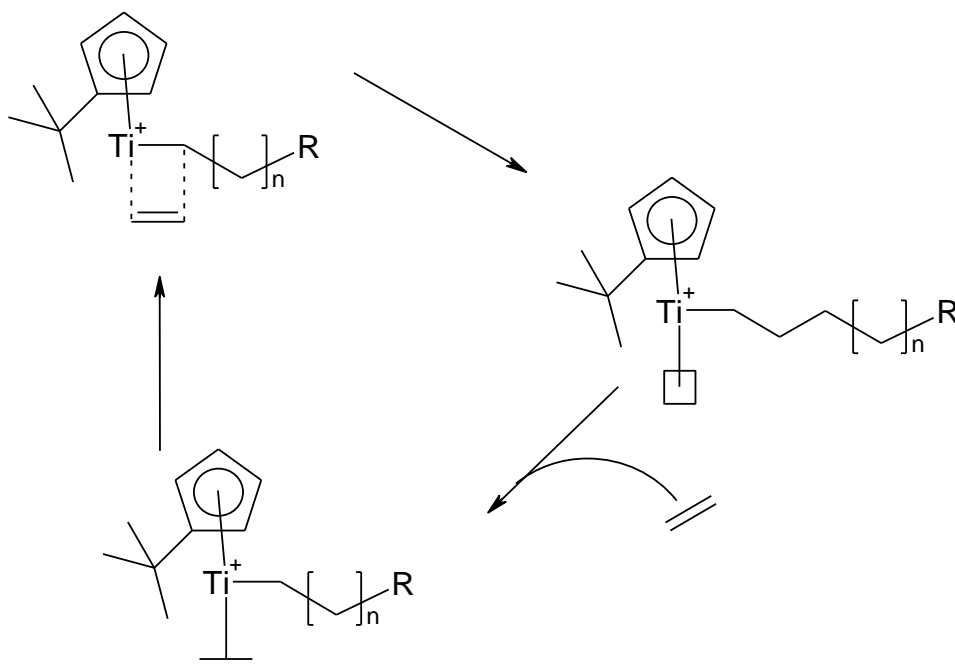


Figure 1.19: Ethylene Polymerization by η^5 -C₅H₄CMe₃TiCl₃/MAO

Where R = Ph, the major product of the reaction is reported to be 1-hexene. A metallacyclic mechanism is proposed.²⁵

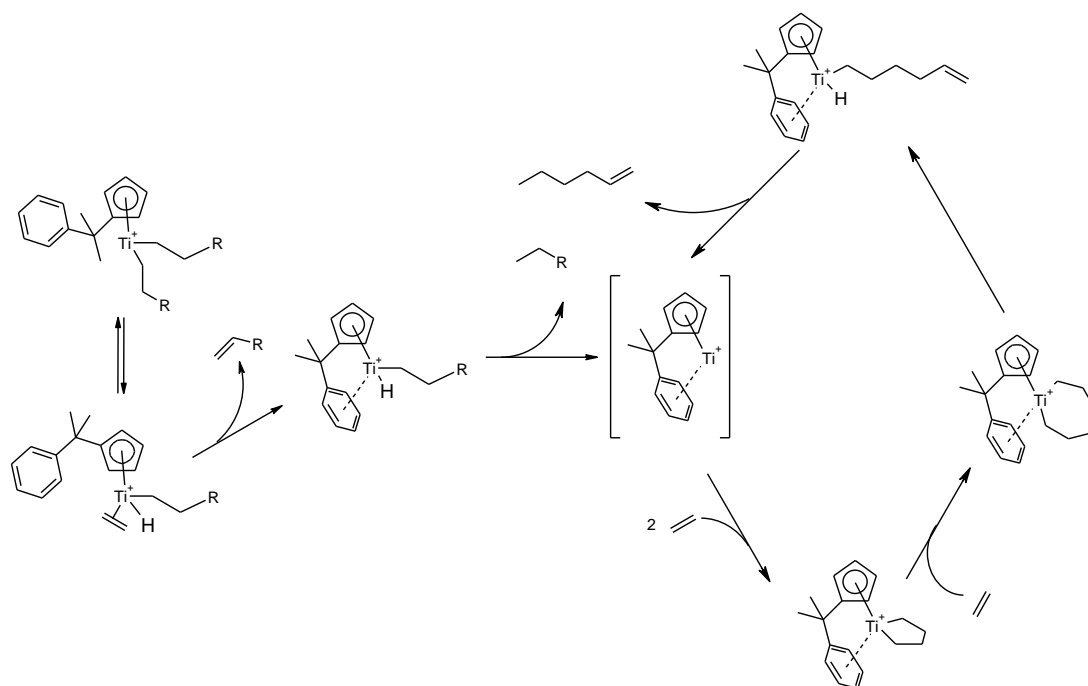


Figure 1.20: Proposed Mechanism of Ethylene Trimerisation by η^5 -
 $\text{C}_5\text{H}_4\text{CMe}_2\text{PhTiCl}_3/\text{MAO}$

The supposition that coordination of the pendent arene was important for trimerisation was tested by use of the analogous ligand by η^5 - $\text{C}_5\text{H}_4\text{CMe}_2\text{RTiCl}_3/\text{MAO}$, where $\text{R} = 3,5\text{-Me}_2\text{C}_6\text{H}_3$. The presence of the methyl substituents renders the arene more electron rich than the unsubstituted phenyl group, and the effect of this is to significantly reduce the activity of the catalyst, although the selectivity for trimerisation is retained.

The productivity of the 3 systems is shown below:²⁵ (where productivity is given in kg C_6 product per mol Ti, per hour). Other products comprise principally C_{10} oligomers: 1-hexene/ethylene co-trimers (mainly 5-methylnon-1-ene), and small quantities of 1-octene and polyethylene.

Catalyst:	C_6 product/g (wt %)	PE product/g (wt%)	Productivity
$\text{R} = \text{Ph}$	20.9	0.5	2787
$\text{R} = (3,5\text{-Me}_2\text{C}_6\text{H}_3)$	7.9	0.1	1053
$\text{R} = \text{Me}$	0.5	2.4	66

This system has further been the subject of a theoretical investigation by Tobisch *et al.*²⁰ which supports the proposed trimerisation mechanism, as does the work of Blok *et al.*²⁶ though with one significant alteration, ie, that 1-hexene elimination occurs via a concerted hydrogen transfer process rather than a two step process of β -elimination followed by reductive elimination of the olefin. (Figure 1.21). This proposal is supported by the absence of products of insertion into the originally proposed alkyl chromium hydride intermediate. (See above- Figure 1.20).

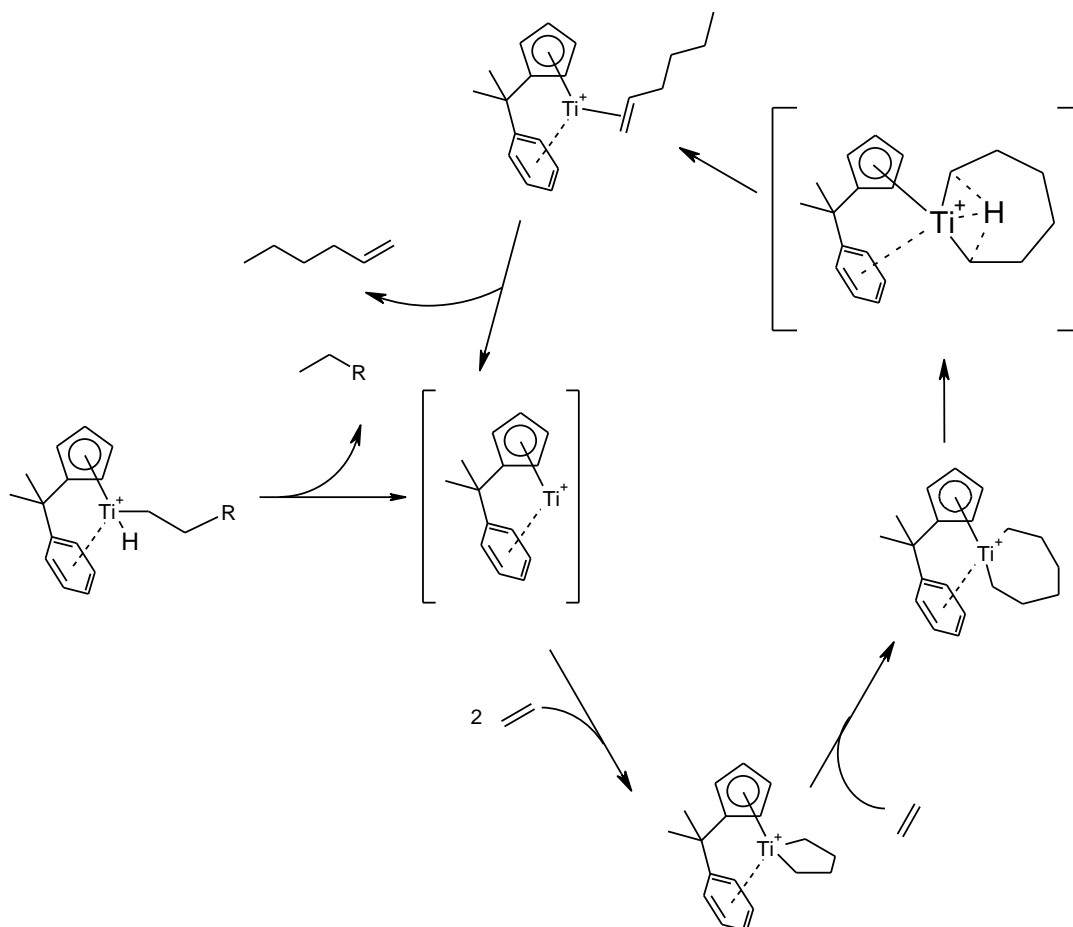


Figure 1.21: Modified mechanism of ethylene trimerisation by η^5 -
 $\text{C}_5\text{H}_4\text{CMe}_2\text{PhTiCl}_3/\text{MAO}$.

They further conclude that, as expected, coordination of the pendent arene reduces olefin coordination energy and thus promotes β -hydrogen transfer over further chain growth.

These findings serve to reinforce the hypothesis that a hemilabile ligand capable of shifting between κ^3 and κ^2 coordination to the metal centre during the catalytic cycle is essential for selective trimerisation by the metallacyclic mechanism.

1.3.2.3 1,2,3,4,5-Pentaphenylcyclopentadienyl Chromium Hexanoate:

Mahomed *et al.*²⁷ report a substituted cyclopentadienyl-chromium (III) system exhibiting selectivity for the trimerisation of ethylene. Cyclopentadienyl chromium systems are more typically associated with ethylene polymerization, but in this case selectivity of up to 76 wt% 1-hexene is reported. The significant features of this system are the substantial steric bulk of the substituted cyclopentadienyl ligand, and the inclusion of a halogen source, (cf. the Phillips Ethylene Trimerisation Catalyst).

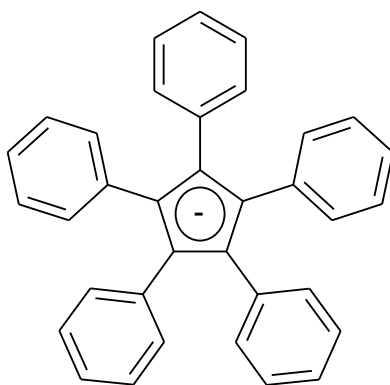


Figure 1.22: 1,2,3,4,5-Pentaphenylcyclopentadienyl Anion.

The system reported comprises 1,2,3,4,5-pentaphenylcyclopenta-1,3-diene, hexachloroethane and triethylaluminium added to Cr(III) 2-ethylhexanoate. The system exhibited catalytic activity in the absence of the halogen source, but the presence of the latter represented a significant enhancement. Studies of analogous complexes employing less sterically bulky Cp ligands also exhibited activity for trimerisation, although to a lesser extent. Slightly greater activity is reported in the case of the more sterically bulky ligand 5-(4-*tert*-butylphenyl)-1,2,3,4-tetraphenyl-1,3-cyclopentadiene, see figure 1.23:

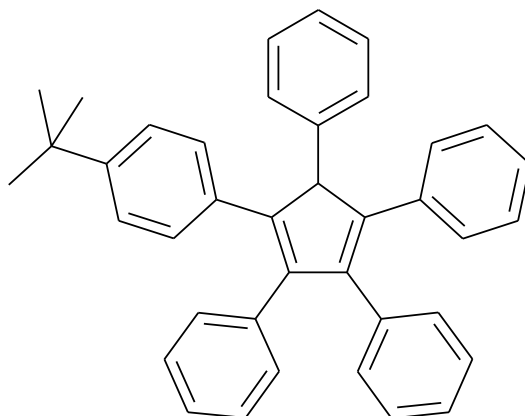


Figure 1.23: 5-(4-*tert*-butylphenyl)-1,2,3,4-tetraphenyl-1,3-cyclopentadiene

In none of the systems studied could the 1-hexene selectivity be altered via changes to the physical environment of the reaction, except by temperature, although improved selectivity at higher temperatures occurred at the expense of reduced catalyst activity.

Consideration of the conformational constraints of this class of ligand precludes a mechanism analogous to that proposed for the cyclopentadienyl titanium system by Deckers *et al.*²⁵ though it is still possible for the ligand to be hemilabile, due to the variable hapticity sometimes exhibited by the cyclopentadienyl anion.

As with the findings of Morgan *et al.*,²³ a mechanistic explanation of the activity of this system must presumably be concerned chiefly with steric effects.

No mechanistic information concerning this system has been established *per se*, but the usual metallacyclic route to 1-hexene is assumed due to the high selectivity for trimerisation and the presence in the product distribution of small amounts of other plausible products of the metallacyclic chain growth mechanism, ie decenes, produced by co-trimerization of 1-hexene with ethylene.

It seems improbable that an active species in which the chromium centre is coordinated to the cyclopentadienyl functionality would exhibit catalytic activity, where the ligand is so sterically hindered, which leads one to speculate that the active species may in fact be zwitterionic; the chromium coordinating to one of the adjacent phenyl substituents, see figure 1.24:

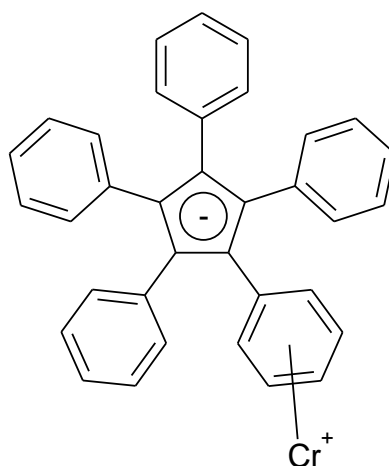


Figure 1.24: Possible Zwitterionic Bonding Mode of Active Species.

1.3.3 Complexes based on Multidentate Ligands:

Besides triazacyclohexanes, a number of bidentate and tridentate ligand types, exhibiting various steric and electronic properties and potential coordination geometries, have been employed in catalytically active chromium complexes. Notable examples follow:

1.3.3.1 1,4,7-Trimethyl-1,4,7-Triazacyclononane Chromium Chloride:

As reported by Wu *et al.*²⁸ the facially coordinating ligand 1,4,7-trimethyl-1,4,7-triazacyclononane, complexed to CrCl_3 and activated by MAO, selectively oligomerises ethylene, producing, in addition to a Flory-Schultz distribution of α -olefins, a disproportionately large quantity of 1-hexene.

This suggests that both a linear chain growth mechanism and a metallacyclic mechanism occur in this system. Use of the analogous unsubstituted complex 1,4,7-triazacyclononane results only in polymerization, supporting the belief that steric bulk is important for the suppression of the linear chain growth mechanism.

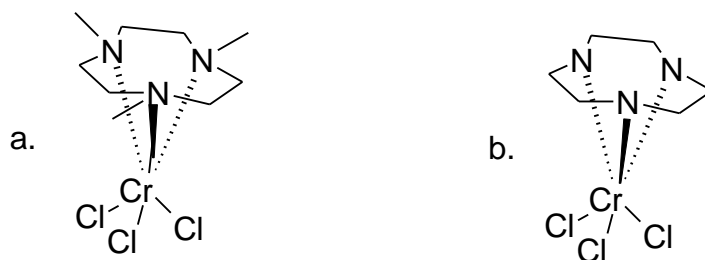


Figure 1.25: 1,4,7-trimethyl-1,4,7-triazacyclononane/ CrCl_3 complex (a) and 1,4,7-triazacyclononane/ CrCl_3 complex (b).

A further distinction between triazacyclononane and triazacyclohexane complexes is that the former are incapable of trimerising higher α -olefins, while the latter are highly selective for α -olefin trimerisation.

1.3.3.2 Tris(pyrazolyl)methane Chromium Chloride:

Tris(pyrazolyl)methane ligands are a (neutral) variant of the original scorpionate ligand (tris(pyrazolyl)hydroborates). Dixon et al.¹⁹ review a patent of the Tosoh Corporation,²⁹ in which complexes of tris(pyrazolyl)methane ligands, activated by MAO or trialkylaluminiums, represent selective ethylene trimerisation catalysts. Complexes tris(3,5- $\text{R,R}'$ -1-pyrazolyl)methane-chromium trichloride, where $\text{R,R}' = \text{Me,Me}$, $\text{R,R}' = \text{Ph,Me}$, $\text{R,R}' = \text{Ph,H}$, and $\text{R,R}' = (4\text{-Tolyl}),\text{H}$ are reported. See figure 26:

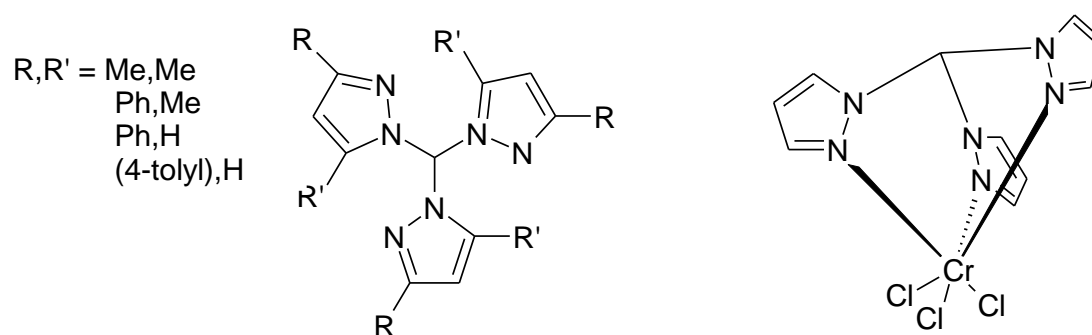


Figure 1.26: Tris(pyrazolyl)methane Ligands, and generic Scorpionate-Chromium Trichloride Complex- substituents omitted for clarity.

The best results were achieved in the case of the ligand tris(3,5-dimethyl-1-pyrazolyl)methane, activated by MAO, where 99.1% selectivity for 1-hexene was reported, for a catalyst activity of 40,100 g/g Cr per hour.

For this type of facially coordinated ligand, it is reasonable to suggest a trimerisation mechanism featuring a switch from κ^3 to κ^2 coordination during the catalytic cycle (cf. triazacyclohexane, see '1.4 Chromium Complexes of 1,3,5-Triazacyclohexanes') See figure 1.27:

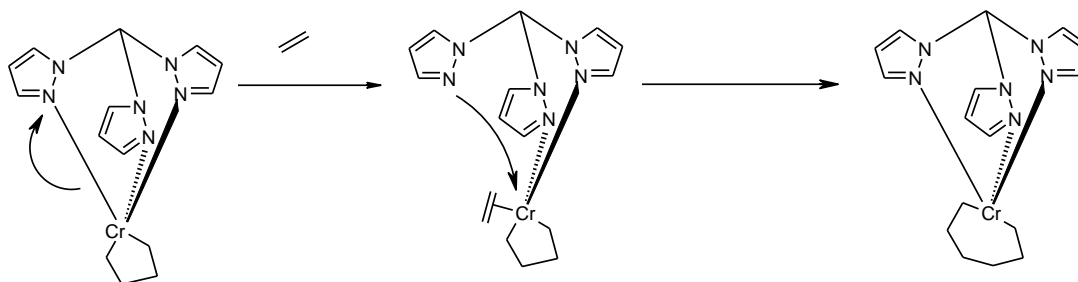


Figure 1.27: Proposed Switch between κ^3 and κ^2 Coordination Modes during Metallacycle insertion. (cf. generic Metallacyclic Trimerisation Mechanism).

1.3.3.3 Methyl-bis(diaryl)phosphinoamine Complexes: $\text{Ar}_2\text{PN}(\text{Me})\text{PAr}_2$:

Carter *et al.*³⁰ report highly active and selective ethylene trimerisation catalysts based on ligands of the type $\text{Ar}_2\text{PN}(\text{Me})\text{PAr}_2$, where R = ortho-methoxy-substituted aryl group, in the presence of a chromium source and MAO activator.

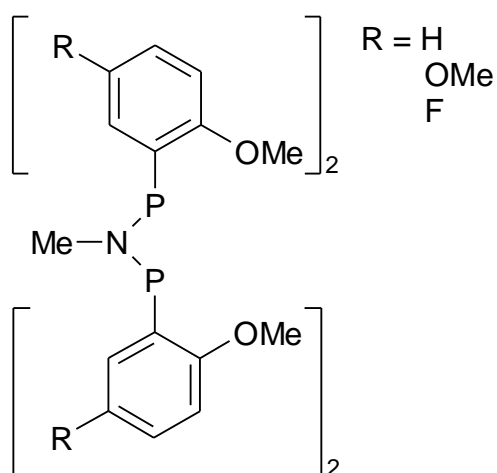


Figure 1.28: Generic ligand $\text{Ar}_2\text{PN}(\text{Me})\text{PAr}_2$.

The following observations were initially reported:

The best activities and selectivities are reported for the ligand, R = H, though reasonable activity and high selectivity is reported for R = OMe, F. The product distribution for catalysis of ethylene trimerisation by these systems is consistent with the metallacyclic mechanism.

Otherwise analogous ligands lacking OMe functionalities in the *ortho*- position showed no activity, nor did ligands in which the bridging NMe group was substituted for (CH₂)_n, n = 1,2.

Substitution of the requisite *ortho*-OMe substituents with Ethyl substituents, which were deemed to be sterically equivalent, did not result in an active complex, suggesting that the influence of the *ortho*-OMe substituents is not sterically derived. The presence of electron withdrawing substituents *para* to the *ortho*-OMe groups reduced the activity of the resultant complex, but did not render it inactive. This suggested that the coordinating properties of the *ortho*-OMe substituents were requirements for trimerisation. It was suggested that they act as pendent donors to the metal centre in the active species. In this case the ligand might be considered to be hemilabile.

However, subsequent research has revealed that the *ortho*-methoxy substituents are not, in fact essential for catalysis; and approximately equivalent activity is reported for the ligand, whether the *ortho*-substituents be methoxy- or hydride-groups.³¹ However, there is a significant difference in the distribution of products, examined in the case of ethylene/styrene co-polymerisation, though this is deemed to be consistent with steric rather than electronic effects.

1.3.3.4 S and N Donor Mixed Systems:

McGuinness *et al.*²² report a class of selective ethylene trimerisation catalysts comprising chromium trichloride complexes of ligands of the type (RS(CH₂)₂)₂NH, where R = Me, Et, n-Bu or n-Dec. In each case selectivity for 1-hexene production was greater than 90%, in the presence of MAO co-catalyst, in toluene solvent. The system where R = n-Decyl was reported to be significantly more active than for the other 3 systems investigated, and the superior solubility of the former in toluene is noted by the authors. This is to be expected given the obvious kinetic advantages of

homogeneous versus heterogeneous catalysis, and in general reinforces the importance of incorporating the largest organic substituents practicable in any given ligand type for an intended homogeneous catalyst system, given that non-polar organic solvents are the preferred environment for trimerisation catalysis in most cases, (and particularly those within the scope of this project).

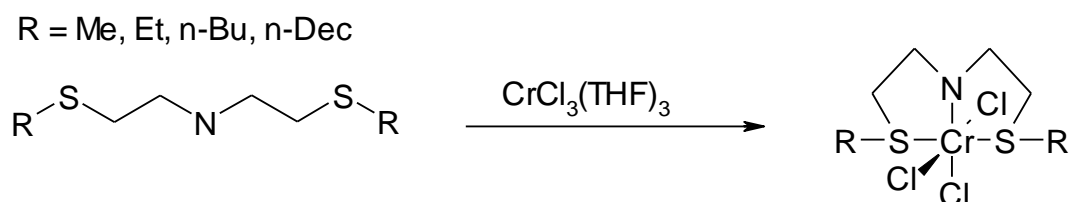


Figure 1.29: Ligand $(\text{RS}(\text{CH}_2)_2)_2\text{NH}$, and derived Chromium Complex.

A crystal structure is reported for the complex $(\text{EtS}(\text{CH}_2)_2)_2\text{NH-CrCl}_3$. The coordination geometry of the ligand is revealed to be meridional, in contrast to, eg triazacyclohexane-or scorpionate complexes. Thioether groups are extremely soft ligands, so it is not unreasonable to propose a mechanism for catalysis in which they are reversibly decomplexed, but the geometry of the complex might be expected to place some conformational constraints on the nature of the metallacyclic intermediates in the assumed trimerisation mechanism. However, the metallacycle growth step is considered to require only κ^2 coordination of the ligand, in which instance the distinction between facial and meridional coordination is nonsensical, see figure 1.30:

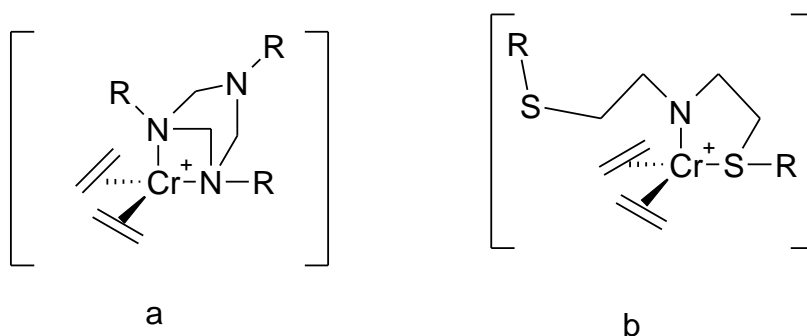


Figure 1.31: Comparison of Metallacycle-Olefin insertion step in Triazacyclohexane-Chromium Trichloride (a) and $(\text{RS}(\text{CH}_2)_2)_2\text{NH}$ -Chromium Trichloride (b) Catalysis.

Bluhm *et al.*³² report a number of ligands of types 1 and 2, see figure 1.32:

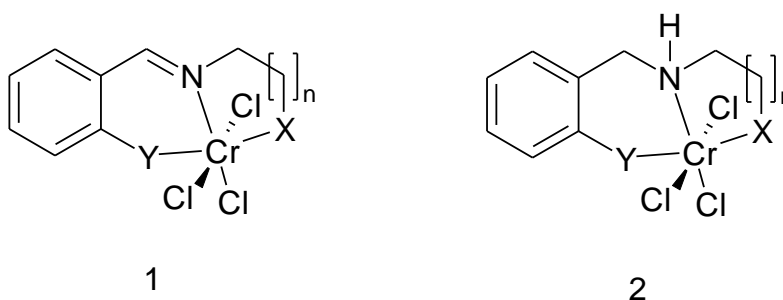


Figure 1.32: Generic Ligand Types.

Where X and Y represent various phosphorous and sulphur based substituents. In the presence of MAO co-catalyst, good selectivity (>98%) and activity for ethylene trimerisation catalysis is reported, for type '1', where $Y = X = PPh_2$, $n = 1$ and where $Y = PPh_2$ and $X = SEt$, $n = 1$. However, for the amine analogues of these ligands, ie for the same substituents on generic ligand backbone '2', though trimerisation does occur, in no case does the selectivity for trimerisation exceed 44 wt% of the product of ethylene catalysis, the majority of product being polyethylene. Crystal structures are reported for a number of variants, revealing, as in comparable work by McGuinness *et al.*²² that the ligands coordinate meridionally, forming complexes possessed of slightly distorted octahedral geometry. The PNP and PNS ligand complexes display very similar chelate bite angles, which differ significantly from that observed for the analogous complex where $Y = SMe$, $X = SEt$, which functions solely as a polymerization catalyst. The ligand $Y = X = PPh_2$, $n = 2$, unsurprisingly shows a more strained coordination geometry, and exhibits substantially reduced trimerisation selectivity.

For ligand type '1', where $X = Y = PPh_2$, but $n = 2$, there is essentially no selectivity for trimerisation and the complex performs as a polymerization catalyst. A recurring theme in this study is that comparatively minor variations in geometry, coordinating ability and steric strain are sufficient to dramatically alter selectivity for trimerisation and in some cases prevent it entirely. By contrast, all of the variants of ligand types '1' and '2' investigated, (of which there were 11 of type 1 and 3 of type 2) exhibited at least some activity for ethylene polymerization.

Zirconium, Vanadium and Tantalum complexes of various types have also been investigated as potential ethylene trimerisation catalysts,^{33,34} but none have exhibited activity or selectivity sufficient to compete with the known chromium-based systems.

A wide variety of ligand types have been shown to be active ethylene trimerisation catalysts, some approaching 100% selectivity; their trimerisation activity is in almost all cases restricted to ethylene and not higher α -olefins, although in some cases cotrimerisation of α -olefins with ethylene may occur. This is probably attributable at least in part to steric constraints, as in the case of triazacyclononane complexes and presumably any of the meridionally bonded ligand types.

The most selective trimerisation catalysts are hemilabile, polydentate ligands, but they exist in sufficient variety to suggest that there remains considerable scope for development of new systems and ligand classes. Given the concerns over steric constraints on higher α -olefin coordination, and since the only homogeneous system for α -olefin trimerisation to which I can find reference is based on the facially coordinated triazacyclohexane-chromium system, it is sensible to focus investigation on similarly facially coordinated ligands.

1.4 Chromium Complexes of 1,3,5-Triazacyclohexanes:

Recent work by Köhn *et al.* has been concerned with the development of 1,3,5-triazacyclohexane complexes of chromium III chloride, see figure 1.33:

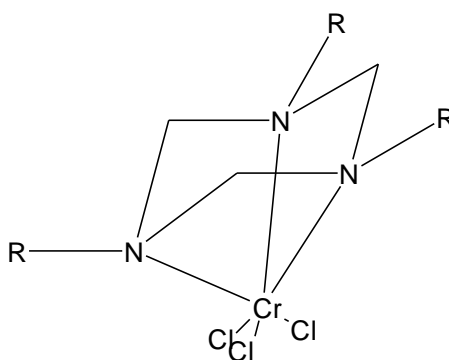


Figure 1.33: 1,3,5-Tris(R)-1,3,5-Triazacyclohexane.

Complexes of this type, when activated by MAO, represent catalysts for the selective polymerization of ethylene. Moderate activity of the poorly soluble (in toluene) 1,3,5-trimethyl-1,3,5-triazacyclohexane chromium chloride complex was

reported, but the much more soluble tris-dodecyl analogue yielded a much higher activity of 13,780 g/g Cr per hour.¹⁶ The resultant polymer exhibited butyl side-chains –indicative of 1-hexene incorporation, and the presence of small amounts of 1-hexene and decenes. This, along with the distribution of end groups in the polymer, is comparable to the products of ethylene polymerization by the Phillips Catalyst, which fact led the authors to suggest that this may represent a homogeneous model system for the latter. It was later discovered³⁵ that, while most trimerisation catalysts were limited to ethylene, these triazacyclohexane-chromium III complexes are capable of trimerising higher α -olefins, such as propene, styrene and 1-hexene.

Iron III chloride and chromium III chloride complexes have in some cases been characterised by single crystal X-ray diffraction,³⁶ and the ligands in both instances are shown to be κ^3 , facially coordinated to the metal centre. The complex $^i\text{Pr}_3\text{TACCrCl}(\text{CH}_2\text{SiMe}_3)_2$, also characterised by X-ray diffraction, exhibits an average Cr-N bond length of 225.7 pm- comparatively long, and comparable to those found in similar triazacyclononane complexes.

The ligand itself shows no unusual distortion of bond length or conformation, and it is thus possible to calculate the angle made by the N-Cr bond relative to the normal (axial) orientation of the lone pairs. For the complex $^i\text{Pr}_3\text{TACCrCl}(\text{CH}_2\text{SiMe}_3)_2$, there was some variation of Cr-N bond length and angle, trans to the chloride, versus the two organic substituents, such that the angle made by the bond trans to the chloride, see figure 31, $\theta = 22.9^\circ$, while that trans to the CH_2SiMe_3 substituents was $\theta = 26.2^\circ$. For comparison, the comparable bond angle in the case of the complex $\text{Me}_3\text{TACCrCl}_3$ was $\theta = 23.6^\circ$. Larger θ values represent poorer orbital overlap and thus weaker bonding interactions between the N lone pair and the chromium centre.

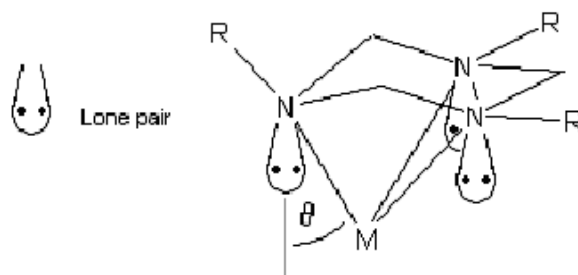


Figure 1.34: Angle between Normal Triazacyclohexane Lone Pair Orientation and N-M Bond Angle.

The postulated active species following addition of MAO is the methylated cationic species, figure 1.35:

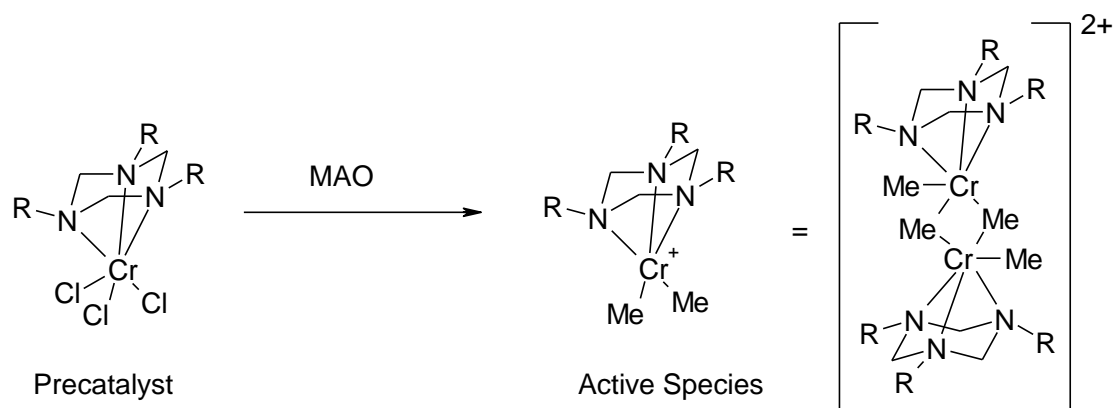


Figure 1.35: Alkylation of Precatalyst to Active Species.

The normal bonding mode for the complex is regarded as κ^3 coordination, but the poor correlation between N-Cr bond angle and the preferred lone pair orientation, is considered to be destabilizing, as evidenced by the elongation of the N-Cr bonds. Consequently, the κ^3 and κ^2 coordination modes are energetically similar, and it is thus postulated that the trimerisation mechanism proceeds via a κ^2 coordinated species, whereby the ligand shifts to the κ^2 mode in order to simultaneously coordinate two α -olefins, prior to metallacycle formation, see figure 1.36:

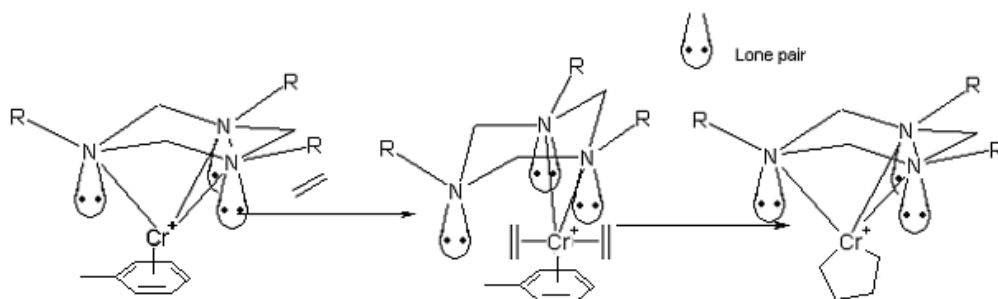


Figure 1.36: Shift of Triazacyclohexane Ligand from κ^3 to κ^2 Bonding Mode during α -Olefin Insertion.

A mechanism incorporating a κ^1 mode may also be proposed, although this is speculative.

It is possible to propose a mechanism for the experimentally determined trimerisation of 1-hexene by 1,3,5- R_3 -1,3,5-triazacyclohexane-chromium trichloride, where R = octyl, dodecyl, which results in a statistical distribution of branched octadecenes, consistent with experimental observations.³⁵ See figure 1.37.

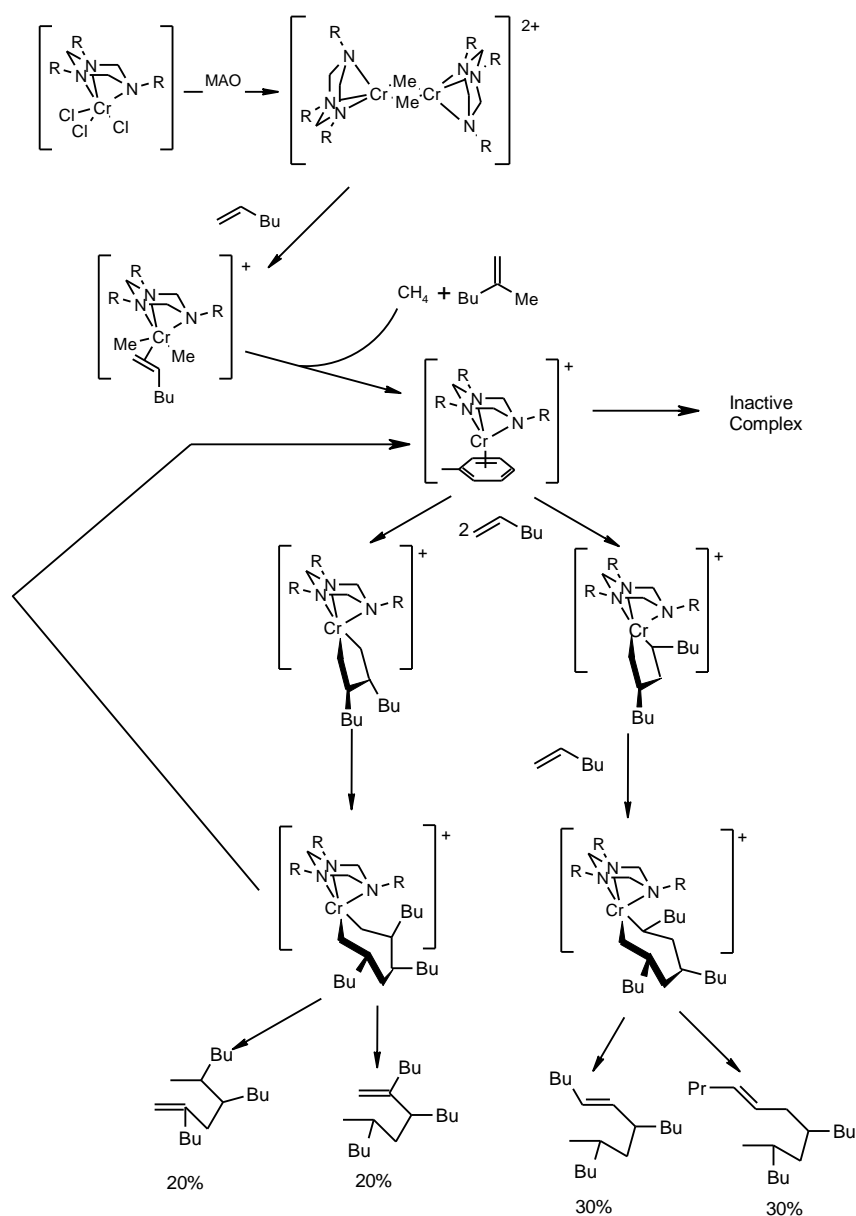


Figure 1.37: Proposed 1-Hexene Trimerisation Mechanism.

Though these systems exhibit good selectivity and are initially highly active, the trimerisation activity ceases after a few hours at room temperature. Reducing the

temperature of the reaction mixture to 0 °C allows up to 90% α -olefin conversion after several days. The cessation of catalytic activity occurs as a consequence of spontaneous degradation of the active catalyst into an inactive species. This species has never been fully characterised, but has been determined (by NMR spectroscopy, employing the Evans Method) to have a magnetic moment of 3.3 μ_B , which is consistent with a bridged, di- or poly-nuclear chromium III complex. It is believed that this deactivation occurs as a consequence of decomplexation of the triazacyclohexane ligand, possibly as a consequence of competitive coordination by the alkyl aluminium cocatalyst. Partially deuterated TAC ligands are observable by 2H NMR spectroscopy, and upon decomposition of the active species, a significant shift in the 2H NMR signals of the ligand is observed. A signal attributed to the diamagnetic and thus de-complexed TAC ligand is also observed, supporting the decomplexation hypothesis.³⁵

In contrast to some of the heterogeneous systems previously reported^{24,28} the presence of coordinating functionalities, in the solvent, on the olefinic monomer starting material, or on the triazacyclohexane ligand itself, results in a substantial loss of activity relative to a comparable system comprising only hydrocarbon substituents.³⁵

1.4.1 The Effect of Paramagnetism on In Situ Characterization of Chromium III Complexes:

In situ investigation of chromium III based catalyst systems has not been widely reported, largely due to the difficulties imposed on conventional NMR spectroscopy by the paramagnetism of the active species.

Octahedral Chromium III has electronic configuration $3d^3$, and as such has 3 unpaired valence electrons, figure 1.38:

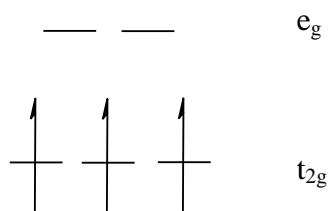


Figure 1.38: d- electron configuration in Octahedral Chromium III.

The presence of unpaired electrons in the valence shell imposes a substantial magnetic moment on the environment around the chromium centre. Since this alters the extent of nuclear shielding, the chemical shift value of NMR signals originating from the vicinity of the paramagnetic nucleus may be dramatically different from that exhibited by a comparable functionality in a diamagnetic environment. The magnitude and direction of this ‘shift shift’ is difficult to predict, being necessarily dependent on the subtleties of spin-delocalisation, distance from and relative orientation to the anisotropic field.

NMR signals also undergo line broadening in a paramagnetic environment. The relaxation rate for a given nucleus is chiefly dependent on the spin-lattice relaxation rate, which is given by:³⁷

$$R_{1M} = \frac{2}{15} \left(\frac{\mu_0}{4\pi} \right)^2 \frac{\gamma_N^2 g_e^2 \mu_B^2 S(S+1)}{r^6}$$

A line width associated with relaxation is directly proportional to the relaxation rate, which is proportional to $1/r^6$. Therefore, NMR signals arising from nuclei sufficiently close to the paramagnetic centre may be broadened to such an extent that they can no longer be resolved.

1.5 1,3,5-Triazacyclohexanes- Synthesis and Reactivity.

1,3,5-tris(alkyl/aryl)-1,3,5-triazacyclohexanes (1,3,5-tri(alkyl/aryl)hexahydro-1,3,5-triazines), or ‘TAC’s are formed readily by the condensation of formaldehyde with primary aliphatic or aromatic amines. This reaction was reported early in the last

century, and given the limited analytical methods available at the time, condensation of primary alkylamines with formaldehyde was originally presumed to yield alkylmethyleimines, see figure 1.39:

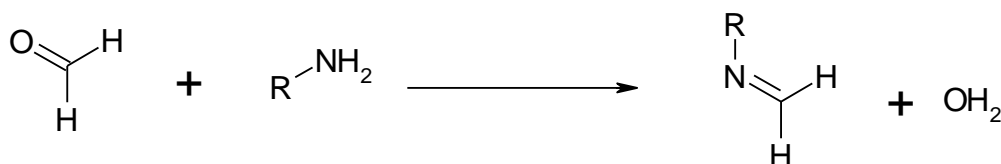


Figure 1.39: Originally Postulated Condensation Reaction.

However, Graymore³⁸ subsequently characterised the products as cyclic triazacyclohexanes, see figure 1.40:

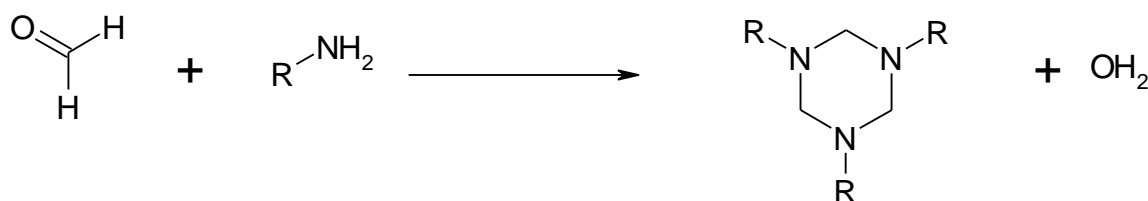


Figure 1.40: Synthesis of Triazacyclohexane by Condensation Reaction.

The heterocycles can be synthesized in almost quantitative yield by condensation of formaldehyde or paraformaldehyde with a wide variety of amines or anilines, in aqueous or organic solvent. Symmetrical trialkyl TACs can be synthesized by combining the amine with 1 equivalent of formaldehyde in aqueous solution. The condensation is also effective, if slower, in aromatic organic solvents, eg toluene.

Condensation of formaldehyde with a mixture of aliphatic primary amines yields a statistical distribution of symmetrical and unsymmetrical triazacyclohexanes, as follows:

If one equivalent of R^1NH_2 , n equivalents of R^2NH_2 and $n+1$ equivalents of formaldehyde are condensed:

The proportion of R^1_3TAC produced statistically is: $1^3 = 1$ eq.

The proportion of $\text{R}^1_2\text{R}^2\text{TAC}$ produced is:

$$(1 \times 1 \times n) + (1 \times n \times 1) + (n \times 1 \times 1) = 3(1 \times 1 \times n) = 3n \text{ eq.}$$

The proportion of $R^1R^2_2\text{TAC}$ is:

$$(1 \times n \times n) + (n \times 1 \times n) + (n \times n \times 1) = 3(1 \times n \times n) = 3n^2 \text{ eq.}$$

The proportion of $R^2_3\text{TAC}$ produced is: $n^3 \text{ eq.}$

Therefore, if a 10-fold excess of $R^2\text{NH}_2$ over $R^1\text{NH}_2$ is employed, the products occur in the ratio 0.08% ($R^1_3\text{TAC}$), 2.25% ($R^1_2R^2\text{TAC}$), 22.54% ($R^1R^2_2\text{TAC}$), 75.13% ($R^2_3\text{TAC}$).

This allows the synthesis of unsymmetric TACs bearing one substituent R^1 and two substituents R^2 , by addition of a large excess of $R^2\text{NH}_2$ relative to $R^1\text{NH}_2$. The reaction produces a large excess of $R^2_3\text{TAC}$ as a by-product.

Thus, by this method the major product may be separated by distillation to leave the desired unsymmetrical TAC species and the other by-products in almost negligible quantities.

Where the condensation of a mixture of aliphatic and aromatic primary amines is attempted, this statistical distribution is observed, where an alcohol solvent or an aromatic solvent in the presence of an added base is employed. However, for example, in the case of condensation of a mixture of aliphatic and aromatic amines with formaldehyde in toluene solution, the condensation of the aliphatic amines is often observed to be preferred. In this case the proportion of unsymmetrical TAC species produced by this method is lower than would be expected from a statistical distribution. This is assumed to be attributable to the difference in basicity of aromatic versus aliphatic amines, i.e. in the case of the aromatic amine, the acidity of the amine protons is enhanced relative to those of the aliphatic amine, by the stabilisation of the conjugate base by delocalisation into the π -system, see figure 1.41:

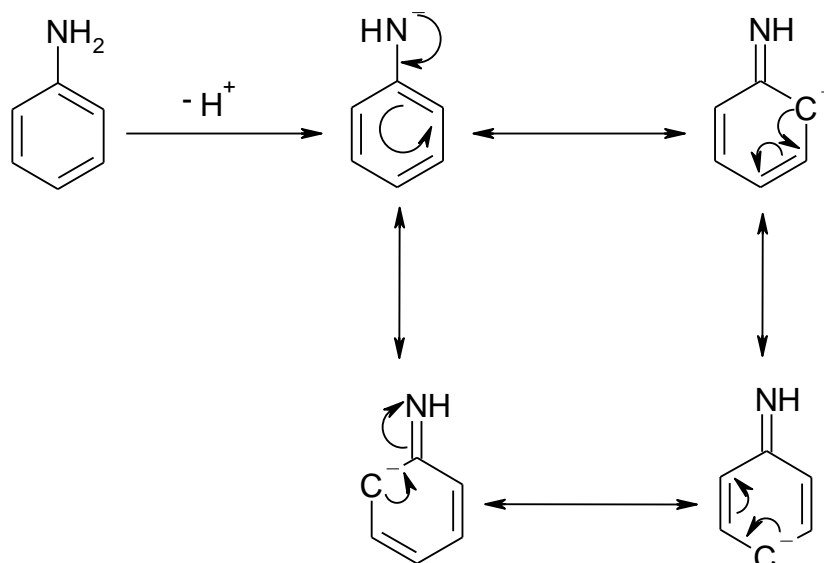


Figure 1.41: Resonance Stabilisation of Deprotonated Aniline.

The pK_a of aniline for example, is 4.63, while that of methylamine is 10.66.³⁹

The addition of a base to the reaction solution results in the deprotonation of the aromatic amines and thus to a statistical distribution of products.

The comparative basicity of protic solvents (other than water) is hypothesised also to be attributable to the relative basicity of such solvents.

TAC molecules are sensitive to various environmental conditions:

Above a certain temperature, which has not been studied systematically, but which we believe to be above ca. 60-70° C, the heterocycles are prone to equilibration, ie a mixture of two or more symmetrical TAC species when heated are converted into a statistical distribution of mixed and symmetrical heterocycles, by exchange of primary amines.

Consequently, it is not possible to separate a mixture of TACs by distillation at any given pressure if their boiling points at that pressure exceed the temperature at which equilibration occurs, as this simply results in formation and distillation of the more volatile symmetric species, leaving a residue comprising the less volatile symmetric species.

TAC molecules are not stable in aqueous acidic conditions:

The heterocycle decomposes rapidly upon the addition of aqueous acids, reverting to formaldehyde and the protonated salt of the relevant primary amine.³⁸ It is possible

to propose plausible mechanisms for the formation and the acidic decomposition of the heterocycles, taking alkylmethyleneimines to be intermediates, see figures 1.42a, 1.42b:

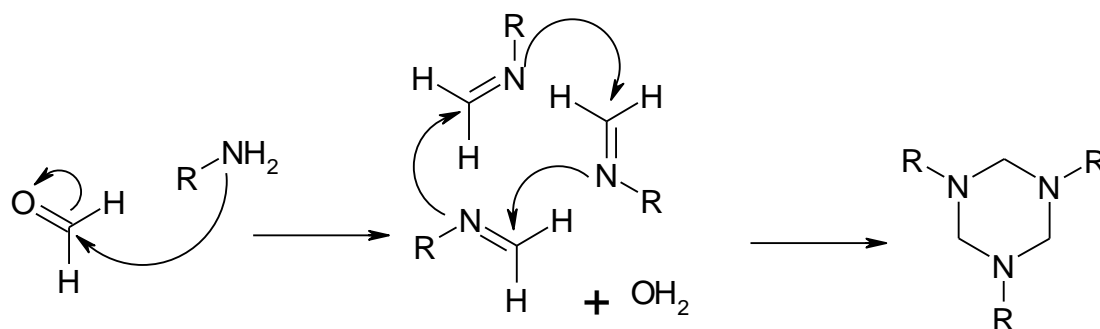


Figure 1.42a: Mechanism of Formation of Heterocycle, via Imine Intermediates.

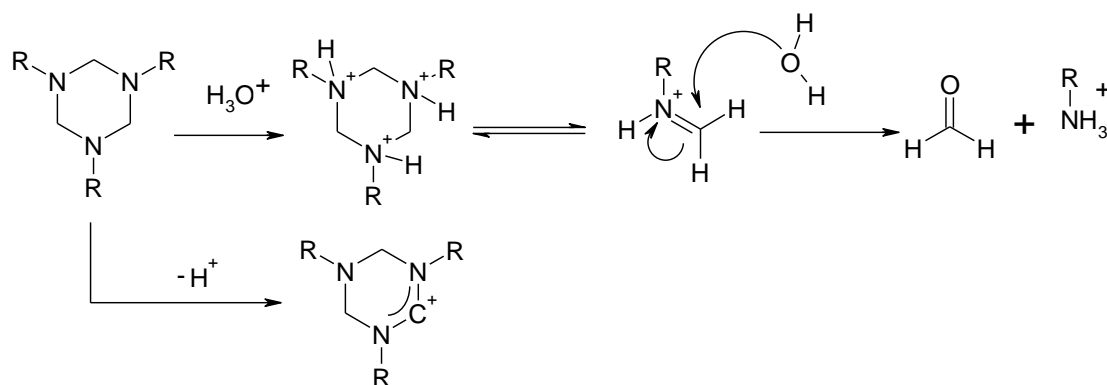


Figure 1.42b: Mechanism of Acid Decomposition of Heterocycle, via Imine Intermediate, and to Amidinium Cation by Hydride Abstraction.

Additionally, we have observed the formation of amidinium cations upon addition of lewis acids to TAC molecules. See ‘2.1 Triazacyclohexanes bearing Tetrarylborate Anionic Functionalities.’ This represents an irreversible decomposition of the cycle.

TAC molecules can be protonated without decomposition, in the absence of an aqueous medium; eg. by direct addition of $\text{HBr}_{(\text{g})}$ to a TAC solution in a non-protic solvent, see figure 1.43:

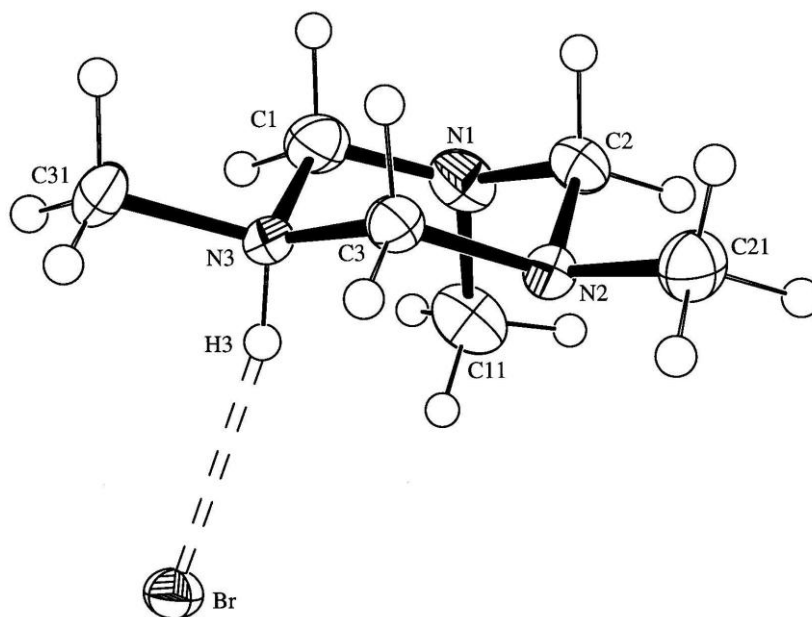


Figure 1.43: Crystal Structure of 1,3,5-Trimethyl-1,3,5-Triazacyclohexane Hydrobromide. (Crystallised from Diethyl Ether, see ‘3.6 Preparation of 1,3,5-trimethyl-1,3,5-triazacyclohexane Hydrobromide Crystals:’).

Recent work has established that TAC molecules are also prone to decomposition in the presence of more general Lewis acids, such as $\text{BF}_3 \cdot \text{Et}_2\text{O}$. (See ‘2.1 Triazacyclohexanes bearing tetrarylborate anionic functionalities’). The irreversibility of decomposition as a consequence of exposure to acidic media suggests the formation of amidinium cations, by hydride abstraction.

The TAC molecule is most stable in the ‘chair’ conformation, and owing to the effects of electrostatic repulsion between substituents, the most stable conformation sees the three substituents ‘R’ oriented in an ‘equatorial, equatorial, axial’ (see figure 1.43), or an ‘equatorial, axial, axial’ arrangement. There is of course no potential for stereoisomerism in TAC molecules, as uncomplexed sp^3 nitrogen centres do not exhibit chirality. Consideration of the relative positions of the nitrogen centres in the chair conformation, (given the tetrahedral arrangement of substituents around sp^3 centres), shows the donor lone pairs to be orientated axially, when substituents ‘R’ are equatorial, see figure 1.44:

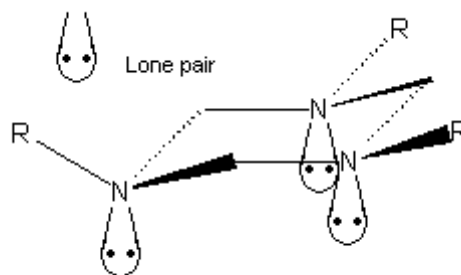


Figure 1.44: TAC Molecule, showing Substituent Orientations with respect to Nitrogen Centres.

While TAC molecules may be readily synthesized incorporating various different hydrocarbon substituents, they are intolerant of a range of other functionalities besides acids:

-Attempts to incorporate alkyl halide functionalities result in decomposition to insoluble materials that are difficult to characterize, but which can reasonably be taken to be a mixture of products of quaternisation of the tertiary amines in the ring, see figure 1.45:

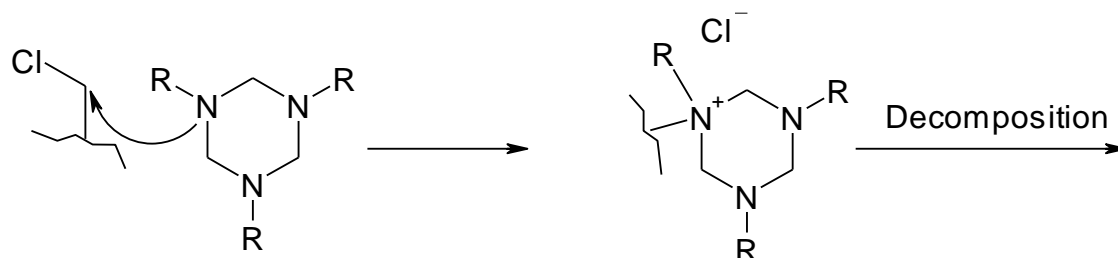


Figure 1.45: Reaction of TAC Ring Nitrogen with Chloroalkyl Functionality.

Aryl species bearing halogen substituents present no such problems however, not being prone to nucleophilic attack.

-Attempts to produce a TAC molecule incorporating 4-hydroxyaniline unexpectedly failed- the reagent did not react with formaldehyde to form TACs as expected, even as its (deprotonated) sodium salt. This suggests that the inductively electron withdrawing effect of the *para*-hydroxyl substituent significantly reduced the reactivity of the amine functionality. Furthermore, phenolic groups are capable of reaction with formaldehyde.

-Most boranes coordinate strongly to amine functionalities, as do similar species such as trialkylaluminiums, and, in the former case, may cause decomposition.

-TAC molecules are tolerant of hydroxyalkyl substituents, but not thiols, as the acidity of the latter causes decomposition.

While aromatic primary amines can be readily incorporated into a TAC molecule, the resultant species is a much weaker electron donor than is the equivalent aliphatic amine based species, as a consequence of the same delocalization effect that renders anilines more acidic than their aliphatic equivalents. (An exception to this effect is seen where the aromatic substituent's p-orbitals are arranged orthogonally to the nitrogen lone pair, thus preventing overlap and hence conjugation. This may occur as a consequence of steric constraints imposed by bulky substituents *ortho* to the nitrogen group). For this reason, and the inherent steric bulk associated with aromatic substituents, TAC molecules derived entirely from anilines have been considered to be poor ligands and thus were not considered to be viable synthetic targets for this project, though unsymmetrical species bearing one aromatic substituent were deemed potentially suitable, (see '1.4.1 Proposed Development of Anionic Ligands').

1.6 Proposed Development of Anionic Ligands:

On the assumption that catalyst degradation in the case of triazacyclohexane complexes occurs as a consequence of decomplexation of the ligand, the project was concerned with attempting to develop ligands, broadly analogous to 1,3,5-triazacyclohexanes in terms of κ^2/κ^3 denticity, that were more strongly associated with the metal centre in the active species. In order to accomplish this, a class of anionic ligands was envisaged.

Peters *et al.*⁴⁰ report the diazaborate anionic ligand $[(\text{Ph}_2\text{B}(\text{CH}_2\text{NMe}_2)_2)]^-$, and hence the synthesis of various zwitterionic rhodium complexes, see figure 1.46:

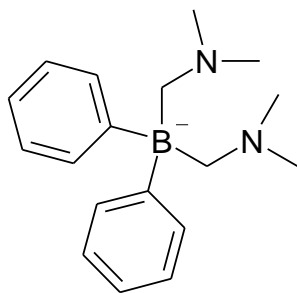


Figure 1.46: Diazaborate Anion.

This ligand is somewhat similar to the previously investigated triazacyclohexane ligands. It was proposed that the attraction between the negatively charged ligand and the positively charged chromium centre on the active species would reduce the tendency towards decomplexation and thus prolong the lifetime of the catalyst. See figure 1.47:

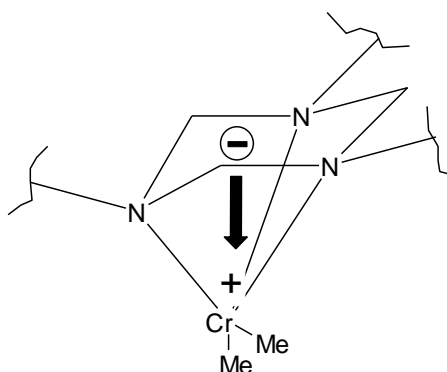


Figure 1.47: Active Species showing Cation/Anion Interaction.

The nature of the active species and the observed behaviour of the triazacyclohexane-chromium chloride system imposed certain requirements. Given that the active species is cationic, the charge on an anionic ligand must be localized- if delocalized it would simply represent an additional bond to the chromium centre, rendering the active species neutral and no longer active. The effect of coordinating functional groups has been shown to be reduction of activity of the catalyst, so any anionic functional group must also be weakly coordinating, which fact complicates the synthetic requirements significantly. Derivatives of tetraphenylborate anions are extensively employed where a weakly coordinating counterion is required in catalyst systems. Thus, the ligands envisaged in this project are all based on anionic tetracoordinated boron centres. They can further be subdivided into two classes:

1. Those which are based closely on 1,3,5-triazacyclohexanes, ie, functionalized variants thereof, or ligands which are structurally dissimilar to triazacyclohexanes but possess comparable donor groups, ie sp^3 hybridised tertiary amines in similar orientations and relative positions to those exhibited by the TAC molecule. See figure 1.48:

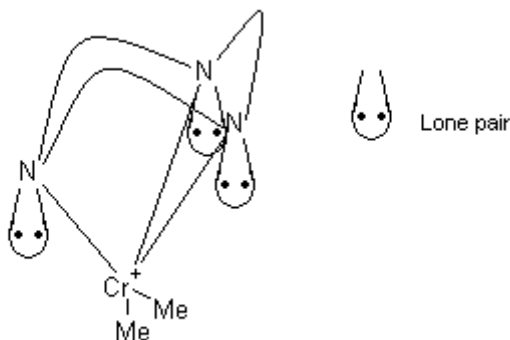


Figure 1.48: Generic Triazacyclohexane Type Bonding Ligand Complex.

2. Ligands structurally and coordinatively distinct from TAC molecules, but still hemilabile as a consequence of possessing two strongly coordinating and one weakly coordinating functionality, allowing κ^2 and κ^3 coordination, see figure 1.49, X = weakly coordinating donor, Y = strongly coordinating donor groups.

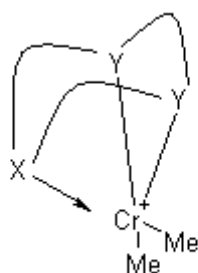


Figure 1.49: Generic Hemilabile Ligand Type. X = weakly coordinating donor, Y = strongly coordinating Donor Groups.

Introduction- Summary:

The selective trimerisation of ethylene and higher α -olefins is believed to proceed via a metallacyclic mechanism.

Of the various catalyst systems known to be active for the selective trimerisation of ethylene and α -olefins, the majority are based on chromium complexes.

The homogeneous catalyst systems for ethylene and α -olefin trimerisation feature hemilabile ligands. This appears to be an essential requirement of the proposed general metallacyclic mechanism.

Heterogeneous ethylene and α -olefin trimerisation catalysts are greatly varied, and often poorly defined.

The synthesis of 1,3,5-triazacyclohexanes is a relatively trivial procedure, though separation of mixed unsymmetrical TAC species poses significant challenges. TAC molecules are of limited stability in acidic environments.

TAC molecules form κ^2 and κ^3 bound complexes to Chromium III centres.

Analogous hemilabile ligand-types may exhibit similar catalytic activity, and the introduction of an anionic functionality may result in an active species less prone to decomposition than are Chromium III complexes of neutral TAC species.

2. Results and Discussion:

2.1 Triazacyclohexanes bearing Tetraarylborate Anionic Functionalities:

Tetraarylborate anions may be synthesized by addition of aryl lithium or Grignard reagents to tris-arylboranes,^{41,42} see figure 2.1:

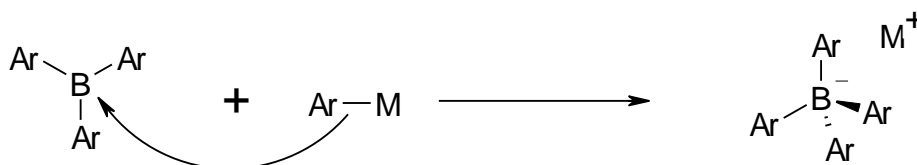


Figure 2.1: Quaternisation of Tris-arylborane by reaction with Aryl Metal.

The ligand class $[\text{Ar}_3\text{BC}_6\text{H}_4\text{R}_2\text{TAC}]^-$ and thus the corresponding chromium III complex was envisaged, see figure 2.2:

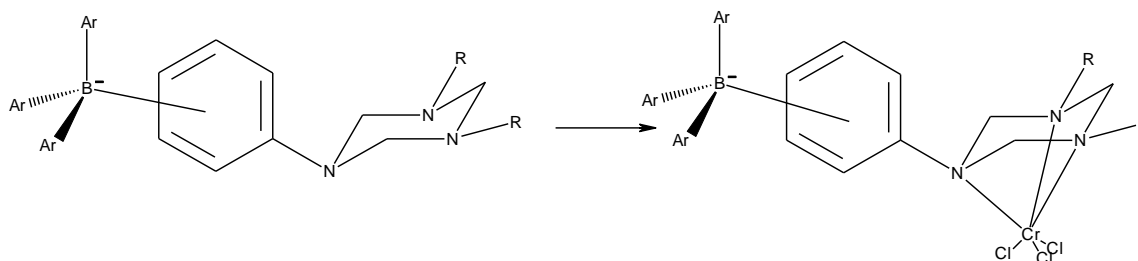


Figure 2.2: Ligand Class $[\text{Ar}_3\text{BC}_6\text{H}_4\text{R}_2\text{TAC}]^-$ and corresponding Chromium III Complex.

Initially, the following synthetic strategy was attempted:

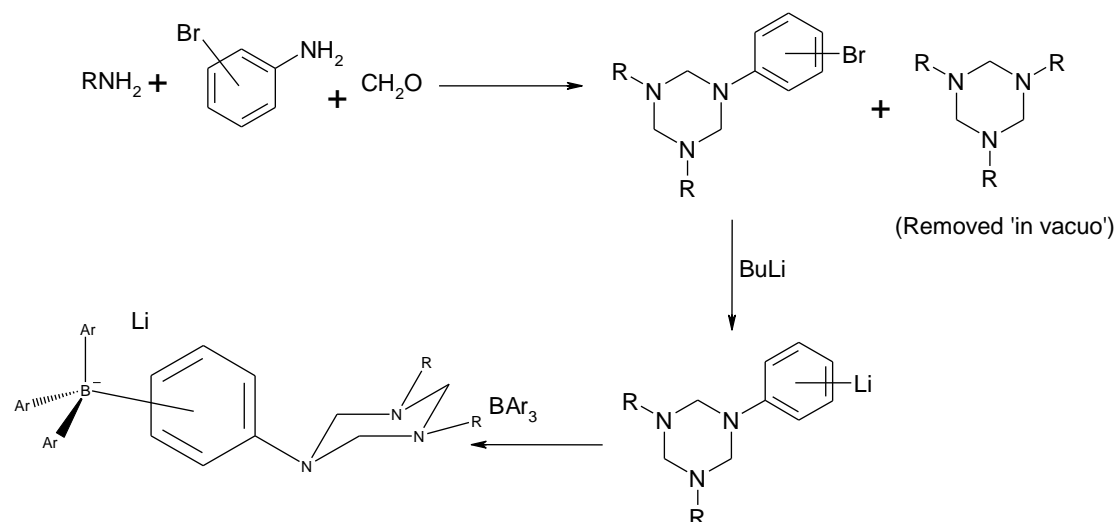


Figure 2.3: Attempted Synthetic Strategy.

The reaction of *p*-bromoaniline with a large excess of paraformaldehyde and methylamine in methanol solution yielded a statistical distribution of products. The major product, 1,3,5-trimethyl-1,3,5-triazacyclohexane was removed under high vacuum at room temperature, leaving 1-(*p*-bromo)phenyl-3,5-dimethyl-1,3,5-triazacyclohexane as a > 90% pure product. The attempted formation of the quaternary borate anion was based on the work of Wittig *et al.*⁴³ The unsymmetrical TAC was dissolved in dry, degassed THF and cooled to $-78\text{ }^{\circ}\text{C}$. To the solution was added *n*-BuLi solution in order to generate the organolithium precursor. One equivalent of tris(pentafluoro)phenylborane was subsequently added as a saturated solution in dry THF, and the resultant solution was stirred at $-78\text{ }^{\circ}\text{C}$ for 1 hour, before being allowed to stir for several hours at room temperature. (See ‘Experimental’ section).

Removal of the solvent from the product yielded a brown, viscous oil, which was ascertained to be soluble in most solvents, with the exception of hexane. Attempts to recrystallise this material were unsuccessful, and attempted characterization by NMR spectroscopy revealed a mixture of products, but no evidence of the continued existence of the triazacyclohexane molecule. Relatively clean ^{19}F NMR spectra suggest no more than two fluorine containing major products, while ^{11}B NMR spectra typically show signals at approximately 0 ppm, depending on the solvent in use. Tetraarylborates typically exhibit sharp singlets between ca. -5 and -15 ppm; signals at 0 ppm are more consistent with N-adducts.

In order to assess the viability of the lithiation step, an attempt was made to silylate the unsymmetrical TAC species, under similar conditions to the attempted reaction with the borane:

The unsymmetrical TAC was dissolved in dry, degassed THF and cooled to -78°C . To the solution was added one equivalent of n-BuLi solution. To this solution, after 1 hour was added one equivalent of chlorotrimethylsilane. The solvent was removed *in vacuo*, the inorganic salts removed by precipitation and the residue characterised by ^1H and ^{13}C NMR spectroscopy. Although the product was not clean, appearing principally to comprise a mixture of the silylated product and the unsilylated starting material, the signals attributable to the heterocycle and the trimethylsilyl functionality were clearly visible in the ^1H and ^{13}C spectra. (See 'Experimental' section). This suggested that the flaw in the synthetic strategy for the synthesis of the borate anion lay in the tris-arylborane addition step.

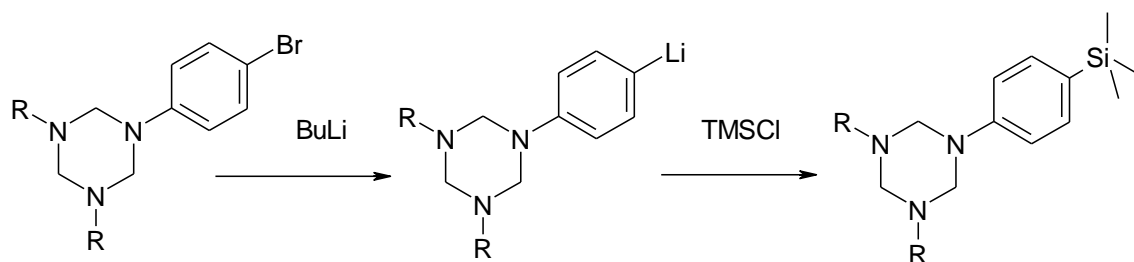


Figure 2.4: Silylation of Unsymmetric TAC.

For tris(pentafluoro)phenylborane in the presence of the lithiated precursor, there are two possible reactions which may occur- the borane may either react with the phenyl lithium substituent, or undergo coordination to the nitrogen lone pairs on the heterocycle, see figure 2.5:

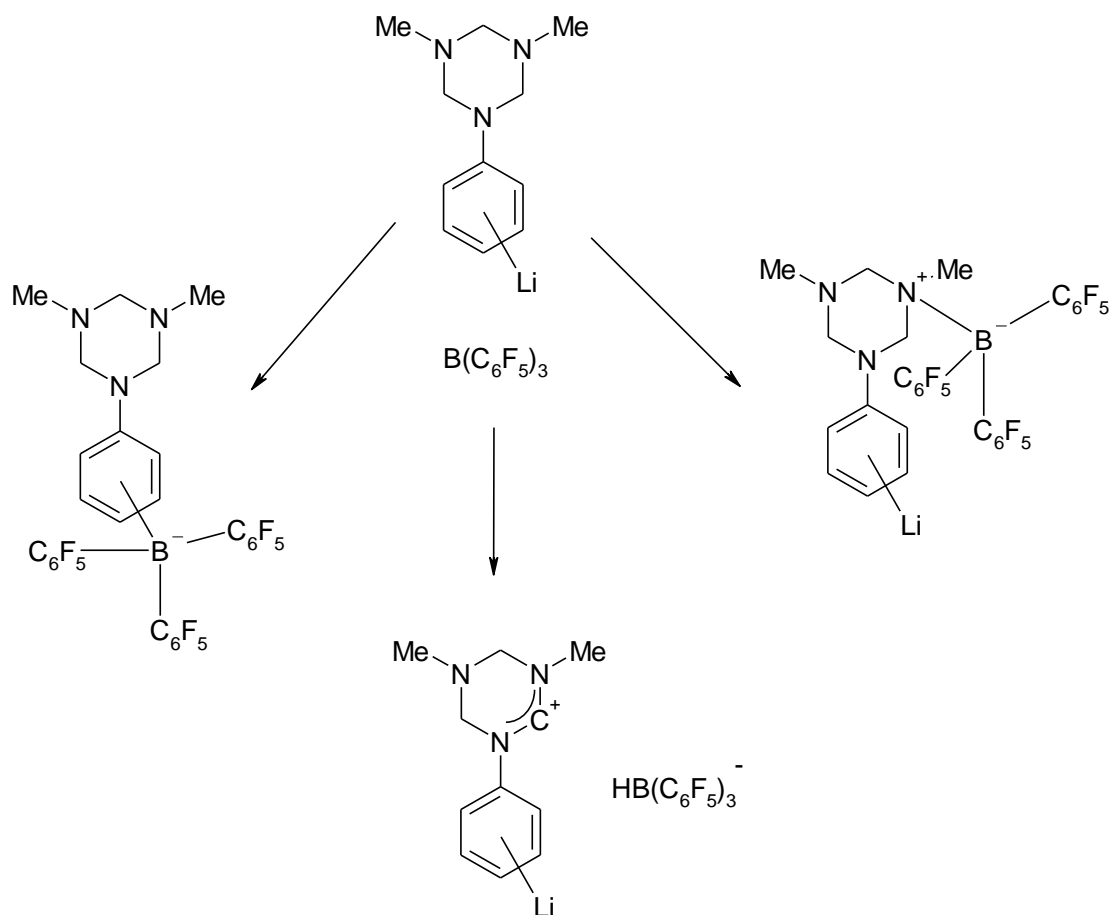


Figure 2.5: Possible Reactions of Tris(pentafluoro)phenylborane with $\text{LiC}_6\text{H}_4\text{Me}_2\text{TAC}$.

Given the apparent loss of the TAC molecule during the course of the reaction, and the lack of spectroscopic evidence of tetraarylborate formation, it was hypothesized that coordination of the borane may result in decomposition of the heterocycle. In order to investigate this possibility, to a solution of 1,3,5-trimethyl-1,3,5-triazacyclohexane in CDCl_3 was added boron trifluoride diethyletherate. The solution was characterised by ^1H , ^{13}C and ^{11}B NMR spectroscopy after a few hours, and signals were exhibited at $\delta = \text{ca. } 7.5 \text{ ppm}$, and 163.0 ppm in the ^1H and ^{13}C NMR spectra respectively, this being characteristic of an amidinium cation.

Similarly, the reaction of 1,3,5-tribenzyl-1,3,5-triazacyclohexane with tris(pentafluoro)phenylborane was investigated. To an excess of 1,3,5-tribenzyl-1,3,5-triazacyclohexane was added a solution of tris(pentafluorophenyl)borane in dry THF. The solution was characterised by ^1H , ^{13}C , ^{11}B and ^{19}F NMR spectroscopy after several hours. The ^{19}F NMR spectrum exhibited signals at $\delta = -131.95$, -158.50 and

-164.78, this being characteristic of a quaternary boron compound. In addition to the aromatic signals, signals were observed at ca. 8.3 ppm and 169 ppm in the ^1H and ^{13}C NMR spectra respectively, again characteristic of an amidinium cation.

Thus hydride elimination is apparent, and the resultant cycle is not expected to be stable- decomposition to an imine is probable.

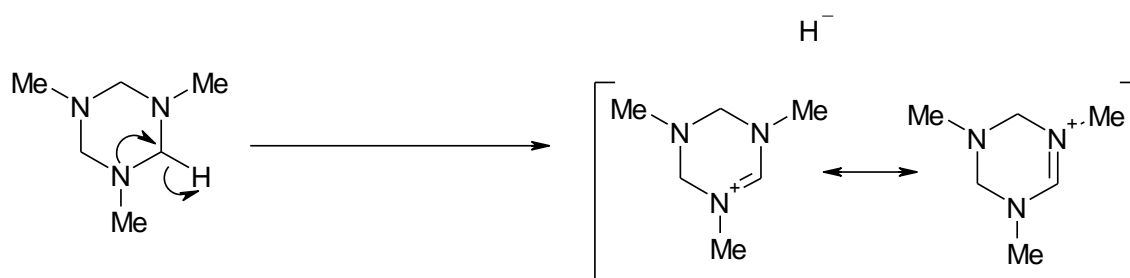


Figure 2.6: Amidinium Cation Formation.

Given the impracticability of a synthetic strategy that involves the addition of trisubstituted boranes to triazacyclohexanes, an alternative strategy is required. Synthesis of the tetraarylborate prior to TAC formation was one possibility, ie lithiation of bromoaniline followed by addition of borane. However, in this case the two aniline protons are certainly more reactive than the arylbromide functionality. The addition of 2-3 equivalents of *n*-BuLi and 2-3 equivalents of tris(pentafluoro)phenylborane might be expected to produce a borane adduct of the target anion, bearing, in addition to the anionic boron centre, 1 or possibly 2 borane species (depending on steric constraints), coordinated to the aniline functionality see figure 2.7:

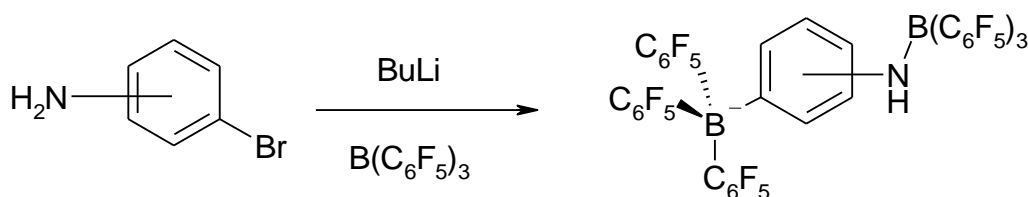


Figure 2.7: Product of Lithiation and Tris(pentafluoro)phenylborane Addition to Bromoaniline.

This strategy would be hugely wasteful of the borane however, and instead the strategy devised comprised the protection of the amine functionality by bis-silylation, followed by lithiation, and the addition of tris(pentafluoro)phenylborane to form the

salt. The silane functionalities can be removed by acidic hydrolysis subsequently. See figure 2.8:

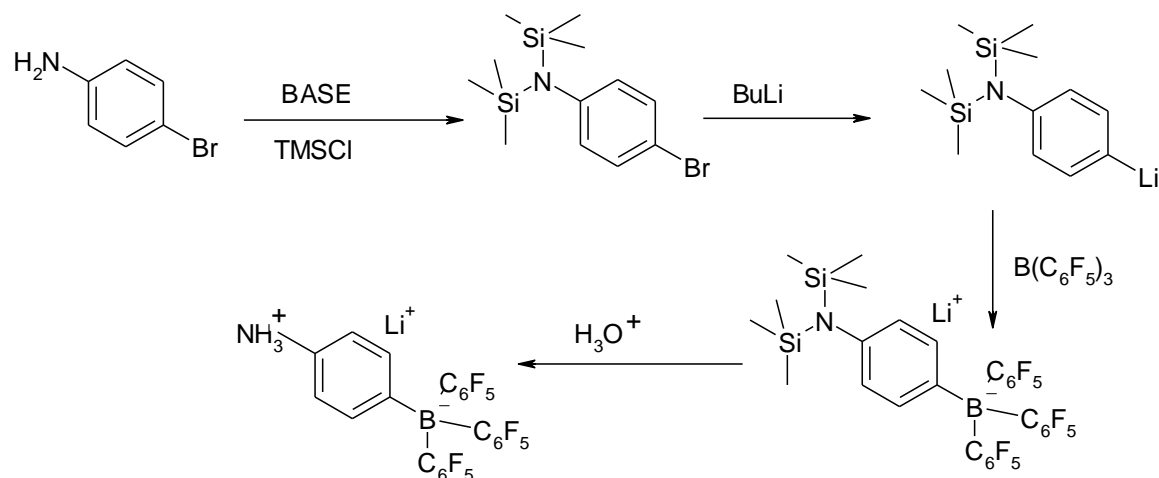


Figure 2.8: Strategy for the Synthesis of Lithium Aminophenyltris(pentafluoro)phenylborate-Acid Salt.

N-(Trimethyl)silyl-p-bromoaniline is readily synthesized by reaction of chlorotrimethylsilane with the aniline in the presence of a mild base, eg triethylamine. Harsher conditions are required to produce the bis-silylated aniline however, and this was accomplished by prolonged reflux with an excess of methylmagnesium chloride in dry THF solution, followed by addition of excess chlorotrimethylsilane and further refluxing, (See ‘Experimental’ section). The result comprised bis(trimethyl)silyl-p-bromoaniline with a few percent (trimethyl)silyl-p-bromoaniline impurity. In order to establish the reactivity of the bromine substituent, a reaction analogous to that envisaged for the synthesis of the borate was attempted, ie silylation of the aniline at the *para* position, see figure 2.9:

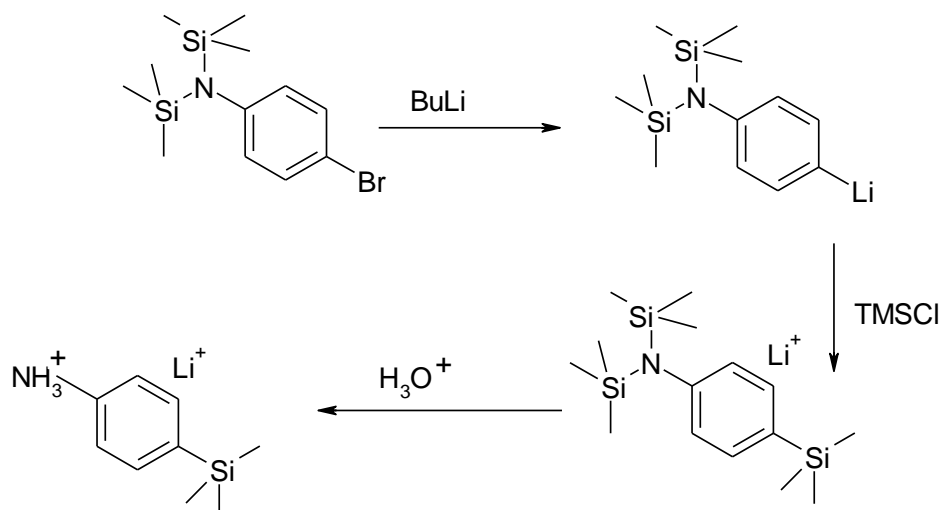


Figure 2.9: *p*-Silylation of Aniline.

The *N,N*-bis-silylated aniline was reacted with *n*-butyl lithium at 0°C , followed by addition of one equivalent of chlorotrimethylsilane. The resultant solution was stirred in aqueous hydrochloric acid overnight, and the volatiles removed *in vacuo* to yield a brown solid. This was characterised by ^1H and ^{13}C NMR spectroscopy, exhibiting in each case a single singlet at 0 ppm attributable to a trimethylsilyl substituent, though the aromatic regions appeared to exhibit 2 sets of peaks, probably attributable to a mixture of the product and unsilylated *p*-bromoaniline. The relative magnitudes of the aromatic and aliphatic integrals are consistent with this (See ‘3.15 Synthesis of 4-(trimethyl)silylaniline hydrochloride:’).

The reaction of the *N,N'*-bis-silylated aniline with one equivalent of *n*-butyl lithium at 0°C , followed by addition of one equivalent of tris(pentafluoro)phenylborane yielded a brown oil. Recrystallisation from diethyl ether was possible, but the resultant crystals were of insufficient quality for analysis by single crystal X-ray diffraction. The crystalline material was characterised by ^1H , ^{13}C , ^{19}F and ^{11}B NMR spectroscopy. Relatively clean ^{19}F , ^{13}C and ^1H spectra were consistent with the synthetic target, and ^{11}B NMR spectra exhibit sharp singlets typically at ca. -14 ppm, as well as broad, shallow peaks evidencing other minor products.

The product was stirred overnight dissolved in an aqueous solution of hydrochloric acid, under $\text{N}_{2(\text{g})}$. The volatiles were removed *in vacuo* and the resultant solid characterised by ^1H , ^{13}C and ^{11}B NMR spectroscopy. The ^{11}B spectrum was largely

unchanged, the sharp singlet indicative of the tetra-aryl borate salt remaining, while the intensities of the signals indicative of the (trimethyl)silyl substituents on the aniline functionality were dramatically reduced in the ^1H and ^{13}C NMR spectra, being eventually eliminated altogether by further exposure to aqueous acid. (See ‘.17 (*Synthesis of Lithium 4-aminophenyltris(pentafluoro)phenylborate hydrochloride*)[Et_2O] $_2$:’). The overall yield for this synthesis is relatively low, and further progress towards the desired functionalized TAC ligand has not been accomplished at the time of writing.

2.2 1-(*p*-(Trisarylboron)oxymethyl)phenyl-3,5-dialkyl-1,3,5-triazacyclohexanes:

As an alternative to tetraarylborate as a weakly coordinating anion, various quaternary species incorporating B-O bonds are known. Of particular interest were species of the type $[\text{ArBOR}]^-$, synthesized by reaction of trisarylborane with a species bearing a hydroxyl substituent.^{44,45}



Figure 2.10: Addition of Alcohol to Trisarylborane.

The synthesis of a TAC molecule bearing a phenolic substituent was attempted, but failed- presumably due to the acidity of the hydroxyaniline starting material, and possibly reaction of the phenolic groups with formaldehyde (see ‘1.5 1,3,5-Triazacyclohexanes- Synthesis and reactivity’). Consequently, the following complex type was proposed:

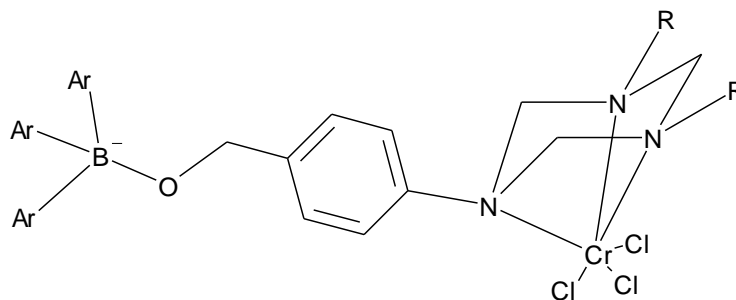


Figure 2.11: (*p*-(Tris(pentafluorophenyl)boron)oxymethyl)phenyl-3,5-dialkyl-1,3,5-triazacyclohexane.

The synthesis of the unsymmetric TAC molecule, 1-(3-hydroxymethyl)phenyl)-2,5-di(2-ethyl)hexyl-1,3,5-triazacyclohexane was attempted by condensation of 4-aminobenzylalcohol with a large excess of 2-ethylhexylamine and paraformaldehyde in methanol solution, followed by reaction of the resultant TAC mixture with sodium in dry THF. The unsymmetric TAC ligand was then separated from the symmetrical by-product by precipitation from hexane solution. The resultant oily solid was characterised by ^1H and ^{13}C NMR spectroscopy. The ^1H NMR spectrum showed a series of peaks, the relative integrals of which initially appeared to be consistent with the bis-arylated heterocyclic species, 1,3-bis(*p*-hydroxymethyl)phenyl)-5-(2-ethyl)hexyl-1,3,5-triazacyclohexane. An attempt was made to complex the product to chromium III chloride. However, after closer inspection of the ^1H and pendent ^{13}C NMR spectra, it was concluded that they were most consistent with a mixture of 1,3,5-tris(2-ethyl)hexyl-1,3,5-triazacyclohexane, and the sodium salt of (3-amino)benzylalcohol. The insolubility of this product in non-polar solvents suggests coordination of the amine functionalities to the sodium counter-ion. The residue of the hexane washings was also characterised, exhibiting 9 signals in the ^{13}C NMR spectrum, and no aromatic signals; as is consistent with the formation of the symmetric 1,3,5-tris(2-ethyl)hexyl-1,3,5-triazacyclohexane. (See ‘3.18 Attempted Synthesis of 1-(3-(sodium oxy)methyl)phenyl-3,5-(2-ethyl)hexyl-1,3,5-triazacyclohexane:’).

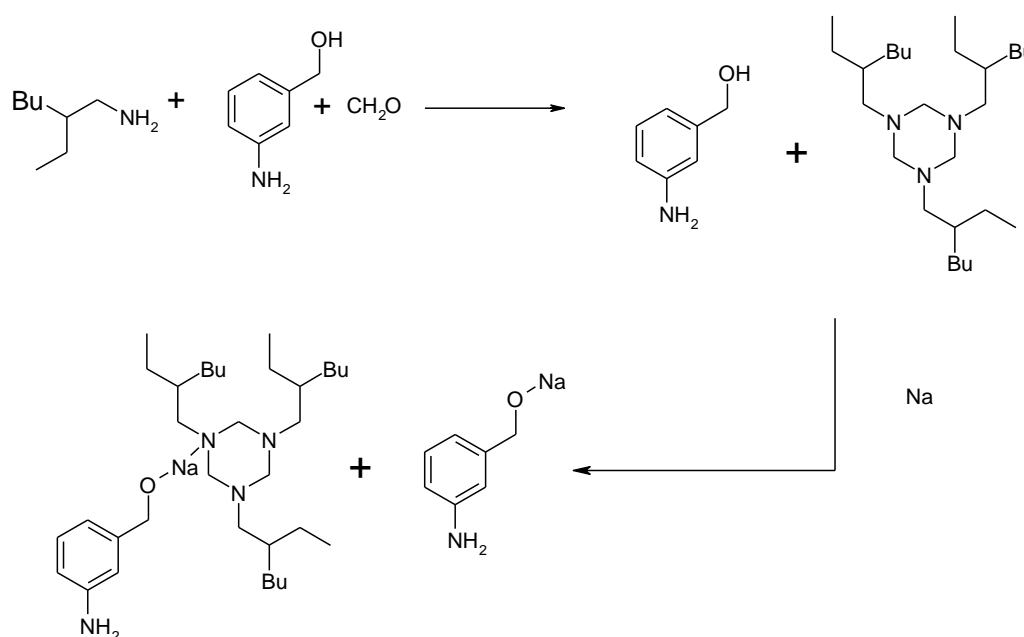


Figure 2.12: Attempted Reaction of 4-aminobenzylalcohol and 2-ethylhexylamine with Paraformaldehyde.

The failure of this reaction to yield the intended unsymmetric product is strange, as such anomalous results do not occur in the case of condensation reactions involving linear aliphatic aminoalcohols, and must therefore be considered a peculiarity of amines bearing benzylic alcohol functionalities.

The catalytic properties of the product, complexed to chromium III chloride, were evaluated in the presence, and absence of tris(pentafluoro)phenylborane. (See ‘**4. Catalysis- NMR interpretation:**’). The characterisation of this chromium system by electro-spray mass spectrometry was attempted, and a cationic mass signal $m/z = 492.40$ was observed, which is consistent with the product of complexation of 3 equivalents of 3-aminobenzylalcohol to CrCl_2^+ : $m/z = 492.40$ (theoretical $m/z = 492.37$, Sigma fits <0.05 indicates high probability of correct MF).

2.3 B-N Bonded Anionic Ligands:

In order to place the anionic functionality of a ligand as close as possible to the nitrogen centres responsible for coordination, quaternary boron centres bearing σ -bonded nitrogen substituents were investigated.

2.3.1 Azaboranes:

The simplest B-N bonded species envisaged comprised an azacyclic ligand bearing a quaternary boron centre, directly bound to a ring nitrogen. Accordingly, the following ligand, and corresponding zwitterionic complex, was envisaged:

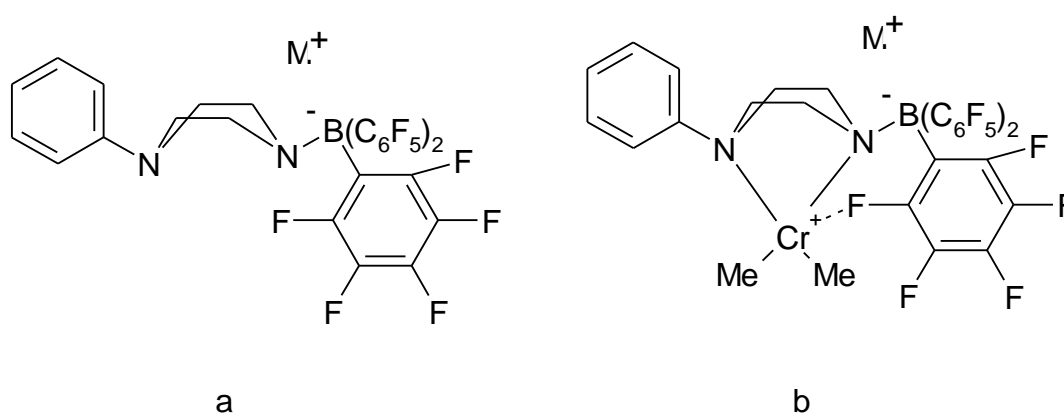


Figure 2.13: 1-(tris(pentafluoro)phenylbora)-4-phenyl-1,4-piperazine Anion (a) and Corresponding Complex (b).

The following synthetic strategy was proposed, in order to generate the anionic ligand:

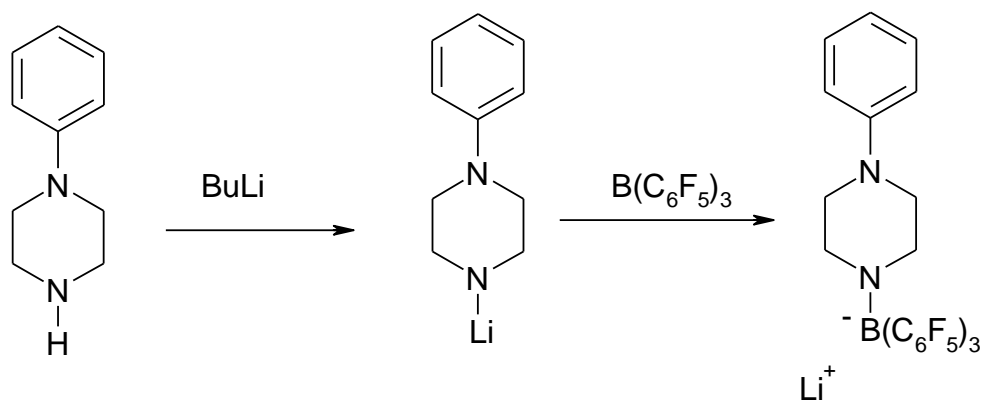


Figure 2.14: Proposed Synthesis of 1-(tris(pentafluorophenyl)bora)-4-phenyl-1,4-piperazine Anion.

In order to test the validity of the strategy, a silyl analogue was synthesised by the following procedure:

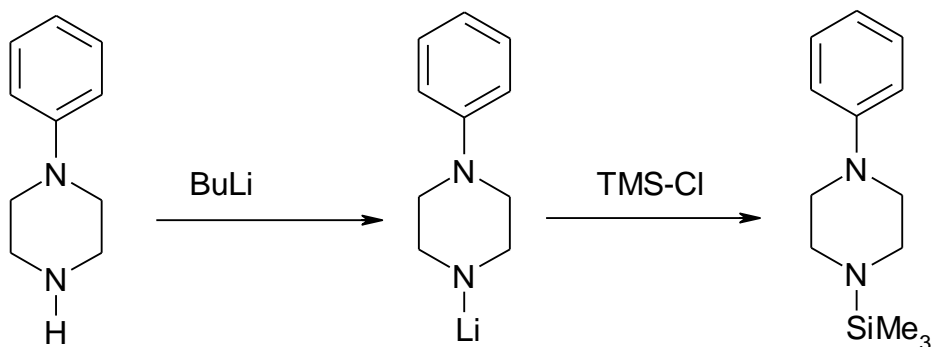


Figure 2.15: Synthesis of 1-(trimethyl)silyl-4-phenyl-1,4-piperazine.

The silane was synthesised in 79% yield, and characterised by ^1H and ^{13}C NMR spectroscopy. (See '3.52 Synthesis of N-phenyl-N'-trimethylsilylpiperazine:'). The analogous reaction was attempted, between N-lithium-N'-phenylpiperazine, and triphenylborane, in an effort to generate an anionic species, see figure 2.16:

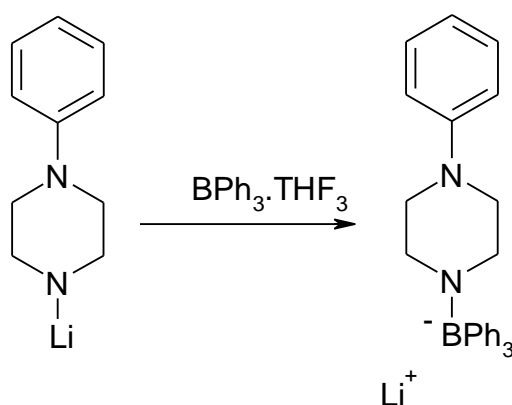


Figure 2.16: Attempted Synthesis of 1-(triphenyl)bora-4-phenyl-1,4-piperazine Anion.

A white solid was precipitated from the THF solution, by addition of dry hexane, but ^{11}B NMR spectroscopy revealed an absence of boron in the precipitated substance, while ^1H and ^{13}C NMR data showed a multitude of unidentified signals. Given the expected weakness of the single B-N σ bond (see ‘2.3.4 Theoretical Considerations of B-N bonded species’), this line of investigation was not continued.

2.3.2 Diazaboranes:

A quaternary boron centre bearing two directly bonded sp^3 hybridised nitrogen substituents and two organic substituents, was considered as a potential class of ligands. The proposed strategy was to synthesise a heterocyclic precursor, of the type 1-aryl-2,5-dialkyl-1-bora-2,5-diazacyclopentane, see figure 2.17:

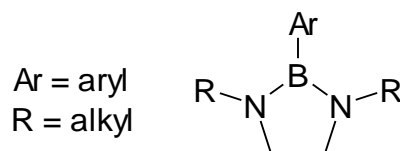


Figure 2.17: Synthetic Precursor, $\text{ArB}(\text{RNCH}_2)_2$.

The reaction of boron trihalides with dialkylethylenediamines is well established,⁴⁶ the product being $\text{XB}(\text{RNCH}_2)_2$, where $\text{X} = \text{Br}, \text{Cl}, \text{I}$.

The synthesis of 1-phenyl-2,5-di-*tert*-butyl-1-bora-2,5-diazacyclopentane by reaction of phenyldichloroborane with two equivalents of N,N'-diethylethylenediamine, see figure 2.18,

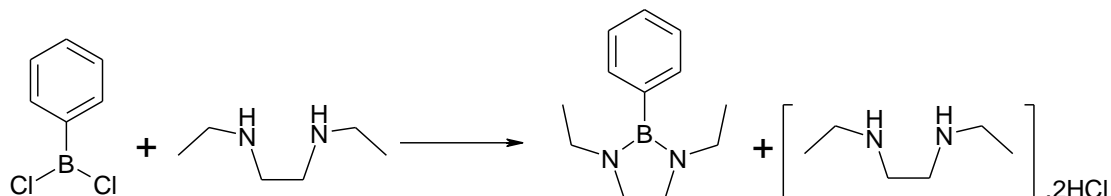


Figure 2.18: Reaction of N,N'-Diethylethylenediamine with Dichlorophenylborane.

produces good yields but is an inefficient strategy in terms of starting materials. For the reactions, both of boron trihalides and dichlorophenylborane with dialkylethylenediamines, the preferred method was to prepare the triethylamine adduct of the relevant borane and reflux this with the diamine in hexane solution, see figure 2.19:

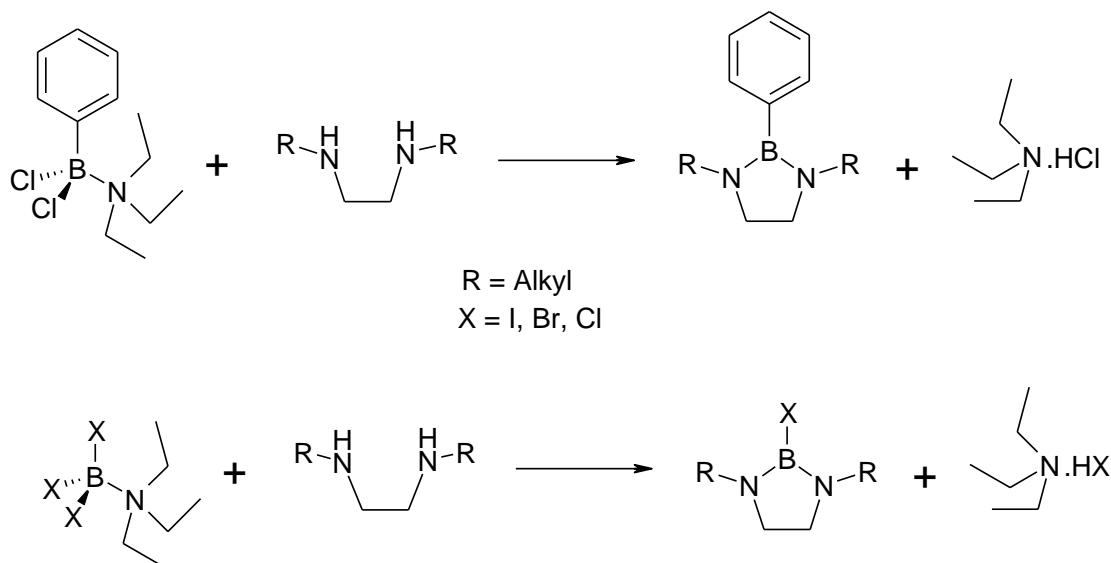


Figure 2.19: Heterocycle Syntheses via Borane-Triethylamine Adducts.

Heterocycles were synthesized based on dibenzyl, diethyl-, di-*n*-propyl- and di-*tert*-butylethylenediamine, of which di-*tert*-butylethylenediamine was deemed most useful as a precursor, as it produced by far the best yields, and the products were

invariably crystalline solids at room temperature. Compounds of the type XB(t-BuNCH₂)₂, where X = Br, Cl, proved to be unstable in THF and diethyl ether solution, decomposing into a brown, insoluble material over a period of hours. This precluded any attempt to alkylate or arylate these species via Grignard reagents, and attempts to do so using butyl lithium in hexane solution also resulted in decomposition.

Following is a table of ¹H, ¹³C and ¹¹B NMR data obtained for the various heterocyclic B-N bonded species that were synthesised, and the analogous silane 1,1-diphenyl-2,5-diethyl-1-sila-2,5-diazacyclopentane (See '**3. Experimental:**')

Compound:	¹ H NMR: δ =
PhB(NEt ₂) ₂ (CDCl ₃):	0.91(t, J=6.9Hz, 12H), 2.83(q, J=6.9Hz, 8H), 7.19(m, 2H), 7.24(m, 3H)
PhB(<i>tert</i> -BuNCH ₂) ₂ (CDCl ₃):	0.89(s, 18H), 3.23(s, 4H), 7.14(m, 3H), 7.23(m, 2H)
PhB(BzNCH ₂) ₂ (CDCl ₃ †):	3.02(s, 4H), 4.10(s, 4H), 7.20(m, 10H)
ClB(<i>tert</i> -BuNCH ₂) ₂ (CDCl ₃):	1.20(s, 18H), 3.11(s, 4H) - -
BrB(<i>tert</i> -BuNCH ₂) ₂ (CDCl ₃):	1.24(s, 18H), 1.45(s, 6H)*, 3.14(s, 4H) -
ClB(EtNCH ₂) ₂ (CDCl ₃):	0.96(t, J=7.2Hz, 6H), 2.93(q, J=7.2Hz, 4H), 3.17(s, 4H)
ClB(n-PrNCH ₂) ₂ (CDCl ₃):	0.78(t, J=7.2Hz), 1.36(q, J= 7.2,6.9Hz), 2.84(t, J= 6.9Hz), 3.15(s)
Ph ₂ Si(EtNCH ₂) ₂ (CDCl ₃):	0.86(t, J=6.9Hz, 6H), 2.68(q, J=6.9Hz,4H), 3.05(s, 4H), 7.28(m, 6H), 7.57(m, 4H)

* This additional signal occurs in the pure substance, and may be a consequence of oligomerisation of the heterocycle, which, curiously, has been observed as both a crystalline solid and a liquid at room temperature- cf. ¹¹B NMR spectrum (below).

† (Additional signals- impurities: δ 0.00 (silicone grease), 1.35, 2.99 (triethylamine)).

Compound:	¹³ C NMR: δ =
PhB(NEt ₂) ₂ (CDCl ₃):	14.6, 41.2 - 125.6, 126.5, 131.6
PhB(<i>tert</i> -BuNCH ₂) ₂ (CDCl ₃):	31.1, 45.3, 52.1, 126.7, 127.3, 132.8
PhB(BzNCH ₂) ₂ (CDCl ₃ †):	45.7, 49.1, 125.8, 126.7, 127.4, 138.7
ClB(<i>tert</i> -BuNCH ₂) ₂ (CDCl ₃):	15.0, 40.5, 46.1
BrB(<i>tert</i> -BuNCH ₂) ₂ (CDCl ₃):	29.1, 30.0, 44.0*, 50.9
ClB(EtNCH ₂) ₂ (CDCl ₃):	15.0, 40.5, 47.0
ClB(n-PrNCH ₂) ₂ (CDCl ₃):	10.2, 20.9, 46.0, 46.5
Ph ₂ Si(EtNCH ₂) ₂ (CDCl ₃):	15.7, 42.5, 49.1, 128.0, 130.1, 136.0

* This additional signal occurs in the pure substance, and may be a consequence of oligomerisation of the heterocycle, which, curiously, has been observed as both a crystalline solid and a liquid at room temperature- cf. ¹¹B NMR spectrum (below).

† (Additional signals- impurities: δ 0.00 (silicone grease), 7.6, 44.8 (triethylamine)).

Compound:	¹¹ B NMR: δ =
PhB(NEt ₂) ₂ (CDCl ₃):	34.05
PhB(<i>tert</i> -BuNCH ₂) ₂ (CDCl ₃):	32.67
PhB(BzNCH ₂) ₂ (CDCl ₃):	25.22
ClB(<i>tert</i> -BuNCH ₂) ₂ (CDCl ₃):	27.96
BrB(<i>tert</i> -BuNCH ₂) ₂ (CDCl ₃):	24.82, 17.29*
ClB(EtNCH ₂) ₂ (CDCl ₃):	27.96
ClB(n-PrNCH ₂) ₂ (CDCl ₃):	28.32
Ph ₂ Si(EtNCH ₂) ₂ (CDCl ₃):	-

*See notes- ¹H spectrum, above

1-phenyl-2,5-di-*tert*-butyl-1-bora-2,5-diazacyclopentane was synthesized in bulk and the properties of the precursor were investigated. X-ray crystallographic data was obtained for the compounds 1-phenyl-2,5-di-*tert*-butyl-1-bora-2,5-diazacyclopentane and 1-bromo-2,5-di-*tert*-butyl-1-bora-2,5-diazacyclopentane. In both cases, the conformation of the nitrogen centres appears to be approximately half way between planar and tetrahedral geometry, which is consistent with a resonance stabilised species, see below. Some ring strain is apparent in both cases, and the boron centres appear trigonal planar.

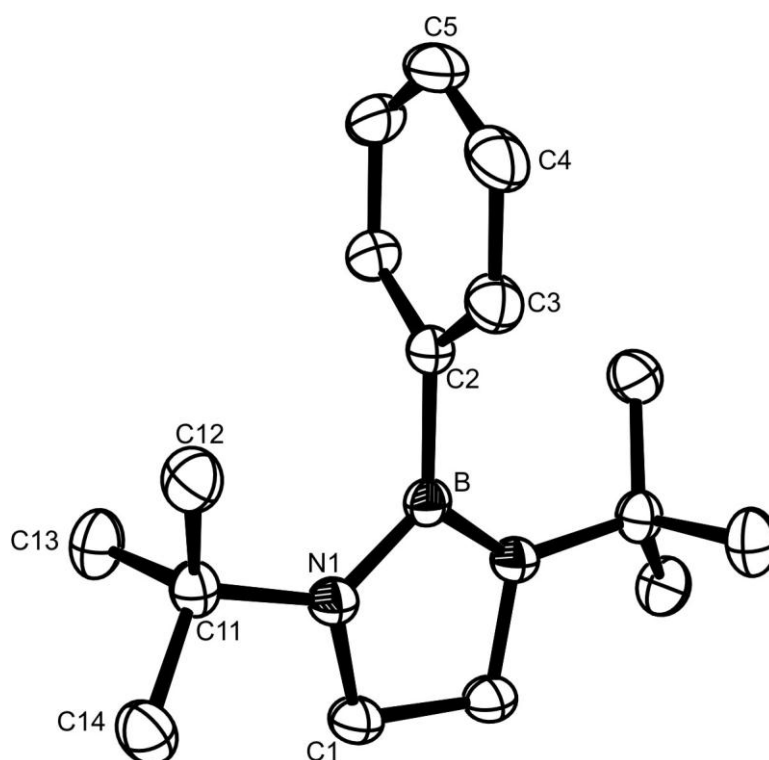


Figure 2.20: Crystal Structure of 1-Phenyl-2,5-di-*tert*-butyl-1-bora-2,5-diazacyclopentane.

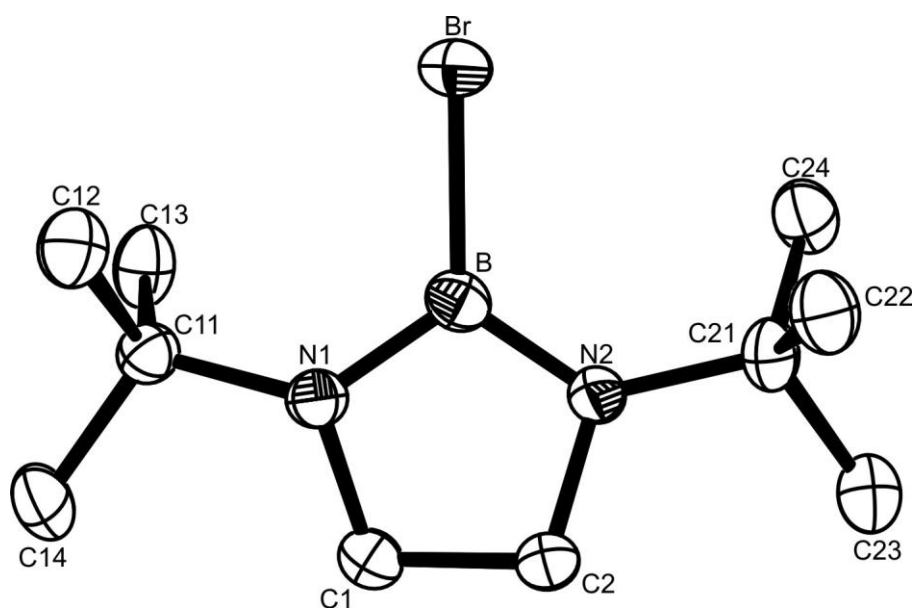


Figure 2.21: Crystal Structure of 1-Bromo-2,5-di-*tert*-butyl-1-bora-2,5-diazacyclopentane.

Below is the crystal structure of a dimeric complex of *N,N'*-di-*tert*-butylethylenediamine and lithium chloride. This structure represents the expected geometry of a heterocyclic species without resonance π -donation between the two nitrogen centres and the bridging group. In contrast to the boradiazacyclic species, ring strain is less pronounced, and tetrahedral geometry is exhibited by the nitrogen centres.

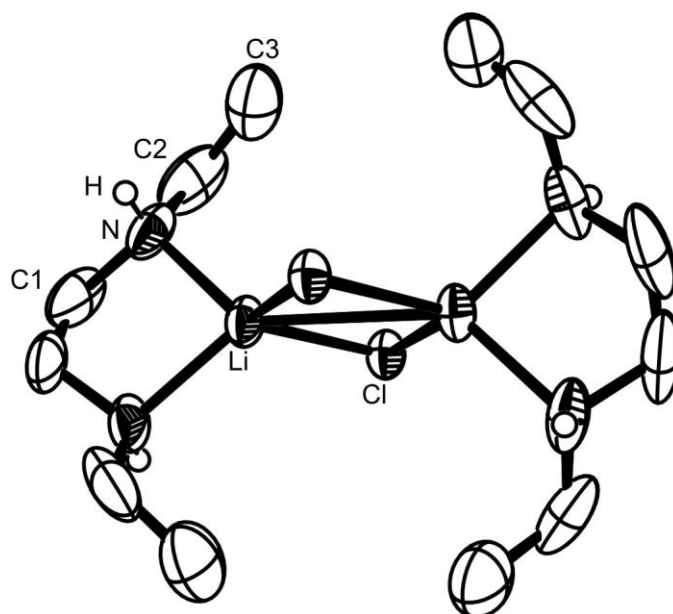


Figure 2.22: Crystal Structure of *N,N'*-di-*tert*-butylethylenediamine and Lithium Chloride.

The boron-nitrogen bond is known to exhibit π -donation of the nitrogen lone pair onto the Lewis-acidic boron centre, an effect which has been widely studied by computer modeling.^{47,48,49,50,51}

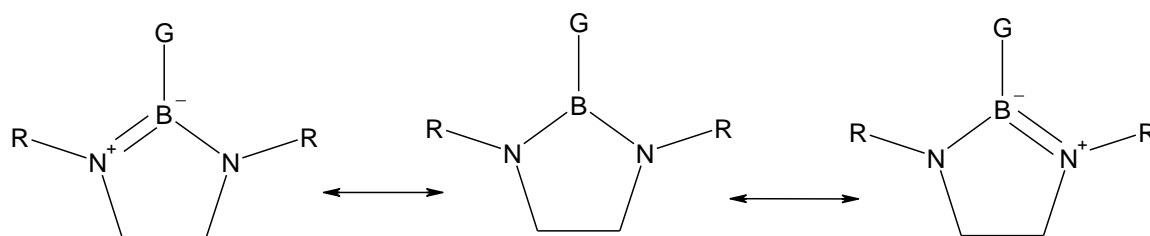


Figure 2.23: Resonance Structures of generic $GB(RNCH_2)_2$ Heterocycle.

This has the effect of stabilizing both centres, ie drastically reducing the Lewis-acidity of the boron, while delocalizing the nitrogen lone pairs. Modification of the species to create a quaternary boron centre however, see figure 2.17, eg by addition of a base, results in a hypothetical structure in which the anionic borate functionality will no longer accept π -electrons from the nitrogen centres, and the lone pairs are hence localized and available for coordination. Hence ligands of this type were considered as potential precursors to zwitterionic Chromium III complexes.

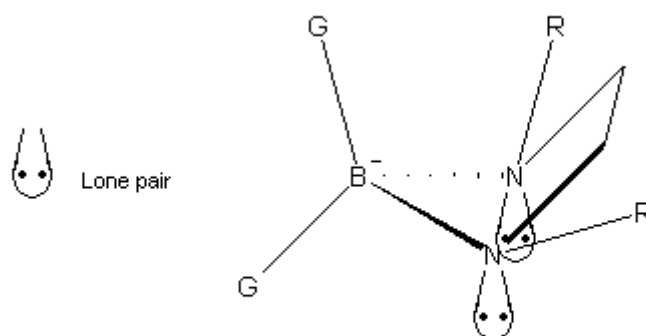


Figure 2.24: Proposed Quaternary Diazaborate Anionic Ligand.

The reactivity of 1-phenyl-2,5-di-*tert*-butyl-1-bora-2,5-diazacyclopentane with various nucleophilic species was investigated, in an attempt to quaternise the boron centre:

2.3.2.1 Reactivity of 1-phenyl-2,5-di-*tert*-butyl-1-bora-2,5-diazacyclopentane with *n*-Butyl Lithium:

It was envisaged that the addition of *n*-butyl lithium to the heterocycle may result in the formation of the lithium salt, $\text{Li}^+ [\text{PhBuB}(\text{tert-BuNCH}_2)_2]^-$, see figure 2.25:

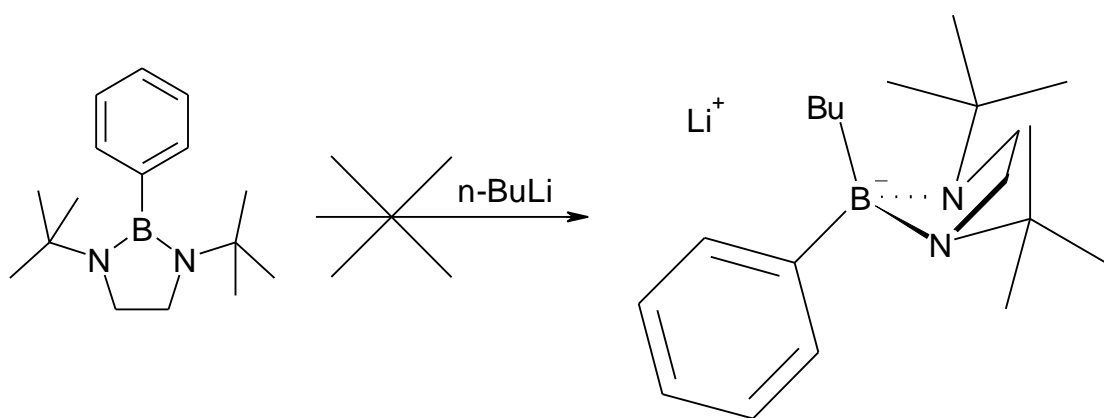


Figure 2.25: Attempted Reaction of *n*-BuLi with $\text{PhB}(\text{tert-BuNCH}_2)_2$.

The product of addition of 1 equivalent of *n*-butyl lithium to the heterocycle in hexane solution was characterised by ^1H , ^{11}B and ^{13}C NMR spectroscopy after several hours. The resultant ^1H and ^{13}C spectra exhibited signals attributable to the two starting materials, while the ^{11}B spectrum exhibited a broad singlet, the chemical shift value of which was within 4 ppm of the signal exhibited by the heterocycle in isolation (See ‘Experimental’ section). Thus the heterocycle is considered to be unreactive towards the organolithium reagent under standard conditions. (NMR data- see ‘3.33 Attempted Reaction of 1-Phenyl-2,5-di-*tert*-butyl-1-bora-2,5-diazacyclopentane with *n*-Butyl Lithium’)

2.3.2.2 Reactivity of 1-phenyl-2,5-di-*tert*-butyl-1-bora-2,5-diazacyclopentane with Hexylmagnesium Bromide:

The synthesis of the salt $\text{BrMg}^+[\text{PhHexB}(\text{tert-BuNCH}_2)_2]^-$ was attempted, see figure 2.26:

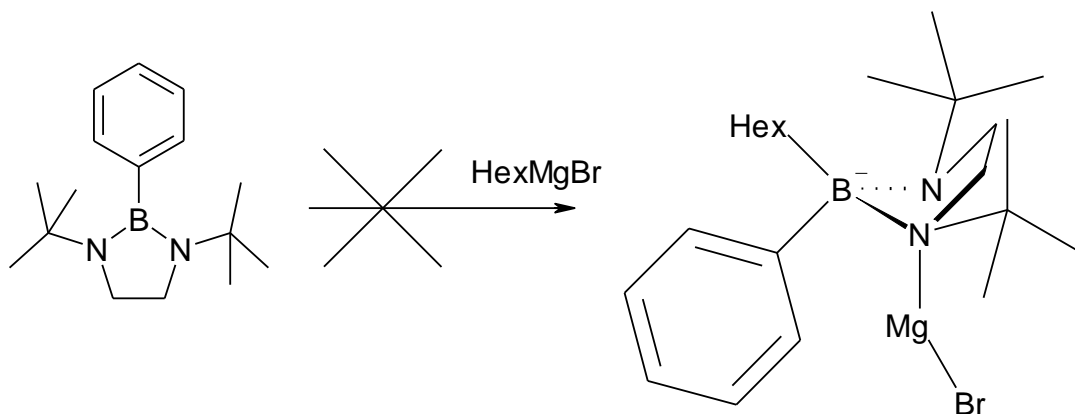


Figure 2.26: Attempted Reaction of HexMgBr with $\text{PhB}(\text{tert-BuNCH}_2)_2$.

A hexylmagnesium bromide solution in THF was prepared, the concentration of which was determined by ^1H NMR spectroscopy. 1 equivalent of this solution with respect to the Grignard reagent, (See ‘3.54 Determination of Concentration of Grignard reagent in THF soln. Example method: Hexylmagnesium bromide in THF:’) was added to a solution of 1-phenyl-2,5-di-*tert*-butyl-1-bora-2,5-diazacyclopentane in THF. After several hours, the resultant solution was characterised by ^1H , ^{13}C and ^{11}B NMR spectroscopy. The resultant spectra were consistent with a mixture of the two starting materials, particularly the ^{11}B spectrum, which exhibited a broad singlet, possessing a chemical shift value within 3 ppm of that exhibited by the heterocycle in isolation. (See ‘Experimental’ section). The heterocycle is hence considered to be unreactive towards Grignard reagents under standard conditions. (NMR data- see ‘3.31 Attempted Reaction of 1-Phenyl -2,5-di-*tert*-butyl-1-bora-2,5-diazacyclopentane with Hexylmagnesium Bromide:’)

2.3.2.3 Reactivity of 1-phenyl-2,5-di-*tert*-butyl-1-bora-2,5-diazacyclopentane with Methanol:

An attempt was made to generate the species $\text{H}^+[\text{Ph}(\text{MeO})\text{B}(\text{tert-BuNCH}_2)_2]^-$, by addition of methanol to the heterocycle, see figure 2.27:

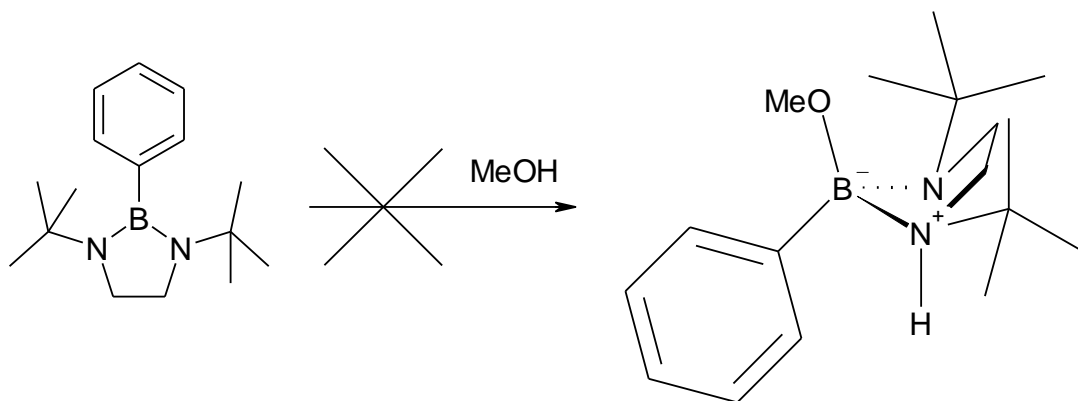


Figure 2.27: Attempted Reaction of Methanol with $\text{PhB}(\text{tert-BuNCH}_2)_2$.

The addition of an excess of dry methanol to a solution of $\text{PhB}(\text{tert-BuNCH}_2)_2$ in chloroform solution resulted in no significant change in the ^1H , ^{13}C or ^{11}B NMR spectra, relative to the corresponding spectra of $\text{PhB}(\text{tert-BuNCH}_2)_2$ in isolation, most significantly the ^{11}B spectra corresponded to within 3 ppm. (See ‘Experimental’ section).

There is thus no detectable coordination of methanol by the heterocycle.
(NMR data- see ‘3.29 Attempted Reaction of 1-Phenyl -2,5-di-*tert*-butyl-1-bora-2,5-diazacyclopentane with Methanol:’)

A sample of $\text{PhB}(\text{tert-BuNCH}_2)_2$ was dissolved in dry methanol, and the resultant solution characterised by ^1H , ^{13}C and ^{11}B NMR spectroscopy. The ^1H and ^{13}C NMR spectra exhibited the expected signals attributable to the heterocycle and the solvent, and the ^{11}B NMR spectrum exhibited a singlet at ca. $\delta = 15.4$ ppm. This differs somewhat from the spectrum of the heterocycle in CDCl_3 soln, but is within the range expected given solvent effects, and thus does not suggest coordination of the borane.

2.3.2.4 Reactivity of 1-phenyl-2,5-di-*tert*-butyl-1-bora-2,5-diazacyclopentane with (De-ionised) Water:

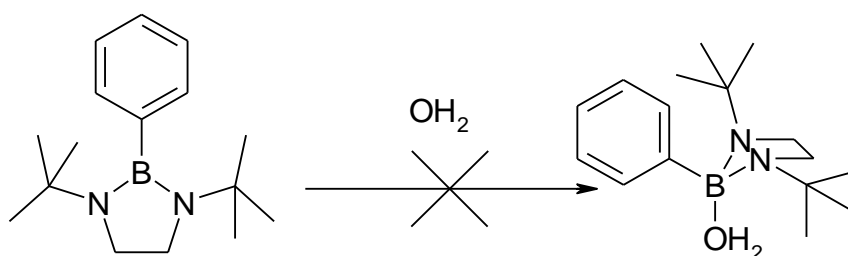


Figure 2.28: Attempted Reaction of 1-phenyl-2,5-di-*tert*-butyl-1-bora-2,5-diazacyclopentane with De-ionised Water.

To a sample of 1-phenyl-2,5-di-*tert*-butyl-1-bora-2,5-diazacyclopentane in CDCl_3 was added a large excess of de-ionised water. The resultant solution was characterised by ^1H , ^{13}C and ^{11}B NMR spectroscopy. The ^1H and ^{13}C NMR spectra exhibited signals consistent with the heterocycle, but the ^{11}B NMR spectrum did not exhibit any strong signals. Very broad, weak signals were observed, centred at ca. 30.0 ppm and -3.8 ppm. This contrasts greatly with the spectrum observed in the presence of methanol, and suggests that the heterocycle is not stable to hydrolysis. (Phenylboronic acid ^{11}B NMR signal in CDCl_3 : $\delta = 9.33$ ppm (See ‘3.44 Synthesis of Sodium Phenyl (Bis-hydroxy)Butoxyborate.’)

(NMR data- see ‘3.28 Reactivity of 1-phenyl-2,5-di-*tert*-butyl-1-bora-2,5-diazacyclopentane with De-ionised Water’).

2.3.2.5 Reactivity of 1-phenyl-2,5-di-*tert*-butyl-1-bora-2,5-diazacyclopentane with Tetramethylammonium Fluoride:

The lack of reactivity of the boron centre was considered to be due to the difficulties of adding further electron density to a species already undergoing a π -

bonding interaction with adjacent nitrogen centres, and it was therefore hypothesized that the highest probability of forming an additional dative bond to the boron would occur where a highly electronegative nucleophile was employed. The fluoride anion represented the most electronegative nucleophile available, and, given that dry tetramethylammonium fluoride is among the few dry organic fluoride salts commercially available, an attempt was made to synthesise the salt $\text{NMe}_4^+[\text{PhFB}(\text{tert-BuNCH}_2)_2]^-$ by reaction of the heterocycle with tetramethylammonium fluoride in DCM solution, see figure 2.29:

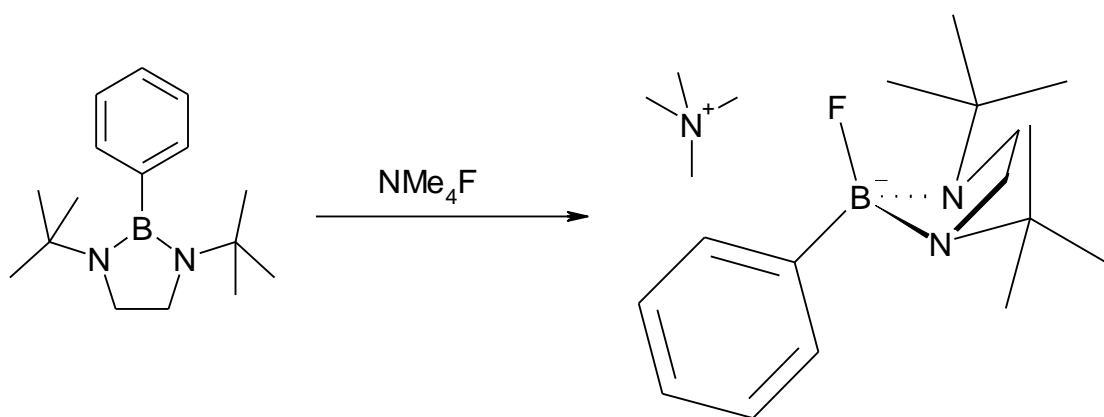


Figure 2.29: Reaction of $\text{PhB}(\text{tert-BuNCH}_2)_2$ with NMe_4F .

The product of addition of 1 eq. of tetramethylammonium fluoride in DCM to a DCM solution of the heterocycle was characterised after several hours, by ^1H , ^{13}C , ^{11}B and ^{19}F NMR spectroscopy. ^1H and ^{13}C NMR spectra in DCM solution exhibited two sets of each aliphatic signal compared to the spectra of the heterocycle in isolation. The ^{11}B spectrum exhibits two signals, the larger being at ca. 35 ppm, which is consistent with the uncoordinated heterocycle, while another signal is observed at ca. 6 ppm, with an approximate intensity 40% that of the larger signal. We can find no previous reports of analogous species, though Das *et al.*⁵² report ^{11}B NMR data for the similar, (though neutral) species $\text{C}_6\text{H}_5\text{FB}(\mu\text{-Pz})_2\text{C}_6\text{H}_5\text{BF}$, (figure 2.21), which exhibits a singlet at $\delta = 3.5$ ppm. The addition of a large excess of tetramethylammonium fluoride to the solution increases the relative size of the smaller peak, up to approximately a 1:1 ratio of signal intensities, as would be expected of an equilibrium, but could not render it the major product.

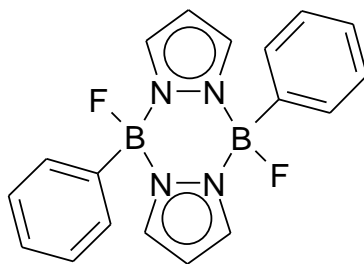


Figure 2.30: $\text{C}_6\text{H}_5\text{FB}(\mu\text{-Pz})_2\text{C}_6\text{H}_5\text{BF}$.

The ^{19}F NMR spectrum exhibited a broad signal and two sharp singlets, at $\delta = \text{ca. } -133, -136 \text{ and } -140 \text{ ppm}$ respectively. Free tetramethylammonium fluoride in DCM exhibits a signal at $\delta = -97 \text{ ppm}$,⁵³ which is not observed here.

The most similar species to the quaternary heterocycle for which ^{19}F NMR data has been reported previously, is the tentative assignment of a signal at $\delta = -156 \text{ ppm}$, to the anion $[(\text{Me}_2\text{N})_3\text{BF}]^-$.⁵⁴

The presence of multiple ^{19}F NMR signals raises the possibility of decomposition of the heterocycle, but this is inconsistent with the NMR data obtained for other nuclei, in particular ^{11}B . The chemical shift value of fluoride anions is known to be extremely sensitive to solvent effects in the case of polar solvents,⁵³ and the presence of additional signals in the ^{19}F spectrum may thus be attributable to interactions of the fluoride with the amine functionalities on the heterocycle. (See ‘Experimental’ section).

Thus the product is considered to be a mixture of the target compound, the neutral precursor and tetramethylammonium fluoride.

Given the apparent lack of reactivity of the heterocycle with dry methanol, and given the greater solubility of tetramethylammonium fluoride in protic solvents, compared to DCM, the alcohol was employed as a solvent. To a solution of the heterocycle in dry methanol, was added a small excess of tetramethylammonium fluoride. The solution was characterised by ^1H , ^{13}C , ^{11}B and ^{19}F NMR spectroscopy. The ^1H and ^{13}C NMR exhibited signals consistent with the heterocycle and the fluoride salt, while the ^{11}B NMR spectrum exhibited a single singlet at $\delta = 8.94$. This is approximately consistent with the signal attributed to the fluoride-complexed boron signal observed for the DCM solution, but for comparison, the ^{11}B signal of the heterocycle in methanol solution, in the absence of fluoride ions, is at ca. 15 ppm –

suggesting that a reduced down-field shift is exhibited in a protic solvent, even in the absence of coordination to the boron centre.

The ^{19}F NMR spectrum exhibited a broad singlet at $\delta = -148.1$. For comparison, free tetramethylammonium fluoride in methanol exhibits a signal at $\delta = -148.0$.⁵⁵ This suggests that solvation of the fluoride ion is more favourable than coordination to the heterocycle.

(NMR data- see '3.26 Reaction of 1-Phenyl-2,5-di-*tert*-butyl-1-bora-2,5-diazacyclopentane with Tetramethylammonium Fluoride')

An attempt was made to complex the product of addition of tetramethylammonium fluoride to the heterocycle, to chromium III chloride, by addition of 1 equivalent, relative to either of the other two reagents, of $\text{CrCl}_3 \cdot \text{THF}_3$. The resultant compound was characterised by elemental analysis, and electro-spray mass spectrometry.

Elemental analysis yielded the following result:

C: 45.6% H: 7.9% N: 8.2%.

This compares to an expected:

C: 47.0% H: 7.9% N: 8.2%.

The cationic electro-spray mass spectrum exhibited, among others, a signal: $m/z = 279.25$, which is a good match for the (protonated) zwitterion:

$[\text{Ph}(\text{F})\text{B}(\text{tert-BuN}(\text{H})\text{CH}_2)_2]^+$ ($m/z = 279.23$). The calibration of the spectrometer is such that m/z within ± 0.05 of the predicted value is considered to be a high probability of a match. A smaller signal was also observed at $m/z = 278.25$, the ratio relative to the first signal being approximately consistent with the $^{10}\text{B}:^{11}\text{B}$ isotopic abundance ratio.

2.3.2.6 Reactivity of 1-phenyl-2,5-di-*tert*-butyl-1-bora-2,5-diazacyclopentane with Sodium n-Butoxide:

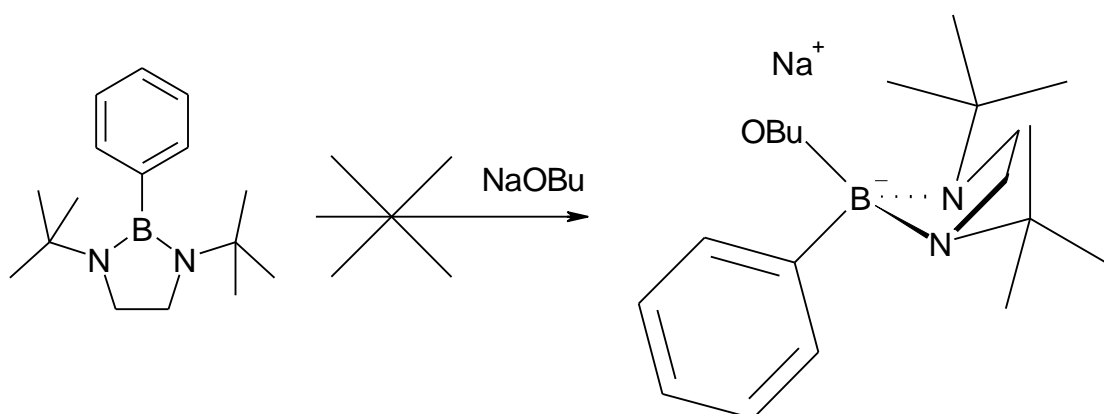


Figure 2.31: Attempted Reaction of Sodium Butoxide with $\text{PhB}(\text{tert-BuNCH}_2)_2$

The greater basicity of sodium alkoxides over the corresponding alcohols led to an attempt to coordinate sodium *n*-butoxide to $\text{PhB}(\text{tert-BuNCH}_2)_2$, despite the observed non-reactivity of the latter towards methanol. However, the product of addition of 1 equivalent of sodium *n*-butoxide to $\text{PhB}(\text{tert-BuNCH}_2)_2$ in THF solution was characterised by ^1H , ^{13}C and ^{11}B NMR spectroscopy and shown to correspond to a mixture of the starting materials. Again, the ^{11}B spectrum of the product corresponded to within 3 ppm to that of the non-coordinated heterocycle, suggesting no reaction had occurred.

Efforts to force a reaction by use of higher temperatures were precluded by the fact that attempts to do so invariably resulted in decomposition of the heterocycle to a brown, insoluble material.

(NMR data- see ‘3.30 Attempted Reaction of 1-Phenyl -2,5-di-tert-butyl-1-bora-2,5-diazacyclopentane with sodium *n*-butoxide’).

2.3.3 Triazaboranes:

Similar problems were encountered when considering a similar class of potential ligands -a quaternary boron centre bearing three directly bonded sp^3 hybridised amine substituents and one organic substituent, see figure 2.32:

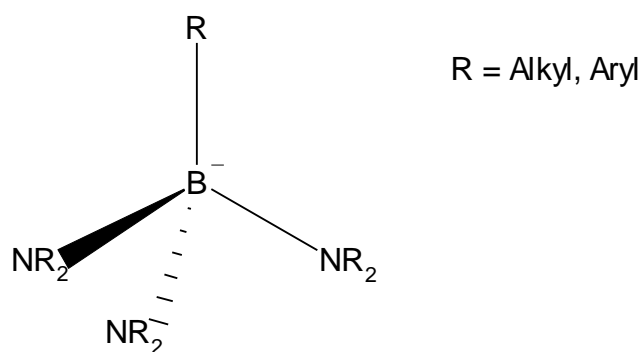


Figure 2.32: Hypothetical Triazaborate.

Such a species would be closely analogous to the triazacyclohexane ligand, in terms of the orientation and relative positions of the amine lone pairs, see figure 2.33:

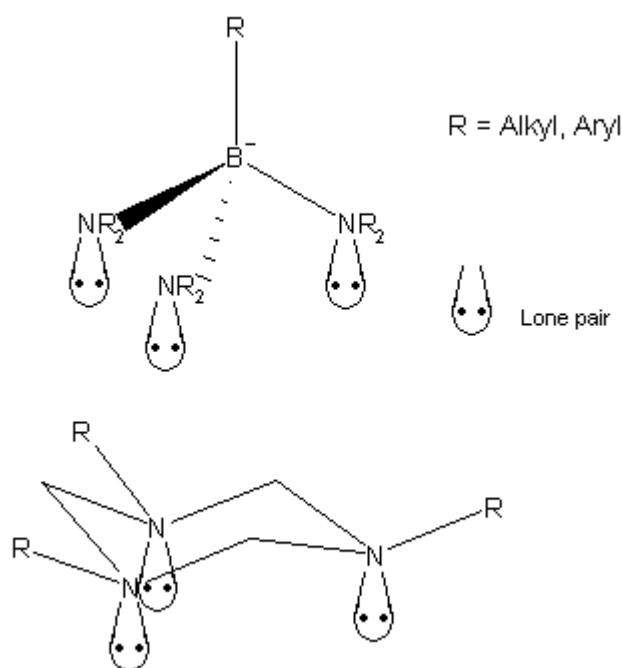


Figure 2.33: Comparison of Lone Pair Arrangement in Target Ligand versus Triazacyclohexane.

No literature precedent exists for species of this type, though the similar ‘scorpionate’ ligand has been widely utilized in catalysis,⁵⁶ indeed the neutral scorpionate ligand tris(pyrazolyl)methane as a chromium III complex, has been previously reported as an ethylene trimerisation catalyst (see ‘1.3.3.2 *Tris(pyrazolyl)methane chromium chloride*’).

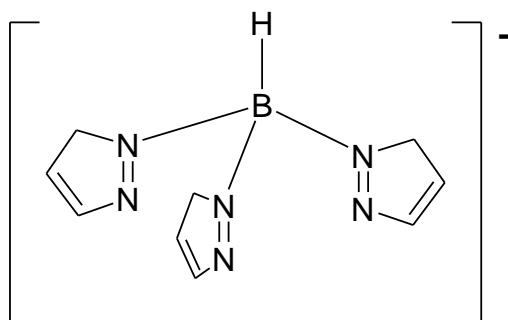


Figure 2.34: Tris(pyrazolyl)hydroborate Anion.⁵⁷

Originally developed by Trofimenko in the 1960s,⁵⁸ tris(pyrazolyl)hydroborates, are the most common ‘scorpionate’ ligand type, but despite their superficial similarity to the proposed triazaborate, some significant differences should be noted. The nitrogen centres in the ligand are sp^2 hybridized and the nitrogen-boron bonds occur via the lone pairs of the attached nitrogens, while the lone pairs of the remaining 3 nitrogen atoms are responsible for the ligands coordinating ability. Consideration of the geometry of the above structure reveals the alignment of lone pairs to be more favourable for coordination to a metal centre than in the case of either triazacyclohexane or the proposed organotrisaminoborate anion, see figure 2.35:

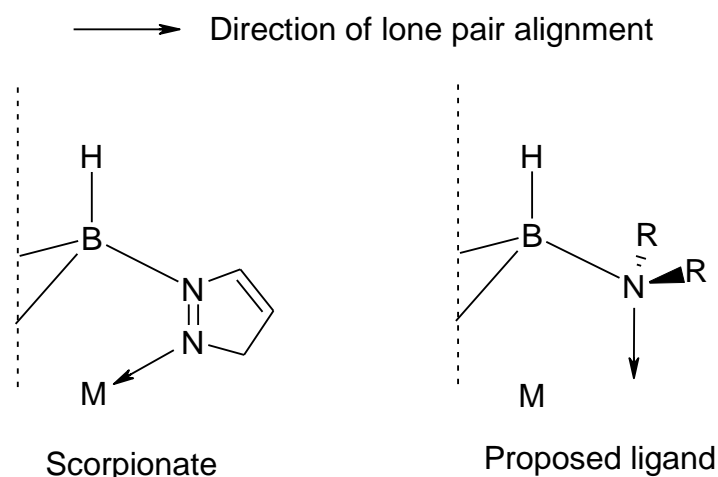


Figure 2.35: Comparison of Lone Pair Orientation in Scorpionate Ligand Versus Proposed Synthetic Target.

Furthermore, the negative charge born by the scorpionate ligand may not be considered to be localized at the boron centre.

The neutral precursor, Tris(diethylamino)borane, was synthesized by reaction of Boron trichloride with diethylamine (see ‘Experimental’ section), figure 2.36:

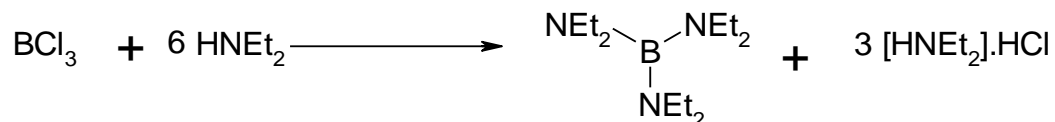


Figure 2.36: Tris(diethylamino)borane Synthesis.

2.3.3.1 Reactivity of Tris(diethyl)aminoborane with Methylmagnesium Chloride:

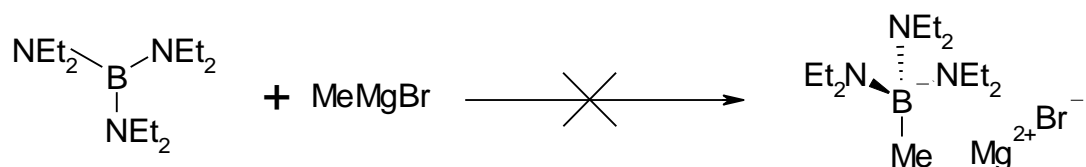


Figure 2.37: Attempted Reaction of Tris(diethyl)aminoborane with Methylmagnesium Bromide.

An attempt was made to generate the species tris(diethyl)aminomethylborate magnesium chloride, by addition of 1 equivalent of methylmagnesium chloride. The product exhibited a diminutive singlet at $\delta = \text{ca. } -16 \text{ ppm}$ in the ^{11}B NMR spectrum, which was attributed to an impurity in the grignard solution, but the only significant signal appeared at ca. 32 ppm, which is consistent with neutral tris(diethyl)aminoborane. Thus there is no detectable reaction with methylmagnesium chloride.

(NMR data- see ‘3.22 Attempted reaction of Tris(diethyl)aminoborane with Methylmagnesium chloride’)

2.3.3.2: Reactivity of Tris(diethyl)aminoborane with n-Butyl Lithium:

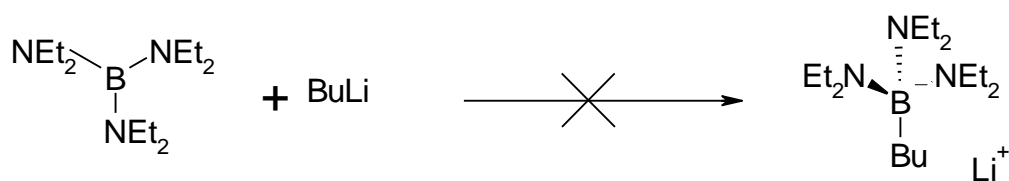


Figure 2.38: Attempted Reaction of Tris(diethyl)aminoborane with n-Butyl Lithium.

An attempt was made to generate the species lithium butyltris(diethyl)aminoborate by addition of 1 equivalent of n-butyl lithium. The product exhibited a signal at $\delta =$ ca. 32 ppm in the ^{11}B NMR spectrum, suggesting no reaction of the neutral precursor with n-butyl lithium.

(NMR data- see ‘3.25 Attempted reaction of Tris(diethyl)aminoborane with n-butyl lithium’)

2.3.2.3: Reactivity of Tris(diethyl)aminoborane with Tetramethylammonium Fluoride:

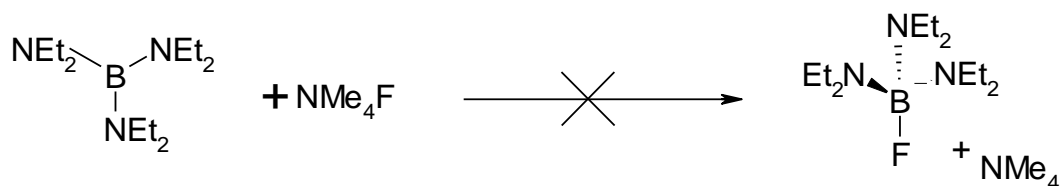


Figure 2.39: Attempted Reaction of Tris(diethyl)aminoborane with Tetramethylammonium Fluoride.

An attempt was made to generate the species tetramethylammonium tris(diethyl)aminofluoroborate by addition of 1 equivalent of tetramethylammonium fluoride. The product exhibited a signal at $\delta =$ ca. 31 ppm in the ^{11}B NMR spectrum, suggesting no coordination of fluoride to the neutral precursor. (See ‘Experimental’ section).

(NMR data- see ‘3.24 Attempted reaction of Tris(diethyl)aminoborane with Tetramethylammonium fluoride’)

2.3.3.4: Reactivity of Tris(diethyl)aminoborane with Lithium Diethylamide:

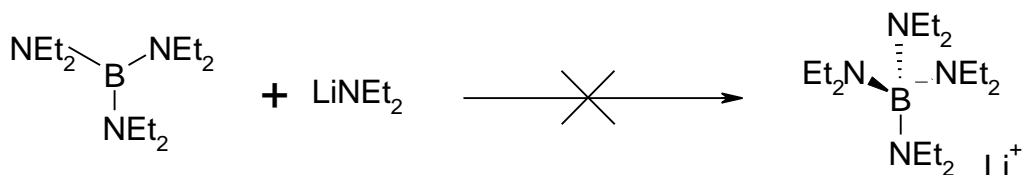


Figure 2.40: Attempted Reaction of Tris(diethyl)aminoborane with Lithium Diethylamide.

An attempt was made to generate the species lithium tetra(diethyl)aminoborate by addition of one equivalent of lithium diethylamide- prepared by 1:1 addition of *n*-butyl lithium to diethylamine in THF solution, to tris(diethyl)aminoborane. This was analogous to the synthesis of potassium tetraethoxyborate by addition of potassium ethoxide to triethylborate as reported by Brown *et al.*,⁵⁹ see figure 2.41:



Figure 2.41: Synthesis of Potassium Tetraethoxyborate.

The product exhibited a signal at $\delta = \text{ca. } 31 \text{ ppm}$ in the ^{11}B NMR spectrum, and thus the tris-aminoborane is shown not to coordinate an additional amine group. (NMR data- see ‘3.23 Attempted reaction of Tris(diethyl)aminoborane with lithium Diethylamide’)

2.3.4 Theoretical Considerations of B-N bonded species:

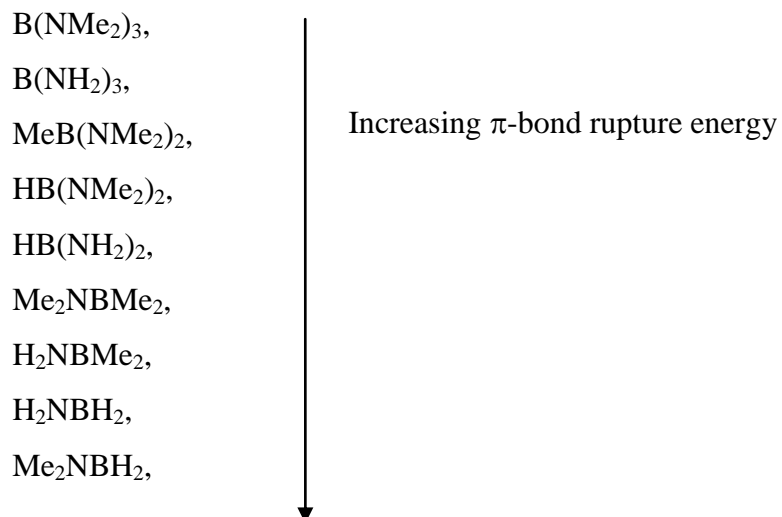
The observed lack of reactivity of the B-N bonded species towards nucleophiles suggests that the stability of the compound is greatly enhanced by the N-B π -bonding interactions. A number of theoretical studies have been carried out, modeling the relative stability of σ - and π -bonding interactions in boron-nitrogen compounds. Østby *et al.*⁶⁰ report a DFT study on the 2 centre, 2 electron π -bonding system for a number of boron-nitrogen species, of which the most relevant here are $\text{B}(\text{NMe}_2)_3$, $\text{B}(\text{NH}_2)_3$, $\text{MeB}(\text{NMe}_2)_2$, $\text{HB}(\text{NMe}_2)_2$ and $\text{HB}(\text{NH}_2)_2$. They calculate the magnitude of

the π -bonding interaction as the 'Mean π - bond rupture energy', thus: The π -bonding interactions result in a computed planar equilibrium structure for any given B-N bonded species, and furthermore the π -bonding interaction can be broken by rotating the B-N centres relative to one another, such that their respective substituents are orthogonally orientated. The calculated difference in energy between the two conformations then allows approximate determination of the total π -bonding energy of the compound.

The calculated energy required to break the dative π -bond in H_2NBH_2 is 136 kJmol^{-1} , which compares closely to the energy of the dative σ -bond in the coordination compound H_3NBH_3 , (experimentally determined as $130 \text{ kJ} \pm 4 \text{ kJmol}^{-1}$). By contrast the estimated energy of covalent B-N bonds exhibited by boron nitride crystal lattices, as determined by measurement of the enthalpy of formation of the cubic and hexagonal forms of the latter, is $368 \pm 8 \text{ kJmol}^{-1}$. (For comparison, the B-C bond energy is given as $459 \pm 11.6 \text{ kJmol}^{-1}$,⁶¹ the C-C σ -bonding interaction 346 kJmol^{-1} ,⁶² and the C-C π -bonding interaction in ethylene is given as $256 \pm 21 \text{ kJmol}^{-1}$).⁶³

The study further predicts that the π -bond rupture energy of a given B-N bond is reduced by the presence of electron releasing substituents on the boron, and increased by their presence on the nitrogen(s) eg, the effect of methyl versus hydrogen substituents. The calculated mean π -bond rupture energies (per bond) for the systems H_2NBH_2 , $\text{HB}(\text{NH}_2)_2$ and $\text{B}(\text{NH}_2)_3$, were calculated as ca. 136 kJmol^{-1} , 101 kJmol^{-1} and 70 kJmol^{-1} respectively, i.e. in the approximate ratio 4:3:2, dependant on the number of centres, not the number of π electrons.

The relevant compounds, in order of increasing π -bond rupture energies are given as follows:



So, for the model system B(NH₂)₃, the total π -bond rupture energy for the molecule = $3 \times 70 \text{ kJmol}^{-1} = 210 \text{ kJmol}^{-1}$.

Therefore, the enthalpy change of reaction of B(NH₂)₃ to form the quaternary species [RB(NH₂)₃]⁻ may be calculated as the enthalpy of formation of a B-C σ -bond (-459 kJmol^{-1}) + the total π -bond rupture energy ($+210 \text{ kJmol}^{-1}$) = -249 kJmol^{-1} . Where alkylation is attempted by addition of RLi, the enthalpy of dissociation, $\text{RLi} \rightarrow \text{R}^- + \text{Li}^+$, must be considered. Bickelhaupt *et al.*⁶⁴ report a calculated value of 182.0 kJmol^{-1} , based on computer modelling. Thus, the total enthalpy change for the reaction is given by $-249 \text{ kJmol}^{-1} + 182.0 \text{ kJmol}^{-1} = -67 \text{ kJmol}^{-1}$. See figure 2.42.

Thus the reaction would appear to be thermodynamically feasible, suggesting that the non-reactivity of the experimentally observed B(NEt₂)₃ species may be attributable to a kinetic barrier- the enthalpy of formation and indeed the possible nature of transition state 'N' being unknown.

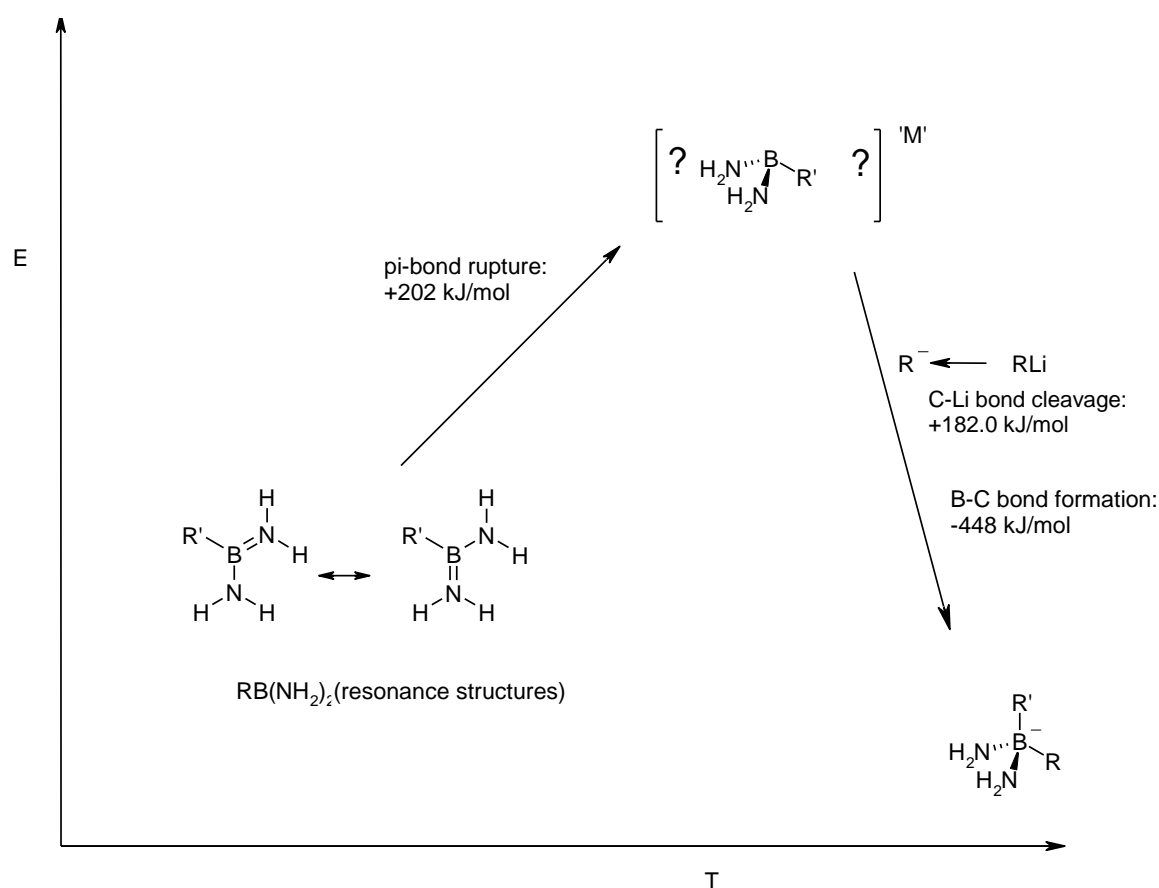


Figure 2.42: Diagram of Hypothetical Reaction $B(NH_2)_3 \rightarrow [RB(NH_2)_3]^-$, showing the relative energies, 'E' of the Reagent, Product and presumed Transition State 'N', plotted against Reaction Time 'T'.

Though the formation of an additional B-C bond to $B(NH_2)_3$ may be thermodynamically feasible, it does not necessarily follow that the product of the addition would be stable. Various values for the energy of the B-N σ bond have been proposed, for example, Østby *et al*'s⁶⁰ value of 368 kJmol^{-1} (see above). The value for the B-N bond as determined for a gaseous diatomic species is given as $448 \pm 29 \text{ kJmol}^{-1}$.⁶⁵

However, these values are determined for species sufficiently different to the compounds herein investigated that they are unlikely to be applicable. For a nitrogen bonded to a quaternary borate centre, there is in fact no distinction between a coordinative and bonding interaction, as can be seen by consideration of the deprotonated secondary amine NH_2^- , see figure 2.43:

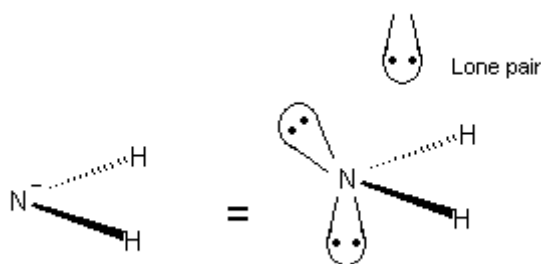


Figure 2.43: NH_2^- Anion

Clearly, there is no distinction between the lone pair and the charge carrying orbital. Therefore, *in the absence of any additional π -bonding interaction*, the B-N bond may be regarded as a dative interaction. The experimentally determined value for the H_3NBH_3 interaction as the energy of a B-N σ -bond in this system (130 kJmol^{-1}), the following reaction of the hypothetical quaternary species must be considered, see figure 2.44:

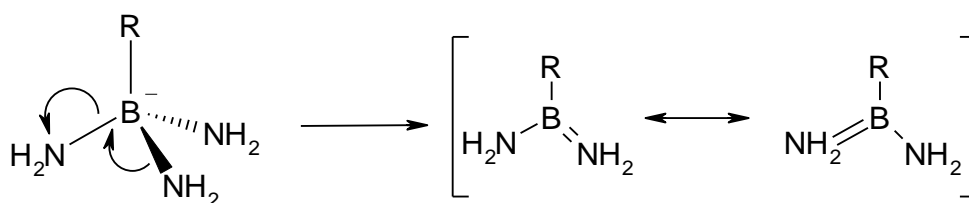


Figure 2.44: Decomposition of Hypothetical Quaternary Species.

The cleavage of a B-N σ -bond on the quaternary species would be energetically unfavourable by an amount equal to the B-N σ -bond energy, 130 kJmol^{-1} , while the π -bonding interaction restored to the resultant neutral species, taking $\text{HB}(\text{NH}_2)_2$ as an approximation to it, equates to an energetically favourable $2 \times -101 \text{ kJmol}^{-1} = -202 \text{ kJmol}^{-1}$. Therefore the enthalpy change of decomposition to the neutral species $= -202 + 130 = -72 \text{ kJmol}^{-1}$. In addition to this, decomposition allows the formation of a new alkyl lithium C-Li bond, which is also energetically favourable. Furthermore, the extreme weakness of the B-N σ -bonds makes it unlikely that any significant energy barrier to decomposition would be observed.

In summary, while given the right conditions it may be thermodynamically viable to alkylate triazaboranes, it is highly improbable that any stable quaternary species of the

the type $[\text{RB}(\text{NR}_2)_3]^-$ could be isolated- if they exist at all, it is likely only as transient intermediates.

The class of compounds $\text{R}'\text{B}(\text{RNCH}_2)_2$ can, for these purposes be approximated to the model species $\text{HB}(\text{NH}_2)_2$. In this case, the alkylation of the boron centre is again deemed to be energetically favourable by -459 kJmol^{-1} , while the resultant loss of B-N π -interactions is disfavoured, by $2 \times 101 \text{ kJmol}^{-1} = 202 \text{ kJmol}^{-1}$.

Therefore, the enthalpy change for the transformation, see figure 2.36 $= 202 \text{ kJmol}^{-1} + -459 \text{ kJmol}^{-1} = -257 \text{ kJmol}^{-1}$. As before, this must be offset against the enthalpy of dissociation of the C-Li bond for alkylation by RLi (182.0 kJmol^{-1}). $-257 \text{ kJmol}^{-1} + 182.0 \text{ kJmol}^{-1} = -75 \text{ kJmol}^{-1}$. Therefore, the quaternisation of the diazaborane appears to be thermodynamically favourable, to an extent approximately equal to that calculated in the case of $\text{B}(\text{NH}_2)_3$, therefore the observed lack of reactivity of the species $\text{PhB}(\text{tert-BuNCH}_2)_2$ is again attributed to a kinetic barrier or steric hindrance. Consideration of the energetic favourability of decomposition in accordance with the following reaction, figure 2.45,

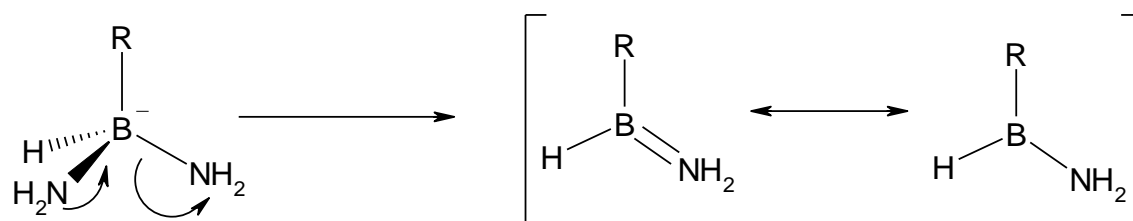


Figure 2.45: Decomposition of Hypothetical Quaternary Species.

results in the following calculation: B-N σ -bond cleavage is energetically disfavoured: 130 kJmol^{-1} , while the resultant restoration of B-N π -bonding is favoured: -136 kJmol^{-1} . Therefore the enthalpy change of decomposition to neutral $\text{RBH}\text{NH}_2 = 130 \text{ kJmol}^{-1} + -136 \text{ kJmol}^{-1} = -6 \text{ kJmol}^{-1}$. In addition to this, decomposition allows the reformation of the alkyllithium C-Li bond, which is also energetically favourable. So again, decomposition of the quaternary boron species appears to be thermodynamically favoured, (albeit to a smaller extent than is the case for triazaboranes), and it is thus improbable that such a species can be rendered stable in isolation.

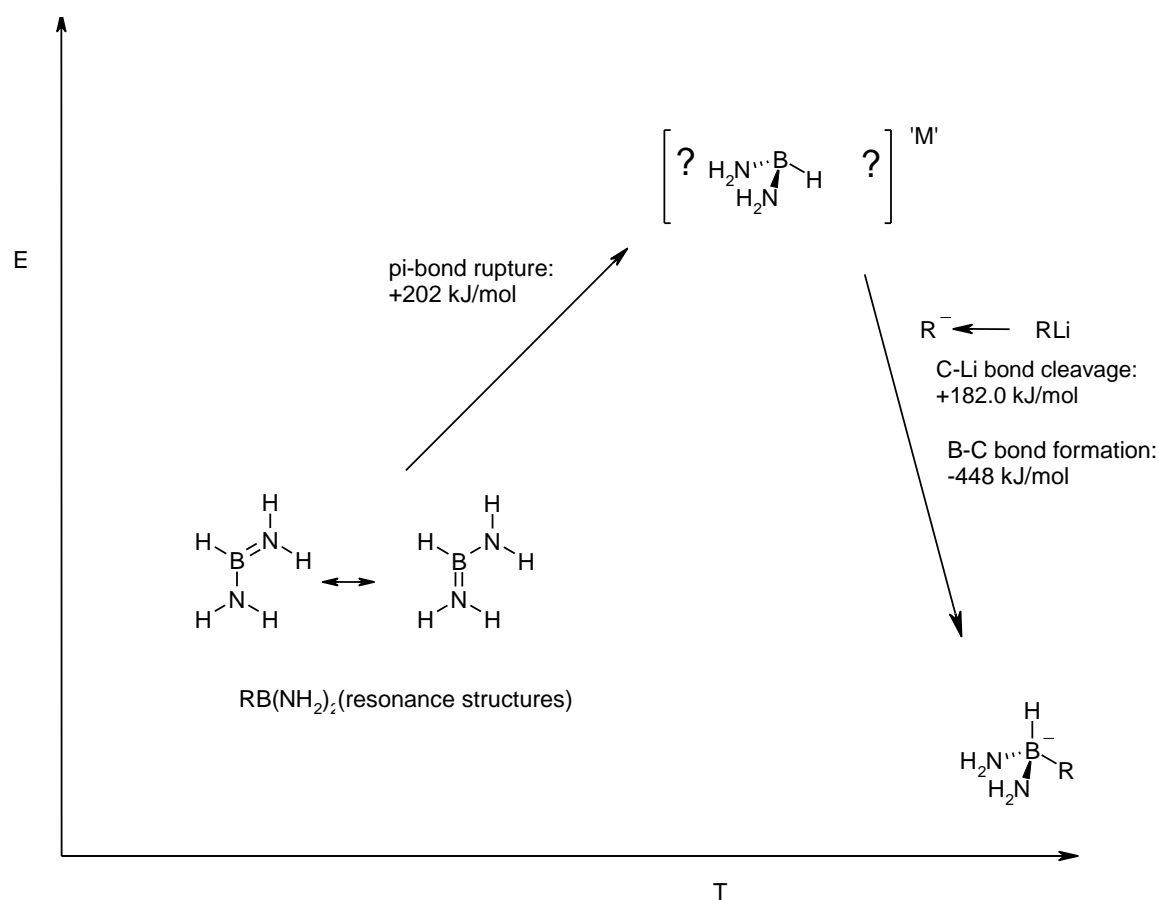


Figure 2.46: Diagram of Hypothetical Reaction $\text{HB}(\text{NH}_2)_2 \rightarrow [\text{RHB}(\text{NH}_2)_2]^-$, showing the Relative Energies, 'E' of the Reagent, Product and presumed Transition state 'M', plotted against Reaction Time 'T'.

While the reactivity of the neutral precursor, $\text{PhB}(\text{tert-BuNCH}_2)_2$ has been thoroughly investigated, analogues bearing other substituents were considered. In particular, substituting phenyl for fluorinated aryl substituents on the boron, see figure 2.47

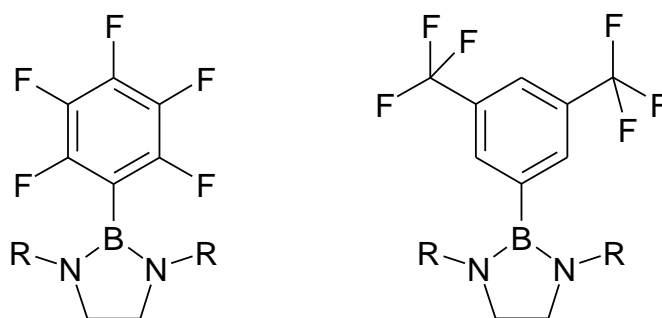


Figure 2.47: Possible Fluorinated Analogues of the Precursor $\text{PhB}(\text{tert-BuNCH}_2)_2$.

Since the lack of reactivity of the neutral species $\text{B}(\text{NEt}_2)_3$ and $\text{PhB}(\text{tert-BuNCH}_2)_2$ was considered to be attributable to electron donation by the nitrogen lone pairs, it was originally hoped that the presence of a strongly electron withdrawing group on the boron centre would negate this effect.

As previously mentioned (see '2.3.1 Diazaboranes'), the synthesis of compounds $\text{RB}(\text{tert-BuNCH}_2)_2$ by alkylation/arylation of $\text{XB}(\text{tert-BuNCH}_2)_2$, $\text{X} = \text{Br}, \text{Cl}$ is not practical. Consequently, efforts to synthesise alternative heterocycles focused on generating precursors of the type RBX_2 , $\text{R} = \text{C}_6\text{F}_5$, $(\text{CF}_3)_2\text{C}_6\text{H}_3$, $\text{X} = \text{Br}, \text{Cl}$.

Several instances have been previously reported of the synthesis of aryldichloro- and aryldibromoboranes, by reaction of the corresponding aryltrimethylsilane with boron trihalides,^{66,67} see figure 2.48:



Figure 2.48: Haloboration of Aryltrimethylsilane.

The following syntheses were attempted:

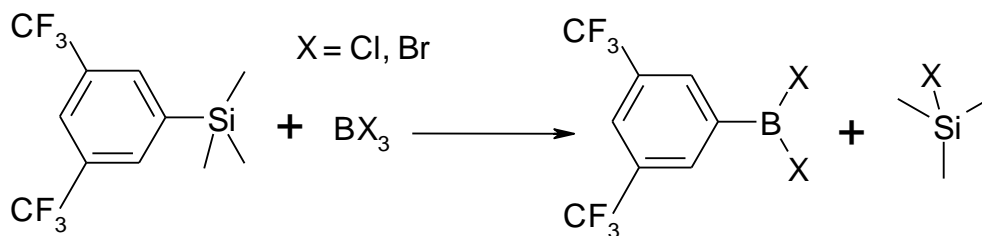


Figure 2.49: Proposed Synthesis of 3,5-Bis(trifluoro)methylphenyldihaloborane.

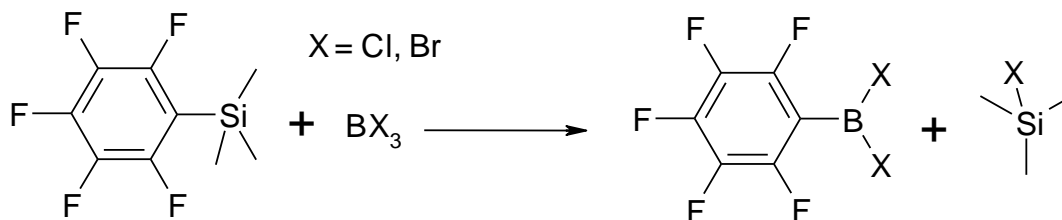


Figure 2.50: Proposed Synthesis of Pentafluorophenyldihaloborane.

An attempt was made to react trimethyl(pentafluoro)phenylsilane, in each of the following conditions. The reaction progress was followed by ^{11}B NMR spectroscopy- spectrum was obtained of each solution prior to reaction and compared with result:

-Refluxing with one equivalent of neat boron tribromide at 80°C for 24 hrs. ^{11}B NMR spectrum showed no change.⁶⁶

-Refluxing with one equivalent of boron tribromide in dichloromethane, at 40°C for 24 hrs. ^{11}B NMR spectrum showed no change.⁶⁸

-Heating with one equivalent of neat boron tribromide at 120°C for 48 hrs in a sealed pressure vessel. ^{11}B NMR spectrum of liquid phase showed no change. A black insoluble decomposition product was formed.

-Refluxing with one equivalent of boron trichloride in dichloromethane, at 40°C for 24 hrs. ^{11}B NMR spectrum showed no change.

-Heating with one equivalent of neat boron trichloride at 120°C for 48 hrs in a sealed pressure vessel. ^{11}B NMR spectrum of liquid phase showed no change. A black insoluble decomposition product was formed.

An attempt was made to react 3,5-bis(trifluoromethyl)phenyltrimethylsilane, in each of the following conditions. The reaction progress was followed by ^{11}B NMR spectroscopy- spectrum was obtained of each solution prior to reaction and compared with result:

-Refluxing with one equivalent of neat boron tribromide at 80°C for 24 hrs.⁶⁶

-Heating with one equivalent of neat boron tribromide at 120°C for 48 hrs in a sealed pressure vessel.⁶⁷

-Heating with one equivalent of boron trichloride at 120°C for 48 hrs in a sealed pressure vessel. ^{11}B NMR spectrum of liquid phase showed no change. A black insoluble decomposition product was formed.

In all 3 of the above cases, ^{11}B NMR spectrum of liquid phase showed no change. A black insoluble decomposition product was formed.

-Refluxing with one equivalent of boron tribromide in dichloromethane, at 40°C for 24 hrs. ^{11}B NMR spectrum showed no change.

-Refluxing with one equivalent of boron trichloride in dichloromethane, at 40°C for 24 hrs. ^{11}B NMR spectrum showed no change.

While there is precedent for the synthesis of a variety of aryldihaloboranes, none of those reported are as inductively electron withdrawing as those attempted here, which fact is supposed to reduce the nucleophilicity of the aryl group to such an extent as to render it unreactive towards the borane. This is consistent with the findings of Frohn *et al.*⁶⁸ who similarly report the non-reactivity of trimethyl(pentafluorophenyl)silane towards boron tribromide.

The susceptibility of the B-N bond strength of a given species to substituent effects has been the subject of computational and Gas Electron Diffraction studies.^{60,69} Of particular note is the analysis of the effect of a strongly electron withdrawing substituent in the model system $\text{ClB}(\text{N}(\text{CH}_3)_2)_2$,⁶⁹ which concludes that the principle effect of an electronegative substituent on the boron centre is to *increase* the extent of π -donation from the nitrogen lone pairs. Therefore, it does not appear that the use of a more electronegative substituent on the neutral precursor would enhance the stability of the quaternary synthetic target.

In order to further investigate the stability of the envisaged zwitterionic complexes, DFT calculations for the model system $\text{Me}_2\text{B}(\text{MeNCH}_2)_2^+$ were carried out,⁷⁰ resulting in the following predictions: For coordination of the neutral species $\text{MeB}(\text{MeNCH}_2)_2$ to AlMe_3 , the migration of the methyl group to the boron centre, to create a zwitterion is not energetically favoured over the singly coordinated, neutral species, see figure 2.51



Figure 2.51: Proposed Addition of Trimethylaluminium to Heterocycle.

By contrast, in the case of coordination of the neutral species to a methyl chromium(III) species, the migration of the methyl group to form the desired zwitterion is slightly energetically favoured.

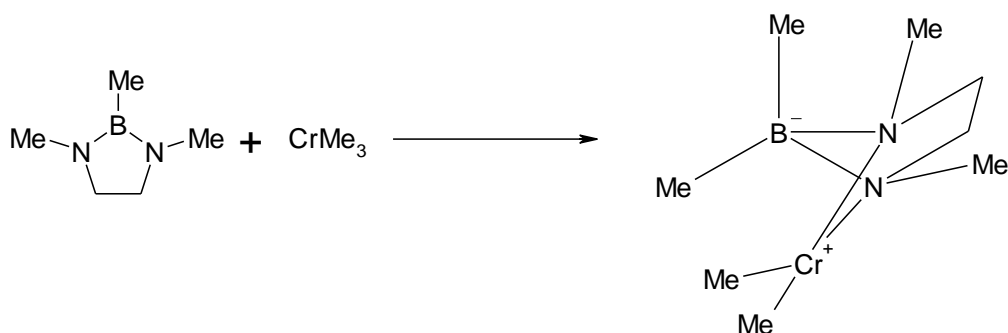


Figure 2.52: Proposed Addition of Trimethylchromium to Heterocycle.

2.3.5 Complexation to Chromium III:

Although both nitrogen lone pairs on the neutral, heterocyclic precursor are capable of π -donation onto the boron centre, consideration of the electronic configuration of the boron centre demonstrates that only the equivalent of one electron pair ($2e^-$) may be donating at any given time, see figure 2.53.

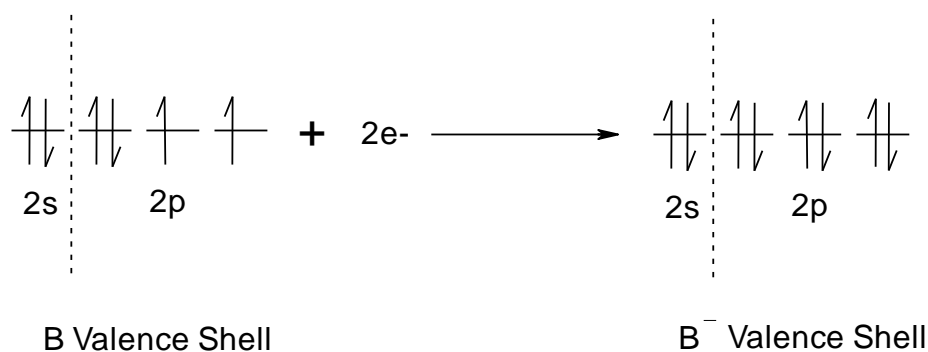


Figure 2.53: Comparative Valence Electronic Configuration for Tertiary Boron Centre, versus Quaternary Borate Centre.

Thus, although the nitrogen centres are equivalent, the molecule is best represented as one of its resonance structures, in which there remains a localized lone pair, see figure 2.54:

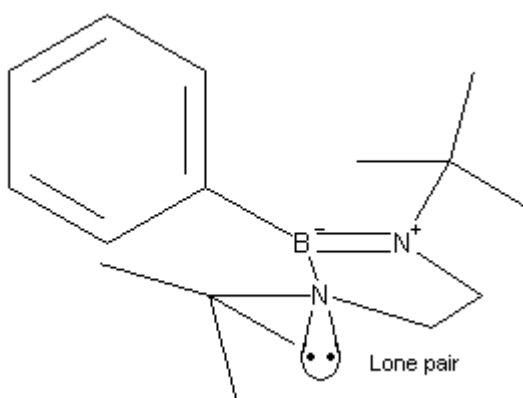


Figure 2.54: Resonance Structure of $\text{PhB}(\text{tert-BuNCH}_2)_2$.

Indeed this effect is alluded to in a number of computational studies of B-N bonded species^{60,69} So, while the compound is a very poor electrophile, it retains some nucleophilicity via the amine functionalities. A number of singly coordinated compounds of this type are noted in the literature, for example, $\text{ClB}(\text{MeNCH}_2)_2 \cdot \text{AlCl}_3$,^{71,72} see figure 2.55a, and $\text{MeB}(\text{MeNCH}_2)_2 \cdot \text{MeBBr}_2$ ⁷³, see figure 2.55b, formed by direct addition of the relevant lewis acid to the neutral, heterocyclic precursor.

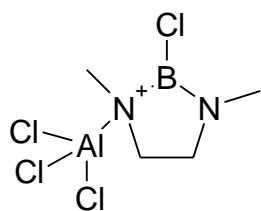


Figure 2.55a:

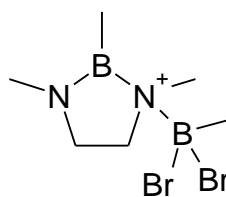


Figure 2.55b



An alternative strategy is thus presented for the formation of a zwitterionic Chromium III complex, ie, attempting to increase the Lewis acidity of the boron centre by coordinating the amine(s) and thus reducing the intramolecular electron density available to it. An attempt was made to coordinate the free ligand to $\text{CrCl}_3(\text{THF})_3$ in THF solution, followed by precipitation of the resultant complex by reducing the polarity of the solution. To a similar solution, containing equimolar quantities of $\text{CrCl}_3(\text{THF})_3$ and $\text{PhB}(\text{tert-BuNCH}_2)_2$ was added 1 equivalent, (with respect to either species) of hexylmagnesium bromide, as a freshly prepared solution in THF. (Concentration determined by ^1H NMR spectroscopy, see ‘Experimental’ section).

The resultant species was also precipitated from the solution. The addition of Grignard reagents to Chromium III chloride in THF solution has been well documented,⁷⁴ and typically results in the alkylation of the Chromium centre.

Where a heterocycle of the type seen here is coordinated, there is no literature precedent for the addition of a Grignard reagent, but there are two likely possibilities, either alkylation of the borane functionality on the ligand, figure 2.56a or alkylation of the chromium centre, figure 2.56b:

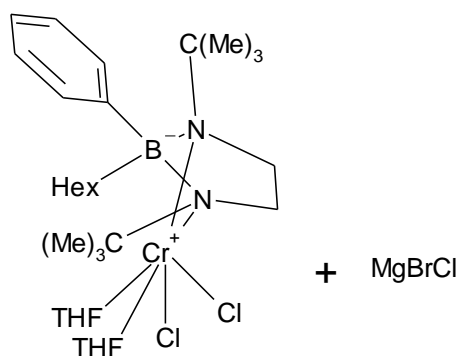


Figure 2.56a: Alkylation of Borane
Functional group

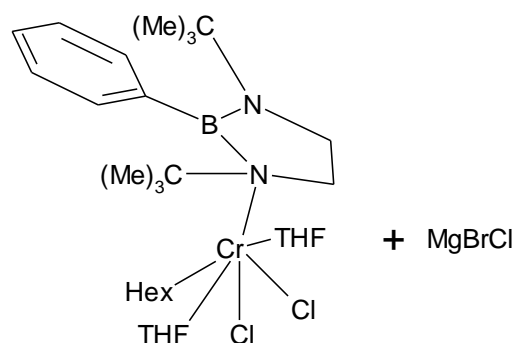


Figure 2.56b: Alkylation of
Chromium Centre

Either case is likely to result in the elimination of magnesium halides, though the former case differs from the latter in that it has the potential to form an active species without the need for an additional co-catalyst, as alkylation would occur at the boron centre, leaving a free site on the chromium centre, following chloride abstraction by the displaced MgBr ion.

Of course the addition of an alkylaluminium or MAO co-catalyst to the non-alkylated $\text{PhB}(\text{tert-BuNCH}_2)_2\text{-CrCl}_3$ complex would be expected to exhibit comparable behaviour, see figure 2.57:

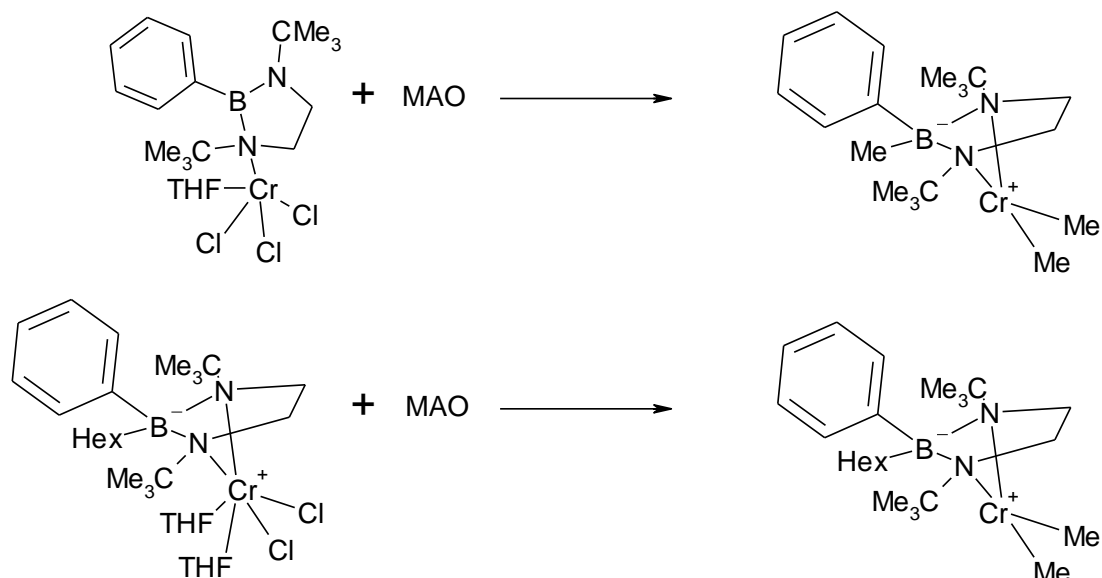


Figure 2.57: Comparison of proposed Reactivity of Neutral versus Alkylated
Complexes with MAO.

Therefore, in the presence of MAO, little distinction is expected between the catalytic properties of the alkylated versus the non-alkylated complex, except that which may be attributable to differences in solubility of the complex owing to the difference in chain length of the methyl- versus hexyl- alkylating species.

2.3.6: Trioxyboranes:

While the synthesis of a quaternary triazaborate was frustrated, analogous compounds based on oxygen are well documented, whether bearing simple hydroxyl substituents,⁷⁵ or esterified analogues.^{76,68} Indeed, the quaternisation of trimethylborate by metal alkoxides is a trivial procedure, while all efforts to synthesise the analogous tetraaminoborate have proved unsuccessful.

While a species bearing 3 alkoxide functionalities could be prepared with relative ease, the weakness of ethers compared to tertiary amines with respect to coordination to metal centres suggests that they would not represent a good model for the Chromium III- triazacyclohexane system. (For example, the coordination of amine ligands by reaction with $\text{CrCl}_3(\text{THF})_3$ is contingent on the comparative weakness of the Cr-(THF) bond). By contrast the direct bonding interaction of oxygen to chromium (as in a chromium alkoxide for example) is more energetically favourable than the corresponding chromium-nitrogen bond, ie. $429.3 \pm 29.3 \text{ kJmol}^{-1}$ versus $377.8 \pm 18.8 \text{ kJmol}^{-1}$.⁷⁷

In accordance with the assumption that the prerequisite for catalytic activity is a ligand which strongly coordinates at least two sites on the chromium centre, and weakly coordinates a third, the following synthetic target was proposed, figure 2.58:

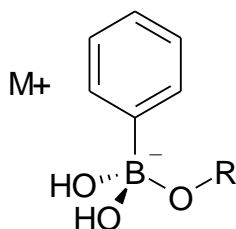


Figure 2.58: Target Ligand.

This concept has certain similarities to the triazacyclohexane ligand, insofar as the distance between and relative positions of the oxygen functionalities compare to the

nitrogen functionalities in the triazacyclohexane molecule, (cf. '2.3.2 Triazaboranes') see figure 2.59:

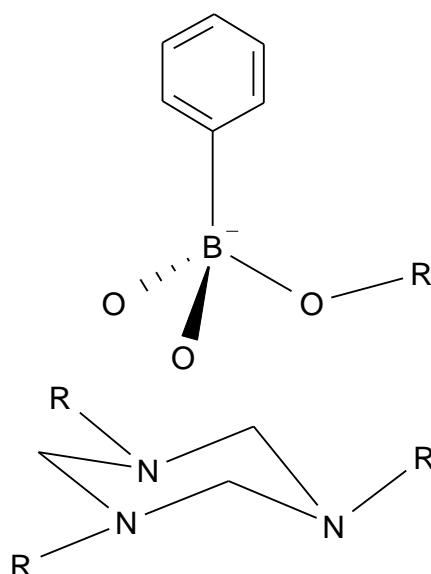


Figure 2.59: Comparison of Target Ligand and Triazacyclohexane.

A significant difference between the two species is the fact that whereas all triazacyclohexane-metal interactions represent dative interaction between lone pairs and the metal centre, there are two distinct kinds of oxygen-metal interaction in the proposed target ligand complex, ie, a dative interaction and two instances of direct sigma bonding, see figure 2.60. The lone pairs on the σ -bonding oxygens are prevented from interaction with the metal centre by steric constraints, and as such are omitted for the sake of clarity.

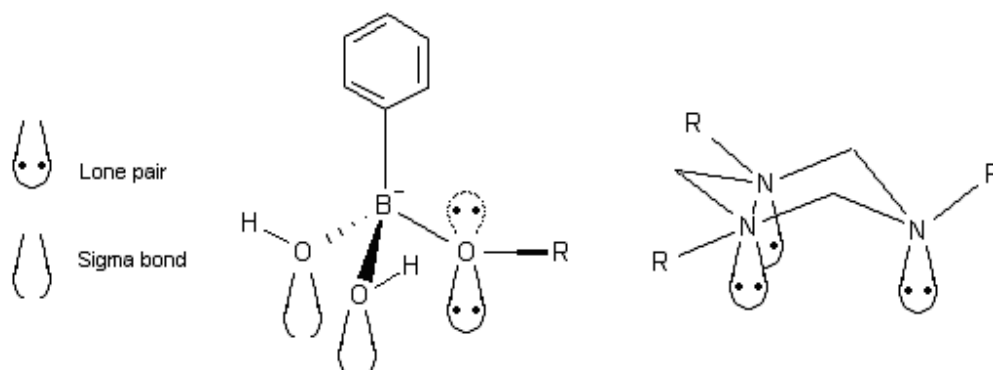


Figure 2.60: Comparison of Bonding Modes in Target Ligand versus Triazacyclohexane. (Non-Bonding Oxygen Lone Pairs omitted).

Clearly, despite their disparate nature, the orientation of the bonding orbitals of the target ligand is comparable to those of the triazacyclohexane. The proximity of the anionic functionality to the chromium centre in the envisaged complex renders it a good potential candidate for improved longevity of the active species, as discussed previously (See ‘1.6 Proposed Development of Anionic Ligands’).

The envisaged complex was as follows, figure 2.61:

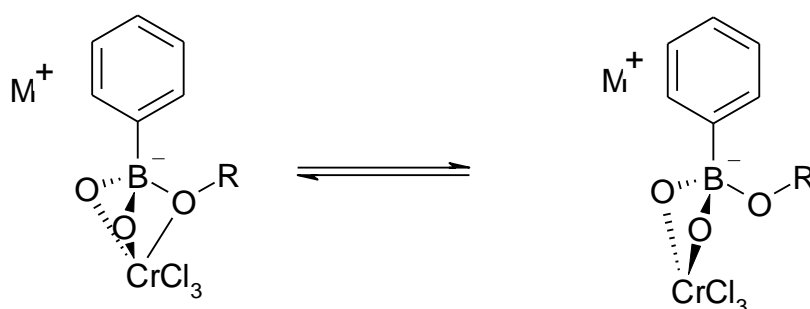


Figure 2.61: Target Complex, showing expected κ^2 and κ^3 Bonding Modes.
(Hydroxyl Protons omitted for Clarity).

Although examples of somewhat similar systems have been recorded.^{78,79} we can find no precedent for this type of complex in the literature.

The ligand $\text{NaPhB(OH)}_2\text{OBu}$, figure 2.62, was prepared by reaction of sodium n-butoxide with phenylboronic acid, (see ‘Experimental’ section).

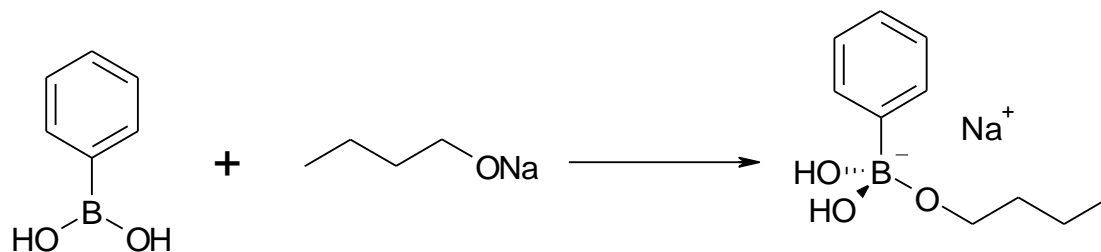


Figure 2.62: Synthesis of $\text{NaPhB(OH)}_2\text{OBu}$.

The resultant oily solid was dissolved in dry THF with 1 equivalent of $\text{CrCl}_3(\text{THF})_3$ and the resultant complex isolated by precipitation. The catalysis of trimerisation of 1-hexene by the complex thus isolated, was attempted. See ‘4. Catalysis- NMR interpretation:’

2.4 Cyclic Ureas:

In keeping with the concept of the B-O bonded quaternary borate anion, the ligand type $[\text{R}(\text{O})\text{B}(\text{R}'\text{NCH}_2)_2]^-$, was considered.

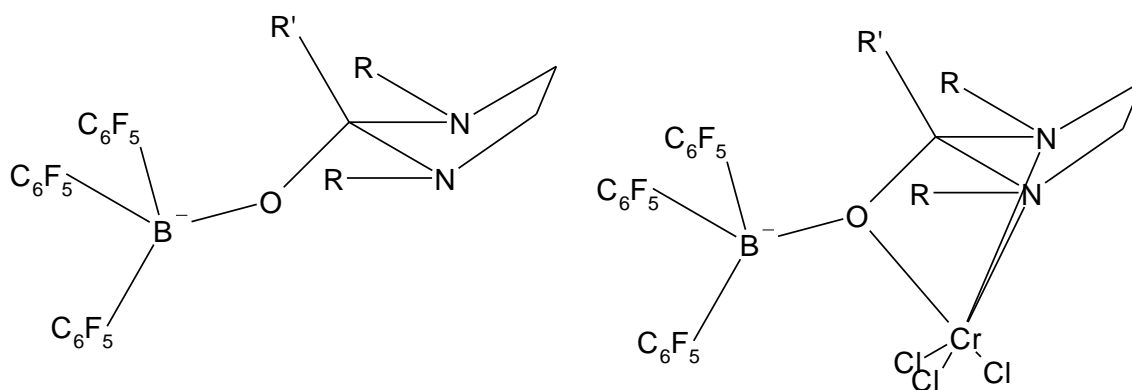


Figure 2.63: Anion Type $[\text{R}(\text{O})\text{B}(\text{R}'\text{NCH}_2)_2]^-$, and corresponding CrCl_3 Complex.

There is some precedent for the synthesis of an alcoholate by addition of metal alkyls to ureas.⁸⁰ Thus, the following synthetic strategy was devised:

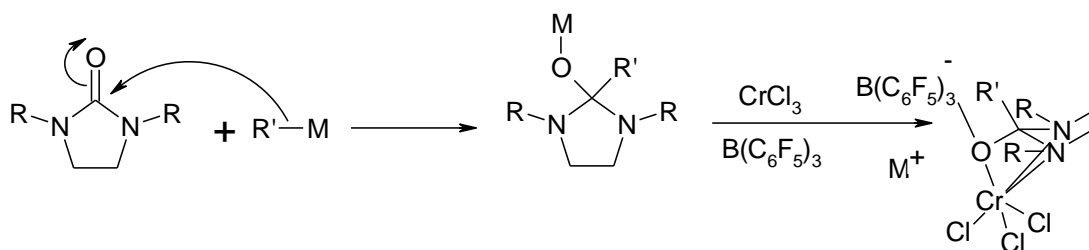


Figure 2.64: Nucleophilic Addition of Metal Alkyl to Cyclic Urea.

The synthesis of the cyclic urea, 1-keto-2,5-di-*tert*-butyl-2,5-diazacyclopentane was effected, as the distinctive ^1H NMR signal attributed to *tert*-butyl substituents improves the reliability of spectroscopic characterization.

One equivalent of N,N'-di-*tert*-butylethylenediamine and one equivalent of diphenylcarbonate were mixed in the absence of solvent, and heated at 190°C for 24 hrs, in a distillation apparatus, under an inert atmosphere.

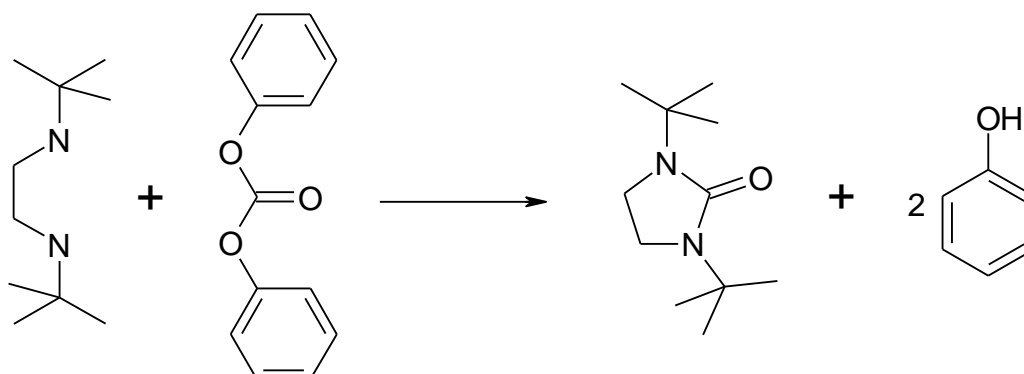


Figure 2.65: Reaction of Diphenylcarbonate with N,N'-Di-*tert*-butylethylenediamine.

The sublimed phenol was discarded, while the residual mixture comprised the product, and approximately one equivalent of phenol. Repeated extraction of a hexane solution of the residue with water resulted in removal of the phenol. The pure 1-keto-2,5-di-*tert*-butyl-2,5-diazacyclopentane was recrystallised from hexane and characterised by ^1H and ^{13}C NMR spectroscopy, and by single crystal X-ray diffraction.

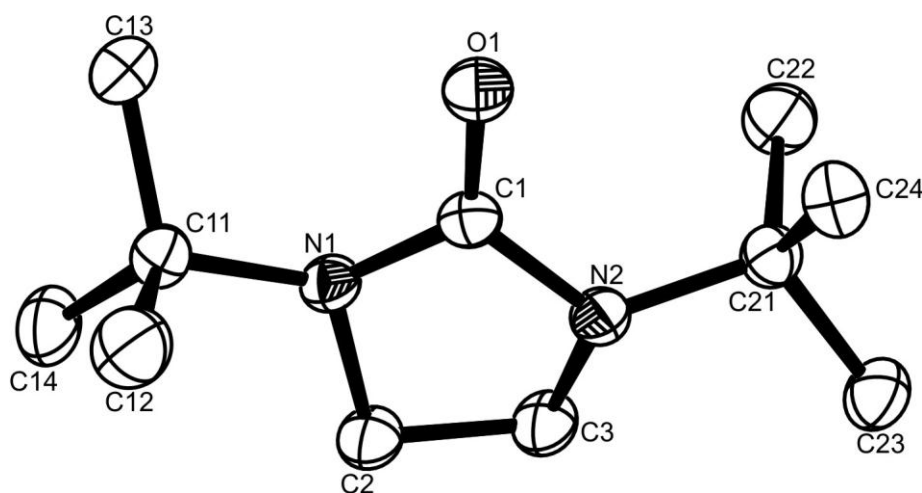


Figure 2.66: Structure of 1-keto-2,5-di-*tert*-butyl-2,5-diazacyclopentane.

As in the case of 1-bora-2,5-diazacyclopentanes, the amine functionalities exhibit a geometry which is neither wholly tetrahedral, nor trigonal planar, suggesting a similar

resonance stabilisation effect, due to donation of the N lone pairs onto the carbonyl functionality. (See below).

The synthesis of this species has been reported previously, by phosgenation of N,N'-di-*tert*-butylethylenediamine⁸¹ and by reaction of the diamine dilithium salt with ethyl chloroformate.⁸² In the latter case, a crystal structure is reported, the bond lengths and angles of which correspond closely to those determined here (see 'Appendix 2')

However, very little information has been previously reported relating to the reactivity of this species.

2.4.1 Reaction of 1-keto-2,5-di-*tert*-butyl-2,5-diazacyclopentane with *n*-butyl Lithium:

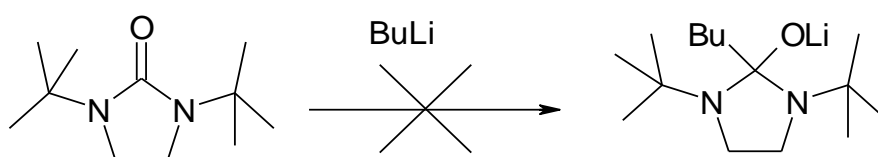


Figure 2.67: Attempted Reaction of Heterocycle with BuLi.

To 1 equivalent of the heterocycle in dry diethylether was added 1 equivalent of *n*-butyl lithium. The solution was stirred overnight at room temperature. The solvent was removed *in vacuo* and the residue characterised as comprising principally the starting material- the ¹³C NMR signal representing the carbonyl functionality is distinctive and was clearly observed. Signals attributable to the heterocycle, *n*-butyl lithium and diethyl ether were exhibited by the ¹H NMR spectrum.

2.4.2 Reaction of 1-keto-2,5-di-*tert*-butyl-2,5-diazacyclopentane with Hexylmagnesium Bromide:

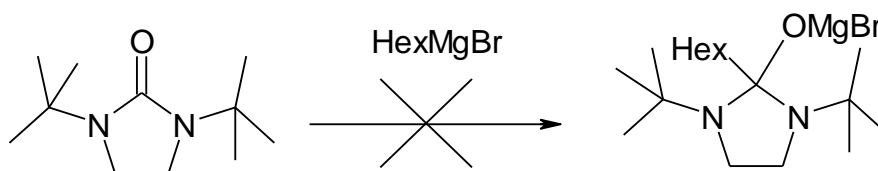


Figure 2.68: Attempted Reaction of Heterocycle with HexMgBr.

To 1 equivalent of the heterocycle in dry THF was added 1 equivalent of a freshly prepared solution of hexylmagnesium bromide. The solution was stirred overnight at room temperature. The resultant solution was characterised by ¹H and ¹³C NMR spectroscopy, and appeared to comprise a mixture of the Grignard reagent and the

starting material- again, the carbonyl functionality was observed in the ^{13}C NMR spectrum.

The lack of reactivity of the diaminomethanal towards nucleophiles may be attributed to stabilization by tautomerism, see figure 2.69:



Figure 2.69: Tautomerism in 1-Keto-2,5-di-*tert*-butyl-2,5-diazacyclopentane.

The carbonyl functionality was expected to be more susceptible to nucleophilic attack when one or both of the adjacent nitrogen lone pairs was coordinated than in the case of the free ligand.

The delocalisation also reduces the nucleophilicity of the nitrogen lone pairs, but there is some precedent for coordination of cyclic diaminomethanals,^{83,84} (cf. ‘2.3.4 *Theoretical Considerations of B-N bonded species:*’).

2.4.3: Attempted Complexation of 1-keto-2,5-di-*tert*-butyl-2,5-diazacyclopentane and hexylmagnesium bromide to Chromium III Chloride:

The ‘one pot’ reaction of 1-keto-2,5-di-*tert*-butyl-2,5-diazacyclopentane, chromium III chloride and hexylmagnesium bromide was attempted.

To a solution of chromium III chloride in dry THF was added 1 equivalent of 1-keto-2,5-di-*tert*-butyl-2,5-diazacyclopentane. To the stirring solution was added dropwise, one equivalent of a freshly prepared solution of hexylmagnesium bromide in THF. The solution was stirred overnight, and the resultant complex precipitated by addition of excess dry diethylether.

For comparison, the complexation of 1-keto-2,5-di-*tert*-butyl-2,5-diazacyclopentane to CrCl_3 in dry THF in the absence of any Grignard reagent was attempted. The product was again obtained by precipitation.

In the case of the addition of hexylmagnesium bromide to a 1-keto-2,5-di-*tert*-butyl-2,5-diazacyclopentane complex of chromium III chloride, the product has not been well characterised, though the continued presence of the heterocyclic precursor is suggested by the presence in the cationic electro-spray mass spectrum, of a signal:

$m/z = 259.22$, consistent with $[\text{Ph}(\text{H})\text{B}(\text{tert-BuNCH}_2)_2]^+$ (259.23), and a signal: $m/z = 277.24$, consistent with $\text{PhB}(\text{tert-BuNCH}_2)_2 \cdot \text{H}_3\text{O}^+$ (277.24). (These signals are also exhibited by the mass spectrum of $\text{PhB}(\text{tert-BuNCH}_2)_2$ in isolation).

There are two functionalities on the precursor which are potentially susceptible to alkylation; the carbonyl carbon, and the chromium centre.

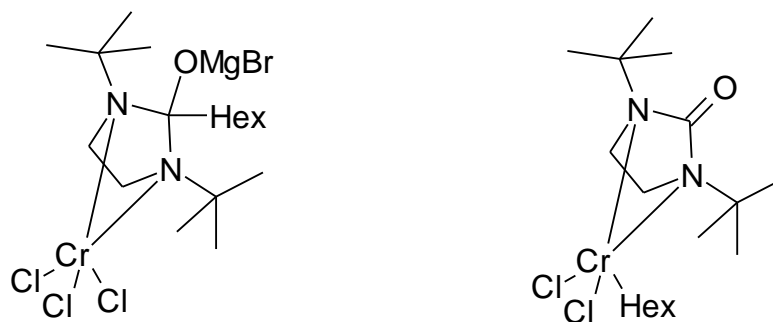


Figure 2.70: The Two possible Alkylation Products.

Whether alkylation of the complex occurs at the carbonyl carbon, at the metal centre or, where the Grignard reagent is omitted; upon activation with excess MAO, similar active species are expected in every case, because in each case the complex is exposed to an excess of alkylating reagents, be they Grignard reagent or aluminium alkyls, and always a large excess of MAO is employed as an activator; likely to alkylate every susceptible functionality. See figure 2.71:

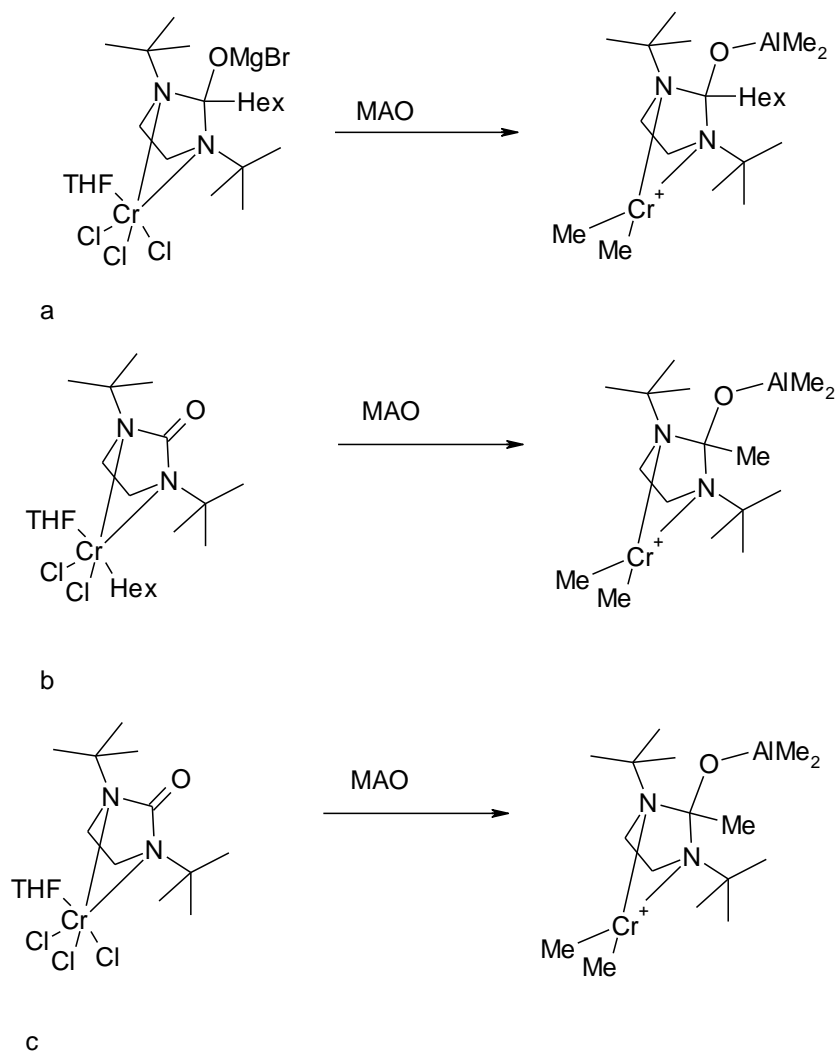


Figure 2.71: The Possible Addition Products of MAO and Hexylmagnesium Bromide

The κ^3 coordination mode for such a complex would be expected to be sterically similar to $\text{PhB}(\text{OH})_2\text{OBu}$ (see ‘2.3.5 *Trioxyboranes*’).

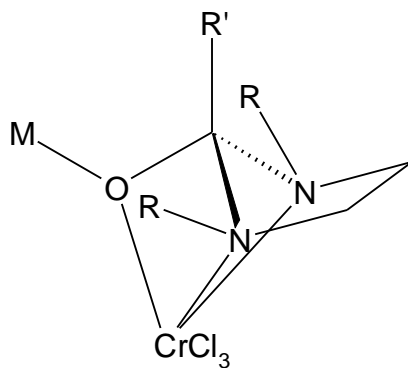


Figure 2.72: κ^3 Coordination Mode for $M[R'(O)C(RNCH_2)_2]_3-CrCl_3$

2.5 Synthesis of N,N'-dialkylethylenediamines:

For the ligand types $[\text{R}(\text{G})\text{B}(\text{R}'\text{NCH}_2)_2]^-$ and $[\text{R}(\text{O})\text{B}(\text{R}'\text{NCH}_2)_2]^-$, the synthetic precursor $(\text{R}'(\text{H})\text{NCH}_2)_2$ is employed. Since the nature of the group R' affects the solubility of the corresponding complex, it is necessary to devise a method by which diamines bearing a range of alkyl or aryl substituents may be synthesized. The following strategy was devised:

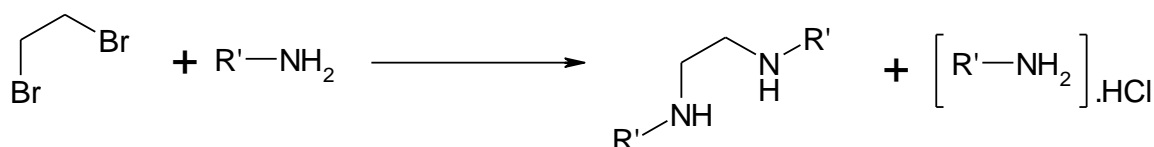


Figure 2.73: Diamine Synthesis.

This synthesis was attempted for $\text{R}' = 2\text{-ethylhexyl}$ and for $\text{R}' = \text{phenethyl}$.

2.5.1 *N,N'*-Bis(2-ethylhexyl)ethylenediamine Synthesis:

4 equivalents of 2-ethylhexylamine were refluxed with 1 equivalent of 1,2-dibromoethane in a mixture of DMSO and water. The solvent was removed by distillation, and the product was then distilled from the residue. The distillate still contained unreacted 2-ethylhexylamine, and this was removed by prolonged distillation at lower temperature. (See 'Experimental' section). The bulk of the 2-ethylhexylamine was separated at the solvent removal stage, as the amine has a lower boiling point than DMSO.

2.5.2 *N,N'*-Bis(phenethyl)ethylenediamine Synthesis:

4 equivalents of phenethylamine were refluxed with 1 equivalent of 1,2-dibromoethane in a mixture of DMSO and water. The solvent was removed by distillation, and the product was then distilled from the residue. The distillate comprised a mixture of the product and phenethylamine. The distillate was dissolved in dodecane, and the solvent removed by distillation. This process was repeated and the residue then redistilled to yield the diamine cleanly. (Dodecylamine bp. is slightly higher than that of phenethylamine).

2.6 Catalytic Properties of Chromium Complexes:

Triazacyclohexane-Chromium Chloride complexes are typically most catalytically active in the presence of 150-200 equivalents of MAO. Consequently 200 equivalents was selected as the ratio of MAO to Chromium complex for all the potential catalysts investigated in this study. (See '4. Catalysis- NMR interpretation:')

Results and Discussion- Summary:

The difficulties inherent in attempting to synthesise quaternary borates in the presence of amines were greater than anticipated, and success in the synthesis of such species has been limited. However, there is spectroscopic evidence supporting the synthesis of a tetra-aryl borate bearing an amine hydrochloride substituent. Potential exists for the synthesis of unsymmetrical TAC molecules bearing tetra-arylborate functionalities, from such a precursor.

The synthesis of various neutral B-N bonded species has been accomplished, and the stability of the B-N bond in these species evaluated. Quaternary, anionic borates bearing multiple B-N σ -bonds are not readily synthesised, and computer modelling suggests that the B-N σ -bond, in the absence of any π resonance stabilisation, is extremely weak. There is spectroscopic evidence to suggest the successful quaternisation of $\text{PhB}(\text{tert-BuNCH}_2)_2$ by the most electronegative of the nucleophiles tested: F^- .

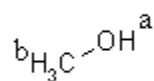
Borates bearing multiple B-O bonds are substantially more stable than their B-N bonded equivalents, and correspondingly easier to synthesise.

The cyclic urea $\text{OC}(\text{tert-BuNCH}_2)_2$ was synthesised, but proved to be of limited utility, as its reactivity towards nucleophiles was significantly impaired compared to other carbonyl-bearing species. The planar N-C(O)-N bonds as observed by X-ray crystallography suggest resonance stabilisation of the functional group.

3. Experimental:

General:

Solvents were used as supplied unless otherwise stated. All manipulations were carried out at room temperature under an inert atmosphere, unless otherwise stated. Degassing of solvents and solutions was accomplished by exposure of the solvents to high vacuum at $-196\text{ }^{\circ}\text{C}$ for ca. 30 minutes. All glass apparatus was pre-dried at $120\text{ }^{\circ}\text{C}$ unless otherwise stated. Toluene, hexane, THF, Et_2O and triethylamine solvents were dried by distillation over metallic sodium, MeOH was dried over anhydrous magnesium sulphate. Otherwise, solvents were used as prepared by solvent purification columns. ‘Reduced pressure’ refers to an oil-pump induced vacuum pressure of ca. 1-5 mBar. ^1H , ^{13}C , ^{19}F and ^{11}B NMR spectra were obtained employing a Bruker 300 MHz NMR spectrometer, (operating at the following frequencies: ^1H : 300.2 MHz, ^{13}C : 75.5 MHz, ^{11}B : 96.3 MHz) or a Bruker 400 MHz spectrometer (operating at the following frequencies: ^1H : 400.1 MHz, ^{13}C : 100.6 MHz, ^{11}B : 128.4 MHz, ^{19}F : 376.5 MHz). NMR interpretation was carried out utilising the XWinNMR software package. Chemical shifts are expressed in ppm, coupling constants in Hz. Chemical shift values are calibrated against the relevant deuterated solvents or, where these are not used, against the conventional solvent signals, eg. THF, Et_2O . Where potentially ambiguous NMR data is presented, for each spectrum, signals are assigned letters, corresponding to the nuclei as they appear on the attendant diagrams for each method. Eg. MeOH: ^1H NMR (CDCl_3): δ 1.09 (a), 3.49 (b):



Mass spectrometric data was obtained employing a Bruker electro-spray mass spectrometer.

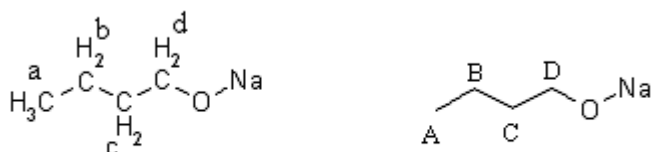
3.1 Synthesis of Sodium n-Butoxide:

To a solution of 1-butanol (3.00 cm^3 , 32.8 mmol) in dry THF (50.0 cm^3), was added sodium metal (1.0 g, 43.5 mmol). The solution was stirred for 12 hrs. The excess sodium was removed by decanting, and the solution reduced *in vacuo* to yield a brown semi-crystalline solid. The solid was washed with hexane, and characterised by ^1H and ^{13}C NMR spectroscopy.

Yield: 2.77 g (88%)

^1H NMR (CDCl_3): δ 0.97 (3H, t, $J = 7.2$ Hz, CH_3) (a), 1.42 (2H, q, $J = 7.2$ Hz, CH_2CH_3) (b), 1.61 (2H, tt, $J = 6.6$ Hz, 4.5 Hz, $\text{CH}_2\text{CH}_2\text{CH}_3$) (c), 3.67 (2H, t, $J = 6.6$ Hz, OCH_2) (d)

^{13}C NMR (CDCl_3): δ 14.2 (CH_3) (A), 19.3 (CH_3CH_2) (B), 35.2 (OCH_2CH_2) (C), 63.0 (OCH_2) (D)

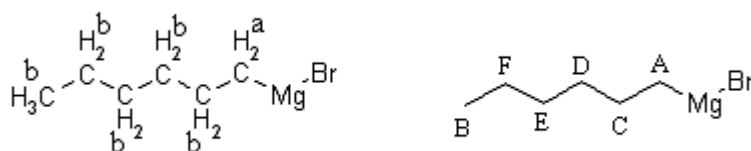


3.2 Synthesis of Hexylmagnesium Bromide :

1-bromohexane (10.0 cm^3 , 0.071 mol) was dissolved in dry THF (50.0 cm^3). To the solution was added magnesium turnings (1.74 g, 0.071 mol). To the mixture was added a crystal of iodine. The mixture was stirred until the magnesium dissolved. The solution was characterised by ^1H and ^{13}C NMR spectroscopy.

^1H NMR: (THF signals discounted) δ -0.46 (2H, t, $J = 7.5$ Hz, MgCH_2) (a), [0.94, 1.34, 1.58] (11H, complex signal, $\text{C}_5\text{H}_{11}\text{CH}_2\text{Mg}$) (b) Sep27-2006 30 1

^{13}C NMR: (THF signals discounted) δ 15.8 (A), 16.1 (B), [23.7, 24.1] (C), [32.4, 32.8] (D), 34.5 (E), 45.2 (F) (Solvent interactions result in multiple signals, see spectrum).



3.3 Synthesis of Bis-phenethylethylenediamine:

Phenethylamine (7.53 cm^3 , 60.0 mmol) and 1,2-dibromoethane (1.17 cm^3 , 13.6 mmol) were dissolved in DMSO (50.0 cm^3) and water (10.0 cm). The solution was refluxed at 120°C for 3 hrs. The solvent was removed by distillation at reduced

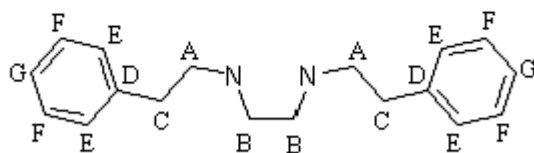
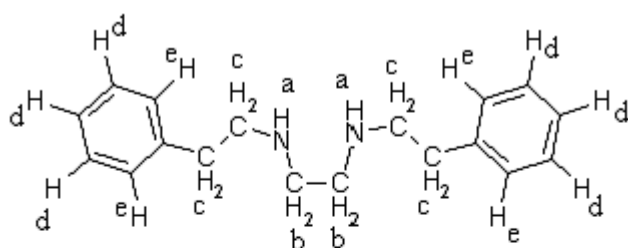
pressure, to yield a viscous oil. 2.0 g of sodium hydroxide was dissolved in water to form a saturated solution. The solution was added to the reaction mixture after the latter had cooled to room temperature. To the soln. was added diethyl ether (50.0 cm³). The biphasic solution was stirred for 1 hr.

The ether phase was separated and the solvent removed *in vacuo* to yield a viscous oil. The residue was distilled at reduced pressure and high temperature (heat-gun) and the product characterised by ¹H and ¹³C NMR spectroscopy, revealing it to contain an excess of phenethylamine. The mixture was dissolved in dodecane (30.0 cm³) and the solvent removed by distillation at reduced pressure at 140°C. The non-volatile material was then characterised by ¹H and ¹³C NMR spectroscopy.

Yield: 2.70 g (37%)

¹H NMR (CDCl₃): δ 1.39 (2H, broad s, NH) (a), 2.58 (4H, s, (NCH₂)₂) (b), 2.61 (8H, complex multiplet, N(CH₂)₂Ph) (c), 7.07 (6H, CH(CH₂)₂) (d) 7.14 (4H, m, CH₂C(CH₂)₂) (e)

¹³C (CDCl₃): δ 34.04 (NCH₂Bz) (A), 49.7 (N(CH₂)₂N) (B), 51.59 (PhCH₂) (C), 126.5 (CH₂C(CH₂)₂) (D), 129.1 (CH₂C(CH₂)₂) (E), 140.5 (CH(CH₂)₂) (F), 140.7 (CH(CH₂)₂) (G) (Additional small peaks: 61.0, 53.6, 34.0: Attributed to residual Et₂O, impurities).



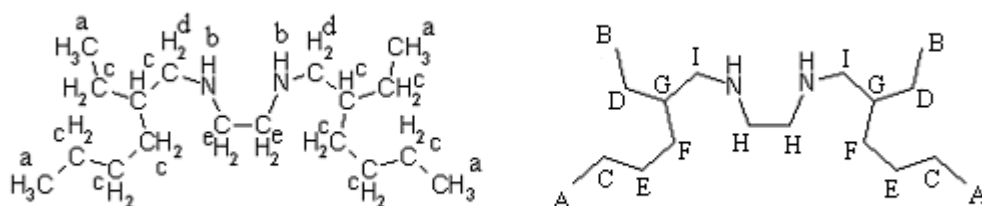
3.4 Synthesis of Bis(2-Ethyl)hexylethylenediamine:

2-Ethylhexylamine (4.97 cm³, 30.0 mmol) and 1,2-dibromoethane (0.59 cm³, 6.8 mmol) were dissolved in a solution of DMSO (37.0 g) and water (5.44 g). The

solution was stirred at 120°C for 3 hrs. The solvent was removed by distillation at reduced pressure. The residue was distilled at 120°C under high vacuum, and remaining 2-ethylhexylamine removed from the distillate by heating for a further 4 hrs. The residual clear liquid was characterised by ^1H and ^{13}C NMR spectroscopy. Yield: 0.76 g (39 %).

^1H NMR (CDCl_3): δ 0.85 (12H, complex m, $\text{NCH}_2\text{CH}(\text{CH}_2\text{CH}_3)\text{CH}_2\text{CH}_2\text{CH}_2\text{CH}_3$) (a), 1.17 (2H, broad s, NH) (b), 1.27 (18H, complex m, $\text{NCH}_2\text{CH}(\text{CH}_2\text{CH}_3)\text{CH}_2\text{CH}_2\text{CH}_2\text{CH}_3$) (c), 2.48 (4H, d, $J = 6.0$ Hz, $((\text{NCH}_2\text{CH}(\text{CH}_2\text{CH}_3)\text{CH}_2\text{CH}_2\text{CH}_2\text{CH}_3)$ (d), 2.69 (4H, s $\text{N}(\text{CH}_2)_2\text{N}$) (e) s (NCH_2)

^{13}C NMR (CDCl_3): δ 11.3 ($\text{CH}_2\text{CH}_2\text{CH}_2\text{CH}_3$) (A), 14.5 ($\text{CH}_3\text{CH}_2\text{CH}(\text{C}_4\text{H}_9)\text{CH}_2\text{N}$) (B), 23.5 ($\text{CH}_2\text{CH}_2\text{CH}_2\text{CH}_3$) (C), 24.9 ($\text{CH}_3\text{CH}_2\text{CH}(\text{C}_4\text{H}_9)\text{CH}_2\text{N}$) (D), 29.4 ($\text{CH}_2\text{CH}_2\text{CH}_2\text{CH}_3$) (E), 31.8 ($\text{CH}_2\text{CH}_2\text{CH}_2\text{CH}_3$) (F), 39.9 (NCH_2CH) (G), 50.1 ($\text{N}(\text{CH}_2)_2\text{N}$) (H), 53.5 (NCH_2CH) (I)



3.5 Example Procedure: Synthesis of Symmetric Triazacyclohexanes- Synthesis of 1,3,5-trimethyl-1,3,5-triazacyclohexane:

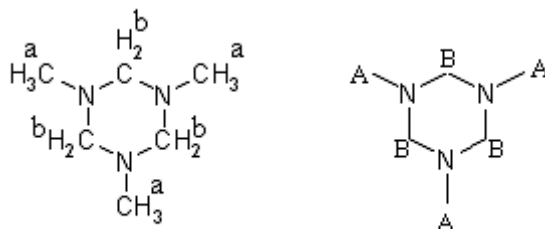
Methylamine (40% w/w aqueous solution, 15.0 cm^3 , 0.17 mol) and paraformaldehyde (5.1 g, 0.17 mol) were dissolved in ethanol (100.0 cm^3) and stirred for 12 hrs.

The solvent was removed *in vacuo* and the residue distilled at reduced pressure, over sodium, at ca. 80°C. The resultant liquid was characterised by ^1H and ^{13}C NMR spectroscopy.

Yield: 6.52 g (89%).

^1H NMR (CDCl_3): δ 2.21 (9H, s, CH_3) (a), 3.13 (6H, broad s, NCH_2N) (b)

^{13}C NMR (CDCl_3): δ 40.6 (A), 77.6 (B)



3.6 Preparation of 1,3,5-trimethyl-1,3,5-triazacyclohexane Hydrobromide Crystals:

1,3,5-trimethyl-1,3,5-triazacyclohexane (0.5 g, 3.87 mmol) and hydrobromic acid (48% w/w aq. soln, 0.23 cm³, 2.0 mmol) were dissolved in THF (10.0 cm³). The solvent was allowed to evaporate over 48 hrs, during which time single crystals of 1,3,5-trimethyl-1,3,5-triazacyclohexane hydrobromide were formed.

X-Ray crystallographic data: see Appendix 2.

3.7 Example procedure: Synthesis of Unsymmetric Triazacyclohexanes- Synthesis of 1,3-dimethyl-5-(4-bromo)phenyl-1,3,5-triazacyclohexane:

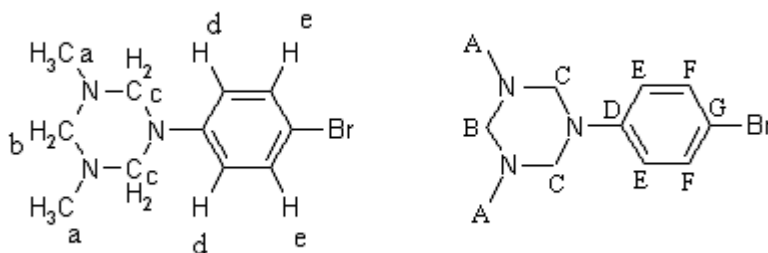
Methylamine (40% w/w aqueous solution, 15.1 cm³, 0.17 mol), 4-bromoaniline (2.0 g, 12 mmol) and paraformaldehyde (6.0 g, 0.20 mol) were dissolved in ethanol (50.0 cm³) and stirred for 12 hrs. All volatiles were removed under high vacuum over a period of 24 hrs, at room temperature, and the residue characterised by ^1H and ^{13}C NMR spectroscopy.

Yield: 2.90 g (89 %).

^1H NMR (CDCl_3): δ 2.15 (6H, s, NCH_3) (a), 3.27 (2H, s, NCH_2N) (b), 3.88 (4H, s, NCH_2N) (c), 6.8 (2H, m, $\text{NC}(\text{CH})_2$) (d), 6.9 (2H, m, $\text{BrC}(\text{CH})_2$) (e)

^{13}C NMR (CDCl_3): 40.8 (NCH_3) (A), 72.5 (NCH_2N) (B), 86.8 (NCH_2) (C), 116.1 ($\text{NC}(\text{CH})_2$) (D), 120.4 ($\text{NC}(\text{CH})_2$) (E), 123.4 ($\text{BrC}(\text{CH})_2$) (F), 131.1 ($\text{BrC}(\text{CH})_2$) (G),

[39.7, 123.8, 152.1]: Diminutive signals- uncharacterised impurity).



3.8 Synthesis of 1,3-dimethyl-5-(4-trimethylsilyl)phenyl-1,3,5-triazacyclohexane:

1,3-dimethyl-5-(4-bromo)phenyl-1,3,5-triazacyclohexane (2.0 g, 7.4 mmol) was dissolved in dry THF (50.0 cm³). The solution was cooled to -78°C, and n-BuLi (2.5 M soln. in hexanes, 3.0 cm³, 7.5 mmol) was added, dropwise by syringe. The solution was stirred for 1 hr, after which time chlorotrimethylsilane (0.94 cm³, 7.4 mmol) was added dropwise by syringe. The solution was stirred for 1 hr, before being allowed to warm to room temperature and stirred for a further 12 hrs. The volatiles were removed *in vacuo* and the residue dissolved in dry hexane (50.0 cm³). The inorganic products were removed by filtration and the filtrate reduced *in vacuo* to yield a viscous oil.

Yield: 0.79 g. This was characterised by ¹H and ¹³C NMR, and found to be impure.

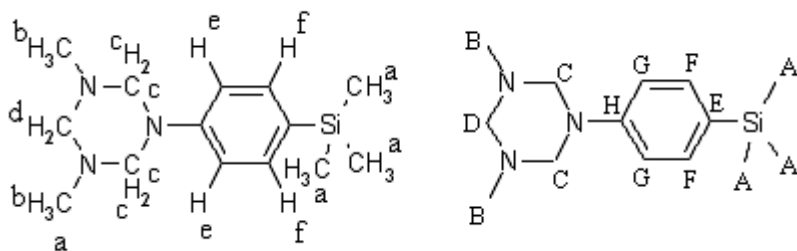
However, the following signals were observed:

¹H NMR (C₆D₆)

[Attributed to 1,3-dimethyl-5-(4-bromo)phenyl-1,3,5-triazacyclohexane]: δ 1.89 (6H, s, CH₃), 3.59 (4H, s, NCH₂N), 3.77 (2H, s, NCH₂N), 6.47 (2H, d, J = 9.0 Hz, NC(CH)₂), 7.15 (2H, m, BrC(CH)₂).

[Attributed to 1,3-dimethyl-5-(4-trimethylsilyl)phenyl-1,3,5-triazacyclohexane: Ratio of integrals- 0.5:1, relative to 1,3-dimethyl-5-(4-bromo)phenyl-1,3,5-triazacyclohexane signals]: δ 0.19 (s, 9H, Si(CH₃)₃) (a), 1.97 (s, 6H, CH₃) (b), 3.03 (s, 4H, NCH₂N) (c), 3.10 (2H, s, NCH₂N) (d), 6.31 (2H, d, J = 9.0 Hz, NC(CH)₂) (e), 7.15 (2H, m, SiC(CH)₂) (f).

¹³C NMR (C₆D₆): δ 0.0 (SiCH₃) (A), 38.8 (NCH₃) (B), 70.7 (NCH₂N) (C), 76.1 (NCH₂N) (D), 115.6 (Me₃SiC) (E), 117.6 (SiC(CH)₂) (F), 118.0 (NC(CH)₂) (G), 130.9 (NC(CH)₂) (H)



3.9 Reaction of 1,3,5-trimethyl-1,3,5-triazacyclohexane with Boron Trifluoride

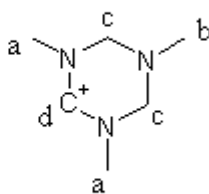
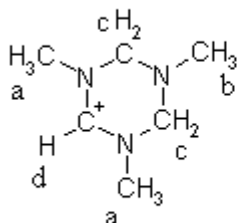
Diethyletherate:

In an NMR tube, to a sample of 1,3,5-trimethyl-1,3,5-triazacyclohexane in CDCl_3 was added ca. 3 equivalents of boron trifluoride diethyletherate. After standing for 12 hrs the sample was characterised by ^1H , ^{13}C and ^{11}B NMR spectroscopy.

^1H NMR (CDCl_3): δ 1.19 (6H, t, $J = 6.9$ Hz, $(\text{CH}_3\text{CH}_2)\text{O}$), 2.35 (6H, s, NCH_3 (adjacent to amidinium)) (a), 2.90 (3H, s, NCH_3 (opposite amidinium) (b), 3.45 (4H, q, $J = 6.9$ Hz, $(\text{CH}_3\text{CH}_2)_2\text{O}$), 3.68 (4H, s, NCH_2N) (c), 7.32, 7.58, 7.71, 7.96 (Amidinium cation: various solvent interactions) (d).

^{13}C NMR (CDCl_3) (Discounting Et_2O and unreacted Me_3TAC signals): δ 40.0 (NCH_3 (adjacent to amidinium)) (a), 43.6 (3H, s, NCH_3 (opposite amidinium) (b), 73.6 (4H, s, NCH_2N) (c), 162.96 (Amidinium cation) (d):

^{11}B NMR (CDCl_3): δ -0.353, 0.48 (multiplet) (Appears to comprise 2 overlapping quartets: B-F coupling. Chemical shifts consistent with B-N coordination).



3.10 Reaction of 1,3,5-tribenzyl-1,3,5-triazacyclohexane with Tris(pentafluoro)phenylborane Diethyletherate:

In an NMR tube, to a sample of *tris*(pentafluoro)phenylborane was added a slight excess of 1,3,5-tribenzyl-1,3,5-triazacyclohexane, in THF soln. After standing for 12 hrs, the sample was characterised by ^1H , ^{13}C , ^{11}B and ^{19}F NMR spectroscopy:

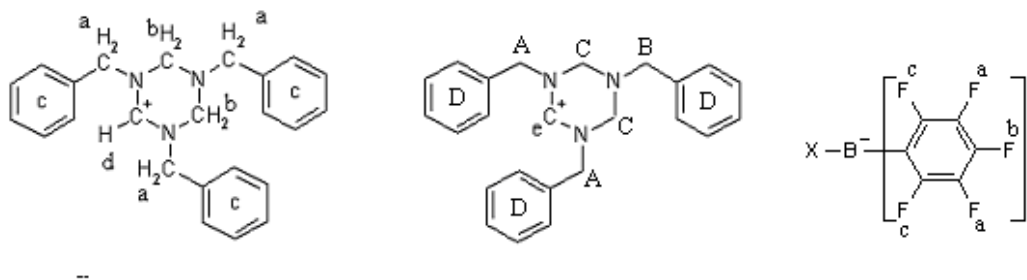
^1H NMR: 2.01 (THF), 3.86 (THF signal masks NCH_2N and PhCH_2N signals) (a), 5.27 (4H, NCH_2N - adjacent to amidinium) (b), 7.45 (complex m, all Ph signals) (c), 8.35 (s, (1H, $\text{N}[\text{CH}]^+\text{N}$) (d).

^{13}C NMR: (THF signals discounted) δ 57.4 ($\text{C}_6\text{H}_5\text{CH}_2$: adjacent to amidinium) (A), 61.8 ($\text{C}_6\text{H}_5\text{CH}_2$: opposite amidinium) (B), 74.4 (NCH_2N) (C), [127.2, 128.4, 128.5, 129.2, 129.3, 139.7] (phenyl carbons) (D), 166.8 ($\text{N}[\text{CH}]^+\text{N}$: amidinium) (E) [^{19}F coupled: 133.6, 136.1, 139.2, 147.1, 150.3]

^{11}B NMR (CDCl_3): δ -1.35 (cf. $\text{PhNMe}_2\text{-B}(\text{C}_6\text{F}_5)_3$: δ -3.0)⁸⁵

^{19}F NMR (CDCl_3): δ -164.78 (6F, s, *meta*- C_6F_5) (a), -158.51 (2F, s *para*- C_6F_5) (b), -131.95 (6F, broad s *ortho*- C_6F_5) (c)

cf. $[\text{MeB}(\text{C}_6\text{F}_5)_3]^-$: δ -166.3 (6F, s, *meta*- C_6F_5), -163.6 (2F, s *para*- C_6F_5), -131.6 (6F, broad s *ortho*- C_6F_5)⁸⁶



3.11 Synthesis of *N*-(trimethyl)silyl-4-bromoaniline:

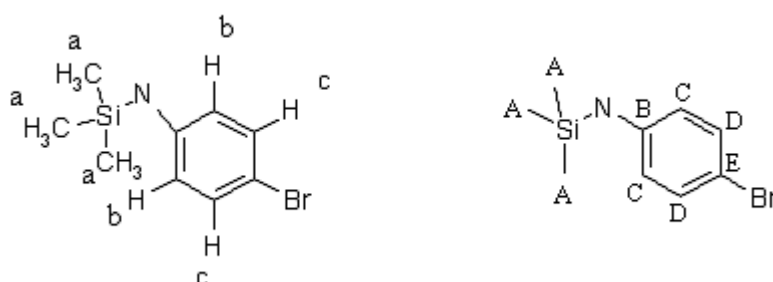
4-bromoaniline (1.0 g, 5.8 mmol) was dissolved in dry diethyl ether (50.0 cm³). To the soln. was added dry triethylamine (0.89 cm³, 6.4 mmol), and chlorotrimethylsilane (0.82 cm³, 6.4 mmol). The soln. was stirred for 12 hrs, during which time a precipitate was formed. This was removed by filtration and the filtrate reduced *in vacuo* to yield

a white solid. The solid was distilled at reduced pressure at 140 °C, and characterised by ^1H and ^{13}C NMR spectroscopy.

Yield: 1.25 g (88 %).

^1H NMR (CDCl_3): δ 0.19 (9H, s, $\text{Si}(\text{CH}_3)_3$) (a), 6.47 (2H, m, $\text{SiC}(\text{CH})_2$) (b), 7.15 (2H, m, $\text{BrC}(\text{CH})_2$) (c)

^{13}C NMR (CDCl_3): 0.0 (A), 11.8 (diminutive signal- impurity), 109.3 (B), 117.8 (C), 132.1 (D), 146.6 (E)



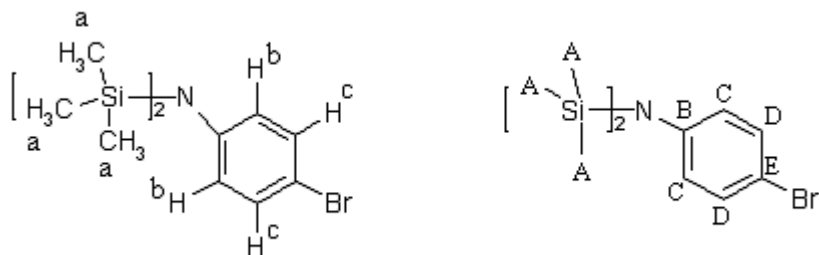
3.12 Synthesis of *N,N*-bis-(trimethyl)silyl-4-bromoaniline:

4-bromoaniline (2.0 g, 11.6 mmol) was dissolved in dry THF (50.0 cm^3). To the solution was added methylmagnesium chloride (22 wt% soln. in THF, 10.5 cm^3 , 34.8 mmol), dropwise by syringe. The soln. was refluxed for 4 hrs at 70°C. To the solution was added chlorotrimethylsilane (4.42 cm^3 , 34.8 mmol). The solution was refluxed at 70°C for a further 12 hrs, during which time a precipitate was formed. The suspension was filtered and the filtrate reduced *in vacuo* to yield a brown oil. This was distilled at reduced pressure at 140°C, to yield a clear, colourless liquid. Characterised by ^1H and ^{13}C NMR spectroscopy.

Yield: 1.24 g (34%).

^1H NMR (CDCl_3): δ -0.01 (s, 18 H, CH_3) (a), 6.71 (d, $J = 8.7$ Hz, 2H, $\text{NC}(\text{CH})_2$) (b), 7.25 (d, $J = 8.7$ Hz, 2H, $\text{BrC}(\text{CH})_2$) (c)

^{13}C NMR (CDCl_3): δ 0.0 (SiCH_3) (A), 114.7 (NC) (B), 127.5 ($\text{NC}(\text{CH})_2$) (C), 131.5 ($\text{BrC}(\text{CH})_2$) (D), 145.3 (BrC) (E)



3.13 Synthesis of 4-(*N,N'*-bis-(trimethyl)silyl)aminophenyl Lithium:

N,N-bis-(trimethyl)silyl-4-bromoaniline (0.5 g, 1.58 mmol) was dissolved in dry Et₂O (30.0 cm³). The solution was cooled to 0°C and *n*-butyl lithium (2.5 M soln. in hexanes, 0.63 cm³, 1.58 mmol) was added, dropwise by syringe. The solution was stirred for 2 hrs. The lithiated product was not isolated, but reacted on immediately.

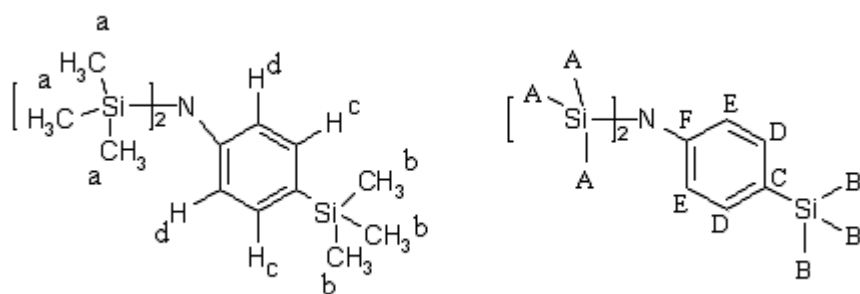
3.14 Synthesis of *N,N*-bis-(trimethylsilyl)-*p*-(trimethyl)silylaniline:

To a solution of 4-(*N,N'*-bis-(trimethyl)silyl)aminophenyl lithium (1.58 mmol) in dry Et₂O (30.0 cm³) at 0°C was added chlorotrimethylsilane (0.20 cm³, 1.58 mmol). The solution was allowed to warm to room temperature and stirred for 12 hrs. The solvent was removed *in vacuo* and the residue dissolved in dry hexane (50 cm³). The inorganic material was removed by filtration and the filtrate reduced *in vacuo* to yield a pale oil. This was distilled at reduced pressure at 140°C, and the distillate characterised by ¹H and ¹³C NMR spectroscopy.

Yield: 0.41 g (41%)

¹H NMR (CDCl₃): δ 0.00 (18H, s, N(Si(CH₃)₃)₂) (a), 0.17 (9H, s, CSi(CH₃)₃) (b), 6.80 (4H, d, *J* = 8.3 Hz, SiC(CH)₂) (c), 7.27 (4H, d, *J* = 8.3 Hz, NC(CH)₂) (d).

¹³C NMR (CDCl₃): δ 0.9 (NSiCH₃) (A), 3.0 (CSiCH₃) (B), 116.5 (SiC) (C), 130.4 (SiC(CH)₂) (D), 132.4 (NC(CH)₂) (E), 149.4 (NC) (F)

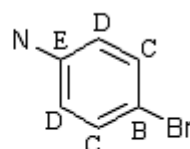
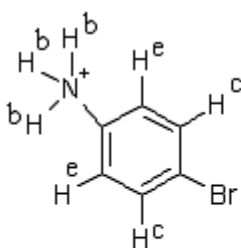
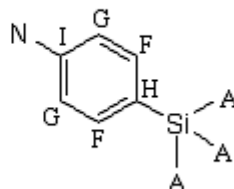
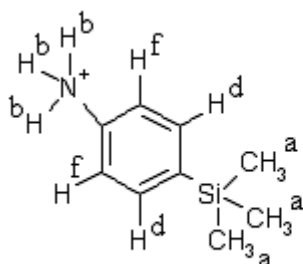


3.15 Synthesis of 4-(trimethyl)silylaniline hydrochloride:

The residue was dissolved in hydrochloric acid (1.2 M aq. soln, 50 cm³, 60 mmol). The solution was stirred for 12 hrs. The solvent was removed *in vacuo* to yield a colourless, semicrystalline solid. Characterised by ¹H and ¹³C NMR spectroscopy. Revealed to be a mixture of *para*-silylated and unsilylated aniline, in an approximate ratio of 2:3, [silylaniline]:[aniline]:
Yield: 0.10 g.

¹H NMR (CDCl₃): δ 0.01 (9H, s, Si(CH₃)₃) (a), 3.44 (3H, broad s, NH₂.HCl) (b), 6.32, 2H, d, J = 4.8 Hz, BrC(CH)₂) (c), 6.46 (2H, d, J = 4.5 Hz, SiC(CH)₂) (d), 7.01 (2H, d, J = 4.8 Hz, BrC(CH)₂(CH)₂) (e), 7.10 (2H, d, J = 4.5 Hz, SiC(CH)₂(CH)₂) (f)

¹³C NMR (CDCl₃): δ -0.15 (A), 111.0 (B), 115.4 (C), 117.6 (D), 129.3 (E), 132.8 (F), 135.4 (G), 146.3 (H), 147.9 (I)
[28.3, and additional diminutive signals- probable solvent impurities].



For comparison, ¹H and ¹³C NMR spectra were obtained for *p*-bromoaniline hydrochloride, but the latter's insolubility in CDCl₃ required that NMR data be obtained in D₂O. This prohibits direct comparison of chemical shift values:

^1H NMR (D_2O): δ 7.09 (2H, d, $J = 8.7$ Hz, $\text{NC}(\text{CH}_2)_2$), 7.43 (2H, d, $J = 8.7$ Hz, $\text{BrC}(\text{CH}_2)_2$)

^{13}C NMR (D_2O): δ 122.8, 125.2, 129.2, 133.4

3.16 (Synthesis of Lithium N,N-bis-(trimethyl)silyl-4-(tris(pentafluorophenylborato)aniline)]Et₂O]₂ :

To a solution of 4-(N,N'-bis-(trimethyl)silyl)phenyl lithium (1.58 mmol) in dry THF (30.0 cm^3) at 0°C was added a freshly prepared solution of tris(pentafluorophenyl)borane-diethyletherate (0.93 g, 1.58 mmol) in dry THF (10.0 cm^3). The solution was allowed to warm to room temperature and stirred for 12 hrs. The solvent was removed *in vacuo* to yield a viscous brown oil. The product was washed repeatedly with dry hexane (5 x 20 cm^3). Residual hexane was removed under high vacuum and the product characterised by ^1H , ^{13}C , ^{11}B and ^{19}F NMR spectroscopy in DCM soln. The ^1H and ^{13}C NMR spectra were not well resolved, ^{11}B and ^{19}F NMR spectra appeared to show multiple products.

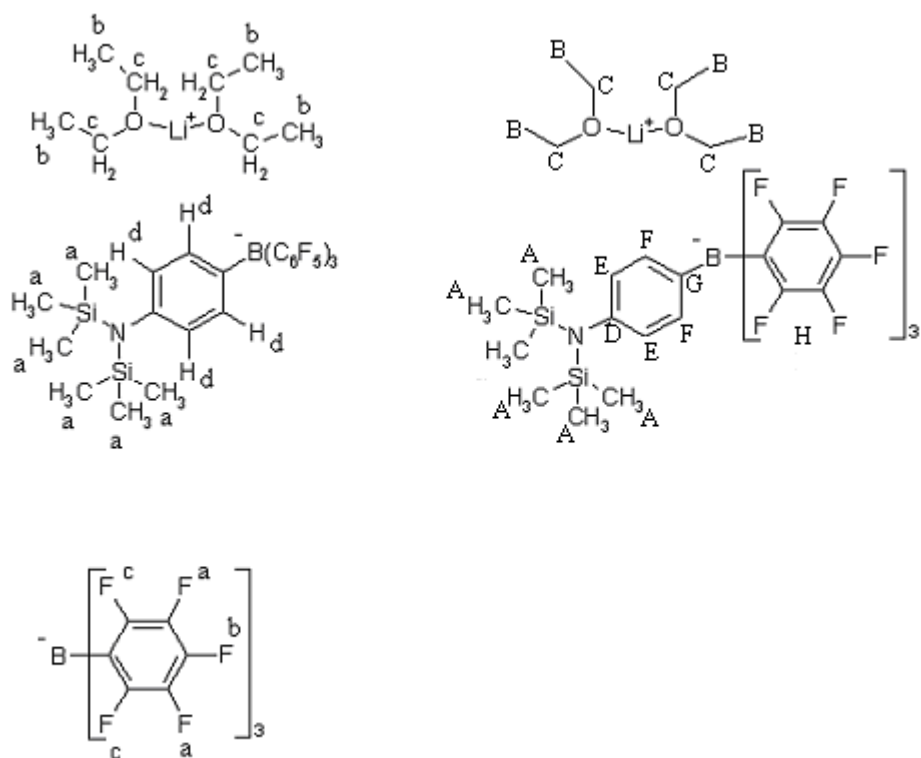
Yield: 0.41 g

^1H NMR: δ 0.20 (~15H, multiple signals, attributed to uncharacterised $\text{Si}(\text{CH}_3)_3$ based impurities), 0.29 (~6H, s, $\text{Si}(\text{CH}_3)_3$) (a), 1.20 (12H, t, $J = 6.9$ Hz, Et_2O) (b), 3.63 (8H, q, $J = 6.9\text{Hz}$, Et_2O) (c), [6.70 (2H, d, $J = 8.4$ Hz), 6.89 (2H, d, $J = 9.0$ Hz), 7.00 (2H, d, $J = 7.2$ Hz), 7.35 (2H, d, $J = 7.2$ Hz), multiple C_6H_4] (d)

^{13}C NMR: -0.3 (uncharacterised $\text{Si}(\text{CH}_3)_3$ impurity), 1.8 (SiCH_3) (A), 14.1 (Et_2O) (B), 54.0, (DCM), 66.5 (Et_2O) (C), 116.4 (NC) (D), 130.3 ($\text{NC}(\text{CH}_2)_2$) (E), 133.9 ($\text{BC}(\text{CH}_2)_2$) (F), 146.7 $\text{BC}(\text{CH}_2)_2$ (G), [F-coupled, 131.6 (s), 136.3 (d, $J = 354.9$ Hz), 148.3 (d, $J = 234.1$ Hz)] (H)

^{11}B NMR: δ [-21.8, -13.7, -10.6] (Consistent with borate anions), [-1.4, 0.1, 4.1] (Consistent with B-N adducts, B-O adducts (eg, etherates)).

^{19}F NMR: δ -167.73 (2F, broad s, $\text{CF}(\text{CF})_2$) (a), -163.76 (1F, t, $J = 19.6$ Hz, $\text{CF}(\text{CF})_2$) (b), -133.12 (2F, broad s, $\text{BC}(\text{CF})_2$) (c)



3.17 (Synthesis of Lithium 4-aminophenyltris(pentafluoro)phenylborate hydrochloride)[Et₂O]₂:

Lithium N,N-bis-(trimethyl)silyl-4-(tris(pentafluoro)phenylborato)aniline[Et₂O]₂ (0.41 g, 0.46 mmol) was dissolved in an excess of ca. 5 M hydrochloric acid soln. The soln. was stirred for 12 hrs, and the volatiles removed *in vacuo*, to yield a pale semi-solid. Characterised by ¹H, ¹³C, ¹¹B and ¹⁹F NMR spectroscopy:

Yield: 0.33 g (89%)

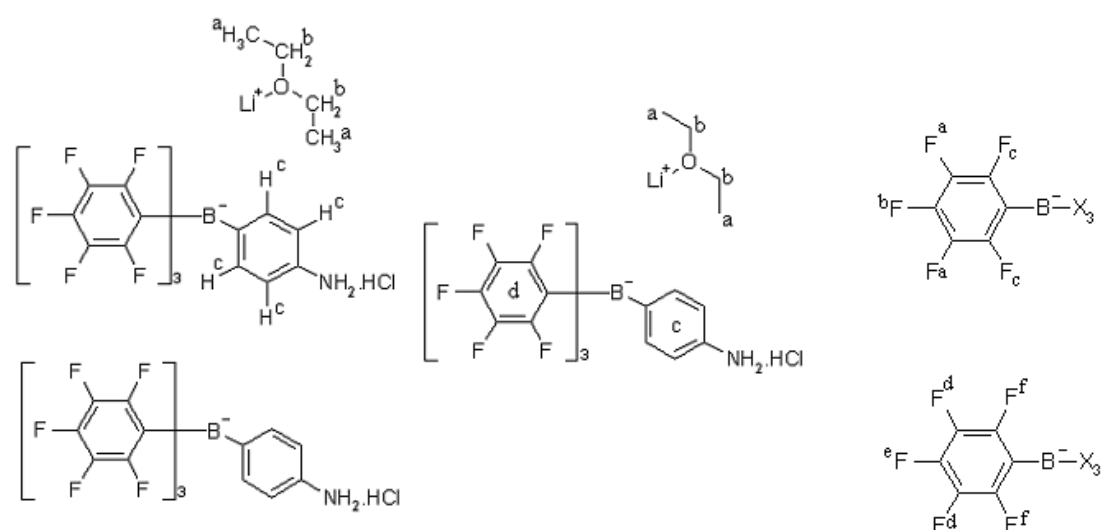
¹H NMR (CDCl₃): δ 0.00 (s, 0.06 H, (CH₃)₃Si) (residual), 1.04 (t, J = 7.2 Hz, 0.6 H, (CH₃CH₂)₂O) (a), 2.27 (s, 0.06 H) (residual impurity), 3.52 (q, J = 7.2 Hz, (CH₃CH₂)₂O) (b), 5.22 (s, 0.03 H) (residual impurity), 7.08 (m, 4H, N-C₆H₄-B) (c)

¹³C NMR (δ 14.7 (Et₂O) (A), 66.7 (Et₂O) (B), [122.9, 124.4, 129.5, 130.3, 1311.4, 133.5, 134.4] (C: NC₆H₄B⁻ anion + aniline/borane adduct), [F-coupled:137.7 (d, J = 249.2 Hz), 148.1 (d, J = 249.2 Hz), 116.5 (broad s)] (D)

^{11}B NMR (CDCl_3): δ -4.4 (broad) $[(\text{BrC}_6\text{H}_4\text{NH}_2\cdot\text{HCl})\text{-(B(C}_6\text{F}_5)_3\text{) adduct}]$, -15.97 (Anion)

^{19}F NMR (CDCl_3): δ -166.26 (2F, broad s, CF(CF)_2) (a), -161.78 (1F, t, $J = 20.7$ Hz, CF(CF)_2) (b), -133.15 (2F, broad s, BC(CF)_2) (c) (cf. 3.16 (*Synthesis of Lithium N,N-bis-(trimethyl)silyl-4-(tris(pentafluoro)phenylborato)aniline*)] $\text{Et}_2\text{O}]_2$: Chemical shift values very similar.

δ -162.37 (2F, t, $J = 18.4$ Hz, CF(CF)_2) (d), -155.46 (1F, t, $J = 19.9$ Hz, CF(CF)_2) (e), -133.15 (2F, m, BC(CF)_2) (f) (Attributed to B-N adduct).



3.18 Attempted Synthesis of 1-(3-(sodium oxy)methyl)phenyl-3,5-(2-ethyl)hexyl-1,3,5-triazacyclohexane:

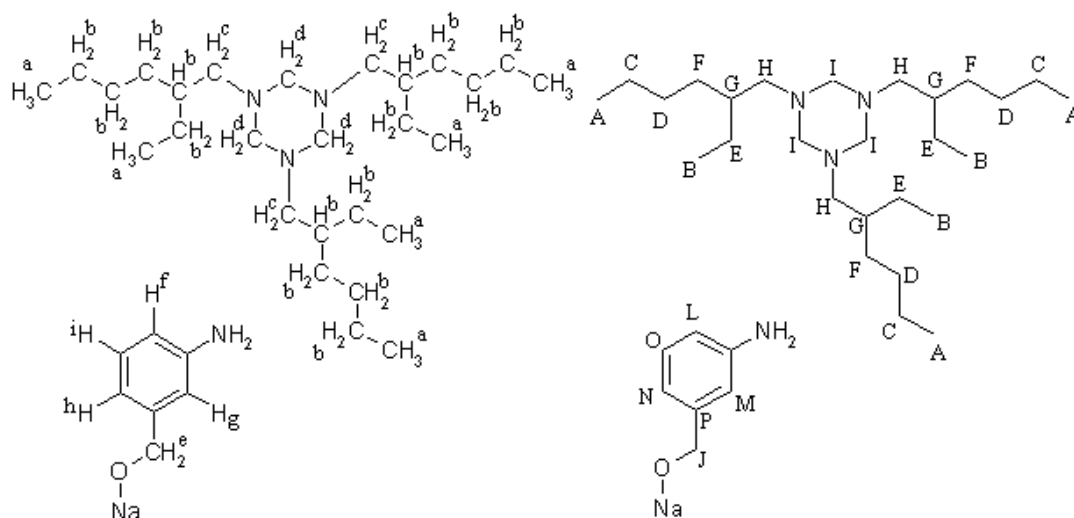
3-aminobenzylalcohol (1 g, 8.12 mmol), 2-ethyl-1-hexylamine (13.5 cm^3 , 0.08 mol) were dissolved in ethanol (30 cm^3). To the solution was added, with stirring, paraformaldehyde (2.7 g, 0.13 mol). The solution was stirred overnight at room temperature. All volatiles were removed *in vacuo* to yield a viscous, colourless oil. The residue was dissolved in dry diethyl ether (50 cm^3) and stirred for 24 hrs in the presence of an excess of metallic sodium. The excess solid sodium was removed and the solvent removed *in vacuo* to yield a viscous oil. To the residue was added dry hexane (50 cm^3). The resultant mixture was stirred for 12 hrs and the resultant precipitate separated by filtration. Volatiles were removed and the resultant oily solid characterised by ^1H and ^{13}C NMR spectroscopy.

Yield: 0.91g.

The NMR data did not appear to show formation of the target unsymmetrical TAC, and was most consistent with a mixture of 1,3,5-tris(2-ethyl)hexyl-1,3,5-triazacyclohexane, and approximately 5 equivalents of 3-aminobenzylalcohol (or the corresponding sodium salt).

^1H NMR (CDCl_3): δ 0.82 (m, 18H, $\text{NCH}_2\text{CH}(\text{CH}_2\text{CH}_3)\text{C}_3\text{H}_6\text{CH}_3$) (a), 1.17 (m, 27H, $\text{NCH}_2\text{CH}(\text{CH}_2\text{CH}_3)\text{C}_3\text{H}_6\text{CH}_3$) (b), 2.21 (d, $J = 4.8$ Hz, 6H, $\text{NCH}_2\text{CH}(\text{CH}_2\text{CH}_3)\text{C}_3\text{H}_6\text{CH}_3$) (c), 3.20 (broad s, 6H, NCH_2CH) (d), 4.52 (s, 10H, OCH_2) (e), 6.55 (m, 5H, *para* to NaOCH_2 -) (f), 6.63 (s, 5H, *ortho* to N-, NaOCH_2 -) (g), 6.67 (d, $J = 7.8$ Hz, 5H, *para* to N-) (h), 7.08 (t, $J = 7.8$ Hz, 5H, *meta* to NaOCH_2) (i)

^{13}C NMR (CDCl_3): δ 11.2 ($\text{NC}_7\text{H}_{14}\text{CH}_3$) (A), 14.6 ($\text{NCH}_2\text{CH}(\text{CH}_2\text{CH}_3)\text{C}_4\text{H}_9$) (B), 23.6 ($\text{NC}_6\text{H}_{12}\text{CH}_2\text{CH}_3$) (C), 25.0 ($\text{CH}_2\text{CH}_2\text{CH}_3$) (D), 29.4 ($\text{NCH}_2\text{CH}(\text{CH}_2\text{CH}_3)\text{C}_4\text{H}_9$) (E), 31.9 ($\text{CH}_2\text{CH}_2\text{CH}_2\text{CH}_3$) (F), 37.8 ($\text{NCH}_2\text{CH}(\text{C}_2\text{H}_5)\text{C}_4\text{H}_9$) (G), 57.2 (NCH_2) (H), 65.6 (NCH_2N) (I), 75.7 (ArCH_2O) (J), 77.4 (CHCl_3) (K), 114.0 (CH) (L), 114.8 (CH) (M), 117.5 (CH) (N), 129.9 (CH) (O), 142.7 (CH) (P)



3.19 Complexation of Product and Chromium III Chloride:

The product of reaction of 3-aminobenzylalcohol, 2-ethyl-1-hexylamine and paraformaldehyde, was dissolved in dry THF (50 cm³). To the resultant solution was added Chromium III Chloride tris-THF (0.70 g, 1.87 mmol). The resultant dark purple

solution was stirred under $N_{2(g)}$ for 12 hrs. The resultant green Chromium compound was isolated by precipitation from soln, by addition of toluene.

Yield: 0.82 g

The chromium III chloride adduct of this product was characterised by electro-spray mass spectrometry, and the cation spectrum exhibited a mass peak attributable to the product of complexation of 3-aminobenzylalcohol to $CrCl_3$: $m/z = 492.40$ (cf.

$[(NH_2C_6H_4CH_2OH)_3CrCl_2]^+$: $m/z = 492.37$).

Elemental Analysis: Expected (for $C_{26}H_{46}N_3NaO_2CrCl_3$):

C: 52.2% H: 7.8% N: 7.0%

Found: C: 41.2% H: 6.7% N: 6.8%

3.20 Synthesis of 1,1-diphenyl-2,5-diethyl-1-sila-2,5-diazacyclopentane:

N,N' -diethylethylenediamine (1.0 cm^3 , 7.0 mmol) was dissolved in dry hexane. The soln. was degassed. To the soln. was added $n\text{-BuLi}$ (2.5 M soln. in hexanes, 5.6 cm^3 , 14.0 mmol), at -78°C . The soln. was allowed to warm to room temperature, and stirred for 12 hrs. To the resultant suspension was added diphenyldichlorosilane (1.47 cm^3 , 7.0 mmol), dropwise by syringe. The suspension was stirred for 48 hrs. The solid was removed by filtration and washed with dry hexane. The filtrate was reduced *in vacuo* to yield the product as a colourless oil. This was characterised by ^1H and ^{13}C NMR spectroscopy.

Yield: 1.63 g, (78%).

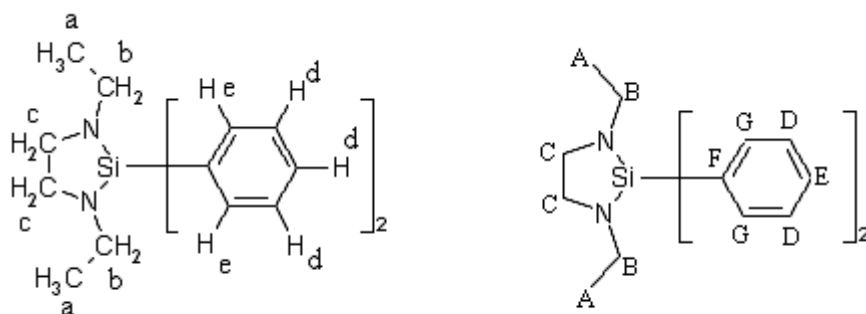
^1H NMR: δ 0.86 (6H, t, $J = 6.9\text{ Hz}$, CH_3) (a), 2.68 (4H, q, $J = 6.9\text{ Hz}$, CH_2CH_3) (b), 3.05 (4H, s, $\text{NCH}_2\text{CH}_2\text{N}$) (c), 7.28 (6H, m, $(\text{CH})_2\text{CH}$) (d), 7.57 (4H, m, $\text{SiC}(\text{CH})_2$) (e)

^{13}C NMR: δ 15.7 (CH_3) (A), 42.5 (CH_3CH_2) (B), 49.1 ($\text{N}(\text{CH}_2)_2\text{N}$) (C), 128.0 ($\text{CH}(\text{CH})_2$) (D), 130.1 ($\text{CH}(\text{CH})_2$) (E), 136.0 (SiC) (F), 136.1 $\text{SiC}(\text{CH})_2$ (G).

Elemental Analysis ($C_{18}H_{24}N_2\text{Si}$):

Expected: C: 72.9% H: 8.2% N: 9.5%

Found: C: 70.4% H: 7.9% N: 7.1%



3.21 Attempted Complexation of 1,1-diphenyl-2,5-diethyl-1-sila-2,5-diazacyclopentane:

1,1-diphenyl-2,5-diethyl-1-sila-2,5-diazacyclopentane (0.40 g, 1.37 mmol) was dissolved in dry THF (10 cm³). CrCl₃.THF₃ (0.50 g, 1.37 mmol) was dissolved in dry THF (20.0 cm³). The two solns. were mixed and stirred at room temperature for 12 hrs. The solvent was removed *in vacuo* and the residue stirred in dry hexane for 12 hrs. The pale, purple solid was removed by filtration, washed with dry hexane and volatiles removed *in vacuo*.

Elemental Analysis (C₁₈H₂₄Cl₃CrN₂Si):

Expected: C: 47.5% H: 5.3% N: 6.2%

Found: C: 37.8% H: 4.9% N: 3.3%

The elemental analysis result is a closer match to the following mixture:

Ph₂Si(EtNCH₂)₂ + 2CrCl₃ + 3 THF: C: 43.4% H: 5.8% N: 3.4%, suggesting only partial complexation of the ligand.

3.22 Example Procedure: Synthesis of 1-Phenyl-2,5-di-tert-butyl-1-bora-2,5-diazacyclopentane:

Dichlorophenylborane (1.44 cm³, 11.1 mmol) was added dropwise to a stirring solution of triethylamine (1.54 cm³, 11.1 mmol) in dry hexane (50.0 cm³). The solution was stirred at room temperature for 10 minutes. To the solution was added N,N'-di-tert-butylethylenediamine (2.0 cm³, 11.1 mmol). The solution was refluxed at 70 °C for 3 hrs. The solid was separated by filtration and the residue reduced *in vacuo* to yield a white solid. The product was recrystallised and characterised by ¹H, ¹³C and

^{11}B NMR spectroscopy, in C_6D_6 and CDCl_3 . A structure was obtained by single crystal X-ray diffraction.

Yield: 1.59 g (84%).

Crystals were obtained by cooling a saturated hexane soln. of the product to -20°C .

Crystals appeared over 24 hrs.

Melting point: $76.9\text{--}78.6^\circ\text{C}$

^1H NMR (C_6D_6) δ 0.94 (s, 18H, $\text{PhB}((\text{CH}_3)_3\text{CNCH}_2)_2$) (a), 3.10 (s, 4H, $\text{PhB}((\text{CH}_3)_3\text{CNCH}_2)_2$) (b), 7.07 (m, 3H, $\text{CH}(\text{CH})_2(\text{CH})_2\text{CB}(\text{t-BuNCH}_2)_2$) (c), (m, 2H, $\text{CH}(\text{CH})_2(\text{CH})_2\text{CB}(\text{t-BuNCH}_2)_2$) (d):

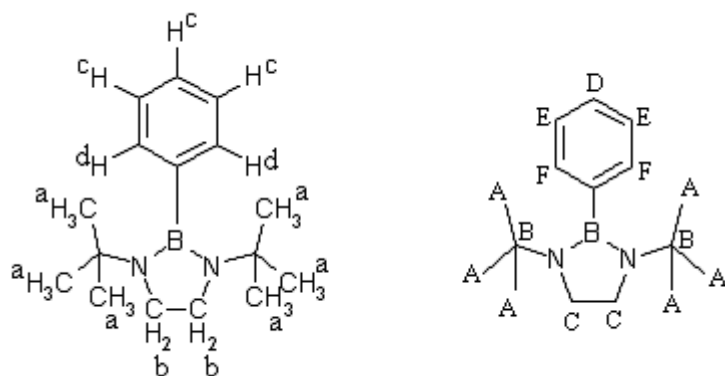
^{13}C NMR: (C_6D_6) δ 29.6 1 ($\text{PhB}((\text{CH}_3)_3\text{CNCH}_2)_2$) (A), 43.8 ($\text{PhB}((\text{CH}_3)_3\text{CNCH}_2)_2$) (B), 50.4 ($\text{PhB}((\text{CH}_3)_3\text{CNCH}_2)_2$) (C), 125.5 ($\text{C}(\text{CH})_2(\text{CH})_2\text{CH}$) (D), 131.3 ($\text{C}(\text{CH})_2(\text{CH})_2\text{CH}$) (E), 134.2 ($\text{C}(\text{CH})_2(\text{CH})_2\text{CH}$) (F):

^{11}B NMR (C_6D_6): δ 31.96.

^1H NMR (CDCl_3): δ 0.89 ((s, 18H, $\text{PhB}((\text{CH}_3)_3\text{CNCH}_2)_2$) (a), 3.23 (s, 4H, $\text{PhB}((\text{CH}_3)_3\text{CNCH}_2)_2$) (b), 7.14 (m, 3H, $\text{CH}(\text{CH})_2(\text{CH})_2\text{CB}(\text{t-BuNCH}_2)_2$) (c), 7.23 (m, 2H, $\text{CH}(\text{CH})_2(\text{CH})_2\text{CB}(\text{t-BuNCH}_2)_2$) (d)

^{13}C NMR (CDCl_3): δ 31.1 ($\text{PhB}((\text{CH}_3)_3\text{CNCH}_2)_2$) (A), 45.3 ($\text{PhB}((\text{CH}_3)_3\text{CNCH}_2)_2$) (B), 52.1 ($\text{PhB}((\text{CH}_3)_3\text{CNCH}_2)_2$) (C), 126.7 ($\text{C}(\text{CH})_2(\text{CH})_2\text{CH}$) (D), 127.3 ($\text{C}(\text{CH})_2(\text{CH})_2\text{CH}$) (E), 132.8 ($\text{C}(\text{CH})_2(\text{CH})_2\text{CH}$) (F)

^{11}B NMR (CDCl_3): δ 32.7



X-Ray Crystallographic Data: See Appendix 2.

Elemental Analysis ($C_{16}H_{27}BN_2$):

Expected:	C: 74.4%	H: 10.5%	N: 10.9%
Found:	C: 73.0%	H: 10.5%	N: 10.8%

Electro-spray mass spectra were obtained. Notable signals in the cation spectrum (Sigma fits <0.05 indicates high probability of correct MF):

$m/z = 259.23$ (cf. $PhB(tert-BuNCH_2)_2.H^+$: $m/z = 259.23$).

$m/z = 277.25$ (and ^{10}B isotope signal at 276.25) (cf. $PhB(tert-BuNCH_2)_2.H_3O^+$: $m/z = 277.24$).

3.23 Attempted Complexation of 1-Phenyl-2,5-di-tert-butyl-1-bora-2,5-diazacyclopentane:

1-Phenyl-2,5-di-*tert*-butyl-1-bora-2,5-diazacyclopentane (0.5 g, 1.94 mmol) was dissolved in dry THF (50.0 cm³). To the solution was added $CrCl_3.THF_3$ (0.73 g, 1.94 mmol). The soln. was stirred for 2 hrs. To the solution was added an excess of dry hexane. A purple precipitate was formed. This was separated by filtration, and the volatiles were removed *in vacuo*.

Yield: 0.63 g (78%).

Elemental analysis:	Expected:	C: 46.0%	H: 6.8%	N: 6.7%
	Found:	C: 37.8%	H: 6.5%	N: 5.0%

Cationic electro-spray mass spectrum exhibited peak: $m/z = 277.25$ (and ^{10}B isotope signal at 276.24) (cf. $\text{PhB}(\text{tert-BuNCH}_2)_2\cdot\text{H}_3\text{O}^+$: $m/z = 277.24$).

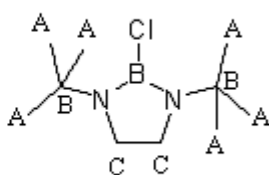
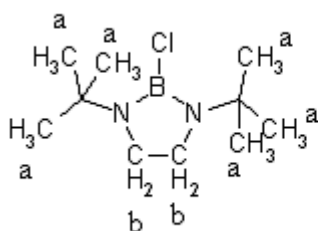
3.24 Example Procedure- Synthesis of 1-chloro-2,5-di-tert-butyl-1-bora-2,5-diazacyclopentane:

To a solution of dry triethylamine (1.94 cm^3 , 13.9 mmol) in dry hexane (20.0 cm^3) was added boron trichloride (1 M soln. in hexanes, 13.9 cm^3 , 13.9 mmol), dropwise by syringe. To the resultant suspension was added di-*tert*-butylethylenediamine (3 cm^3 , 13.9 mmol). The suspension was refluxed for 3 hrs. The resultant suspension was allowed to cool to room temperature, filtered and the solvent removed *in vacuo* to yield a crystalline solid. Characterised by ^1H , ^{13}C and ^{11}B NMR spectroscopy. Yield: 1.43 g (48 %).

^1H NMR (CDCl_3): δ 1.20 (18H, s, $\text{C}(\text{CH}_3)_3$) (a), 3.11 (4H, s, $\text{N}(\text{CH}_2)_2\text{N}$) (b)

^{13}C NMR (CDCl_3): δ 30.2 (CH_3) (A), 44.7 ($\text{C}(\text{CH}_3)_3$) (B), 51.9 ($\text{N}(\text{CH}_2)_2\text{N}$) (C)

^{11}B NMR (CDCl_3): δ 27.6



3.25 Preparation of 1-bromo-2,5-di-tert-butyl-1-bora-2,5-diazacyclopentane

Crystals:

A saturated solution of 1-bromo-2,5-di-*tert*-butyl-1-bora-2,5-diazacyclopentane in dry, degassed hexane was prepared. The solution was cooled to $-20\text{ }^\circ\text{C}$. Colourless crystals appeared over 24 hrs.

X-Ray Crystallographic Data: See Appendix 2.

3.26 Synthesis of Bis(diethyl)aminophenylborane:

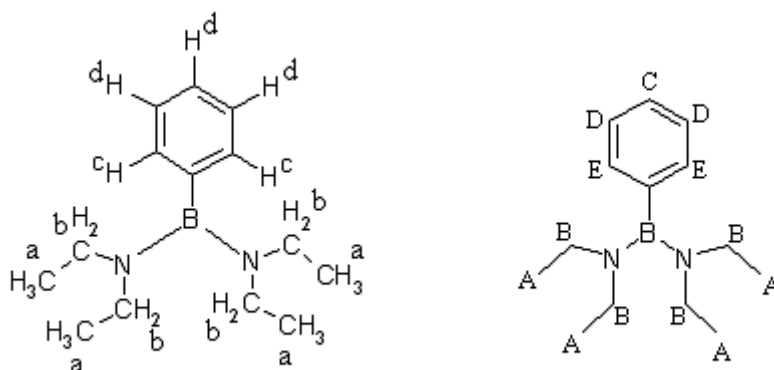
To a stirring solution of diethylamine (3.19 cm³, 30.8 mmol) in dry hexane (50 cm³), was added dichlorophenylborane (1.0 cm³, 7.7 mmol), dropwise by syringe. The solution was stirred for 12 hrs. The precipitate was removed by filtration, and the filtrate reduced *in vacuo* to yield a pale yellow oil. The product was distilled at reduced pressure, at high temperature (heat-gun), and characterised by ¹H, ¹³C and ¹¹B NMR spectroscopy.

Yield: 1.08 g (61%)

¹H NMR (CDCl₃): δ 0.91 (12H, t, J=6.9Hz, CH₃) (a), 2.83 (8H, q, J=6.9Hz, CH₂) (b), 7.19 (2H, m, BC(CH₂)₂) (c), 7.24(3H, m, CH(CH)₂) (d).

¹³C NMR (CDCl₃): δ 14.6 (CH₃) (A), 41.2 (CH₂CH₃) (B), 125.6 (BC(CH)₂) (C), 126.5 (CH(CH)₂) (D), 131.6 (C(CH)₂) (E)

¹¹B NMR (CDCl₃): δ 34.05



3.27 Synthesis of Tris(diethyl)aminoborane:

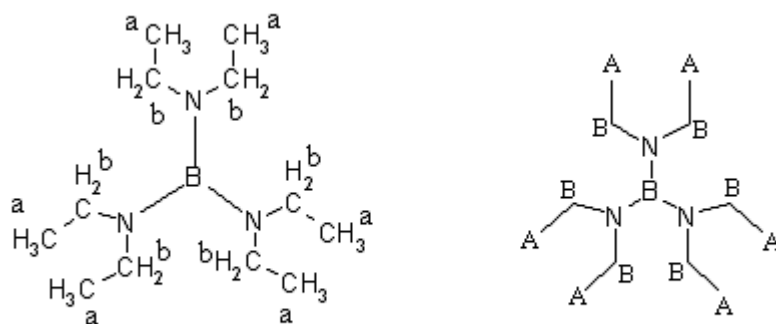
Boron trichloride (1 M soln. in heptane, 8.00 cm³, 8.0 mmol, was added dropwise to a stirring soln. of diethylamine (4.97 cm³, 48.0 mmol), in dry hexane (50.0 cm³). The soln. was stirred overnight. The resultant suspension was filtered and the filtrate reduced *in vacuo* to yield a viscous brown oil. This was distilled under reduced pressure at 120 °C to yield a clear, colourless liquid, characterised by ¹H, ¹³C and ¹¹B NMR spectroscopy.

Yield: 1.16 g (64 %)

^1H NMR (CDCl_3): δ 0.94 (9H, t, $J = 6.9$ Hz, CH_3) (a), 2.80 (6H, q, $J = 6.9$ Hz, CH_2) (b)

^{13}C NMR (CDCl_3): δ 15.7 (CH_2CH_3) (A), 40.7 (CH_2CH_3) (B)

^{11}B NMR (CDCl_3): δ 29.5



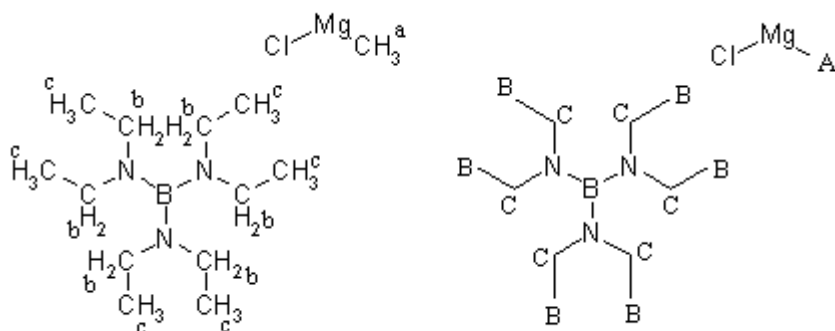
3.28 Attempted Reaction of Tris(diethyl)aminoborane with Methylmagnesium Chloride:

Tris(diethyl)aminoborane (0.2 g, 1.4 mmol) was dissolved in dry THF (10.0 cm^3). Methylmagnesium chloride (22 wt% soln in THF, 0.47 cm^3 , 1.4 mmol) was added dropwise, by syringe. The solution was stirred for 12 hrs, and characterised by ^1H , ^{13}C and ^{11}B NMR spectroscopy.

^1H NMR: (Discounting THF signals) δ -2.00 (3H, broad s, MgCH_3) (a), 0.81 (18H, t, $J = 7.2$ Hz, NCH_2CH_3) (b), 2.70 (12H, q, $J = 7.2$ Hz, NCH_2CH_3) (c)

^{13}C NMR: (Discounting THF signals) δ -17.2 (MgCH_3) (A), 14.5 (CH_3) (B), 40.2 (CH_2) (C)

^{11}B NMR: -16.6, 31.7(diminutive, possible trace decomposition product).



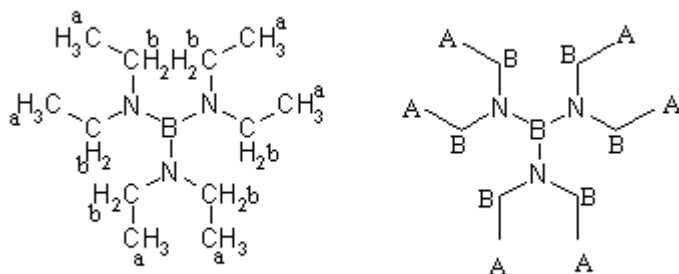
3.29 Attempted Reaction of Tris(diethyl)aminoborane with Lithium Diethylamide:

Diethylamine (0.14 cm³, 1.4 mmol) was dissolved in dry THF (10.0 cm³). To the solution was added n-butyl lithium (2.5 M soln in hexanes, 0.56 cm³, 1.4 mmol). The soln was stirred for 1 hr. To the solution was added tris(diethyl)aminoborane (0.2 g, 1.4 mmol). The solution was stirred for 12 hrs and the volatiles removed *in vacuo*. The residue was characterised by ¹H, ¹³C and ¹¹B NMR spectroscopy, in THF solution, revealing only tris(diethyl)aminoborane.

¹H NMR: (Discounting THF signals) δ 1.09 (18H, t, J = 7.2 Hz, NCH₂CH₃) (a), 3.00 (12H, q, J = 7.2 Hz, NCH₂CH₃) (b)

¹³C NMR: (Discounting THF signals) δ 14.2 (CH₃) (A), 39.9 (CH₂CH₃) (B)

¹¹B NMR: δ 31.4



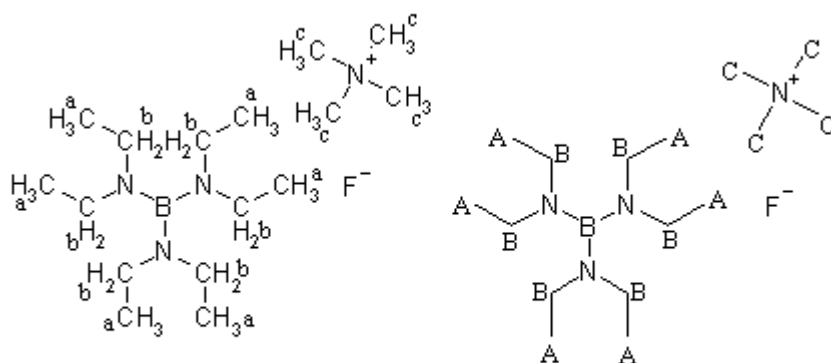
3.30 Attempted Reaction of Tris(diethyl)aminoborane with Tetramethylammonium Fluoride:

Tris(diethyl)aminoborane (0.2 g, 1.4 mmol) was dissolved in dry DCM (10.0 cm³). To the solution was added tetramethylammonium fluoride (0.13 g, 1.4 mmol). The solution was stirred for 12 hrs, and characterised by ¹H, ¹³C and ¹¹B NMR spectroscopy.

¹H NMR: δ 0.73 (18H, t, J = 6.9 Hz, NCH₂CH₃) (a), 2.63 (12H, q, J = 6.9 Hz, NCH₂CH₃) (b), 3.32 (9H, s, N(CH₃)₄) (c)

¹³C NMR: δ 14.2 (CH₃) (A), 39.6 (CH₂CH₃) (B), 55.0 (NCH₃) (C)

¹¹B NMR: δ 31.6



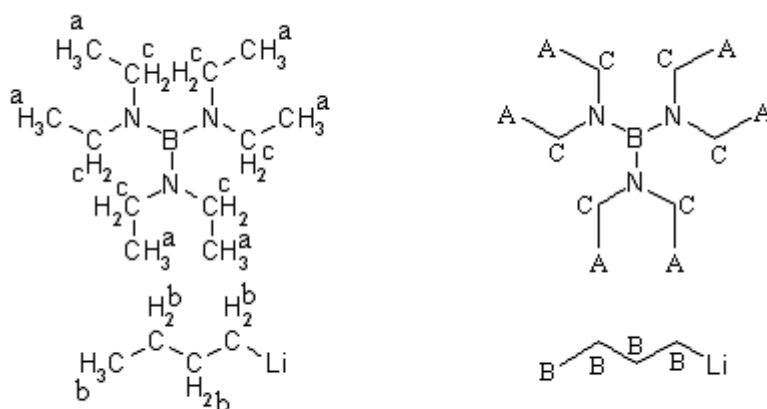
3.31 Attempted Reaction of Tris(diethyl)aminoborane with *n*-butyl Lithium:

Tris(diethyl)aminoborane (0.2 g, 1.4 mmol) was dissolved in dry hexane (20.0 cm³). To the solution was added *n*-Butyl Lithium (2.5 M soln. in hexanes, 0.56 cm³, 1.4 mmol). The solution was stirred for 12 hrs, and characterised by ¹H, ¹³C and ¹¹B NMR spectroscopy.

¹H NMR (C₆D₆): δ 0.84 (18H, t, J = 6.9 Hz, NCH₂CH₃) (a), 1.20 (9H, broad m, *BuLi*) (b) 2.74 (12H, q, J = 6.9 Hz, NCH₂CH₃) (c)

¹³C NMR (C₆D₆): δ 13.8 (NCH₂CH₃) (A), [13.0, 14.6, 21.8, 25.5, 27.3, 28.2, 30.7, 31.0, 39.3] (*BuLi* dimer, trimer, tetramer) (B), 41.2 (NCH₂CH₃) (C)

^{11}B NMR (C_6D_6): δ 29.7



3.32 Reaction of 1-Phenyl-2,5-di-tert-butyl-1-bora-2,5-diazacyclopentane with Tetramethylammonium Fluoride:

1-Phenyl-2,5-di-*tert*-butyl-1-bora-2,5-diazacyclopentane (0.20 g, 0.77 mmol) and tetramethylammonium fluoride (0.07 g, 0.77 mmol) were dissolved in dry DCM (10.0 cm^3). The solution was stirred overnight. The solution was reduced *in vacuo* to ca. 3 cm^3 and characterised by ^1H , ^{13}C , ^{11}B and ^{19}F NMR spectroscopy, in DCM soln.

^1H NMR- 2 sets of signals, set 'A' and set 'B'. Approx ratio A:B = 2:1; signal ratios within each set are relative to other signals within the set, and not between sets. As they are not otherwise distinguishable, the aromatic signal intensities are given relative to the sum of the integrals of set 'A' and set 'B':

[A: δ 0.87 (s, 18H, $\text{NC}(\text{CH}_3)_3$) (a) , 2.81 (s, 4H, $\text{N}(\text{CH}_2)_2\text{N}$) (b)],

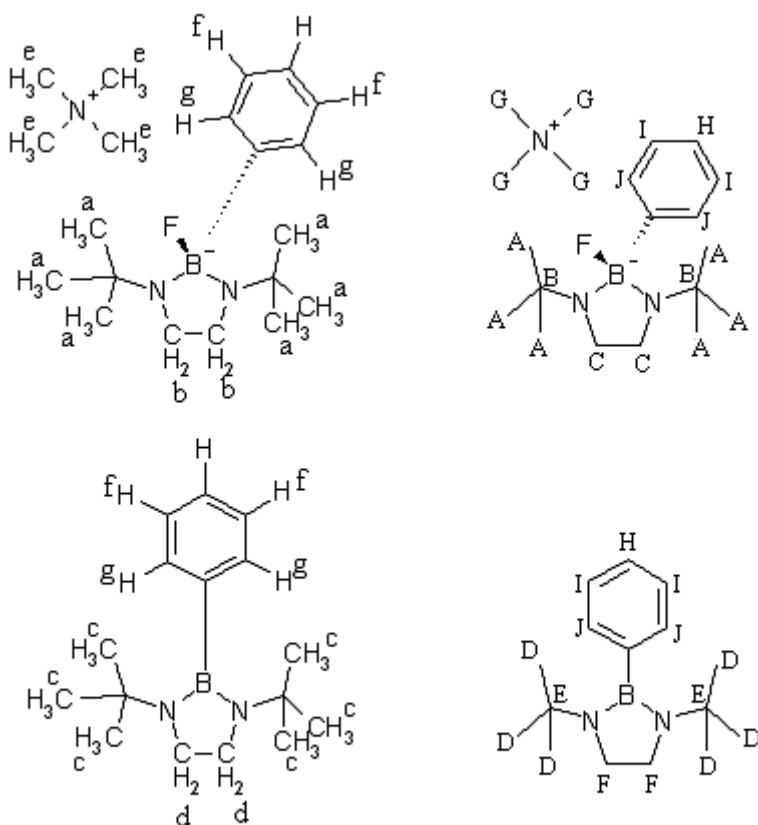
[B: δ 0.97 (s, 18H, $\text{NC}(\text{CH}_3)_3$) (c), 2.52 (s, 4H, $\text{N}(\text{CH}_2)_2\text{N}$) (d)],

3.21 (s, 12H, $\text{N}(\text{CH}_3)_4$) (e), 7.13 (d, 2H, $J = 4.4$ Hz, $\text{CH}(\text{CH})_2(\text{CH})_2\text{CB}$) (f), 7.21 (2H, d, $J = 4.4$ Hz, $\text{CH}(\text{CH})_2(\text{CH})_2\text{CB}$) (g).

^{13}C NMR: [A: δ 30.2 (A), 44.6 (B), 49.5 (C)], [B: δ 28.6 (D), 43.0 (E), 49.5 (F)], 55.3 (G), 126.0 (H), 126.5 (I), 132.1 (J)

^{11}B NMR: 7.1, 35.3

^{19}F NMR: δ -139.8 (25F, s), -135.9 (10F, s), -133.0 (13F, broad s)



The ^{11}B NMR spectrum of 1-phenyl-2,5-di-*tert*-butyl-1-bora-2,5-diazacyclopentane in DCM with one eq. of tetramethylammonium fluoride (1) was compared to that of 1-phenyl-2,5-di-*tert*-butyl-1-bora-2,5-diazacyclopentane in DCM with a large excess of tetramethylammonium fluoride (2). In both cases 2 signals were observed, and their relative ratios were determined as follows:

^{11}B NMR (1) (CDCl_3): δ 34.9 (relative integral: 1.00), 6.6 (d, $J = 56.6$ Hz, relative integral: 0.41).

^{11}B NMR (2) (CDCl_3): δ 34.6 (relative integral: 1.00), 6.5 (d, $J = 53.6$ Hz, relative integral: 0.95).

A sample of 1-phenyl-2,5-di-*tert*-butyl-1-bora-2,5-diazacyclopentane, and an excess of tetramethylammonium fluoride were dissolved in dry methanol, and characterised by ^1H , ^{13}C and ^{11}B NMR spectroscopy:

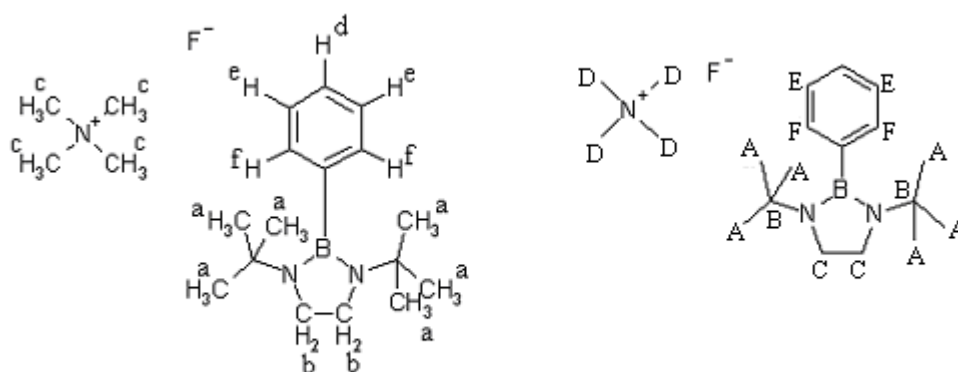
^1H NMR (CDCl_3) (Methanol solvent signals discounted): δ -0.32 (18H, s, CH_3) (a), 1.26 (4H, s, $\text{N}(\text{CH}_2)_2\text{N}$) (b), 1.67 (9H, s, $\text{N}(\text{CH}_3)_4$) (c), 5.55 (1H, d, $J = 7.2$ Hz,

(CH)₂CH) (d), 5.62 (2H, t, J = 7.2 Hz, (CH)₂CH) (e), 5.99 (2H, d, J = 6.6 Hz, (BC(CH)₂) (f)

¹³C NMR (CDCl₃) (Methanol solvent signals discounted): δ 22.0 (CH₃) (A), 42.3 C(CH₃)₃ (B), 52.3 N(CH₂)₂N (C), 55.4 (NCH₃) (D), 127.1 (CH(CH)₂) (E), 133.5 BC(CH)₂) (F)

¹¹B NMR (CDCl₃): δ 8.9

¹⁹F NMR (CDCl₃): δ -148.1 (broad s)



3.33 Complexation of 1-Phenyl-2,5-di-tert-butyl-1-bora-2,5-diazacyclopentane and Tetramethylammonium Fluoride, with Chromium III Chloride:

1-Phenyl-2,5-di-tert-butyl-1-bora-2,5-diazacyclopentane (1.0 g, 3.87 mmol) was dissolved in a mixture of dry DCM (30.0 cm³) and dry THF (30.0 cm³). To the solution was added NMe₄F (0.36 g, 3.87 mmol). The solution was stirred for 1 hr. To the resultant solution was added CrCl₃.THF₃ (1.45 g, 3.87 mmol). The soln. was stirred for 1 hr, and to the solution was added an excess of dry hexane. A bright purple solid was precipitated, which was removed by filtration, and the volatiles removed *in vacuo*.

Yield: 1.60 g (81%).

Elemental analysis (C₂₀H₃₉BCl₃CrFN₃):

Expected: C: 47.0%	H: 7.9%	N: 8.2%
Found: C: 45.6%	H: 7.9%	N: 8.2%

Electro-spray mass spectra were obtained. Notable signals in the cation spectrum (Sigma fits <0.05 indicates high probability of correct MF):

$m/z = 277.25$ (and ^{10}B isotope at 276.25) (cf. $\text{PhB}(\text{tert-BuNCH}_2)_2\cdot\text{H}_3\text{O}^+$: $m/z = 277.24$).

$m/z = 279.25$ (and ^{10}B isotope at 278.25) (cf. $[\text{Ph}(\text{F})\text{B}(\text{tert-BuN}(\text{H})\text{CH}_2)_2]^+$: $m/z = 279.23$).

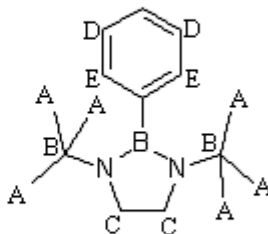
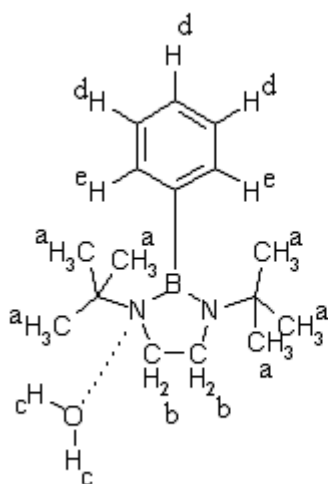
3.34 Reactivity of 1-phenyl-2,5-di-tert-butyl-1-bora-2,5-diazacyclopentane with De-ionised Water:

To a sample of 1-phenyl-2,5-di-tert-butyl-1-bora-2,5-diazacyclopentane in CDCl_3 was added an excess of de-ionised water. The resultant solution was characterised by ^1H , ^{13}C and ^{11}B NMR spectroscopy.

^1H NMR (CDCl_3): 1.08 (18 H, s, CH_3) (a), 2.67 (4H, s, $\text{N}(\text{CH}_2)_2\text{N}$) (b), 2.81 (4H, broad s, H_2O (coordinated)) (c), 4.78 (60H, s, H_2O), 7.27 (3H, broad s, $\text{CH}(\text{CH}_2)_2$) (d), 7.97 (2H, broad s, $\text{BC}(\text{CH}_2)_2$) (e):

^{13}C NMR (CDCl_3): 29.0 ($\text{C}(\text{CH}_3)_3$) (A), 42.8 ($\text{C}(\text{CH}_3)_3$) (B), 51.5 ($\text{N}(\text{CH}_2)_2\text{N}$) (C), 127.8 ($\text{CH}(\text{CH}_2)_2$) (D), 134.2 ($\text{BC}(\text{CH}_2)_2$) (E)

^{11}B NMR (CDCl_3): -3.9, 30.0



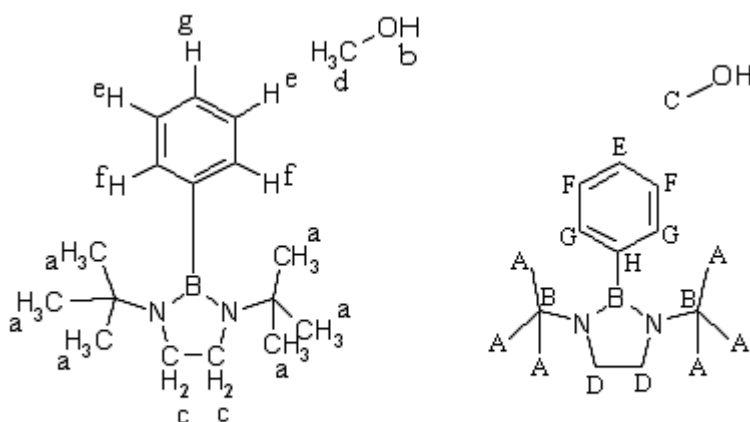
3.35 Attempted Reaction of 1-Phenyl -2,5-di-*tert*-butyl-1-bora-2,5-diazacyclopentane with Methanol:

1-Phenyl-2,5-di-*tert*-butyl-1-bora-2,5-diazacyclopentane (ca. 10 mg, 0.04 mmol) was dissolved in CDCl_3 (1.0 cm^3) in an NMR tube. To the solution was added ca. 5 eq. of dry methanol, dropwise by syringe. After standing for 12 hrs, the soln was characterised by ^1H , ^{13}C and ^{11}B NMR spectroscopy.

^1H NMR (CDCl_3): 1.11 (18H, s, $\text{NC}(\text{CH}_3)_3$) (a), 2.60 (5H, s, CH_3OH) (b), 2.64 (4H, s, $\text{N}(\text{CH}_2)_2\text{N}$) (c), 3.52 (s, 15 H, CH_3OH) (d), 7.36 (m, 2H, $\text{CH}(\text{CH})_2(\text{CH})_2\text{CB}$) (e), 7.61 (d, $J = 1.50 \text{ Hz}$, $\text{CH}(\text{CH})_2(\text{CH})_2\text{CB}$) (f), 7.97 (1H, m, $\text{CH}(\text{CH})_2(\text{CH})_2\text{CB}$) (g):

^{13}C NMR (CDCl_3): δ 29.2 (CH_3) (A), 43.1 ($\text{C}(\text{CH}_3)$) (B), 50.9 (CH_3OH) (C), 51.3 ($\text{N}(\text{CH}_2)_2\text{N}$) (D), 127.5 ($\text{CH}(\text{CH})_2$) (E), 128.1 ($\text{CH}(\text{CH})_2$) (F), 130.1 ($\text{BC}(\text{CH})_2$) (G), 133.8 (BC) (H)

^{11}B NMR (CDCl_3): δ 29.3

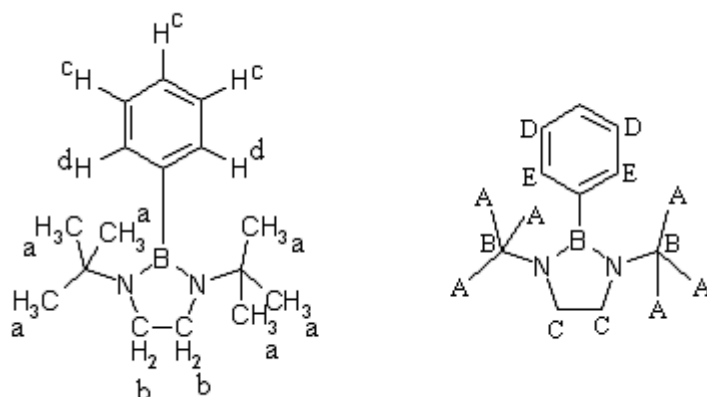


For comparison, a spectrum of the heterocycle was obtained in dry methanol solution:

^1H NMR: (MeOH signals discounted) δ 1.35 (18H, s, CH_3) (a), 2.98 (4H, s, $\text{N}(\text{CH}_2)_2\text{N}$) (b), 7.33 (3H, m, $\text{CH}(\text{CH})_2$) (c), 7.66 (2H, d, $J = 6.0 \text{ Hz}$, $\text{BC}(\text{CH})_2$) (d)

^{13}C NMR: δ 28.3 (CH_3) (A), 42.7 ($\text{C}(\text{CH}_3)_3$) (B), 54.1 ($\text{N}(\text{CH}_2)_2\text{N}$) (C), 128.1 ($\text{CH}(\text{CH})_2$) (D), 134.7 ($\text{BC}(\text{CH})_2$) (E)

^{11}B NMR: δ 15.5



3.36 Attempted Reaction of 1-Phenyl -2,5-di-tert-butyl-1-bora-2,5-diazacyclopentane with Sodium *n*-butoxide:

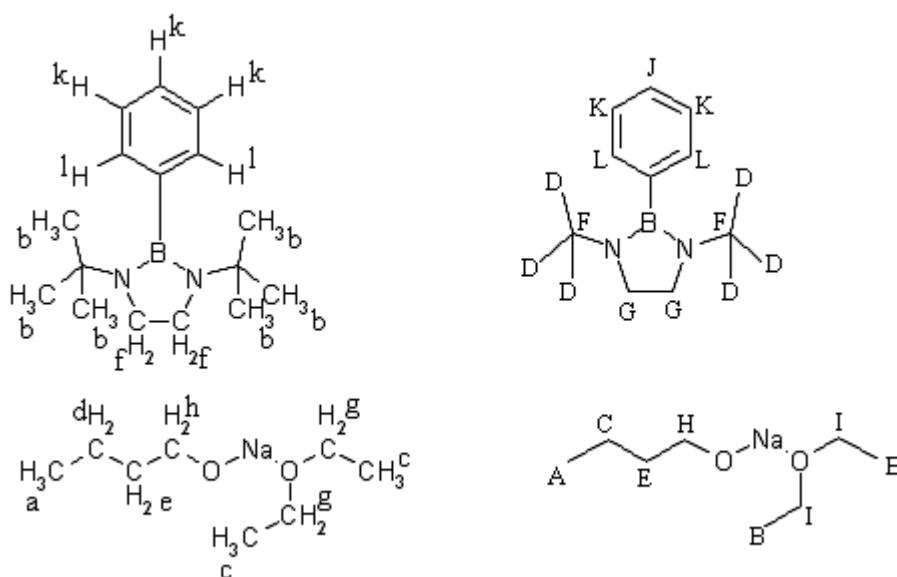
1-Phenyl -2,5-di-tert-butyl-1-bora-2,5-diazacyclopentane (0.10 g, 0.38 mmol) and sodium *n*-butoxide (0.38 mmol, 0.04 g), was dissolved in dry Et_2O (10.0 cm^3). The solution was stirred overnight. The solvent was removed *in vacuo* to yield a white solid. Characterised by ^1H , ^{13}C and ^{11}B NMR spectroscopy.

^1H NMR (CDCl_3): δ 0.87 (3H, t, $J = 7.5\text{ Hz}$, $\text{OC}_3\text{H}_6\text{CH}_3$) (a), 0.90 (18H, s, $\text{NC}(\text{CH}_3)_3$) (b), 1.14 (6H, s, diethyl ether) (c), 1.14 (2H, t, $J = 7.5\text{ Hz}$, $\text{OC}_2\text{H}_6\text{CH}_2\text{CH}_3$) (d), 1.48 (2H, t, $J = 7.5\text{ Hz}$, $\text{OCH}_2\text{CH}_2\text{C}_2\text{H}_5$) (e), 3.24 (4H, s, $\text{N}(\text{CH}_2)_2\text{N}$) (f), 3.42 (4H, s, diethyl ether) (g), 3.56 (2H, t, $J = 6.3\text{ Hz}$, OCH_2) (h), 7.15 (2H, m, $\text{CH}(\text{CH})_2(\text{CH})_2\text{CB}$) (i), 7.23 (2H, m, $\text{CH}(\text{CH})_2(\text{CH})_2\text{CB}$) (j).

Additional small peaks: 1.03 (7H, s), 2.57 (2H, s) [Consistent with free N,N' -di-tert-butylethylenediamine: δ 1.04, 2.57]⁸⁷

^{13}C NMR (CDCl_3): δ 14.3 ($\text{CH}_3\text{C}_3\text{H}_6\text{O}$) (A), 15.7 ($\text{CH}_3\text{CH}_2\text{O}$) (B), 19.3 ($\text{CH}_3\text{CH}_2\text{C}_2\text{H}_4\text{O}$) (C), 31.1 ($\text{C}(\text{CH}_3)_3$) (D), 35.3 ($\text{C}_2\text{H}_5\text{CH}_2\text{CH}_2\text{O}$) (E), 45.3 ($\text{C}(\text{CH}_3)_3$) (F), 52.1 ($\text{N}(\text{CH}_2)_2\text{N}$) (G), 62.9 ($\text{C}_3\text{H}_7\text{CH}_2\text{O}$) (H), 66.2 ($\text{CH}_3\text{CH}_2\text{O}$) (I), 126.7 ($\text{CH}(\text{CH})_2$) (J), 127.25 ($\text{CH}(\text{CH})_2$) (L), 132.8, ($\text{BC}(\text{CH})_2$) (L) (Additional small peaks: 29.5, 43.6, 50.4, [Consistent with free N,N' -di-tert-butylethylenediamine: δ 29.4, 43.6, 49.8]⁸⁷

^{11}B NMR (CDCl_3): δ 32.4



3.37 Attempted Reaction of 1-Phenyl -2,5-di-tert-butyl-1-bora-2,5-diazacyclopentane with Hexylmagnesium Bromide:

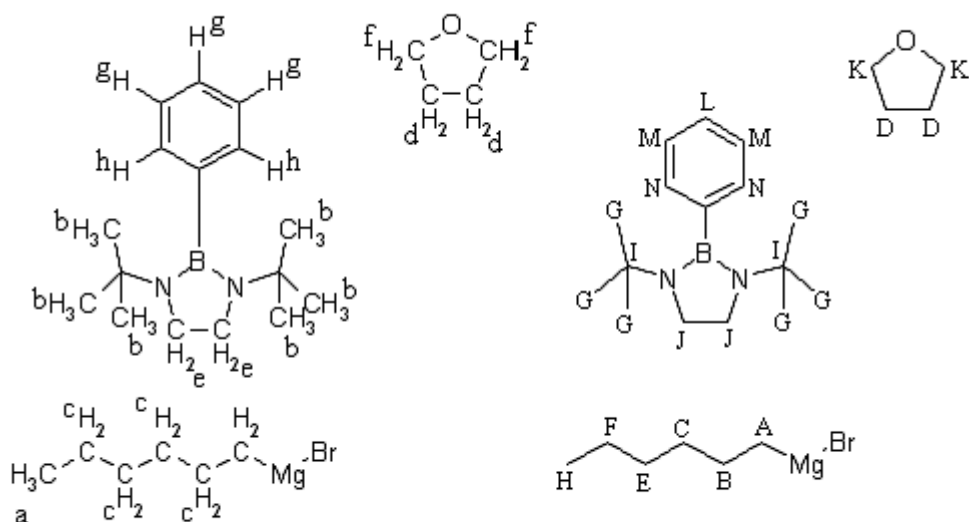
1-Phenyl -2,5-di-tert-butyl-1-bora-2,5-diazacyclopentane (0.10 g, 0.38 mmol) was dissolved in dry THF (10.0 cm³). To the solution was added dropwise, one equivalent of a freshly prepared soln of hexylmagnesium bromide in THF. (concentration determined by ¹H NMR spectroscopy, see ‘3.54 Determination of Concentration of Grignard Reagent in THF soln. Example method: Hexylmagnesium Bromide in THF’). The soln was stirred for 12 hrs, and characterised by ¹H, ¹³C and ¹¹B NMR spectroscopy.

¹H NMR: δ 1.01 (3H, t, J = 6.2 Hz, MgC₅H₁₀CH₃) (a), 1.08 (18H, s, C(CH₃)₃) (b), 1.41 (8H, broad m, MgCH₂C₄H₈) (c), 1.88 (THF) (d), 3.41 (4H, s, (NCH₂)₂N) (e), 3.76 (THF) (f), 7.30 (3H, m, BC(CH)₂(CH)₂CH) (g), 7.38 (m, 2H, BC(CH)₂(CH)₂CH) (h)

¹³C NMR: δ 14.1 (A), [23.2, 23.4] (B), [25.8, 26.0] (C), 26.2 (D), [29.9, 30.2] (E), 30.2, (F) 30.8 (G), [32.5, 32.7] (H), 45.3 (I), 51.9 (J), 68.0 (K), 126.9 (L), 127.3 (M), 132.8 (N)

(Where multiple signals are bracketed, they are attributed to the same carbon; such multiplicity is frequently observed in Grignard reagent THF soln, and is attributed to solvent effects).

^{11}B NMR: δ 35.1



3.38 Complexation of 1-Phenyl-2,5-di-tert-butyl-1-bora-2,5-diazacyclopentane and hexylmagnesium bromide to Chromium III Chloride:

1-Phenyl-2,5-di-tert-butyl-1-bora-2,5-diazacyclopentane (0.50 g, 1.94 mmol) was dissolved in dry THF (50.0 cm³). To the solution was added CrCl₃.THF₃ (0.73 g, 1.94 mmol). The soln. was stirred for 1 hr, after which one equivalent of a freshly prepared soln of hexylmagnesium bromide in THF was added, dropwise by syringe. The resultant soln. was stirred for 2 hrs. To the solution was added an excess of dry hexane. A pale green precipitate was formed. This was separated by filtration, and the volatiles removed *in vacuo*.

Yield: 0.92 g (78%).

Elemental Analysis (C₂₂H₄₀BBBrCl₃CrMgN₂):

Expected: C: 43.5%	H: 6.8%	N: 4.6%
Found: C: 26.7%	H: 5.2%	N: 0.7%

Electro-spray mass spectra were obtained. Notable signals in the cation spectrum (Sigma fits <0.05 indicates high probability of correct MF):

$m/z = 259.22$ (cf. $\text{PhB}(\text{tert-BuNCH}_2)_2.\text{H}^+$: $m/z = 259.23$).

$m/z = 277.24$ (and ^{10}B isotope at 276.22) (cf. $\text{PhB}(\text{tert-BuNCH}_2)_2.\text{H}_3\text{O}^+$: $m/z = 277.24$).

3.39 Attempted Reaction of 1-Phenyl-2,5-di-tert-butyl-1-bora-2,5-diazacyclopentane with n-Butyl Lithium:

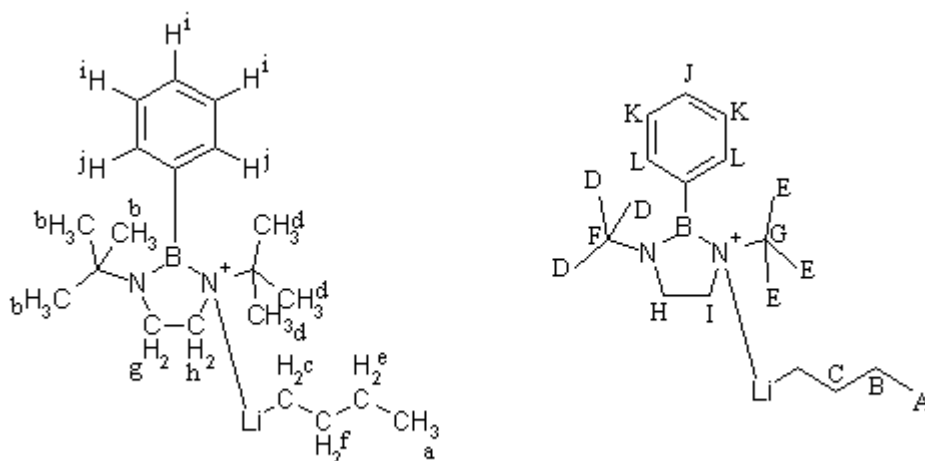
1-Phenyl-2,5-di-tert-butyl-1-bora-2,5-diazacyclopentane (0.10 g, 0.38 mmol) was dissolved in dry THF (10.0 cm³). To the solution was added n-butyl lithium (0.15 cm³). The solution was stirred for 12 hrs. Volatiles were removed in vacuo and the residue redissolved in dry C₆D₆ and characterised by ¹H, ¹³C and ¹¹B NMR spectroscopy.

¹H NMR (C₆D₆): δ 0.89 (3H, t, $J = 7.5$ Hz, CH₂CH₃) (a), 0.94 (s, 9H, NC(CH₃)₃) (b), 1.11 (2H, complex m, LiCH₂) (c), 1.16 (s, 9H, N⁺C(CH₃)₃) (d), 1.36 (2H, q, $J = 7.5$ Hz, CH₃CH₂) (e), 1.50 (2H, complex m, LiCH₂CH₂) (f), 2.94 (2H, s, NCH₂CH₂N⁺) (g), 3.10 (2H, s, NCH₂CH₂N⁺) (h), 7.09 (3H, complex m, CH(CH₂)₂) (i), 7.34 (2H, m, BC(CH)₂) (j).

¹³C NMR (C₆D₆): δ 12.7 (CH₂CH₃) (A), 25.7 (CH₂CH₃) (B), 27.7 (LiCH₂CH₂) (C), 29.3 (NC(CH₃)₃) (D), 29.6 (N⁺C(CH₃)) (E), 43.8 (NC(CH₃)₃) (F), 43.8 (N⁺C(CH₃)₃) (G), 50.3 (NCH₂) (H), 50.4 (N⁺CH₂) (I), 125.5 (CH(CH)₂) (J), 131.3 (CH(CH)₂) (K), (BC(CH)₂) (L).

(LiCH₂ signal is expected at ca. 10 ppm, but is not visible)

¹¹B NMR: δ 36.2



The ^1H and ^{13}C NMR spectra showed duplication of the heterocycle's aliphatic signals, suggesting a loss of symmetry. The ^{11}B NMR spectrum exhibited only a single signal. This suggests that coordination of the heterocycle occurs via one of the two nitrogen centres. The absence of additional aromatic signals suggests no coordination via the boron centre however.

3.40 Attempted Reaction of Trimethyl(pentafluoro)phenylsilane with Boron Tribromide:

The reaction was attempted by the following methods, but in all cases no reaction was observed:

Trimethyl(pentafluoro)phenylsilane (1.0 cm^3 , 5.2 mmol) and boron tribromide (0.50 cm^3 , 5.2 mmol) were heated at 80°C for 24 hrs in a distillation apparatus. The resultant mixture was characterised by ^{11}B NMR spectroscopy.

Trimethyl(pentafluoro)phenylsilane (1.0 cm^3 , 5.2 mmol) and boron tribromide (0.50 cm^3 , 5.2 mmol) were dissolved in dry DCM (10.00 cm^3) and heated at 40°C for 24 hrs in a distillation apparatus. The resultant mixture was characterised by ^{11}B NMR spectroscopy.

Trimethyl(pentafluoro)phenylsilane (1.0 cm^3 , 5.2 mmol) and boron tribromide (0.50 cm^3 , 5.2 mmol) were heated at 120°C for 48 hrs, with stirring, in a sealed pressure vessel. A black insoluble residue was formed. The remaining liquid was characterised by ^{11}B NMR spectroscopy.

3.41 Attempted Reaction of Trimethyl(pentafluoro)phenylsilane with Boron

Trichloride:

The reaction was attempted by the following methods, but in each case no reaction was observed:

Trimethyl(pentafluoro)phenylsilane (1.0 cm³, 5.2 mmol) and boron trichloride (1 M soln. in hexanes, 5.2 cm³, 5.2 mmol) were dissolved in dry DCM (30.00 cm³) and heated at 40°C for 24 hrs in a distillation apparatus. The resultant mixture was characterised by ¹¹B NMR spectroscopy.

Trimethyl(pentafluoro)phenylsilane (1.0 cm³, 5.2 mmol) and boron trichloride (1 M soln. in hexanes, 5.2 cm³, 5.2 cm³, 5.2 mmol) were heated at 120°C for 48 hrs, with stirring, in a sealed pressure vessel. A black insoluble residue was formed. The remaining liquid was characterised by ¹¹B NMR spectroscopy.

3.42 Attempted Reaction of 3,5-bis(trifluoromethyl)phenyltrimethylsilane with Boron tribromide:

The reaction was attempted by the following methods, but in each case no reaction was observed:

3,5-bis(trifluoromethyl)phenyltrimethylsilane (1.49g, 5.2 mmol) and boron tribromide (0.50 cm³, 5.2 mmol) were heated at 80°C for 24 hrs in a distillation apparatus. A black insoluble residue was formed. The remaining liquid was characterised by ¹¹B NMR spectroscopy.

3,5-bis(trifluoromethyl)phenyltrimethylsilane (1.49g, 5.2 mmol) and boron tribromide (0.50 cm³, 5.2 mmol) were dissolved in dry DCM (10.00 cm³) and heated at 40°C for 24 hrs in a distillation apparatus. A black insoluble residue was formed. The remaining liquid was characterised by ¹¹B NMR spectroscopy.

3,5-bis(trifluoromethyl)phenyltrimethylsilane (1.49g, 5.2 mmol) and boron tribromide (0.50 cm³, 5.2 mmol) were heated at 120°C for 48 hrs, with stirring, in a sealed pressure vessel. A black insoluble residue was formed. The remaining liquid was characterised by ¹¹B NMR spectroscopy.

3.43 Attempted Reaction of 3,5-bis(trifluoromethyl)phenyltrimethylsilane with Boron Trichloride:

The reaction was attempted by the following methods, but in each case no reaction was observed:

3,5-bis(trifluoromethyl)phenyltrimethylsilane (1.49g, 5.2 mmol) and boron trichloride (1 M soln. in hexanes, 5.2 cm³, 5.2 mmol) were dissolved in dry DCM (30.00 cm³) and heated at 40°C for 24 hrs in a distillation apparatus. A black insoluble residue was formed. The remaining liquid was characterised by ¹¹B NMR spectroscopy.

3,5-bis(trifluoromethyl)phenyltrimethylsilane (1.49g, 5.2 mmol) and boron trichloride (1 M soln. in hexanes, 5.2 cm³, 5.2 cm³, 5.2 mmol) were heated at 120°C for 48 hrs, with stirring, in a sealed pressure vessel. A black insoluble residue was formed. The remaining liquid was characterised by ¹¹B NMR spectroscopy.

3.44 Synthesis of Sodium Phenyl(Bis-hydroxy)Butoxyborate:

Phenylboronic acid (1.27 g, 10.4 mmol) and sodium n-butoxide (1.0 g, 10.4 mmol), were dissolved in dry THF (50.0 cm³). The solution was stirred for 12 hrs. The solvent was removed *in vacuo* and the resultant semi-crystalline solid characterised by ¹H and ¹³C NMR spectroscopy.

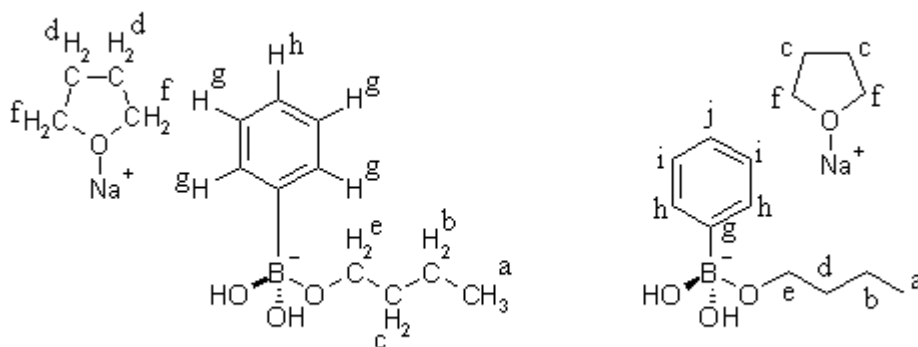
Yield: 1.89 g (83%).

¹H NMR (CDCl₃) (Poorly resolved): δ 0.66 (3H, t, J = 6.6 Hz, OC₃H₆CH₃) (a), 1.04 (2H, broad s, OC₂H₄CH₂CH₃) (b), 1.17 (2H, broad s, OCH₂CH₂C₂H₅) (c), 1.58 (4H, t, J = 6.3 Hz, THF) (d), 3.24 (2H, broad s, OCH₂) (e), 3.47 (4H, t, J = 6.3 Hz, THF) (f), 7.10 (4H, m, CH(CH)₂(CH)₂CB) (g), 7.72 (1H, d, J = 6.3 Hz, CH(CH)₂(CH)₂CB) (h)

¹³C NMR (CDCl₃): δ 14.2 (CH₃) (a), 19.1 (CH₂CH₃) (b), 25.9 (THF) (c), 35.1 (OCH₂CH₂) (d), 63.2 (OCH₂) (e), 68.4 (THF) (f), 128.2 (g), 130.8 (h), 131.3 (i), 134.9 (j)

¹¹B NMR (CDCl₃): δ 4.47, 29.39 (diminutive)

[¹¹B NMR spectrum of phenylboronic acid, for comparison (CDCl₃): δ 9.33] ⁸⁸



3.45 Complexation of Sodium Phenyl (Bis-hydroxy)butoxyborate:

Sodium Phenyl (Bis-hydroxy)butoxyborate (1.0 g, 4.59 mmol), was dissolved in dry THF (50.0 cm³). To the solution was added CrCl₃.THF₃ (1.72 g, 4.59 mmol). The soln was stirred for 2 hrs. The solution was reduced *in vacuo* to ca. 5 cm³, and an excess of dry diethyl ether added. A green precipitate was formed. This was separated by filtration and volatiles removed *in vacuo*.

Yield: 0.91 g (53%).

Elemental Analysis (C₁₀H₁₄BCl₃CrNaO₃):

Expected:	C: 31.9%	H: 4.3%	N: 0.0%
Found:	C: 22.8%	H: 4.6%	N: 0.16%

3.46 Synthesis of 1-keto-2,5-di-tert-butyl-2,5-diazacyclopentane:

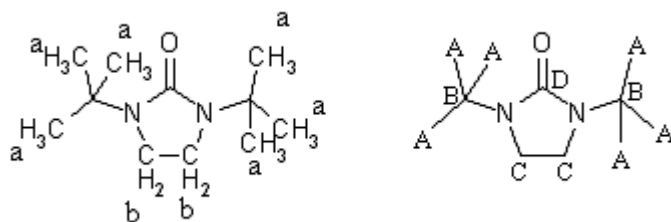
A mixture of N,N'-di-tert-butylethylenediamine (3.00 cm³, 13.9 mmol) and diphenylcarbonate (3.0 g, 14.0 mmol) was stirred at 190°C for 48 hrs, in a distillation apparatus. Phenol was produced and was removed by sublimation. The resultant mixture was cooled to room temperature and characterised by ¹H and ¹³C NMR spectroscopy, showing a mixture of the desired product and phenol. The mixture was dissolved in hexane and the solution extracted with water (15 x 20 cm³). The hexane fraction was reduced *in vacuo* to yield a white crystalline solid. This was characterised by ¹H and ¹³C NMR spectroscopy, and by single crystal X-ray diffraction: A saturated soln. was prepared in hexane, and the solution cooled to -18°C. Crystals formed over a period of 24 hrs.

Yield: 1.10 g (40%).

Melting Point: 73.9-75.1 °C

^1H NMR (C_6D_6): δ 1.22 (18H, s, $\text{C}(\text{CH}_3)_3$) (a), 2.57 (4H, s, NCH_2) (b)

^{13}C NMR (C_6D_6): δ 26.0 (CH_3) (A), 39.0 ($\text{C}(\text{CH}_3)_3$) (B), 51.4 ($\text{N}(\text{CH}_2)_2\text{N}$) (C), 160.3 (CO) (D)



X-Ray Crystallographic Data: See Appendix 2.

3.47 Complexation of 1-keto-2,5-di-tert-butyl-2,5-diazacyclopentane:

1-keto-2,5-di-tert-butyl-2,5-diazacyclopentane (0.5 g, 2.52 mmol) was dissolved in dry THF (50.0 cm^3). To the solution was added $\text{CrCl}_3 \cdot \text{THF}_3$ (0.94 g, 2.52 mmol). The solution was stirred for 2 hrs. To the solution was added an excess of dry hexane. A purple precipitate was formed. This was separated by filtration, and the volatiles removed *in vacuo*.

Yield: 0.35 g (39%).

Elemental Analysis ($\text{C}_{11}\text{H}_{22}\text{Cl}_3\text{CrN}_2\text{O}$):

Expected: C: 41.9% H: 7.3% N: 6.5%

Found: C: 26.3% H: 5.6% N: 0.7%

(Low N content suggests poor complexation- majority of product is likely to be $\text{CrCl}_3 \cdot \text{THF}_3$).

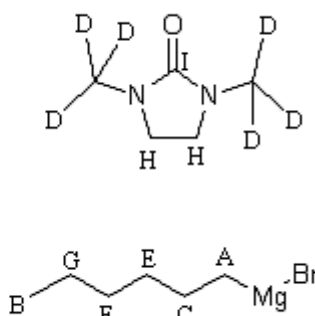
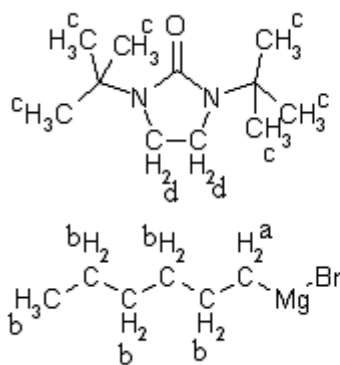
3.48 Attempted Reaction of 1-keto-2,5-di-tert-butyl-2,5-diazacyclopentane with Hexylmagnesium Bromide:

1-keto-2,5-di-tert-butyl-2,5-diazacyclopentane (0.20 g, 1.00 mmol) was dissolved in dry Et_2O (10.0 cm^3). To this solution was added one equivalent of a freshly prepared solution of hexylmagnesium bromide in dry THF (concentration determined

by ^1H NMR spectroscopy, see '3.54 Determination of Concentration of Grignard reagent in THF soln. Example Method: Hexylmagnesium Bromide in THF'. The solution was stirred for 12 hrs, then characterised by ^1H and ^{13}C NMR spectroscopy. ^1H NMR: Most reagent signals cannot be properly resolved. [δ 1.18 (45H, t, $J = 6.6$ Hz), 3.43 (30H, q, $J = 6.6$ Hz): Et_2O] [δ 1.85 (113H, broad s), 3.73 (113H, broad s): THF],

δ -0.47 (2H, t, $J = 6.9$ Hz, MgCH_2) (a), 0.98 (broad s, 11H, $\text{MgCH}_2\text{C}_5\text{H}_{11}$) (b), 1.39 (broad s, ~18H, $\text{C}(\text{CH}_3)_3$) (c), 1.63 (broad s, ~4H, $\text{N}(\text{CH}_2)_2\text{N}$) (d).

^{13}C NMR (THF and Et_2O signals discounted): δ 14.0 (MgCH_2) (A), 14.4 (CH_2CH_3) (B), [23.1, 23.5] (MgCH_2CH_2) (C), 27.3 ($\text{C}(\text{CH}_3)_3$) (D), [29.8, 30.1] ($\text{MgC}_2\text{H}_4\text{CH}_2$) (E), 32.1 ($\text{CH}_2\text{C}_2\text{H}_5$) (F), [32.4, 32.7] (CH_3CH_2) (G), 40.8 $\text{N}(\text{CH}_2)_2\text{N}$ (H), 161.8 (CO) (I) (Multiplicity of signals assumed to be due to solvent effects).



3.49 Complexation of 1-keto-2,5-di-tert-butyl-2,5-diazacyclopentane and Hexylmagnesium Bromide with Chromium III Chloride:

1-keto-2,5-di-tert-butyl-2,5-diazacyclopentane (0.5 g, 2.52 mmol) was dissolved in dry THF (50.0 cm^3). To the soln was added $\text{CrCl}_3 \cdot \text{THF}_3$ (0.94 g, 2.52 mmol). The solution was stirred for 2 hrs. To the soln was added 1 equivalent of a freshly prepared soln. of hexylmagnesium bromide in THF, dropwise by syringe. The soln was stirred for 2 hrs. To the solution was added excess dry hexane. A pale green precipitate was formed. This was separated by filtration, and volatiles removed *in vacuo*.

Yield: 0.73 g (53%).

Elemental Analysis ($C_{17}H_{35}BrCl_3CrMgN_2O$):

Expected: C: 37.3% H: 6.8% N: 5.1%

Found: C: 25.0% H: 3.0% N: 5.7%

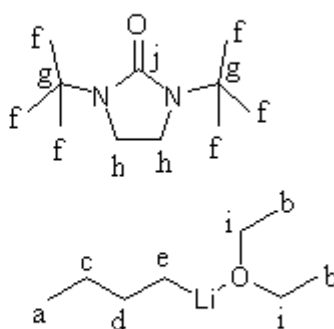
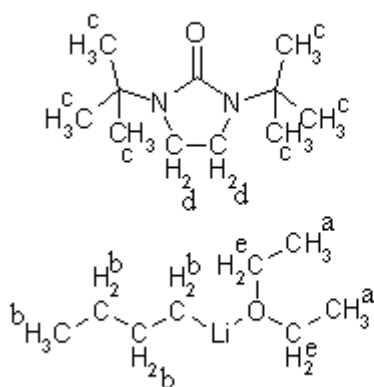
(Low C and N values suggest excess $CrCl_3$ and Mg content).

3.50 Attempted Reaction of 1-keto-2,5-di-tert-butyl-2,5-diazacyclopentane with n-butyl Lithium:

1-keto-2,5-di-*tert*-butyl-2,5-diazacyclopentane (0.20 g, 1.0 mmol) was dissolved in dry diethyl ether (10.0 cm^3). *N*-Butyl lithium (2.5 M soln in hexanes, 0.40 cm^3 , 1.0 mmol) was added dropwise to the solution, which was then stirred at room temperature for 12 hrs. The solvent was removed *in vacuo* and the residue characterised by 1H and ^{13}C NMR spectroscopy.

1H NMR (C_6D_6): 1.17 (6H, t, $J = 6.9\text{ Hz}$, Et_2O) (a), 1.31 (9H, m, *n*-BuLi) (b), 1.37 (18H, s, $C(CH_3)_3$) (c), 2.76 (4H, s, $N(CH_2)_2N$) (d), 3.33 (4H, q, $J = 6.9\text{ Hz}$, Et_2O) (e).

^{13}C (C_6D_6): 12.6 ($CH_3C_3H_6Li$) (a), 13.5 (Et_2O) (b), 14.2 ($CH_2C_2H_4Li$) (c), 21.7 (CH_2CH_2Li) (d), 23.8 (CH_2Li) (e), 26.1 ($C(CH_3)_3$) (f), 39.0 ($C(CH_3)_3$) (g), 51.5 ($N(CH_2)_2N$) (h), 64.5 (Et_2O) (i), 160.3 (CO) (j)



3.51 Synthesis of *N*-lithium-*N'*-phenylpiperazine:

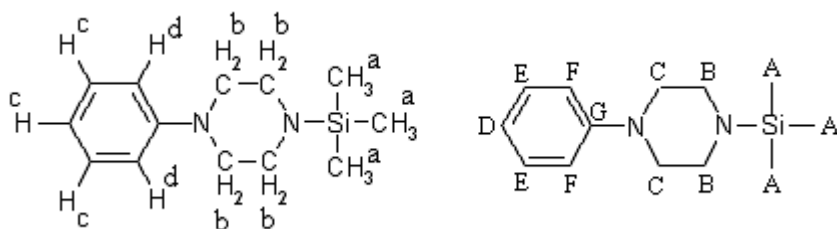
1-Phenylpiperazine (2.0 cm³, 13.1 mmol) was dissolved in dry hexane (50 cm³). To the solution was added *n*-butyl lithium (2.5 M soln. in hexanes, 5.24 cm³, 13.1 mmol). The resulting suspension was stirred overnight. The lithiated species was not isolated, but was reacted directly with chlorotrimethylsilane to produce *N*-phenyl-*N'*-trimethylsilylpiperazine.

3.52 Synthesis of *N*-phenyl-*N'*-trimethylsilylpiperazine:

To a suspension of *N*-lithium-*N'*-phenylpiperazine (13.1 mmol) in hexane (50 cm³) was added freshly distilled chlorotrimethylsilane (1.67 cm³, 13.1 mmol), dropwise at room temperature. The suspension was stirred overnight. The suspension was filtered and the filtrate reduced *in vacuo* and distilled at reduced pressure at 120 °C to yield a colourless oil. Characterised by ¹H and ¹³C NMR spectroscopy. Yield: 2.44 g (79%).

¹H NMR (CDCl₃): δ 0.00 (9H, s, Si(CH₃)₃) (a), 2.92 (8H, broad s, N(CH₂)₂N) (b), 6.84 (3H, m, NC(CH₂)₂(C₃H₃)) (c), 7.17 (m, 2H, NC(CH₂)₂(C₃H₃)) (d):

¹³C NMR (CDCl₃): δ 0.0 (SiCH₃) (A), 46.3 (SiN(CH₂)₂) (B), 51.8 (PhN(CH₂)₂) (C), 117.0 (CH(CH₂)₂) (D), 120.4 (CH(CH₂)₂) (E), 130.0 (NC(CH₂)₂) (F), 153.1 (NC(CH₂)₂) (G)



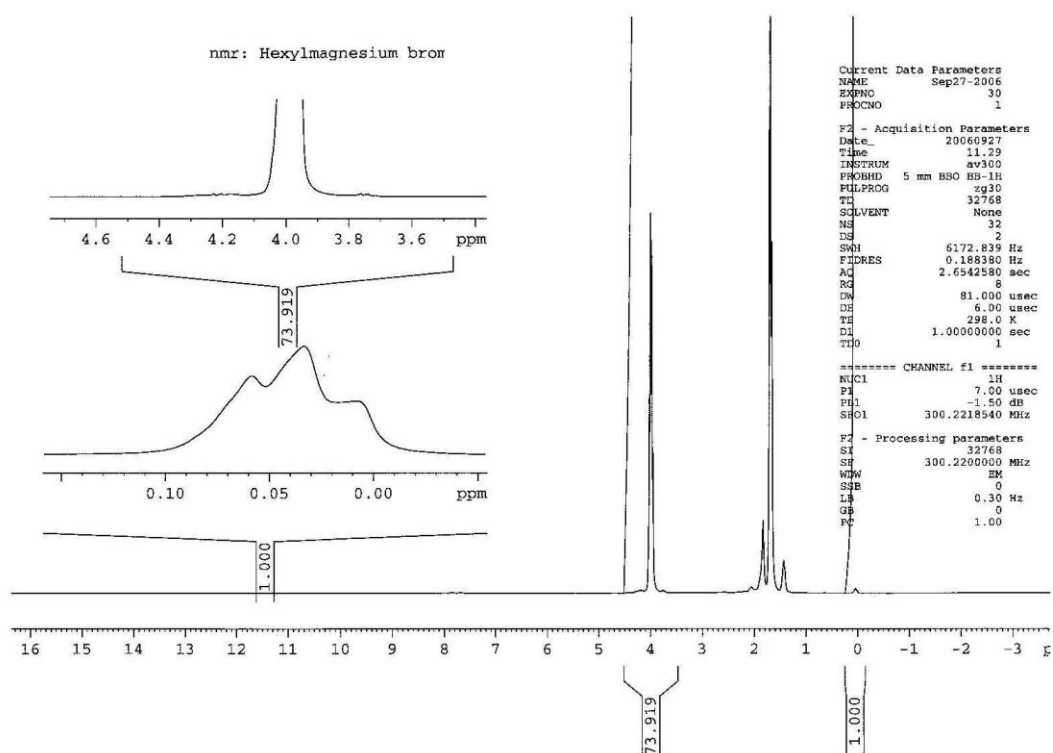
3.53 Attempted Synthesis of Lithium *N*-triphenylborato-*N'*-phenylpiperazine:

1-Phenylpiperazine (1.0 cm³, 6.6 mmol) was dissolved in dry THF (50 cm³). To the solution was added *n*-butyl lithium (2.5 M soln. in hexanes, 2.62 cm³, 6.6 mmol). The resulting solution was stirred overnight. The solution was cooled to -78 °C and to

it was added dropwise a solution of triphenylborane (1.58 g, 6.6 mmol) in dry THF (10 cm³). The solution was allowed to warm to room temperature and stirred overnight. An attempt was made to isolate the product by precipitation upon addition of hexane. No boron containing species could be identified in the resultant solid.

3.54 Determination of Concentration of Grignard Reagent in THF soln. Example method: Hexylmagnesium Bromide in THF:

Example method:



For ¹H NMR spectrum of a solution of Hexylmagnesium Bromide in THF, signal MgCH₂ is distinct- at -0.46 ppm, integral = 1.00, (2H). Relative integral of THF signal at 3.76 ppm = 73.92 (4H).

$$\therefore \text{THF (1H)} = 73.92/4 = 18.48$$

$$\text{Grignard (1H)} = \frac{1}{2} = 0.5$$

$$\text{Ratio of Grignard reagent to solvent} = 5:18.48 = 1:36.96$$

Concentration of neat THF = 889 gdm^{-3} , = 12.3 moldm^{-3} .

\therefore Concentration of Grignard reagent = $12.33/36.96 = \underline{0.33 \text{ moldm}^{-3}}$.

3.55 Determination of Magnetic Moment (and hence Oxidation State) of a Chromium Complex in Solution, by an Approximation of the Evans Method:

The relationship between chemical shift of a solution of a given substance(s), relative to the chemical shift of the neat solvent; and the magnetic moment of the substance, is given thus:

$$\frac{3\delta[\text{ppm}]}{4\pi} = \frac{m_x}{V} \chi_x^{\text{para}} + \frac{m_x}{V} \chi_x^{\text{dia}} + \frac{m_y}{V} \chi_y + \left(\frac{m_L}{V} - d_L \right) \chi_L$$

Where:

$$\chi_x^{\text{para}} [10^{-6} \text{ cgs}] = 10^6 \frac{(\mu_{\text{eff}} / \mu_B)^2}{8.066 \cdot T \cdot M_w^x} \dots \text{and} \dots \chi^{\text{dia}} [10^{-6} \text{ cgs}] = \frac{\chi_M^{\text{dia}}}{M_w}$$

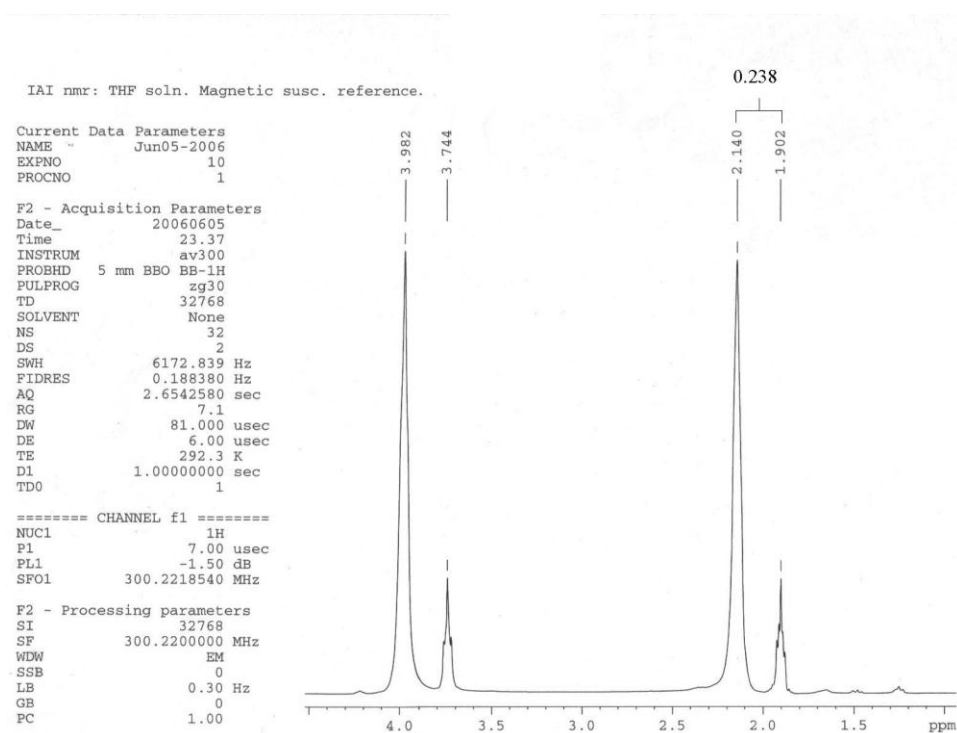
For a solution of a paramagnetic substance, this equation may be approximated thus:

$$\frac{3\delta[\text{ppm}]}{4\pi} = \frac{m_x}{V} \chi_x^{\text{para}}$$

$$\chi_x^{\text{para}} [10^{-6} \text{ cgs}] = 10^6 \frac{(\mu_{\text{eff}} / \mu_B)^2}{8.066 \cdot T \cdot M_w^x}$$

Eg.

A soln. of Dodecyl₃TAC.CrCl₃. (0.50g) in THF soln. (76 cm³) was prepared. The following ¹H NMR spectrum was obtained subsequently, where the smaller set of signals = neat THF, obtained by addition of a sealed capillary tube of THF to the NMR sample. (M = RMM for Dodecyl₃TAC.CrCl₃. = 750.46)



Thus: $3\delta[\text{ppm}]/4\pi = (m/V)\chi$

$$\chi [10^{-6} \text{ cgs}] = 10^6(\mu/\mu_B)^2/8.066.T.M$$

$$3(0.238)/4\pi = [(0.50 \text{ g})/(76 \text{ cm}^3)]\chi$$

$$8.64[10^{-6} \text{ cgs}] = 10^6(\mu/\mu_B)^2/8.066(298)(750.46)$$

$$\therefore \chi = 8.64$$

$$\therefore (\mu/\mu_B)^2 = 15.59$$

$$(\mu/\mu_B) = 3.95$$

$(\mu/\mu_B)^2 = N(N+2)$, where N = no. of unpaired electrons. $N(N+2) = 15.59$, where $N =$ ca. 3. Therefore, Chromium in the sample exists in d^3 configuration. ie, Chromium(III).

4. Catalysis- NMR Interpretation:

In an effort to evaluate the trimerisation properties of some of the chromium-based systems thus far devised, catalytic (small) amounts of the various mixtures/complexes were added, along with an activator, to a solution of 1-hexene in hexane/toluene. The resultant sample was characterised by ^1H NMR spectroscopy at measured time intervals, up until a sufficient period had elapsed to ensure that any trimerisation reaction had gone to completion. By measuring the relative integrals of the various signals in the ^1H NMR spectra, the extent of reaction, and the mean product chain length was estimated in each case. (1-hexene may undergo isomerisation to internal hexenes, as well as oligomerisation; calculation of mean chain length of product allows the extent of trimerisation versus isomerisation to be evaluated).

The following systems were investigated:

Dodecyl₃TAC.CrCl₃ (For comparison).

OC(*tert*-BuNCH₂)₂ + CrCl₃.THF₃ + HexylMgBr

OC(*tert*-BuNCH₂)₂ + CrCl₃.THF₃

(2-Et)Hex₃TAC + NH₂C₆H₄CH₂ONa + CrCl₃.THF₃

(2-Et)Hex₃TAC + NH₂C₆H₄CH₂ONa + CrCl₃.THF₃ + B(C₆F₅)₃.Et₂O

PhB(*tert*-BuNCH₂)₂ + NMe₄F + CrCl₃.THF₃

PhB(*tert*-BuNCH₂)₂ + CrCl₃.THF₃

Na PhB(OH)₂OBu + CrCl₃.THF₃

For a given solution comprising toluene, MAO, 1-hexene and trimers and isomers thereof, (discounting the negligible concentration of catalytic species), the ratio of 1-hexene to products may be determined by ^1H NMR spectroscopy, by measurement of the integrals of the aliphatic versus the olefinic proton signals. Furthermore, the conversion of 1-hexene to products with time may be calculated, where a reference at $t = 0$ is available, by comparison of the olefinic signals to those of the toluene solvent.

Calculation of Mass % Conversion of 1-hexene to Products- Example Spectrum:
Catalysis of Ethylene Trimerisation by 1,3,5-Tris-dodecyl-1,3,5-triazacyclohexane:

The ^1H solution spectrum for a given system comprises the following signals, in order of increasing chemical shift:

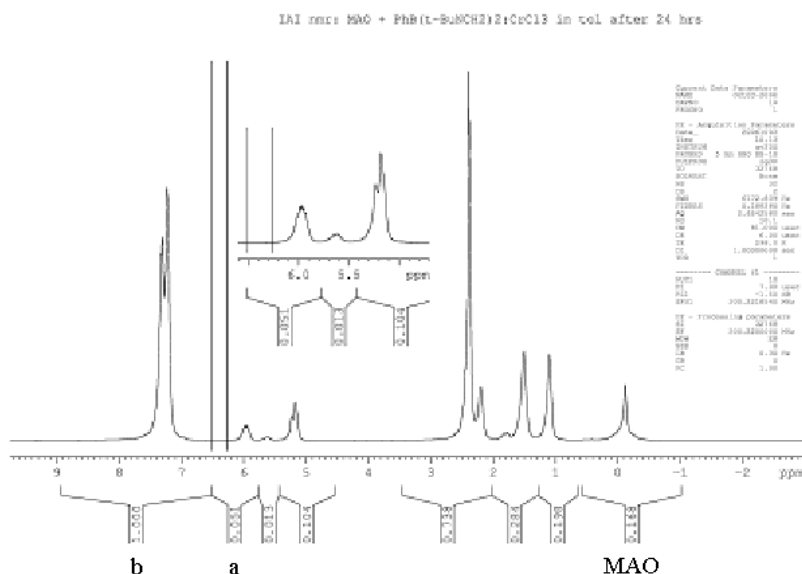


Figure 4.1: Typical ^1H NMR solution spectrum.

MAO aluminoxane

Aliphatic signals, representing 1-hexene, trimers, isomers and toluene CH_3 singlet.

All olefinic $\text{CH}_n=\text{CH}_n$ signals

Toluene aromatic signals (5H, m).

The starting material, 1-hexene, $\text{CH}_2=\text{CH}-\text{C}_4\text{H}_9$ exhibits 3 olefinic signals and 9 aliphatic signals in the ^1H NMR spectrum, of which the internal olefinic proton exhibits a distinct signal at ca. 6.2 ppm, to the left of the remaining olefinic signals. This signal is not exhibited by internal olefins.

1. The sum of the integrals of the signals attributable to 1-hexene (12 protons) may be given by $12 \times a = A$, where 'a' is the integral of the signal attributed to 1-hexene's lone, internal-olefinic proton.

2. The integral of the sum toluene aromatic signal 'b', can be measured separately, and represents 5 protons. Therefore, the integral of the aliphatic toluene signal = $3b/5$. Subtracting the aliphatic toluene signal from the total integral of the aliphatic and olefinic regions of the spectrum, 'c' (excluding the separate MAO signal), gives the sum of the protons of 1-hexene and all products, 'd'.

$$c - 3b/5 = d$$

3. Subtracting the previously determined integral of 1-hexene 'a', gives the total integral of the products of conversion of 1-hexene, 'e'.

$$d - A = e$$

4. The percentage conversion of 1-hexene to products, by mass is then given by $e/d \times 100\%$

Eg. For the trimerisation of 1-hexene by 1,3,5-Tris-dodecyl-1,3,5-triazacyclohexane, at $t = 0$,

$$1. A = 12 \times 10.00 = 120.00 \pm 1\%$$

$$2. b = 374.70,$$

$$c = 353.07 \pm 0.03\%$$

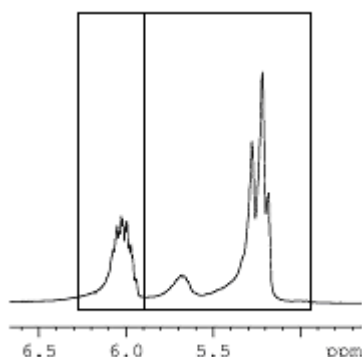
$$d = c - 3b/5 = 353.07 - 3(374.70)/5 = 128.25 \pm 0.14\%$$

$$3. e = d - A = 128.25 - 120.00 = 8.25 \pm 14.5\%$$

$$4. e/d \times 100\% = 6.40\% \pm 0.97\% \text{ (mass) conversion.}$$

Calculation of Mean Olefinic to Aliphatic Proton Ratio in 1-hexene Reaction Products:

The olefinic region comprises the characteristic 1-hexene signal at ca. 6.2 ppm, 'a' and a separate, complex signal, 'f' see figure 4.2:



a f
Figure 4.2:

The complex signal comprises the 2-proton, terminal olefinic signal of 1-hexene, and the total olefinic signals of all oligomerisation and isomerisation products. The integral of the 1-hexene terminal olefinic signal is given by $2 \times a$. Therefore, the total integral of the olefinic signals of the isomerisation and oligomerisation products, 'g', is given by

$$g = f - 2a$$

Similarly, the sum of the integrals of the aliphatic signals of the isomerisation and oligomerisation products can be determined by measuring 'h', the combined integral of all the aliphatic signals in the spectrum, after subtracting the integral of the toluene solvent aliphatic signal, $3b/5$ (see above). The sum of the 9 aliphatic proton signals attributable to 1-hexene is given by $9 \times a$.

Therefore, the total integral of the aliphatic signals of the isomerisation and oligomerisation products, 'i', is given

$$i = h - 9a$$

Eg. For the trimerisation of 1-hexene by 1,3,5-Tris-dodecyl-1,3,5-triazacyclohexane, at $t = 0$,

$$f = 20.64$$

$$g = f - 2a = 20.64 - 2(10.00) = 0.64$$

$$\text{Error margin for integrals} \sim \pm 0.1. \therefore g_{\text{minimum}} = 20.54 - 2(10.10) = 0.34$$

$$g_{\text{maximum}} = 20.74 - 2(9.9) = 0.94$$

$$\text{Therefore, error margin for } g = (0.94 - 0.64) / 0.64 \times 100 = \pm 47.00\%$$

$$h = 97.61 \pm 0.17\%$$

$$i = h - 9a = 97.61 - 90.00 = 7.61 \pm 14.00\%$$

Therefore, ratio of olefinic to aliphatic protons in the product = $0.64:7.61 = 1:11.9 \pm 41.50\%$

All products represent internal olefins, ie, comprise 2 olefinic protons, 2 CH₃ groups (6 aliphatic protons), and n CH₂ groups in the chain (2n aliphatic protons), see figure 4.3:

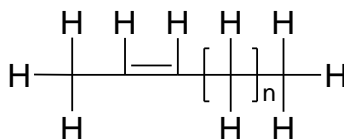


Figure 4.3:

Therefore, internal olefins possess a ratio of olefinic to aliphatic protons, given by the formula,

$2 : (6 + 2n)$, where the mean number of carbon atoms in the chain = $n + 4$, or where the mean number of hexene monomeric units = $(n + 4)/6$.

In this case, $1:11.9 = 2: 23.8$.

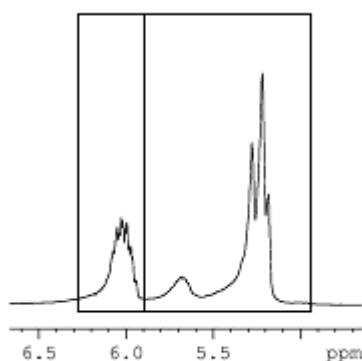
$$\therefore 6 + 2n = 23.8, 2n = 17.8, n = 8.9 \pm 41.50\%$$

This corresponds to an average chain-length of 12.9 carbons, or 2.2 1-hexene monomer units. $\pm 41.50\%$

Comparative Estimate of Product Chain Length:

Where the initial concentration of 1-hexene in solution is known, the mean chain-length of the products after a given time 't', can be estimated by comparison of the integrals of the olefinic signals of the initial spectrum, and the spectrum at time 't' (relative to the toluene solvent):

Initially, 1-hexene is taken to be the sole constituent of the olefinic signals.



N_1 M_1

Figure 4.4

The signals can be split into ' N_1 ', attributed to the single, internal olefinic proton, and ' M_1 ', attributed to the 2 terminal olefinic protons.

At time 't', the relative intensities of these signals will change- isomerisation does not alter the intensity of signal ' M_1 ', but does reduce the intensity of signal ' N_1 ', as the product contains no terminal olefinic protons.

Oligomerisation also causes a reduction in the intensity of signal ' N_1 ', and also reduces the intensity of signal ' M_1 '. Formation of an oligomer comprising 'x' monomer units, reduces the intensity of the olefin signal from $2x \rightarrow 2$. Therefore, for a given change in the intensity of signal ' N_1 ', the change in signal intensity of signal ' M_1 ', $= 2x - 2$.

Therefore, where the two signals for the spectrum at time 't' are given by ' N_2 ' and ' M_2 ',

$$\Delta M = (M_1 - M_2) = (2x - 2) \Delta N = (2x - 2)(N_1 - N_2).$$

$$((M_1 - M_2)/(N_1 - N_2) + 2)/2 = n$$

Eg. For the trimerisation of 1-hexene by 1,3,5-Tris-dodecyl-1,3,5-triazacyclohexane, from $t = 0$ to $t = 24$ hrs.

$$(7.09/5.50 + 2)/2 = n = 1.64 \text{ 1-hexene monomer units.}$$

Comparative Analysis of Trimerisation Properties 1,3,5-Tris-Dodecyl-1,3,5-triazacyclohexene- Chromium III Chloride Complex:

The complex was prepared by addition of 1,3,5-Tris-Dodecyl-1,3,5-triazacyclohexene to $\text{CrCl}_3 \cdot \text{THF}_3$ in THF solution, see 'Experimental' section.

A sample of 1,3,5-Tris-Dodecyl-1,3,5-triazacyclohexene- Chromium III Chloride (0.058 g) was dissolved in dry, degassed toluene (10.3 cm^3) To an NMR tube was added 0.244 g of this soln. (2.099×10^{-6} mol. To the resultant solution was added 200 eq. MAO (10% w/w soln. in toluene). To this solution was added dry, degassed 1-hexene, and the resultant sample characterized by ^1H NMR spectroscopy at intervals of 0, 3 and 24 hrs.

At $t = 0$:

See examples, above.

At $t = 3$ hrs:

Mass % conversion of 1-hexene to products:

$$1. a = 12 \times 1.00 = 12.00 \pm 1\%$$

$$2. b = 41.05$$

$$c = 42.5 \pm 0.02\%$$

$$d = c - 3b/5 = 42.50 - 3(41.05)/5 = 17.87 \pm 0.06\%$$

$$3. e = d - a = 17.87 - 12.00 = 5.87 \pm 2.2\%$$

$$4. e/d \times 100\% = \underline{32.8\% \pm 0.75\% \text{ mass conversion.}}$$

Mean olefinic to aliphatic proton ratio in 1-hexene reaction products:

$$f = 2.35 \pm 0.42\%$$

$$g = f - 2a = 2.35 - 2(1.00) = 0.35 \pm 6.50\%$$

$$h = 14.52 \pm 0.07\%$$

$$i = h - 9a = 14.52 - 9(1.00) = 5.52 \pm 10.00\%$$

Therefore, ratio of olefinic to aliphatic protons in the product = $0.35:5.52 = 1:15.8$

$$2 : (6 + 2n) = 2:31.5, n = 12.8 \pm 15.43\%.$$

Mean chain length = 16.8 carbons = 2.8 monomer units:

Comparative estimate of Product Chain Length 0 hrs \rightarrow 3hrs:

See examples, above.

At $t = 24$ hrs:

Mass % conversion of 1-hexene to products:

$$1. a = 12 \times 10.00 = 120.00 \pm 1\%$$

$$2. b = 435.01$$

$$c = 549.65 \pm 0.02\%$$

$$d = c - 3b/5 = 549.65 - 3(435.01)/5 = 288.64$$

$$3. e = d - a = 288.59 - 120.00 = 168.64 \pm 0.71\%$$

4. $e/d \times 100\% = \underline{58.4\% \pm 0.44\%}$ mass conversion.

Mean olefinic to aliphatic proton ratio in 1-hexene reaction products:

1:15.6 = 2:31.2

$n = 12.61 \pm 3.85\%$

Average chain-length of 16.6 carbons, or 2.8 1-hexene monomer units.

Comparative estimate of Product Chain Length 0 hrs \rightarrow 24hrs:

$n = 1.6$ 1-hexene monomer units.

Trimerisation Properties of 1-keto-2,5-di-*tert*-butyl-2,5-diazacyclopentane-Chromium III Chloride complex + Hexylmagnesium Bromide:

The complex was prepared by addition of 1-keto-2,5-di-*tert*-butyl-2,5-diazacyclopentane to $\text{CrCl}_3 \cdot \text{THF}_3$ in THF solution, and the subsequent addition of hexylmagnesium bromide solution in THF, see 'Experimental' section.

To an NMR tube containing 0.5 cm^3 of dry, degassed toluene was added 1-keto-2,5-di-*tert*-butyl-2,5-diazacyclopentane- Chromium III Chloride + Hexylmagnesium bromide (0.0027 g, $4.93 \times 10^{-6} \text{ mol}$ (calculation assumes $\text{OC}(\text{t-BuNCH}_2)_2\text{CrCl}_2\text{HexMgCl}_2$)). To the resultant suspension was added 200 eq. MAO (10% w/w soln. in toluene). To this suspension was added dry, degassed 1-hexene, and the resultant sample characterized by ^1H NMR spectroscopy at intervals of 0, 10 mins and 24 hrs.

At $t = 0 \text{ hrs}$:

Mass % conversion of 1-hexene to products: $22.60\% \pm 0.95\%$

*Mean olefinic to aliphatic proton ratio in 1-hexene reaction products: 1:12.5
±16.01%*

Average chain-length of 13.5 carbons, or 2.3 1-hexene monomer units.

At t = 10 mins:

Mass % conversion of 1-hexene to products: 16.90% ±0.89%

Mean olefinic to aliphatic proton ratio in 1-hexene reaction products: 1:14.5 ±19.6%

Average chain-length of 15.5 carbons, or 2.6 1-hexene monomer units.

At t = 48 hrs:

Mass % conversion of 1-hexene to products: 25.27% ±0.83%

*Mean olefinic to aliphatic proton ratio in 1-hexene reaction products: 1:16.10
±11.99%*

Average chain-length of 17.1 carbons, or 2.9 1-hexene monomer units.

Comparative estimate of Product Chain Length 0 hrs → 48 hrs: n = 2.3 1-hexene monomer units.

Trimerisation Properties of 1-keto-2,5-di-*tert*-butyl-2,5-diazacyclopentane-Chromium III Chloride Complex:

The complex was prepared by addition of 1-keto-2,5-di-*tert*-butyl-2,5-diazacyclopentane to CrCl₃.THF₃ in THF solution, see 'Experimental' section.

To an NMR tube containing 0.5 cm³ of dry, degassed toluene was added 1-keto-2,5-di-*tert*-butyl-2,5-diazacyclopentane- Chromium III Chloride (0.0016 g, 4.46 x 10⁻⁶ mol (calculation assumes OC(t-BuNCH₂)₂CrCl₃)). To the resultant suspension was added 200 eq. MAO (10% w/w soln. in toluene). To this suspension was added dry,

degassed 1-hexene, and the resultant sample characterized by ^1H NMR spectroscopy at intervals of 0, 24 and 48 hrs.

At t = 0 hrs:

Mass % conversion of 1-hexene to products: 9.46% \pm 1.02%

Mean olefinic to aliphatic proton ratio in 1-hexene reaction products:
(Signal intensities prohibit meaningful measurement).

At t = 24 hrs:

Mass % conversion of 1-hexene to products: 21.76% \pm 1.50%

Mean olefinic to aliphatic proton ratio in 1-hexene reaction products: 1:11.7
 \pm 17.89%

Average chain-length of 12.7 carbons, or 2.1 1-hexene monomer units.

At t = 48 hrs:

Mass % conversion of 1-hexene to products: 27.78% \pm 0.87%

Mean olefinic to aliphatic proton ratio in 1-hexene reaction products: 1:10.4
 \pm 10.63%

Average chain-length of 11.4 carbons, or 1.9 1-hexene monomer units.

Comparative estimate of Product Chain Length 0 hrs \rightarrow 24 hrs: n = 1.5 1-hexene monomer units.

**Trimerisation Properties of 1,3,5-tris(2-ethyl)hexyl-1,3,5-triazacyclohexane,
sodium 3-aminobenzylalcoholate + Chromium III Chloride:**

The system was prepared by addition of the 1,3,5-tris(2-ethyl)hexyl-1,3,5-triazacyclohexane, sodium 3-aminobenzylalcoholate mixture to $\text{CrCl}_3 \cdot \text{THF}_3$. (See 'Experimental' section).

To an NMR tube containing 0.5 cm^3 of dry, degassed toluene was added 1,3,5-tris(2-ethyl)hexyl-1,3,5-triazacyclohexane, sodium 3-aminobenzylalcoholate - CrCl_3 complex (0.0023g, $3.83 \times 10^{-6} \text{ mol}$). To the resultant suspension was added 200 eq. MAO (10% w/w soln. in toluene). To this suspension was added dry, degassed 1-hexene, and the resultant sample characterized by ^1H NMR spectroscopy at intervals of 0, 24 and 48 hrs.

At $t = 0$ hrs:

Mass % conversion of 1-hexene to products: $17.2\% \pm 0.93\%$

Mean olefinic to aliphatic proton ratio in 1-hexene reaction products: $1:17.8 \pm 3.15\%$

Average chain-length of 18.5 carbons, or 3.1 1-hexene monomer units.

At $t = 24$ hrs:

Mass % conversion of 1-hexene to products: $31.2\% \pm 0.72\%$

Mean olefinic to aliphatic proton ratio in 1-hexene reaction products: $1:7.6 \pm 5.52\%$

Average chain-length of 8.6 carbons, or 1.4 1-hexene monomer units.

At $t = 48$ hrs:

Mass % conversion of 1-hexene to products: $45.5\% \pm 0.60\%$

Mean olefinic to aliphatic proton ratio in 1-hexene reaction products: $1:9.7 \pm 2.30\%$

Average chain-length of 10.7 carbons, or 1.8 1-hexene monomer units.

Comparative estimate of Product Chain Length 0 hrs → 48 hrs: n = 2.3 1-hexene monomer units.

Trimerisation Properties of 1,3,5-tris(2-ethyl)hexyl-1,3,5-triazacyclohexane, sodium 3-aminobenzylalcoholate + Chromium III Chloride + 1 eq. Tris(pentafluoro)phenylborane:

The complex was prepared by addition of 1,3,5-tris(2-ethyl)hexyl-1,3,5-triazacyclohexane, sodium 3-aminobenzylalcoholate to CrCl₃.THF₃. (See 'Experimental' section).

To an NMR tube containing 0.5 cm³ of dry, degassed toluene was added 1-(4-Sodium oxymethyl)phenyl-3,5-(2-ethyl)hexyl-1,3,5-triazacyclohexane-CrCl₃ complex (0.0029 g, 4.83 x 10⁻⁶ mol). To the resultant suspension was added tris(pentafluorophenylborane diethyletherate (0.0030 g, ca. 1 eq), and 200 eq. MAO (10% w/w soln. in toluene). To this suspension was added dry, degassed 1-hexene, and the resultant sample characterized by ¹H NMR spectroscopy at intervals of 0 and 48 hrs.

At t = 0 hrs:

Mass % conversion of 1-hexene to products: 23.09% ±0.83%

Mean olefinic to aliphatic proton ratio in 1-hexene reaction products: 1:22.4 ±18.56%

Average chain-length of 23.4 carbons, or 3.9 1-hexene monomer units.

At t = 48 hrs:

Mass % conversion of 1-hexene to products: 43.18% ±0.66%

Mean olefinic to aliphatic proton ratio in 1-hexene reaction products: 1:8.7 ±4.54%

Average chain-length of 9.7 carbons, or 1.6 1-hexene monomer units.

Comparative estimate of Product Chain Length 0 hrs → 48 hrs: n = 1.00 1-hexene monomer units.

The suspension was characterised by ^{19}F NMR spectroscopy: ^{19}F NMR: δ -162.0, -161.0, -155.4, -152.4, -122.0. The major constituent appeared to be represented by δ -161.0 (s, 2F), -152.4 (s, 1F), -122.0 (s, 2F). cf. (Tris(pentafluoro)phenyl)borane: δ -164.6 (*m*), -144.3 (*p*), -128.6 (*o*)⁸⁹

Trimerisation Properties of 1-phenyl-2,5-di-*tert*-butyl-1-bora-2,5-diazacyclopentane- Chromium III Chloride Complex + Tetramethylammonium Fluoride:

The complex was prepared by addition of 1:1 1-phenyl-2,5-di-*tert*-butyl-1-bora-2,5-diazacyclopentane: tetramethylammonium fluoride to $\text{CrCl}_3 \cdot \text{THF}_3$ in THF solution, see 'Experimental' section.

To an NMR tube containing 0.5 cm^3 of dry, degassed toluene was added 1-phenyl-1-bora-2,5-di-*tert*-butyl-2,5-diazacyclopentane- Chromium III Chloride + tetramethylammonium fluoride (0.0023 g, 4.49×10^{-6} mol (calculation assumes $\text{PhBF}(\text{t-BuNCH}_2)_2\text{CrCl}_3\text{NMe}_4$)). To the resultant suspension was added 200 eq. MAO (10% w/w soln. in toluene). To this suspension was added dry, degassed 1-hexene, and the resultant sample characterized by ^{19}F and ^{11}B NMR spectroscopy, and by ^1H NMR spectroscopy at intervals of 0 and 24 hrs.

At $t = 0$ hrs:

Mass % conversion of 1-hexene to products: 9.15% \pm 1.04%

Mean olefinic to aliphatic proton ratio in 1-hexene reaction products: $1:6.1 \pm 32.32\%$

Average chain-length of 7.1 carbons, or 1.2 1-hexene monomer units.

At $t = 24$ hrs:

Mass % conversion of 1-hexene to products: 10.00% \pm 0.88%

Mean olefinic to aliphatic proton ratio in 1-hexene reaction products: 1:10.9
 \pm 20.58%

Average chain-length of 11.9 carbons, or 2.0 1-hexene monomer units.

Comparative estimate of Product Chain Length 0 hrs \rightarrow 48 hrs: $n = 3.5$ 1-hexene monomer units.

The suspension was characterised by ^{19}F and ^{11}B NMR spectroscopy.

^{11}B NMR: δ 4.68, 32.04, 86.73. The signals at $\delta = 4.68$ and 32.04 approximately correspond with those observed in the case of the free ligand, but the signal at 86.73 does not. It is hypothesized that this signal represents a boron compound in close proximity to the chromium centre.

^{19}F NMR: δ -175.7, -137.1, -82.0. cf. free ligand δ -139.8, -135.9, -133.0

A solution of $\text{PhB}(\text{tert-BuNCH}_2)_2 + \text{NMe}_4\text{F} + \text{MAO}$ in toluene was characterised by ^{11}B and ^{19}F NMR spectroscopy.

^{11}B NMR: δ 7.46, 36.8 cf. free ligand δ 7.1, 35.3. In the case of the free ligand, the signal at $\delta = \text{ca. } 35$ ppm represents the uncoordinated heterocycle, and is the major constituent. In the presence of MAO, the major boron signal occurs at 7.46 ppm, which is believed to be attributable to the quaternary species $[\text{NMe}_4]^+[\text{PhFB}(\text{tert-BuNCH}_2)_2]^-$.

^{19}F NMR: δ -81.5 cf. free ligand δ -139.8, -135.9, -133.0

Trimerisation Properties of 1-Phenyl-2,5-di-*tert*-butyl-1-bora-2,5-diazacyclopentane- Chromium III Chloride Complex:

The complex was prepared by addition of 1-Phenyl-2,5-di-*tert*-butyl-1-bora-2,5-diazacyclopentane to $\text{CrCl}_3 \cdot \text{THF}_3$ in THF solution, see 'Experimental' section.

To an NMR tube containing 0.5 cm³ of dry, degassed toluene was added 1-Phenyl-2,5-di-tert-butyl-1-bora-2,5-diazacyclopentane- Chromium III Chloride complex (0.0020 g, 4.55 x 10⁻⁶ mol (calculation assumes PhB(t-BuNCH₂)₂CrCl₃)). To the resultant suspension was added 200 eq. MAO (10% w/W soln. in toluene). To this suspension was added dry, degassed 1-hexene, and the resultant sample characterized by ¹¹B NMR spectroscopy and by ¹H NMR spectroscopy at intervals of 0, 24 and 48 hrs.

At t = 0 hrs:

Mass % conversion of 1-hexene to products: 13.33% ±15.09%

Mean olefinic to aliphatic proton ratio in 1-hexene reaction products: 1:12.9
±41.05%

Average chain-length of 13.9 carbons, or 2.3 1-hexene monomer units.

At t = 24 hrs:

Mass % conversion of 1-hexene to products: 22.33% ±1.87%

Mean olefinic to aliphatic proton ratio in 1-hexene reaction products: 1:10.8
±19.01%

Average chain-length of 11.8 carbons, or 2.0 1-hexene monomer units.

At t = 48 hrs:

Mass % conversion of 1-hexene to products: 25.29% ±1.89%

Mean olefinic to aliphatic proton ratio in 1-hexene reaction products: 1:10.1 ±7.75%
Average chain-length of 11.1 carbons, or 1.9 1-hexene monomer units.

Comparative estimate of Product Chain Length 0 hrs → 48 hrs: n = 1.2 1-hexene monomer units.

The suspension was characterised by ^{11}B NMR spectroscopy.

^{11}B NMR: δ 89.9, which compares closely to a signal exhibited by the suspension $\text{PhB}(\text{tert-BuNCH}_2)_2 + \text{NMe}_4\text{F} + \text{CrCl}_3$ (See previous), which was attributed to a boron compound in close proximity to the chromium centre.

For comparison, a solution of $\text{PhB}(\text{tert-BuNCH}_2)_2 + \text{MAO}$ in toluene was characterised by ^{11}B NMR spectroscopy.

^{11}B NMR: δ -91.8, -9.01

Trimerisation Properties of 1-phenyl-2,5-di-*tert*-butyl-1-boro-2,5-diazacyclopentane- Chromium III Chloride Complex + Hexylmagnesium Bromide:

The complex was prepared by addition of 1-phenyl-2,5-di-*tert*-butyl-1-boro-2,5-diazacyclopentane to $\text{CrCl}_3 \cdot \text{THF}_3$ in THF solution, and the subsequent addition of hexylmagnesium bromide solution in THF, see 'Experimental' section.

To an NMR tube containing 0.5 cm³ of dry, degassed toluene was added 1-phenyl-2,5-di-*tert*-butyl-1-boro-2,5-diazacyclopentane - Chromium III Chloride + Hexylmagnesium bromide (0.0020 g, 4.79×10^{-6} mol). To the resultant suspension was added 200 eq. MAO (10% w/w soln. in toluene). To this suspension was added dry, degassed 1-hexene, and the resultant sample characterized by ^1H NMR spectroscopy at intervals of 0, 10 mins and 24 hrs.

At $t = 0$ hrs:

Mass % conversion of 1-hexene to products: 24.30% \pm 0.70%

Mean olefinic to aliphatic proton ratio in 1-hexene reaction products: 1:52.0
 \pm 37.18%

Average chain-length of 53.0 carbons, or 8.8 1-hexene monomer units.

At $t = 24$ hrs:

Mass % conversion of 1-hexene to products: 36.03% \pm 2.26%

Mean olefinic to aliphatic proton ratio in 1-hexene reaction products: 1:18.6 \pm 7.87%

Average chain-length of 19.6 carbons, or 3.3 1-hexene monomer units.

At t = 48 hrs:

Mass % conversion of 1-hexene to products: 31.97% \pm 0.63%

Mean olefinic to aliphatic proton ratio in 1-hexene reaction products: 1:17.5

\pm 11.75%

Average chain-length of 18.5 carbons, or 3.1 1-hexene monomer units.

Comparative estimate of Product Chain Length 0 hrs \rightarrow 48 hrs: n = 5.5 1-hexene monomer units.

Trimerisation Properties of Sodium Phenyl(bis-hydroxy)butoxyborate-Chromium III Chloride Complex:

The complex was prepared by addition of Sodium Phenyl(bis-hydroxy)butoxyborate to CrCl₃.THF₃ in THF solution, see 'Experimental' section.

To an NMR tube containing 0.5 cm³ of dry, degassed toluene was added Sodium Phenyl(bis-hydroxy)butoxyborate- Chromium III Chloride complex (0.0021 g, 4.68×10^{-6} mol (calculation assumes NaPhB(OH)₂Ot-BuCrCl₃)). The complex was poorly soluble, and to the resultant suspension was added 200 eq. MAO (10% w/W soln. in toluene). To this suspension was added dry, degassed 1-hexene, and the resultant sample characterized by ¹¹B NMR spectroscopy and by ¹H NMR spectroscopy at intervals of 0, 24 and 48 hrs.

At t = 0 hrs:

Mass % conversion of 1-hexene to products: 5.67% \pm 1.10%

Mean olefinic to aliphatic proton ratio in 1-hexene reaction products:

(Signal intensities prohibit meaningful measurement).

At t = 24 hrs:

Mass % conversion of 1-hexene to products: 19.05% \pm 0.99%

Mean olefinic to aliphatic proton ratio in 1-hexene reaction products: 1:5.6 \pm 12.80%

Average chain-length of 6.6 carbons, or 1.1 1-hexene monomer units.

At t = 48 hrs:

Mass % conversion of 1-hexene to products: 30.21% \pm 0.83%

Mean olefinic to aliphatic proton ratio in 1-hexene reaction products: 1:8.0 \pm 7.56%

Average chain-length of 9.0 carbons, or 1.5 1-hexene monomer units.

Comparative estimate of Product Chain Length 0 hrs \rightarrow 48 hrs: n = 1.9 1-hexene monomer units.

The solution was characterised by ^{11}B NMR spectroscopy, revealing a small singlet at δ = ca. 87 ppm. Cf. δ = 4.47 for free ligand, 9.33 for phenylboronic acid.⁸⁸

Conclusion:

A number of synthetic pathways have been investigated, to various distinct classes of chromium ligand, and precursors thereof. Principally:

1: $\text{RB}(\text{R}'\text{NCH}_2)_2 + \text{E}^+\text{N}^-$ where E^+ and N^- are electrophilic and nucleophilic groups respectively. In particular there is reasonably compelling evidence for the formation of the anionic species, $[\text{Ph}(\text{F})\text{B}(\text{tert-BuNCH}_2)_2]^-$.

2: $[\text{PhB}(\text{OH})_2\text{OBu}]^-$.

3: $\text{OC}(\text{RNCH}_2)_2 + \text{E}^+\text{N}^-$ where E^+ and N^- are electrophilic and nucleophilic groups respectively.

4. $[(\text{C}_6\text{F}_5)_3\text{BC}_6\text{H}_4\text{NH}_2\cdot\text{HCl}]^-$, as a potential precursor to $[(\text{C}_6\text{F}_5)_3\text{BC}_6\text{H}_4\text{R}_2\text{TAC}]^-$.

The catalytic properties of several chromium-based systems have been tested.

The strategy by which a *para*-lithiated aniline was added to tris(pentafluoro)phenylborane shows some promise, but otherwise the difficulty inherent in synthesising borates in the presence of amine functionalities; which proved to be greater than originally anticipated; limits the potential for development of nitrogen based chromium ligands incorporating boron centres; unless perhaps this was accomplished by a radically different strategy, such as functionalisation of a previously synthesised tetra-arylborate, see figure C.1

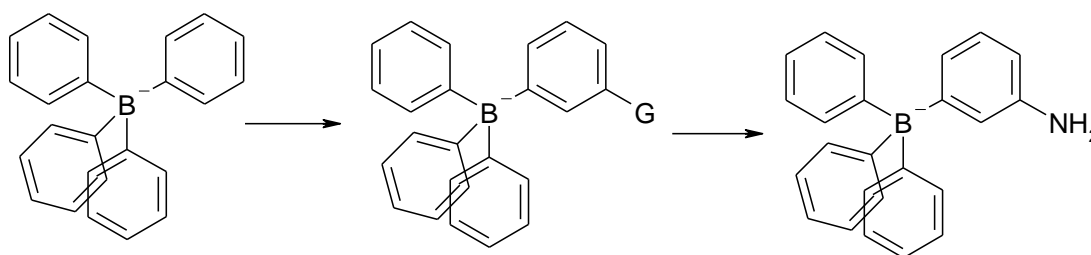


Figure C.1: Alternative Synthetic Pathway to Amine-substituted Borate Anion.

The synthesis of a variety of boron-nitrogen bonded species was accomplished, and the resultant species characterised convincingly, but the available evidence is

consistent with the expected stabilisation of the neutral species by π -electron donation- an observation well illustrated by the N-B-N bond angles in the relevant crystal structures. The B-N σ -bond, in the absence of additional π -interactions, is comparatively weak, which fact is considered to have prevented the isolation of quaternary B-N bonded, anionic species. Neutral B-N bonded species in general, appear largely unreactive towards nucleophiles, except under conditions sufficiently harsh to result in decomposition, although there is evidence of coordination of fluoride anions to diazaboranes.

The formation of quaternary B-O bonded species is, by contrast, a relatively less challenging procedure.

NMR characterisation of chromium III complexes remains impracticable, due to the complications imposed by the paramagnetic centre (see '*1.4.1 The Effect of Paramagnetism on In Situ Characterization of Chromium III Complexes:*'), while attempts to crystallise complexes from the chromium systems investigated were unsuccessful. Thus, as has often been the case for chromium(III)-based catalyst systems, neither the pre-catalysts, nor the proposed active species have been definitively characterised.

Some data has been obtained by elemental analysis and electro-spray mass spectrometry. Besides evidencing the continued presence of $\text{PhB}(\text{tert-BuNCH}_2)_2$ in chromium based systems isolated by precipitation, of particular note is evidence of a cationic derivative of the anion $[\text{Ph}(\text{F})\text{B}(\text{tert-BuNCH}_2)_2]^-$, (the existence of which is also supported by NMR spectroscopy). However, no fragment containing the heterocycle and a chromium centre has been identified, and the presence of such complexes thus remains unconfirmed.

The catalytic activity with respect to 1-hexene in toluene solution of seven distinct systems was investigated, and ^1H NMR analysis of the resultant solutions suggested trimerisation activity in several of these. In none of these systems did the activity match or surpass that exhibited by 1,3,5-*tris*-dodecyl-1,3,5-triazacyclohexane-Chromium(III) chloride however, and in all cases significant isomerisation of the 1-hexene starting material was observed. This apparent deficiency may in part be attributable to the low solubility of the catalysts in toluene/MAO, relative to 1,3,5-*tris*-dodecyl-1,3,5-triazacyclohexane-chromium(III) chloride.

Because the short alkyl substituents on the $\text{PhB}(\text{tert-BuNCH}_2)_2$ based systems restrict the potential solubility of the resultant complexes, methods were devised for the synthesis of $\text{N,N}'$ -*bis*-phenethyl- and $\text{N,N}'$ -di-*tert*-butylethylenediamine, as precursors to heterocycles, and thus complexes, of greater potential solubility in non-polar solvents.

The results of the catalytic tests, after a sufficient duration as to allow the assumption that the reaction has reached completion, are summarised in the table below:

	Mass % conversion of 1-hexene to products:	Average chain-length of Products (no. monomer units):
a. $(\text{Dodecyl})_3\text{TAC} + \text{CrCl}_3 + \text{MAO}$	58.4%	2.8
1. $\text{PhB}(\text{tert-BuNCH}_2)_2 + \text{CrCl}_3 + \text{MAO}$	25.3%	1.9
2. $\text{PhB}(\text{tert-BuNCH}_2)_2 + \text{CrCl}_3 + \text{HexylMgBr} + \text{MAO}$	32.0%	3.1
3. $\text{PhB}(\text{tert-BuNCH}_2)_2 + \text{CrCl}_3 + \text{NMe}_4\text{F MAO}$	10.0%	2.0
4. $(2\text{-Et})\text{Hex}_3\text{TAC} + \text{NH}_2\text{C}_6\text{H}_4\text{CH}_2\text{ONa}$ + $\text{CrCl}_3, \text{THF}_3 + \text{MAO}$	45.5%	1.8
5. $(2\text{-Et})\text{Hex}_3\text{TAC} + \text{NH}_2\text{C}_6\text{H}_4\text{CH}_2\text{ONa}$ + $\text{CrCl}_3, \text{THF}_3 + \text{B}(\text{C}_6\text{F}_5)_3, \text{Et}_2\text{O}$	43.2%	1.6
6. $\text{OC}(\text{tert-BuNCH}_2)_2 + \text{CrCl}_3 + \text{MAO}$	27.8%	1.9
7. $\text{OC}(\text{tert-BuNCH}_2)_2 + \text{HexMgBr} + \text{CrCl}_3 + \text{MAO}$	25.3%	2.6
8. $\text{NaPhB}(\text{OH})_2\text{OBu} + \text{CrCl}_3 + \text{MAO}$	30.2%	1.5

Evidence for the formation of a quaternary B-N bonded anionic species- as a free ligand, is only observed in the case of addition of $\text{PhB}(\text{tert-BuNCH}_2)_2$ to NMe_4F (See '3.32 Reaction of 1-Phenyl-2,5-di-*tert*-butyl-1-bora-2,5-diazacyclopentane with Tetramethylammonium Fluoride: '). It is noteworthy that the catalyst system based on this combination is not one of the more effective of those studied and that quaternary borate anions of this type must be considered of questionable stability, and thus the fluoride substituents potentially labile.

The system $\text{NaPhB}(\text{OH})_2\text{OBu} + \text{CrCl}_3$ appeared to show moderate activity for the conversion of 1-hexene, but the average chain length of the products suggests that they comprise mostly internal hexenes. It should be noted that this ligand, even when

complexed to CrCl_3 as envisaged, exhibits uncoordinated lone pairs, a feature that is in contrast to the various nitrogen based ligand types. This, like the presence of free F^- , may result in reduction of activity.

The largest conversion, proportionately, of 1-hexene, occurs in the case of the systems 4 and 5 (see above), but these also exhibit the shortest average chain length of products, suggesting that the majority of the product in these cases comprise internal hexenes. The relatively poor activity exhibited by these systems compared to $(\text{Dodecyl})_3\text{TAC-CrCl}_3$ is consistent with the previously reported³⁷ impairment of trimerisation activity of TACs in the presence of electron donating functionalities (aminobenzylalcohols in this case). The addition of $\text{B}(\text{C}_6\text{F}_5)_3 \cdot \text{Et}_2\text{O}$ to the complex in the case of '5' was expected to result in coordination to the oxygen-based substituents, potentially reducing the effective electron donor strength of the latter, and increasing the resultant complex's efficacy as a trimerisation catalyst.

The observed activity in the case of '5' versus '4' in fact shows an approximately 2% reduction in the extent of conversion of 1-hexene, which is within the margin of error, but based on the calculated average chain length of products, suggests an approximately 33% improvement in trimerisation activity. This suggests that the coordination of $\text{B}(\text{C}_6\text{F}_5)_3$ may indeed serve to reduce the impairment of trimerisation activity by electron donor groups.

The best observed activity of a novel catalyst system occurs in the case of $\text{PhB}(\text{tert-BuNCH}_2)_2 + \text{CrCl}_3 + \text{HexylMgBr}$, this system having exhibited the highest proportionate conversion of 1-hexene to products, and an average chain length corresponding well to the production of a trimer. This system represents a significant improvement over the observed activity of the equivalent system '1', in the absence of the alkylating reagent.

A similar correspondence is noted between the activity of the $\text{OC}(\text{tert-BuNCH}_2)_2\text{-CrCl}_3$ systems, in the presence, versus the absence, of the alkylating reagent, though the overall 1-hexene conversion remained lower than in the case of $\text{PhB}(\text{tert-BuNCH}_2)_2 + \text{CrCl}_3 + \text{HexylMgBr}$.

References:

1. http://www.exxonmobilchemical.com/public_products/Polyethylene/Polyethylene/Europe/PE_ProductFrontPage.asp **11/07/07**
2. <http://en.wikipedia.org/wiki/Polyethene> **26/05/04**
3. S.K. Kim, H.K. Kim, M.H. Lee, S.W. Yoon, and Y. Do, *Angewandte Chemie International Edition*, **45**, 6163-6166, **2006**
4. *Inorganic Chemistry: Third Edition*, D.F. Shriver, P.W. Atkins, **1999**
5. <http://www.chee.iit.edu/~m1/ziegler.html> **10/06/04**
6. <http://www.akzonobel-polymerchemicals.com/ProductGroups/What+are+Ziegler-Natta+Catalysts.htm> **13/11/06**
7. http://www.chem.ucalgary.ca/groups/ziegler/met_intro.html **10/06/04**
8. A. Zecchina, S. Bertarione, A. Damin, D. Scarano, C. Lamberti, C. Prestipino, G. Spoto, S. Bordiga, *Physical Chemistry Chemical Physics*, **5** (20), 4414, **2003**
9. Ø. Espelid, K.J. Børve, *Journal of Catalysis*, **206**, 331-338, **2002**
10. A.K. Tomov, J.J. Chirinos, D.J. Jones, R.J. Long, V.C. Gibson, *Journal of the American Chemical Society*, **127**, 10166-10167, **2005**
11. L.A. MacAdams, G.P. Buffone, C.D. Incarvito, A.L. Rheingold, K.H. Theopold, *Journal of the American Chemical Society*, **127**, 1082-1083, **2005**
12. W.K. Kim, M.J. Fevola, L.M. Liable-Sands, A.L. Rheingold, K.H. Theopold, *Organometallics*, **17**, 4541-4543, **1998**
13. T. Hanmura, M. Ichihashi, T. Monoi, K. Matsuura, T. Kondow, *Journal of Physical Chemistry A*, **109**, 6465-6470, **2005**
14. Theopold, *European Journal of Inorganic Chemistry*, **1**, 15-24, **1998**
15. R. Emrich, O. Heinemann, P.W. Jolly, C. Krüger, G.P.J. Verhovnik, *Organometallics*, **1997**, **16**, 1511, **1997**
16. J.T. Dixon, M.J. Green, F.M. Hess, D.H. Morgan, *Journal of Organometallic Chemistry*, **689**, 3641-3668, **2004**
17. http://en.wikipedia.org/wiki/Linear_alpha_olefins **11/07/07**
18. http://nexant.ecnext.com/coms2/gi_0255-148/Alpha-Olefins.html **11/07/07**
19. http://www.cpchem.com/enu/press_releases_785.asp **11/07/07**

20. S. Tobisch, T. Ziegler, *Organometallics*, 23 (17) 4077-4088, **2004**
21. R.D. Köhn, M. Haufe, S. Mihan, D. Lilge, *Chemical Communications*, 1927-1928, **2000**
22. D.S. McGuinness, P. Wasserscheid, W. Keim, D. Morgan, J.T. Dixon, A. Bollmann, H. Maumela, F. Hess, U. Englert, *Journal of the American Chemical Society*, 125, 18, 5273, **2003**
23. D.H. Morgan, S.L. Schwikkard, J.T. Dixon, J.J. Nair, R. Hunter, *Advanced Synthesis & Catalysis*, 345, 939-942, **2003**
24. B. Hessen, *Journal of Molecular Catalysis A: Chemical*, 213, 129-135, **2004**
25. P.J.W. Deckers, B. Hessen, J.H. Teuben, *Angewandte Chemie International Edition*, 40, 13, 2516-2519, **2001**
26. A.N.J. Blok, P.H.M. Budzelaar, A.W. Gal, *Organometallics*, 22, 2564, **2003**
27. H. Mahomed, A. Bollmann, J.T. Dixon, V. Gokul, L. Griesel, C. Grove, F. Hess, H. Maumela, L. Pepler, *Applied catalysis A: General*, 255, 355-359, **2003**
28. F.J. Wu, EP 0537609 (Albermarle Corporation) July 10, **1992**.
29. T. Yoshida, T. Yamamoto, H. Okada, H. Murakita, US2002/0035029 (Tosoh Corporation), March 21, **2002**.
30. A. Carter, S.A. Cohen, N.A. Cooley, A. Murphy, J. Scutt, D.F. Wass, *Chemical Communications*, 858-859, **2002**
31. L.E. Bowen, D.F. Wass, *Organometallics*, 25 (3), 555-557, **2006**
32. M.E. Bluhm, O. Walter, M. Döring, *Journal of Organometallic Chemistry*, 690 713-721, **2005**
33. W.K. Reagan, J.W. Freeman, B.K. Conroy, T.M. Pettijohn, E.A. Benham, US 5,451,645 (Phillips Petroleum Company), September 19, **1995**.
34. S. Murtaza, S.B. Harkins, G.S. Long, A. Sen, *Journal of the American Chemical Society*, 122, 1867, **2000**
35. R.D. Köhn, M. Haufe, G. Kociok-Köhn, S. Grimm, P. Wasserscheid, W. Keim, *Angewandte Chemie International Edition*, 39, 23, **2000**
36. R.D. Köhn, G. Kociok-Köhn, *Angewandte Chemie International Edition*, 33, 18, 1877-1878, **1994**
37. <http://www.cerm.unifi.it/relax/tutor2.html> **29/3/2007**
38. J. Graymore, *Journal of the Chemical Society*, 1353-1357, **1932**
39. <http://www.chromatography.co.uk/TECHNIQS/Other/buffers.htm> **10/06/04**

40. T.A. Betley, J.C. Peters, *Inorganic Chemistry*, 41 (25) 6541-6543, **2002**
- 41: M.A. Grassberger, R. Koester, *Angewandte Chemie*, 81, 261, **1969**
- 42: K. Ren, J.H. Malpert, H. Li, H. Gu, D.C. Neckers, *Macromolecules*, 35, 5, 1632-1637, **2002**
- 43: Wittig *et al.* *Justus Liebigs Annalen der Chemie*, 563, 110-122, **1949**
- 44: S.P. Lewis, N.J. Taylor, W.E. Piers, S. Collins, *Journal of the American Chemical Society*, 125, 48, 14686-14687, **2003**
- 45: C. Bergquist, B.M. Bridgewater, C.J. Harlan, J.R. Norton, R.A. Friesner, G. Parkin, *Journal of the American Chemical Society*, 122, 43, 10581-10590, **2000**
- 46: M.P. Brown, A.E. Dann, D.W. Hunt, H.B. Silver, *Journal of the Chemical Society*, 4648-4652, **1962**
- 47: K.A. Østby, A. Haaland, G. Gundersen, *Organometallics*, 24, 5318-5328, **2005**
- 48: K.A. Østby, G. Gundersen, A. Haaland, H. Nöth, *Dalton Transactions*, 13, 2284-2291, **2005**
- 49: B.L. Kormos, C.J. Cramer, *Inorganic Chemistry*, 42, 6691-6700, **2003**
- 50: J. Zhang, Q.S. Li, S. Zhang, *Diamond and Related Materials*, 14, 1654-1662, **2005**
- 51: P.W. Fowler, E. Steiner, *Journal of Physical Chemistry A*, 101 (7), 1409-1413, **1996**
52. M.K. Das, A.L. DeGraffenreid, K.D. Edwards, L. Komorowski, J.F. Mariategui, B.W. Miller, M.T. Mojesky, K. Niedenzu, *Inorganic chemistry*, 27, 3085-3089, **1988**
53. K.O. Christe, W.W. Wilson, R.D. Wilson, R. Bau, J. Feng, *Journal of the American Chemical Society*, 112, 7619-7625, **1990**
54. A.H. Cowley, D. J. Pagel, M.L. Walker, *Journal of the American Chemical society*, 100, 7065-7066, **1978**
- 55: K. O. Christe, W. W. Wilson, R. D. Wilson, R. Bau, J. Feng, *Journal of the American Chemical Society*, 112 (21) 7619-7625, **1990**
56. S. Trofimenko, *Journal of the American Chemical Society*, 88 (8) 1842-1844, **1966**
57. B Benkmil, M. Ji, H. Vahrenkamp, *Inorganic Chemistry*, 43 (26) 8212-8214, **2004**
- 58: S. Trofimenko, *Journal of the American Chemical Society*, 88 (8) 1842, **1966**
59. H.C. Brown, E.J. Mead, *Journal of the American Chemical Society*, 78, 3614-3616, **1956**

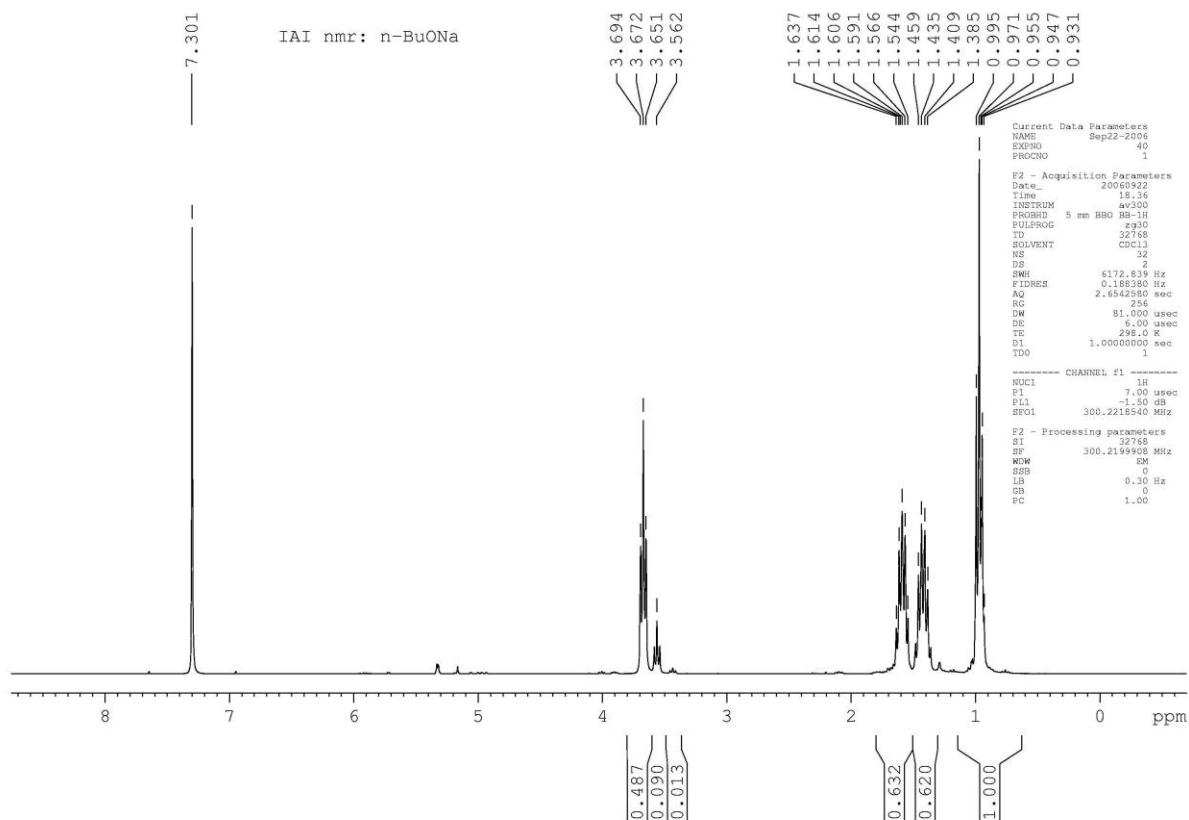
60. K.A. Østby, A. Haaland, G. Gundersen, *Organometallics*, 24, 5318-5328, **2005**
61. S.W. Govorchin, A.S. Kana'an, J.M. Kanameuller, *Journal of Chemical Thermodynamics*, 16, 8, 703-709, **1984**
62. <http://www.webelements.com/webelements/elements/text/B/enth.html> **23/10/06**
63. <http://chemviz.ncsa.uiuc.edu/content/doc-resources-bond.html> **23/10/06**
64. F.M. Bickelhaupt, N.J.R. van Eikema Hommes, C.F. Guerra, E.J. Baerends, *Organometallics*, 15 (13) 2923-2931, **1996**.
65. <http://www.webelements.com/webelements/elements/text/B/enth.html> **23/10/06**
66. W. Haubold, J. Herdtle, W. Gollinger, W. Einholz, *Journal of Organometallic Chemistry*, 315, 1, **1986**.
67. E. Hupe, M.I. Calaza, P. Knochel, *Journal of Organometallic Chemistry*, 680, 1-2, 136-142, **2003**
68. H.J. Frohn, H. Franke, P. Fritzen, V.V. Bardin, *Journal of Organometallic Chemistry*, 598, 127-135, **2000**
69. K. Østby, G. Gundersen, *Journal of Molecular Structure*, 691, 1-24, **2004**
70. Personal Communication, Dr. R.D. Köhn, University of Bath.
71. K. Anton, C. Euringer, H. Noeth, *Chemische Berichte*, 117, 1222-1234, **1984**
72. C.K. Narula, H. Noeth, *Inorganic Chemistry*, 23, 4147-4152, **1984**
73. K. Anton, H. Noeth, H. Pommerening, *Chemische Berichte*, 117, 2479-2494, **1984**
74. T. Kauffman, A. Hamsen, C. Beirich, *Angewandte Chemie*, 94, 145-146, **1982**
75. Rudakova *et al.* *Soviet Journal of Bioorganic Chemistry*, 1, **1975**, 475-476
76. W. Gerrard, M.F. Lappert, W. Shafferman, *Journal of the Chemical Society*, 3648-3652, **1958**
77. <http://www.webelements.com/webelements/elements/text/Cr/enth.html> **16/10/06**
78. P.K. Hurlburst, O.P. Anderson, S.H. Strauss, *Journal of the American Chemical Society*, 113, 6277-6278, **1991**
79. Y.A. Lysenko, I.V. Nevechera, S.P. Pridat'ko, E.A. Troshima. *Journal of General Chemistry*, USSR, 60, 505-510, **1990**
80. W. Ried, U. Reiher, J.W. Bats, *Helvetica Chimica Acta*, 70, 1255-1260, **1987**
81. J.N. Tilley, A.A.R. Sayigh, *Journal of Organic Chemistry*, 28, 2076-2079, **1963**
82. M.K. Denk, J.M. Rodezno, S. Gupta, A.J. Lough, *Journal of Organometallic Chemistry*, 617-618, 242-253, **2001**
83. A.R. Bassindale, T. Stout, *Tetrahedron Letters*, 26, 28, 3403-3406, **1985**
84. H. Meerwein *et al.* *Justus Liebigs Annalen der Chemie*, 641, 1-39, **1961**

- 85: N. Millot, C.C. Santini, B. Fenet, J.M. Basset, *European Journal of Inorganic Chemistry*, 3328, **2002**
- 86: S. Dagorne, I.A. Guzei, M.P. Coles, R.F. Jordan, *Journal of the American Chemical Society*, 122, 274-289, **2000**
- 87: M.K. Denk, M.J. Krause, D.F. Niyogi, N.K. Eill, *Tetrahedron*, 59, 38, 7565-7570, **2003**
- 88: H.C. Beachell, D.W. Beistel, *Inorganic Chemistry*, 3, 1028, **1964**
- 89: S.A. Llewellyn, M.L.H. Green, A.R. Cowley, *Dalton Transactions*, 1776-1783, **2006**

Appendix 1: Selected NMR Spectra:

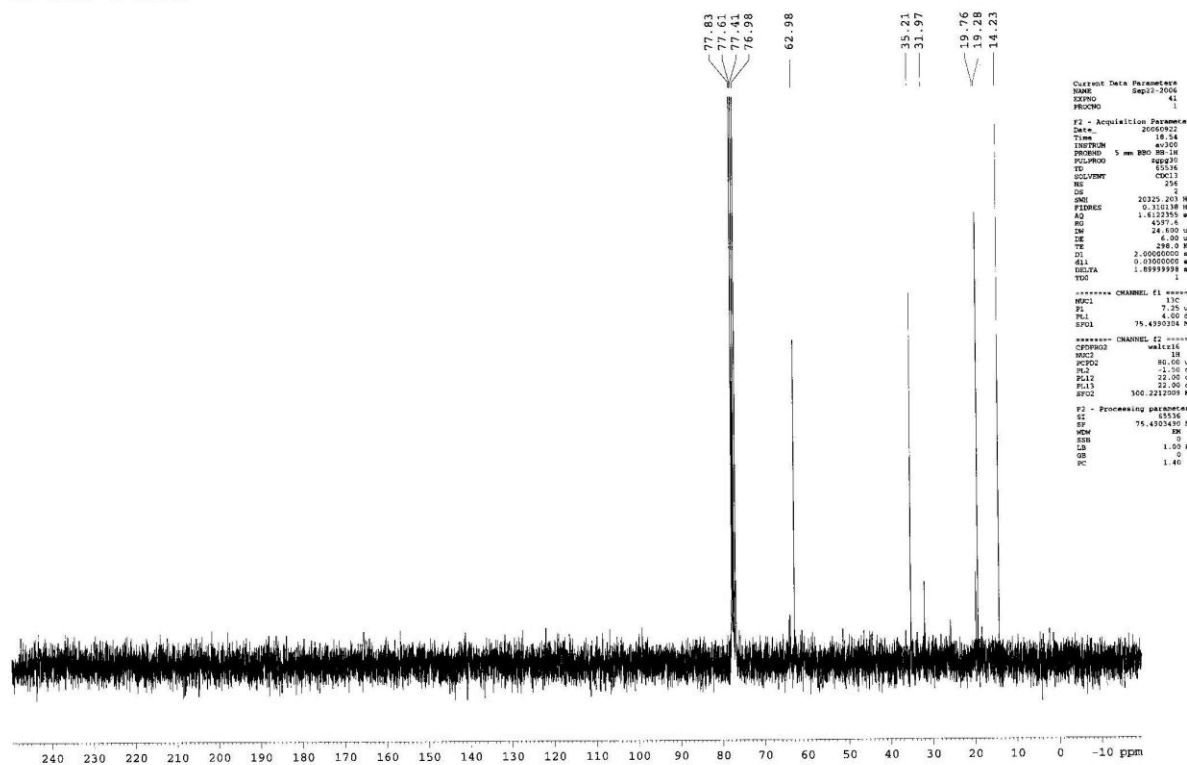
3.1:

Sodium n-Butoxide: ^1H

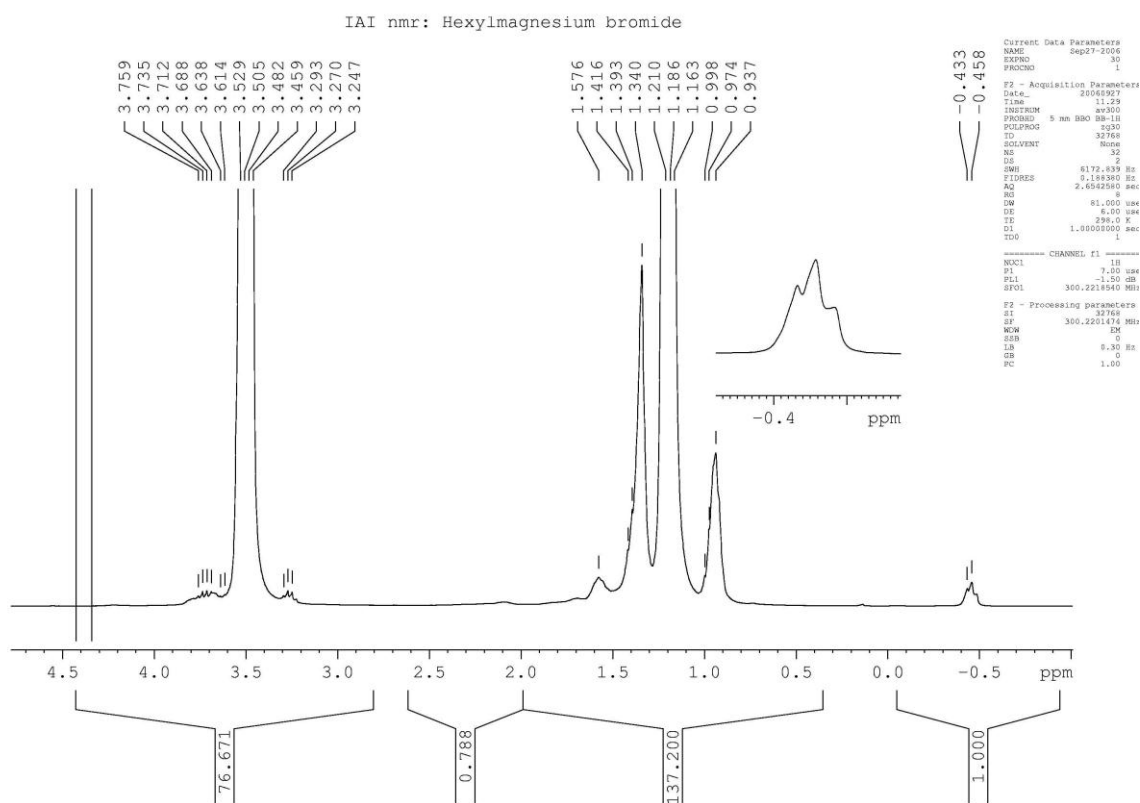
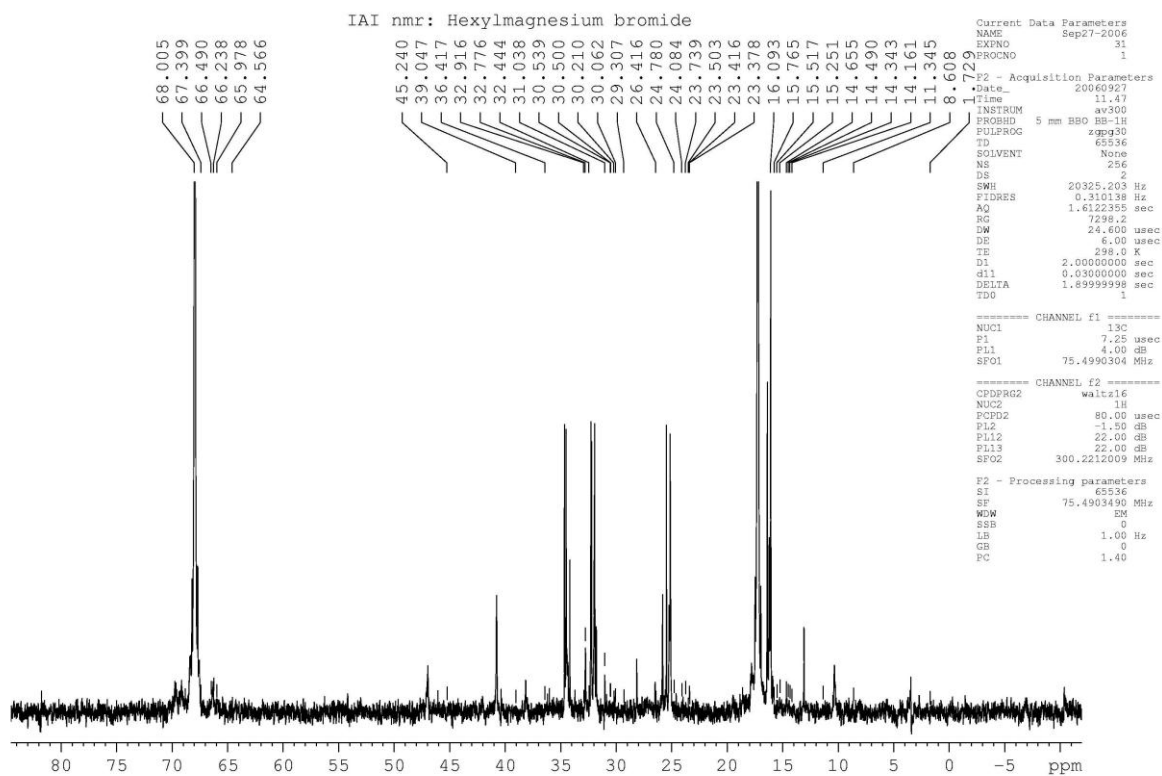


Sodium n-Butoxide: ^{13}C

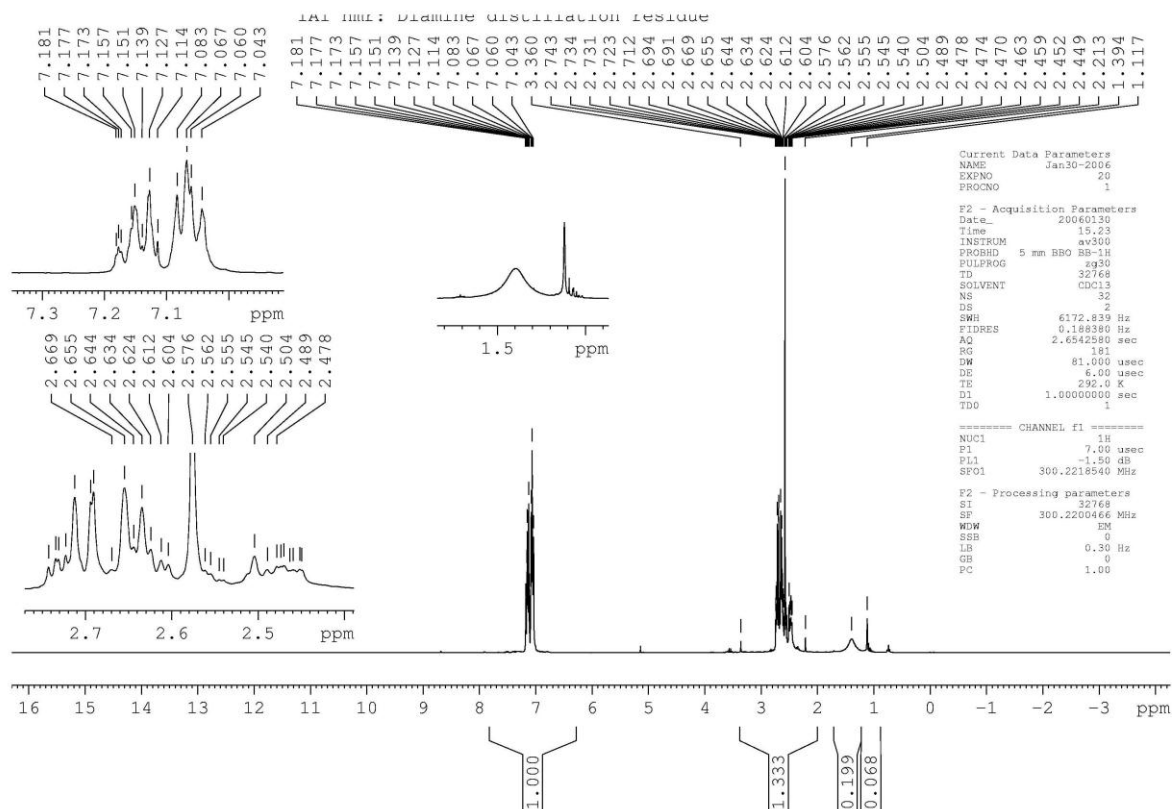
IAI nmr: n-BuONa



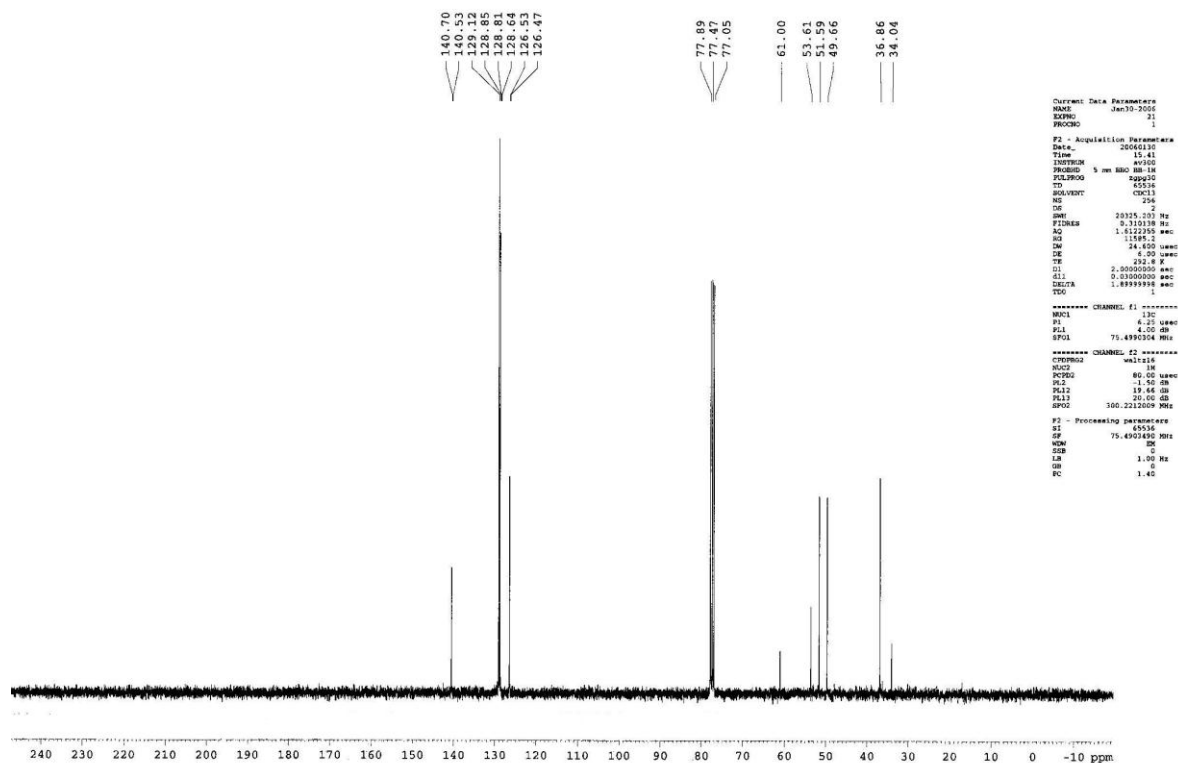
3.2:

Hexylmagnesium Bromide: ^1H Hexylmagnesium Bromide: ^{13}C 

3.3:

Synthesis of Bis-phenethylethylenediamine: ^1H Synthesis of Bis-phenethylethylenediamine: ^{13}C

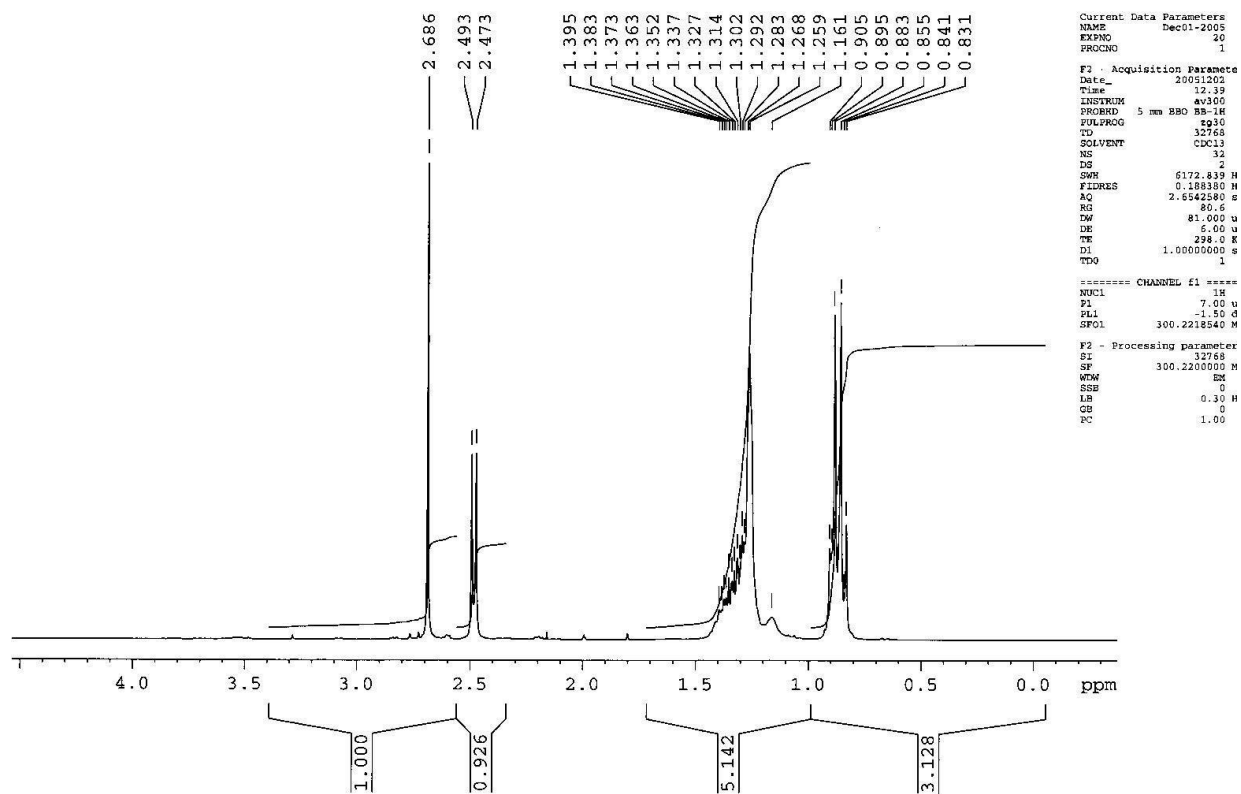
IAI nmr: Diamine distillation residue



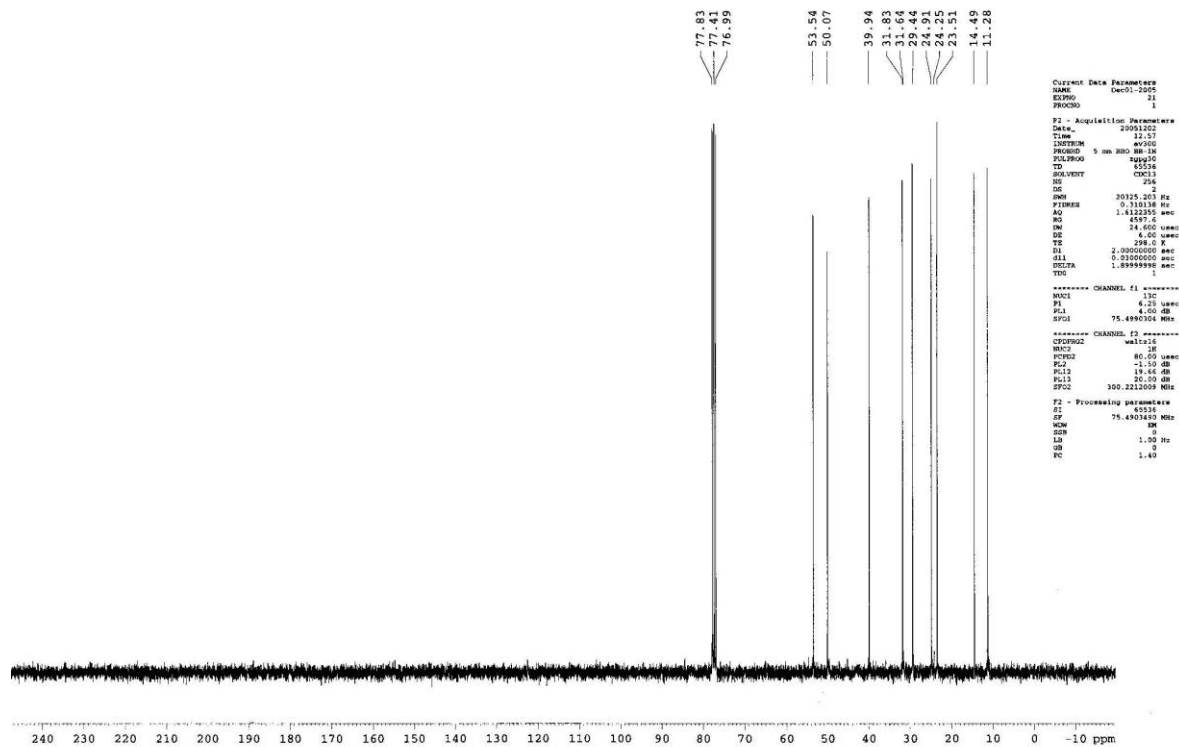
3.4:

Bis(2-Ethyl)hexylethylenediamine: ^1H :

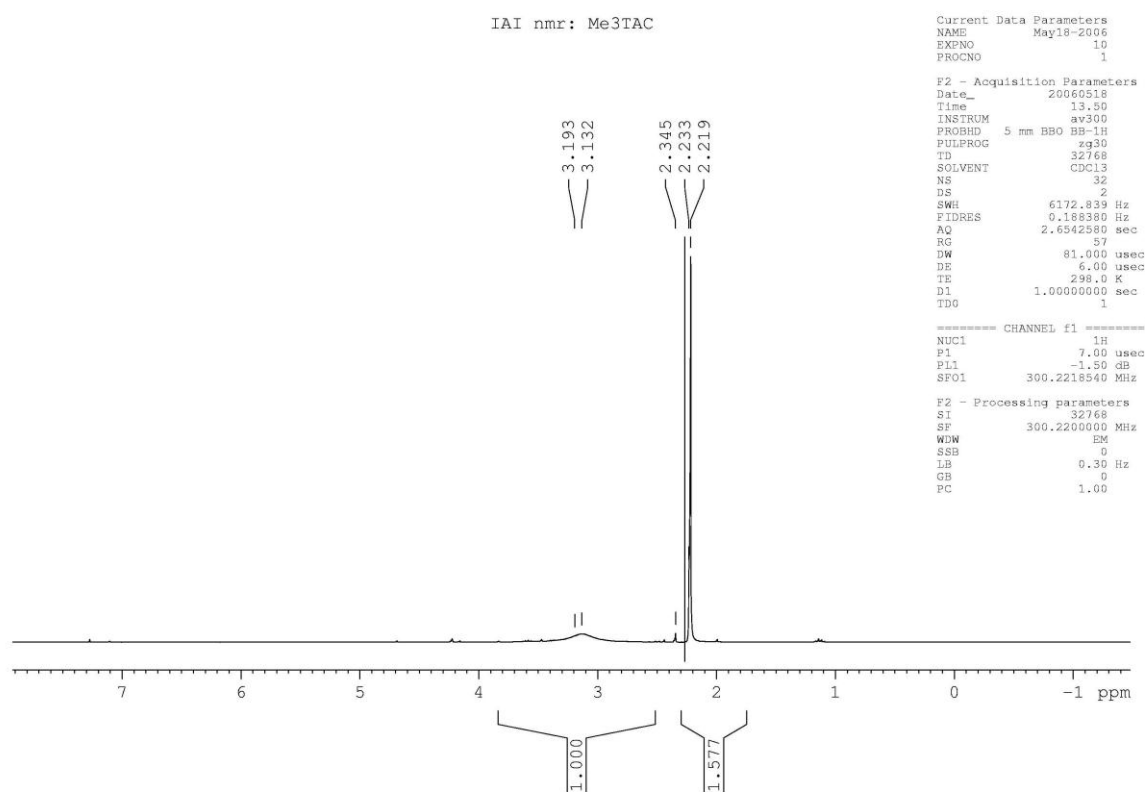
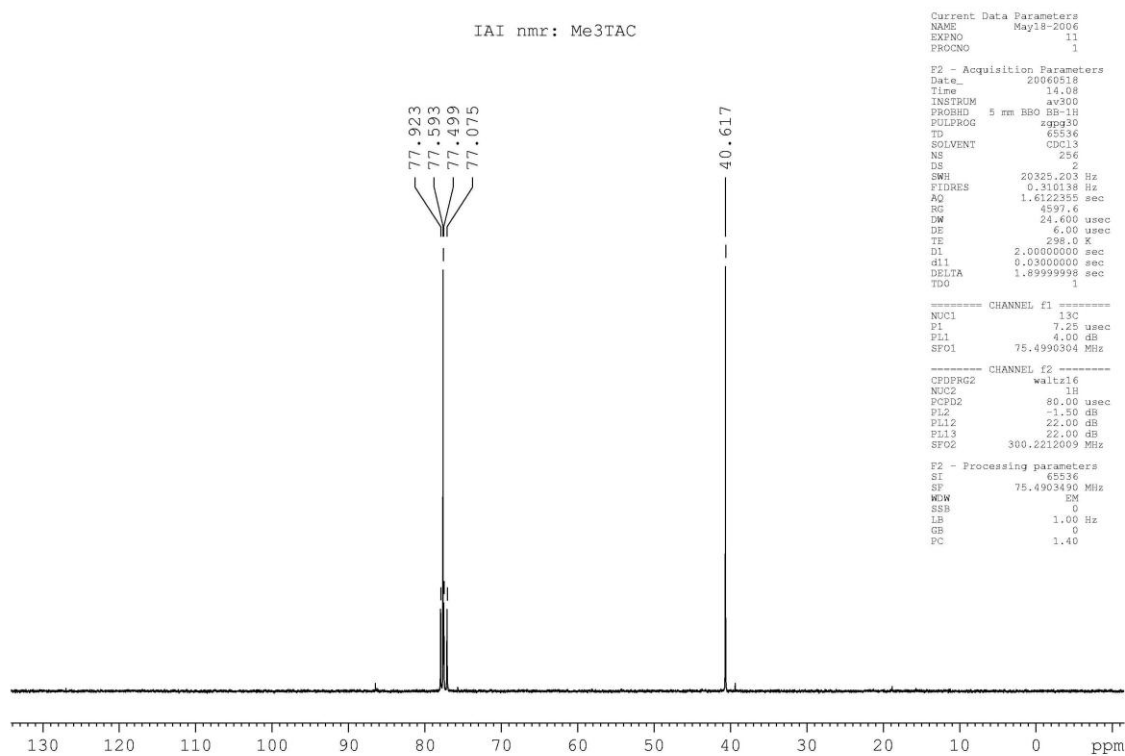
IAI nmr: Diamine

Bis(2-Ethyl)hexylethylenediamine: ^{13}C

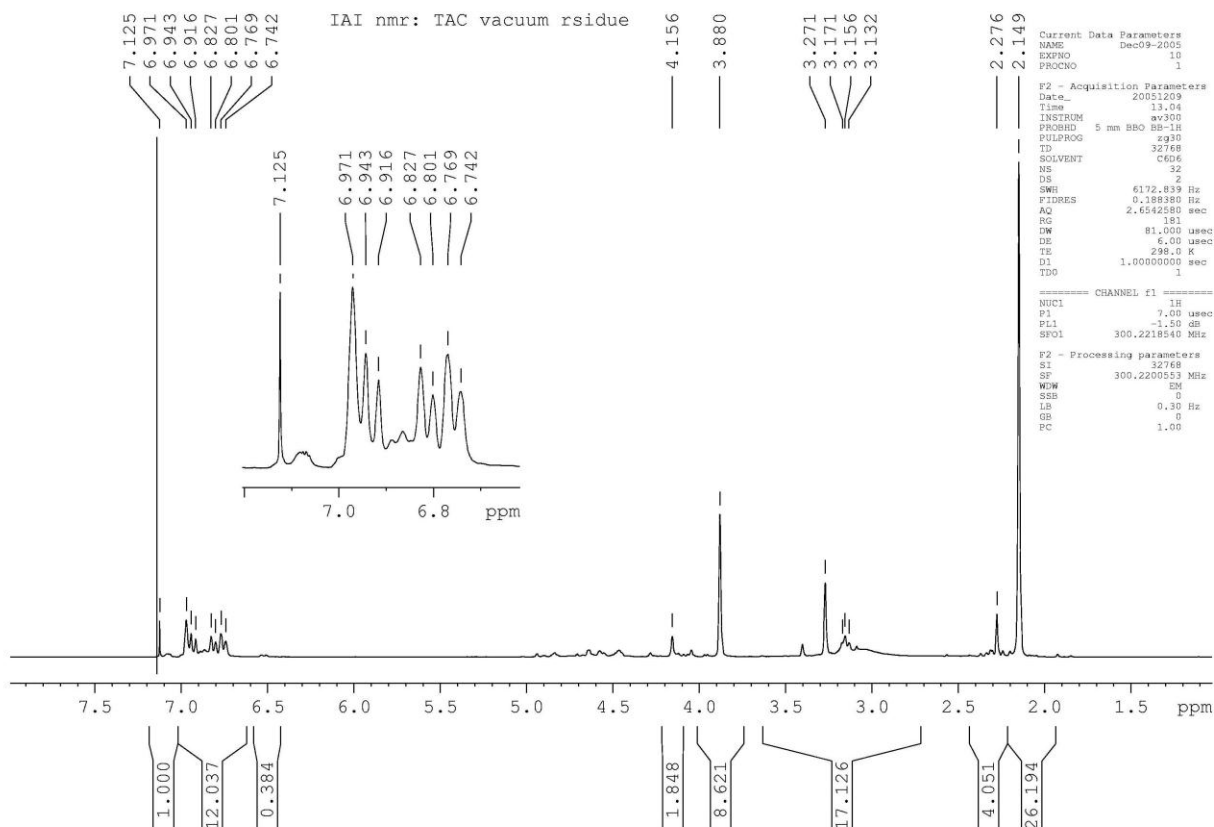
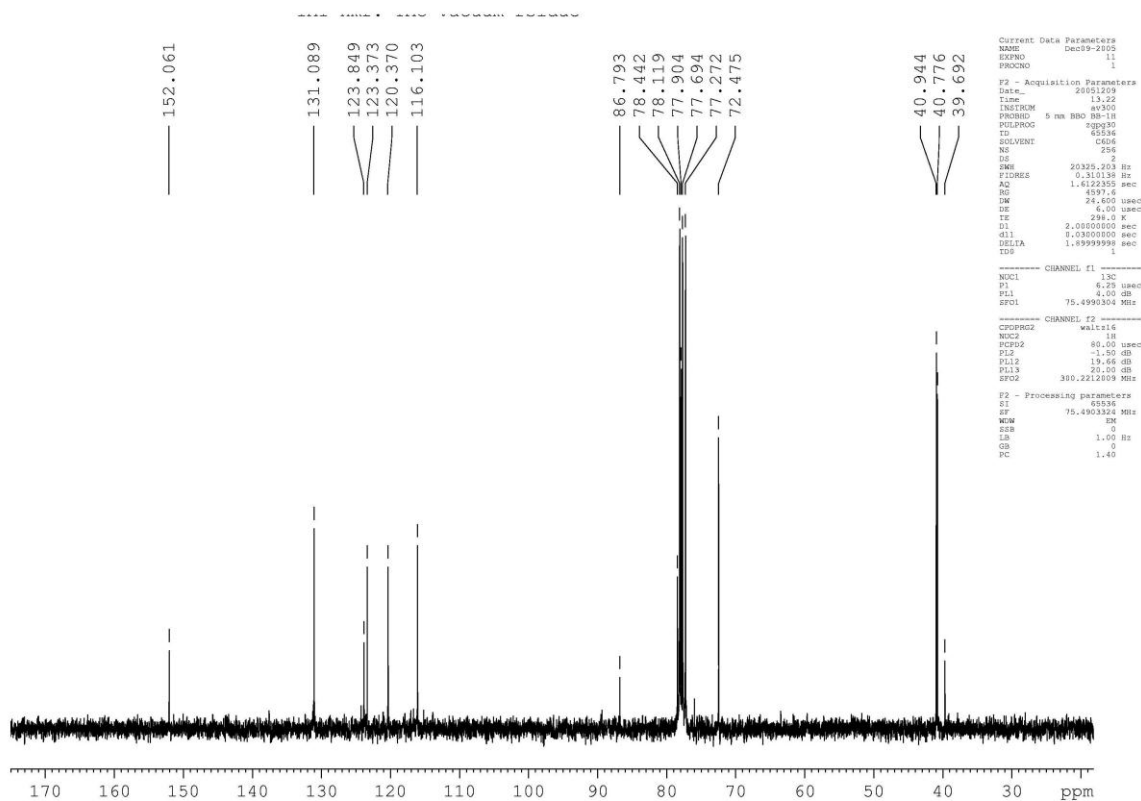
IAI nmr: Diamine



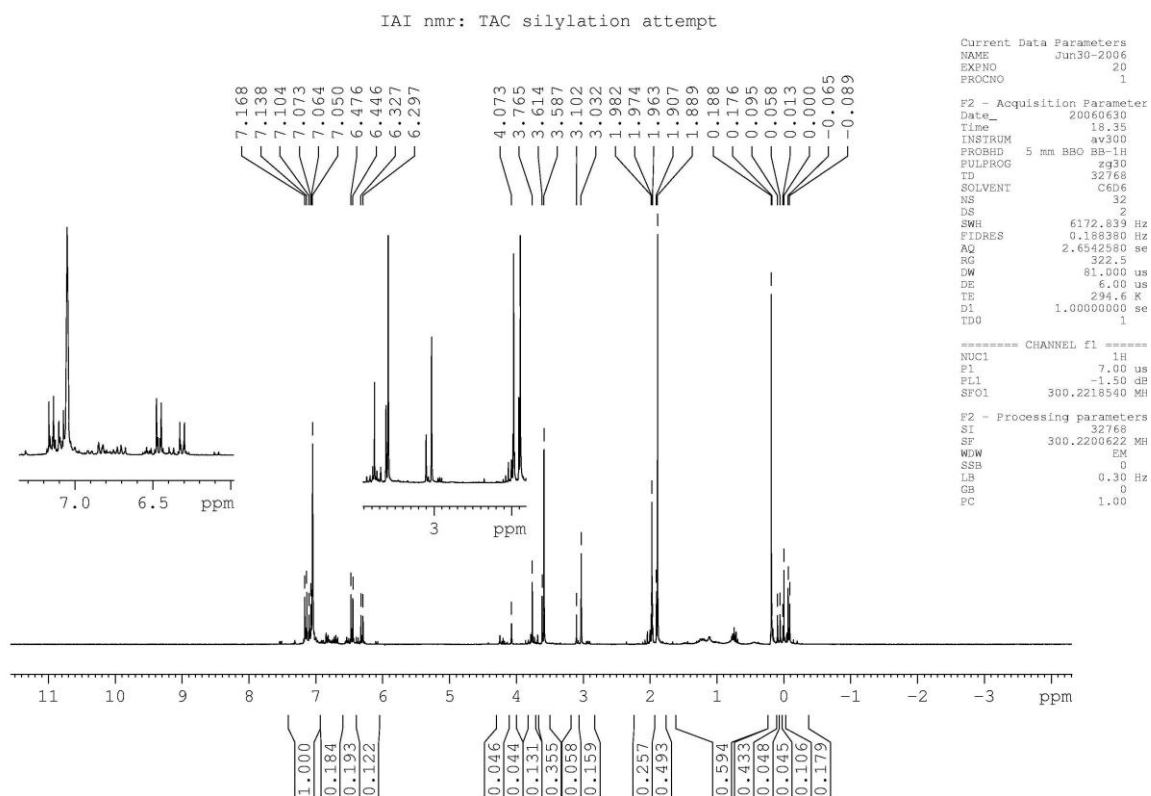
3.5:

1,3,5-trimethyl-1,3,5-triazacyclohexane: ^1H 1,3,5-trimethyl-1,3,5-triazacyclohexane: ^{13}C 

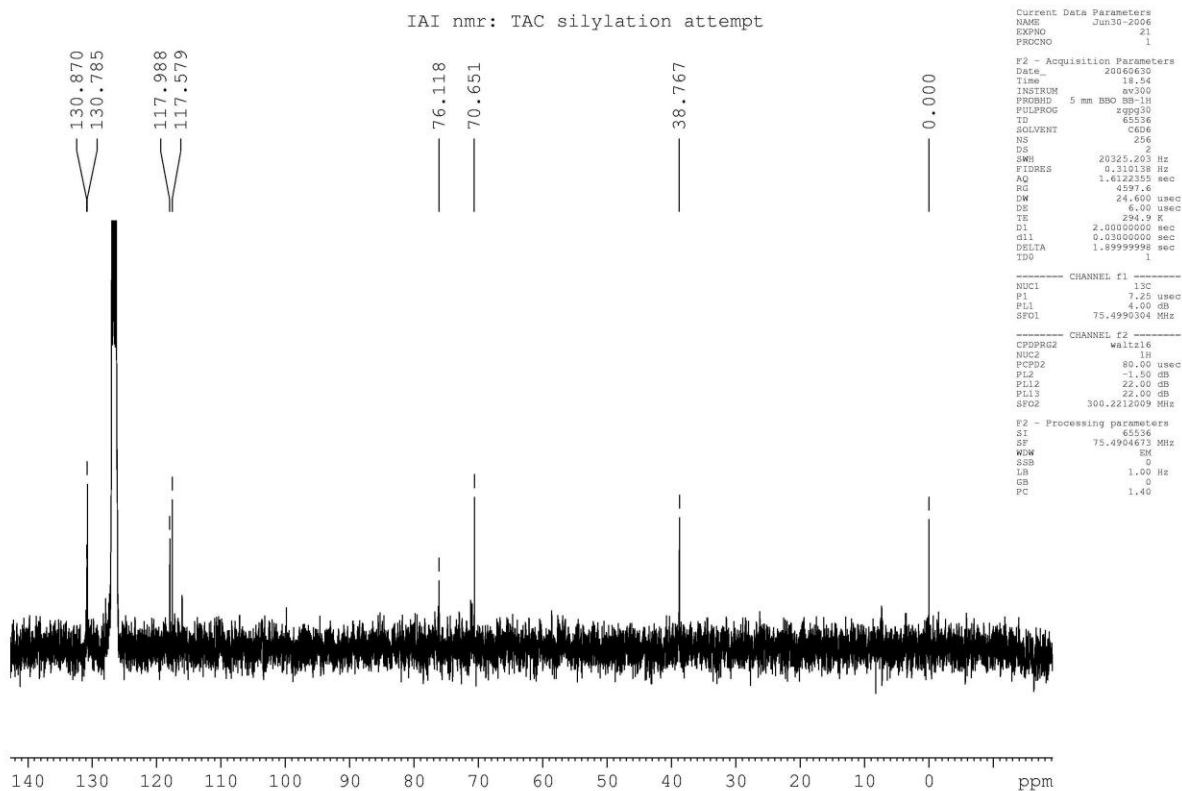
3.7:

1,3-dimethyl-5-(4-bromo)phenyl-1,3,5-triazacyclohexane: ^1H 1,3-dimethyl-5-(4-bromo)phenyl-1,3,5-triazacyclohexane: ^{13}C 

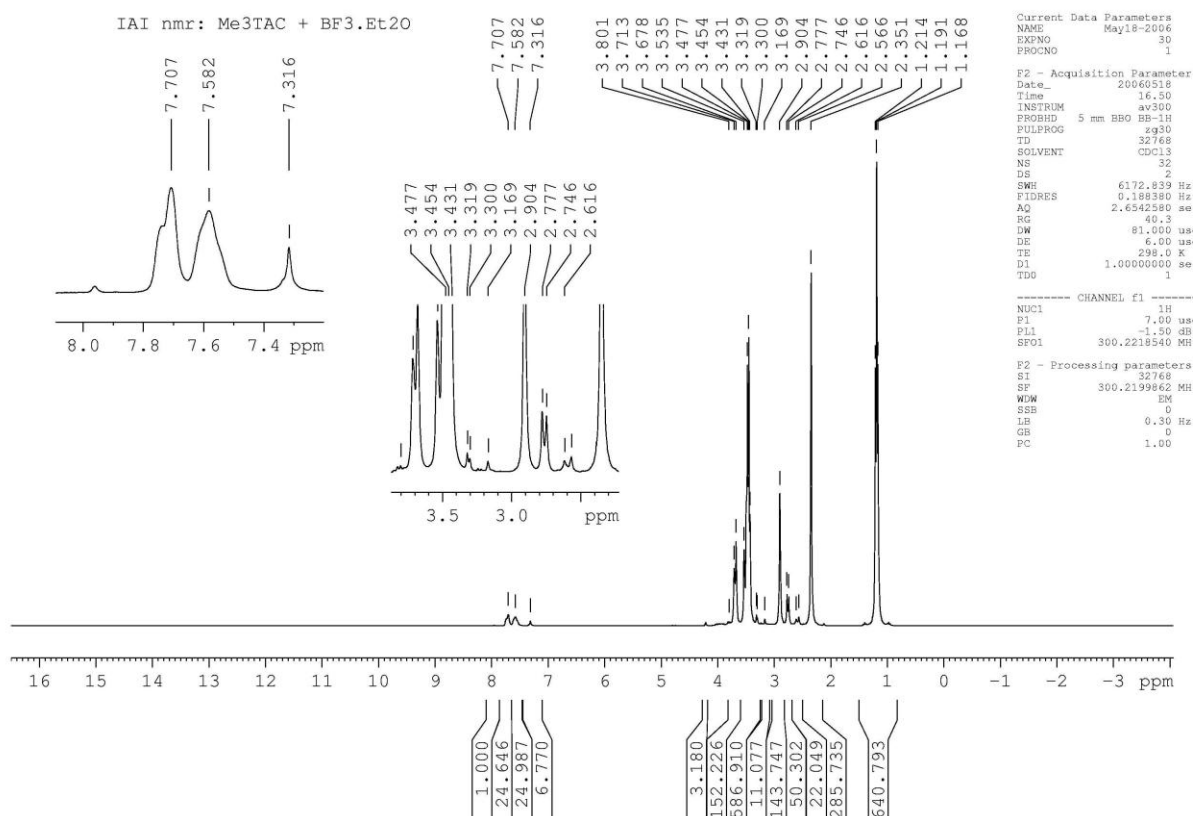
3.8: 1,3-dimethyl-5-(4-trimethylsilyl)phenyl-1,3,5-triazacyclohexane: ^1H



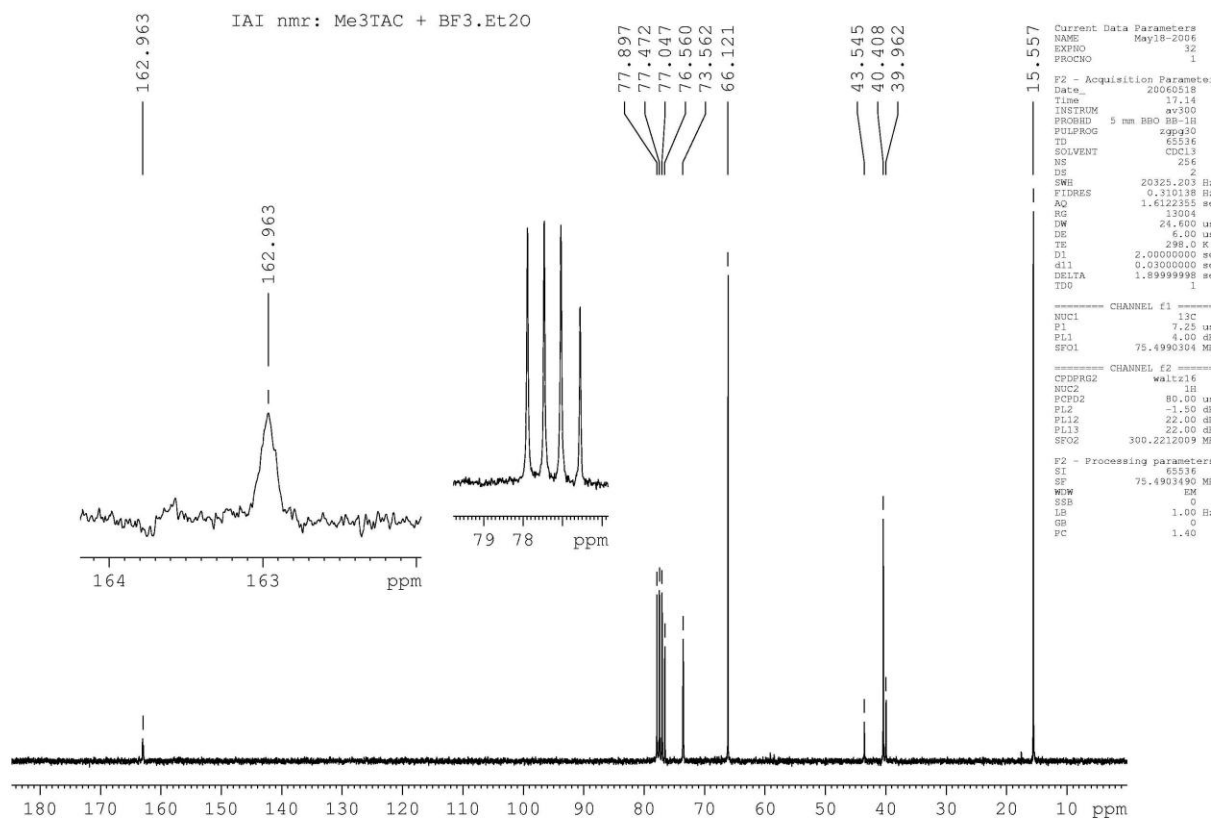
1,3-dimethyl-5-(4-trimethylsilyl)phenyl-1,3,5-triazacyclohexane: ^{13}C



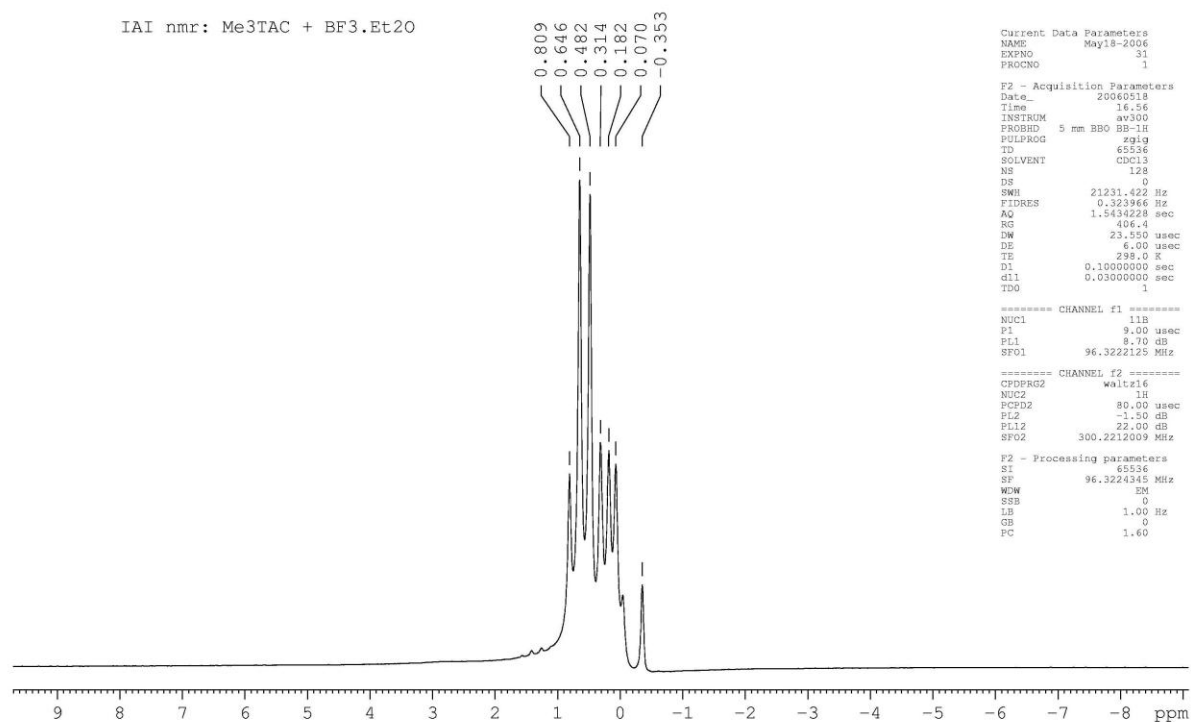
3.9: 1,3,5-trimethyl-1,3,5-triazacyclohexane with boron trifluoride diethyletherate: ^1H



1,3,5-trimethyl-1,3,5-triazacyclohexane with boron trifluoride diethyletherate: ^{13}C

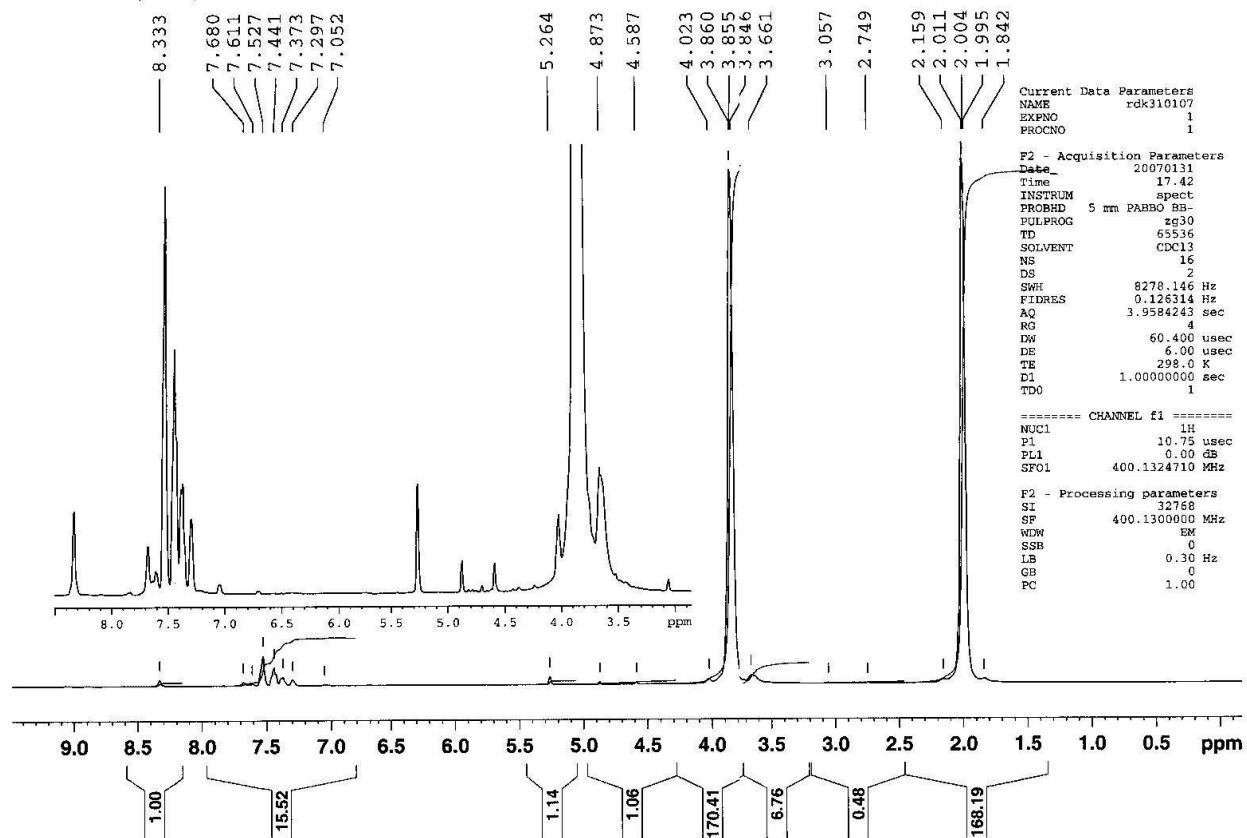


1,3,5-trimethyl-1,3,5-triazacyclohexane with boron trifluoride diethyletherate: ^{11}B



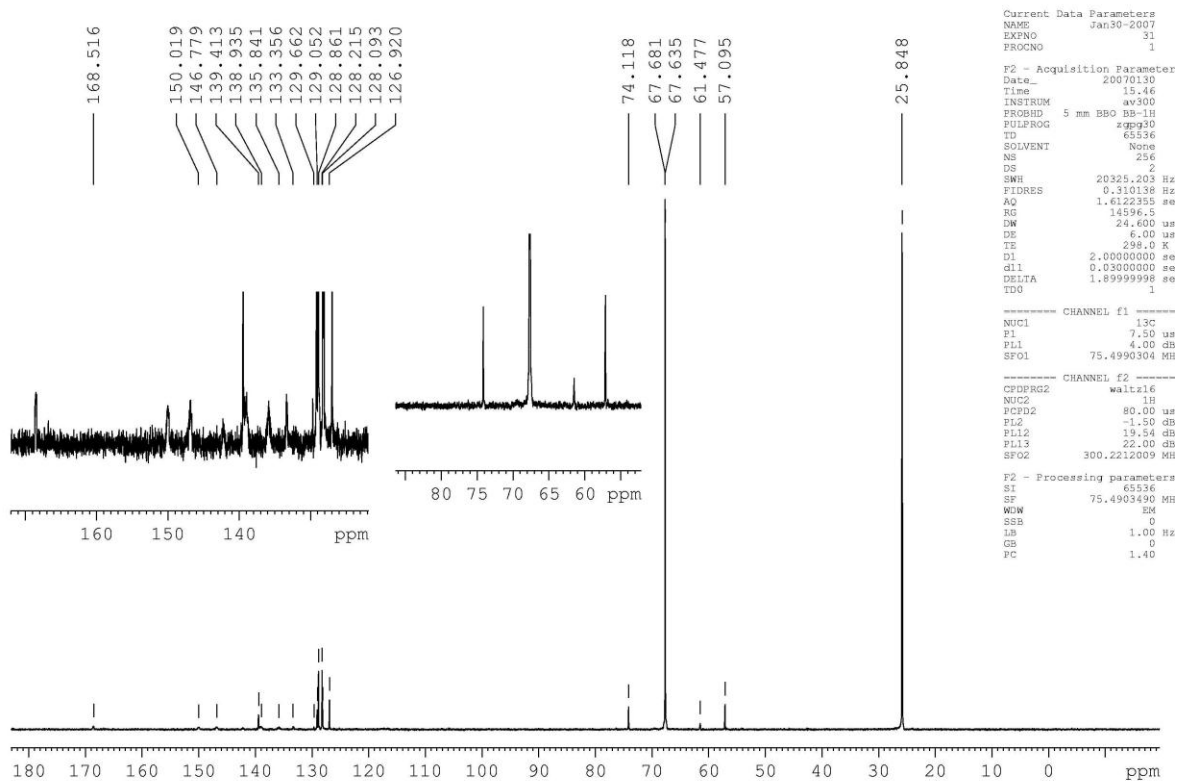
3.10: 1,3,5-tribenzyl-1,3,5-triazacyclohexane with tris(pentafluoro)phenylborane diethyletherate: ^1H

Bz3TAC + B(C6F5)3 in THF

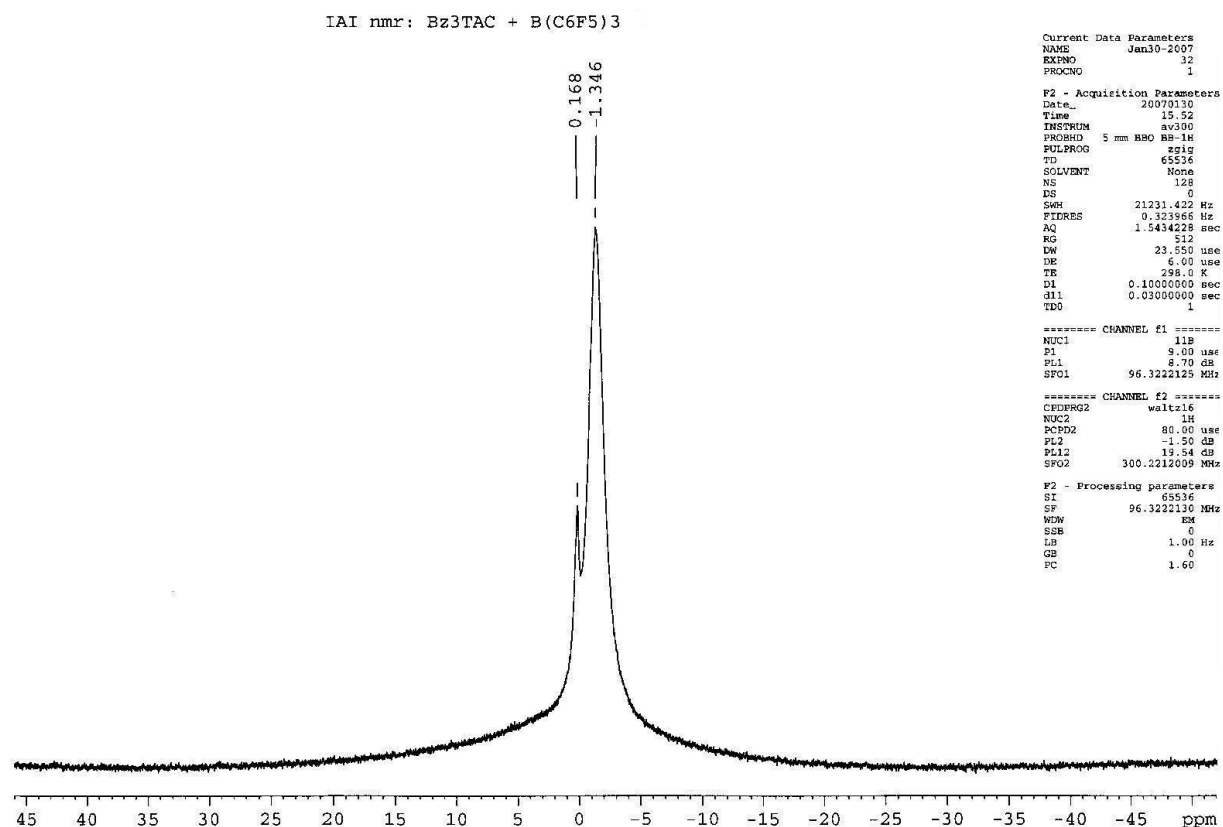


1,3,5-tribenzyl-1,3,5-triazacyclohexane with tris(pentafluoro)phenylborane diethyletherate: ^{13}C

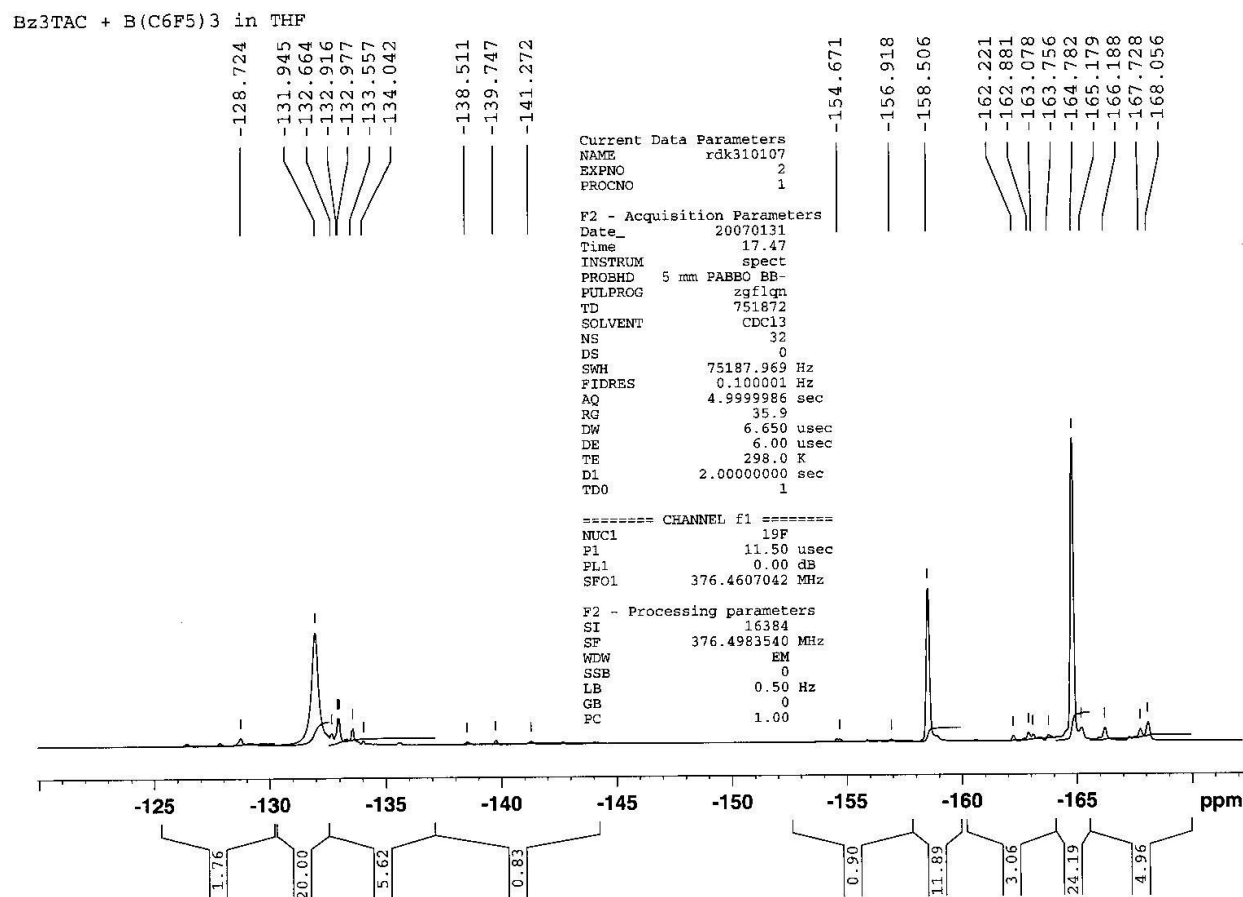
IAI nmr: Bz3TAC + B(C6F5)3 in Et2O



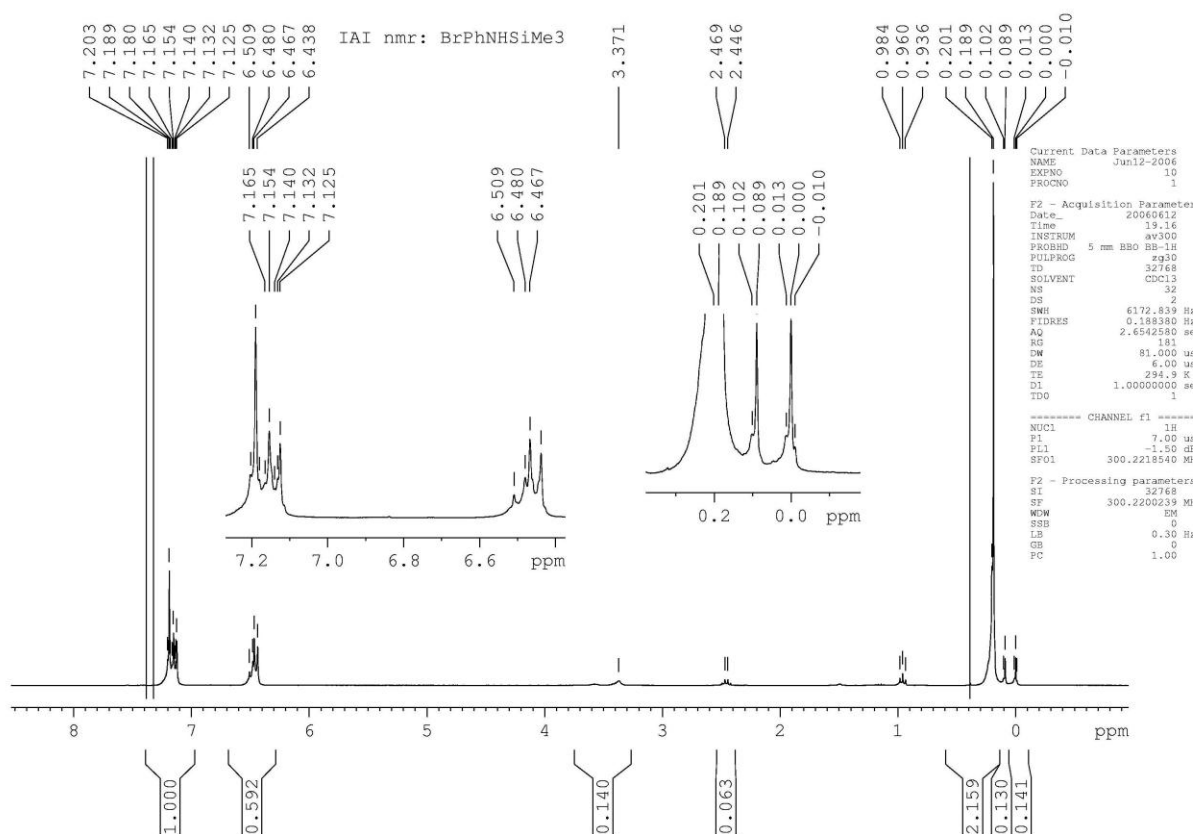
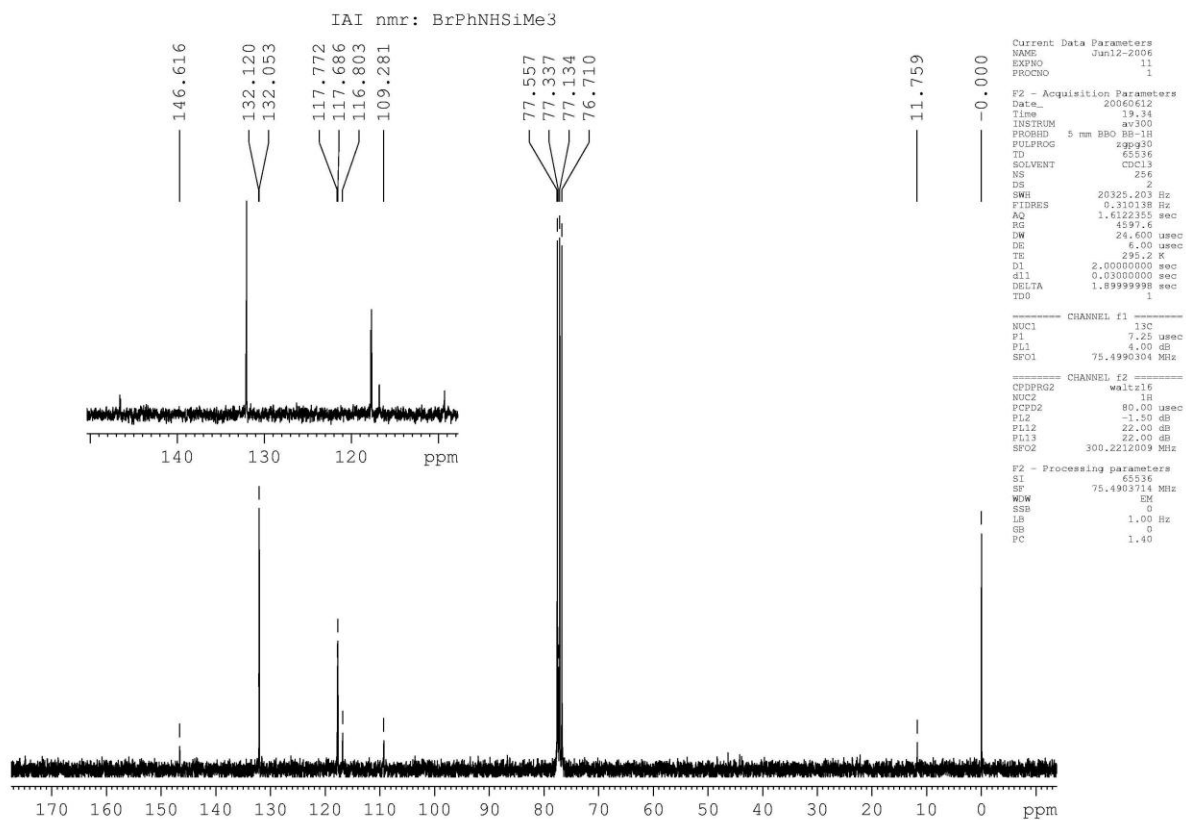
1,3,5-tribenzyl-1,3,5-triazacyclohexane with tris(pentafluoro)phenylborane diethyletherate: ^{11}B



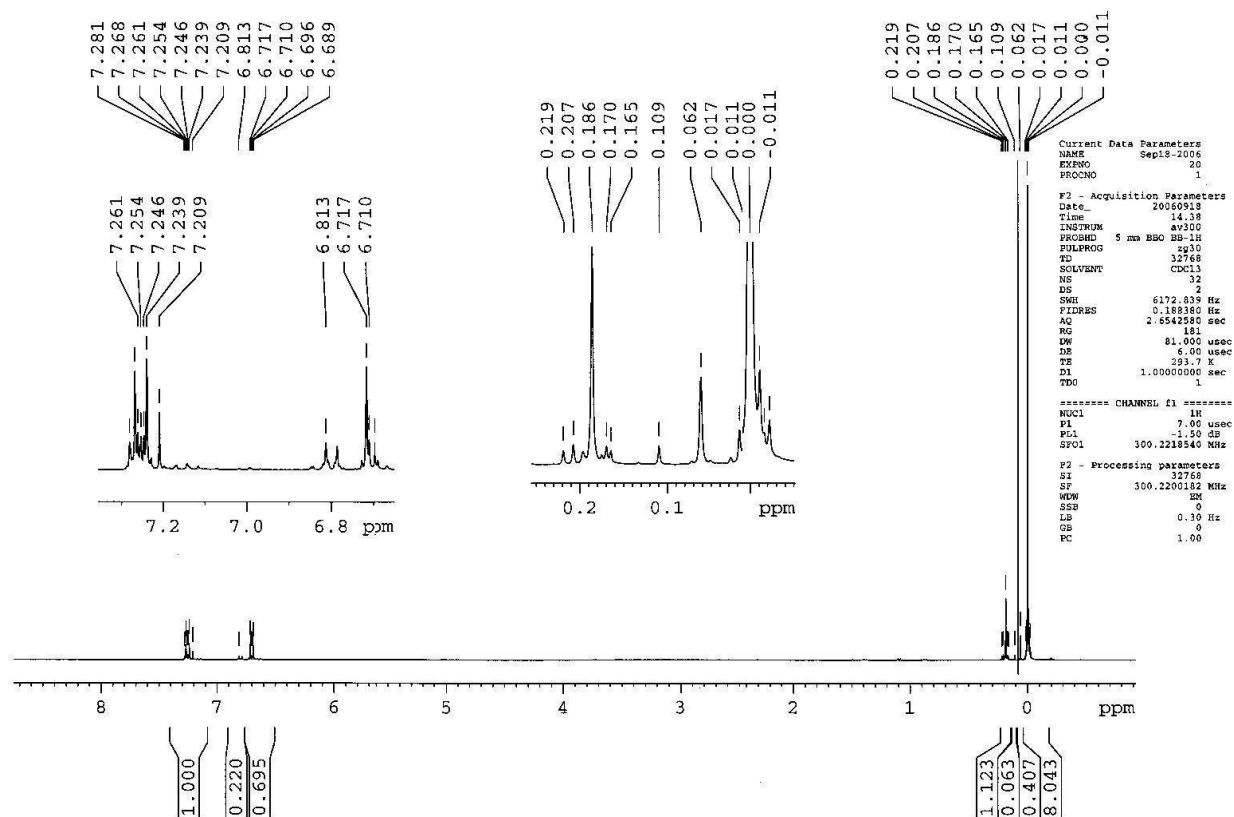
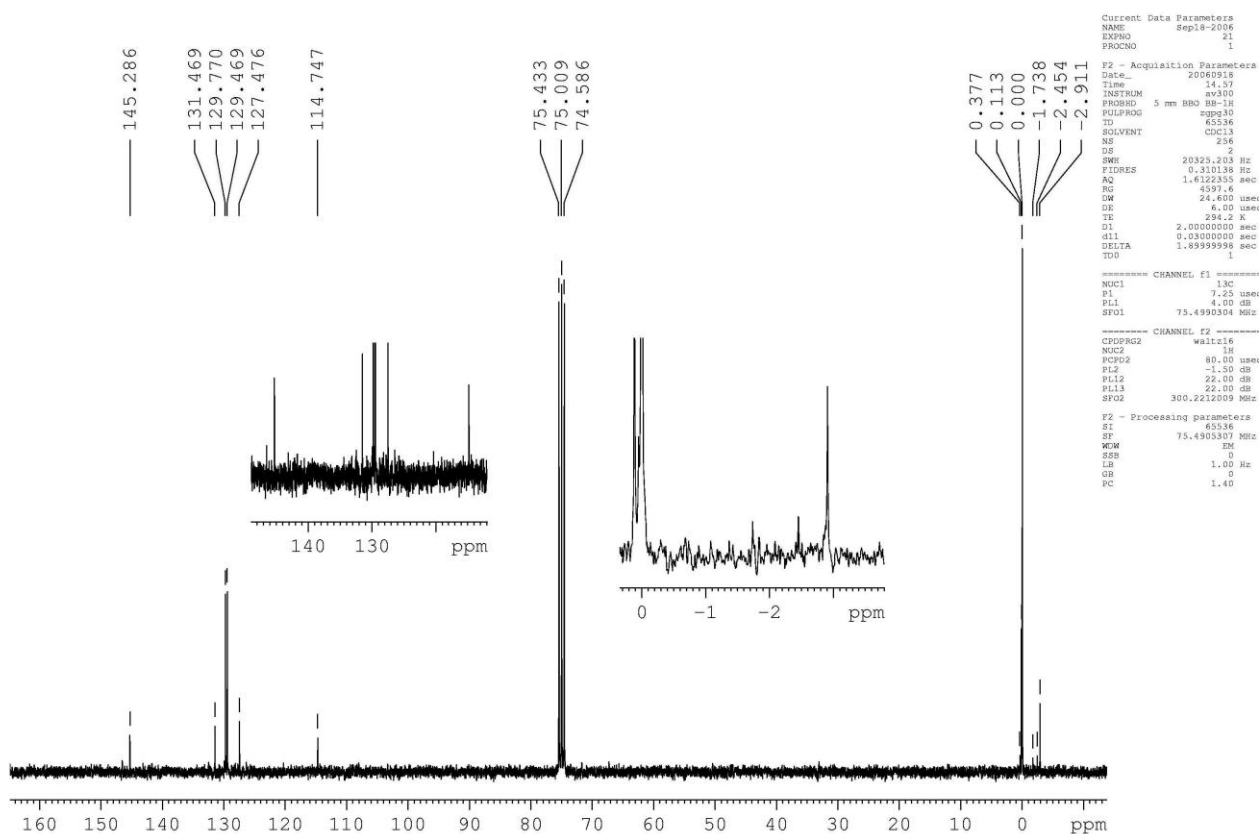
1,3,5-tribenzyl-1,3,5-triazacyclohexane with tris(pentafluoro)phenylborane diethyletherate: ^{19}F



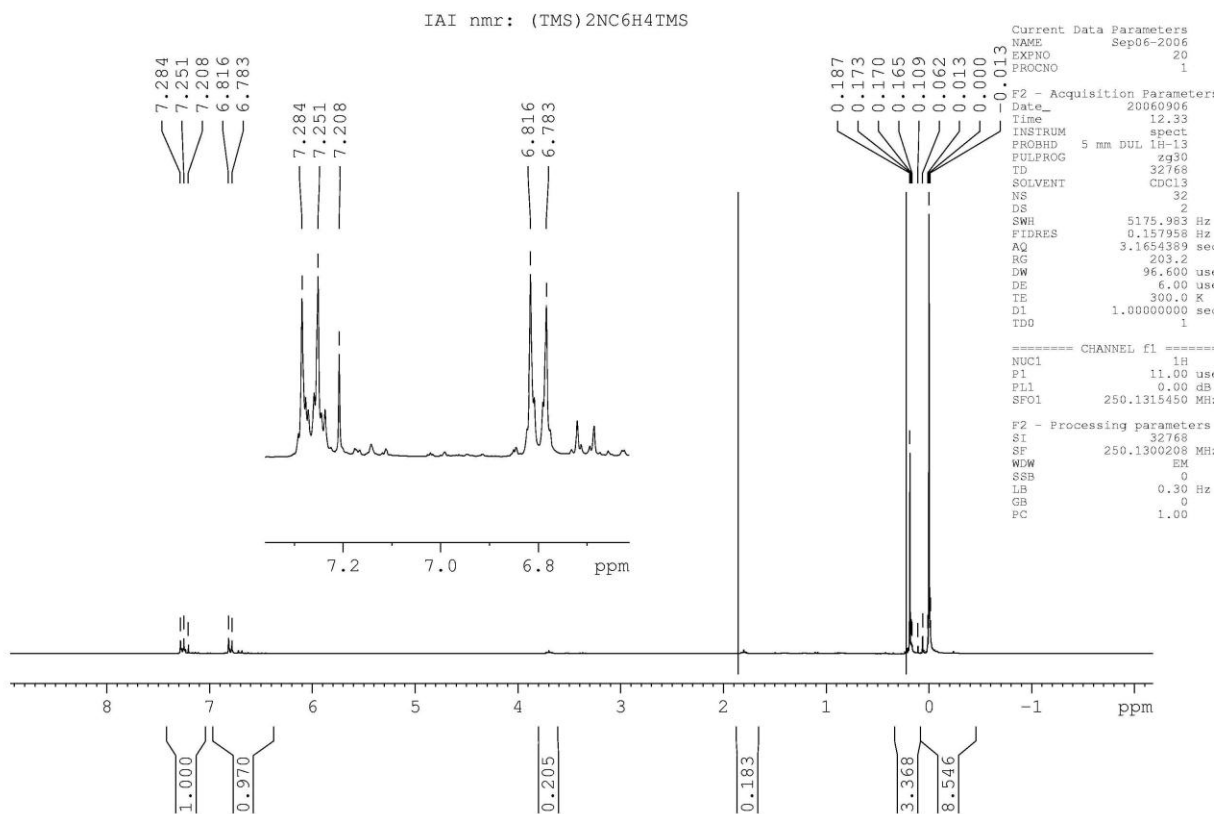
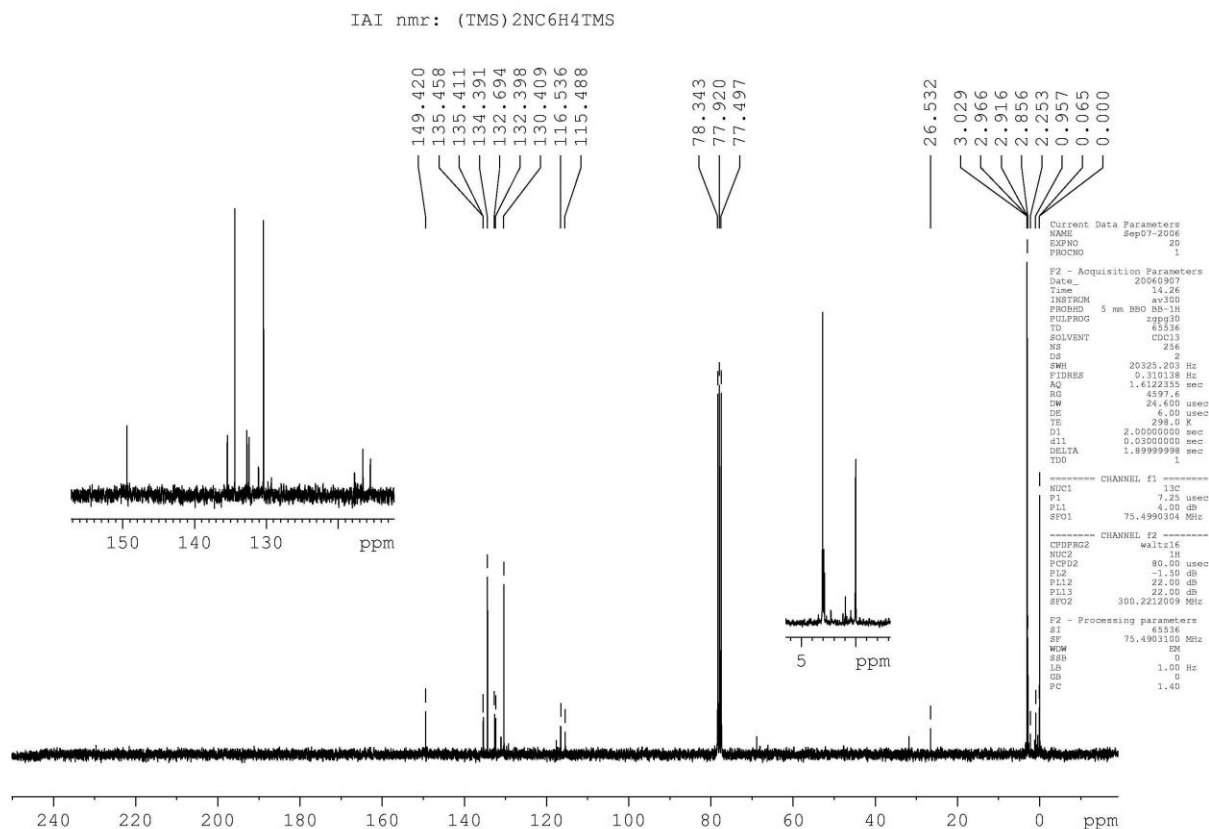
3.11:

N-(trimethyl)silyl-4-bromoaniline: ^1H N-(trimethyl)silyl-4-bromoaniline: ^{13}C 

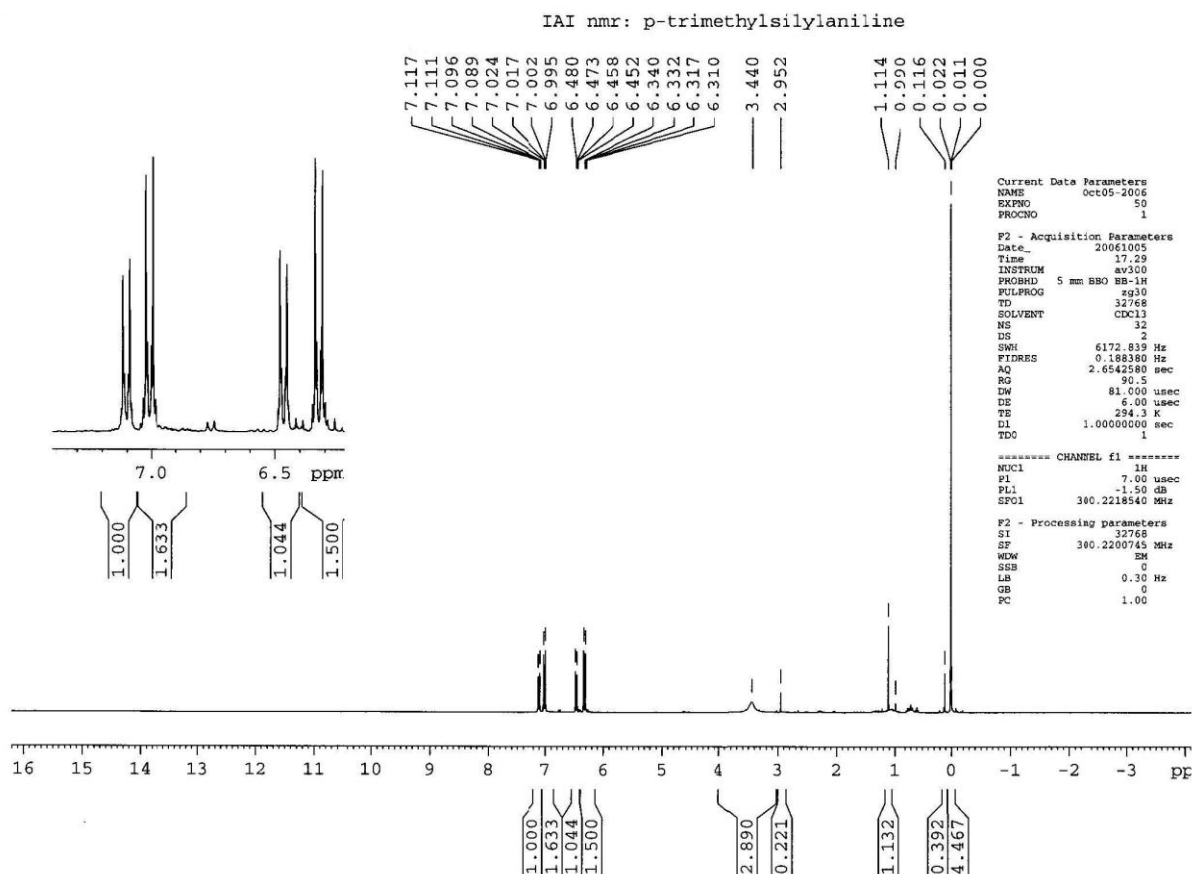
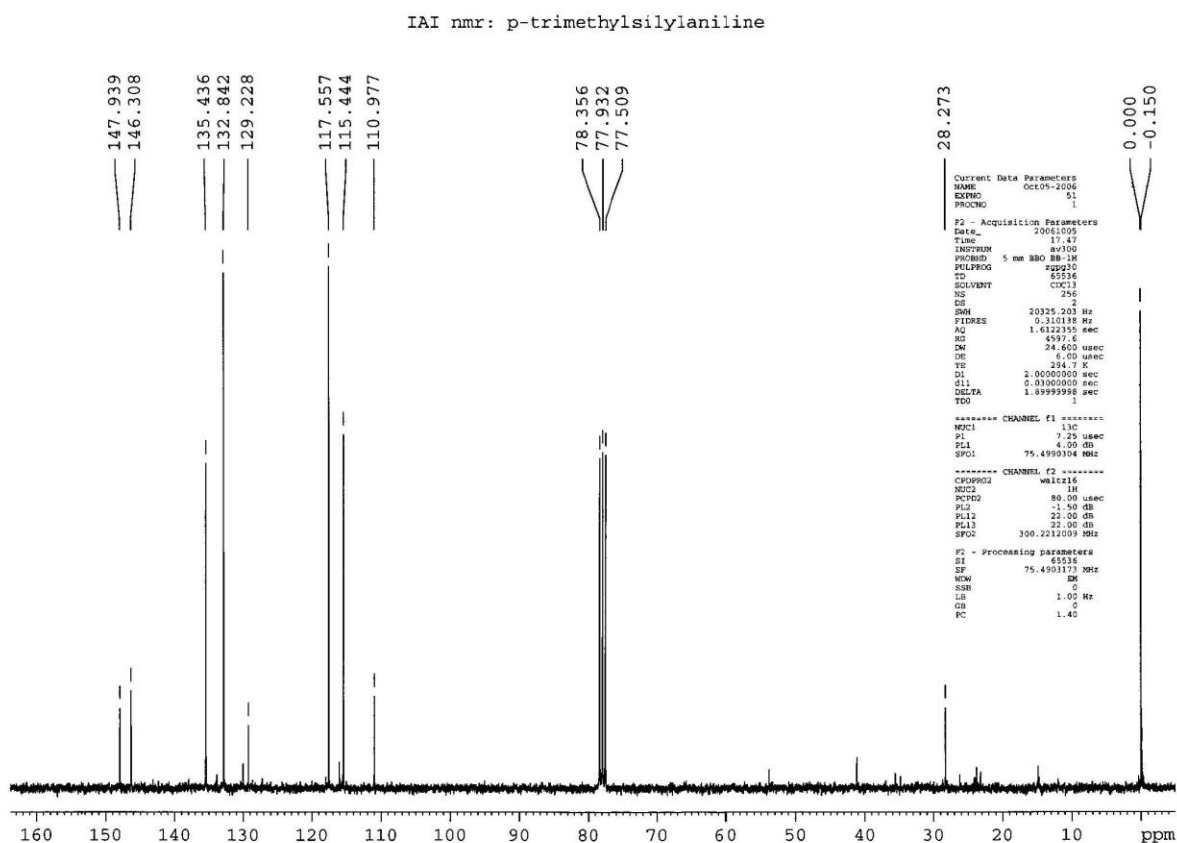
3.12:

N,N-bis-(trimethyl)silyl-4-bromoaniline: ^1H N,N-bis-(trimethyl)silyl-4-bromoaniline: ^{13}C 

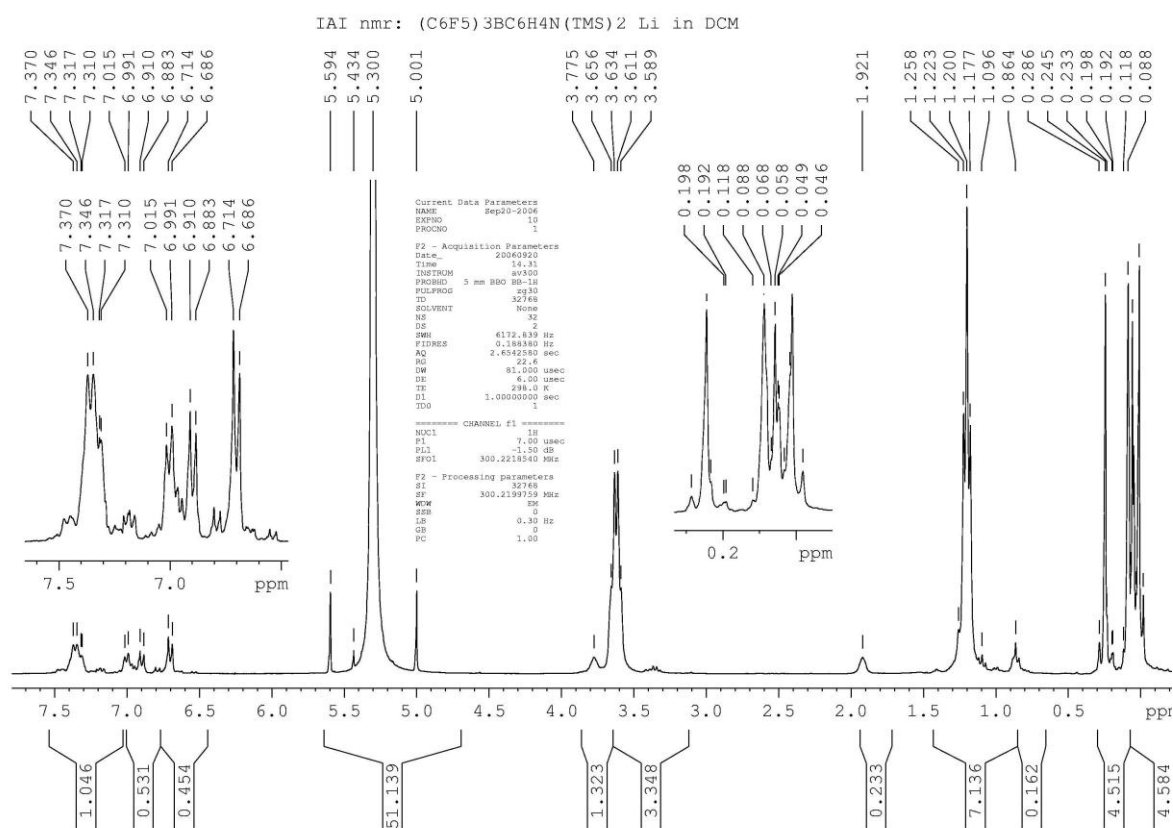
3.14:

N,N-bis-(trimethylsilyl)-p-(trimethyl)silylaniline: ^1H N,N-bis-(trimethylsilyl)-p-(trimethyl)silylaniline: ^{13}C 

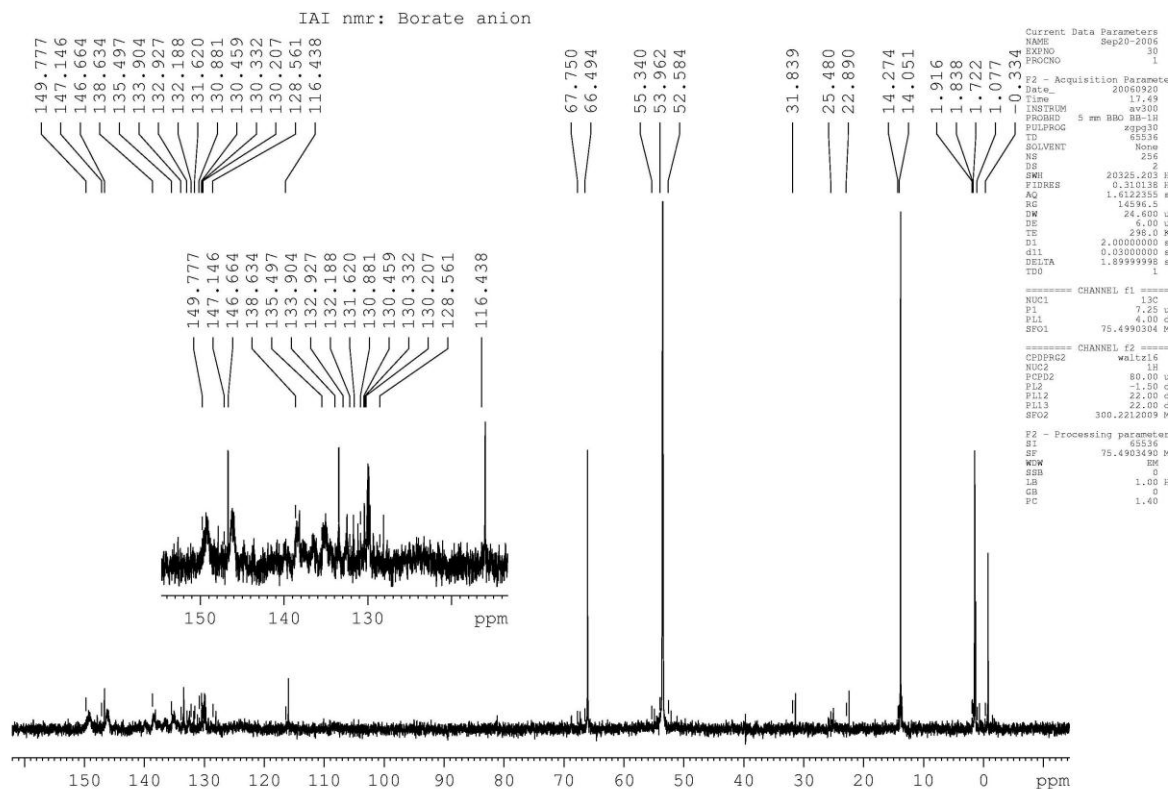
3.15:

4-(trimethyl)silylaniline hydrochloride: ^1H 4-(trimethyl)silylaniline hydrochloride: ^{13}C 

3.16: Lithium N,N-bis-(trimethyl)silyl-4-(tris(pentafluoro)phenylborato)aniline[Et₂O]₂: ¹H

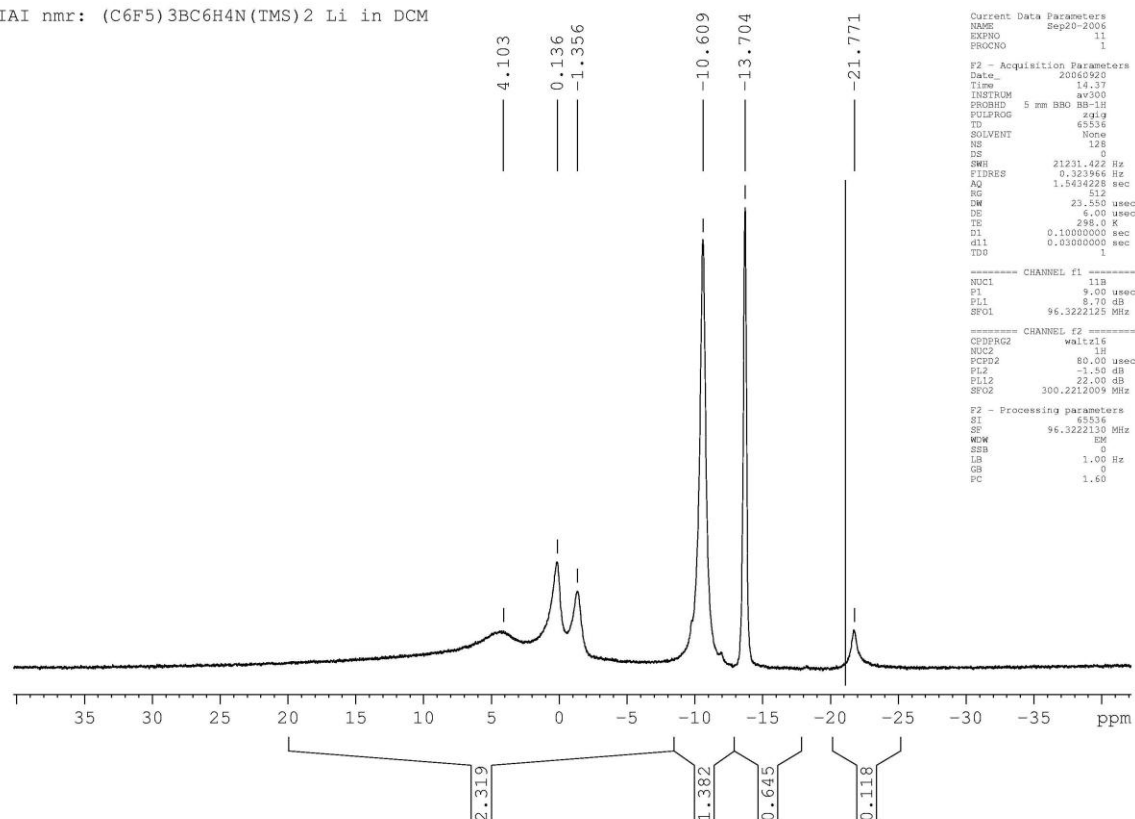


Lithium N,N-bis-(trimethyl)silyl-4-(tris(pentafluoro)phenylborato)aniline[Et₂O]₂: ¹³C



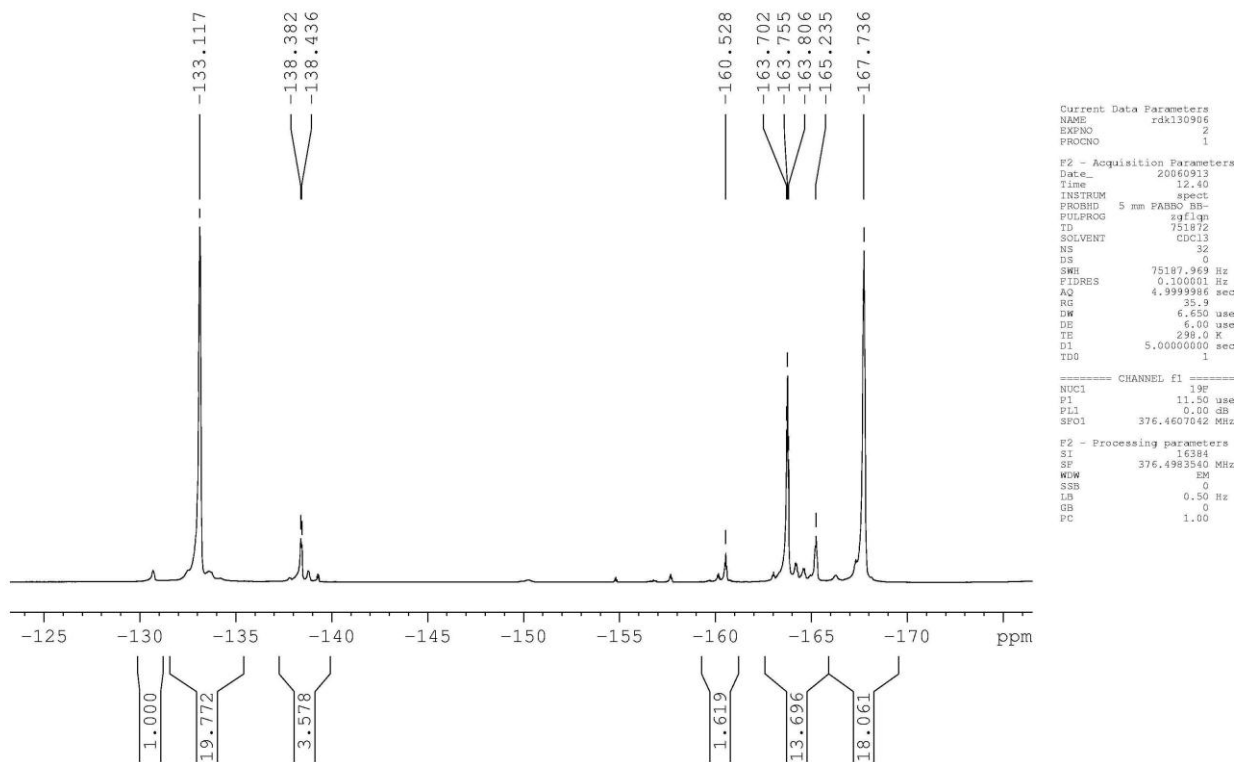
Lithium N,N-bis-(trimethyl)silyl-4-(tris(pentafluoro)phenylborato)aniline[Et₂O]₂ : ¹¹B

IAI nmr: (C6F5)3BC6H4N(TMS)2 Li in DCM

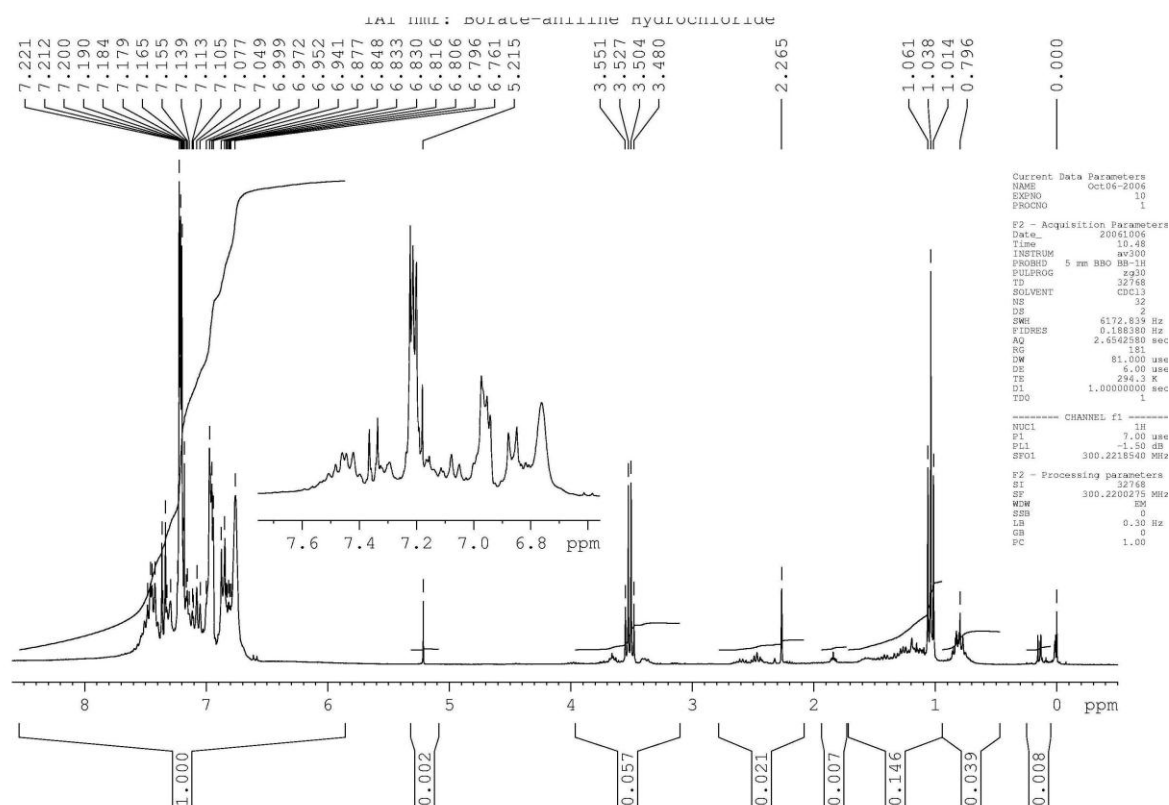


Lithium N,N-bis-(trimethyl)silyl-4-(tris(pentafluoro)phenylborato)aniline[Et₂O]₂ : ¹⁹F

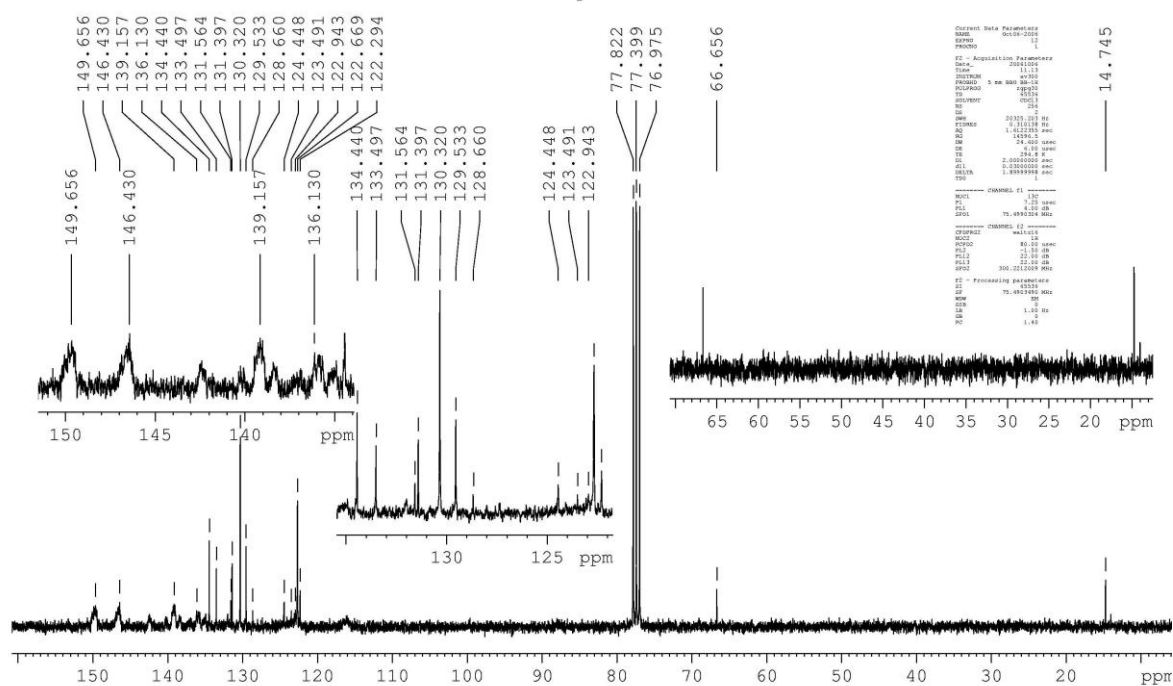
(C6F5)3B(C6H4NTMS2 Li) in DCM



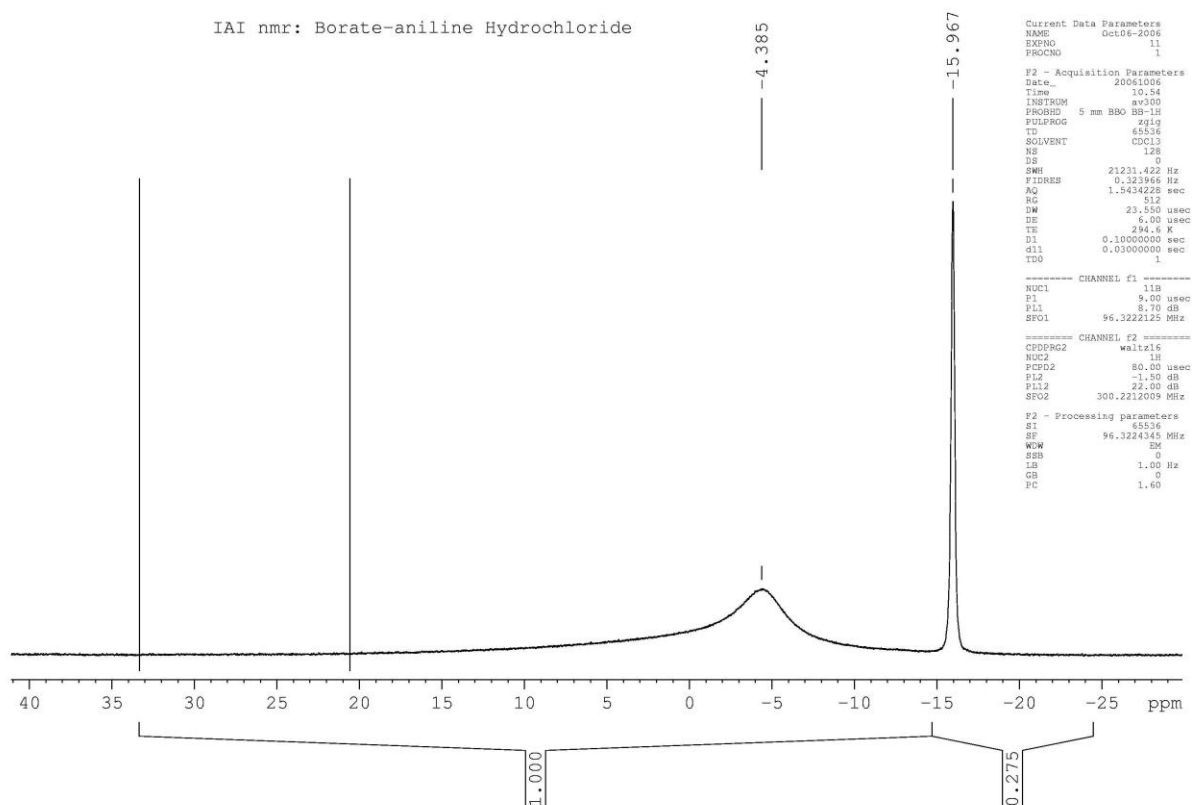
3.17: Lithium 4-aminophenyltris(pentafluoro)phenylborate hydrochloride)[Et₂O]₂: ¹H
Oct06-2006 10 1



Lithium 4-aminophenyltris(pentafluoro)phenylborate hydrochloride)[Et₂O]₂: ¹³C

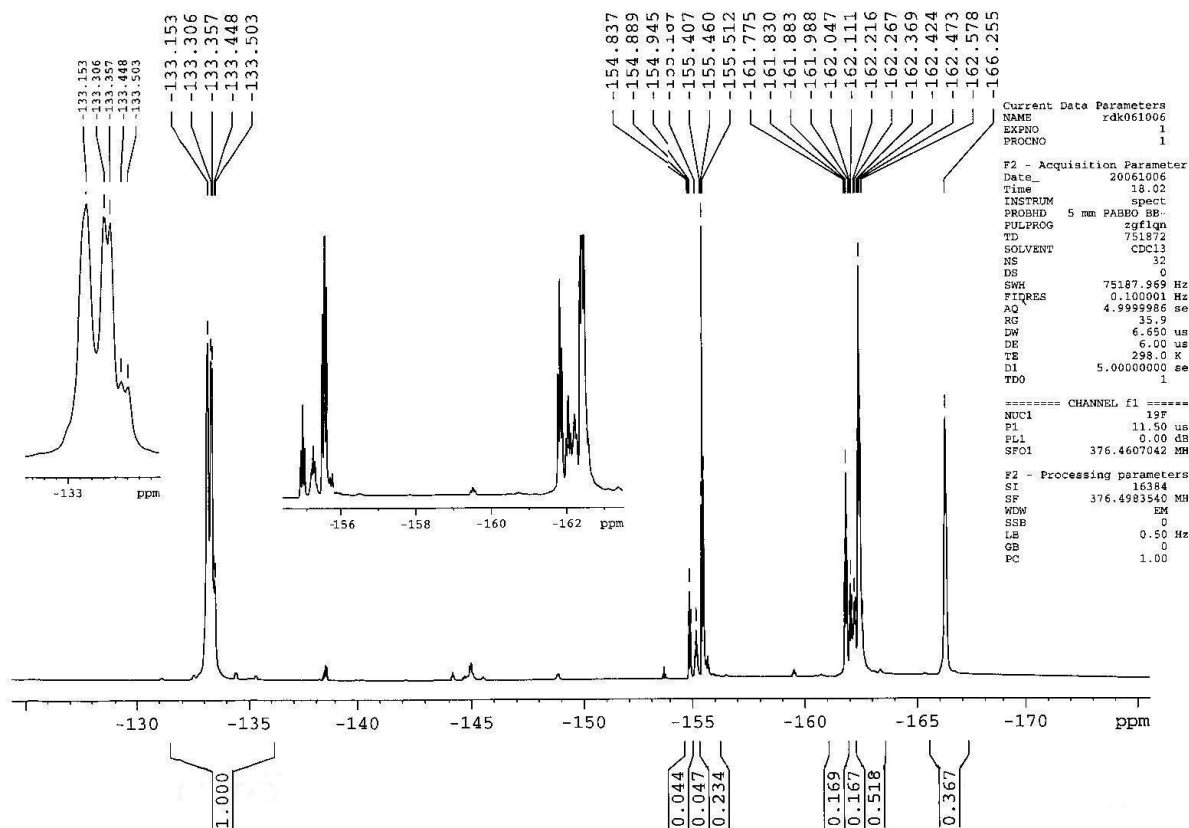


Lithium 4-aminophenyltris(pentafluoro)phenylborate hydrochloride)[Et₂O]₂: ¹¹B

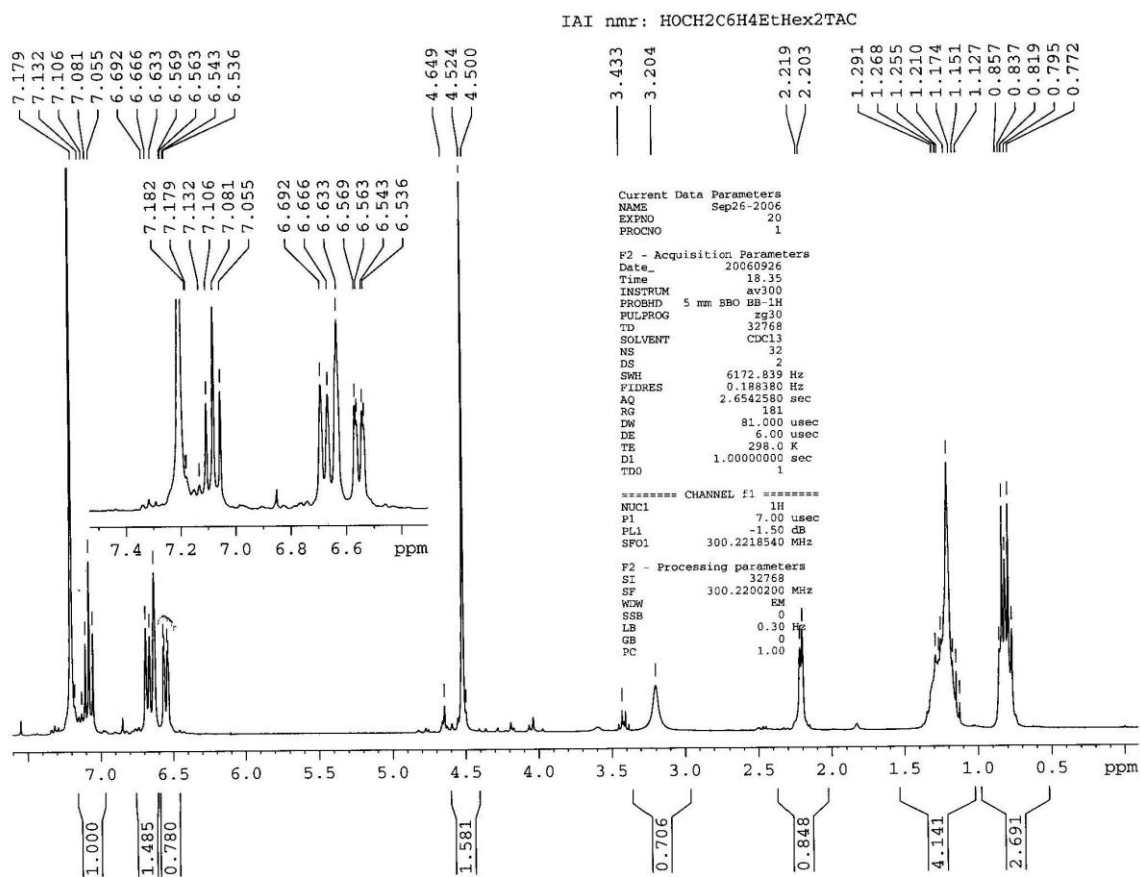


Lithium 4-aminophenyltris(pentafluoro)phenylborate hydrochloride)[Et₂O]₂: ¹⁹F:

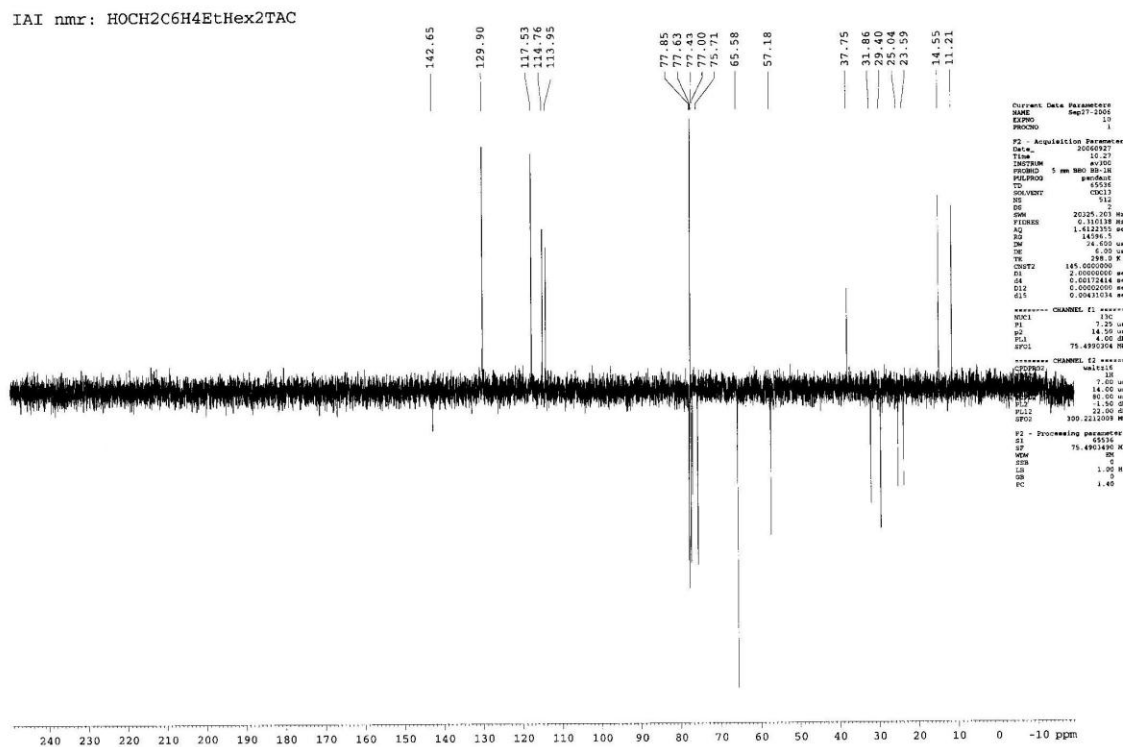
(C6F5)₃B(C6H4NH₃) in CDCl₃



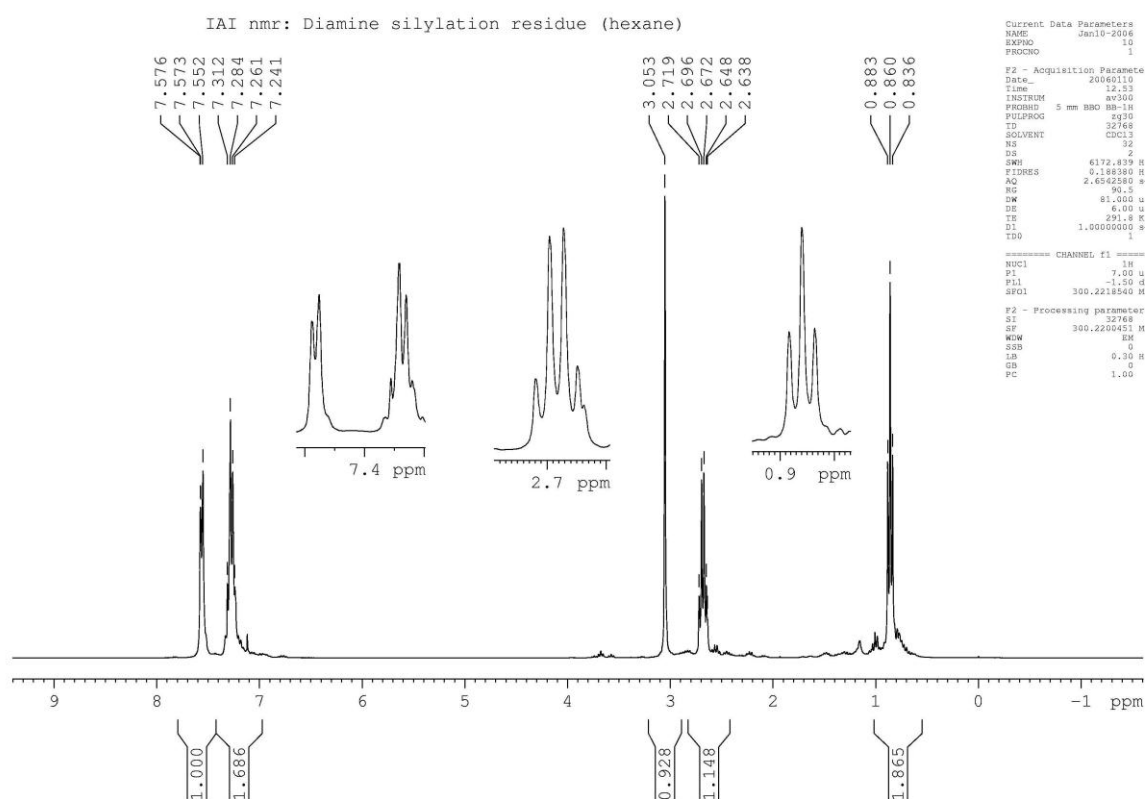
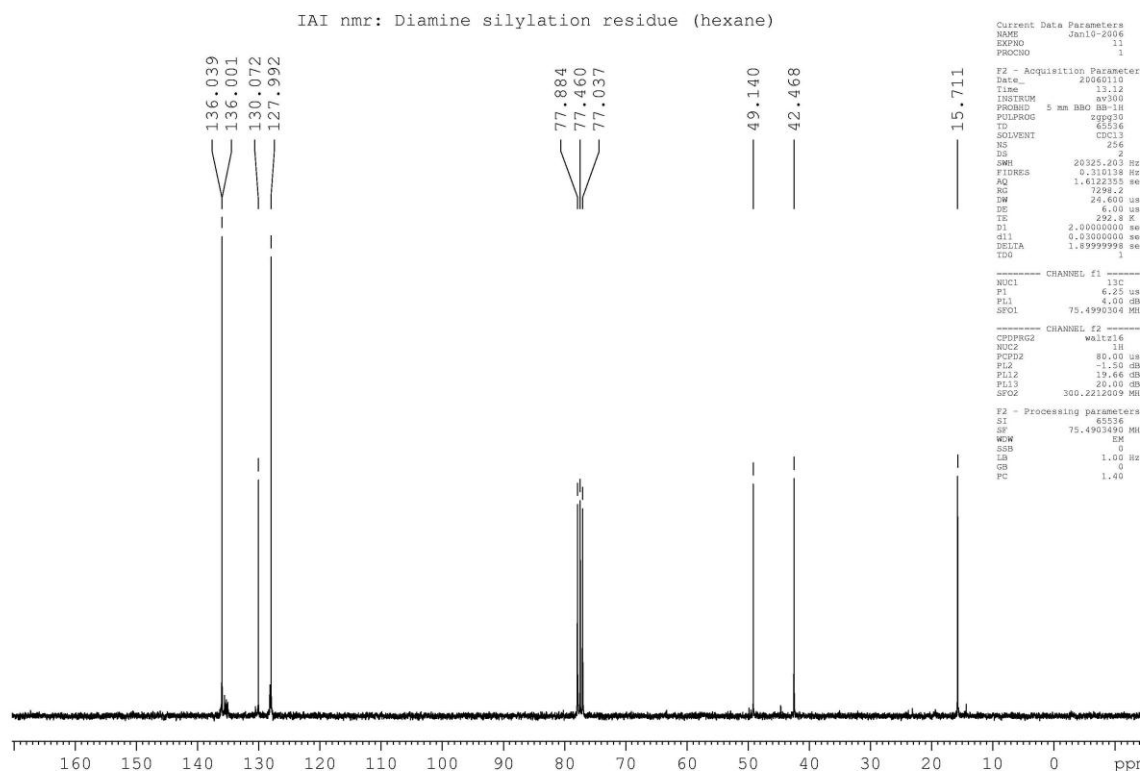
3.18: 1,3,5-tris(2-ethyl)hexyl-1,3,5-triazacyclohexane + sodium 3-aminobenzylalcoholate: ^1H



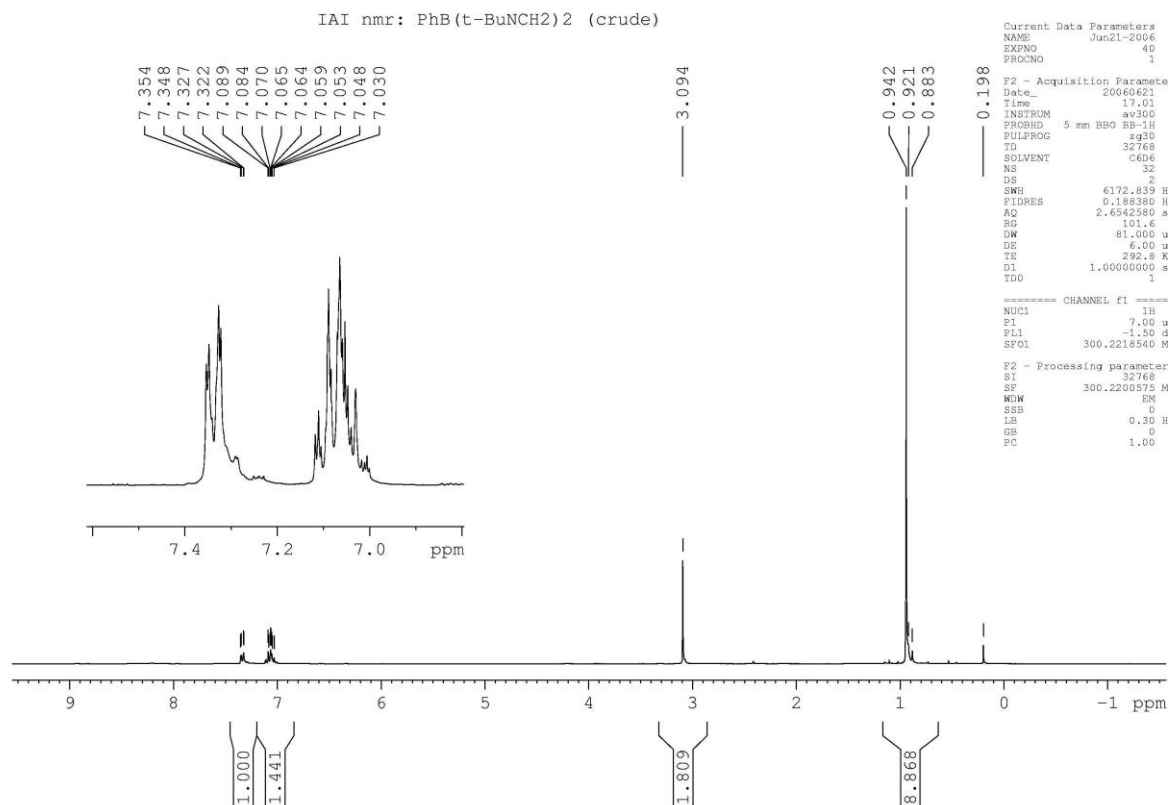
1,3,5-tris(2-ethyl)hexyl-1,3,5-triazacyclohexane + sodium 3-aminobenzylalcoholate: ^{13}C



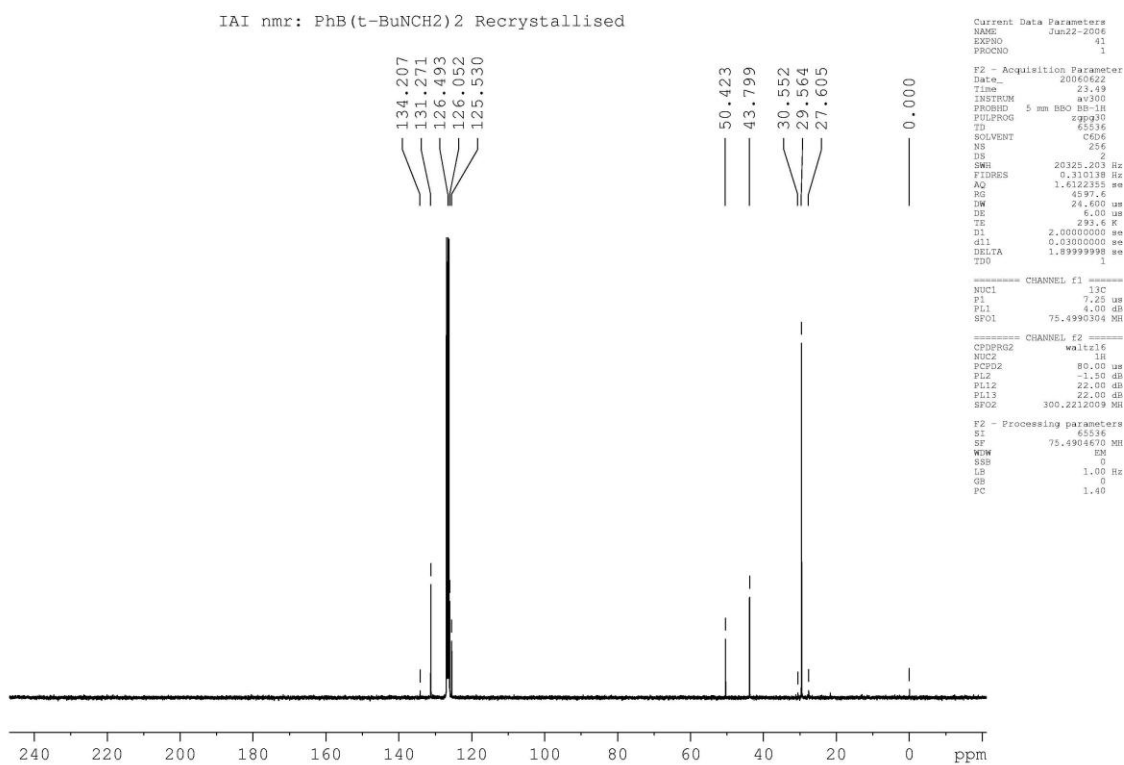
3.20:

1,1-diphenyl-2,5-diethyl-1-sila-2,5-diazacyclopentane: ^1H :1,1-diphenyl-2,5-diethyl-1-sila-2,5-diazacyclopentane: ^{13}C :

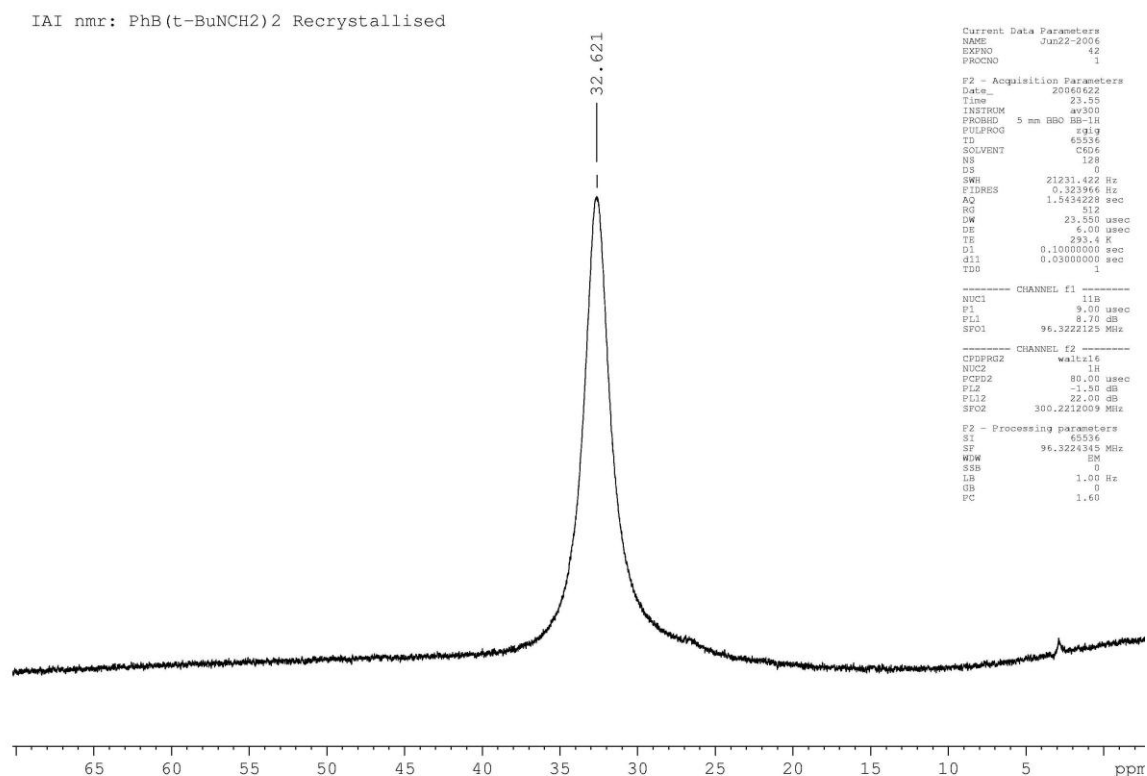
3.22: 1-Phenyl-2,5-di-*tert*-butyl-1-bora-2,5-diazacyclopentane: ^1H (C_6D_6):



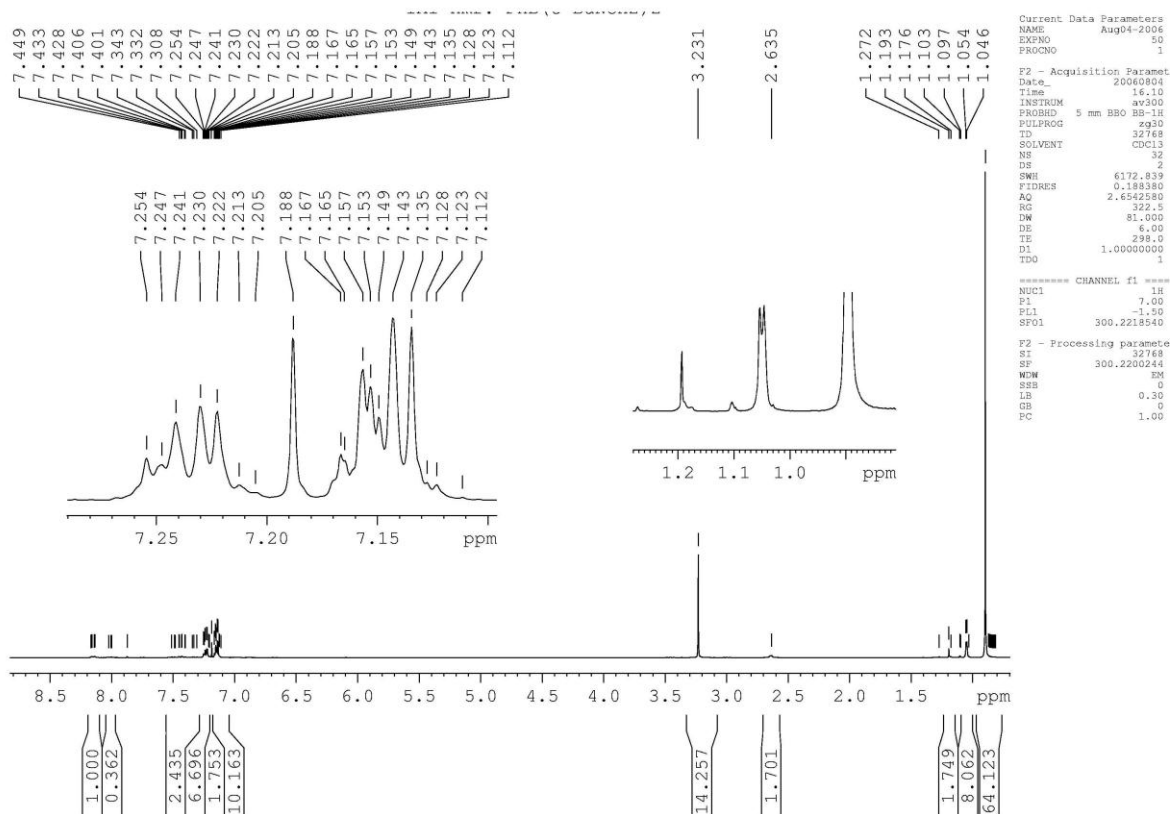
1-Phenyl-2,5-di-*tert*-butyl-1-bora-2,5-diazacyclopentane: ^{13}C : (C_6D_6)



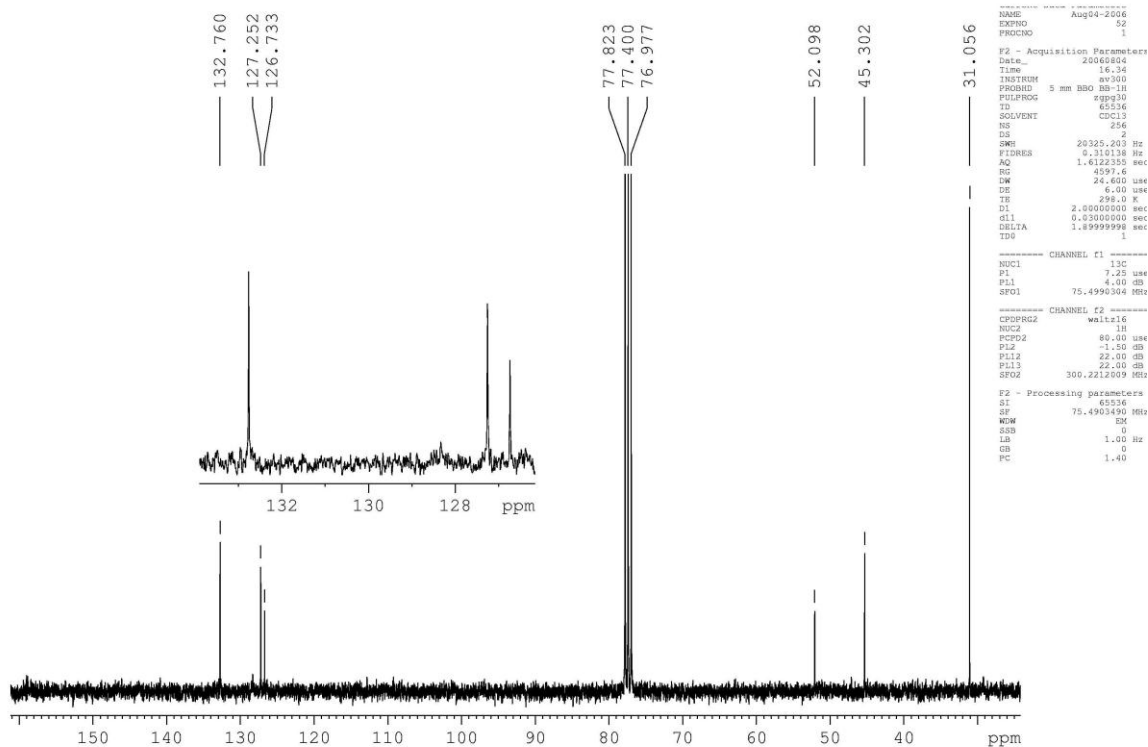
1-Phenyl-2,5-di-*tert*-butyl-1-bora-2,5-diazacyclopentane: ^{11}B : (C_6D_6):



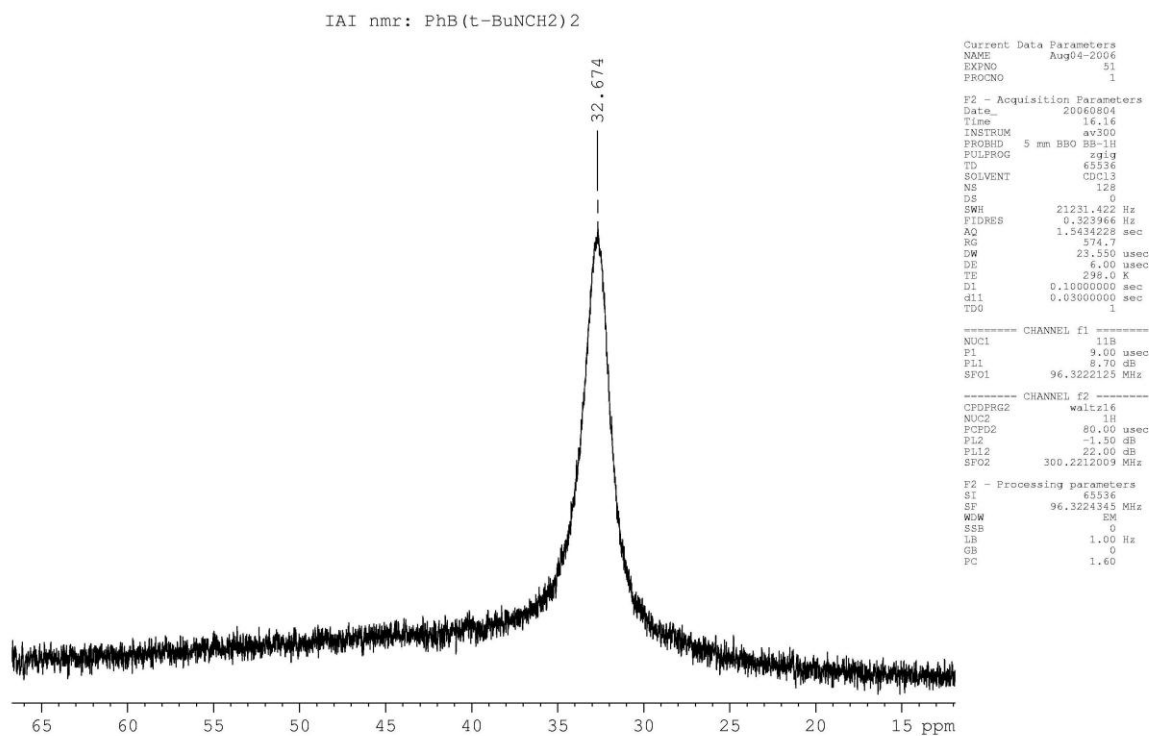
1-Phenyl-2,5-di-*tert*-butyl-1-bora-2,5-diazacyclopentane: ^1H : (CDCl_3)



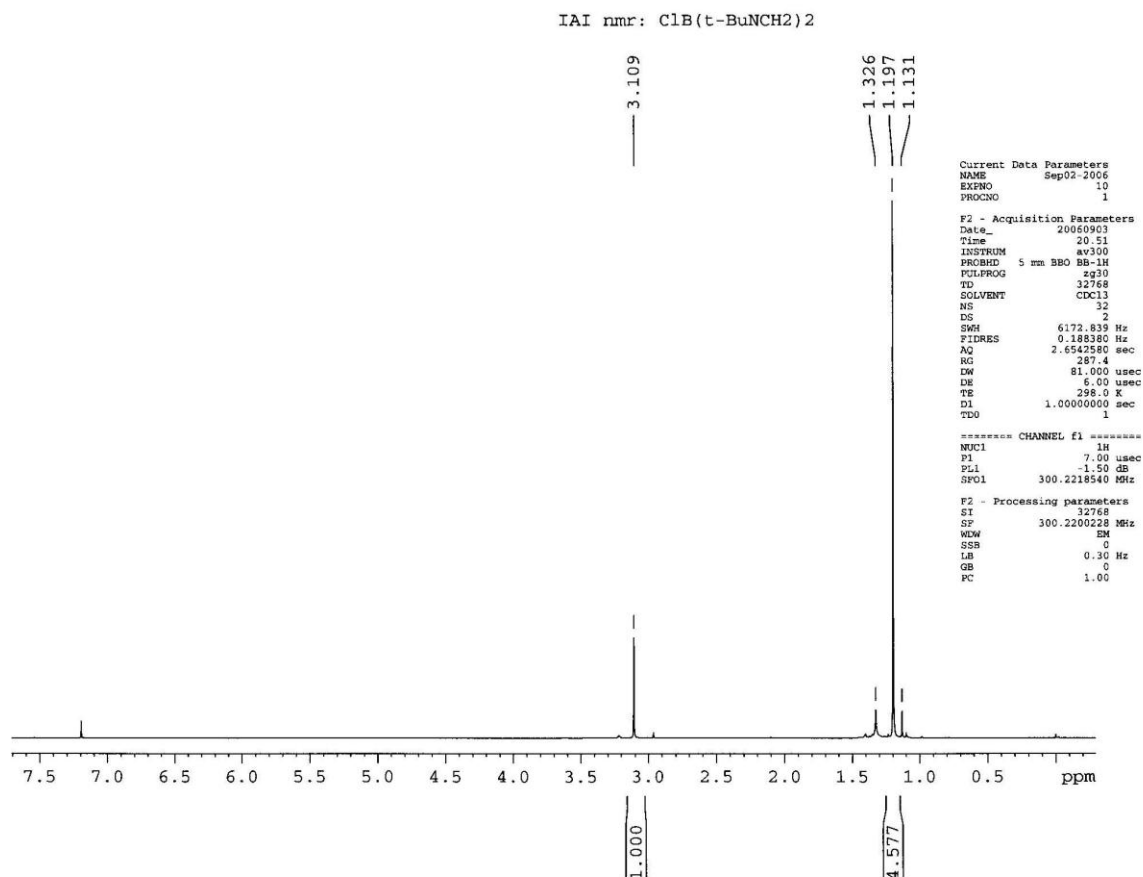
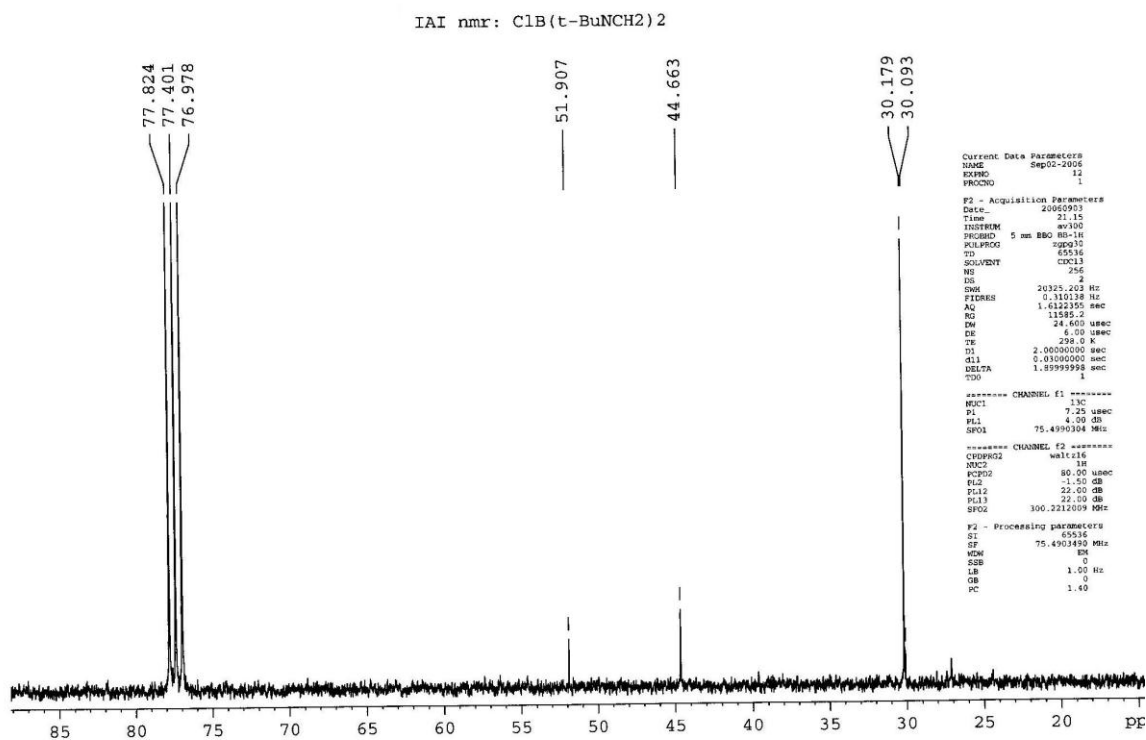
1-Phenyl-2,5-di-*tert*-butyl-1-bora-2,5-diazacyclopentane: ^{13}C : (CDCl_3)



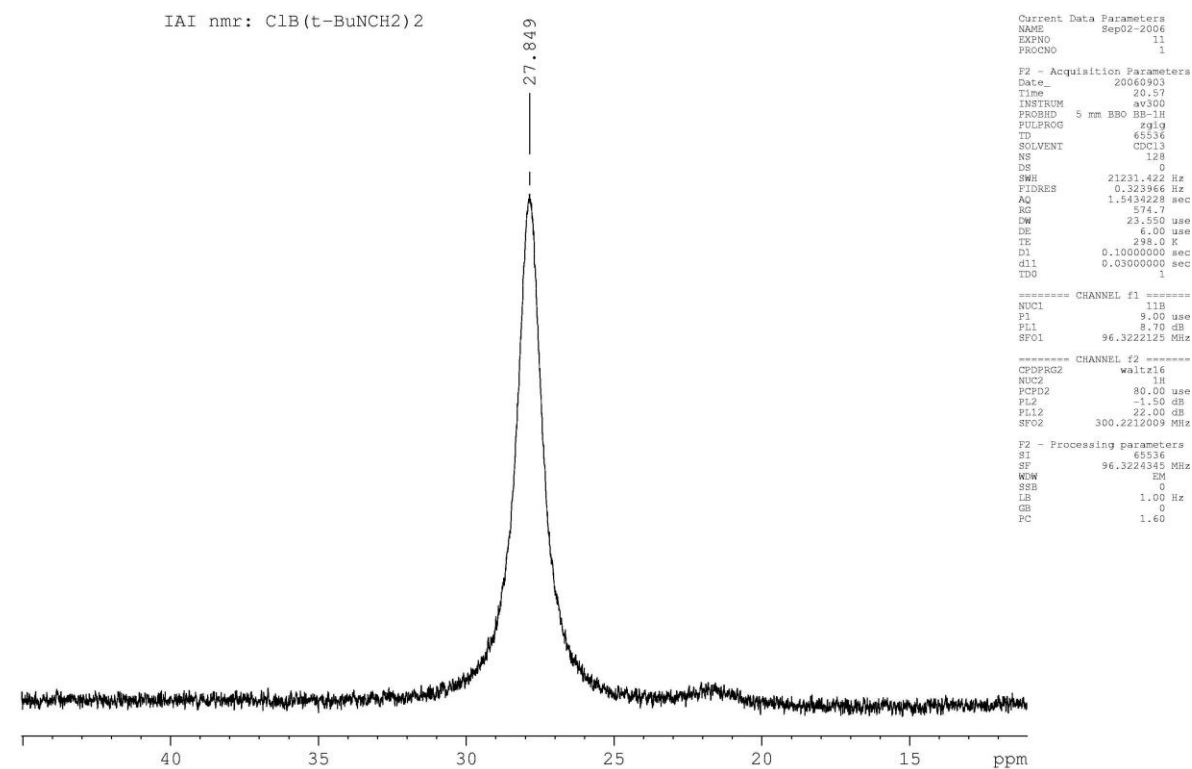
1-Phenyl-2,5-di-*tert*-butyl-1-bora-2,5-diazacyclopentane: ^{11}B : (CDCl_3)



3.24:

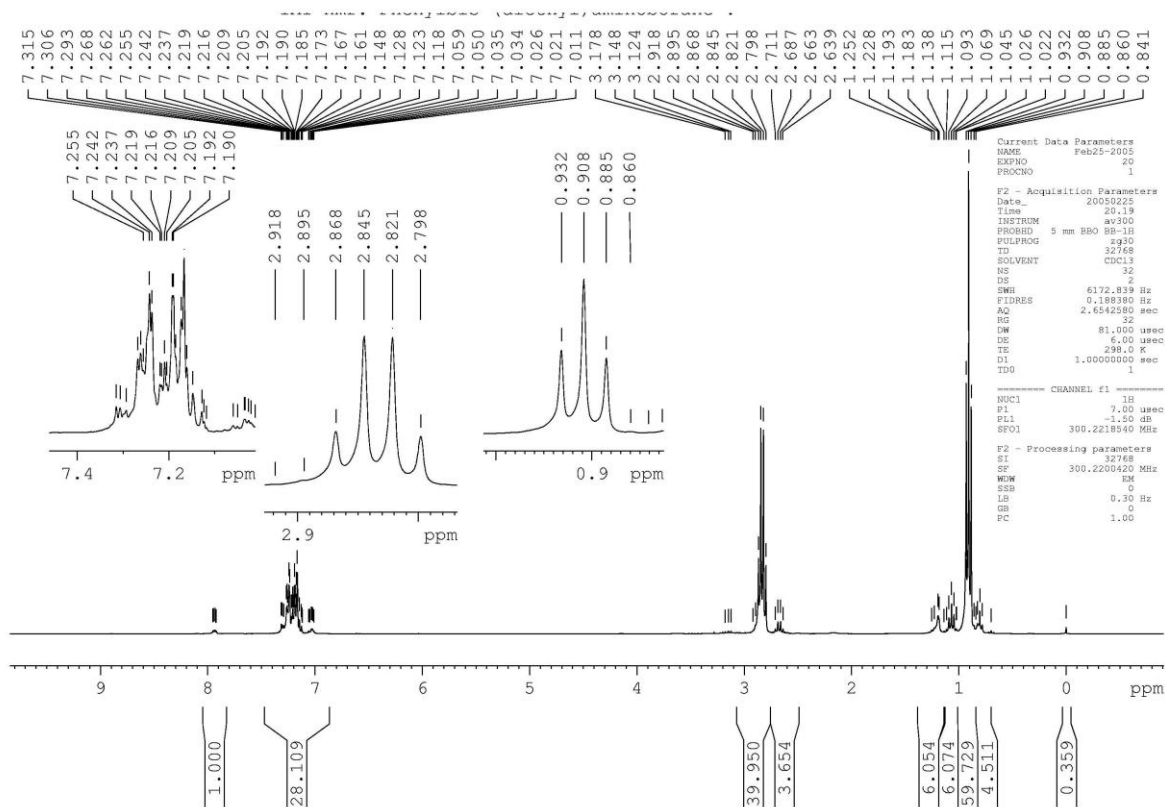
1-chloro-2,5-di-*tert*-butyl-1-bora-2,5-diazacyclopentane: ^1H :1-chloro-2,5-di-*tert*-butyl-1-bora-2,5-diazacyclopentane: ^{13}C 

1-chloro-2,5-di-*tert*-butyl-1-bora-2,5-diazacyclopentane: ^{11}B

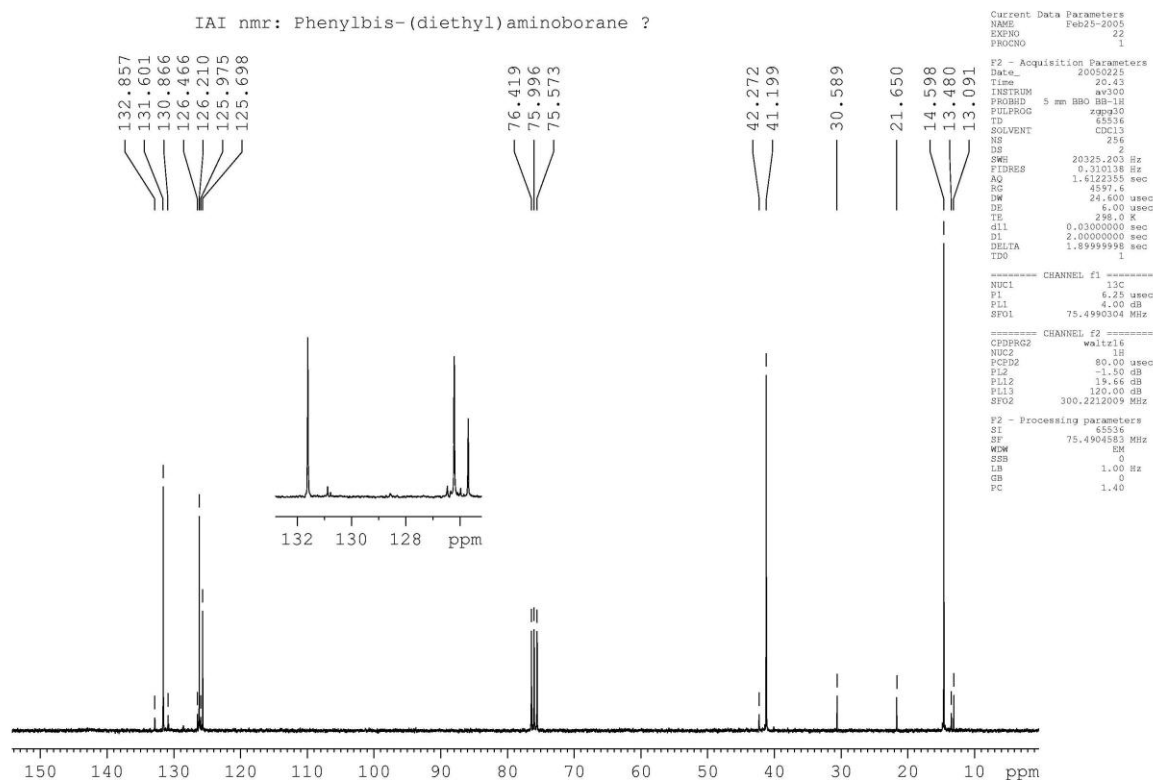


3.26:

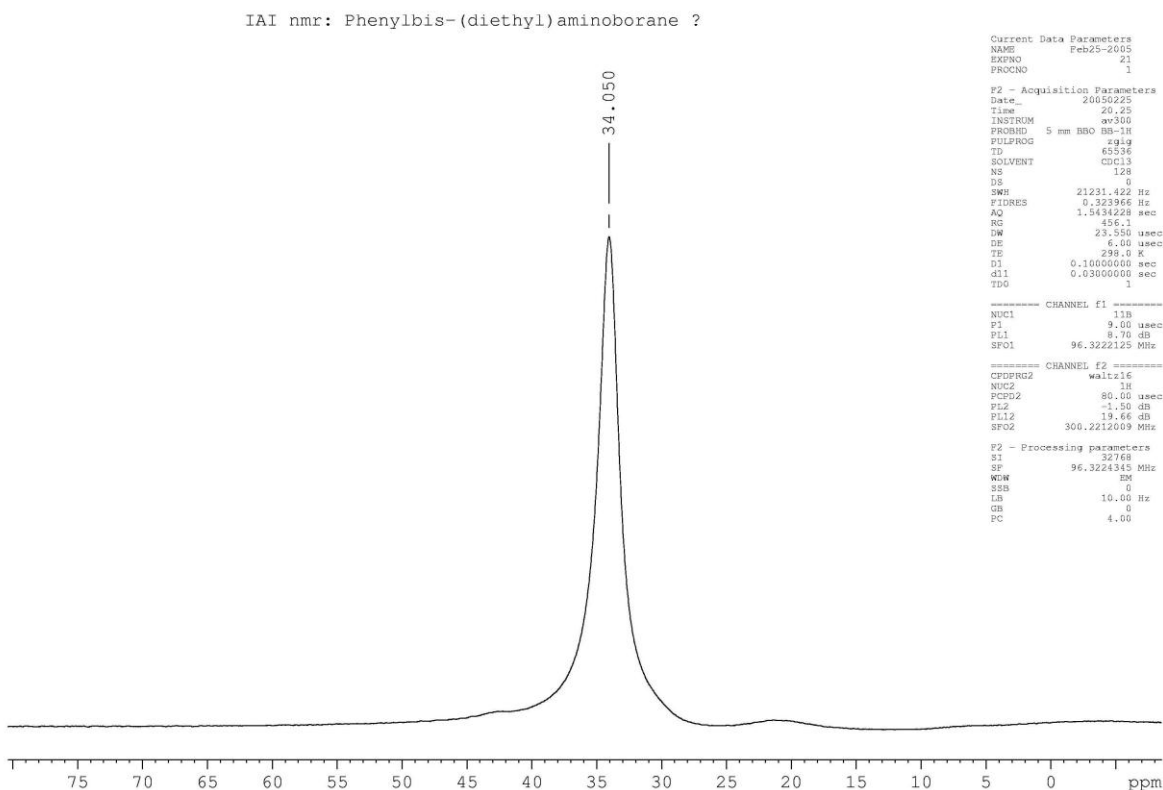
Bis-(diethyl)aminophenylborane: ^1H :



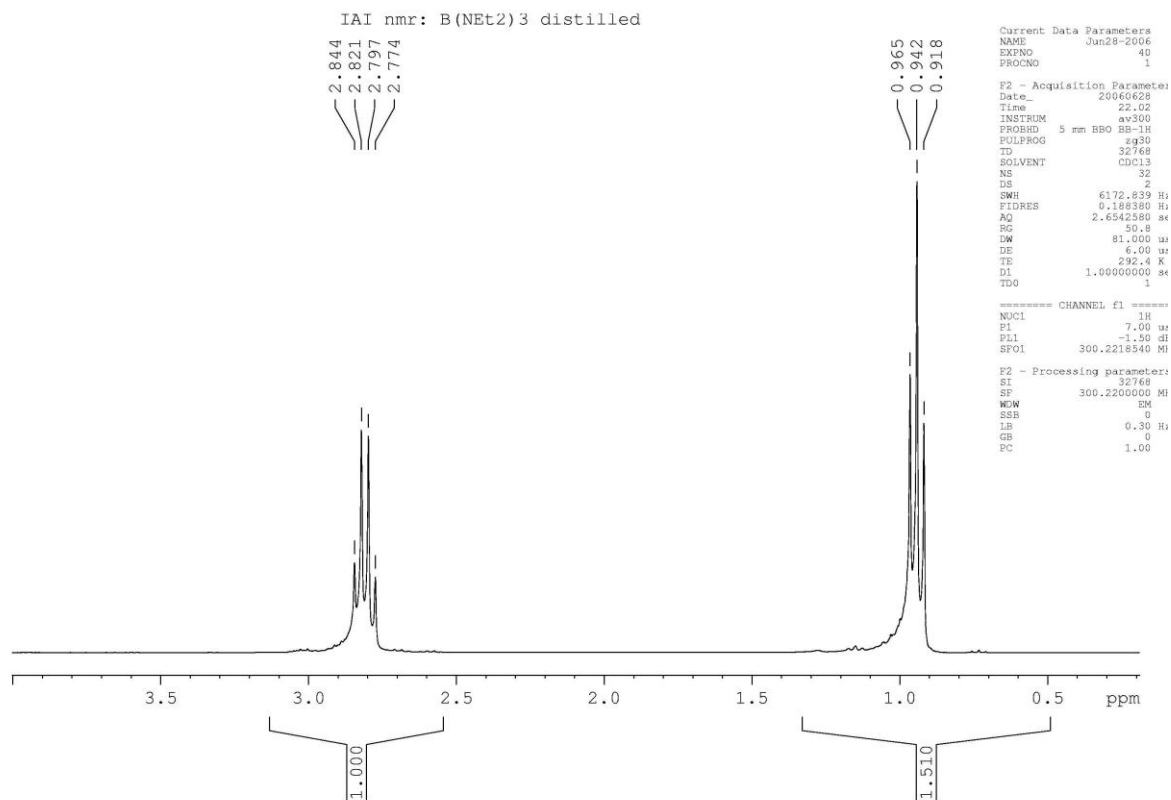
Bis-(diethyl)aminophenylborane: ^{13}C :



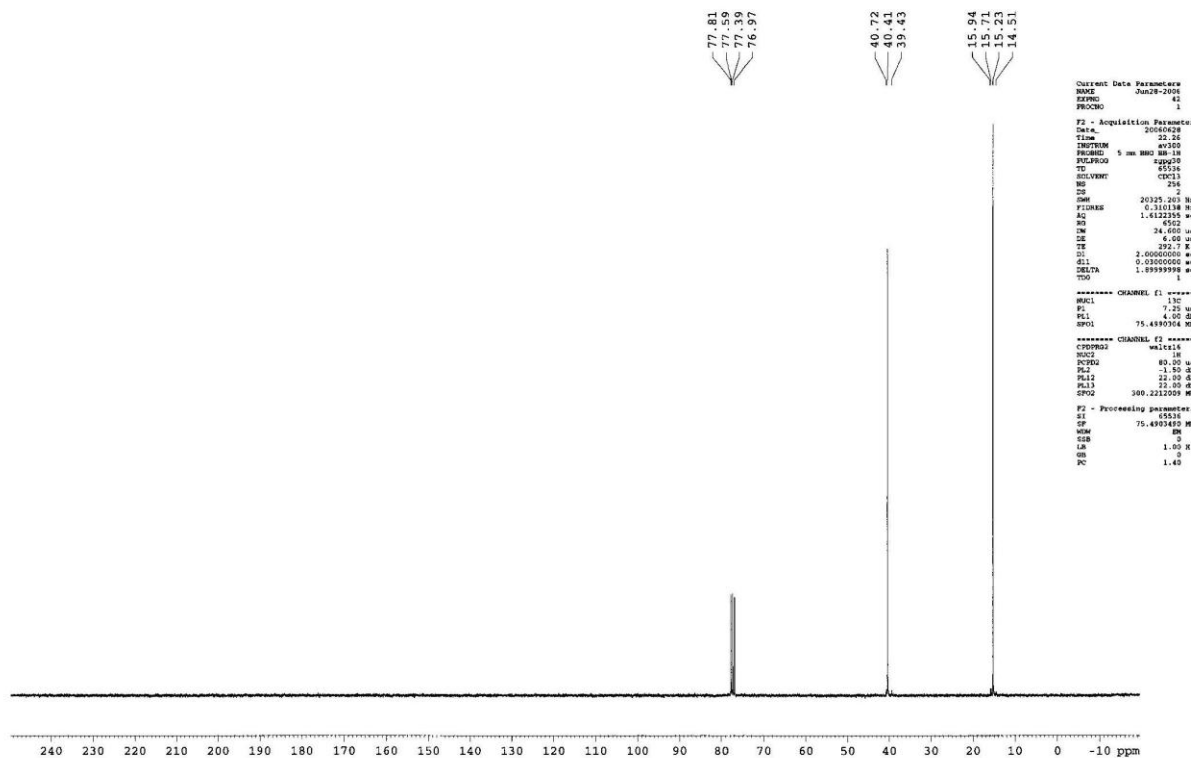
Bis-(diethyl)aminophenylborane: ^{11}B :



3.27:

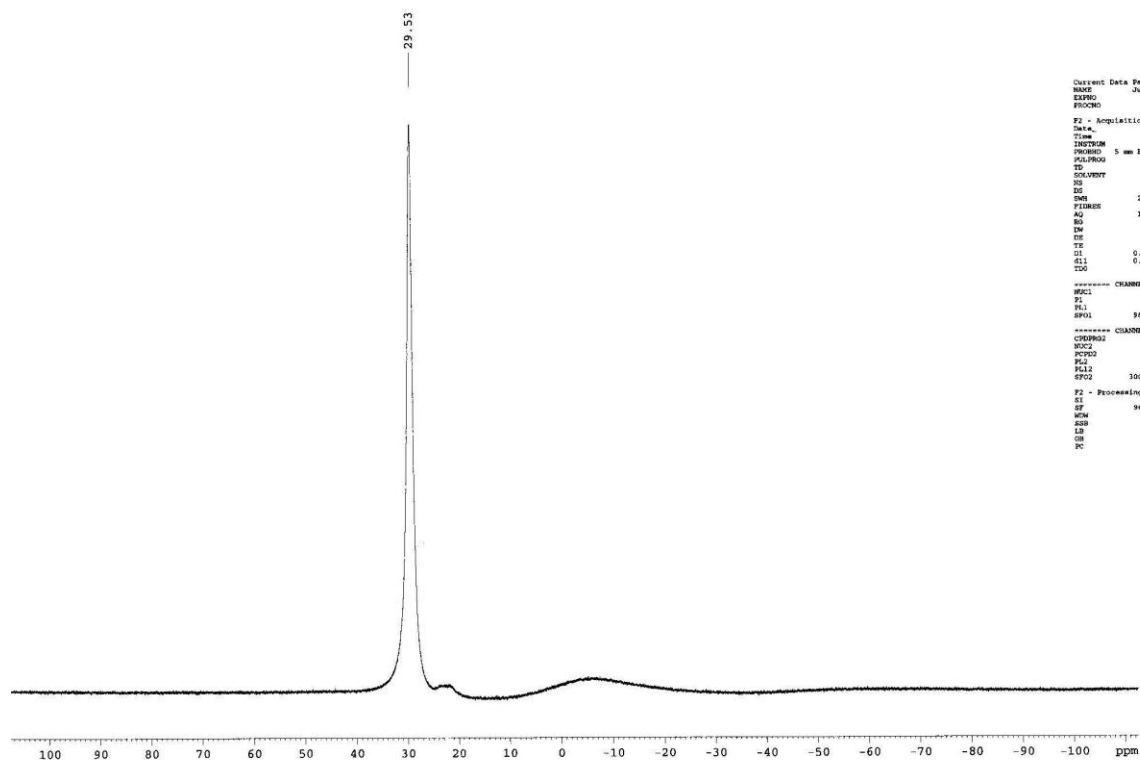
Tris(diethyl)aminoborane: ^1H Tris(diethyl)aminoborane: ^{13}C

IAI nmr: B(NEt2)3 distilled



Tris(diethyl)aminoborane: ^{11}B

IAI nmr: B(NEt₂)₃ distilled



```

Current Data Parameters
NAME      JNM-BL-200
EXPNO     41
PROCNO    1

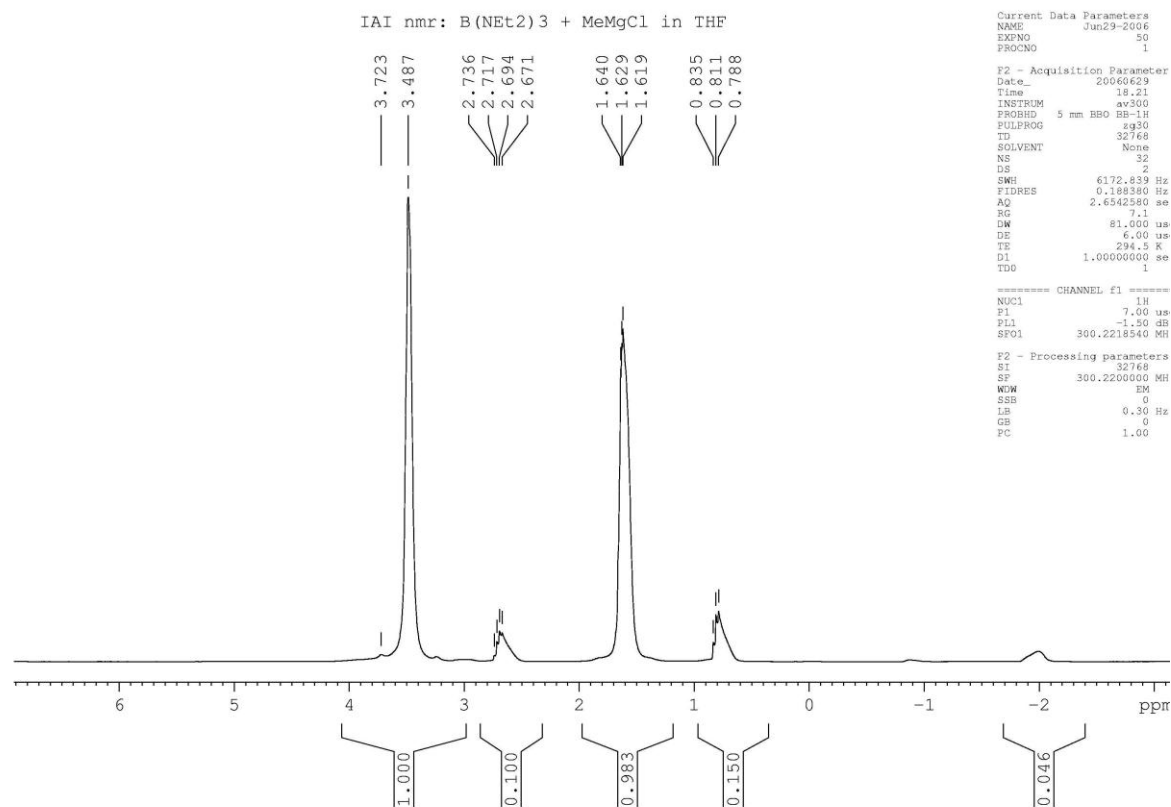
F2 - Acquisition Parameters
Date_     20060628
Time      22.08
INSTRUM   av200
PROBHD    5 mm BBO
PULPROG   zgpg30
PC        65516
TD         65536
SOLVENT   CDCl3
DS         4
DMS        21231.422 Hz
FIDRES    0.227866 Hz
AQ        1.5464228 sec
RG         656.1
BW         20.550 usec
DE         4.00 usec
TE         292.2 K
QT         0.1000000 sec
EI1        0.0300000 sec
TSD        1

===== CHANNEL f1 =====
NUC1       11B
P1         9.00 usec
PL1        0.70 dB
SFO1       96.322123 MHz

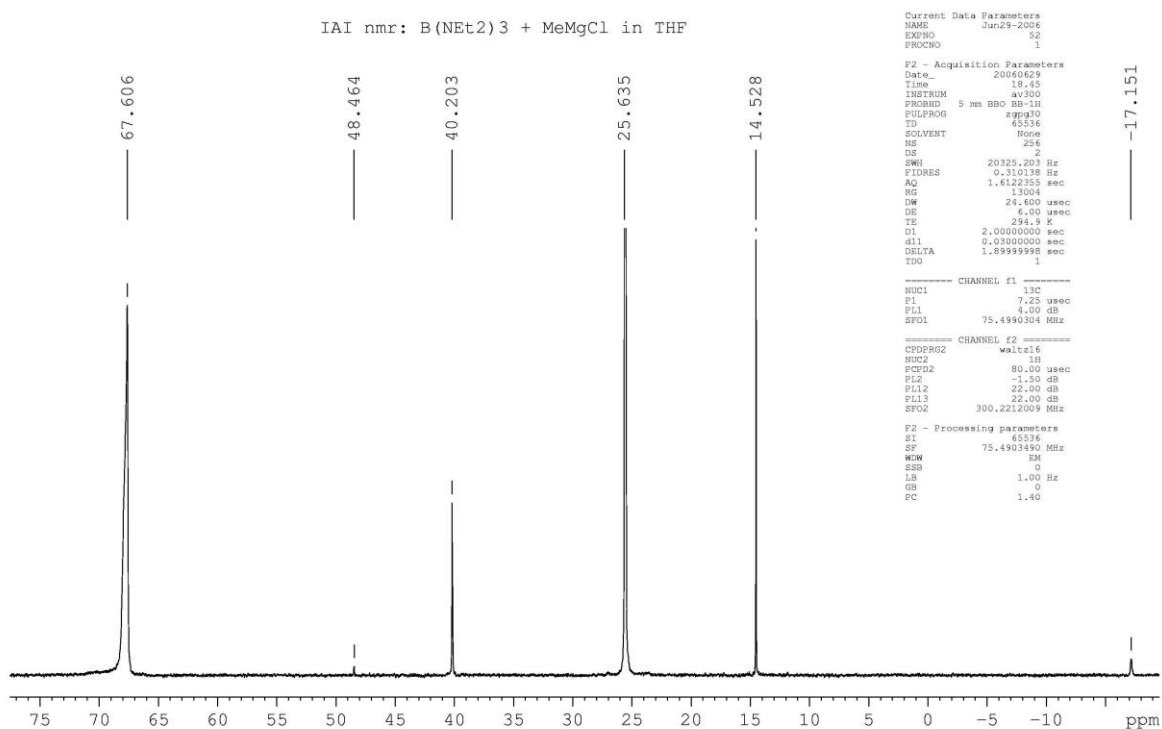
===== CHANNEL f2 =====
CPDPRG2    waltz16
NUC2       1H
PCPD2      80.00 usec
PL2         1.30 dB
PL12       22.00 dB
SFO2      300.2112609 MHz

F2 - Processing parameters
SI         65536
SF         96.322445 MHz
WDW        EM
SSB         0
LB          1.00 Hz
GB          0
PC          1.00
    
```

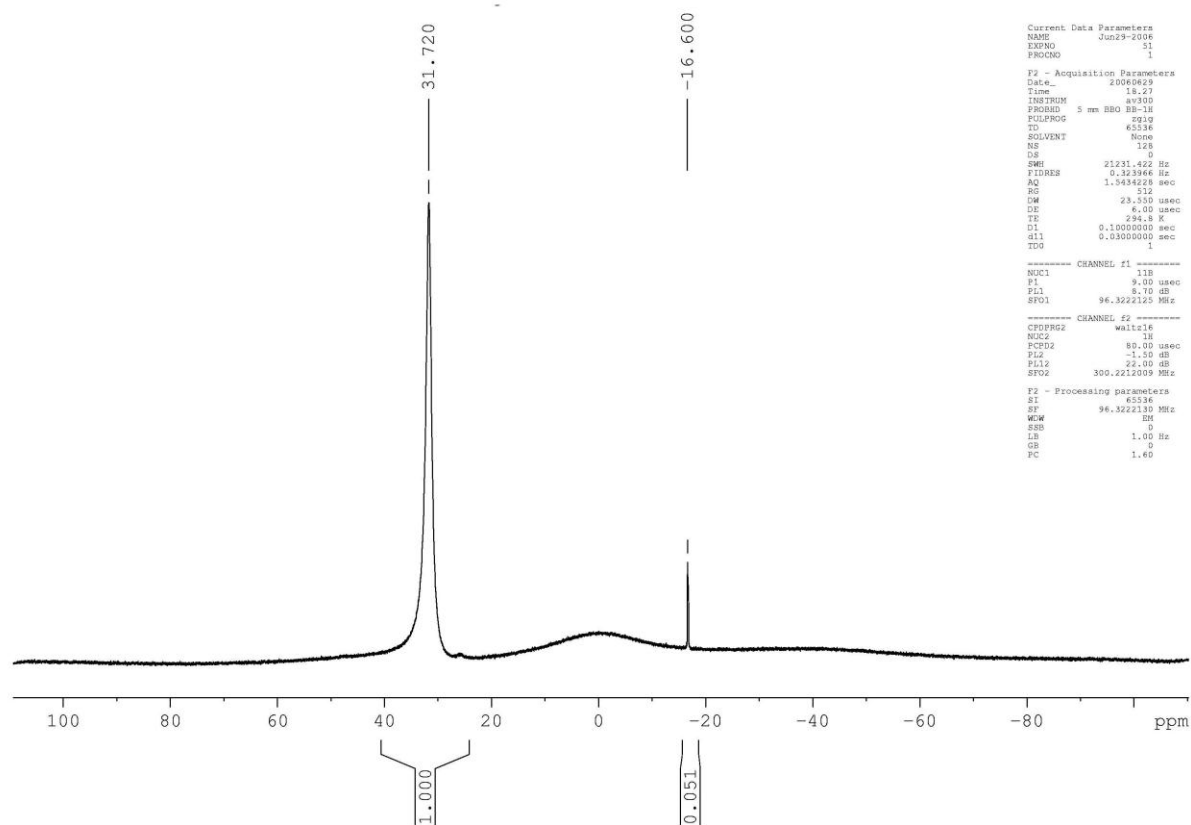

3.28: Attempted reaction of Tris(diethyl)aminoborane with Methylmagnesium chloride: ^1H



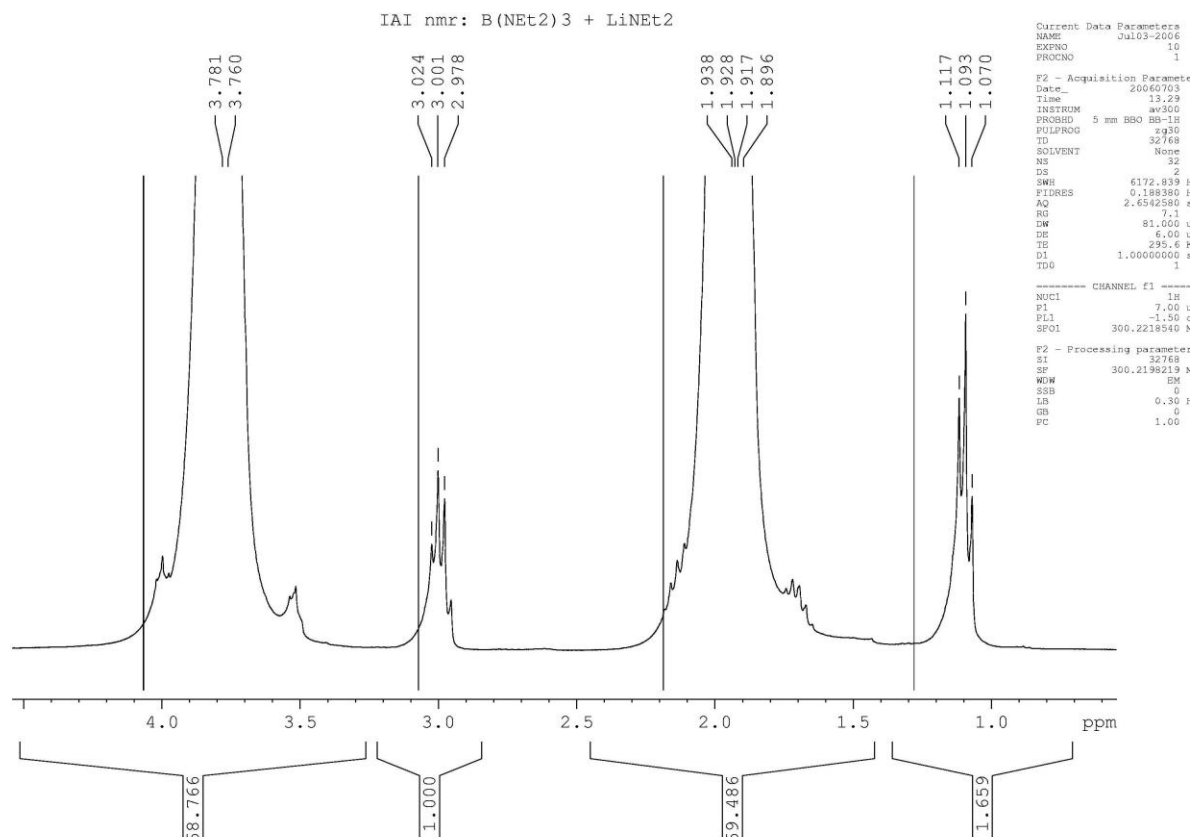
Attempted reaction of Tris(diethyl)aminoborane with Methylmagnesium Chloride: ^{13}C



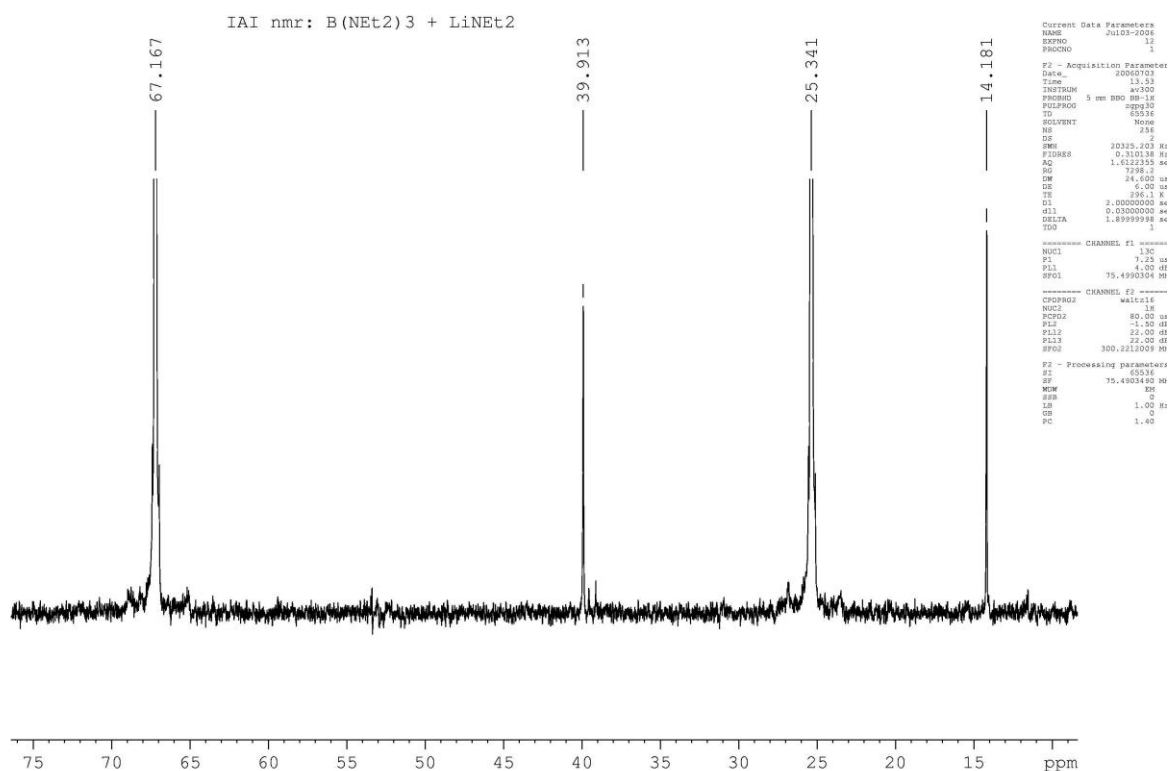
Attempted reaction of Tris(diethyl)aminoborane with Methylmagnesium chloride: ^{11}B



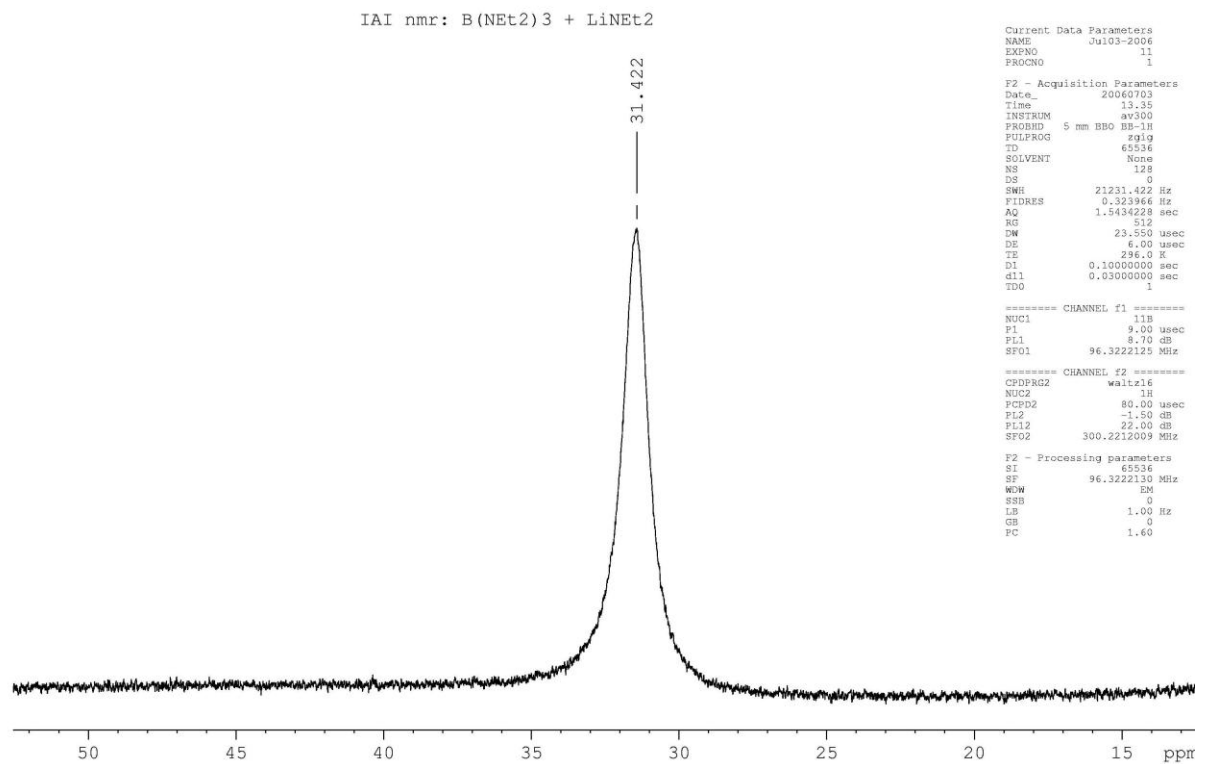
3.29: Attempted reaction of Tris(diethyl)aminoborane with lithium diethylamide: ^1H



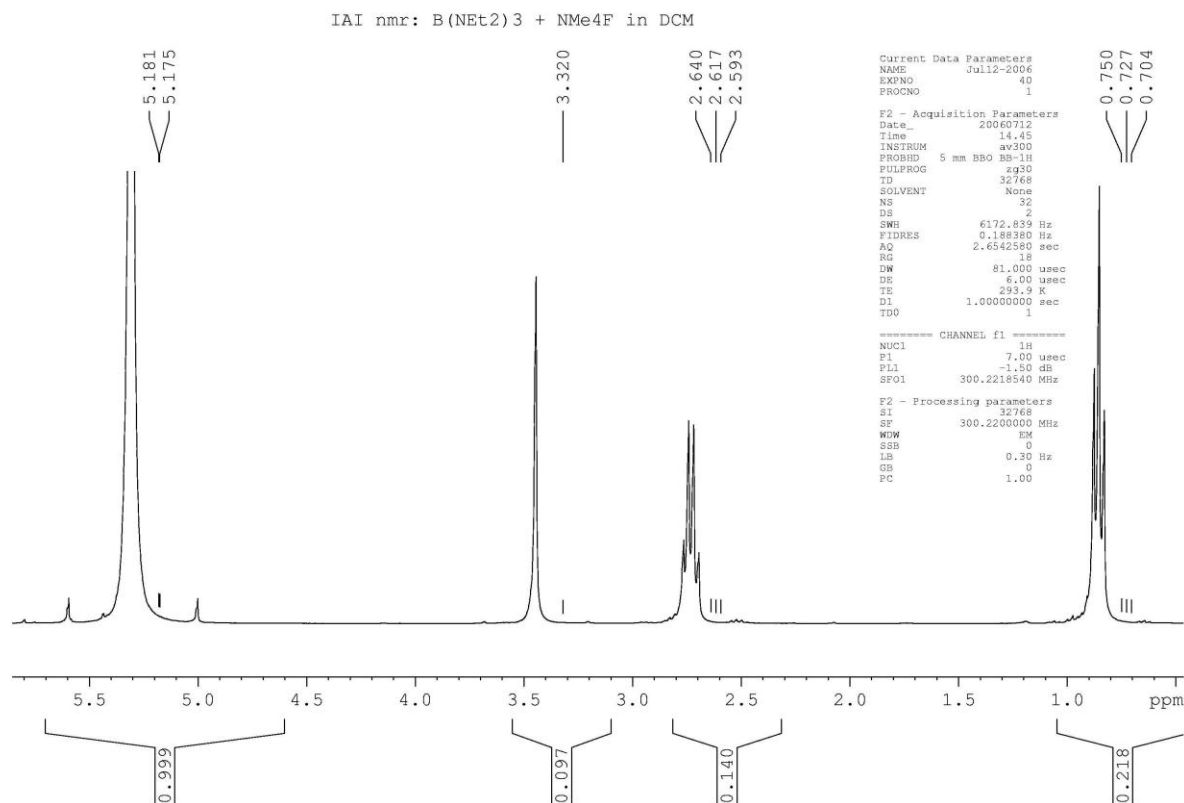
Attempted reaction of Tris(diethyl)aminoborane with lithium diethylamide: ^{13}C



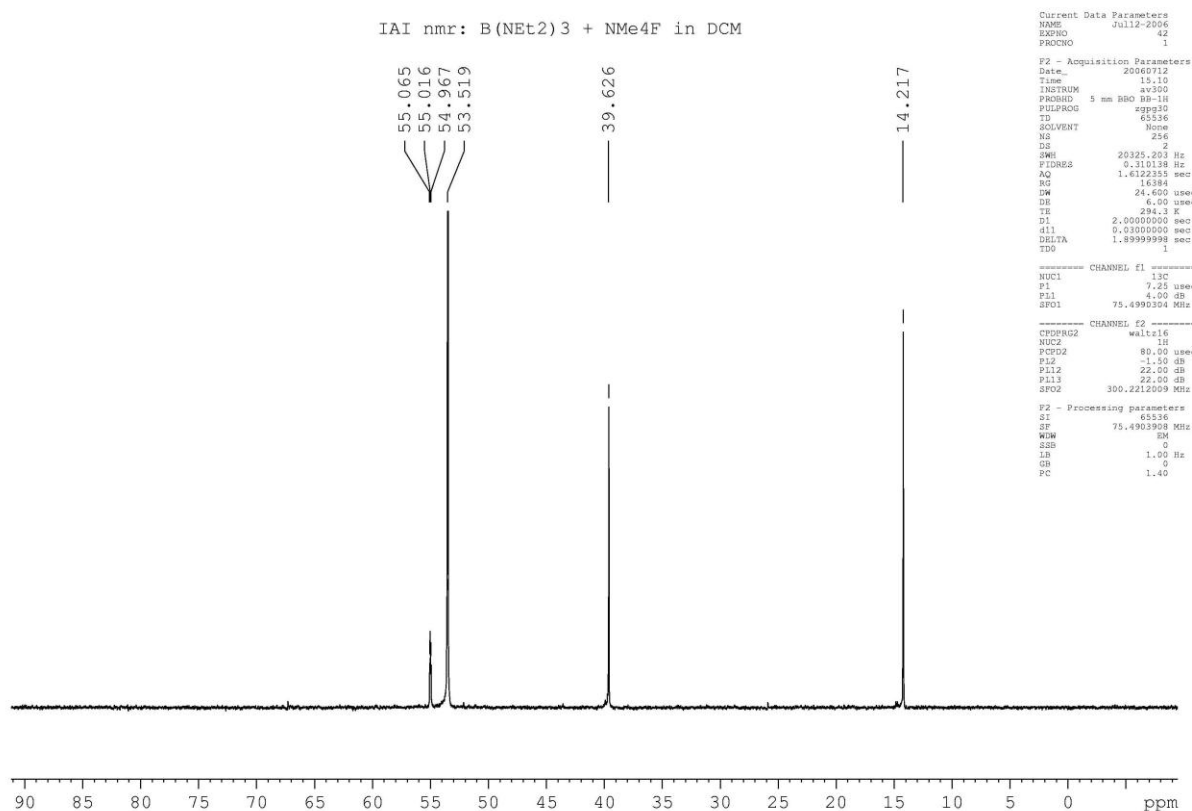
Attempted reaction of Tris(diethyl)aminoborane with lithium diethylamide: ^{11}B



3.30: Attempted reaction of Tris(diethyl)aminoborane with Tetramethylammonium fluoride: ^1H

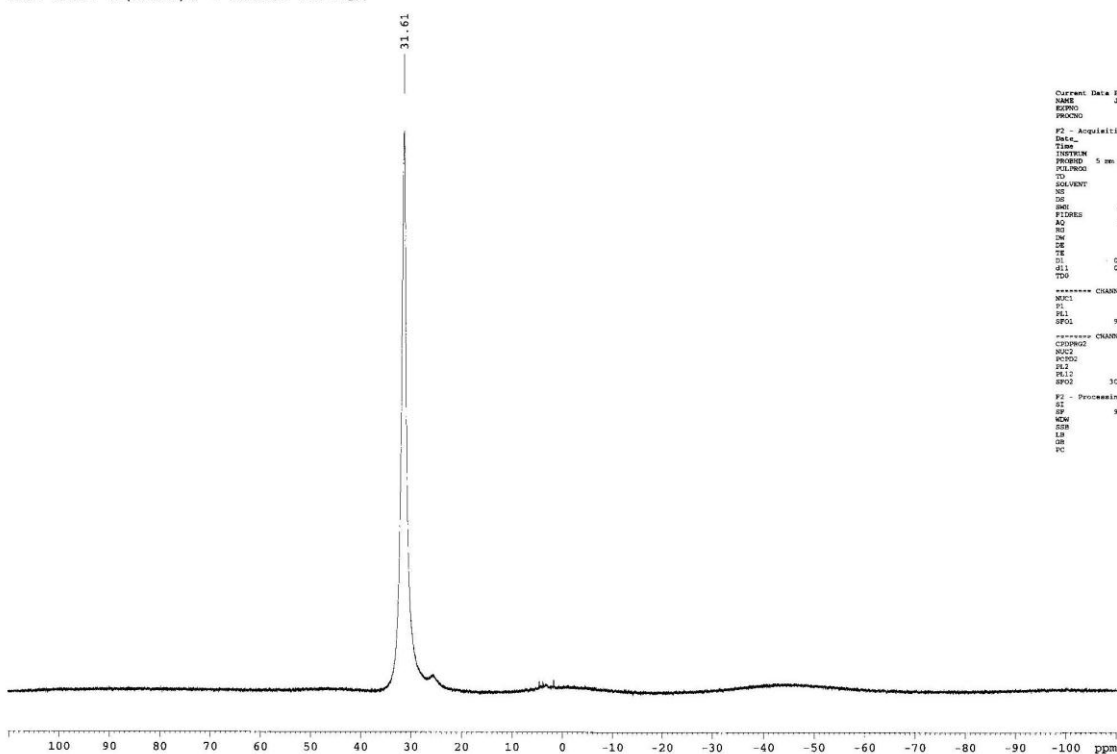


Attempted reaction of Tris(diethyl)aminoborane with Tetramethylammonium fluoride: ^{13}C



Attempted reaction of Tris(diethyl)aminoborane with Tetramethylammonium fluoride: ¹¹B

IAI nmr: B(NEt₂)₃ + NMe₄F in DCM



```

Current Data Parameters
NAME      Jul12-2006
EXPNO     41
PROCNO    1

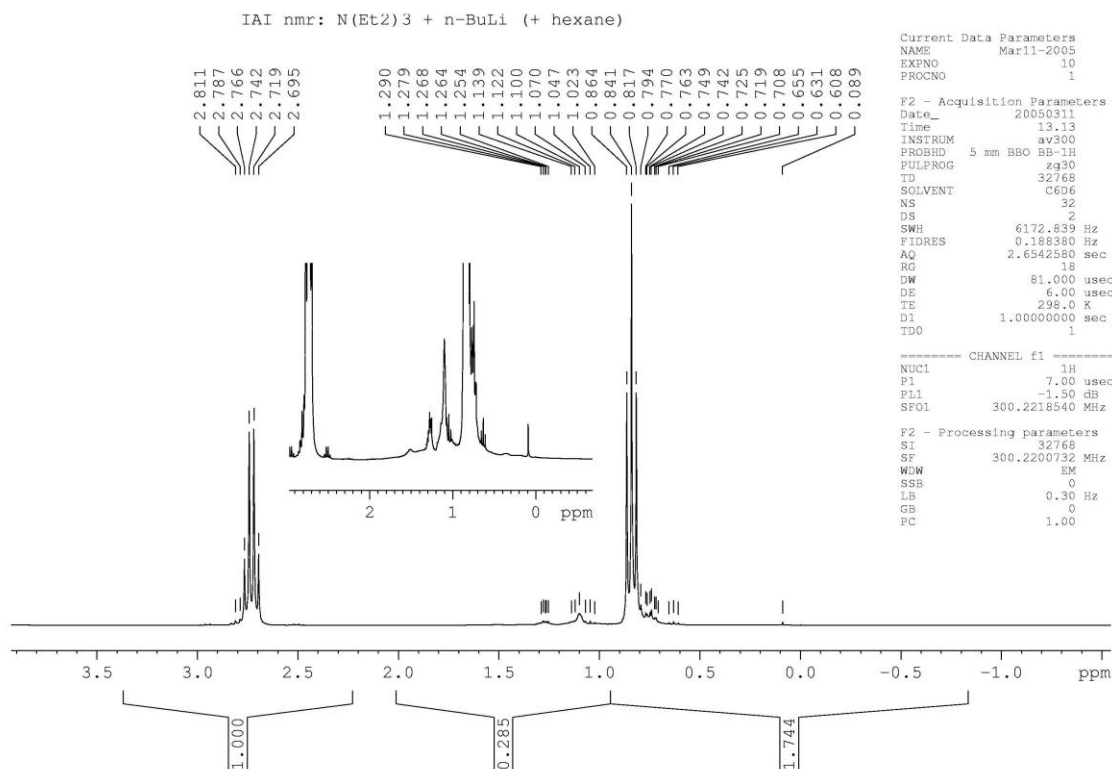
F2 - Acquisition Parameters
Date_     20060712
Time      14.51
INSTRUM   avn500
PROBHD    5 mm BBO BB-1H
PULPROG   zgpg30
TD        65536
SOLVENT   MeCN
NS         2
DS         4
SWH        21511.422 Hz
FIDRES     0.3223966 Hz
AQ         1.5474226 s
RG         512
WDW        33.150 us
SSB         0.00 us
GB         0.00 us
TE         300.2 K
D1         0.16000000 s
d11        0.03000000 s
TD0        1

===== CHANNEL f1 =====
NUC1       11B
P1         9.00 us
PL1        0.70 dB
SFO1       96.2222123 MHz

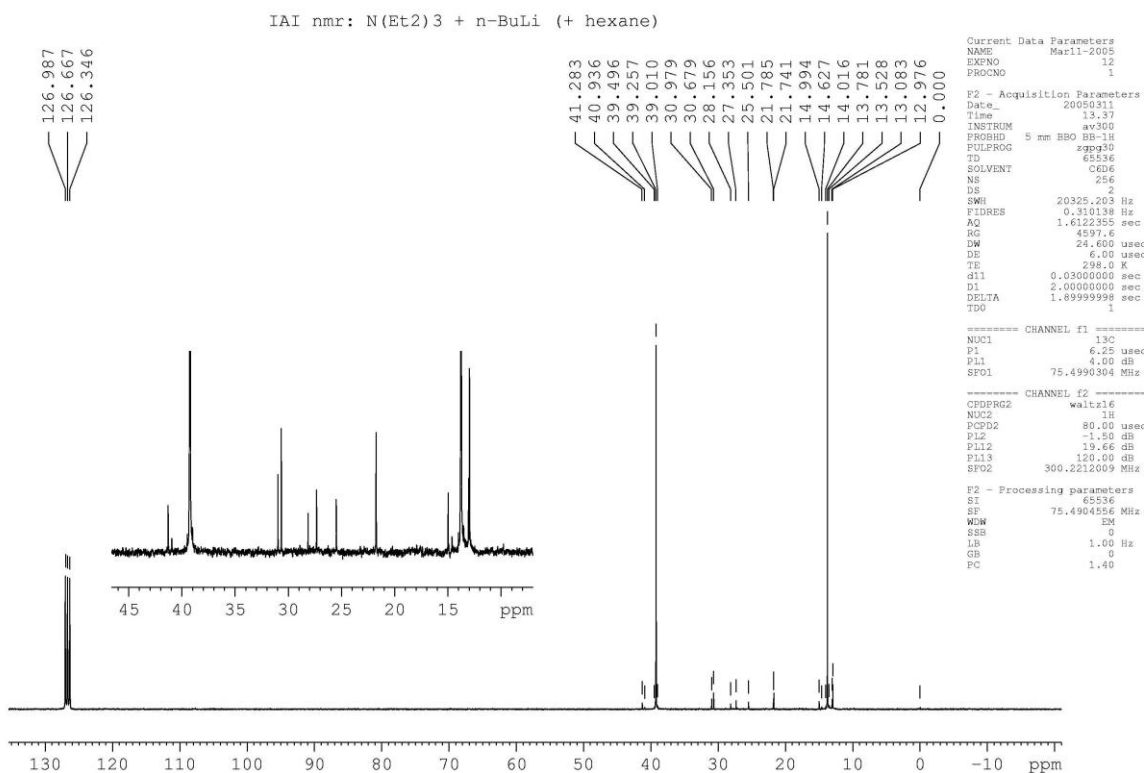
===== CHANNEL f2 =====
CPDPRG2   waltz16
NUC2       1H
P2         80.00 us
PL2        1.50 dB
PL12       22.00 dB
SFO2       300.1311009 MHz

F2 - Processing parameters
SI         85536
SF         96.1222135 MHz
WDW        0
SSB         0.00 us
GB         0.00 us
TE         300.2 K
D1         0.16000000 s
d11        0.03000000 s
TD0        1
    
```

3.31: Attempted reaction of Tris(diethyl)aminoborane with n-butyl lithium: ^1H

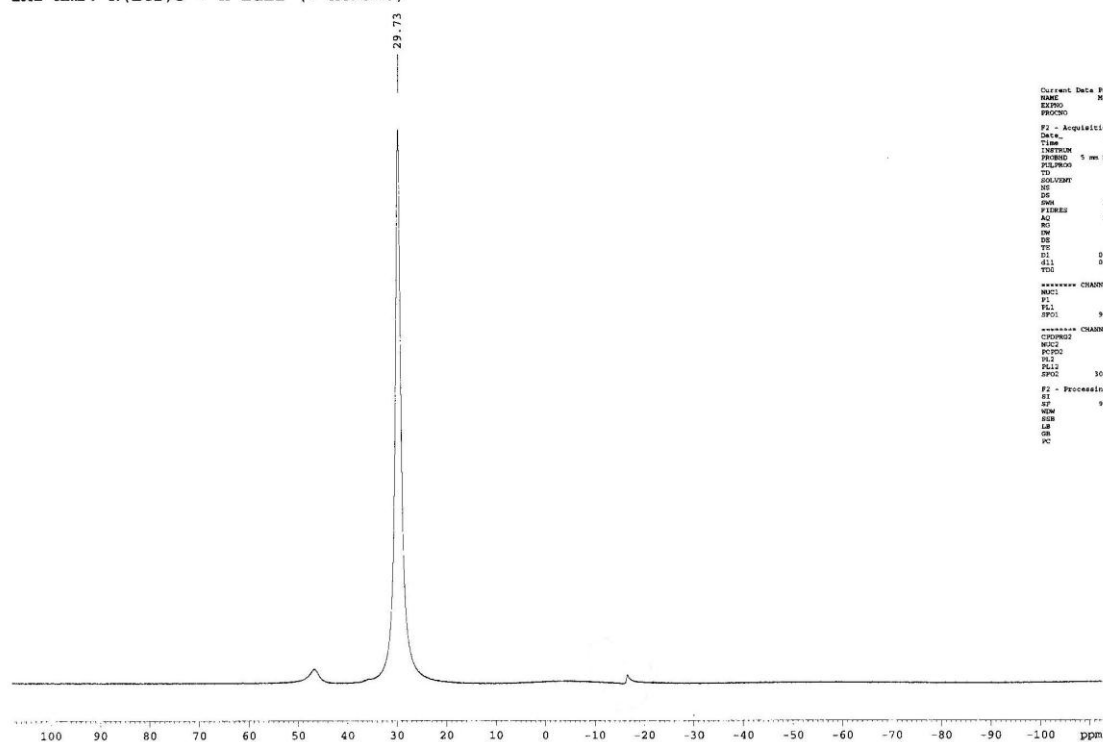


Attempted reaction of Tris(diethyl)aminoborane with n-butyl lithium: ^{13}C

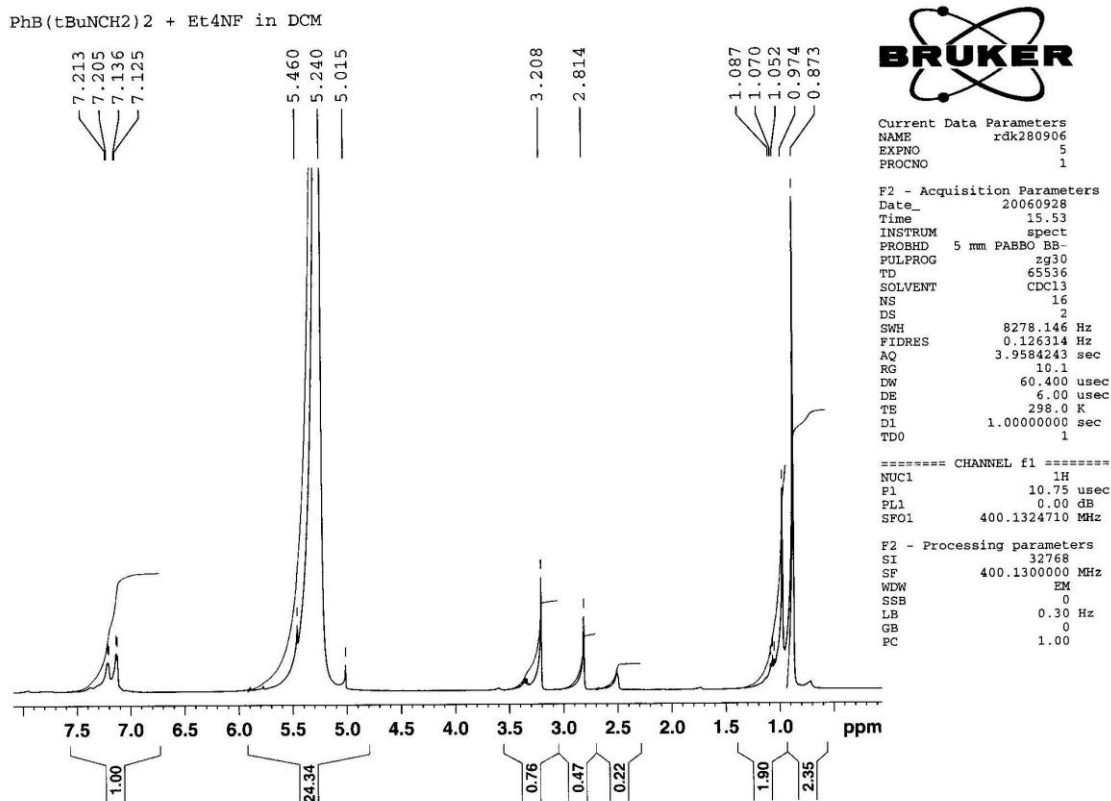


Attempted reaction of Tris(diethyl)aminoborane with n-butyl lithium: ^{11}B

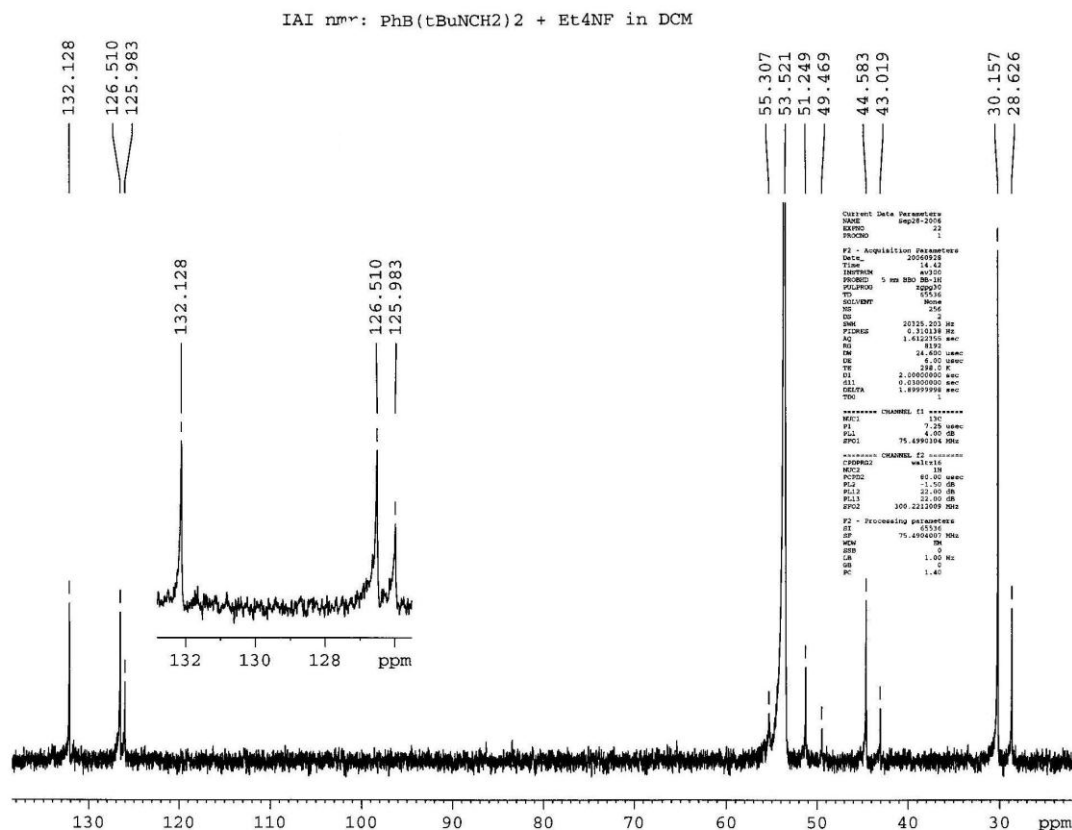
IAI nmr: N(Et2)3 + n-BuLi (+ hexane)



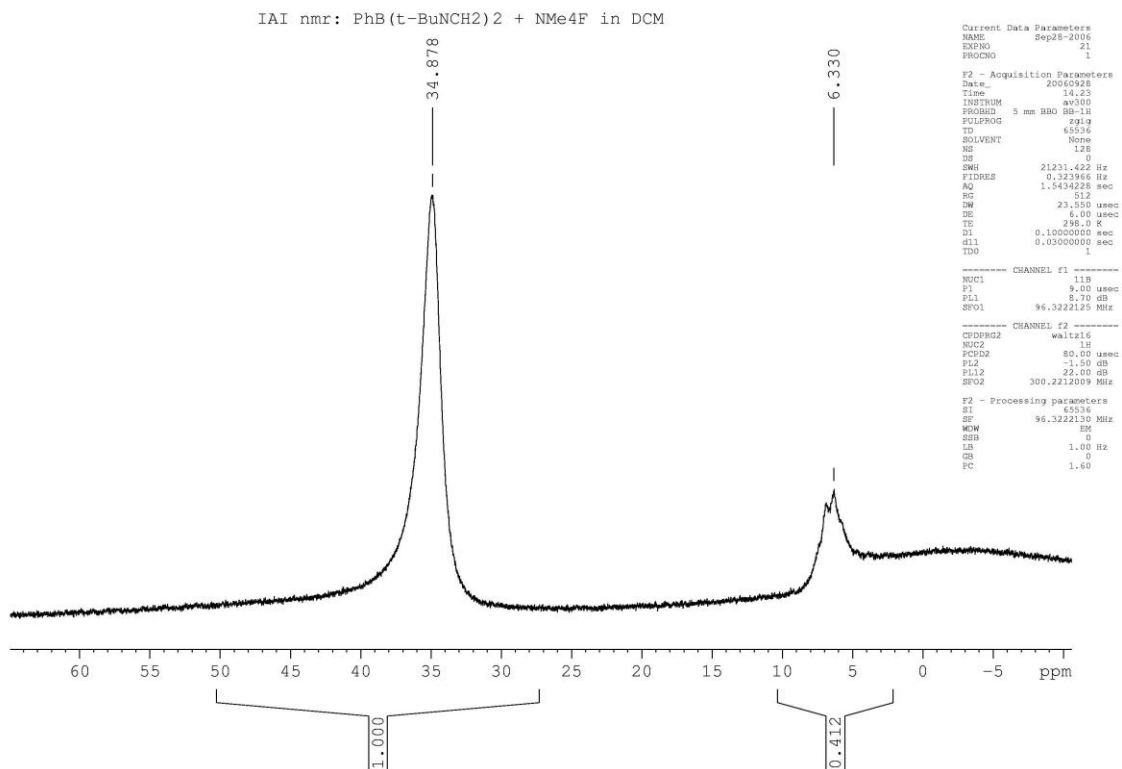
3.32: Reaction of 1-Phenyl-2,5-di-*tert*-butyl-1-bora-2,5-diazacyclopentane with Tetramethylammonium Fluoride: ^1H



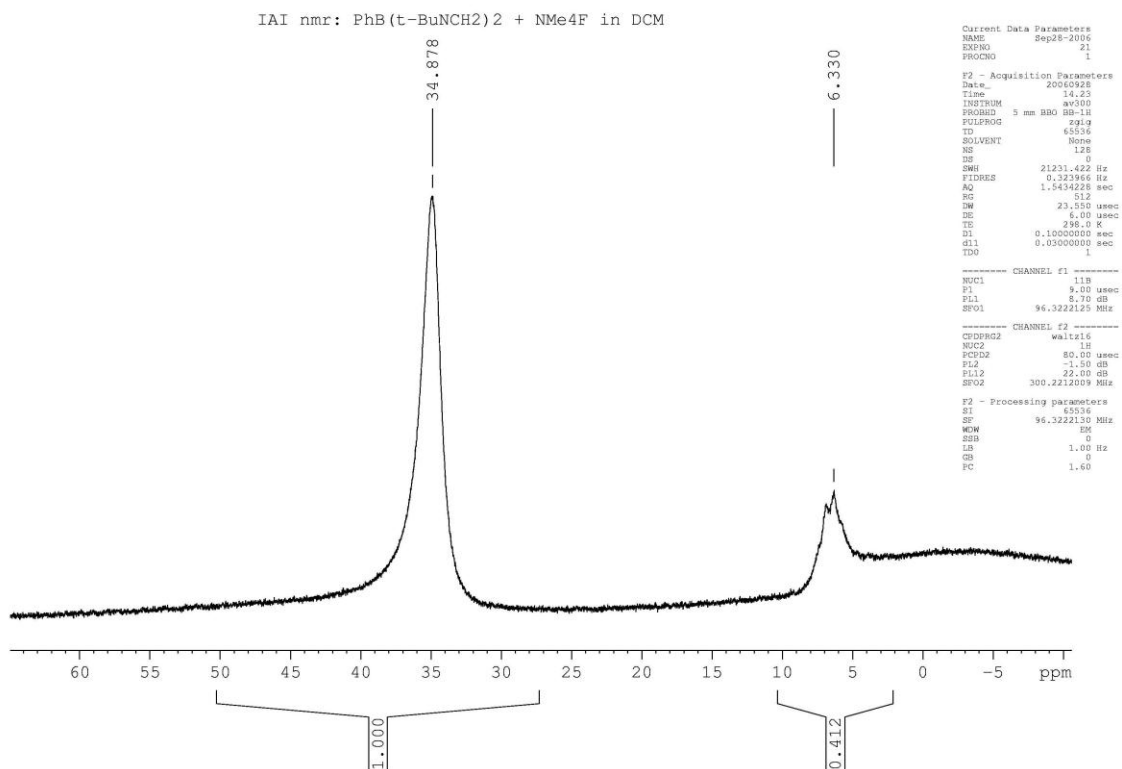
Reaction of 1-Phenyl-2,5-di-*tert*-butyl-1-bora-2,5-diazacyclopentane with Tetramethylammonium Fluoride: ^{13}C



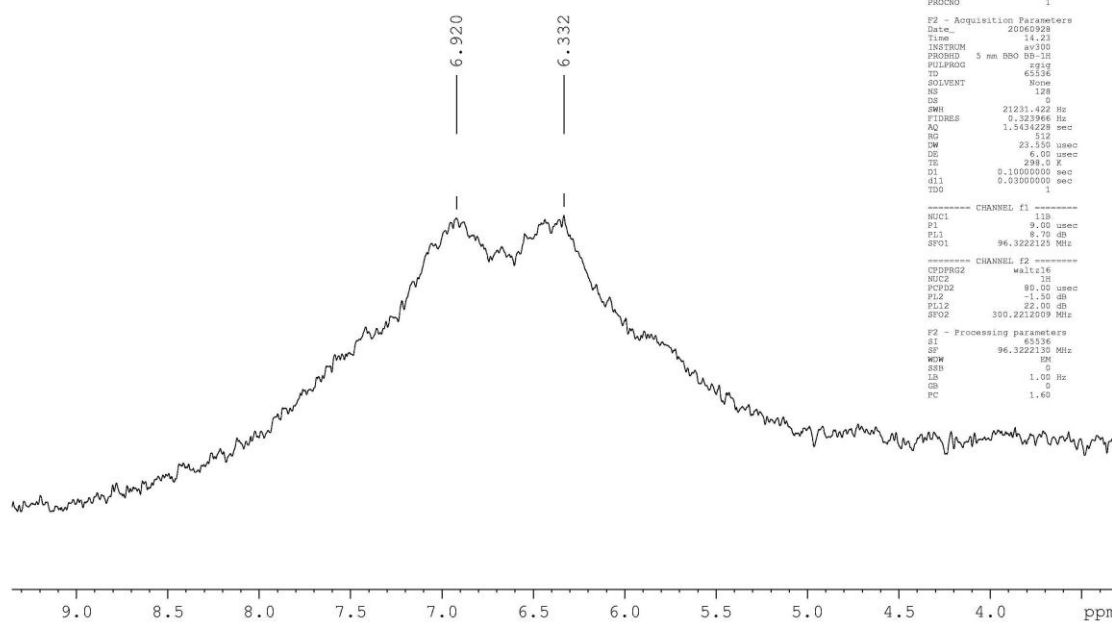
Reaction of 1-Phenyl-2,5-di-*tert*-butyl-1-bora-2,5-diazacyclopentane with Tetramethylammonium Fluoride: ^{11}B



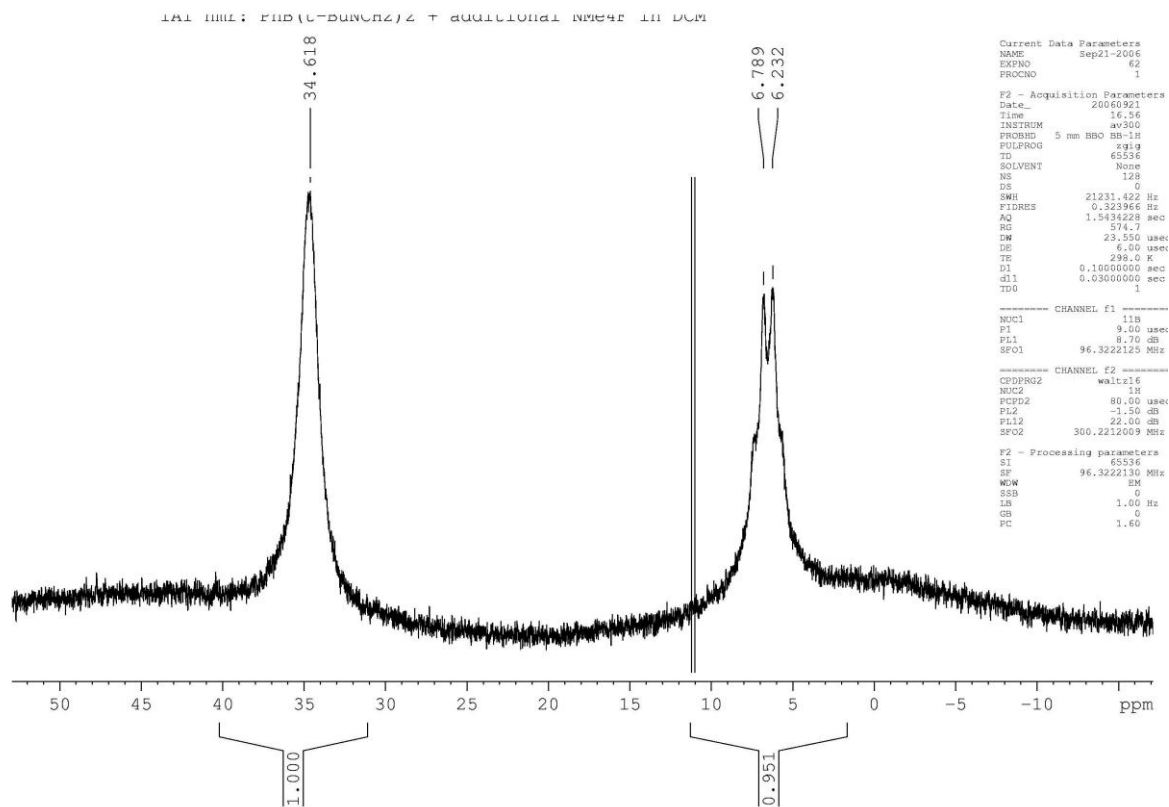
Upon addition of 1 Equivalent Tetramethylammonium Fluoride:
 ^{11}B :



IAI nmr: PhB(t-BuNCH₂)₂ + NMe₄F in DCM

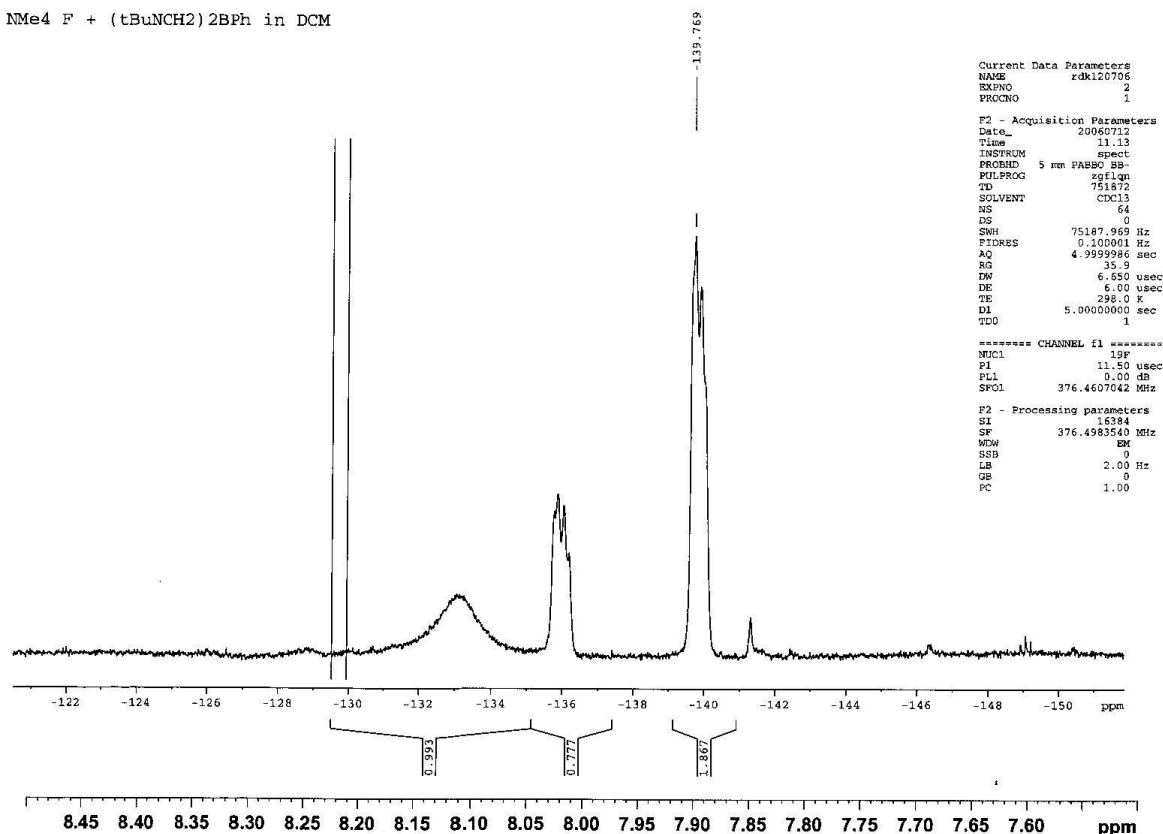


Upon Addition of Large Excess Tetramethylammonium Fluoride:

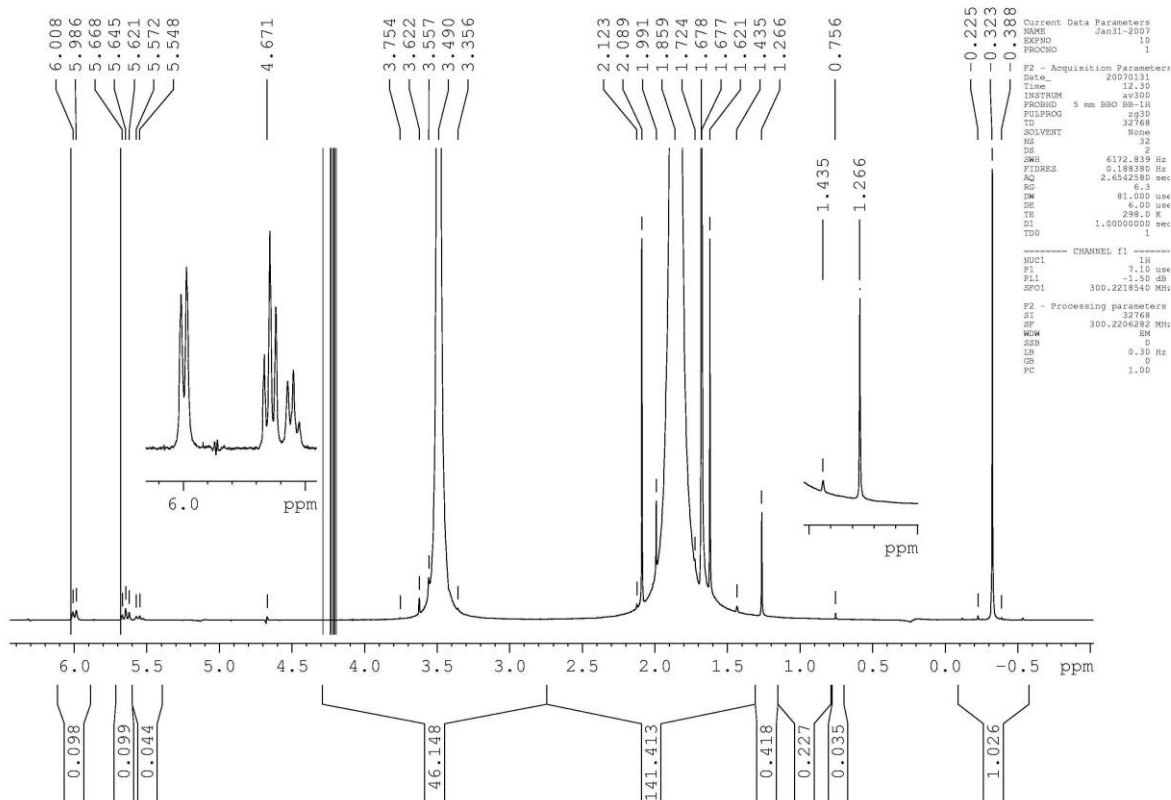


Reaction of 1-Phenyl-2,5-di-*tert*-butyl-1-bora-2,5-diazacyclopentane with Tetramethylammonium Fluoride: ^{19}F

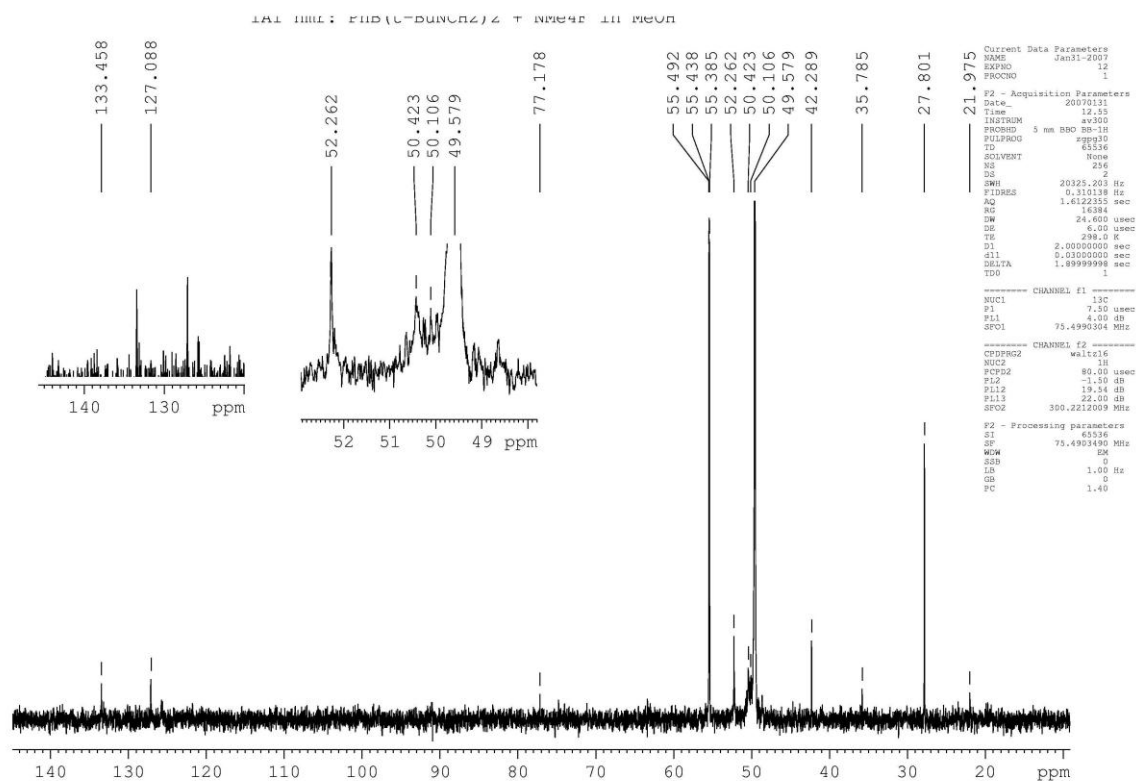
NMe₄ F + (tBuNCH₂)₂BPh in DCM



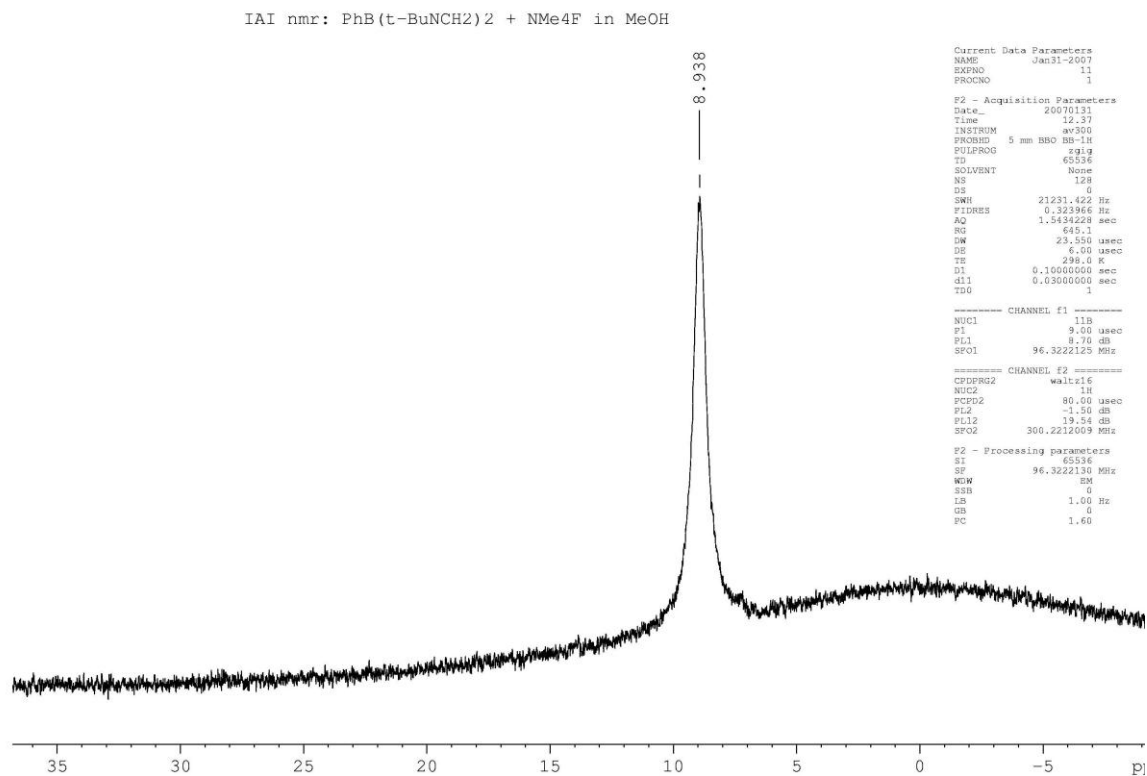
Reaction of 1-Phenyl-2,5-di-*tert*-butyl-1-bora-2,5-diazacyclopentane with Tetramethylammonium Fluoride in Methanol Soln: ^1H :



Reaction of 1-Phenyl-2,5-di-*tert*-butyl-1-bora-2,5-diazacyclopentane with Tetramethylammonium Fluoride in Methanol Soln: ^{13}C :

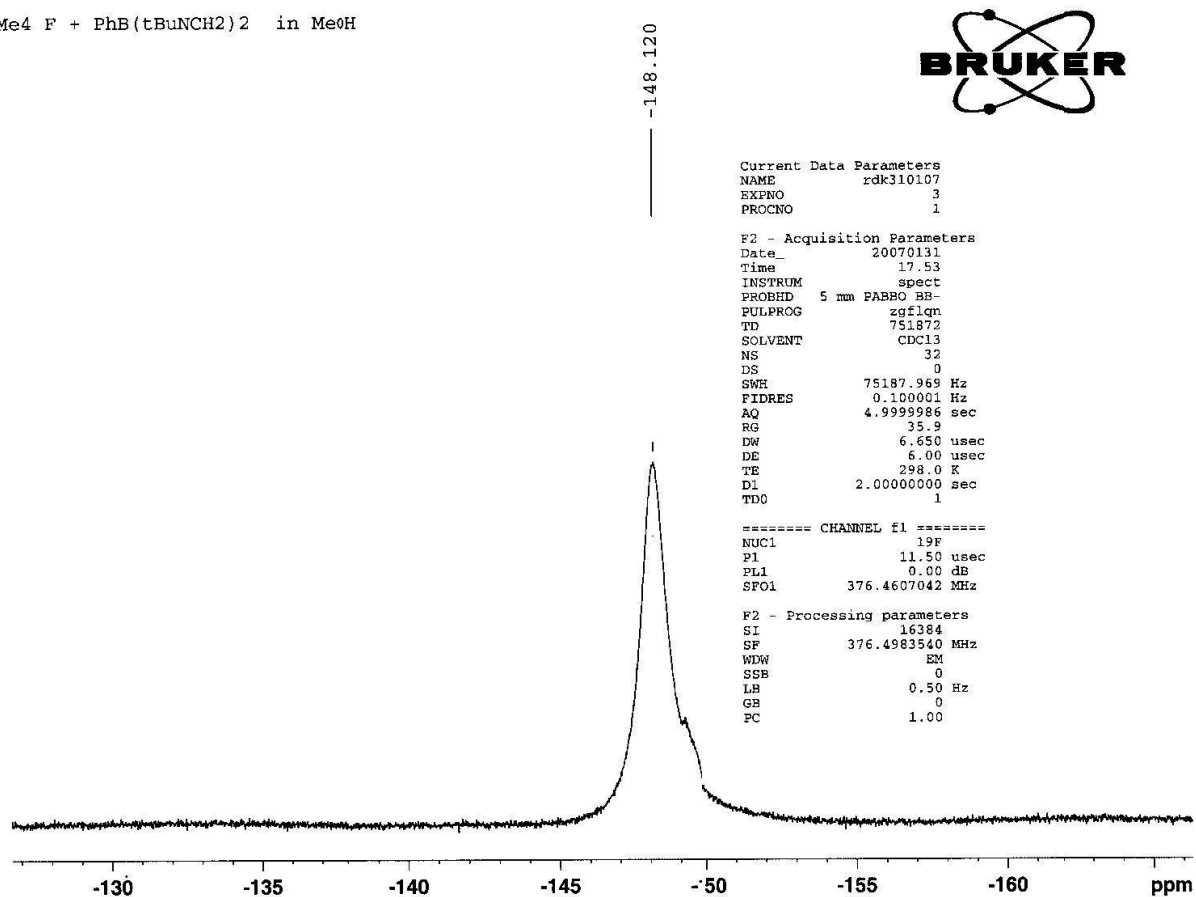


Reaction of 1-Phenyl-2,5-di-*tert*-butyl-1-bora-2,5-diazacyclopentane with Tetramethylammonium Fluoride in Methanol Soln: ^{11}B :

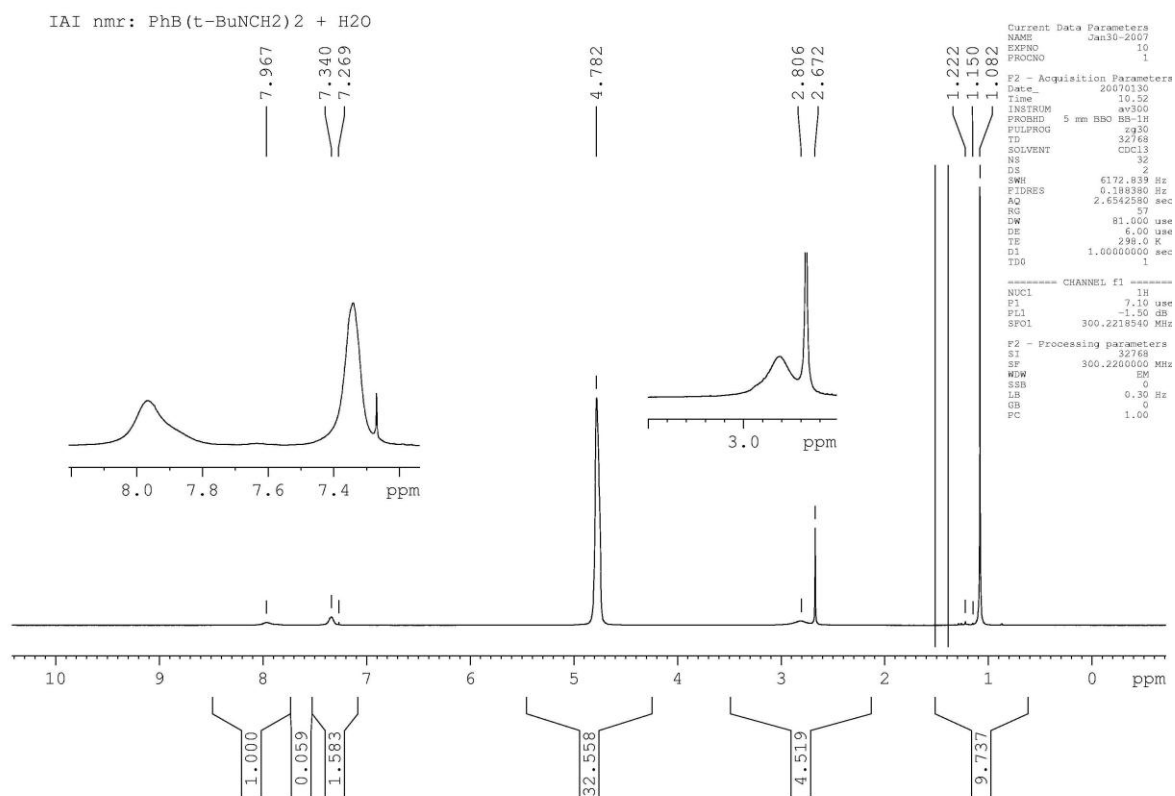


Reaction of 1-Phenyl-2,5-di-*tert*-butyl-1-bora-2,5-diazacyclopentane with Tetramethylammonium Fluoride in Methanol Soln: ^{19}F :

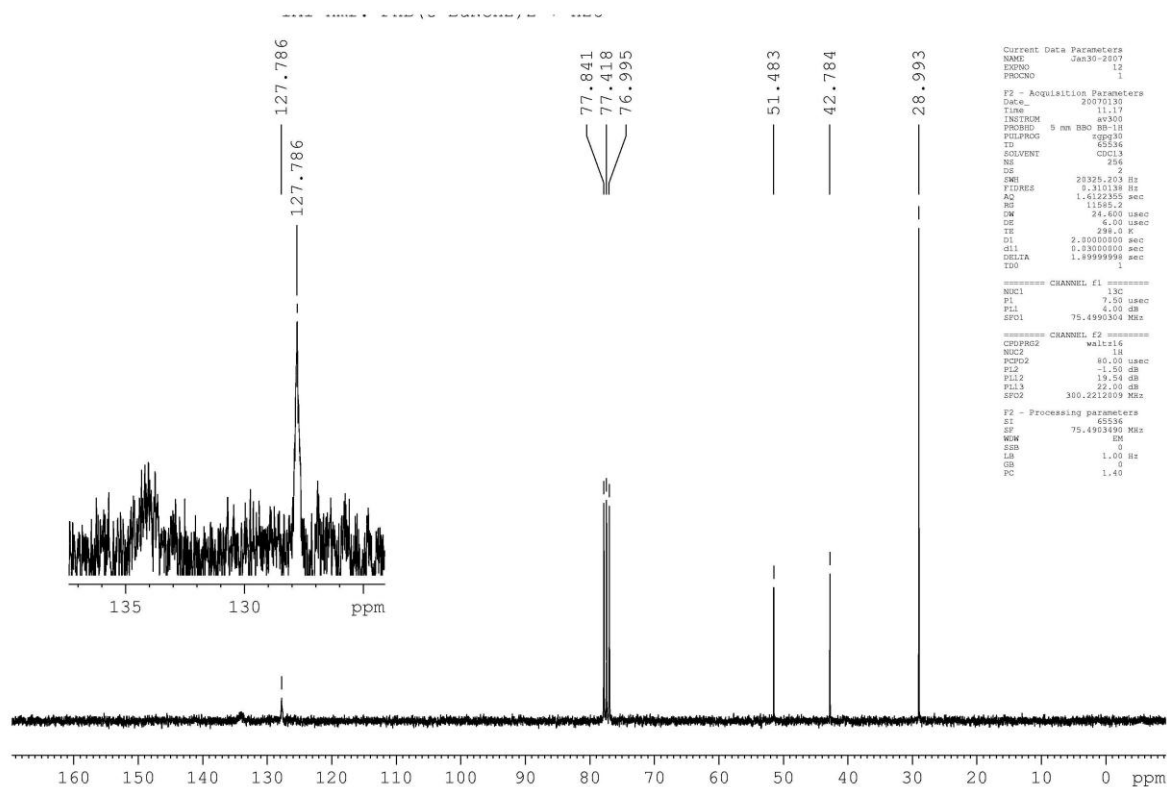
$\text{NMe}_4^+ \text{F}^- + \text{PhB}(\text{tBuNCH}_2)_2$ in MeOH



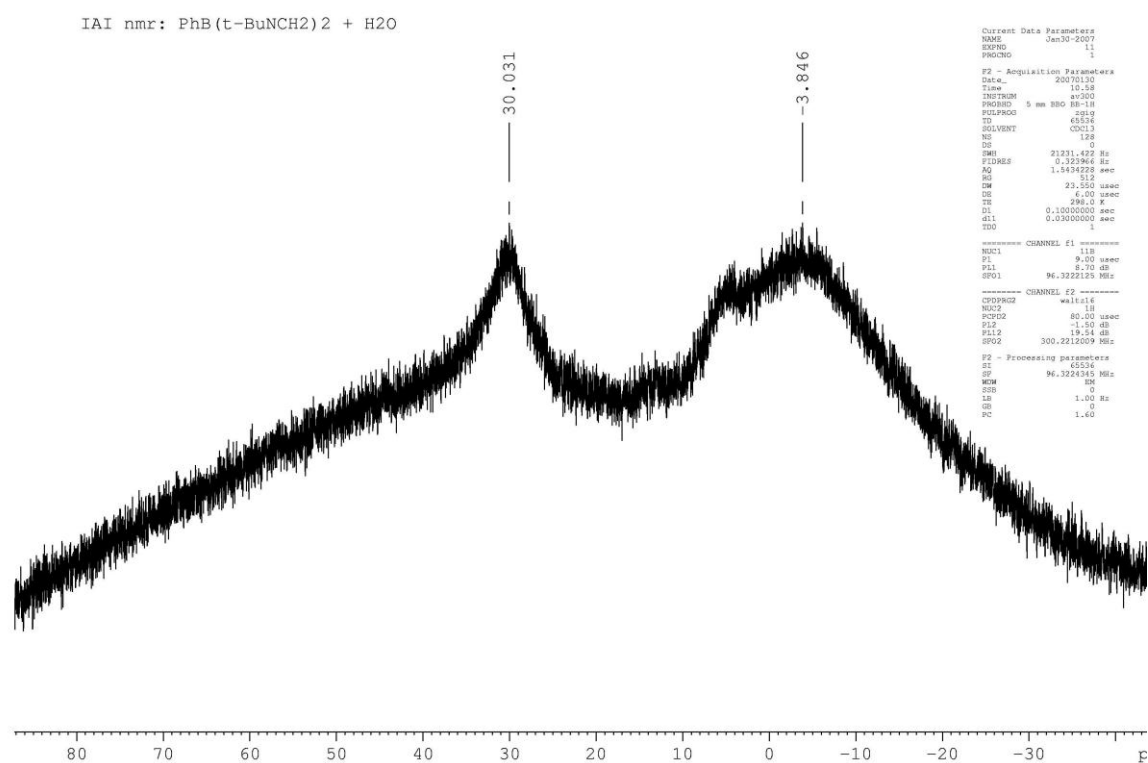
3.34: Reactivity of 1-phenyl-2,5-di-*tert*-butyl-1-bora-2,5-diazacyclopentane with De-ionised Water: ^1H :



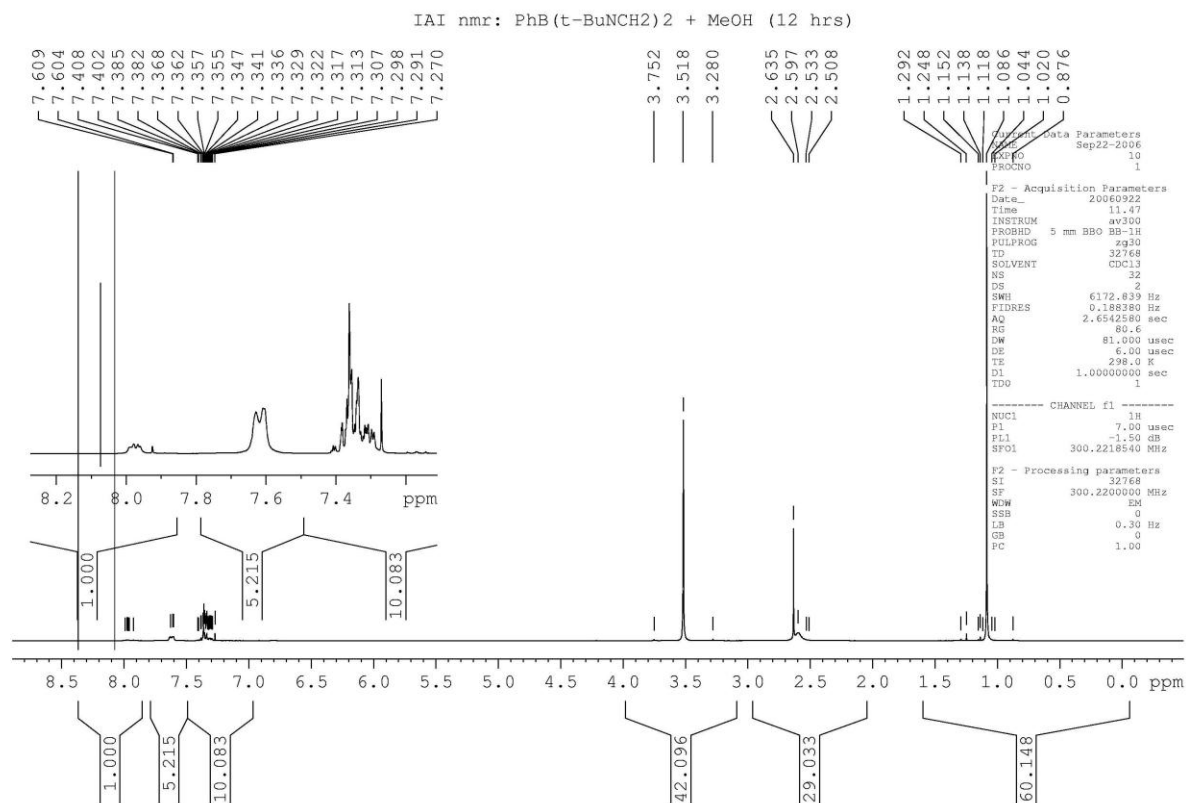
Reactivity of 1-phenyl-2,5-di-*tert*-butyl-1-bora-2,5-diazacyclopentane with De-ionised Water: ^{13}C :



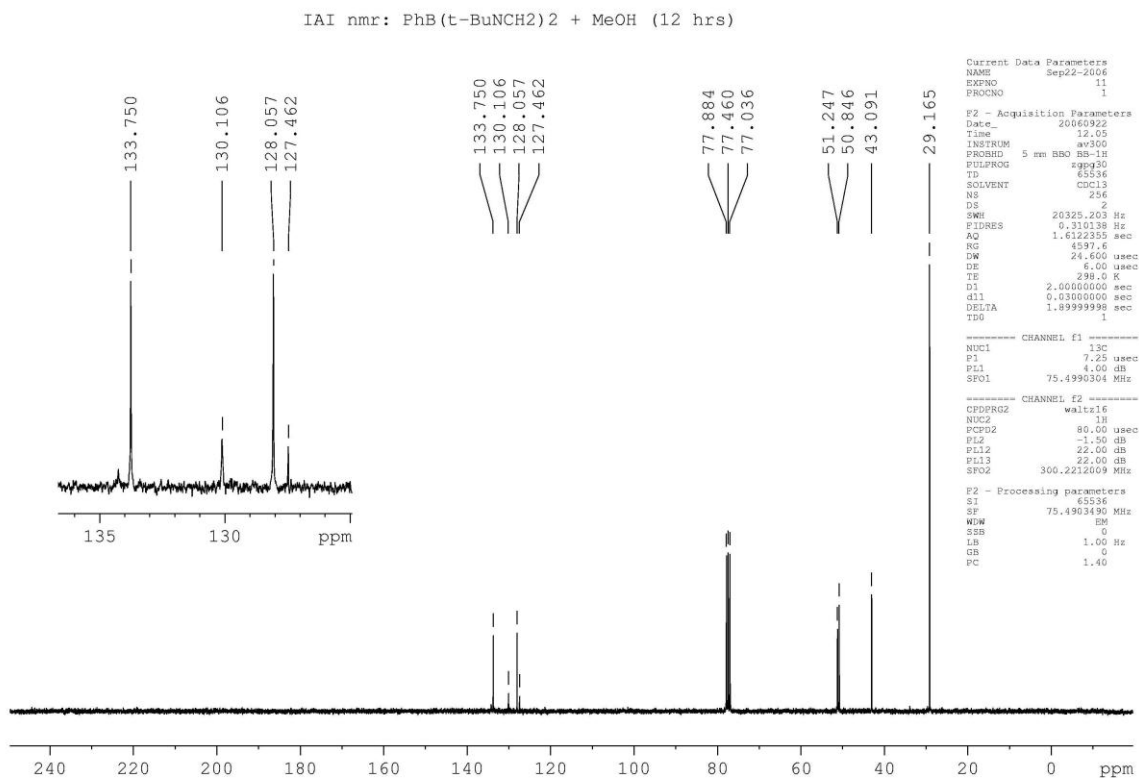
Reactivity of 1-phenyl-2,5-di-*tert*-butyl-1-bora-2,5-diazacyclopentane with De-ionised Water: ^{11}B :



3.35: Attempted Reaction of 1-Phenyl-2,5-di-*tert*-butyl-1-bora-2,5-diazacyclopentane with Methanol: ^1H

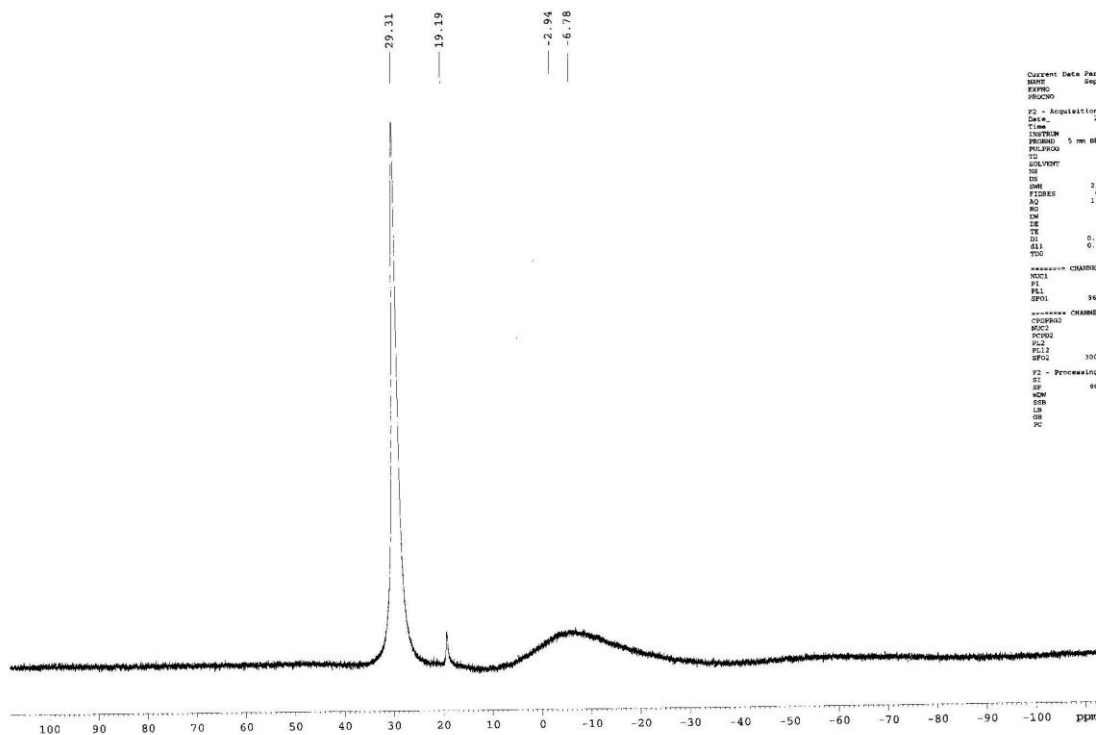


Attempted Reaction of 1-Phenyl-2,5-di-*tert*-butyl-1-bora-2,5-diazacyclopentane with Methanol: ^{13}C



Attempted Reaction of 1-Phenyl -2,5-di-*tert*-butyl-1-bora-2,5-diazacyclopentane with Methanol: ^{11}B

IAI nmr: PhB(t-BuNCH₂)₂ + MeOH (12 hrs)



```

Current Data Parameters
NAME      Sep27-2006
EXPNO     12
PROCNO    1

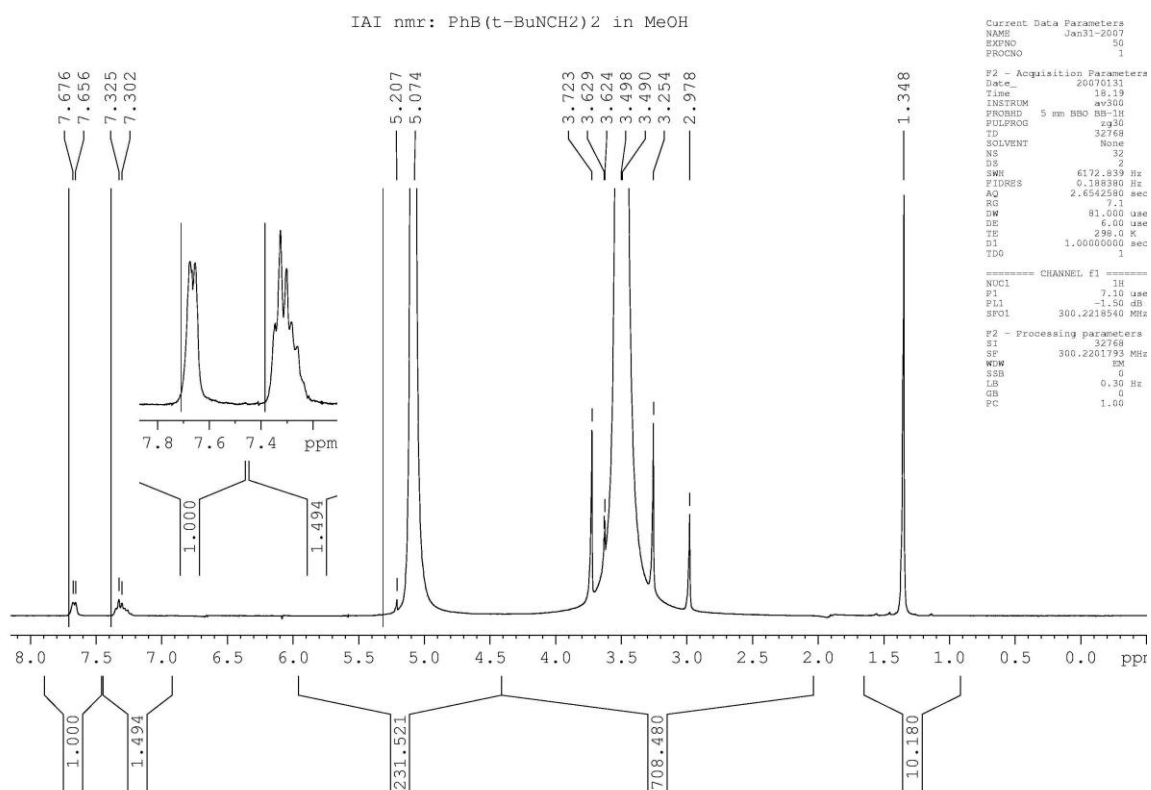
F2 - Acquisition Parameters
Date_     20060822
Time      17.12
INSTRUM   spect
PROBHD    5 mm BBO MM-1H
PULPROG   zgpg30
TD         65536
SOLVENT   CDCl3
NS         128
DS         4
SWH        21231.422 Hz
FIDRES     0.337866 Hz
AQ         1.5434228 sec
RG         512
EW         23.555 uHz
DE         6.00 uHz
TE         300.2 K
DQ         0.10000000 sec
SLL        0.03000000 sec
TPO        1

===== CHANNEL f1 =====
NUC1       11B
P1         9.00 uSec
PL1        0.10 dB
SFO1       96.2222125 MHz

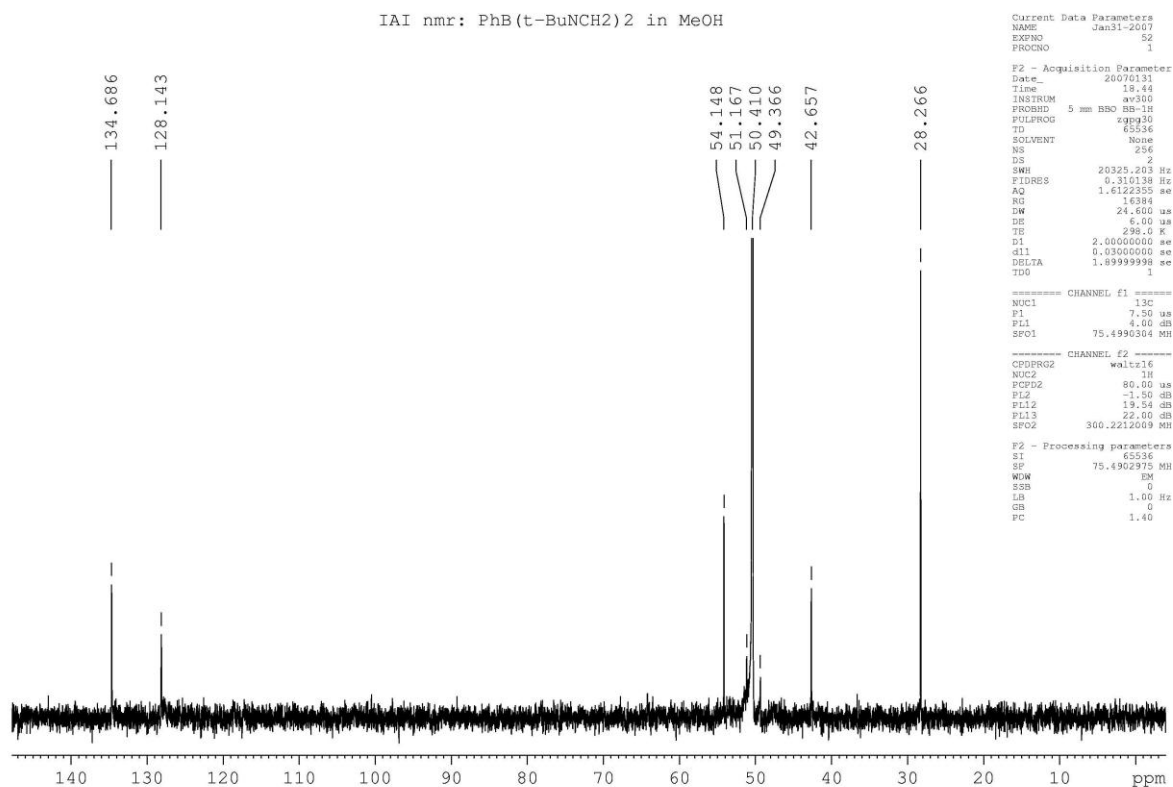
===== CHANNEL f2 =====
CPDPRG2    waltz16
NUC2       1H
P2         80.00 uSec
PL2        -1.50 dB
PL12       19.00 dB
SFO2       300.2212009 MHz

F2 - Processing parameters
SI         32768
SF         96.224145 MHz
WDW         EM
SSB         0
LB         1.00 Hz
GB         0
PC         1.60
    
```

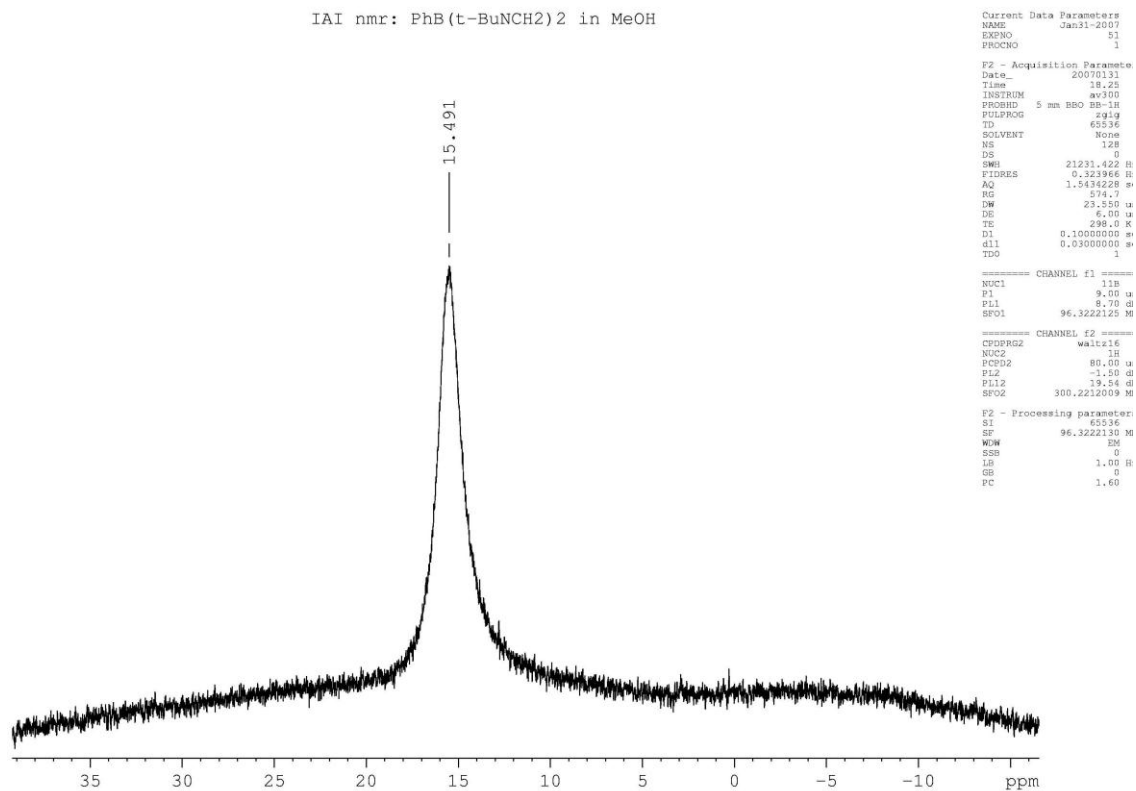
1-Phenyl -2,5-di-*tert*-butyl-1-bora-2,5-diazacyclopentane in Methanol Soln: ^1H :



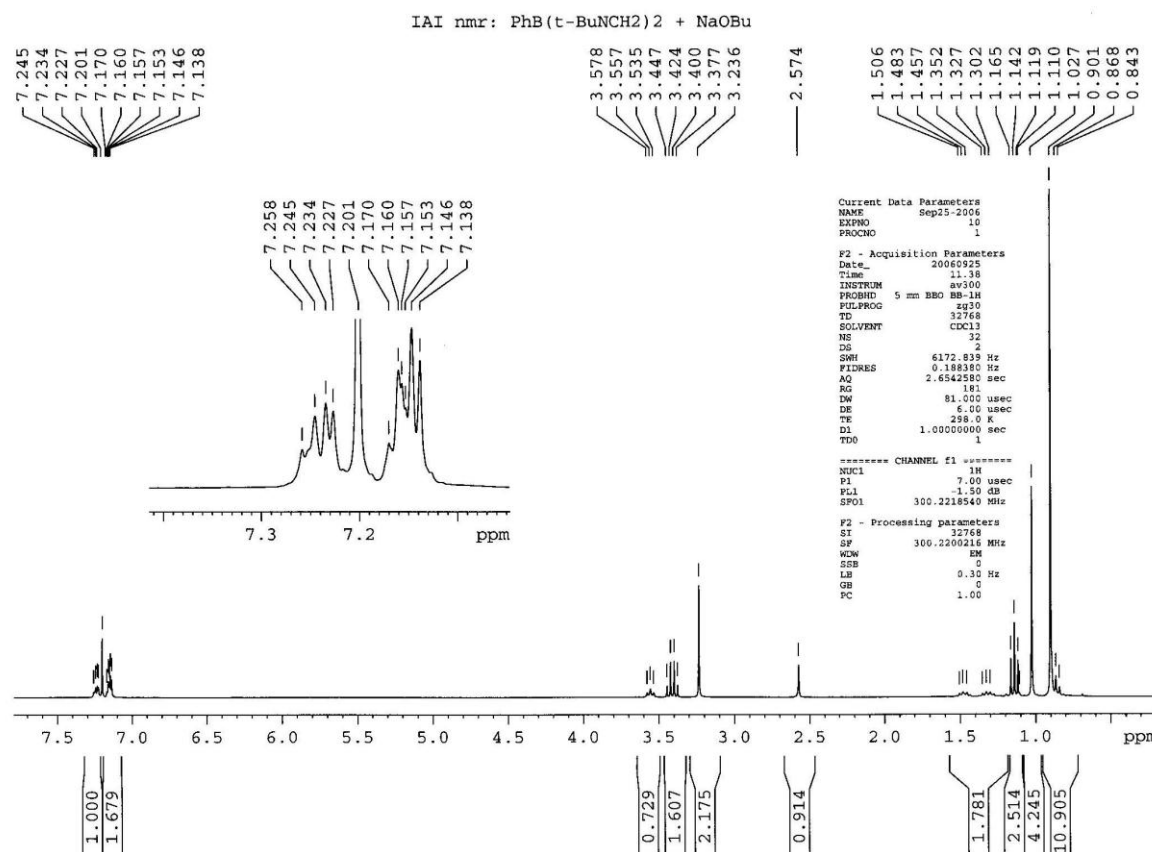
1-Phenyl -2,5-di-*tert*-butyl-1-bora-2,5-diazacyclopentane in Methanol Soln: ^{13}C :



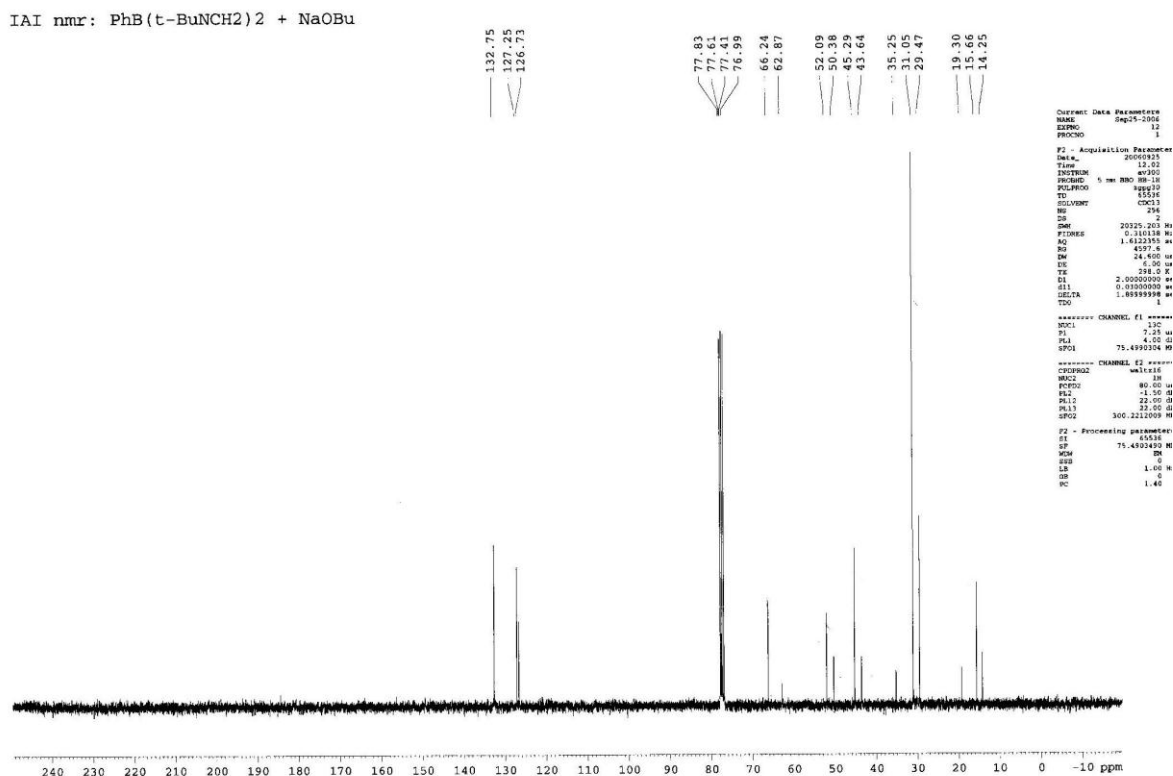
1-Phenyl -2,5-di-*tert*-butyl-1-bora-2,5-diazacyclopentane in Methanol Soln: ¹¹B:



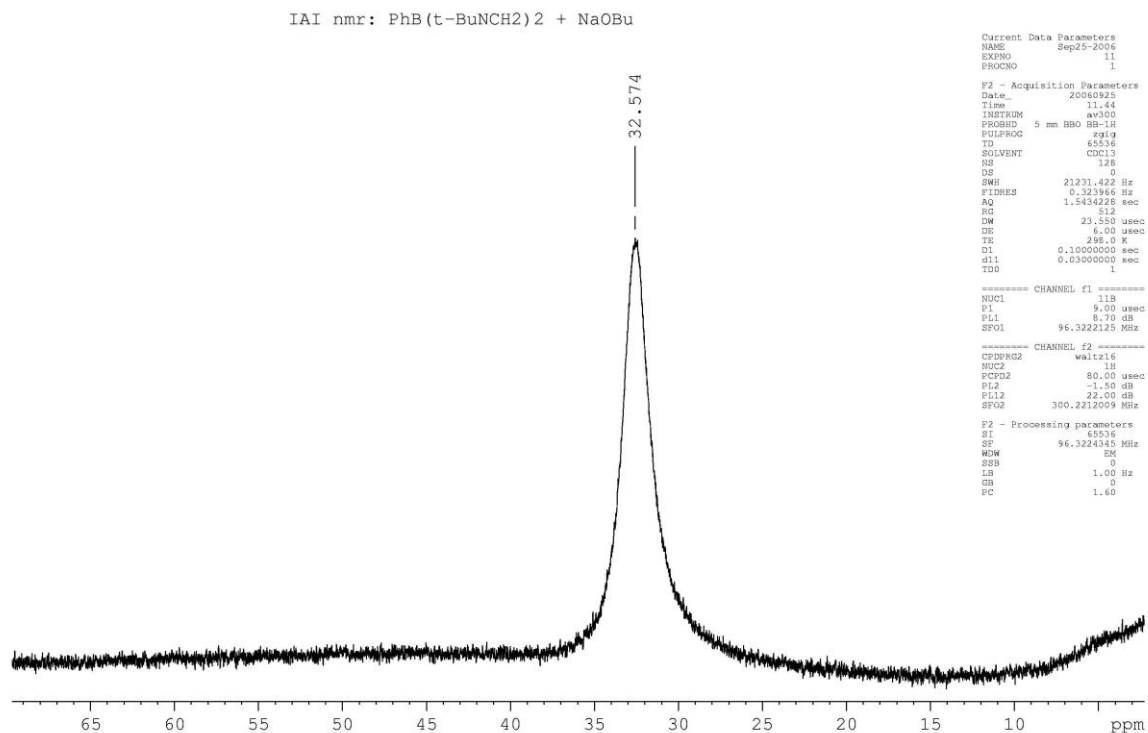
3.36: Attempted Reaction of 1-Phenyl -2,5-di-*tert*-butyl-1-bora-2,5-diazacyclopentane with sodium n-butoxide: ^1H



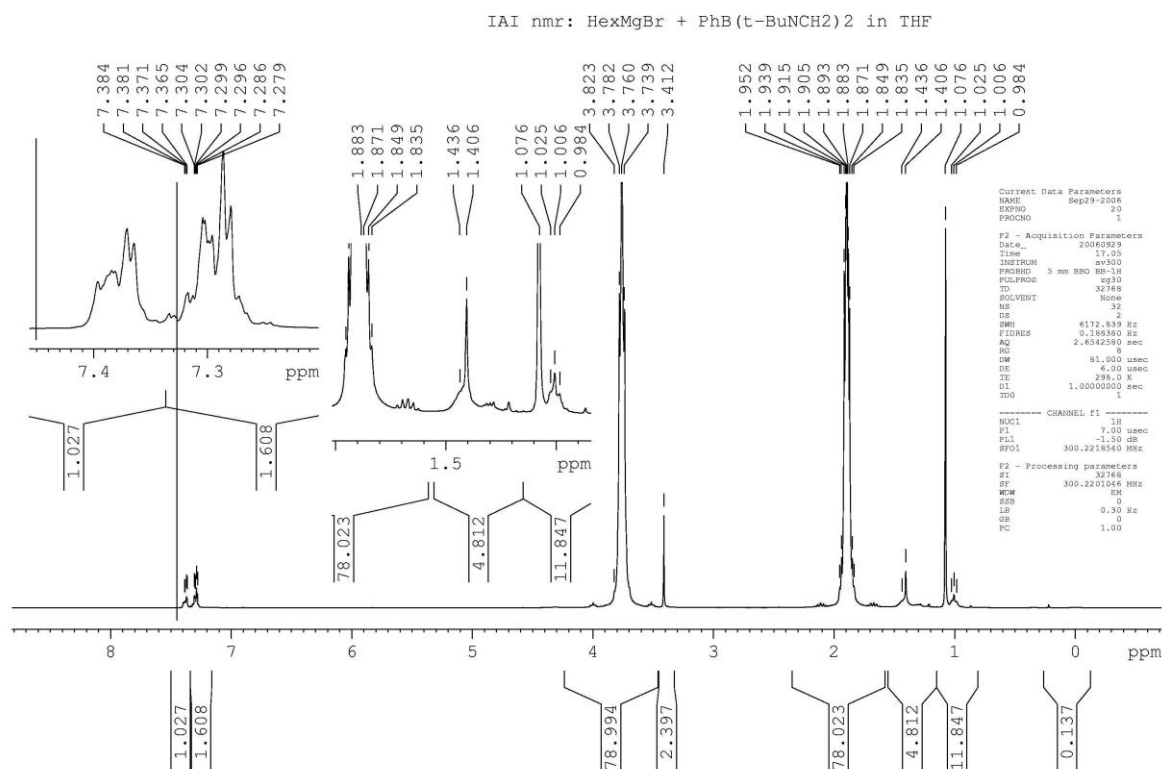
Attempted Reaction of 1-Phenyl -2,5-di-*tert*-butyl-1-bora-2,5-diazacyclopentane with sodium n-butoxide: ^{13}C



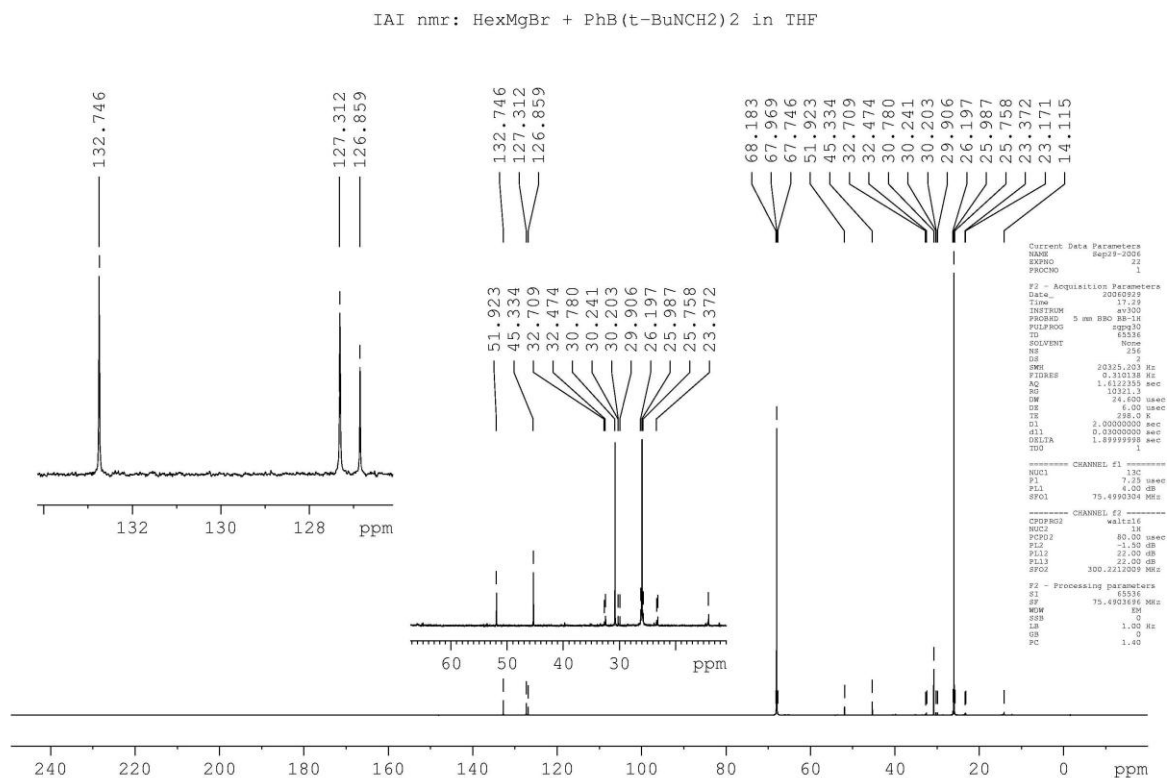
Attempted Reaction of 1-Phenyl -2,5-di-*tert*-butyl-1-bora-2,5-diazacyclopentane with sodium n-butoxide: ^{11}B



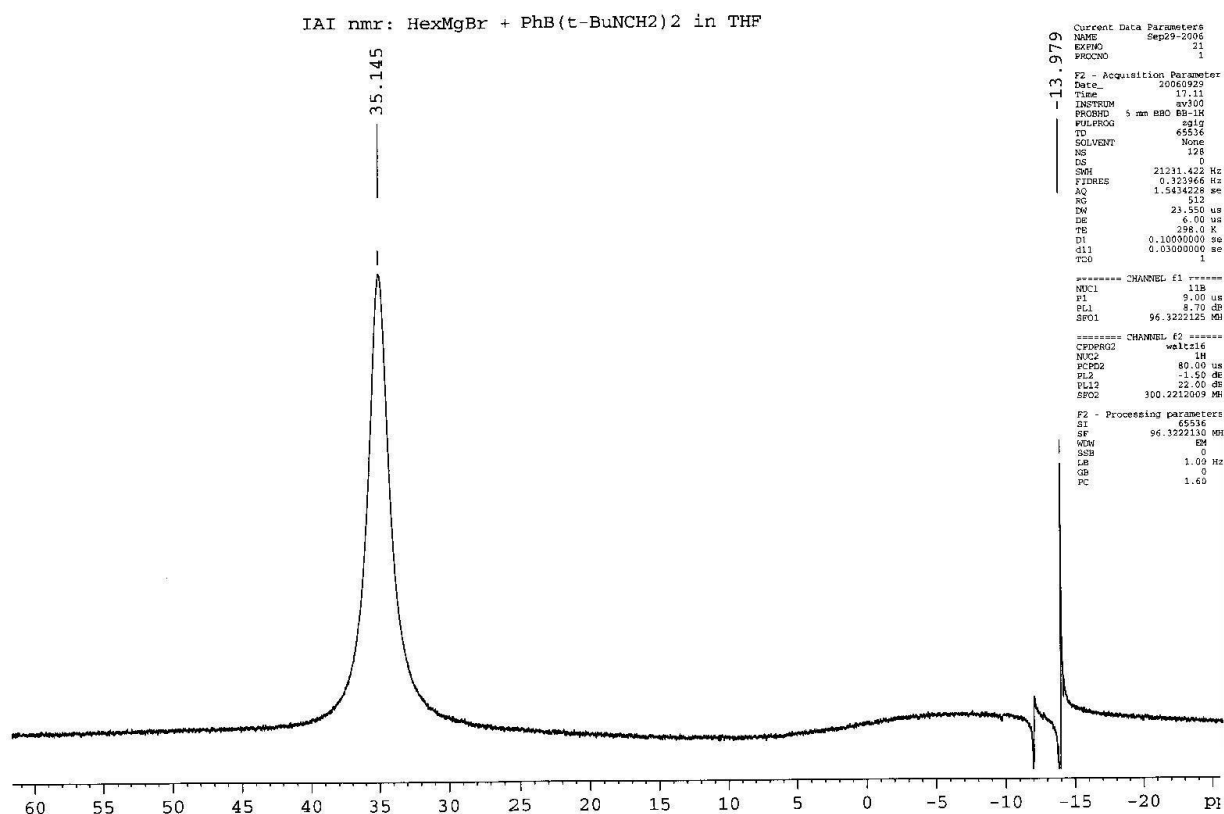
3.37: Attempted Reaction of 1-Phenyl-2,5-di-*tert*-butyl-1-bora-2,5-diazacyclopentane with Hexylmagnesium Bromide: ¹H



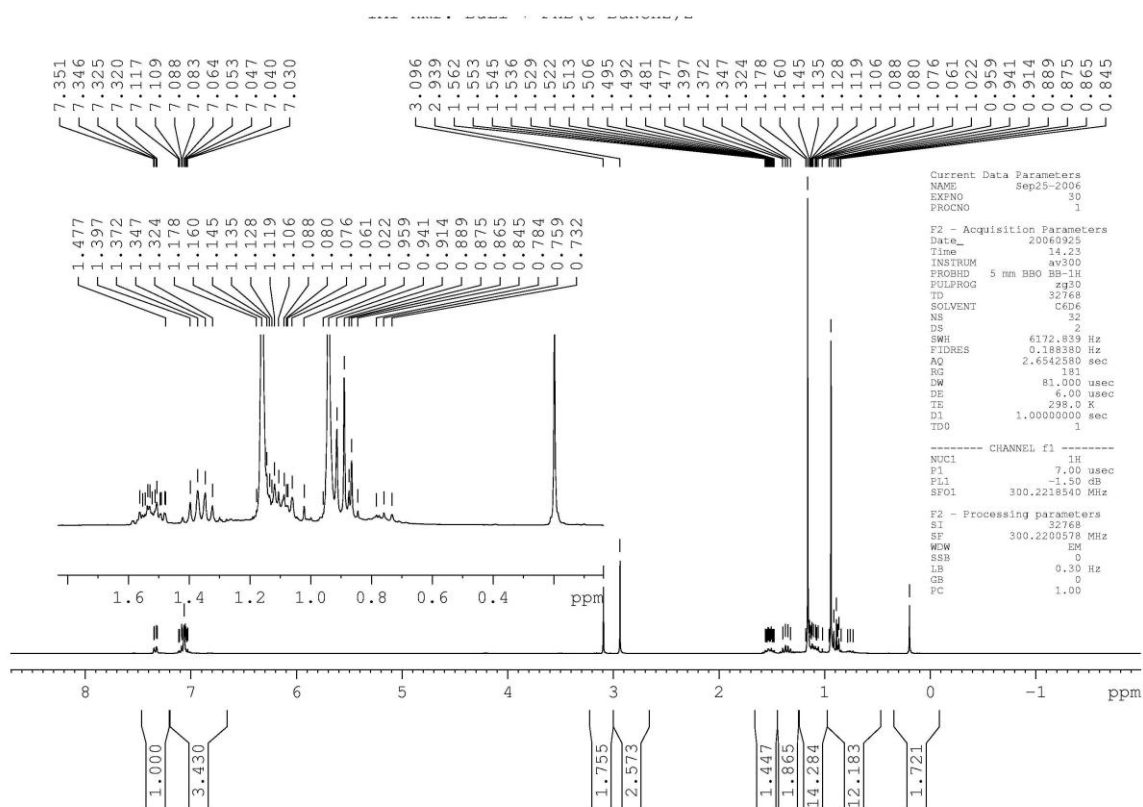
Attempted Reaction of 1-Phenyl-2,5-di-*tert*-butyl-1-bora-2,5-diazacyclopentane with Hexylmagnesium Bromide: ^{13}C



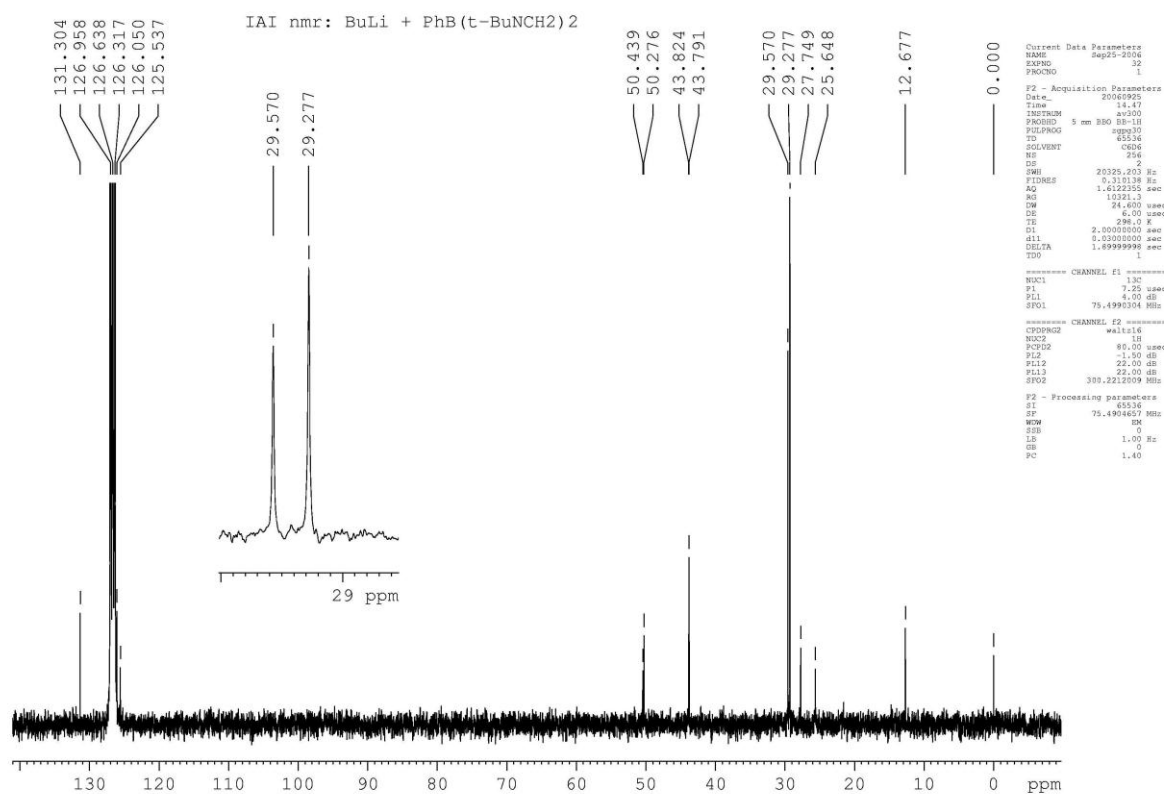
Attempted Reaction of 1-Phenyl-2,5-di-*tert*-butyl-1-bora-2,5-diazacyclopentane with Hexylmagnesium Bromide: ^{11}B



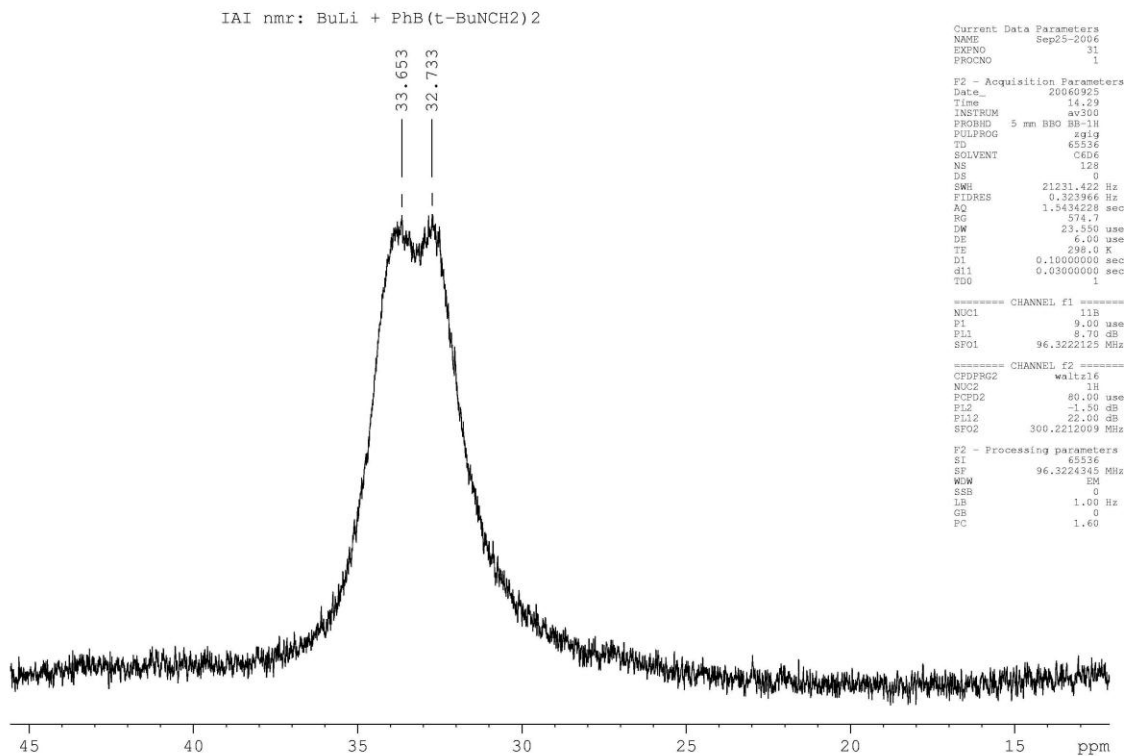
3.39: Attempted Reaction of 1-Phenyl-2,5-di-*tert*-butyl-1-bora-2,5-diazacyclopentane with *n*-Butyl Lithium: ^1H



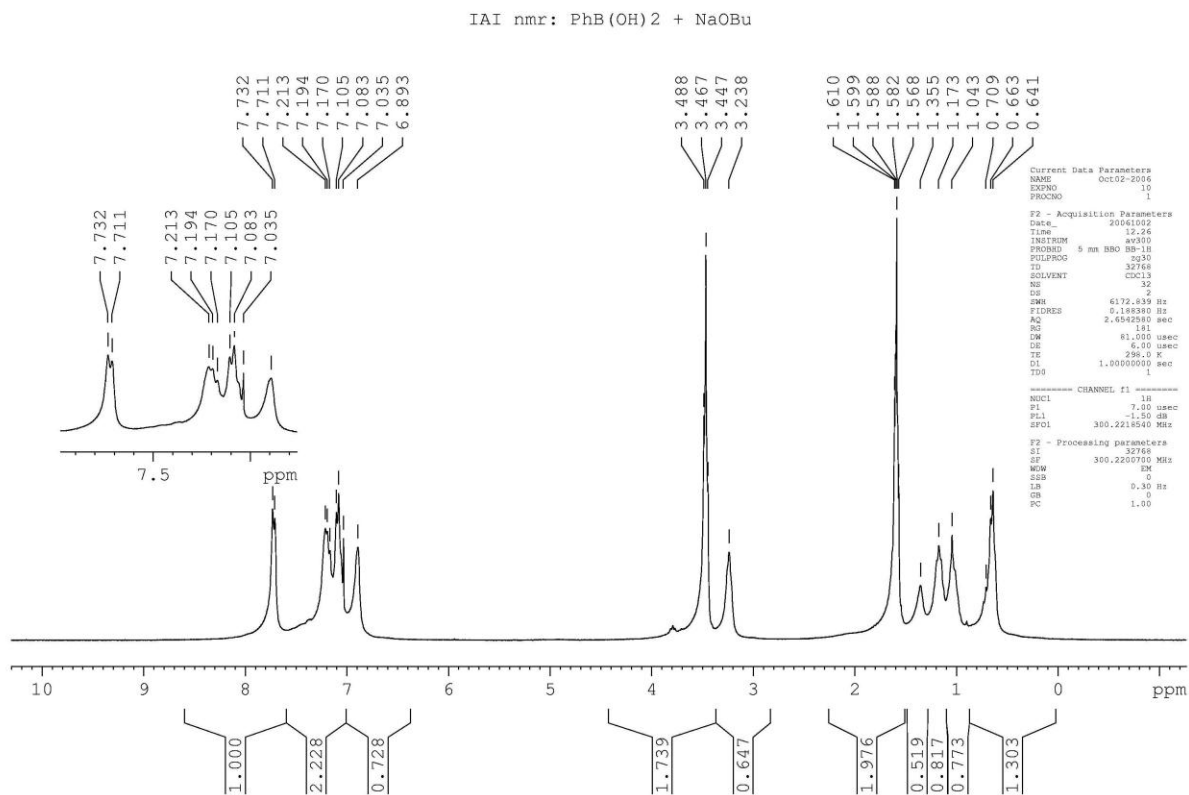
Attempted Reaction of 1-Phenyl-2,5-di-*tert*-butyl-1-bora-2,5-diazacyclopentane with *n*-Butyl Lithium:
¹³C



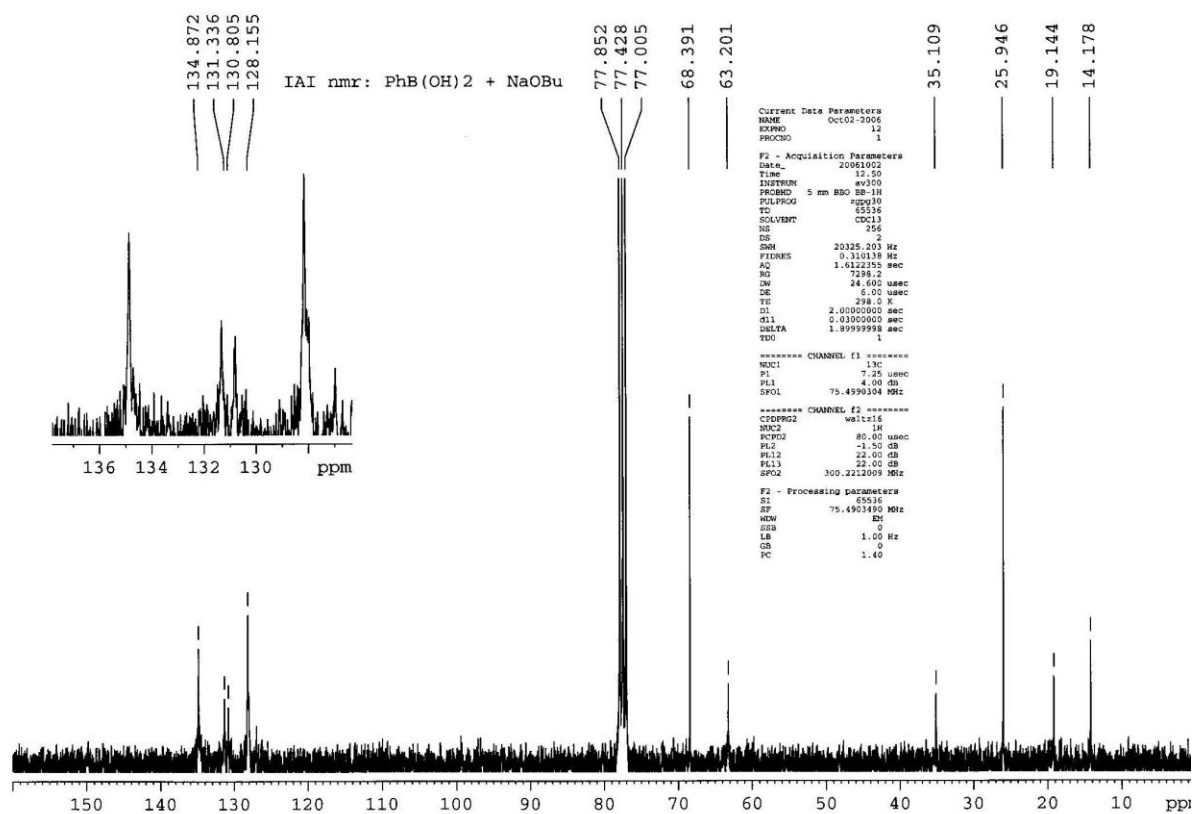
Attempted Reaction of 1-Phenyl-2,5-di-*tert*-butyl-1-bora-2,5-diazacyclopentane with *n*-Butyl Lithium:
¹¹B



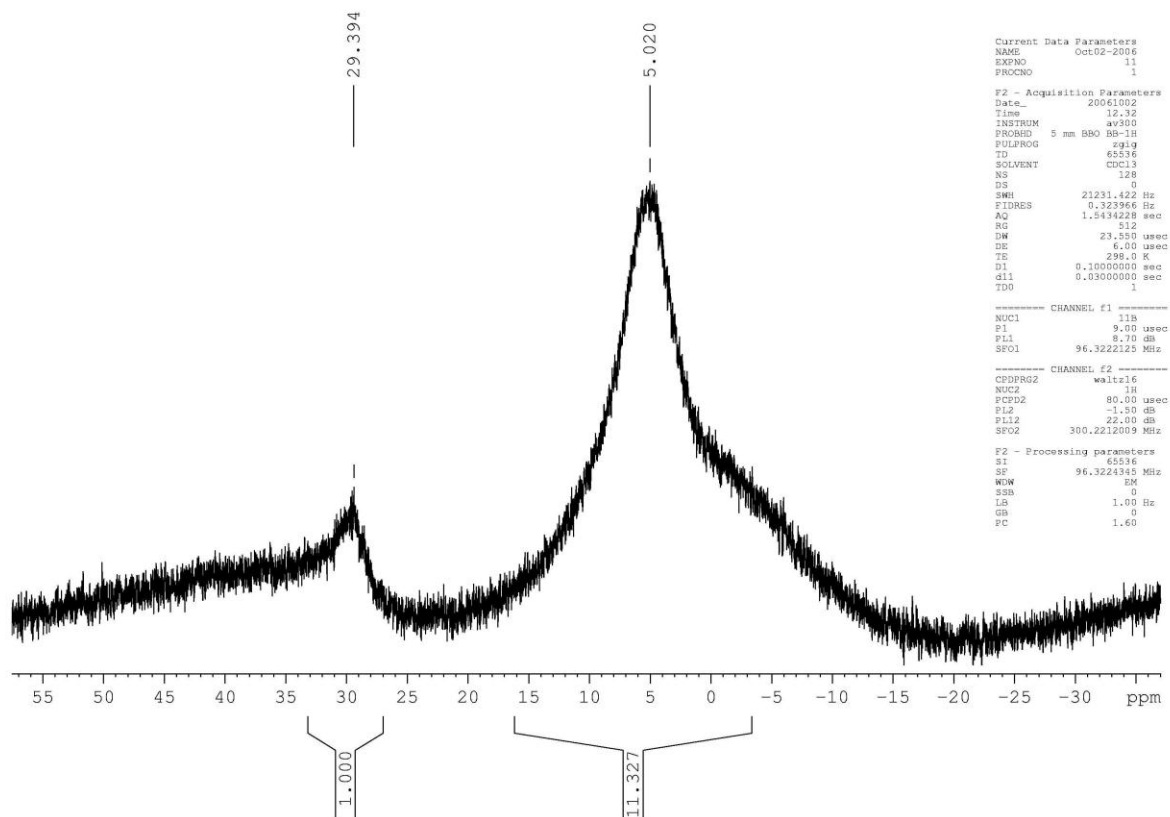
3.44: Sodium Phenyl (Bis-hydroxy)Butoxyborate: ¹H



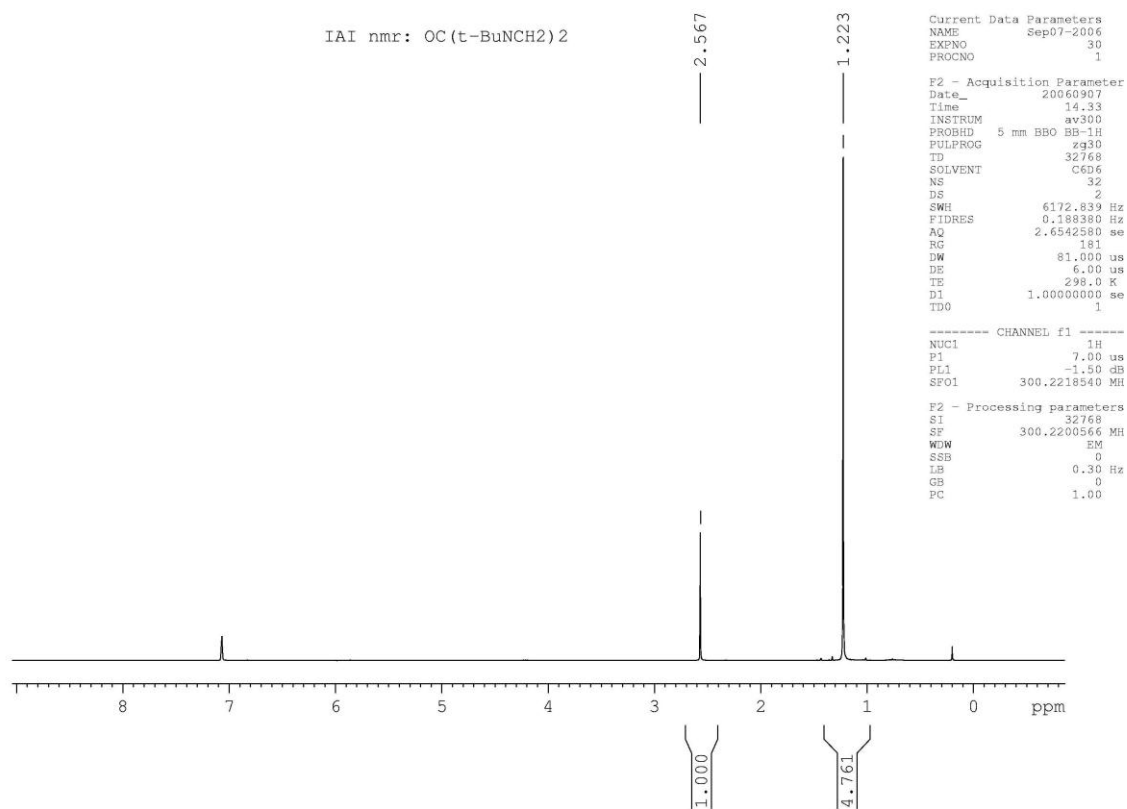
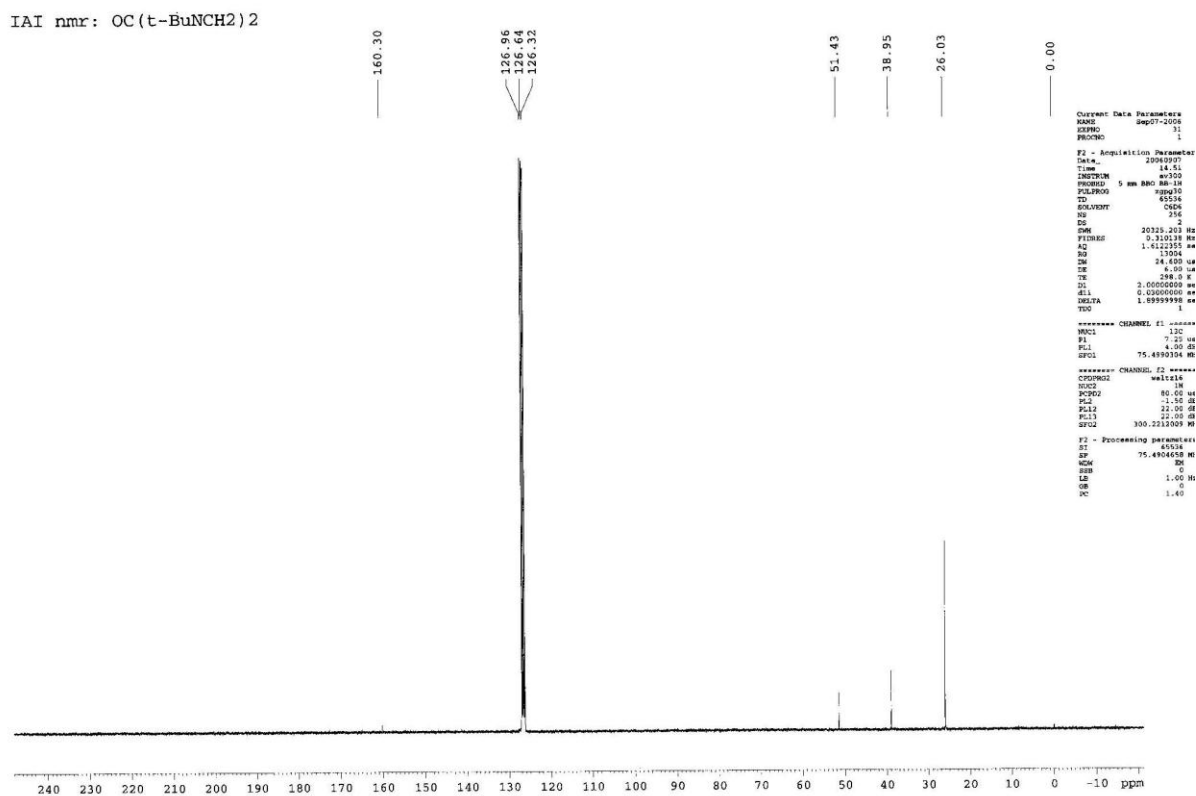
Sodium Phenyl (Bis-hydroxy)Butoxyborate: ¹³C



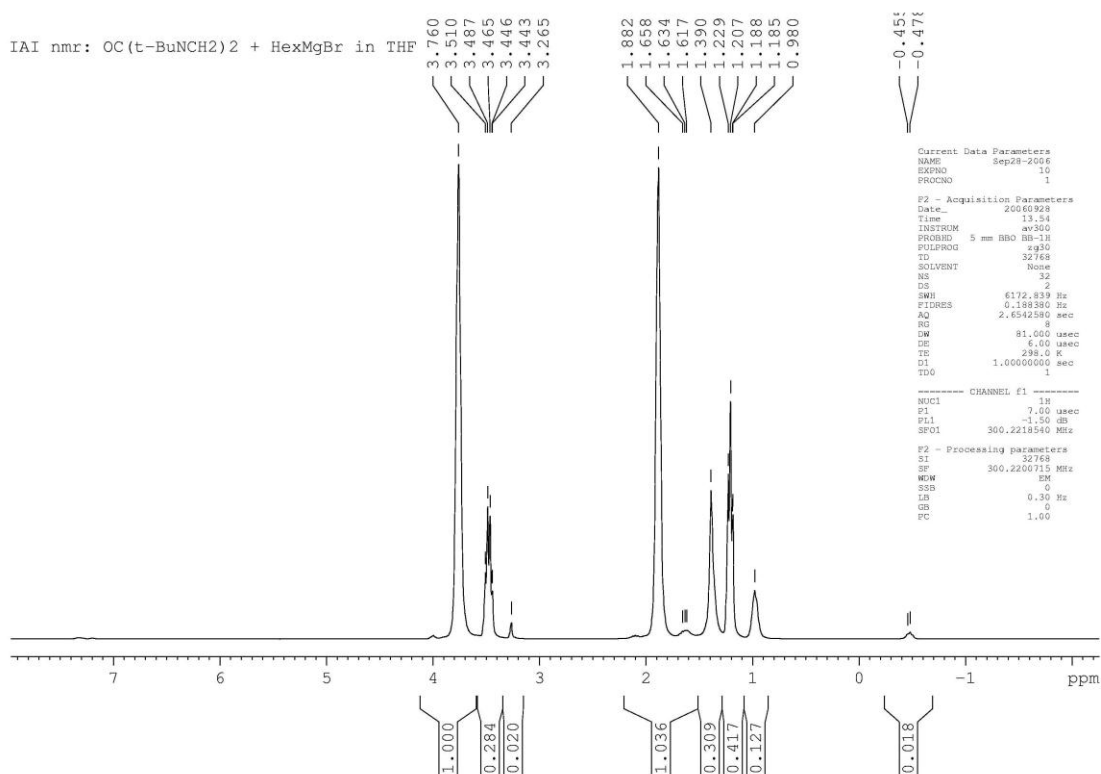
Sodium Phenyl(Bis-hydroxy)Butoxyborate: ¹¹B



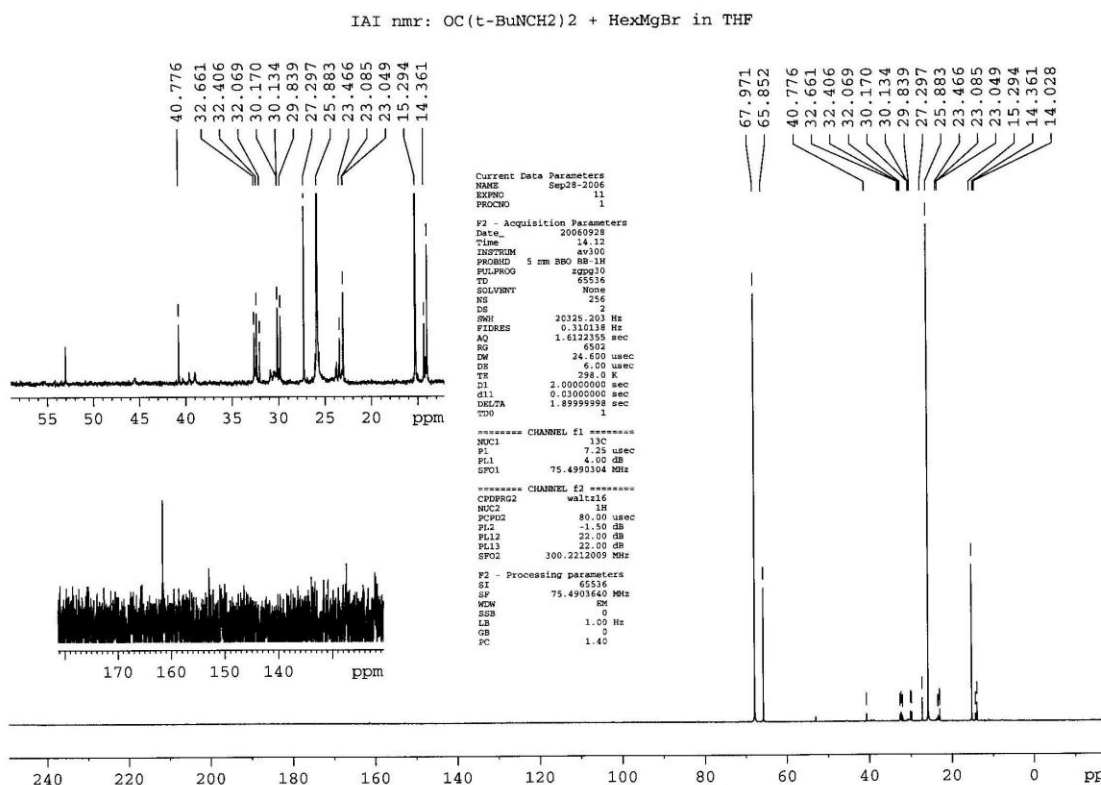
3.46:

1-keto-2,5-di-*tert*-butyl-2,5-diazacyclopentane: ^1H Synthesis of 1-keto-2,5-di-*tert*-butyl-2,5-diazacyclopentane: ^{13}C 

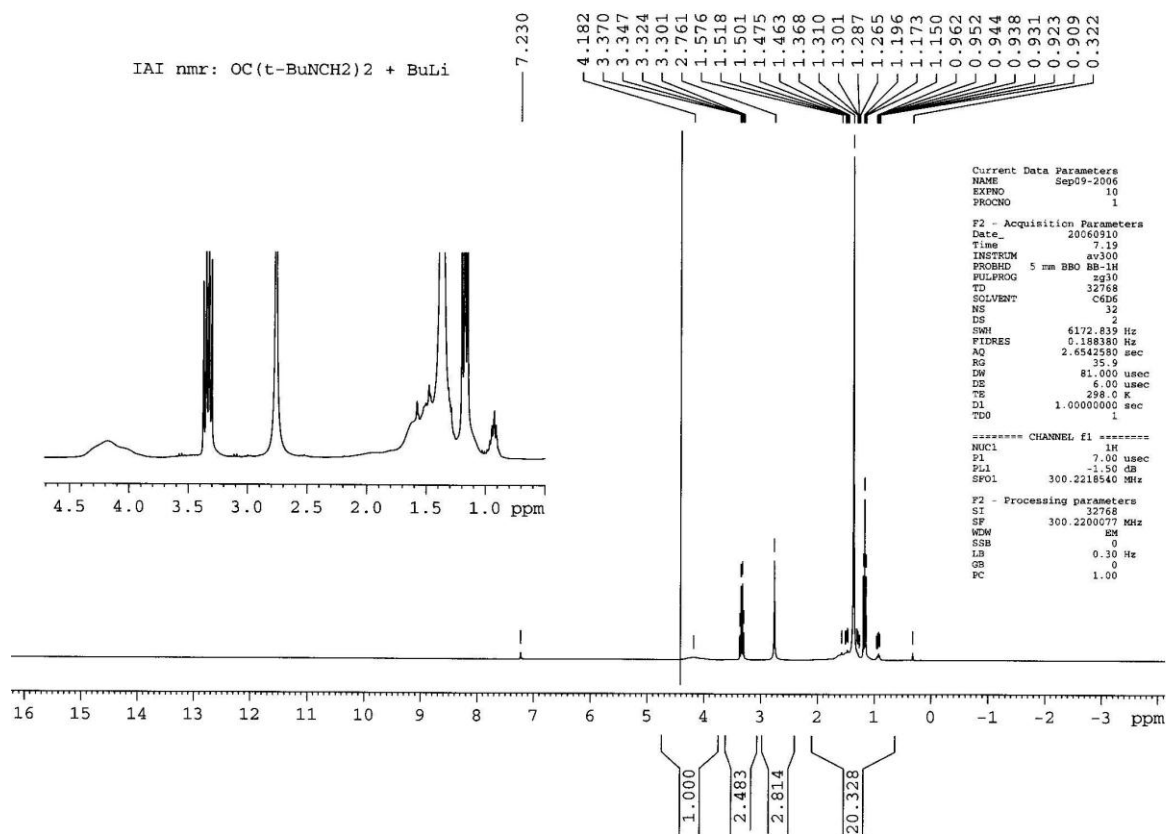
3.48: Attempted reaction of 1-keto-2,5-di-*tert*-butyl-2,5-diazacyclopentane with hexylmagnesium bromide: ^1H



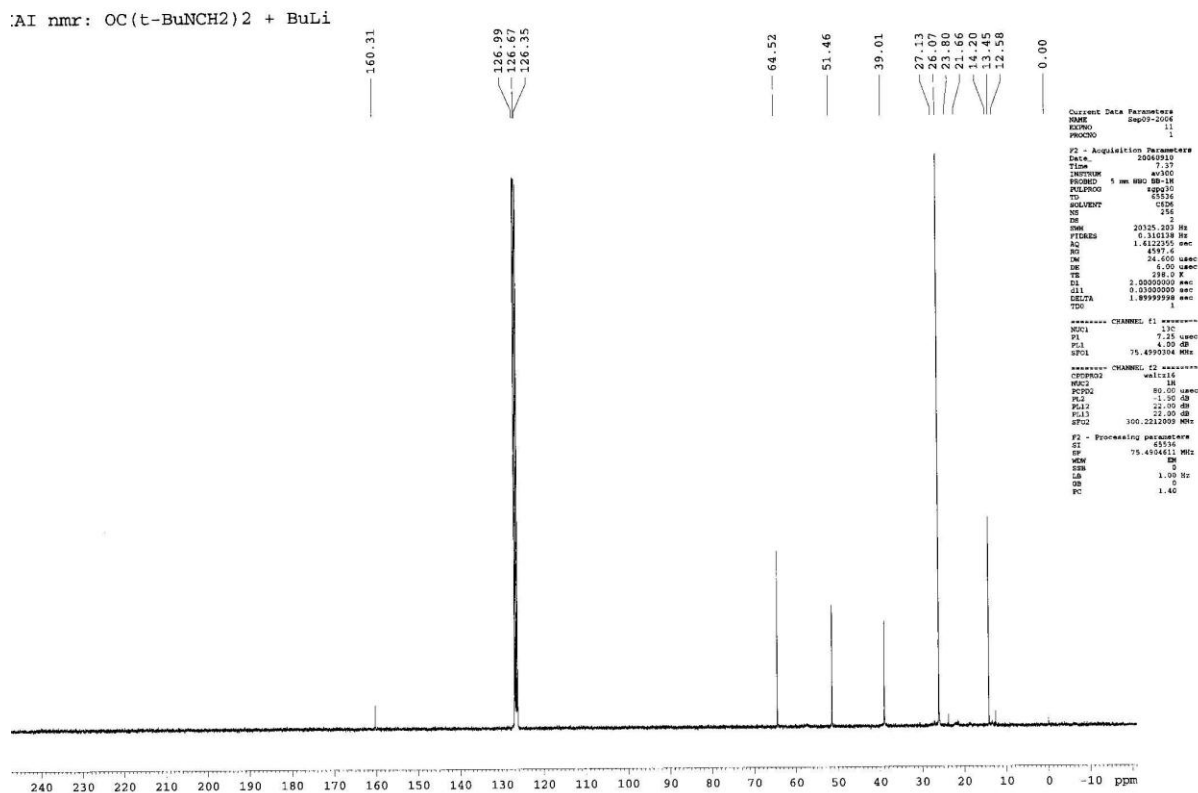
Attempted reaction of 1-keto-2,5-di-*tert*-butyl-2,5-diazacyclopentane with hexylmagnesium bromide: ^{13}C



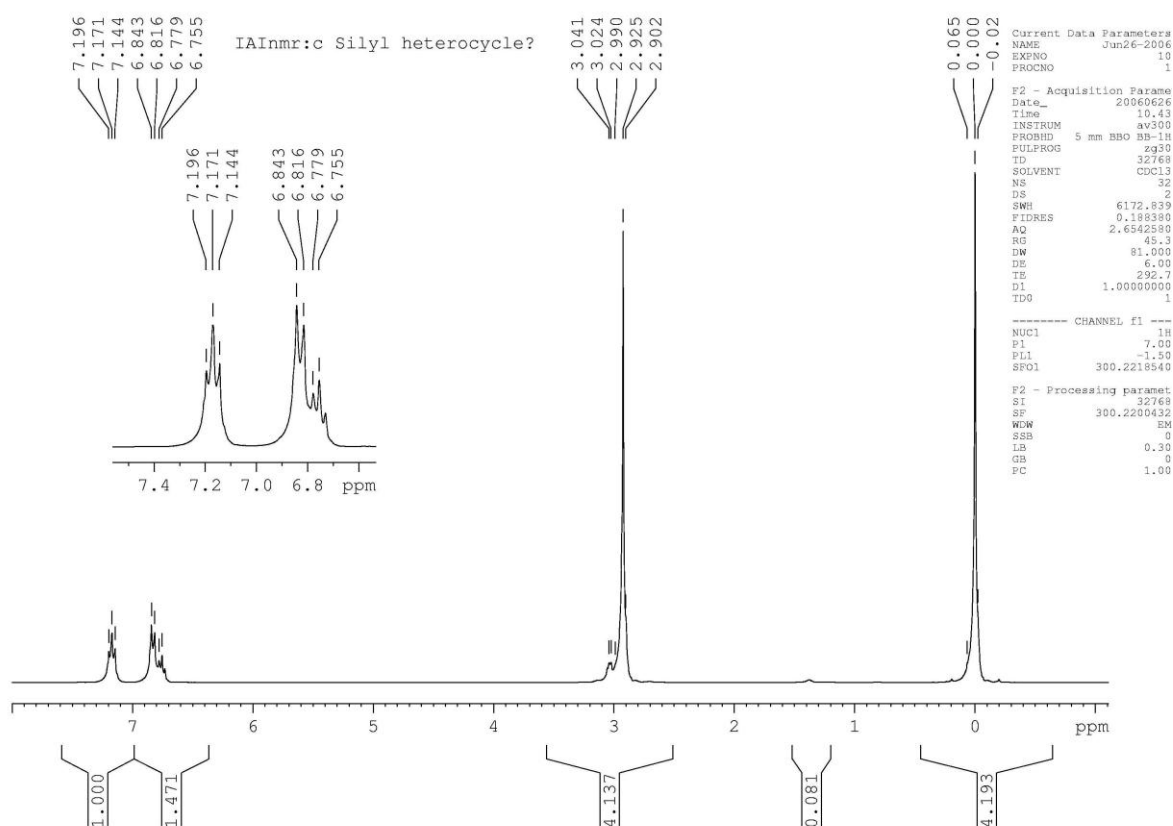
3.50: Attempted reaction of 1-keto-2,5-di-*tert*-butyl-2,5-diazacyclopentane with *n*-butyl lithium: ^1H



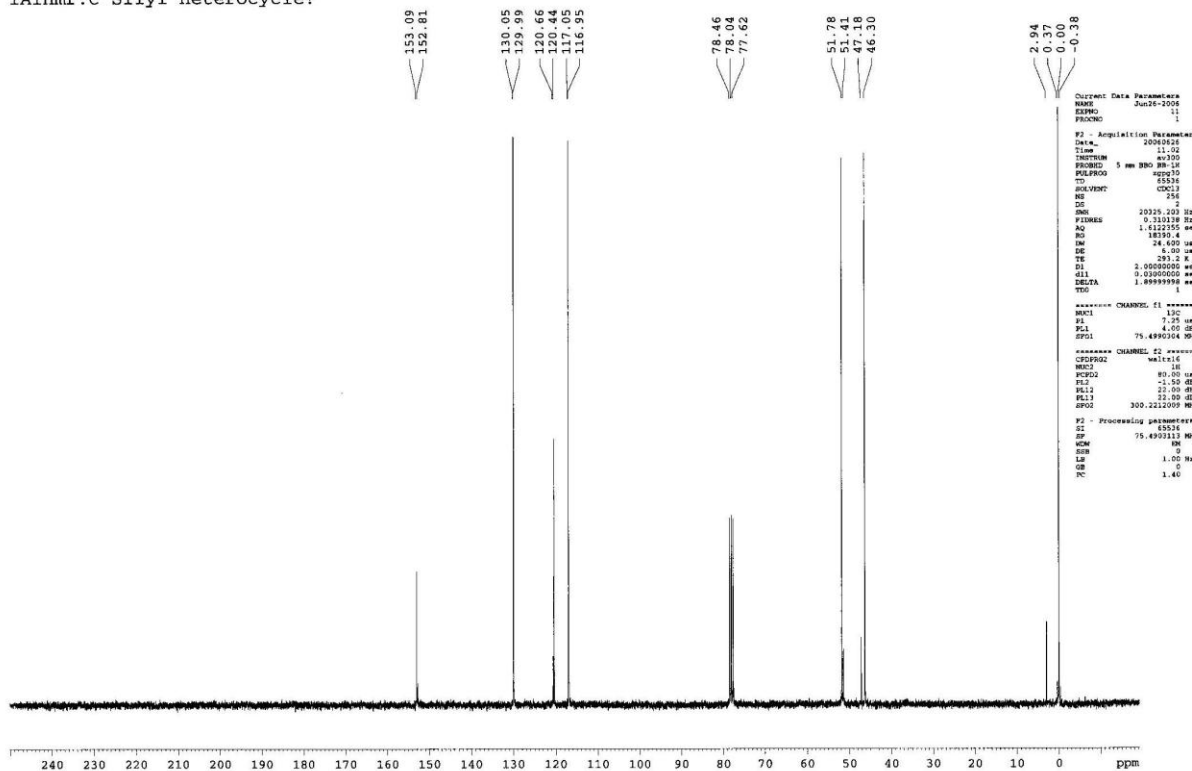
Attempted reaction of 1-keto-2,5-di-*tert*-butyl-2,5-diazacyclopentane with *n*-butyl lithium: ^{13}C



3.52:

N-phenyl-N'-trimethylsilylpiperazine: ^1H :N-phenyl-N'-trimethylsilylpiperazine: ^{13}C :

IAInmr:c Silyl heterocycle?



Appendix 2: X-Ray Crystallography Data:

1. Crystal Structure: 1,3,5-trimethyl-1,3,5-triazacyclohexane Hydrobromide:

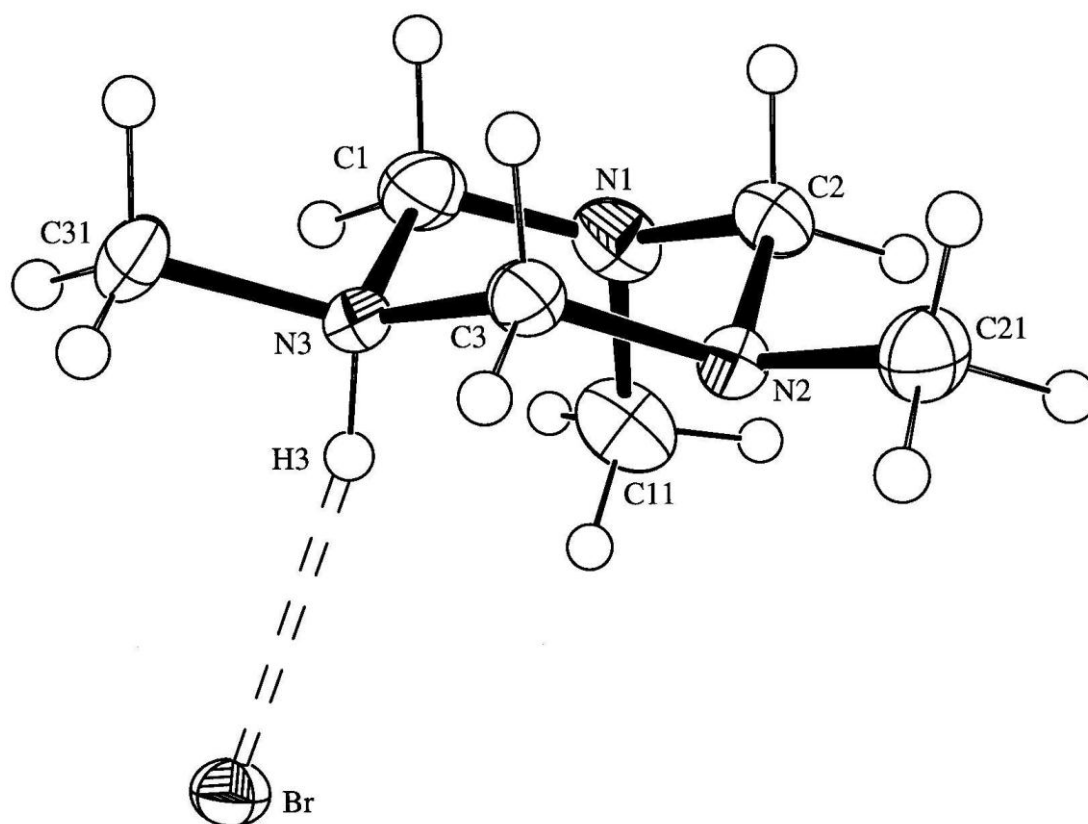


Table 1. Crystal data and structure refinement for k03rdk9.

Identification code	k03rdk9
Empirical formula	C6 H16 Br N3
Formula weight	210.13
Temperature	150(2) K
Wavelength	0.71073 Å
Crystal system	monoclinic
Space group	P 2 ₁ /n
Unit cell dimensions	a = 6.6140(2) Å alpha = 90 deg. b = 11.0640(3) Å beta = 97.1510(10) deg. c = 12.9120(4) Å gamma = 90 deg.
Volume	937.52(5) Å ³
Z, Calculated density	4, 1.489 Mg/m ³
Absorption coefficient	4.325 mm ⁻¹
F(000)	432
Crystal size	0.50 x 0.45 x 0.03 mm
Colour, shape	colourless plate
Theta range for data collection	3.68 to 30.06 deg.
Limiting indices	-9<=h<=9, -14<=k<=15, -18<=l<=18
Reflections collected / unique	12488 / 2720 [R(int) = 0.0958]
Completeness to theta = 30.06	98.8 %
Max. and min. transmission	0.8812 and 0.2210
Refinement method	Full-matrix least-squares on F ²
Data / restraints / parameters	2720 / 0 / 155
Goodness-of-fit on F ²	1.034
Final R indices [I>2sigma(I)]	R1 = 0.0424, wR2 = 0.0990
R indices (all data)	R1 = 0.0622, wR2 = 0.1093
Largest diff. peak and hole	0.901 and -1.118 e.Å ⁻³

Table 2. Atomic coordinates ($\times 10^4$) and equivalent isotropic displacement parameters ($\text{\AA}^2 \times 10^3$) for k03rdk9. $U(\text{eq})$ is defined as one third of the trace of the orthogonalized U_{ij} tensor.

	x	y	z	$U(\text{eq})$
Br	7980 (1)	7082 (1)	424 (1)	26 (1)
C (1)	5156 (6)	4439 (3)	1956 (3)	36 (1)
N (1)	3976 (4)	5229 (3)	2511 (2)	33 (1)
C (11)	3336 (6)	6360 (4)	1959 (3)	41 (1)
C (2)	4983 (4)	5423 (3)	3561 (2)	26 (1)
N (2)	7029 (4)	5934 (2)	3541 (2)	22 (1)
C (21)	7977 (5)	6197 (3)	4604 (2)	31 (1)
C (3)	8264 (5)	5085 (3)	3052 (2)	25 (1)
N (3)	7329 (4)	4881 (2)	1957 (2)	27 (1)
C (31)	8585 (8)	4021 (3)	1412 (3)	45 (1)

Table 3. Bond lengths [\AA] for k03rdk9.

Br-H (3)	2.34 (4)
C (1)-N (1)	1.424 (5)
C (1)-N (3)	1.519 (4)
C (1)-H (1A)	0.99 (4)
C (1)-H (1B)	1.04 (4)
N (1)-C (2)	1.450 (4)
N (1)-C (11)	1.476 (5)
C (11)-H (11A)	1.02 (5)
C (11)-H (11B)	0.89 (5)
C (11)-H (11C)	0.99 (5)
C (2)-N (2)	1.470 (4)
C (2)-H (2A)	0.95 (3)
C (2)-H (2B)	0.98 (3)
N (2)-C (3)	1.441 (4)
N (2)-C (21)	1.466 (4)
C (21)-H (21A)	1.03 (5)
C (21)-H (21B)	0.98 (4)
C (21)-H (21C)	0.88 (5)
C (3)-N (3)	1.488 (4)
C (3)-H (3A)	0.97 (3)
C (3)-H (3B)	0.96 (4)
N (3)-C (31)	1.496 (4)
N (3)-H (3)	0.89 (4)
C (31)-H (31A)	0.95 (5)
C (31)-H (31B)	0.95 (5)
C (31)-H (31C)	0.97 (6)

Table 4. Bond angles [deg] for k03rdk9.

N(3)-H(3)-BR	164(3)
N(1)-C(1)-N(3)	112.3(2)
N(1)-C(1)-H(1A)	112(2)
N(3)-C(1)-H(1A)	104(2)
N(1)-C(1)-H(1B)	111(2)
N(3)-C(1)-H(1B)	102(2)
H(1A)-C(1)-H(1B)	115(3)
C(1)-N(1)-C(2)	110.1(3)
C(1)-N(1)-C(11)	114.8(3)
C(2)-N(1)-C(11)	113.4(3)
N(1)-C(11)-H(11A)	109(3)
N(1)-C(11)-H(11B)	108(3)
H(11A)-C(11)-H(11B)	108(4)
N(1)-C(11)-H(11C)	115(3)
H(11A)-C(11)-H(11C)	109(4)
H(11B)-C(11)-H(11C)	108(4)
N(1)-C(2)-N(2)	110.9(2)
N(1)-C(2)-H(2A)	112(2)
N(2)-C(2)-H(2A)	106(2)
N(1)-C(2)-H(2B)	104.6(19)
N(2)-C(2)-H(2B)	112.0(19)
H(2A)-C(2)-H(2B)	111(3)
C(3)-N(2)-C(21)	109.9(2)
C(3)-N(2)-C(2)	109.3(2)
C(21)-N(2)-C(2)	110.3(2)
N(2)-C(21)-H(21A)	110(3)
N(2)-C(21)-H(21B)	108(2)
H(21A)-C(21)-H(21B)	107(3)
N(2)-C(21)-H(21C)	118(3)
H(21A)-C(21)-H(21C)	106(4)
H(21B)-C(21)-H(21C)	107(3)
N(2)-C(3)-N(3)	108.9(2)
N(2)-C(3)-H(3A)	117(2)
N(3)-C(3)-H(3A)	103(2)
N(2)-C(3)-H(3B)	111(2)
N(3)-C(3)-H(3B)	107(2)
H(3A)-C(3)-H(3B)	110(3)
C(3)-N(3)-C(31)	110.7(3)
C(3)-N(3)-C(1)	109.3(2)
C(31)-N(3)-C(1)	112.1(3)
C(3)-N(3)-H(3)	108(2)
C(31)-N(3)-H(3)	106(2)
C(1)-N(3)-H(3)	111(2)
N(3)-C(31)-H(31A)	110(3)
N(3)-C(31)-H(31B)	108(3)
H(31A)-C(31)-H(31B)	105(4)
N(3)-C(31)-H(31C)	109(3)
H(31A)-C(31)-H(31C)	108(4)
H(31B)-C(31)-H(31C)	117(4)

Table 5. Anisotropic displacement parameters ($\text{\AA}^2 \times 10^3$) for k03rdk9.
The anisotropic displacement factor exponent takes the form:
 $-2 \pi^2 [h^2 a^{*2} U_{11} + \dots + 2 h k a^* b^* U_{12}]$

	U11	U22	U33	U23	U13	U12
Br	28 (1)	21 (1)	30 (1)	4 (1)	8 (1)	0 (1)
C (1)	48 (2)	29 (2)	29 (2)	-4 (1)	2 (1)	-13 (1)
N (1)	27 (1)	41 (2)	30 (1)	4 (1)	0 (1)	-7 (1)
C (11)	30 (2)	54 (2)	37 (2)	13 (2)	-2 (1)	3 (2)
C (2)	25 (1)	29 (2)	26 (1)	4 (1)	6 (1)	-1 (1)
N (2)	24 (1)	21 (1)	22 (1)	-1 (1)	4 (1)	0 (1)
C (21)	34 (2)	31 (2)	27 (2)	-3 (1)	-2 (1)	-2 (1)
C (3)	28 (1)	22 (1)	27 (1)	2 (1)	8 (1)	2 (1)
N (3)	44 (2)	16 (1)	24 (1)	-1 (1)	12 (1)	-1 (1)
C (31)	82 (3)	20 (2)	39 (2)	-2 (1)	28 (2)	11 (2)

Table 6. Hydrogen coordinates ($\times 10^4$) and isotropic displacement parameters ($\text{\AA}^2 \times 10^3$) for k03rdk9.

	x	y	z	U(eq)
H (1A)	4610 (60)	4390 (40)	1210 (30)	44 (11)
H (1B)	5360 (60)	3610 (40)	2340 (30)	43 (11)
H (11A)	2470 (80)	6850 (40)	2410 (40)	58 (13)
H (11B)	2560 (80)	6170 (40)	1370 (40)	66 (15)
H (11C)	4460 (70)	6880 (40)	1770 (30)	48 (12)
H (2A)	4260 (50)	5980 (30)	3940 (30)	25 (8)
H (2B)	5030 (50)	4620 (30)	3880 (30)	22 (8)
H (21A)	7080 (70)	6790 (40)	4960 (40)	52 (12)
H (21B)	9280 (60)	6600 (40)	4560 (30)	38 (10)
H (21C)	8230 (60)	5580 (40)	5030 (30)	44 (11)
H (3A)	8360 (50)	4280 (30)	3340 (30)	22 (8)
H (3B)	9600 (60)	5400 (30)	3020 (30)	33 (9)
H (3)	7360 (50)	5580 (30)	1610 (30)	24 (8)
H (31A)	8030 (60)	3950 (40)	700 (40)	44 (11)
H (31B)	8450 (70)	3240 (40)	1700 (30)	47 (11)
H (31C)	9950 (90)	4340 (50)	1430 (40)	71 (16)

2. Crystal Structure: 1-Phenyl-2,5-di-*tert*-butyl-1-bora-2,5-diazacyclopentane:

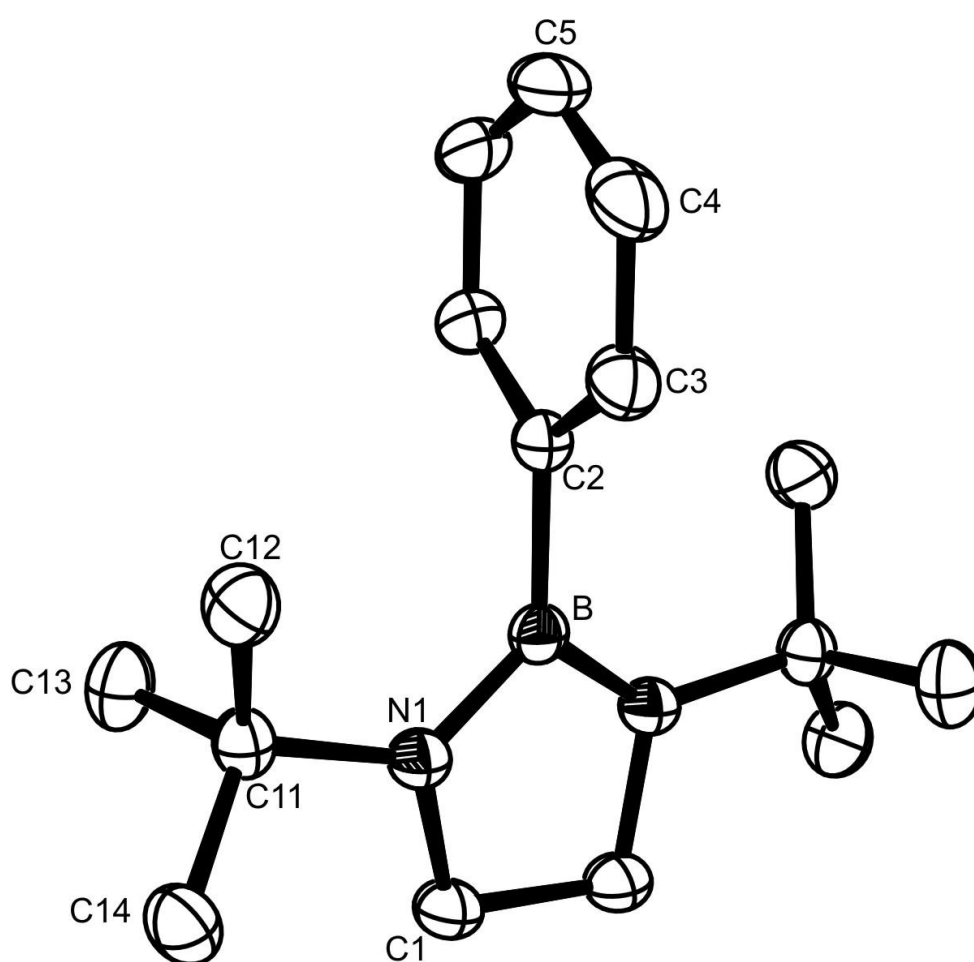


Table 1. Crystal data and structure refinement for h06rdk10.

Identification code	h06rdk10		
Empirical formula	C16 H27 B N2		
Formula weight	258.21		
Temperature	150(2) K		
Wavelength	0.71073 Å		
Crystal system	monoclinic		
Space group	C 2/c		
Unit cell dimensions	a = 14.5180(6) Å	alpha = 90 deg.	
	b = 10.3240(6) Å	beta = 110.844(2) deg.	
	c = 11.1910(5) Å	gamma = 90 deg.	
Volume	1567.57(13) Å ³		
Z, Calculated density	4, 1.094 Mg/m ³		
Absorption coefficient	0.063 mm ⁻¹		
F(000)	568		
Crystal size	0.50 x 0.50 x 0.15 mm		
Theta range for data collection	5.61 to 27.50 deg.		
Limiting indices	-18<=h<=18, -13<=k<=13, -14<=l<=14		
Reflections collected / unique	8946 / 1793 [R(int) = 0.0520]		
Completeness to theta = 27.50	98.8 %		
Max. and min. transmission	0.9906 and 0.9692		
Refinement method	Full-matrix least-squares on F ²		
Data / restraints / parameters	1793 / 0 / 91		
Goodness-of-fit on F ²	1.079		
Final R indices [I>2sigma(I)]	R1 = 0.0406, wR2 = 0.1045		

R indices (all data)

$R_1 = 0.0561$, $wR_2 = 0.1139$

Largest diff. peak and hole

0.187 and -0.180 e.Å⁻³

Table 2. Atomic coordinates ($\times 10^4$) and equivalent isotropic displacement parameters ($\text{\AA}^2 \times 10^3$) for h06rdk10. U(eq) is defined as one third of the trace of the orthogonalized Uij tensor.

	x	y	z	U(eq)
B	0	1399 (2)	2500	23 (1)
C (1)	481 (1)	-750 (1)	2368 (1)	30 (1)
N (1)	626 (1)	602 (1)	2074 (1)	26 (1)
C (11)	1554 (1)	900 (1)	1861 (1)	27 (1)
C (12)	1473 (1)	2180 (1)	1149 (1)	36 (1)
C (13)	2412 (1)	982 (1)	3143 (1)	38 (1)
C (14)	1765 (1)	-164 (1)	1040 (1)	37 (1)
C (2)	0	2925 (1)	2500	25 (1)
C (3)	-506 (1)	3626 (1)	1391 (1)	33 (1)
C (4)	-502 (1)	4969 (1)	1386 (2)	45 (1)
C (5)	0	5637 (2)	2500	49 (1)

Table 3. Bond lengths [\AA] for h06rdk10.

B-N (1)	1.4279 (13)
B-N (1) #1	1.4279 (13)
B-C (2)	1.575 (2)
C (1)-N (1)	1.4665 (13)
C (1)-C (1) #1	1.526 (2)
N (1)-C (11)	1.4821 (13)
C (11)-C (12)	1.5265 (16)
C (11)-C (14)	1.5309 (15)
C (11)-C (13)	1.5312 (16)
C (2)-C (3) #1	1.3983 (14)
C (2)-C (3)	1.3983 (14)
C (3)-C (4)	1.3863 (17)
C (4)-C (5)	1.3837 (18)
C (5)-C (4) #1	1.3837 (18)

Symmetry transformations used to generate equivalent atoms:
 #1 -x,y,-z+1/2

Table 4. Bond angles [deg] for h06rdk10.

N(1)-B-N(1)#1	109.59(12)
N(1)-B-C(2)	125.20(6)
N(1)#1-B-C(2)	125.20(6)
N(1)-C(1)-C(1)#1	104.94(6)
B-N(1)-C(1)	108.32(9)
B-N(1)-C(11)	131.09(9)
C(1)-N(1)-C(11)	116.43(8)
N(1)-C(11)-C(12)	110.94(9)
N(1)-C(11)-C(14)	109.58(9)
C(12)-C(11)-C(14)	107.62(9)
N(1)-C(11)-C(13)	110.09(9)
C(12)-C(11)-C(13)	109.13(10)
C(14)-C(11)-C(13)	109.44(9)
C(3)#1-C(2)-C(3)	117.65(14)
C(3)#1-C(2)-B	121.18(7)
C(3)-C(2)-B	121.18(7)
C(4)-C(3)-C(2)	121.32(12)
C(5)-C(4)-C(3)	119.74(13)
C(4)-C(5)-C(4)#1	120.24(16)

Symmetry transformations used to generate equivalent atoms:
 #1 -x,y,-z+1/2

Table 5. Anisotropic displacement parameters ($\text{\AA}^2 \times 10^3$) for h06rdk10.
 The anisotropic displacement factor exponent takes the form:
 $-2 \pi^2 [h^2 a^2 U_{11} + \dots + 2 h k a^* b^* U_{12}]$

	U11	U22	U33	U23	U13	U12
B	22(1)	23(1)	22(1)	0	5(1)	0
C(1)	33(1)	22(1)	37(1)	0(1)	14(1)	2(1)
N(1)	26(1)	22(1)	30(1)	0(1)	11(1)	0(1)
C(11)	24(1)	31(1)	28(1)	0(1)	11(1)	1(1)
C(12)	35(1)	36(1)	41(1)	4(1)	20(1)	-1(1)
C(13)	28(1)	52(1)	32(1)	-1(1)	7(1)	-3(1)
C(14)	36(1)	41(1)	37(1)	-3(1)	17(1)	5(1)
C(2)	23(1)	23(1)	31(1)	0	11(1)	0
C(3)	31(1)	29(1)	39(1)	7(1)	12(1)	3(1)
C(4)	39(1)	31(1)	69(1)	19(1)	25(1)	9(1)
C(5)	44(1)	20(1)	95(2)	0	38(1)	0

Table 6. Hydrogen coordinates ($\times 10^4$) and isotropic displacement parameters ($\text{\AA}^2 \times 10^3$) for h06rdk10.

	x	y	z	U(eq)
H(1A)	1035	-1052	3128	36
H(1B)	429	-1320	1636	36
H(12A)	891	2160	361	54
H(12B)	2065	2309	935	54
H(12C)	1410	2893	1693	54
H(13A)	2284	1676	3662	57
H(13B)	3023	1167	2992	57
H(13C)	2476	155	3597	57
H(14A)	1910	-977	1523	55
H(14B)	2333	86	812	55
H(14C)	1187	-281	259	55
H(3)	-860	3173	626	40
H(4)	-841	5429	620	53
H(5)	0	6557	2500	59

3. Crystal Structure: 1-bromo-2,5-di-*tert*-butyl-1-bora-2,5-diazacyclopentane:

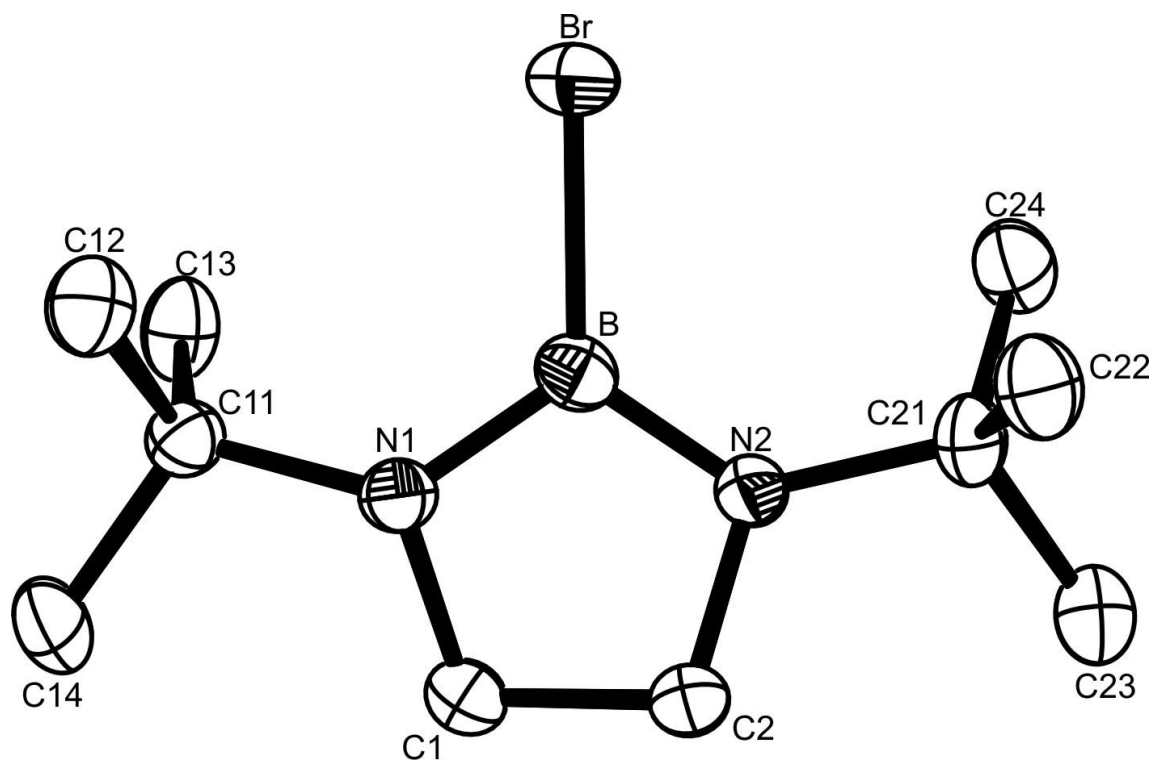


Table 1. Crystal data and structure refinement for h06rdk6.

Identification code	h06rdk6 alias Ian	
Empirical formula	C10 H20 B Br N2	
Formula weight	259.00	
Temperature	150(2) K	
Wavelength	0.71073 Å	
Crystal system	orthorhombic	
Space group	P c 2 ₁ b	
Unit cell dimensions	a = 9.4920(6) Å	alpha = 90 deg.
	b = 11.3280(6) Å	beta = 90 deg.
	c = 11.8200(7) Å	gamma = 90 deg.
Volume	1270.95(13) Å ³	
Z, Calculated density	4, 1.354 Mg/m ³	
Absorption coefficient	3.202 mm ⁻¹	
F(000)	536	
Crystal size	0.50 x 0.50 x 0.30 mm	
Theta range for data collection	4.99 to 27.46 deg.	
Limiting indices	-12<=h<=12, -14<=k<=14, -13<=l<=15	
Reflections collected / unique	7555 / 2722 [R(int) = 0.0440]	
Completeness to theta = 27.46	98.9 %	
Max. and min. transmission	0.4468 and 0.2974	
Refinement method	Full-matrix least-squares on F ²	
Data / restraints / parameters	2722 / 1 / 134	
Goodness-of-fit on F ²	1.029	
Final R indices [I>2sigma(I)]	R1 = 0.0406, wR2 = 0.1021	
R indices (all data)	R1 = 0.0552, wR2 = 0.1141	
Absolute structure parameter	0.38(2)	
Largest diff. peak and hole	0.409 and -0.584 e.Å ⁻³	

Table 2. Atomic coordinates ($\times 10^4$) and equivalent isotropic displacement parameters ($\text{\AA}^2 \times 10^3$) for h06rdk6. U(eq) is defined as one third of the trace of the orthogonalized Uij tensor.

	x	y	z	U(eq)
Br	7492(1)	2327(1)	941(1)	37(1)
B	7615(4)	3949(4)	443(4)	27(1)
N(1)	8510(4)	4812(3)	962(2)	27(1)
N(2)	6820(3)	4447(3)	-452(3)	26(1)
C(1)	8377(4)	5875(4)	279(3)	33(1)
C(2)	6994(5)	5728(4)	-344(4)	32(1)
C(11)	9758(4)	4646(4)	1704(3)	28(1)
C(12)	9294(5)	4163(4)	2854(3)	37(1)
C(13)	10823(4)	3814(5)	1137(4)	38(1)
C(14)	10501(5)	5829(4)	1919(4)	41(1)
C(21)	5552(4)	3997(4)	-1060(3)	31(1)
C(22)	4301(4)	3899(4)	-227(4)	36(1)
C(23)	5147(5)	4835(4)	-2016(4)	39(1)
C(24)	5847(5)	2790(4)	-1582(4)	38(1)

Table 3. Bond lengths [Å] for h06rdk6.

Br-B	1.933(5)
B-N(2)	1.417(6)
B-N(1)	1.433(6)
N(1)-C(1)	1.455(5)
N(1)-C(11)	1.486(5)
N(2)-C(2)	1.466(5)
N(2)-C(21)	1.492(5)
C(1)-C(2)	1.515(6)
C(11)-C(12)	1.530(6)
C(11)-C(13)	1.535(6)
C(11)-C(14)	1.536(6)
C(21)-C(23)	1.525(6)
C(21)-C(24)	1.526(6)
C(21)-C(22)	1.546(5)

Table 4. Bond angles [deg] for h06rdk6.

N(2)-B-N(1)	111.3(4)
N(2)-B-Br	125.0(3)
N(1)-B-Br	123.6(3)
B-N(1)-C(1)	106.0(3)
B-N(1)-C(11)	129.7(4)
C(1)-N(1)-C(11)	120.1(3)
B-N(2)-C(2)	105.6(3)
B-N(2)-C(21)	130.8(3)
C(2)-N(2)-C(21)	118.1(3)
N(1)-C(1)-C(2)	104.7(3)
N(2)-C(2)-C(1)	104.4(3)
N(1)-C(11)-C(12)	109.8(3)
N(1)-C(11)-C(13)	110.2(3)
C(12)-C(11)-C(13)	111.0(4)
N(1)-C(11)-C(14)	110.7(3)
C(12)-C(11)-C(14)	107.3(3)
C(13)-C(11)-C(14)	107.8(4)
N(2)-C(21)-C(23)	110.3(3)
N(2)-C(21)-C(24)	110.7(3)
C(23)-C(21)-C(24)	107.7(3)
N(2)-C(21)-C(22)	109.8(3)
C(23)-C(21)-C(22)	108.8(4)
C(24)-C(21)-C(22)	109.5(4)

Table 5. Anisotropic displacement parameters ($\text{\AA}^2 \times 10^3$) for h06rdk6. The anisotropic displacement factor exponent takes the form:
 $-2 \pi^2 [h^2 a^{*2} U_{11} + \dots + 2 h k a^* b^* U_{12}]$

	U11	U22	U33	U23	U13	U12
Br	39(1)	25(1)	47(1)	6(1)	-5(1)	-3(1)
B	26(2)	27(2)	30(2)	0(2)	4(2)	-3(2)
N(1)	28(2)	24(2)	27(2)	1(1)	0(1)	0(1)
N(2)	24(2)	23(2)	32(2)	-1(1)	-3(1)	0(1)
C(1)	33(2)	27(2)	40(2)	4(2)	-5(2)	-7(2)
C(2)	32(2)	23(2)	42(2)	-2(2)	-8(2)	4(2)
C(11)	27(2)	28(2)	30(2)	1(2)	-1(2)	1(2)
C(12)	39(2)	42(3)	31(2)	-1(2)	-2(2)	0(2)
C(13)	27(2)	53(3)	34(2)	-8(2)	-1(2)	8(2)
C(14)	38(2)	41(3)	43(2)	-4(2)	-10(2)	-12(2)
C(21)	22(2)	38(3)	33(2)	-3(2)	-2(1)	0(2)
C(22)	27(2)	43(3)	37(2)	-3(2)	1(2)	-2(2)
C(23)	35(2)	46(3)	37(2)	-2(2)	-6(2)	-3(2)
C(24)	32(2)	39(2)	44(2)	-7(2)	-2(2)	-1(2)

Table 6. Hydrogen coordinates ($\times 10^4$) and isotropic displacement parameters ($\text{\AA}^2 \times 10^3$) for h06rdk6.

	x	y	z	U(eq)
H(1)	9016	6519	234	40
H(2)	6377	6330	-605	39
H(12A)	8656	4728	3216	56
H(12B)	10123	4044	3334	56
H(12C)	8807	3409	2747	56
H(13A)	10427	3016	1100	57
H(13B)	11696	3800	1580	57
H(13C)	11025	4095	370	57
H(14A)	10827	6159	1199	61
H(14B)	11310	5704	2421	61
H(14C)	9841	6380	2276	61
H(22A)	4532	3330	369	54
H(22B)	3461	3632	-636	54
H(22C)	4117	4673	112	54
H(23A)	4907	5609	-1700	59
H(23B)	4332	4516	-2423	59
H(23C)	5942	4918	-2539	59
H(24A)	6681	2840	-2068	57
H(24B)	5033	2541	-2034	57
H(24C)	6015	2213	-979	57

4. Crystal Structure: N,N-diethylethylenediamine Lithium Chloride Complex.

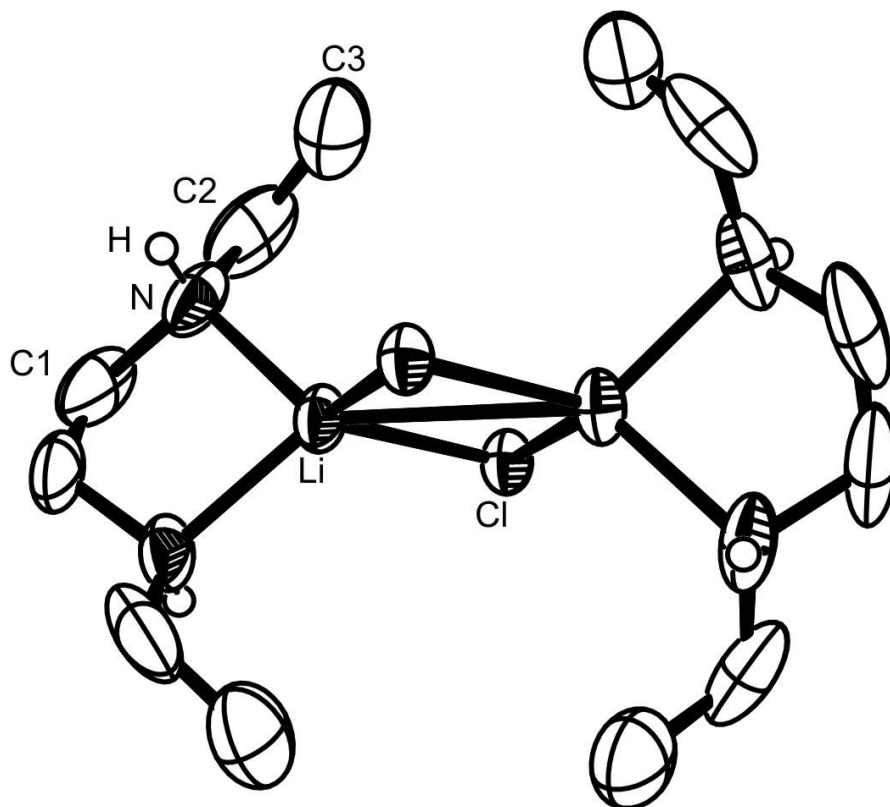


Table 1. Crystal data and structure refinement for k06rdk2.

Identification code	k06rdk2
Empirical formula	C ₂₄ H ₆₄ Cl ₄ Li ₄ N ₈
Formula weight	634.39
Temperature	150(2) K
Wavelength	0.71073 Å
Crystal system	orthorhombic
Space group	F d d d (70)
Unit cell dimensions	a = 13.0000(4) Å alpha = 90 deg. b = 16.0990(6) Å beta = 90 deg. c = 19.3650(7) Å gamma = 90 deg.
Volume	4052.8(2) Å ³
Z, Calculated density	4, 1.040 Mg/m ³
Absorption coefficient	0.315 mm ⁻¹
F(000)	1376
Crystal size	0.25 x 0.25 x 0.08 mm
Theta range for data collection	3.29 to 27.47 deg.
Limiting indices	-15 ≤ h ≤ 16, -19 ≤ k ≤ 20, -25 ≤ l ≤ 25
Reflections collected / unique	7463 / 1171 [R(int) = 0.0581]
Completeness to theta = 27.47	99.8 %
Max. and min. transmission	0.9752 and 0.9254
Refinement method	Full-matrix least-squares on F ²
Data / restraints / parameters	1171 / 0 / 51
Goodness-of-fit on F ²	1.047
Final R indices [I > 2sigma(I)]	R1 = 0.0434, wR2 = 0.1037
R indices (all data)	R1 = 0.0652, wR2 = 0.1150
Largest diff. peak and hole	0.213 and -0.284 e.Å ⁻³

Table 2. Atomic coordinates ($\times 10^4$) and equivalent isotropic displacement parameters ($\text{\AA}^2 \times 10^3$) for k06rdk2. U(eq) is defined as one third of the trace of the orthogonalized Uij tensor.

	x	y	z	U(eq)
Li	1250	1250	480 (2)	42 (1)
Cl	1250	117 (1)	1250	39 (1)
N	2352 (2)	1152 (1)	-310 (1)	61 (1)
C (1)	1707 (2)	984 (2)	-915 (1)	97 (1)
C (2)	3197 (3)	541 (2)	-203 (2)	92 (1)
C (3)	3934 (3)	828 (2)	327 (1)	95 (1)

Table 3. Bond lengths [\AA] for k06rdk2.

Li-N	2.101 (3)
Li-N#1	2.101 (3)
Li-Cl#1	2.356 (2)
Li-Cl	2.356 (2)
Li-Li#2	2.983 (7)
Cl-Li#2	2.356 (2)
N-C (1)	1.466 (3)
N-C (2)	1.489 (4)
N-H	0.82 (2)
C (1)-C (1) #1	1.465 (7)
C (2)-C (3)	1.479 (4)

Symmetry transformations used to generate equivalent atoms:
 #1 $-x+1/4, -y+1/4, z$ #2 $x, -y+1/4, -z+1/4$

Table 4. Bond angles [deg] for k06rdk2.

N-Li-N#1	86.60 (18)
N-Li-Cl#1	121.24 (5)
N#1-Li-Cl#1	113.75 (6)
N-Li-Cl	113.75 (6)
N#1-Li-Cl	121.24 (5)
Cl#1-Li-Cl	101.44 (14)
N-Li-Li#2	136.70 (9)
N#1-Li-Li#2	136.70 (9)
Cl#1-Li-Li#2	50.72 (7)
Cl-Li-Li#2	50.72 (7)
Li#2-Cl-Li	78.56 (14)
C (1) -N-C (2)	114.2 (2)
C (1) -N-Li	101.87 (16)
C (2) -N-Li	116.84 (15)
C (1) -N-H	105.6 (15)
C (2) -N-H	109.7 (15)
Li-N-H	107.8 (15)
C (1) #1-C (1) -N	110.9 (2)
C (3) -C (2) -N	111.5 (2)

Symmetry transformations used to generate equivalent atoms:

#1 $-x+1/4, -y+1/4, z$ #2 $x, -y+1/4, -z+1/4$

Table 5. Anisotropic displacement parameters ($\text{\AA}^2 \times 10^3$) for k06rdk2.
The anisotropic displacement factor exponent takes the form:
 $-2 \pi^2 [h^2 a^{*2} U_{11} + \dots + 2 h k a^* b^* U_{12}]$

	U11	U22	U33	U23	U13	U12
Li	57(2)	43(2)	26(2)	0	0	-9(2)
Cl	50(1)	38(1)	29(1)	0	0(1)	0
N	84(1)	65(1)	34(1)	-9(1)	17(1)	-34(1)
C(1)	113(2)	146(3)	32(1)	-26(1)	20(1)	-76(2)
C(2)	108(2)	87(2)	81(2)	-24(2)	58(2)	-11(2)
C(3)	110(2)	110(2)	65(2)	11(2)	14(2)	14(2)

Table 6. Hydrogen coordinates ($\times 10^4$) and isotropic displacement parameters ($\text{\AA}^2 \times 10^3$) for k06rdk2.

	x	y	z	U(eq)
H	2597(16)	1617(15)	-374(11)	54(6)
H(1A)	2110	1085	-1341	116
H(1B)	1493	394	-912	116
H(2A)	2899	2	-59	110
H(2B)	3565	454	-645	110
H(3A)	4475	411	387	142
H(3B)	3572	909	766	142
H(3C)	4242	1355	180	142

5. Crystal Structure: 1-keto-2,5-di-*tert*-butyl-2,5-diazacyclopentane.

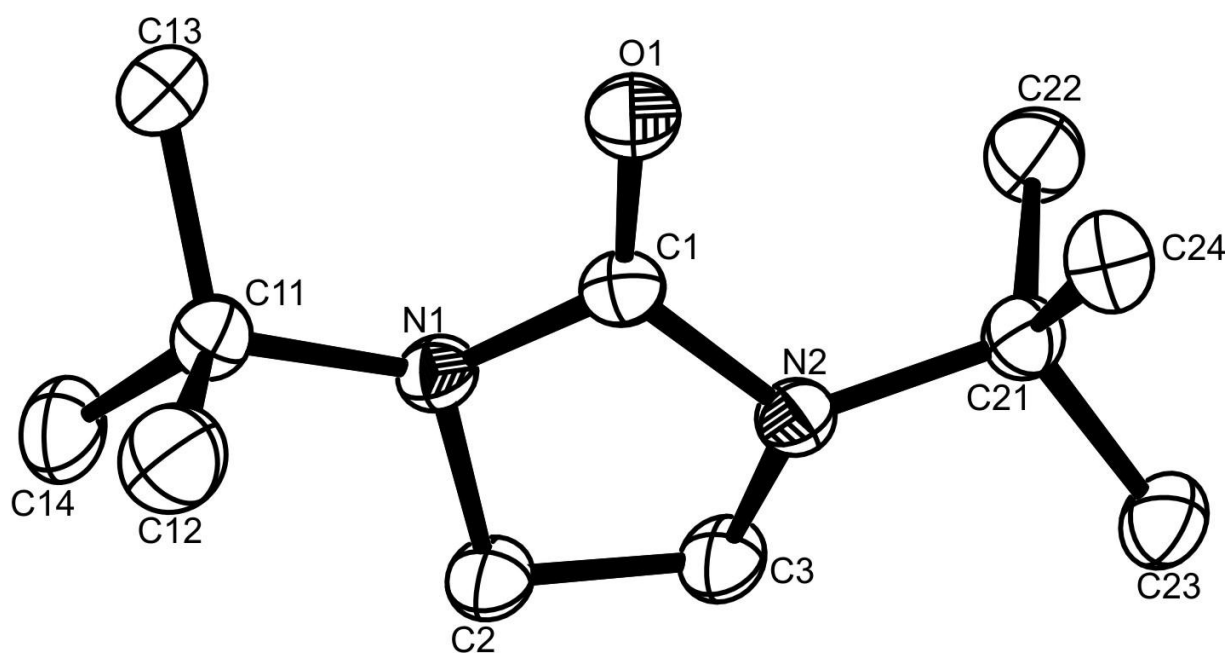


Table 1. Crystal data and structure refinement for h06rdk13.

Identification code	h06rdk13
Empirical formula	C11 H22 N2 O
Formula weight	198.31
Temperature	150(2) K
Wavelength	0.71073 Å
Crystal system	monoclinic
Space group	P 2 ₁ /n
Unit cell dimensions	a = 6.33300(10) Å alpha = 90 deg. b = 18.9270(5) Å beta = 94.851(2) deg. c = 9.9100(2) Å gamma = 90 deg.
Volume	1183.60(4) Å ³
Z, Calculated density	4, 1.113 Mg/m ³
Absorption coefficient	0.072 mm ⁻¹
F(000)	440
Crystal size	0.60 x 0.50 x 0.50 mm
Theta range for data collection	4.13 to 27.46 deg.
Limiting indices	-8<=h<=8, -24<=k<=24, -12<=l<=12
Reflections collected / unique	19001 / 2685 [R(int) = 0.0515]
Completeness to theta = 27.46	99.3 %
Max. and min. transmission	0.9651 and 0.9583
Refinement method	Full-matrix least-squares on F ²
Data / restraints / parameters	2685 / 0 / 133
Goodness-of-fit on F ²	1.037
Final R indices [I>2sigma(I)]	R1 = 0.0383, wR2 = 0.0935
R indices (all data)	R1 = 0.0519, wR2 = 0.1016
Largest diff. peak and hole	0.238 and -0.169 e.Å ⁻³

Table 2. Atomic coordinates ($\times 10^4$) and equivalent isotropic displacement parameters ($\text{\AA}^2 \times 10^3$) for h06rdk13. U(eq) is defined as one third of the trace of the orthogonalized U_{ij} tensor.

	x	y	z	U(eq)
O(1)	-1275(1)	1407(1)	1666(1)	34(1)
C(1)	548(2)	1365(1)	1345(1)	24(1)
C(2)	3948(2)	954(1)	1157(1)	32(1)
C(3)	3618(2)	1629(1)	345(1)	32(1)
N(1)	1780(1)	759(1)	1408(1)	25(1)
C(11)	1445(2)	177(1)	2376(1)	28(1)
C(12)	1966(2)	435(1)	3826(1)	40(1)
C(13)	-833(2)	-92(1)	2188(1)	35(1)
C(14)	2905(2)	-432(1)	2062(2)	42(1)
N(2)	1701(1)	1913(1)	854(1)	25(1)
C(21)	671(2)	2558(1)	247(1)	28(1)
C(22)	-743(2)	2360(1)	-1027(1)	40(1)
C(23)	2411(2)	3065(1)	-120(1)	36(1)
C(24)	-630(2)	2920(1)	1281(1)	34(1)

Table 3. Bond lengths [Å] for h06rdk13.

O(1)-C(1)	1.2253(13)
C(1)-N(2)	1.3807(13)
C(1)-N(1)	1.3855(13)
C(2)-N(1)	1.4626(13)
C(2)-C(3)	1.5159(16)
C(3)-N(2)	1.4559(14)
N(1)-C(11)	1.4877(13)
C(11)-C(14)	1.5261(16)
C(11)-C(13)	1.5264(15)
C(11)-C(12)	1.5273(16)
N(2)-C(21)	1.4864(14)
C(21)-C(23)	1.5277(15)
C(21)-C(24)	1.5304(16)
C(21)-C(22)	1.5313(15)

Table 4. Bond angles [deg] for h06rdk13.

O(1)-C(1)-N(2)	125.47(10)
O(1)-C(1)-N(1)	125.57(10)
N(2)-C(1)-N(1)	108.95(9)
N(1)-C(2)-C(3)	102.30(9)
N(2)-C(3)-C(2)	102.07(8)
C(1)-N(1)-C(2)	108.50(8)
C(1)-N(1)-C(11)	122.08(8)
C(2)-N(1)-C(11)	118.87(9)
N(1)-C(11)-C(14)	107.77(9)
N(1)-C(11)-C(13)	110.68(9)
C(14)-C(11)-C(13)	107.78(10)
N(1)-C(11)-C(12)	109.81(9)
C(14)-C(11)-C(12)	110.31(10)
C(13)-C(11)-C(12)	110.43(10)
C(1)-N(2)-C(3)	109.04(8)
C(1)-N(2)-C(21)	122.16(9)
C(3)-N(2)-C(21)	120.86(8)
N(2)-C(21)-C(23)	108.15(9)
N(2)-C(21)-C(24)	109.82(8)
C(23)-C(21)-C(24)	108.52(9)
N(2)-C(21)-C(22)	109.82(9)
C(23)-C(21)-C(22)	109.93(9)
C(24)-C(21)-C(22)	110.56(10)

Table 5. Anisotropic displacement parameters ($\text{\AA}^2 \times 10^3$) for h06rdk13.
The anisotropic displacement factor exponent takes the form:
 $-2 \pi^2 [h^2 a^{*2} U_{11} + \dots + 2 h k a^* b^* U_{12}]$

	U11	U22	U33	U23	U13	U12
O(1)	23(1)	34(1)	48(1)	7(1)	9(1)	1(1)
C(1)	22(1)	27(1)	23(1)	-1(1)	1(1)	-2(1)
C(2)	24(1)	31(1)	41(1)	2(1)	11(1)	0(1)
C(3)	28(1)	32(1)	38(1)	2(1)	11(1)	-2(1)
N(1)	22(1)	26(1)	29(1)	1(1)	5(1)	-1(1)
C(11)	27(1)	26(1)	30(1)	3(1)	4(1)	-1(1)
C(12)	45(1)	44(1)	30(1)	3(1)	0(1)	-7(1)
C(13)	32(1)	33(1)	42(1)	7(1)	2(1)	-7(1)
C(14)	40(1)	29(1)	57(1)	8(1)	14(1)	5(1)
N(2)	23(1)	26(1)	26(1)	2(1)	4(1)	-1(1)
C(21)	30(1)	28(1)	26(1)	4(1)	-1(1)	-2(1)
C(22)	44(1)	43(1)	31(1)	4(1)	-9(1)	-5(1)
C(23)	39(1)	31(1)	38(1)	7(1)	4(1)	-6(1)
C(24)	35(1)	28(1)	38(1)	2(1)	2(1)	4(1)

Table 6. Hydrogen coordinates ($\times 10^4$) and isotropic displacement parameters ($\text{\AA}^2 \times 10^3$) for h06rdk13.

	x	y	z	U(eq)
H(2A)	4621	584	632	38
H(2B)	4829	1037	2016	38
H(3A)	4829	1956	521	39
H(3B)	3408	1530	-638	39
H(12A)	3434	604	3933	60
H(12B)	1791	46	4458	60
H(12C)	1008	822	4018	60
H(13A)	-1796	274	2469	53
H(13B)	-971	-516	2741	53
H(13C)	-1193	-208	1232	53
H(14A)	2630	-567	1109	62
H(14B)	2639	-836	2640	62
H(14C)	4385	-282	2234	62
H(22A)	116	2133	-1681	60
H(22B)	-1402	2788	-1430	60
H(22C)	-1849	2033	-786	60
H(23A)	3391	3152	682	54
H(23B)	1771	3512	-439	54
H(23C)	3185	2856	-836	54
H(24A)	-1815	2614	1477	50
H(24B)	-1180	3370	911	50
H(24C)	273	3007	2117	50

Appendix 3:

^1H NMR Spectra of 1-Hexene Catalysis: Mathematical Interpretation:

The catalysis of 1-hexene trimerisation by the following systems was attempted:

1. Dodecyl₃TAC-CrCl₃:
2. OC(*tert*-BuNCH₂)₂ + HexylMgBr + CrCl₃.THF₃
3. OC(*tert*-BuNCH₂)₂ + CrCl₃.THF₃
4. (2-Et)Hex₃TAC/NaOCH₂C₆H₄NH₂ + CrCl₃.THF₃
5. (2-Et)Hex₃TAC/NaOCH₂C₆H₄NH₂ + CrCl₃.THF₃ + B(C₆F₅)₃.Et₂O
6. PhB(*tert*-BuNCH₂)₂ + NMe₄F + CrCl₃.THF₃
7. PhB(*tert*-BuNCH₂)₂ + CrCl₃.THF₃
8. PhB(*tert*-BuNCH₂)₂ + HexylMgBr + CrCl₃.THF₃
9. Na⁺[PhB(OH)₂OBu] + CrCl₃.THF₃

For derivation of calculations, see '4. Catalysis- NMR interpretation:'

For a given ^1H NMR spectrum:

a = integral: 1-hexene, CH₂=CHC₄H₉.

A = 12a: magnitude of sum of integrals of 1-hexene protons.

b = 3/5 sum integral toluene solvent aromatic signals. (Equates to toluene CH₃ signal).

c = sum of all integrals, (excluding toluene aromatic signal and hexane/MAO integral).

d = c - (3/5)b

e = d - A = sum of integrals of oligomerisation and isomerisation products.

f = sum of olefinic signals (excluding 'a').

g = f - 2a = sum of olefinic signals of oligomerisation and isomerisation products.

h = sum integrals of aliphatic signals, (excluding toluene aromatic signal and hexane/MAO integral).

i = h - 9a = sum integrals of aliphatic signals of oligomerisation and isomerisation products.

Error margins:

For each spectrum, error in determination of integrals was estimated as ca. 1% of magnitude of integral 'a'.

% error for each calculation is then defined as $[(N_L - N)/N]100\%$, where N is the calculated value, N_L is the largest possible value of N, within the accuracy limits imposed on the previous calculation, eg.

For the calculation:

$$200(\pm 10\%) - 100(\pm 10\%) = N,$$

$$N = 200 - 100 = 100$$

$$N_L = 200(1.10) - 100(0.90) = 220 - 90 = 130$$

$$\therefore [(N_L - N)/N]100\% = [(130 - 100)/100]100\% = \pm 30\%$$

Error margins based on comparative estimate of product chain length across spectra, $T_0 \rightarrow T_i$, are ca. '0' to 3 significant figures, and as such, are not listed in the following calculations. While the limited accuracy of measurement in the comparative calculation is not significant, the latter is extremely sensitive to any change in relative concentration of solvent, which represent unquantified potential error factors. (All error margins $<0.01\%$ are also unlisted).

1. Calculation of mass % conversion of 1-hexene to products- Example spectrum: Catalysis of ethylene trimerisation by 1,3,5-Tris-dodecyl-1,3,5-triazacyclohexane:

$$T = 0$$

$$1. a = 10.00$$

$$A = 12a = 12(10.00) = 120.00 \pm 1\%$$

$$2. c = 353.07 \pm 0.03\%$$

$$(3/5)b = (3/5)(374.70) = 224.82 \pm 0.03\%$$

$$d = c - (3/5)b = 353.07 - 224.82 = 128.25 \pm 0.14\%$$

$$3. e = d - A = 128.25 - 120.00 = 8.25 \pm 14.5\%$$

$$4. e/d \times 100\% = 6.4\% \pm 0.97\% \text{ (mass) conversion.}$$

Calculation of mean olefinic to aliphatic proton ratio in 1-hexene reaction products:

$$f = 20.64 \pm 0.48\%$$

$$g = f - 2a = 20.64 - 2(10.00) = 0.64 \pm 47.00\%$$

$$h = 322.43 - 224.82 = 97.61 \pm 0.17\%$$

$$i = 97.61 - 9(10.00) = 7.61 \pm 14.00\%$$

$$\text{ratio } g : i = 0.64 \pm 47.00\% : 7.61 \pm 14.00\%$$

$$= 2 : 23.8$$

$$6 + 2n = 23.8$$

$$2n = 17.8$$

$$n = 8.9 \pm 41.50\%$$

$$\underline{x = n + 4 = 12.9 \text{ carbons, or } 2.15 \text{ 1-hexene monomer units.}}$$

$$T = 3 \text{ hrs}$$

$$1. a = 1.00$$

$$A = 12a = 12(1.00) = 12.0 \pm 1\%$$

$$2. c = 42.5 \pm 0.02\%$$

$$(3/5)b = (3/5)(41.05) = 24.63 \pm 0.02\%$$

$$d = c - (3/5)b = 42.50 - 24.63 = 17.87 \pm 0.06\%$$

$$3. e = d - A = 17.87 - 12.0 = 5.87 \pm 2.2\%$$

$$4. e/d \times 100\% = 32.8\% \pm 0.75\% \text{ (mass) conversion.}$$

Calculation of mean olefinic to aliphatic proton ratio in 1-hexene reaction products:

$$f = 2.35 \pm 0.42\%$$

$$g = f - 2a = 2.35 - 2(1.00) = 0.35 \pm 6.50\%$$

$$h = 14.52 \pm 0.07\%$$

$$i = h - 9a = 14.52 - 9(1.00) = 5.52 \pm 10.00\%$$

$$\text{ratio } g : i = 0.35 \pm 6.5\% : 5.52 \pm 10.00\%$$

$$= 2 : 31.5$$

$$6 + 2n = 31.5$$

$$2n = 25.5$$

$$n = 12.8 \pm 15.43\%$$

$$x = n + 4 = 16.8 \text{ carbons, or } 2.8 \text{ 1-hexene monomer units.}$$

$$T = 24 \text{ hrs}$$

$$1. a = 10.00$$

$$A = 12a = 12(10.00) = 120.00 \pm 1\%$$

$$2. c = 549.65 \pm 0.02\%$$

$$(3/5)b = (3/5)(435.01) = 261.01 \pm 0.04\%$$

$$d = c - (3/5)b = 549.65 - 261.01 = 288.64$$

$$3. e = d - A = 288.64 - 120.00 = 168.64 \pm 0.71\%$$

$$4. e/d \times 100\% = 58.4\% \pm 0.44\% \text{ (mass) conversion.}$$

Calculation of mean olefinic to aliphatic proton ratio in 1-hexene reaction products:

$$f = 30.15 \pm 0.33\%$$

$$g = f - 2a = 30.15 - 2(10.00) = 10.15 \pm 3.00\%$$

$$h = 509.5 - 261.01 = 248.49 \pm 0.08\%$$

$$i = h - 9a = 248.49 - 9(10.00) = 158.49 \pm 0.69\%$$

$$\text{ratio } g : i = 10.15 \pm 3.00\% : 158.49 \pm 0.69\%$$

$$= 2 : 31.22$$

$$6 + 2n = 31.22$$

$$2n = 25.22$$

$$n = 12.61 \pm 3.85\%$$

$$x = n + 4 = 16.6 \text{ carbons, or } 2.8 \text{ 1-hexene monomer units.}$$

Comparative estimate of Product Chain Length:

(See '4. Catalysis- NMR interpretation:')

$$T = 0 \text{ hrs} \rightarrow T = 24 \text{ hrs}$$

$$(\Delta M / \Delta N + 2) / 2 = (7.09 / 5.50 + 2) / 2 = \underline{1.64 \text{ 1-hexene monomer units.}}$$

Trimerisation Properties of 1-keto-2,5-di-*tert*-butyl-2,5-diazacyclopentane-Chromium III Chloride complex + Hexylmagnesium Bromide:

$$T = 0$$

$$1. a = 32.43$$

$$A = 12a = 12(32.43) = 389.16 \pm 1\%$$

$$2. c = 563.07 \pm 0.06\%$$

$$(3/5)b = (3/5)(100.00) = 60.00 \pm 0.32\%$$

$$d = c - (3/5)b = 563.07 - 60.00 = 503.07 \pm 0.11\%$$

$$3. e = d - A = 503.07 - 389.16 = 113.91 \pm 3.90\%$$

$$4. e/d \times 100\% = 22.60\% \pm 0.95\% \text{ (mass) conversion.}$$

Calculation of mean olefinic to aliphatic proton ratio in 1-hexene reaction products:

$$f = 73.29 \pm 0.44\%$$

$$g = f - 2a = 73.29 - 2(32.43) = 8.43 \pm 11.4\%$$

$$h = 397.35 \pm 0.08\%$$

$$i = h - 9a = 397.35 - 9(32.43) = 105.48 \pm 2.73\%$$

$$\text{ratio } g : i = 8.43 \pm 11.40\% : 105.48 \pm 2.73\%$$

$$= 2 : 25.0$$

$$6 + 2n = 25.0$$

$$2n = 19.0$$

$$n = 9.5 \pm 16.01\%$$

$$\underline{x = n + 4 = 13.5 \text{ carbons, or } 2.3 \text{ 1-hexene monomer units.}}$$

$$T = 0.2 \text{ hrs}$$

$$1. a = 32.31$$

$$A = 12a = 12(32.31) = 387.72 \pm 1\%$$

$$2. c = 526.57 \pm 0.32\%$$

$$(3/5)b = (3/5)(100.00) = 60.00 \pm 0.32\%$$

$$d = c - (3/5)b = 526.57 - 60.00 = 466.57 \pm 0.04\%$$

$$3. e = d - A = 466.57 - 387.72 = 78.85 \pm 5.16\%$$

$$4. e/d \times 100\% = 16.90\% \pm 0.89\% \text{ (mass) conversion.}$$

Calculation of mean olefinic to aliphatic proton ratio in 1-hexene reaction products:

$$f = 69.72 \pm 0.46\%$$

$$g = f - 2a = 69.72 - 2(32.31) = 5.10 \pm 18.82\%$$

$$h = 364.54 \pm 0.09\%$$

$$i = h - 9a = 364.54 - 9(32.31) = 73.75 \pm 4.46\%$$

$$\text{ratio } g : i = 5.10 \pm 18.82\% : 73.75 \pm 4.46\%$$

$$= 2 : 28.9$$

$$6 + 2n = 28.9$$

$$2n = 22.9$$

$$n = 11.5 \pm 19.6\%$$

$$\underline{x = n + 4 = 15.5 \text{ carbons, or } 2.58 \text{ 1-hexene monomer units.}}$$

T = 48 hrs

1. $a = 30.70$

$$A = 12a = 12(30.70) = 368.40 \pm 1\%$$

2. $c = 552.99 \pm 0.06\%$

$$(3/5)b = (3/5)(100.00) = 60.00 \pm 0.31\%$$

$$d = c - (3/5)b = 552.99 - 60.00 = 492.99 \pm 0.11\%$$

3. $e = d - A = 492.99 - 368.40 = 124.59 \pm 3.39\%$

4. $e/d \times 100\% = 25.27\% \pm 0.83\%$ (mass) conversion.

Calculation of mean olefinic to aliphatic proton ratio in 1-hexene reaction products:

$$f = 68.69 \pm 0.45\%$$

$$g = f - 2a = 68.69 - 2(30.70) = 7.29 \pm 8.42\%$$

$$h = 393.60 \pm 0.08\%$$

$$i = h - 9a = 393.6 - 9(30.70) = 117.3 \pm 2.61\%$$

$$\text{ratio } g : i = 7.29 \pm 8.42\% : 117.3 \pm 2.61\%$$

$$= 2 : 32.2$$

$$6 + 2n = 32.2$$

$$2n = 26.2$$

$$n = 13.1 \pm 11.99\%$$

$$\underline{x = n + 4 = 17.1 \text{ carbons, or } 2.9 \text{ 1-hexene monomer units.}}$$

Comparative estimate of Product Chain Length:

$$T = 0 \text{ hrs} \rightarrow T = 48 \text{ hrs}$$

$$(\Delta M / \Delta N + 2) / 2 = (4.60 / 1.73 + 2) / 2 = \underline{2.33 \text{ 1-hexene monomer units.}}$$

Trimerisation Properties of 1-keto-2,5-di-*tert*-butyl-2,5-diazacyclopentane-Chromium III Chloride complex:

T = 0

1. $a = 1704.33$

$$A = 12a = 12(1704.33) = 20451.92 \pm 1\%$$

2. $c = 31191.45 \pm 0.05\%$

$$(3/5)b = (3/5)(14338.70) = 8603.22 \pm 0.12\%$$

$$d = c - (3/5)b = 31191.45 - 8603.22 = 22588.23 \pm 0.11\%$$

3. $e = d - A = 22588.23 - 20451.92 = 2136.31 \pm 10.74\%$

4. $e/d \times 100\% = 9.46\% \pm 1.02\%$ (mass) conversion.

Calculation of mean olefinic to aliphatic proton ratio in 1-hexene reaction products:

Signal intensities prohibit meaningful measurement.

T = 24 hrs

1. $a = 0.080$

$$A = 12a = 12(0.080) = 0.960 \pm 1\%$$

2. $c = 1.827 \pm 0.04\%$

$$(3/5)b = (3/5)(1.000) = 0.600 \pm 0.08\%$$

$$d = c - (3/5)b = 1.827 - 0.600 = 1.227 \pm 0.57\%$$

3. $e = d - A = 1.227 - 0.960 = 0.267 \pm 6.37\%$

4. $e/d \times 100\% = 21.76\% \pm 1.50\%$ (mass) conversion.

Calculation of mean olefinic to aliphatic proton ratio in 1-hexene reaction products:

$$f = 0.181 \pm 0.44\%$$

$$g = f - 2a = 0.181 - 2(0.080) = 0.021 \pm 12.38\%$$

$$h = 0.966 \pm 0.08\%$$

$$i = h - 9a = 0.966 - 9(0.080) = 0.246 \pm 3.25\%$$

$$\text{ratio } g : i = 0.021 \pm 12.38\% : 0.246 \pm 3.25\%$$

$$= 2 : 23.42$$

$$6 + 2n = 23.42$$

$$2n = 17.42$$

$$n = 8.71 \pm 17.89\%$$

$$\underline{x = n + 4 = 12.7 \text{ carbons, or } 2.12 \text{ 1-hexene monomer units.}}$$

$$T = 48 \text{ hrs}$$

$$1. a = 7.66$$

$$A = 12a = 12(7.66) = 91.92 \pm 1\%$$

$$2. c = 187.27 \pm 0.04\%$$

$$(3/5)b = (3/5)(100.00) = 60.00 \pm 0.08\%$$

$$d = c - (3/5)b = 187.27 - 60.00 = 127.27 \pm 0.53\%$$

$$3. e = d - A = 127.27 - 91.92 = 35.35 \pm 2.60\%$$

$$4. e/d \times 100\% = 27.78\% \pm 0.87\% \text{ (mass) conversion.}$$

Calculation of mean olefinic to aliphatic proton ratio in 1-hexene reaction products:

$$f = 18.42 \pm 0.42\%$$

$$g = f - 2a = 18.42 - 2(7.66) = 3.10 \pm 7.52\%$$

$$h = 101.19 \pm 0.08\%$$

$$i = h - 9a = 101.19 - 9(7.66) = 32.25 \pm 2.39\%$$

$$\text{ratio } g : i = 3.10 \pm 7.52\% : 32.25 \pm 2.39\%$$

$$= 2 : 20.81$$

$$6 + 2n = 20.81$$

$$2n = 14.81$$

$$n = 7.41 \pm 10.63\%$$

$$x = n + 4 = 11.4 \text{ carbons, or } 1.9 \text{ 1-hexene monomer units.}$$

Comparative estimate of Product Chain Length:

$$T = 0 \text{ hrs} \rightarrow T = 48 \text{ hrs}$$

$$(\Delta M / \Delta N + 2) / 2 = (0.064 / 0.060 + 2) / 2 = \underline{1.53 \text{ 1-hexene monomer units.}}$$

Trimerisation Properties of 1,3,5-tris(2-ethyl)hexyl-1,3,5-triazacyclohexane, sodium 3-aminobenzylalcoholate + Chromium III Chloride:

$$T = 0$$

$$1. a = 0.060$$

$$A = 12a = 12(0.060) = 0.720 \pm 1\%$$

$$2. c = 1.470 \pm 0.04\%$$

$$(3/5)b = (3/5)(1.000) = 0.600 \pm 0.06\%$$

$$d = c - (3/5)b = 1.470 - 0.600 = 0.870 \pm 0.16\%$$

$$3. e = d - A = 0.870 - 0.72 = 0.15 \pm 5.33\%$$

$$4. e/d \times 100\% = 17.2\% \pm 0.93\% \text{ (mass) conversion.}$$

Calculation of mean olefinic to aliphatic proton ratio in 1-hexene reaction products:

$$f = 0.128 \pm 0.47\%$$

$$g = f - 2a = 0.128 - 2(0.060) = 0.008 \pm 12.5\%$$

$$h = 0.682 \pm 0.09\%$$

$$i = h - 9a = 0.682 - 9(0.060) = 0.14 \pm 6.00\%$$

$$\text{ratio } g : i = 0.008 \pm 12.5\% : 0.14 \pm 6.00\%$$

$$= 2 : 35.0$$

$$6 + 2n = 35.0$$

$$2n = 29.0$$

$$n = 14.5 \pm 3.15\%$$

$$\underline{x = n + 4 = 18.5 \text{ carbons, or 3.1 1-hexene monomer units.}}$$

$$T = 24 \text{ hrs}$$

$$1. a = 0.046$$

$$A = 12a = 12(0.046) = 0.552 \pm 1\%$$

$$2. c = 1.402 \pm 0.03\%$$

$$(3/5)b = (3/5)(1.000) = 0.600 \pm 0.05\%$$

$$d = c - (3/5)b = 1.402 - 0.600 = 0.802$$

$$3. e = d - A = 0.802 - 0.552 = 0.25 \pm 2.4\%$$

$$4. e/d \times 100\% = 31.2\% \pm 0.72\% \text{ (mass) conversion.}$$

Calculation of mean olefinic to aliphatic proton ratio in 1-hexene reaction products:

$$f = 0.121 \pm 0.38\%$$

$$g = f - 2a = 0.121 - 2(0.046) = 0.029 \pm 3.45\%$$

$$h = 0.635 \pm 0.07\%$$

$$i = h - 9a = 0.635 - 9(0.046) = 0.221 \pm 1.87\%$$

$$\text{ratio } g : i = 0.029 \pm 3.45\% : 0.221 \pm 1.87\%$$

$$= 2 : 15.24$$

$$6 + 2n = 15.24$$

$$2n = 9.24$$

$$n = 4.62 \pm 5.52\%$$

$$\underline{x = n + 4 = 8.62 \text{ carbons, or 1.4 1-hexene monomer units.}}$$

$$T = 48 \text{ hrs}$$

$$1. a = 0.038$$

$$A = 12a = 12(0.038) = 0.456 \pm 1\%$$

$$2. c = 1.437 \pm 0.03\%$$

$$(3/5)b = (3/5)(1.000) = 0.600 \pm 0.04\%$$

$$d = c - (3/5)b = 1.437 - 0.600 = 0.837$$

$$3. e = d - A = 0.837 - 0.456 = 0.381 \pm 1.31\%$$

$$4. e/d \times 100\% = 45.5\% \pm 0.60\% \text{ (mass) conversion.}$$

Calculation of mean olefinic to aliphatic proton ratio in 1-hexene reaction products:

$$f = 0.127 \pm 0.30\%$$

$$g = f - 2a = 0.127 - 2(0.038) = 0.051 \pm 1.57\%$$

$$h = 0.837 \pm 0.05\%$$

$$i = h - 9a = 0.837 - 9(0.038) = 0.495 \pm 0.34\%$$

$$\text{ratio } g : i = 0.051 \pm 1.57\% : 0.495 \pm 0.34\%$$

$$= 2 : 19.41$$

$$6 + 2n = 19.41$$

$$2n = 13.41$$

$$n = 6.71 \pm 2.30\%$$

$$\underline{x = n + 4 = 10.7 \text{ carbons, or } 1.8 \text{ 1-hexene monomer units.}}$$

Comparative estimate of Product Chain Length:

$$T = 0 \text{ hrs} \rightarrow T = 48 \text{ hrs}$$

$$(\Delta M / \Delta N + 2) / 2 = (0.053 / 0.020 + 2) / 2 = \underline{2.33 \text{ 1-hexene monomer units.}}$$

**Trimerisation Properties of 1,3,5-tris(2-ethyl)hexyl-1,3,5-triazacyclohexane,
sodium 3-aminobenzylalcoholate + Chromium III Chloride + 1 eq.**

Tris(pentafluoro)phenylborane:

$$T = 0$$

$$1. a = 3.05$$

$$A = 12a = 12(3.05) = 36.6 \pm 1\%$$

$$2. c = 107.59 \pm 0.03\%$$

$$(3/5)b = (3/5)(100.00) = 60.00 \pm 0.03\%$$

$$d = c - (3/5)b = 107.59 - 60.00 = 47.59 \pm 0.04\%$$

$$3. e = d - A = 47.59 - 36.6 = 10.99 \pm 3.55\%$$

$$4. e/d \times 100\% = 23.09\% \pm 0.83\% \text{ (mass) conversion.}$$

**Calculation of mean olefinic to aliphatic proton ratio in 1-hexene reaction
products:**

$$f = 6.57 \pm 0.47\%$$

$$g = f - 2a = 6.57 - 2(3.05) = 0.47 \pm 19.36\%$$

$$h = 37.97 \pm 0.08\%$$

$$i = h - 9a = 37.97 - 9(3.05) = 10.52 \pm 2.89\%$$

$$\text{ratio } g : i = 0.47 \pm 19.36\% : 10.52 \pm 2.89\%$$

$$= 2 : 44.8$$

$$6 + 2n = 44.8$$

$$2n = 38.8$$

$$n = 19.4 \pm 18.56\%$$

$$\underline{x = n + 4 = 23.4 \text{ carbons, or } 3.9 \text{ 1-hexene monomer units.}}$$

$$T = 48 \text{ hrs}$$

$$1. a = 3.01$$

$$A = 12a = 12(3.01) = 36.12 \pm 1\%$$

$$2. c = 123.57 \pm 0.02\%$$

$$(3/5)b = (3/5)(100.00) = 60.00 \pm 0.03\%$$

$$d = c - (3/5)b = 123.57 - 60.00 = 63.57 \pm 0.06\%$$

$$3. e = d - A = 63.57 - 36.12 = 27.45 \pm 1.46\%$$

$$4. e/d \times 100\% = 43.18\% \pm 0.66\% \text{ (mass) conversion.}$$

Calculation of mean olefinic to aliphatic proton ratio in 1-hexene reaction products:

$$f = 8.85 \pm 0.34\%$$

$$g = f - 2a = 8.85 - 2(3.01) = 2.83 \pm 3.18\%$$

$$h = 51.71 \pm 0.06\%$$

$$i = h - 9a = 51.71 - 9(3.01) = 24.62 \pm 1.22\%$$

$$\text{ratio } g : i = 2.83 \pm 3.18\% : 24.62 \pm 1.22\%$$

$$= 2 : 17.4$$

$$6 + 2n = 17.4$$

$$2n = 11.4$$

$$n = 5.7 \pm 4.54\%$$

$$\underline{x = n + 4 = 9.7 \text{ carbons, or 1.6 1-hexene monomer units.}}$$

Comparative estimate of Product Chain Length:

$$T = 0 \text{ hrs} \rightarrow T = 48 \text{ hrs}$$

$$(\Delta M / \Delta N + 2) / 2 = (0.014 / 1.077 + 2) / 2 = \underline{1.00 \text{ 1-hexene monomer units.}}$$

Trimerisation Properties of 1-phenyl-2,5-di-*tert*-butyl-1-bora-2,5-diazacyclopentane- Chromium III Chloride complex + Tetramethylammonium Fluoride:

$$T = 0$$

$$1. a = 6.25$$

$$A = 12a = 12(6.25) = 75.00 \pm 1\%$$

$$2. c = 142.55 \pm 0.04\%$$

$$(3/5)b = (3/5)(100.00) = 60.00 \pm 0.06\%$$

$$d = c - (3/5)b = 82.55 \pm 0.12\%$$

$$3. e = d - A = 82.55 - 75.00 = 7.55 \pm 11.26\%$$

$$4. e/d \times 100\% = 9.15\% \pm 1.04\% \text{ (mass) conversion.}$$

Calculation of mean olefinic to aliphatic proton ratio in 1-hexene reaction products:

$$f = 13.57 \pm 0.46\%$$

$$g = f - 2a = 1.07 \pm 17.29\%$$

$$h = 62.73 - 9(6.25) = 6.48 \pm 9.61\%$$

$$i = h - 9a = 62.73 - 9(6.25) = 6.48 \pm 9.61\%$$

$$\text{ratio } g : i = 1.07 \pm 17.29\% : 6.48 \pm 9.61\%$$

$$= 2 : 12.2$$

$$6 + 2n = 12.2$$

$$2n = 6.2$$

$$n = 3.1 \pm 32.32\%$$

$$\underline{x = n + 4 = 7.1 \text{ carbons, or } 1.2 \text{ 1-hexene monomer units.}}$$

$$T = 24 \text{ hrs}$$

$$1. a = 0.062$$

$$A = 12a = 12(0.062) = 0.744 \pm 1\%$$

$$2. c = 1.427 \pm 0.04\%$$

$$(3/5)b = (3/5)(1.000) = 0.600 \pm 0.06\%$$

$$d = c - (3/5)b = 1.427 - 0.600 = 0.827$$

$$3. e = d - A = 0.827 - 0.744 = 0.083 \pm 8.43\%$$

$$4. e/d \times 100\% = 10.00\% \pm 0.88\% \text{ (mass) conversion.}$$

Calculation of mean olefinic to aliphatic proton ratio in 1-hexene reaction products:

$$f = 0.131 \pm 0.47\%$$

$$g = f - 2a = 0.131 - 2(0.062) = 0.007 \pm 14.3\%$$

$$h = 0.634 \pm 0.10\%$$

$$i = h - 9a = 0.634 - 9(0.062) = 0.076 \pm 9.21\%$$

$$\text{ratio } g : i = 0.007 \pm 14.3\% : 0.076 \pm 9.21\%$$

$$= 2 : 21.7$$

$$6 + 2n = 21.7$$

$$2n = 15.7$$

$$n = 7.9 \pm 20.58\%$$

$$\underline{x = n + 4 = 11.9 \text{ carbons, or } 2.0 \text{ 1-hexene monomer units.}}$$

Comparative estimate of Product Chain Length:

$$T = 0 \text{ hrs} \rightarrow T = 24 \text{ hrs}$$

$$(\Delta M / \Delta N + 2) / 2 = (0.005 / 0.001 + 2) / 2 = \underline{3.5 \text{ 1-hexene monomer units.}}$$

Trimerisation Properties of 1-Phenyl-2,5-di-*tert*-butyl-1-bora-2,5-diazacyclopentane- Chromium III Chloride complex:

T = 0

1. $a = 0.057$

$$A = 12a = 12(0.057) = 0.684 \pm 1\%$$

2. $c = 1.389 \pm 0.04\%$

$$(3/5)b = (3/5)(1.000) = 0.600 \pm 0.06\%$$

$$d = c - (3/5)b = 1.389 - 0.600 = 0.789 \pm 0.89\%$$

3. $e = d - A = 0.789 - 0.684 = 0.105 \pm 13.33\%$

4. $e/d \times 100\% = 13.33\% \pm 15.09\%$ (mass) conversion.

Calculation of mean olefinic to aliphatic proton ratio in 1-hexene reaction products:

$$f = 0.122 \pm 0.47\%$$

$$g = f - 2a = 0.122 - 2(0.057) = 0.008 \pm 25.00\%$$

$$h = 1.216 - 0.600 = 0.616 \pm 0.09\%$$

$$i = h - 9a = 0.616 - 9(0.057) = 0.103 \pm 5.83\%$$

$$\text{ratio } g : i = 0.008 \pm 25.00\% : 0.103 \pm 5.83\%$$

$$= 2 : 25.8$$

$$6 + 2n = 25.8$$

$$2n = 19.8$$

$$n = 9.9 \pm 41.05\%$$

$$\underline{x = n + 4 = 13.9 \text{ carbons, or } 2.3 \text{ 1-hexene monomer units.}}$$

T = 24 hrs

1. $a = 0.051$

$$A = 12a = 12(0.051) = 0.612 \pm 1\%$$

2. $c = 1.388 \pm 0.04\%$

$$(3/5)b = (3/5)(1.000) = 0.600 \pm 0.05\%$$

$$d = c - (3/5)b = 1.388 - 0.600 = 0.788 \pm 0.89\%$$

$$3. e = d - A = 0.788 - 0.612 = 0.176 \pm 7.39\%$$

$$4. e/d \times 100\% = 22.33\% \pm 1.87\% \text{ (mass) conversion.}$$

Calculation of mean olefinic to aliphatic proton ratio in 1-hexene reaction products:

$$f = 0.117 \pm 0.44\%$$

$$g = f - 2a = 0.117 - 2(0.051) = 0.015 \pm 13.33\%$$

$$h = 0.620 \pm 0.08\%$$

$$i = h - 9a = 0.620 - 9(0.051) = 0.161 \pm 3.11\%$$

$$\text{ratio } g : i = 0.015 \pm 13.33\% : 0.161 \pm 3.11\%$$

$$= 2 : 21.5$$

$$6 + 2n = 21.5$$

$$2n = 15.5$$

$$n = 7.7 \pm 19.01\%$$

$$\underline{x = n + 4 = 11.7 \text{ carbons, or 2.0 1-hexene monomer units.}}$$

$$T = 48 \text{ hrs}$$

$$1. a = 0.049$$

$$A = 12a = 12(0.049) = 0.588 \pm 1\%$$

$$2. c = 1.387 \pm 0.04\%$$

$$(3/5)b = (3/5)(1.000) = 0.600 \pm 0.05\%$$

$$d = c - (3/5)b = 1.387 - 0.600 = 0.787 \pm 0.89\%$$

$$3. e = d - A = 0.787 - 0.588 = 0.199 \pm 6.53\%$$

$$4. e/d \times 100\% = 25.29\% \pm 1.89\% \text{ (mass) conversion.}$$

Calculation of mean olefinic to aliphatic proton ratio in 1-hexene reaction products:

$$f = 0.116 \pm 0.42\%$$

$$g = f - 2a = 0.116 - 2(0.049) = 0.018 \pm 5.56\%$$

$$h = 0.622 \pm 0.08\%$$

$$i = h - 9a = 0.622 - 9(0.049) = 0.181 \pm 2.21\%$$

$$\text{ratio } g : i = 0.018 \pm 5.56\% : 0.181 \pm 2.21\%$$

$$= 2 : 20.2$$

$$6 + 2n = 20.2$$

$$2n = 14.2$$

$$n = 7.1 \pm 7.75\%$$

$$\underline{x = n + 4 = 11.1 \text{ carbons, or } 1.9 \text{ 1-hexene monomer units.}}$$

Comparative estimate of Product Chain Length:

$$T = 0 \text{ hrs} \rightarrow T = 48 \text{ hrs}$$

$$(\Delta M / \Delta N + 2) / 2 = (0.003 / 0.008 + 2) / 2 = \underline{1.2 \text{ 1-hexene monomer units.}}$$

Trimerisation Properties of 1-phenyl-2,5-di-*tert*-butyl-1-bora-2,5-diazacyclopentane- Chromium III Chloride complex + Hexylmagnesium bromide:

$$T = 0$$

$$1. a = 0.027$$

$$A = 12a = 12(0.027) = 0.324 \pm 1\%$$

$$2. c = 1.028 \pm 0.03\%$$

$$(3/5)b = (3/5)(1.000) = 0.600 \pm 0.03\%$$

$$d = c - (3/5)b = 1.028 - 0.600 = 0.428$$

$$3. e = d - A = 0.428 - 0.324 = 0.104 \pm 2.88\%$$

$$4. e/d \times 100\% = 24.30\% \pm 0.70\% \text{ (mass) conversion.}$$

Calculation of mean olefinic to aliphatic proton ratio in 1-hexene reaction products:

$$f = 0.057 \pm 0.47\%$$

$$g = f - 2a = 0.057 - 2(0.027) = 0.003 \pm 33.33\%$$

$$h = 0.347 \pm 0.08\%$$

$$i = h - 9a = 0.347 - 9(0.027) = 0.104 \pm 2.88\%$$

$$\text{ratio } g : i = 0.002 \pm 25.00\% : 0.104 \pm 2.88\%$$

$$= 2 : 104$$

$$6 + 2n = 104$$

$$2n = 98$$

$$n = 49 \pm 37.18\%$$

$$\underline{x = n + 4 = 53 \text{ carbons, or } 8.8 \text{ 1-hexene monomer units.}}$$

$$T = 24 \text{ hrs}$$

$$1. a = 0.029$$

$$A = 12a = 12(0.029) = 0.348 \pm 1\%$$

$$2. c = 1.144 \pm 0.03\%$$

$$(3/5)b = (3/5)(1.000) = 0.600 \pm 0.03\%$$

$$d = c - (3/5)b = 1.144 - 0.600 = 0.544 \pm 1.10\%$$

$$3. e = d - A = 0.544 - 0.348 = 0.196 \pm 4.85\%$$

$$4. e/d \times 100\% = 36.03\% \pm 2.26\% \text{ (mass) conversion.}$$

Calculation of mean olefinic to aliphatic proton ratio in 1-hexene reaction products:

$$f = 0.068 \pm 0.43\%$$

$$g = f - 2a = 0.068 - 2(0.029) = 0.01 \pm 5.80\%$$

$$h = 0.447 \pm 0.06\%$$

$$i = h - 9a = 0.447 - 9(0.029) = 0.186 \pm 1.61\%$$

$$\text{ratio } g : i = 0.01 \pm 5.80\% : 0.186 \pm 1.61\%$$

$$= 2 : 37.2$$

$$6 + 2n = 37.2$$

$$2n = 31.2$$

$$n = 15.6 \pm 7.87\%$$

$$x = n + 4 = 19.6 \text{ carbons, or } 3.3 \text{ 1-hexene monomer units.}$$

$$T = 48 \text{ hrs}$$

$$1. a = 0.036$$

$$A = 12a = 12(0.036) = 0.432 \pm 1\%$$

$$2. c = 1.235 \pm 0.03\%$$

$$(3/5)b = (3/5)(1.000) = 0.600 \pm 0.04\%$$

$$d = c - (3/5)b = 1.235 - 0.600 = 0.635$$

$$3. e = d - A = 0.635 - 0.432 = 0.203 \pm 1.97\%$$

$$4. e/d \times 100\% = 31.97\% \pm 0.63\% \text{ (mas) conversion.}$$

Calculation of mean olefinic to aliphatic proton ratio in 1-hexene reaction products:

$$f = 0.083 \pm 0.43\%$$

$$g = f - 2a = 0.083 - 2(0.036) = 0.011 \pm 9.09\%$$

$$h = 0.516 \pm 0.07\%$$

$$i = h - 9a = 0.516 - 9(0.036) = 0.192 \pm 1.56\%$$

$$\text{ratio } g : i = 0.011 \pm 9.09\% : 0.192 \pm 1.56\%$$

$$= 2 : 34.9$$

$$6 + 2n = 34.9$$

$$2n = 28.9$$

$$n = 14.5 \pm 1.75\%$$

$$x = n + 4 = 18.5 \text{ carbons, or } 3.1 \text{ 1-hexene monomer units.}$$

Comparative estimate of Product Chain Length:

$$T = 0 \text{ hrs} \rightarrow T = 24 \text{ hrs}$$

$$(\Delta M / \Delta N + 2) / 2 = (0.027 / 0.003 + 2) / 2 = \underline{5.5 \text{ 1-hexene monomer units.}}$$

Trimerisation Properties of Sodium Phenyl(bis-hydroxy)butoxyborate-Chromium III Chloride complex:

$$T = 0$$

$$1. a = 427.828$$

$$A = 12a = 12(427.828) = 5133.94 \pm 1\%$$

$$2. c = 6639.064 \pm 0.06\%$$

$$(3/5)b = (3/5)(1994.717) = 1196.830 \pm 0.36\%$$

$$d = c - (3/5)b = 5442.234 \pm 0.15\%$$

$$3. e = d - A = 5442.234 - 5133.94 = 308.294 \pm 19.3\%$$

$$4. e/d \times 100\% = 5.67\% \pm 1.10\% \text{ (mass) conversion.}$$

Calculation of mean olefinic to aliphatic proton ratio in 1-hexene reaction products:

Signal intensities prohibit meaningful measurement.

$$T = 24 \text{ hrs}$$

$$1. a = 0.091$$

$$A = 12a = 12(0.091) = 1.092 \pm 1\%$$

$$2. c = 1.949 \pm 0.05\%$$

$$(3/5)b = (3/5)(1.000) = 0.600 \pm 0.09\%$$

$$d = c - (3/5)b = 1.949 - 0.600 = 1.349 \pm 0.15\%$$

$$3. e = d - A = 1.349 - 1.092 = 0.257 \pm 5.06\%$$

$$4. e/d \times 100\% = 19.05\% \pm 0.99\% \text{ (mass) conversion.}$$

Calculation of mean olefinic to aliphatic proton ratio in 1-hexene reaction products:

$$f = 0.221 \pm 0.41\%$$

$$g = f - 2a = 0.221 - 2(0.091) = 0.039 \pm 7.23\%$$

$$h = 1.037 \pm 0.09\%$$

$$i = h - 9a = 1.037 - 9(0.091) = 0.218 \pm 4.13\%$$

$$\text{ratio } g : i = 0.039 \pm 7.23\% : 0.218 \pm 4.13\%$$

$$= 2 : 11.2$$

$$6 + 2n = 11.2$$

$$2n = 5.2$$

$$n = 2.6 \pm 12.80\%$$

$$\underline{x = n + 4 = 6.6 \text{ carbons, or 1.1 1-hexene monomer units.}}$$

$$T = 48 \text{ hrs}$$

$$1. a = 8.49$$

$$A = 12a = 12(8.49) = 101.88 \pm 1\%$$

$$2. c = 205.99 \pm 0.04\%$$

$$(3/5)b = (3/5)(100.00) = 60.00 \pm 0.09\%$$

$$d = c - (3/5)b = 205.99 - 60.00 = 145.99 \pm 0.09\%$$

$$3. e = d - A = 145.99 - 101.88 = 44.11 \pm 2.60\%$$

$$4. e/d \times 100\% = 30.21\% \pm 0.83\% \text{ (mass) conversion.}$$

Calculation of mean olefinic to aliphatic proton ratio in 1-hexene reaction products:

$$f = 21.9 \pm 0.39\%$$

$$g = f - 2a = 21.99 - 2(8.49) = 4.92 \pm 5.18\%$$

$$h = 115.6 \pm 0.07\%$$

$$i = h - 9a = 115.6 - 9(8.49) = 39.19 \pm 2.15\%$$

$$\text{ratio } g : i = 4.92 \pm 5.18\% : 39.19 \pm 2.15\%$$

$$= 2 : 15.9$$

$$6 + 2n = 15.9$$

$$2n = 9.9$$

$$n = 5.0 \pm 7.56\%$$

$$\underline{x = n + 4 = 9.0 \text{ carbons, or } 1.5 \text{ 1-hexene monomer units.}}$$

Comparative estimate of Product Chain Length:

$$T = 0 \text{ hrs} \rightarrow T = 24 \text{ hrs}$$

$$(\Delta M / \Delta N + 2) / 2 = (0.374 / 0.214 + 2) / 2 = \underline{1.9 \text{ 1-hexene monomer units.}}$$